
FUNDAMENTALS OF THE ELUTION OF GOLD CYANIDE FROM ACTIVATED CARBON

PIETER F. VAN DER MERWE



DISSERTATION PRESENTED FOR THE DEGREE OF DOCTOR OF PHILOSOPHY
IN ENGINEERING AT THE UNIVERSITY OF STELLENBOSCH

SUPERVISOR : PROF. J.S.J. VAN DEVENTER

JUNE 1991

*Aan Rebecca,
omdat jy geweet het dat alles sal regkom.*

DECLARATION

I the undersigned declare that the work contained in this thesis is my own original work and has not previously in its entirety or in part been submitted at any University for a degree.

P.F. van der Merwe

30 June 1991

ABSTRACT

Most research work on activated carbon systems has been concerned only with the adsorption process. Nevertheless, controversy still exists on the mechanism by which metal cyanide complexes such as $\text{Au}(\text{CN})_2^-$ are adsorbed onto activated carbon, and whether these complexes are decomposed to irreversibly adsorbed species, such as AuCN and $\text{Au}^{(0)}$. As these species determine directly the need for cyanide during the elution process, the first part of this thesis was devoted to a study of the reversibility of adsorption of metal cyanides on activated carbon and the role that oxygen plays in the adsorption reactions.

It was found that the formation of AuCN was mainly a function of the type of carbon used and that oxygen did not promote the decomposition of $\text{Au}(\text{CN})_2^-$ to AuCN . Although the dissolved oxygen level affected the equilibrium loading of anionic metal cyanides, it did not participate directly in the adsorption reaction. $\text{Au}^{(0)}$ was formed only under drastic conditions of low pH's and high temperatures. It was now possible to select a carbon on which no irreversibly adsorbed species were formed in order to study the mechanism of the desorption of gold cyanide and to determine the need for cyanide in the elution process.

Although the loaded carbon contained only $\text{Au}(\text{CN})_2^-$, the presence of cyanide was found to drastically enhance the elution of the gold. It was shown that the cyanide present in the elution step of an AARL elution was less important than the cyanide in the pretreatment solution. It was concluded that the cyanide passivates the carbon for the adsorption of anionic metal cyanides by reacting with the functional groups on the carbon surface. However, the presence of high concentrations of cations promotes the formation of neutral ion-pairs with the anionic metal cyanide on the carbon and thereby hinders the desorption of the metal cyanide in the pretreatment solution. Once the bulk of the cations are removed in the elution stage, the desorption of the gold increases rapidly.

As the concentrations of cyanide and the spectator cations, as well as their reactions, were found to affect the gold cyanide equilibrium, these

factors had to be accounted for in modelling the gold elution process. The system was simplified by using only one cation, namely potassium. Models were then developed to simulate the changes in cyanide and potassium concentrations during the elution of the gold cyanide. This enabled the calculation of a shifting gold cyanide equilibrium isotherm as a function of time and position in the column. The elution of the gold cyanide was found to be diffusion controlled only under conditions of weak desorption. Under these conditions, the desorption of the gold cyanide was simulated with a model accounting for mass transfer between the micropores and the macropores of the carbon, surface diffusion in the macropores, and film diffusion through the liquid layer surrounding the carbon particles. Under strong elution conditions (i.e. high temperatures and efficient pretreatments) the resistance to mass transfer became negligible and the desorption of the gold could be modelled with an equilibrium model. The equilibrium model was shown to be applicable to both the Zadra and the AARL elution processes.

Simulations of experimental data were presented as evidence of the validity of the models. Furthermore, the models were used to perform a parametric sensitivity analysis and to predict the elution profiles during a continuous elution process.

SAMEVATTING

Die meeste navorsingswerk op geaktiveerde koolstof het tot dusver gekonsentreer op die adsorpsie proses. Daar heers egter nog heelwat polemieke oor die meganisme waarmee metaalsianied komplekse soos $\text{Au}(\text{CN})_2^-$ op koolstof geadsorbeer word, en of hierdie komplekse afgebreek word na onomkeerbaar geadsorbeerde spesies soos AuCN en $\text{Au}^{(0)}$. Aangesien die noodsaaklikheid van sianied in die elueringsproses bepaal word deur die teenwoordigheid van hierdie spesies, is die eerste gedeelte van hierdie proefskrif afgestaan aan 'n studie van die omkeerbaarheid van die adsorpsie van metaalsianiede op geaktiveerde koolstof, en die rol wat suurstof in die adsorpsiereaksies speel.

Daar is gevind dat die vorming van AuCN hoofsaaklik 'n funksie is van die tipe koolstof wat gebruik word en dat die afbreking van $\text{Au}(\text{CN})_2^-$ na AuCN nie deur suurstof bevorder word nie. Alhoewel die opgeloste suurstofvlak die ewewigslading van anioniese metaalsianiede beïnvloed het, het dit nie direk deelgeneem aan die adsorpsiereaksies nie. $\text{Au}^{(0)}$ is slegs onder die uiterste kondisies van lae pH en hoë temperatuur gevorm. Met hierdie kennis was dit toe moontlik om 'n koolstof te kies waarop geen onomkeerbaar geadsorbeerde spesies gevorm word nie ten einde die meganisme van desorpsie en die noodsaaklikheid van sianied in die elueringsproses te bestudeer.

Dit is gevind dat selfs met net $\text{Au}(\text{CN})_2^-$ teenwoordig op die gelaaië koolstof, die desorpsie van goud drasties verhoog word deur die teenwoordigheid van sianied. Daar is verder aangetoon dat die sianied in die elueringstap van 'n AARL elueringsprosedure nie so belangrik is as die sianied wat in die voorafbehandeling gebruik word nie. Hieruit is afgelei dat die sianied die koolstof passiver vir die adsorpsie van anioniese metaalsianiede deur die reaksie daarvan met die funksionele groepe op die oppervlak van die koolstof. Min desorpsie van goud vind egter in die voorafbehandelingstap plaas, omdat die hoë kation konsentrasie die vorming van neutrale ionpare met die anioniese metaalsianied bevorder. Dit is eers nadat die grootste gedeelte van die katione verwyder is in die elueringstap, dat die desorpsie van die goud vinnig toeneem.

Aangesien dit gevind is dat die konsentrasies van die sianied en toeskouer katione, asook hulle reaksies, die goudsianied ewewig beïnvloed, moes hierdie faktore in ag geneem word in die modellering van die desorpsie van die goudsianied. Om die model te vereenvoudig, is slegs een kation, naamlik kalium, gebruik. Modelle is toe ontwikkel waarmee die veranderinge in die sianied- en kaliumkonsentrasie gedurende die desorpsie van die goudsianied beskryf kon word. Hierdie modelle het dit moontlik gemaak om 'n verskuivende goudsianied ewewigsisoterm te bereken as 'n funksie van tyd en hoogte in die kolom. Dit is gevind dat die desorpsie van die goudsianied slegs onder kondisies van swak desorpsie diffusiebeherend was. Onder sulke toestande kon die desorpsie van die goud beskryf word met 'n model wat voorsiening maak vir massa-oordrag tussen die mikro- en makroporieë van die koolstof, oppervlakdiffusie in die makroporieë, en diffusie deur die vloeistoflagie om die koolstofkorrels. Hoë temperature en effektiewe voorafbehandelings (d.w.s. sterk elueringskondisies) het die weerstand teen massa-oordrag sodanig verlaag dat die desorpsie van die goudsianied met 'n ewewigmodel beskryf kon word. Die ewewigmodel was van toepassing op beide die AARL en Zadra elueringsprosesse.

Simulasies van eksperimenteel gemete elueringsprofiele is voorgelê as bewys van die geldigheid van die verskillende modelle. Die modelle is verder gebruik in 'n sensitiviteitsanalise en ook om die elueringsprofiele van 'n kontinue elueringsproses te voorspel.

ACKNOWLEDGEMENTS

The experimental work described in this thesis was carried out in the Department of Metallurgical Engineering at the University of Stellenbosch between March 1986 and December 1989. The modelling work and writing of the dissertation were conducted on a part-time basis from March 1990 to June 1991. A large number of people and organizations were directly or indirectly involved in this work, but the following deserve special credit :

I wish to thank my supervisor, Prof. J.S.J. van Deventer, for his continued encouragement and interest in my career. It was a pleasure to work with someone whom I could consider a friend, and also respect as an authority in his profession.

Gratitude is expressed to Genmin Ltd. for their financial sponsorship of this project and to the Foundation of Research and Development for bursaries awarded to me.

I am thankful to the Department of Chemistry and the Department of Physics at the University of Stellenbosch for the use of their analytical instruments, and for their help with the FTIR and SEM studies.

I would like to thank Mr F. Petersen and Mrs A. Posthumus for their administrative assistance with the thesis and for not making me feel like a nuisance.

The workshop staff of the Department of Chemical and Metallurgical Engineering at the University of Stellenbosch have assisted me on a continuous basis with the building and maintenance of apparatus. I would like to thank them for their patience with all the little jobs I had to have finished by the day-before-yesterday.

Sincere thanks are due to my employer, Caltex Oil (S.A.) (Pty) Ltd., for the use of their reproduction equipment to print out this document.

I would also like to thank my wife, Rebecca, for her continued support, love, and trust in my abilities at times when I felt like giving up. I promise to reward this by catching up on all the years of back-log on painting, lawn-mowing, and all the other chores that husbands do.

CONTENTS

	PAGE
ABSTRACT	i
ACKNOWLEDGEMENTS	v
CONTENTS	vi
LIST OF FIGURES	x
LIST OF TABLES	xix
1 INTRODUCTION	1
1.1 Description of the CIP process	1
1.2 Existing elution procedures	3
1.2.1 AARL elution steps	4
1.2.2 Zadra elution steps	6
1.3 Characteristics of activated carbon	6
1.4 The mechanism of adsorption	8
1.5 The inter-relationship between adsorption and elution	12
1.6 Objectives of this study	13
2 OXYGEN AND THE NATURE OF THE ADSORBED SPECIES	19
2.1 Experimental	19
2.1.1 Chemicals	19
2.1.2 Carbon	20
2.1.3 Analytical methods	21
2.1.4 pH of adsorption	22
2.1.5 Equilibrium adsorption experiments	22
2.1.6 General	23
2.2 Effect of oxygen on adsorption of metal cyanides	23
2.2.1 Equilibrium studies	23
2.2.2 Chemisorbed vs. dissolved oxygen	25
2.2.3 Adsorption of Hg(CN) ₂	26
2.2.4 Ion-exchange	26
2.2.5 Lowering of [O ₂] during adsorption	27
2.3 Consumption of oxygen	28
2.4 Reversibility of adsorption in an alkaline medium	32
2.4.1 Desorption with distilled water	33
2.4.2 Fourier Transform Infrared scans	34
2.4.3 Equilibrium isotherms	34
2.4.4 X-ray photoelectron scans	34
2.5 Effect of temperature and pH on form of adsorbed species	35
2.6 Summary of results	38
3 SUB-PROCESSES OF ELUTION	62
3.1 Experimental	63
3.1.1 Activated carbon	63
3.1.2 Columns	63
3.1.3 Chemicals	65
3.1.4 Equilibrium tests	65
3.2 Sub-processes	66
3.3 Modified Freundlich isotherm	67

3.4	Factors influencing the elution of aurocyanide	68
3.4.1.	Temperature	68
3.4.2	pH of solution	69
3.4.3	Cyanide concentration	70
3.4.4	Cation concentration	71
3.4.5	Cyanide pretreatment in an AARL elution	72
3.4.6	Presence of irreversibly adsorbed species	76
3.4.7	h/d Ratio	77
3.4.8	Flow rate	77
3.4.9	Distribution of adsorbed gold	78
3.4.10	Organic solvents	79
3.4.11	Acid washing	80
3.5	Inter-relationship of effects on gold equilibrium	81
3.6	Decomposition of cyanide	82
3.7	Adsorption and desorption of cations	86
3.8	Mechanism of gold elution	87
3.9	Summary of findings	90
4	MODELLING OF CYANIDE PROFILES DURING GOLD ELUTION	114
4.1	Assumptions	115
4.2	Formulation of model	116
4.3	Numerical solution procedure	117
4.4	Evaluation of model	119
4.5	Summary	120
5	MODELLING OF POTASSIUM PROFILES DURING GOLD ELUTION	126
5.1	Levenspiel's dispersion model	126
5.2	"Stagnant region" model	127
5.3	Pore diffusion model	127
5.4	Nonideal flow model	129
5.4.1	Material balance equations	130
5.4.2	Numerical solution procedure	131
5.4.3	Evaluation of nonideal flow model	132
5.5	Summary	134
6	MATHEMATICAL MODELS FOR ELUTION OF GOLD CYANIDE	149
6.1	Discussion of existing gold elution models	149
6.2	Pore and surface diffusion models	152
6.3	Formulation of combination model	154
6.3.1	Macropore mass balance	155
6.3.2	Micropore mass balance	156
6.3.3	Mass balance at external particle surface	156
6.3.4	Combination model with linear isotherm	157
6.4	Surface diffusion model	158
6.4.1	Formulation of model	158
6.4.2	Numerical solution	162
6.5	Equilibrium model	162
6.5.1	Formulation of model	163
6.5.2	Numerical solution	164
6.6	Reactor configurations	165
6.6.1	Definition of column	165
6.6.2	Batch reactor	165

6.6.3	CSTR	166
6.6.4	Drained carbon beds	166
6.6.5	Continuous elution	167
6.7	Summary	168
7	EVALUATION OF GOLD ELUTION MODELS	171
7.1	Batch kinetic studies	171
7.2	Elution from packed beds of carbon	175
7.2.1	Constant equilibrium	175
7.2.2	AARL elution	175
7.2.3	Zadra elution	184
7.3	Summary	185
8	SENSITIVITY ANALYSIS	210
8.1	Numerical integration constants	211
8.2	Column geometry	212
8.3	Aurocyanide equilibrium	213
8.4	Operating variables	214
8.5	Carbon properties	215
8.6	Reactor configuration	218
8.6.1	Continuous Stirred Tank reactor	218
8.6.2	Batch elution in a column	218
8.6.3	Continuous counter-current elution	219
8.7	Summary	221
9	CONCLUSIONS	245
9.1	Conclusions and significance	245
9.2	Recommendations for future research	248
	REFERENCES	251
	APPENDIX A	259
	Levenspiel's dispersion model	
	APPENDIX B	261
	"Stagnant region" model	
	APPENDIX C	264
	Pore diffusion model with no resistance to film transport	
	APPENDIX D	268
	Example of 4th-order Runge Kutta method	
	APPENDIX E	269
	Solution of combination model with a linear isotherm	
	APPENDIX F	274
	The relationship between α and β	
	APPENDIX G	276
	Turbo Pascal program for combination model with linear isotherm	

APPENDIX H	287
Turbo Pascal program for surface diffusion model	
APPENDIX I	307
Turbo Pascal program for equilibrium model	
APPENDIX J	321
Turbo Pascal sub-routines for menu's and graphics	
APPENDIX K	335
Tabulation of experimental results	
APPENDIX L	428
Publication of results from oxygen related work	
APPENDIX M	439
Conference presentation of results with surface diffusion model	
LIST OF SYMBOLS	451

LIST OF FIGURE CAPTIONS

- Figure 1.1 Overview of a typical CIP plant. (Fleming, 1983)
- Figure 1.2 Flow diagram of the AARL elution system (Brittan, 1988)
- Figure 1.3 Flow diagram of the Zadra elution system (Bailey, 1985)
- Figure 1.4 Schematic representation of pore structure of activated carbon (Acton, 1982).
- Figure 2.1 Zeta potential of carbons A and B as a function of solution pH. (Exp.1)
- Figure 2.2 Particle size distribution of carbon BTX. (Exp.2)
- Figure 2.3 Equilibrium adsorption of $\text{Au}(\text{CN})_2^-$ on carbon A at different constant oxygen concentrations. (Exp. 3,4,5 and 6)
- Figure 2.4 Equilibrium adsorption of $\text{Ag}(\text{CN})_2^-$ on carbon A at different constant oxygen concentrations. (Exp. 7,8 and 9)
- Figure 2.5 The detrimental effect of oxygen concentrations higher than 9 mg/l on the equilibrium adsorption of $\text{Ag}(\text{CN})_2^-$ on carbon A. (Exp. 7 and 10)
- Figure 2.6 Equilibrium adsorption of $\text{Au}(\text{CN})_2^-$ on carbon B at different constant oxygen concentrations. (Exp. 11, 12 and 13)
- Figure 2.7 Equilibrium adsorption of $\text{Ag}(\text{CN})_2^-$ on carbon B at different constant oxygen concentrations. (Exp. 14, 15 and 16)
- Figure 2.8 The effect of the dissolved oxygen level on the equilibrium adsorption of $\text{Au}(\text{CN})_2^-$ and $\text{Ag}(\text{CN})_2^-$ on carbons A and B at a constant liquid phase metal concentration of $C_e = 10 \text{ g.m}^{-3}$.
- Figure 2.9 The detrimental effect of purging with pure oxygen on the adsorption of $\text{Au}(\text{CN})_2^-$ onto carbon A. (Exp.17)
- Figure 2.10 The effect of pure oxygen on the adsorption of $\text{Au}(\text{CN})_2^-$ onto carbon A from a solution with a pH = 3.5. (Exp.18)
- Figure 2.11 Lowering of the oxygen concentration during the adsorption of $\text{Au}(\text{CN})_2^-$ from an aerated solution. (Exp.22)
- Figure 2.12 Desorption of $\text{Au}(\text{CN})_2^-$ at different constant oxygen concentrations after adsorption from aerated solutions. (Exp.23)
- Figure 2.13 Desorption of $\text{Au}(\text{CN})_2^-$ at different constant oxygen concentrations after adsorption from deaerated solutions. (Exp.24)
- Figure 2.14(a) Measurement of the consumption of oxygen during the adsorption of $\text{Au}(\text{CN})_2^-$ onto carbon A in a closed vessel. (Exp.26)
- Figure 2.14(b) The reproducibility of the continuous monitoring of the dissolved O_2 level during the adsorption of $\text{Au}(\text{CN})_2^-$ in a closed vessel. (Exp.26)

- Figure 2.15 Measurement of the dissolved oxygen concentration during the adsorption of $\text{Au}(\text{CN})_2^-$ in a packed bed of carbon A. (Exp. 28)
- Figure 2.16 FTIR scan of $\text{KAu}(\text{CN})_2$ powder.
- Figure 2.17 FTIR scan of carbon A loaded with gold cyanide from an aerated alkaline solution.
- Figure 2.18 FTIR scan of carbon B loaded with gold cyanide from an aerated alkaline solution.
- Figure 2.19 Equilibrium isotherms for gold cyanide on carbon B as determined by adsorption and desorption. (Exp. 11 and 34)
- Figure 2.20 Equilibrium isotherms for gold cyanide on carbon A as determined by adsorption and desorption. (Exp. 3 and 35)
- Figure 2.21 Equilibrium isotherms for gold cyanide on carbon BTX as determined by adsorption and desorption. (Exp. 36 and 37)
- Figure 2.22 Molar ratio of CN : Au on carbons A and B as determined by XPS measurement.
- Figure 2.23 FTIR scan of carbon A loaded with gold cyanide from an acidic solution.
- Figure 2.24 FTIR scan of carbon B loaded with gold cyanide from an acidic solution.
- Figure 2.25 SEM photograph of surface of carbon BTX loaded with $\text{Au}^{(0)}$ from an AuCl solution. (Magnified 2000 x)
- Figure 2.26 SEM photograph of surface of carbon BTX loaded with gold cyanide from an $\text{Au}(\text{CN})_2^-$ solution. (1 g of carbon stirred for 7 h in a solution with $C_{iG} = 200 \text{ g.m}^{-3}$). Soaked loaded carbon in a cold 0.1 M KOH solution for 5 h. (Magnified 2000 x)
- Figure 2.27(a) SEM photograph of surface of carbon BTX loaded with gold cyanide from an $\text{Au}(\text{CN})_2^-$ solution. (1 g of carbon stirred for 7 h in a solution with $C_{iG} = 200 \text{ g.m}^{-3}$). Boiled loaded carbon in a 0.1 M KOH solution for 5 h. (Magnified 2000 x)
- Figure 2.27(b) X-ray scan of sample of carbon used in Figure 2.27(a).
- Figure 2.28 SEM photograph of surface of carbon BTX loaded with gold cyanide from an $\text{Au}(\text{CN})_2^-$ solution. (1 g of carbon stirred for 7 h in a solution with $C_{iG} = 200 \text{ g.m}^{-3}$). Boiled loaded carbon in distilled water for 5 h. (Magnified 2000 x)
- Figure 2.29(a) SEM photograph of surface of carbon BTX loaded with gold cyanide from an $\text{Au}(\text{CN})_2^-$ solution. (1 g of carbon stirred for 7 h in a solution with $C_{iG} = 200 \text{ g.m}^{-3}$). Boiled loaded carbon in 3 vol.% of a 33 mass % HCl solution for 5 h. (Magnified 200 x)
- Figure 2.29(b) SEM photograph of sample of carbon in Figure 2.29(a) (Magnified 2000 x)
- Figure 2.29(c) X-ray scan of sample of carbon used in Figure 2.29(a)
- Figure 3.1 Experimental arrangement for elutions in glass column.
- Figure 3.2 Experimental arrangement for elutions in stainless steel column.
- Figure 3.3 Normalized AARL elution profiles. $C_G = 140.Y \text{ g.m}^{-3}$, $C_K = 3500.Y \text{ g.m}^{-3}$, $C_N = 1500.Y \text{ g.m}^{-3}$, $\text{pH} = 14.Y$. (Exp.40)

- Figure 3.4 Freundlich isotherm parameters for the equilibrium adsorption of $\text{Au}(\text{CN})_2^-$ onto various carbons. (Exp.41)
- Figure 3.5 Equilibrium adsorption of $\text{Au}(\text{CN})_2^-$ onto carbon BTX at different temperatures. (Exp. 36, 42, 43 and 44)
- Figure 3.6 Equilibrium isotherms for the adsorption of $\text{Au}(\text{CN})_2^-$ onto carbon BTX. Curves calculated from average A-values with $n = -0.002688.A + 0.2902$. (Exp. 36, 42, 43 and 44)
- Figure 3.7 Effect of temperature on the Freundlich constant, A, for adsorption of $\text{Au}(\text{CN})_2^-$ onto carbon BTX. (Exp. 36, 42, 43 and 44)
- Figure 3.8 Effect of pH on equilibrium adsorption of $\text{Au}(\text{CN})_2^-$ onto carbon BTX at room temperature. (Exp. 45)
- Figure 3.9 Effect of pH on equilibrium adsorption of $\text{Au}(\text{CN})_2^-$ onto carbon BTX at 40 °C. (Exp. 46)
- Figure 3.10 Effect of cyanide concentration on the equilibrium adsorption of $\text{Au}(\text{CN})_2^-$ onto carbon BTX. (Exp. 47)
- Figure 3.11 The effect of cations (Cat) on the equilibrium adsorption of $\text{Au}(\text{CN})_2^-$ onto carbon BTX. (Exp. 48 and 49)
- Figure 3.12 Gold elution profiles after pretreatments with equimolar NaCN and KCN solutions. (Exp. 50 and 51)
- Figure 3.13 Gold elution profiles after pretreatments with KCN and KOH solutions with the same pH and potassium concentration. (Exp.50 and 52)
- Figure 3.14 The prolonged effect of a cyanide pretreatment on the elution of gold cyanide. $C_G = 220.Y \text{ g.m}^{-3}$, $C_K = 2500.Y \text{ g.m}^{-3}$. (Exp.53)
- Figure 3.15 Illustration of the effect of the deactivation of carbon towards aurocyanide by cyanide. (Exp.54)
- Figure 3.16 The effect of cyanide age on the gold cyanide equilibrium on carbon BTX at 70 °C. (Exp.55)
- Figure 3.17 Reactivation of carbon BTX towards aurocyanide after a cyanide pretreatment. (Exp.56)
- Figure 3.18 The effect of an irreversibly adsorbed gold species on elution with cyanide, but without a cyanide pretreatment. (Exp.57)
- Figure 3.19 Effect of particle size on elution in batch with $\text{Au}^{(0)}$ or AuCN present on the carbon. (Exp.58)
- Figure 3.20 Gold elution profiles from columns with different geometry and size. (Exp.59,60)
- Figure 3.21 The elution of gold cyanide from carbon BTX at different flow rates. (Exp.50,61 and 62)
- Figure 3.22 Effect of flow rate on the adsorption of $\text{Ag}(\text{CN})_2^-$. pH = 8.5, $d = 0.031 \text{ m}$, $h = 0.25 \text{ m}$, $C_{FG} = 4.5 \text{ g.m}^{-3}$. (Exp. 25 and 27 of Jansen van Rensburg, 1986)
- Figure 3.23 Effect of flow rate on the adsorption of $\text{Ag}(\text{CN})_2^-$. pH = 11.5, $d = 0.031 \text{ m}$, $h = 0.4 \text{ m}$, $C_{FG} = 5.1 \text{ g.m}^{-3}$. (Exp. 28 and 30 of Jansen van Rensburg, 1986)
- Figure 3.24 Effect of radial distribution of adsorbed gold cyanide on the kinetics of elution in batch. (Exp.63)
- Figure 3.25 The insensitivity of elution to the radial distribution of the adsorbed gold under conditions of strong desorption. (Exp. 40 and 50)

- Figure 3.26 The detrimental effect of an acid wash on the elution of gold adsorbed from solutions without Mg and Ca. (Exp.64 and 65)
- Figure 3.27 The decomposition of cyanide at different temperatures in the absence of carbon. (Exp. 66)
- Figure 3.28 Arrhenius plot of the rate constant for the decomposition of cyanide in the absence of carbon. (Exp.66)
- Figure 3.29 The sensitivity of the adsorption and decomposition of cyanide on the particle size of carbon BTX. (Exp.67)
- Figure 3.30 The sensitivity of the adsorption and decomposition of cyanide on carbon BTX to mixing speed. (Exp.68)
- Figure 3.31 Profile of cyanide concentration in eluate of a Zadra elution. (Exp.69)
- Figure 3.32 The deactivation of carbon BTX towards cyanide by cyanide. (Exp.70)
- Figure 3.33 The decrease in the kinetics of the decomposition of cyanide with an increase in cyanide age of carbon BTX. (Exp.70)
- Figure 3.34 The insensitivity of the elution of potassium to temperature and flow rate. (Exp.50, 61, 62 and 73)
- Figure 3.35 The influence of the counter anion on the elution of potassium from carbon BTX. (Exp.71 and 73)
- Figure 3.36 The effect of the temperature of the cyanide pretreatment on the elution of gold cyanide from carbon BTX. (Exp.50 and 64)
- Figure 4.1 Definition of column and graphical presentation of elution model for cyanide.
- Figure 4.2 Simulation of the cyanide profile in the eluate of a Zadra elution. (Exp.69)
- Figure 4.3 Simulation of the cyanide profile in the eluate of a Zadra elution with a cyanide pretreatment. (Exp.74)
- Figure 4.4 Simulation of the cyanide profile in the eluate of an AARL elution. (Exp.40, 50 and 75)
- Figure 4.5 Predictions of the contribution of the decomposition of cyanide in the interparticle solution.
- Figure 4.6 Predictions of cyanide profiles during AARL elutions at different temperatures.
- Figure 5.1(a) Fit of Levenspiel's dispersion model to the potassium profile of an AARL elution. (Exp.59)
- Figure 5.1(b) Tail section of potassium profile shown in Figure 5.1(a).
- Figure 5.2(a) Fit of the Stagnant region model to the potassium profile of an AARL elution. (Exp.76)
- Figure 5.2(b) Tail section of potassium profile shown in Figure 5.2(a).
- Figure 5.3(a) Fit of the Pore diffusion model to the potassium profile of an AARL elution. Accounted for one type of pore only. (Exp.50)
- Figure 5.3(b) Tail section of potassium profile shown in Figure 5.3(a).
- Figure 5.4(a) Fit of the Pore diffusion model to the potassium profile of an AARL elution. Accounted for macropores and micropores. (Exp.50)

- Figure 5.4(b) Tail section of potassium profile shown in Figure 5.4(a).
- Figure 5.5 Fit of the Pore diffusion model to the potassium profile of an AARL elution at a flow rate of 37 bed volumes per hour. (Exp.62)
- Figure 5.6(a) Levenspiel's nonideal flow model for long tails.
- Figure 5.6(b) Adapted nonideal flow model with two deadwater regions per stage.
- Figure 5.7(a) Fit of the Nonideal flow model to the potassium profile of an AARL elution. Accounted for two deadwater regions. $V = 1.367 \times 10^{-8} \text{ m}^3 \cdot \text{s}^{-1}$, $C_{K_{pi}} = 14000 \text{ g} \cdot \text{m}^{-3}$, $C_{K_{bi}} = 0 \text{ g} \cdot \text{m}^{-3}$, $C_{K_{F}} = 0 \text{ g} \cdot \text{m}^{-3}$. (Exp.50)
- Figure 5.7(b) Tail section of potassium profile shown in Figure 5.7(a).
- Figure 5.8 Sensitivity of the nonideal model for the elution of potassium to the number of mixed reactor sections. $V = 1.367 \times 10^{-8} \text{ m}^3 \cdot \text{s}^{-1}$, $C_{K_{pi}} = 14000 \text{ g} \cdot \text{m}^{-3}$, $C_{K_{bi}} = 0 \text{ g} \cdot \text{m}^{-3}$, $C_{K_{F}} = 0 \text{ g} \cdot \text{m}^{-3}$, $\Delta t = 5 \text{ s}$.
- Figure 5.9 Simulation of potassium profiles with nonideal flow model with different cross flow parameters. $V = 1.367 \times 10^{-8} \text{ m}^3 \cdot \text{s}^{-1}$, $C_{K_{pi}} = 14000 \text{ g} \cdot \text{m}^{-3}$, $C_{K_{bi}} = 0 \text{ g} \cdot \text{m}^{-3}$, $C_{K_{F}} = 0 \text{ g} \cdot \text{m}^{-3}$, $\Delta t = 5 \text{ s}$.
- Figure 5.10 Simulations with Levenspiel's nonideal flow model with one stagnant region per stage. $V = 1.367 \times 10^{-8} \text{ m}^3 \cdot \text{s}^{-1}$, $C_{K_{pi}} = 14000 \text{ g} \cdot \text{m}^{-3}$, $C_{K_{bi}} = 0 \text{ g} \cdot \text{m}^{-3}$, $C_{K_{F}} = 0 \text{ g} \cdot \text{m}^{-3}$, $X_b = 0$, $\beta_K = 0.999$. (Exp.50)
- Figure 5.11(a) Fit of the nonideal flow model to the potassium profile of an AARL elution at a flow rate of 5.9 bed volumes per hour. $V = 2.89 \times 10^{-8} \text{ m}^3 \cdot \text{s}^{-1}$, $C_{K_{pi}} = 14000 \text{ g} \cdot \text{m}^{-3}$, $C_{K_{bi}} = 0 \text{ g} \cdot \text{m}^{-3}$, $C_{K_{F}} = 0 \text{ g} \cdot \text{m}^{-3}$. (Exp.61)
- Figure 5.11(b) Tail section of potassium profile shown in Figure 5.11(a).
- Figure 5.12 Insensitivity of the nonideal flow model for the elution of potassium to the geometry of the elution column. (Exp.59 and 60)
- Figure 5.13 Simulation of the potassium profile during an AARL elution with a constant concentration of potassium in the feed. $V = 1.376 \times 10^{-8} \text{ m}^3 \cdot \text{s}^{-1}$, $C_{K_{pi}} = 14000 \text{ g} \cdot \text{m}^{-3}$, $C_{K_{bi}} = 559 \text{ g} \cdot \text{m}^{-3}$, $C_{K_{F}} = 559 \text{ g} \cdot \text{m}^{-3}$. (Exp.75)
- Figure 5.14(a) Fit of the nonideal flow model to the profile of potassium eluted from carbon that was soaked in a KCl solution. $V = 1.361 \times 10^{-8} \text{ m}^3 \cdot \text{s}^{-1}$, $C_{K_{pi}} = 12740 \text{ g} \cdot \text{m}^{-3}$, $C_{K_{bi}} = 0 \text{ g} \cdot \text{m}^{-3}$, $C_{K_{F}} = 0 \text{ g} \cdot \text{m}^{-3}$. (Exp.71)
- Figure 5.14(b) Tail section of potassium profile shown in Figure 5.14(a).
- Figure 5.15 Simulation of the potassium profile during a Zadra elution. $V = 1.315 \times 10^{-8} \text{ m}^3 \cdot \text{s}^{-1}$, $C_{K_{pi}} = 0 \text{ g} \cdot \text{m}^{-3}$, $C_{K_{bi}} = 260 \text{ g} \cdot \text{m}^{-3}$, $C_{K_{F}} = 260 \text{ g} \cdot \text{m}^{-3}$. (Exp.69)
- Figure 6.1 The continuous atmospheric elution column (Paterson, 1987).
- Figure 7.1 Simulation of adsorption of gold in batch with surface diffusion model. (Exp.77)
- Figure 7.2 Simulation of adsorption of gold in batch with surface diffusion model. (Exp.78)

- Figure 7.3 Simulation of adsorption of gold in batch with surface diffusion model. (Exp.79)
- Figure 7.4 Simulation of adsorption of gold in batch with surface diffusion model. (Exp.80)
- Figure 7.5 Attempt to simulate desorption of gold in batch with kinetic parameters as determined for adsorption. (Exp.77)
- Figure 7.6 Simulation of desorption of gold in batch with surface diffusion model. (Exp.77)
- Figure 7.7 Simulation of desorption of gold in batch with surface diffusion model. (Exp.78)
- Figure 7.8 Simulation of desorption of gold in batch with surface diffusion model. (Exp.79)
- Figure 7.9 Simulation of desorption of gold in batch with surface diffusion model. (Exp.80)
- Figure 7.10 Simulation of desorption of gold after adsorption to equilibrium. Modelled in batch with surface diffusion model. (Exp.81)
- Figure 7.11 Simulation of desorption of gold in the presence of free cyanide. Modelled in batch with surface diffusion model. (Exp.82)
- Figure 7.12 Simulation of desorption of gold in batch at 52 °C. Modelled with surface diffusion model. (Exp.83)
- Figure 7.13 Simulation of desorption of gold in batch at 90 °C. Modelled with surface diffusion model. (Exp.84)
- Figure 7.14 The effect of the equilibrium isotherm constant on the value of the combined macropore diffusion coefficient. ($\text{Diff} = \Gamma_m \times 10^{12} \text{ m}^2 \cdot \text{s}^{-1}$) (Exp.77-82)
- Figure 7.15(a) Simulation of elution of gold from a packed bed of carbon with the surface diffusion model. No pretreatment, constant equilibrium. (Exp.85)
- Figure 7.15(b) Attempt to simulate the elution in Fig.7.15(a) with the equilibrium model. (Exp.85)
- Figure 7.16 Simulation of an AARL elution at a flow rate of 2.9 bed volumes/h with the surface diffusion model. (Exp.50)
- Figure 7.17 Simulation of an AARL elution at a flow rate of 5.9 bed volumes/h with the surface diffusion model. (Exp.61)
- Figure 7.18 The relationship between the surface diffusion and equilibrium models for the elution of gold cyanide. Surface diffusion (1) : $\Gamma_m = 1 \times 10^{-10} \text{ m}^2 \cdot \text{s}^{-1}$, Surface diffusion (2) : $\Gamma_m = 1 \times 10^{-11} \text{ m}^2 \cdot \text{s}^{-1}$
- Figure 7.19 Estimation of the A-value in the shifting isotherm during an AARL elution. (Exp.50)
- Figure 7.20 Quantification of the effect of potassium on the gold elution equilibrium after a cyanide pretreatment. (Exp.50)
- Figure 7.21 Estimation of the A-value for a constant concentration of potassium in the eluant. (Exp.86)
- Figure 7.22 Simulation of the AARL elution in Figure 7.16 with the equilibrium model. Potassium concentration in feed = $0 \text{ g} \cdot \text{m}^{-3}$, Adsorption period = 22 h, $T = 70 \text{ }^\circ\text{C}$. (Exp.50)

- Figure 7.23 Simulation of an AARL elution with the equilibrium model. Potassium concentration in feed = 559 g.m^{-3} . (Exp.75)
- Figure 7.24 Simulation of an AARL elution with the equilibrium model. Potassium concentration in feed = 2100 g.m^{-3} . (Exp.87)
- Figure 7.25 Simulation of an AARL elution with the equilibrium model. Potassium concentration in feed = 6300 g.m^{-3} . (Exp.86)
- Figure 7.26 Simulation of an AARL elution with the equilibrium model. Adsorption period = 7 h. (Exp.88)
- Figure 7.27 Simulation of an AARL elution with the equilibrium model. Adsorption period = 72 h. (Exp.40)
- Figure 7.28 Simulation of an AARL elution with the equilibrium model. $Q_{Gi} = 12.16 \text{ g.kg}^{-1}$. (Exp.89)
- Figure 7.29 Simulation of an AARL elution with the equilibrium model. Pretreatment with 4 g KCN/l at $20 \text{ }^{\circ}\text{C}$. (Exp.90)
- Figure 7.30 Simulation of an AARL elution with the equilibrium model. Pretreatment with 20 g KCN/l at $100 \text{ }^{\circ}\text{C}$. (Exp.64)
- Figure 7.31 Simulation of an AARL elution with the equilibrium model. Step change in potassium concentration in eluant. (Exp.53)
- Figure 7.32 Simulation of an AARL elution at $50 \text{ }^{\circ}\text{C}$ with the equilibrium model. (Exp.91)
- Figure 7.33 Simulation of an AARL elution at $80 \text{ }^{\circ}\text{C}$ with the equilibrium model. (Exp.92)
- Figure 7.34 Simulation of an AARL elution in the stainless steel column at $130 \text{ }^{\circ}\text{C}$ with the equilibrium model. (Exp.93)
- Figure 7.35 Simulation of an AARL elution at $20 \text{ }^{\circ}\text{C}$ with the surface diffusion model. (Exp.94)
- Figure 7.36 Quantification of the effect of temperature on the gold elution equilibrium after a cyanide pretreatment as done in Exp.50, 91 and 92.
- Figure 7.37 Simulation of a Zadra elution with the equilibrium model. (Exp.69)
- Figure 7.38 Equilibrium model simulation of a Zadra elution with a pretreatment. (Exp.74)
- Figure 8.1 Sensitivity of the equilibrium model to changes in the number of height sections in a column operation.
- Figure 8.2 Sensitivity of the nonideal flow model for the elution of potassium to column geometry with a constant Δh .
- Figure 8.3 Sensitivity of the equilibrium model for the elution of gold cyanide to column geometry with a constant Δh .
- Figure 8.4 Sensitivity of the equilibrium model for the elution of gold cyanide to the equilibrium constant A_0 .
- Figure 8.5 Sensitivity of the equilibrium model for the elution of gold cyanide to the equilibrium constant b .
- Figure 8.6 Sensitivity of the equilibrium model for the elution of gold cyanide to the equilibrium constant B .
- Figure 8.7 Sensitivity of the equilibrium model for the elution of gold cyanide to the equilibrium dependency on the potassium concentration, p .

- Figure 8.8 Sensitivity of the equilibrium model for the elution of gold cyanide to the extent of reactivation, q .
- Figure 8.9 Sensitivity of the equilibrium model for the elution of gold cyanide to the flow rate of the eluant.
- Figure 8.10 Behaviour of the nonideal flow model for the elution of potassium at different initial potassium concentrations in the pore liquid.
- Figure 8.11 Sensitivity of the equilibrium model for the elution of gold cyanide to the initial potassium concentration in the pore liquid.
- Figure 8.12 Sensitivity of the equilibrium model for the elution of gold cyanide to the initial potassium concentration in the interparticle solution.
- Figure 8.13 Sensitivity of the equilibrium model for the elution of gold cyanide to the potassium concentration in the eluant. $C(F) = C_{KF}$ = feed concentration of potassium.
- Figure 8.14 The effect of the concentration of KCN on the Zadra elution profiles predicted with the equilibrium model. $A_o = 2.82$, $p = 0.088$, $C_{Kpi} = C_{Kbi} = C_{KF}$, Cyanide parameters as for Fig. 4.2.
- Figure 8.15 The effect of the concentration of KCN on the Zadra elution profiles predicted with the equilibrium model. $A_o = 1.10$, $p = 0.2$, $C_{Kpi} = C_{Kbi} = C_{KF}$, Cyanide parameters as for Fig. 4.2.
- Figure 8.16 Sensitivity of the equilibrium model for the elution of gold cyanide to the gold cyanide concentration in the eluant. $C(F) = C_{GF}$ = feed concentration of gold cyanide.
- Figure 8.17 Sensitivity of the equilibrium model for the elution of gold cyanide to the initial gold loading on the carbon.
- Figure 8.18 Sensitivity of the surface diffusion model for the elution of gold cyanide to the initial distribution of gold between the micropores and the macropores.
- Figure 8.19 Sensitivity of the equilibrium model for the elution of gold cyanide to ϵ , the void fraction of the carbon bed.
- Figure 8.20 Sensitivity of the nonideal flow model for the elution of potassium to V_o , the pore volume of the carbon.
- Figure 8.21 Sensitivity of the equilibrium model for the elution of gold cyanide to V_o , the pore volume of the carbon.
- Figure 8.22 Sensitivity of the surface diffusion model for the elution of gold cyanide to α_g (alfa), the fraction of the pores available as macropores.
- Figure 8.23 Sensitivity of the surface diffusion model for the elution of gold cyanide to k_s , the film diffusion coefficient.
- Figure 8.24 Sensitivity of the surface diffusion model for the elution of gold cyanide to Γ_m (tau), the combined macropore diffusivity.
- Figure 8.25 Sensitivity of the surface diffusion model for the elution of gold cyanide to k_b , the coefficient for mass transfer between the macropores and the micropores.

- Figure 8.26 Illustration of similarity between equilibrium model and surface diffusion model with high mass transfer coefficients.
- Figure 8.27 Elution profiles for potassium with the nonideal flow model for a column and a CSTR.
- Figure 8.28 Elution profiles for gold cyanide with the equilibrium model for a column and a CSTR.
- Figure 8.29 Gold loading profile through carbon bed at various points of time as predicted by equilibrium model.
- Figure 8.30 Elution profiles of potassium with nonideal flow model for initially full and drained beds of carbon.
- Figure 8.31 Elution profiles of gold cyanide with equilibrium model for initially full and drained beds of carbon.
- Figure 8.32 Equilibrium model simulation of the gold cyanide profile for a continuous counter-current elution.
- Figure 8.33 Equilibrium model simulation of the eluted carbon loading for a continuous counter-current elution.
- Figure 8.34 Nonideal flow model simulation of the potassium profile for a continuous counter-current elution.
- Figure 8.35 Equilibrium model simulation of the gold cyanide profile for a continuous counter-current elution with a lower frequency of carbon transfer than in Figure 8.32.
- Figure 8.36 Equilibrium model simulation of the eluted carbon loading for the continuous counter-current elution of Figure 8.35.
- Figure 8.37 Equilibrium model simulation of the gold cyanide profile for a continuous counter-current elution with twice the carbon flow rate as for Figure 8.32.
- Figure 8.38 Equilibrium model simulation of the eluted carbon loading for the continuous counter-current elution of Figure 8.37.
- Figure 8.39 Equilibrium model simulation of the gold cyanide profile from a continuous counter-current elution column of twice the height of that in Figure 8.32.
- Figure 8.40 Equilibrium model simulation of the eluted carbon loading for the continuous counter-current elution of Figure 8.39.

LIST OF TABLES

<u>Table 2.1</u>	AA settings for determination of various elements.
<u>Table 2.2</u>	Freundlich isotherm constants for adsorption onto carbon A.
<u>Table 2.3</u>	Freundlich isotherm constants for adsorption onto carbon B.
<u>Table 2.4</u>	The consumption of oxygen by activated carbon in the presence and absence of metal cyanides.
<u>Table 2.5</u>	Determination of adsorbed species by elution with distilled water.
<u>Table 3.1</u>	Dimensions of columns.
<u>Table 3.2</u>	Accuracy of predicted Freundlich isotherm exponents for equilibrium gold adsorption on carbon BTX.
<u>Table 3.3</u>	Relationships between A and pH determined from published data.
<u>Table 3.4</u>	Typical metal loadings encountered on activated carbon in different stages of the CIP circuit (Davidson, 1974).
<u>Table 3.5</u>	Determination of accuracy of predictions of A-values with Equation 3.12.
<u>Table 3.6</u>	Rate constants and activation energies (E_a) for the hydrolysis and oxidation reactions of cyanide in the absence of carbon at a pH of 10.5 (Muir and Hoecker, 1988).
<u>Table 4.1</u>	Parameters and conditions used in simulations of cyanide profiles.
<u>Table 6.1</u>	Simulations of gold elution profiles in a batch stirred tank reactor with the combination model and a linear isotherm
<u>Table 7.1</u>	Parameters used in simulations of gold adsorption profiles in batch reactors.
<u>Table 7.2(a)</u>	Parameters used in simulations of gold elution profiles in batch reactors.
<u>Table 7.2(b)</u>	Parameters used in simulations of gold elution profiles in batch reactors.
<u>Table 7.3</u>	Parameters used in surface diffusion model simulations of gold elution profiles from packed bed reactors.
<u>Table 7.4(a)</u>	Parameters used in equilibrium model simulations of gold elution profiles from packed bed reactors.
<u>Table 7.4(b)</u>	Parameters used in equilibrium model simulations of gold elution profiles from packed bed reactors.
<u>Table 8.1</u>	The effect of Δt on the mass balance of gold cyanide after 15 bed volumes with the equilibrium model and a constant equilibrium.

1

INTRODUCTION

Charcoal (or activated carbon) has long been highly valued for its unique properties as an adsorbent. Today, the applications of activated carbon range from the treatment of drinking water to the filtering of cigarette smoke. One of these present day uses of activated carbon is the recovery of precious metals from solution.

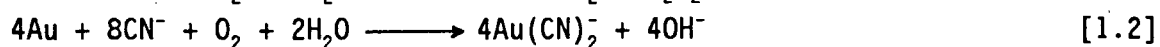
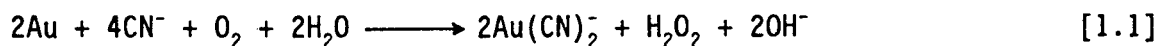
Although the ability of activated carbon to adsorb gold from leach liquors was discovered as early as the middle of the nineteenth century (Acton, 1982), it was not economical to apply the technology, because the carbon had to be smelted to recover the adsorbed metal. This was changed in 1952 with the development of the Zadra process for the elution of gold and silver from activated carbon. Since then, numerous gold extraction plants have employed the carbon-in-pulp (CIP) process or variations thereof.

1.1 DESCRIPTION OF THE CIP PROCESS

Bailey (1987) described the CIP process as follows : "The carbon-in-pulp process recovers gold in solution from slurry streams by contacting the carbon with the pulp and separating the two by screening." Figure 1.1 shows how this is achieved on a typical CIP plant. The following discussion of the CIP process flow sheet was obtained from Fleming (1983), Jackson (1986), Van Deventer (1984a), and Bailey (1987).

The milled ore is screened at 0.6 mm to remove impurities such as woodchips and ore grains larger than the carbon particles (1 to 3 mm). This ensures that only the carbon would be retained on the screens in the adsorption section.

The screened pulp is then fed to the leaching section where gold is believed to react with cyanide via the following reactions (Finkelstein, 1972) :



Sodium cyanide and lime are added to each of the leach tanks. (The lime is added to stabilize the cyanide.) Air is sparged into the tanks to supply oxygen for the dissolution reaction. A retention time of 12 to 24 hours is provided for the leaching reactions by passing the ore through a number of leach tanks in series. The pulp is agitated by rubber-coated impellers.

The gold adsorption section consists of a further number of tanks in series through which the pulp flows counter-current to the charcoal. The pulp flows through a series of interstage screens via a launder into the next adsorption vessel which is on a lower level. The barren pulp (tailings) is discharged from the last stage. Because of the larger particle size of the carbon, it is retained by the screens. The carbon is pumped batchwise in the opposite direction. The loaded carbon from the first tank is screened and washed before being transferred to the stripping (or elution) section.

The gold is eluted from the loaded carbon by washing it with a strong caustic cyanide solution in an elution column at temperatures higher than 90 °C. The different elution techniques are discussed in more detail in the next section. Gold and silver are recovered from the concentrated eluate either by electrowinning or zinc cementation.

The eluted carbon is regenerated by heating it to at least 650 °C for 30 minutes in the absence of air. This removes organic contaminants adsorbed on the carbon surface and thereby restores the activity of the carbon. The reactivated carbon is screened to remove the fines before it is recycled to the last stage of the adsorption circuit.

1.2 EXISTING ELUTION PROCEDURES

Adams and Nicol (1986) identified mainly three methods of elution which are employed at present. These methods are :

- (1) the Zadra (or Homestake) method in which a warm cyanide solution is being circulated through an elution column and one or more electrowinning cells in series (Zadra, 1950),
- (2) the Anglo American Research Laboratory (AARL) method which involves a pretreatment step with a hot cyanide solution followed by elution with hot deionised water (Davidson, 1986a), and
- (3) the organic solvent methods, which are variations of (1) and (2), but with large quantities of organic solvents such as methanol, ethanol, acetone or acetonitrile in the eluate (Espiel *et al.*, 1987, 1988; Muir *et al.*, 1985b).

Muir *et al.* (1985a) published the most recent innovation for the recovery of gold from activated carbon, called the Micron Solvent Distillation Procedure. As in the AARL method, the carbon is first presoaked in about 1 bed volume of 5% NaCN, 1% NaOH solution. The subsequent elution step involves the distillation at total reflux of an organic solvent/water mixture with a column of loaded carbon acting as the fractionating medium. As the organic solvent condenses, it washes the gold off the carbon and into the boiler below. One of the advantages of the process is that it concentrates the eluted gold in less than 1 bed volume of eluant. This method is not recommended by Costello *et al.* (1988) for the elution of large tonnages of carbon.

Comparisons of the different elution procedures by Muir *et al.* (1985a) and Davidson (1986a) indicated that neither the Zadra elution nor the elution with polar organic solvents could compete favourably with the AARL elution procedure in terms of operating costs. Although studies by Paterson (1987) showed insignificant differences in operating and capital costs between the AARL and Zadra systems, the AARL process was preferred for its shorter elution time. According to Costello *et al.* (1988) and La Brooy and Ariti (1988), the AARL elution system proves to be very useful

in the expansion of existing plants, because

- (a) 2-3 elution cycles per day can be performed in a single column, and
- (b) the recovery of the gold by electrowinning or zinc cementation is independent of the elution.

Plant upgrades can thus be accomplished fairly easily by an increase in the number of eluate tanks and recovery capacity.

Davidson (1986a) reported that the AARL elution process was successfully tested on pilot plant scale at the Vaal Reefs Mining and Exploration Company (1975) and the Fairview Gold Mine (1978). The President Brand Gold Mine was the first mine to use the process on a large scale (1980). Most of the early C.I.P. plants in Australia used the Zadra elution technique, whereas the AARL process tends to be preferred on the newer and larger plants (La Brooy and Ariti, 1988).

1.2.1 AARL elution steps (Davidson, 1986a; Brittan, 1988)

A flow diagram for the basic AARL elution system is shown in Figure 1.2.

The elution column is filled via gravity with loaded carbon from a flooded carbon storage hopper. The carbon is then washed with approximately 1 bed volume of dilute hydrochloric acid, followed by 2 to 4 bed volumes of water. The acid requirement will depend largely on the calcium carbonate content of the carbon. Experience has showed that 1 bed volume containing 3 vol.% of a 33 mass % HCl solution effectively removes calcium from the carbon. Cold acid will remove calcium and zinc, whereas hot acid (90 °C) will remove calcium, zinc, nickel, and large portions of iron and silica. No gold, silver or copper are eluted by the acid. During the acid wash and the subsequent rinse with water, the system is brought to its operational temperature (110-120 °C) and pressure (200-300 kPa).

The main benefits of a hot acid wash can be summarized (Davidson, 1986a) as follows :

- (a) The removal of calcium carbonate can be seen as part of the regeneration of the carbon. Calcium carbonate clogs the carbon

- pores and leads to both poor adsorption as well as poor elution,
- (b) A hot acid wash ensures that the system will be at or near the operational temperature for the cyanide pretreatment and elution,
 - (c) The acid washed carbon is less sensitive to water quality, and efficient gold elution can be achieved using a good quality regional water,
 - (d) It is claimed that hot acid washing reduces the mass loss of carbon during the thermal regeneration, and
 - (e) Fewer impurities such as organic contaminants and ferrocyanides are transferred to electrowinning or zinc precipitation.

It was found (Briggs, 1983), however, that the elution efficiency was unaffected by performing the acid wash only after the carbon regeneration step. This eliminated the risk of mixing hydrochloric acid and sodium cyanide solution.

After the carbon has been rinsed with water, one bed volume of the pretreatment solution is pumped into the column and the carbon allowed to soak for approximately 30 min. at the operating temperature. Most plants use a pretreatment solution containing 3 mass % NaCN and 1 to 3 mass % NaOH. The reagent cyanide requirement was found to be insensitive to the gold loading on the carbon (Briggs, 1983).

Elution of the gold is accomplished with 5 to 8 bed volumes of a high quality softened water at a flowrate of 2 bed volumes per hour. The water should contain preferably less than 300 mg/l sodium. Softening of the water will also prevent the choking of the primary heat exchangers. Flow is usually in an upward direction to remove gas evolved in the acid wash and to facilitate the servicing of choked eluate collectors at the top rather than the bottom of the column.

At the end of the elution, the column is cooled to below the boiling point by having the final bed volume enter the column at ambient temperature.

In areas where the availability of good quality water is a problem, the water consumption of the AARL process can be reduced by the use of split elution (La Brooy and Ariti, 1988). This involves the use of the last 4

bed volumes of eluate as part of the feed for the next elution. To prevent the build up of dissolved salts in the system, occasional strips have to be carried out with only fresh water.

1.2.2 Zadra elution steps (Bailey, 1985)

Figure 1.3 contains the flow scheme for a Zadra elution system (Zadra, 1950) as published by Bailey (1985).

The Zadra elution technique differs from the AARL process in that no cyanide pretreatment is conducted and that the eluant is recycled through electrowinning cells in series with the column. The eluate contains 0.2 to 0.5% NaCN and 1 to 2% NaOH. Before being fed to the column, the eluate is preheated to 120 °C in a eluate/eluant heat exchanger and a steam heater in series. The hot eluant leaving the column is cooled to below its ambient boiling point in the eluate/eluant heat exchanger and a water cooler. The solution normally gravitates to the electrowinning cells where the gold is recovered from the solution which is then pumped back to the elution column. The build-up of contaminants is prevented by replacing all or part of the eluting solution with fresh eluate.

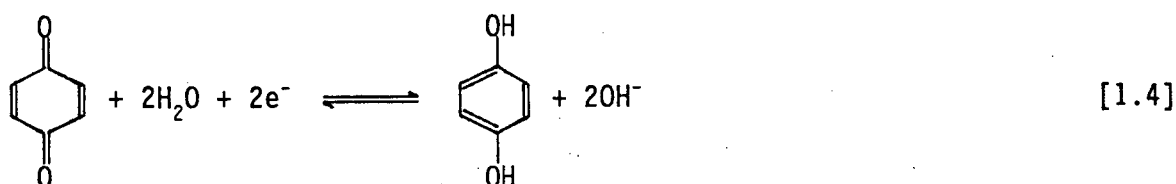
1.3 CHARACTERISTICS OF ACTIVATED CARBON

Activated carbon is manufactured from a large variety of carbonaceous materials such as peach pips and coconut shells. The raw material is first carbonized in the absence of air at 400 to 500 °C to form a char. It is then heated further to temperatures in the region of 1000 °C in an oxidizing atmosphere (such as steam) to activate the carbon. This produces a highly porous structure with a surface area of up to 1400 m².g⁻¹ and a pore volume of 0.5 to 1.8 ml.g⁻¹. The oxidation process also results in the formation of oxygen-containing functional groups on the carbon surface which are believed to contribute to the adsorption process (Acton, 1982).

McDougall and Fleming (1986) presented the structures of some surface oxides that were proposed to be present on activated carbon. These included carboxyl groups, phenolic hydroxyl groups, quinone-type carbonyl

groups and lactones.

It is believed that oxygen or quinone/hydroquinone type couples are responsible for the redox potential of activated carbon (Tsuchida and Muir, 1986a) :



The potential of the carbon will be determined by the potential of the functional groups exhibiting redox behaviour, as well as the pH of the solution in the pores of the carbon.

While the activation process determines mainly the functional groups on the carbon surface, the structure of the pores is a function of the source material (McDougall and Fleming, 1986). The pores are usually classified in terms of their diameters as follows :

Macropores 500 - 20000 nm

Mesopores 100 - 500 nm

Micropores 8 - 100 nm

A graphical presentation of the porous structure of activated carbon is shown in Figure 1.4. It can be seen that the smaller pores are assumed to branch off the macropores.

Clauss and Weiss (1977) stated that adsorption may be associated with the available carbon surface, or with specific parts of it (such as the basal planes or the edges of the crystallites), with micropores or other local imperfections, or with specific functional groups. They measured the adsorption of $\text{Au}(\text{CN})_2^-$ on graphite and a variety of carbons pretreated with different reagents. Although the study did not reveal the exact method of fixation, it was concluded that adsorption is related to specific sites and is not a property of the surface as such. Adsorption of gold cyanide was proved not to be related to the basal graphitic

planes, carboxylic groups or basic surface oxides.

However, in a titrimetric study on activated carbon (Parentich and Kinsella, 1984), it was found that both basic and acid surface groups are involved in the adsorption of gold onto activated carbon.

1.4 THE MECHANISM OF ADSORPTION

No agreement has yet been reached regarding the mechanism by which metal cyanides are adsorbed onto activated carbon. The following factors are believed to contribute to the disagreement among researchers on this subject (McDougall and Fleming, 1987) :

- (a) The complexity of the carbon surface hinders the instrumental analysis thereof by techniques such as infrared spectroscopy,
- (b) Different types of carbons have been used in the various investigations, and
- (c) The adsorption reaction has been studied at different experimental conditions, for example degrees of agitation or the concentrations of other reagents.

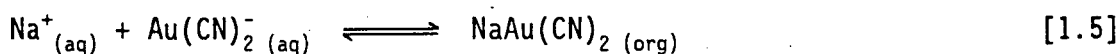
All of the proposed mechanisms for the adsorption of gold or silver cyanide from alkaline solutions at room temperature that have been published since 1974, can be grouped into mainly five categories :

- (a) Adsorption as $M^{n+}(Au(CN)_2^-)_n$

Davidson (1974) proposed a mechanism in which the extent of adsorption depends on the concentration and character of the "spectator" cations (M^{n+}) present in the solution. The calcium aurocyanide was reported as the most strongly adsorbed species in the series : $Ca^{2+} > Mg^{2+} > H^+ > Li^+ > Na^+ > K^+$. The differences in the behaviour of these cations could not be explained in terms of ionic strength alone. His theory is supported by a series of three publications (McDougall *et al.*, 1987, Adams *et al.*, 1987a, Adams *et al.*, 1987b), comparing the mechanisms for the extraction of

aurocyanide by 1-pentanol, polymeric adsorbents and activated carbon.

These mechanisms propose the formation of a neutral ion-pair species in the organic phase or on the adsorbent. As can be expected from Le Chatelier's principle, the equilibrium :



was found (McDougall *et al.*, 1987) to be shifted to the right by an increase in the cation concentration. (In the above equation, org denotes the adsorbent phase.) For the case of the activated carbon (Adams *et al.*, 1987b), the improved capacity for gold in the presence of larger cations was explained by the lower aqueous solubilities of aurocyanide salts with these cations, thus favouring the formation of an ion-pair. The even higher gold capacity in the presence of small (but strongly electrophilic) cations like H^+ , Li^+ and Be^{2+} was attributed to the interaction between these cations and the electron-donating cyanide groups of the aurocyanide anion by polarization of the surrounding water molecules. At low pH values, it was found (Adams and Fleming, 1989) that the gold is initially loaded as $\text{K}^+[\text{Au}(\text{CN})_2^-]$ or $\text{Ca}^{2+}[\text{Au}(\text{CN})_2^-]_2$, with the K^+ and Ca^{2+} slowly being displaced by H^+ as equilibrium is approached.

(b) Adsorption as $\text{M}^{n+}(\text{Au}(\text{CN})_2^-)_n$ followed by partial reduction

McDougall *et al.* (1980) suggested that the initial stage of adsorption involves the adsorption of the less soluble $\text{M}^{n+}(\text{Au}(\text{CN})_2^-)_n$ complex ($\text{M}^{n+} = \text{Ca}^{2+}, \text{H}^+, \text{Na}^+, \text{K}^+$). This is followed by a reduction step in which part of the $\text{Au}(\text{CN})_2^-$ is converted into an irreversibly adsorbed species. Even though the exact character of the reduced species could not be determined, the existence thereof was indicated by XPS studies of the loaded carbons. From the XPS spectra, an oxidation number of 0.3 was calculated for the gold

adsorbed on the carbon. Two possible gold species were proposed :
(i) A sub-stoichiometric $\text{Au}(\text{CN})_x$ species (i.e. a chain of gold atoms with CN^- acting as a bridging group). Because of strong interaction with the carbon, the gold will be in an oxidation state between 0 and 1.

(ii) A cluster-type compound of gold, such as $[\text{Au}_{11}(\text{CN})_3\text{L}_7]$, where $\text{L} = \text{P}(\text{C}_6\text{H}_5)_3$. Such a cluster will contain both $\text{Au}^{(0)}$ and $\text{Au}^{(I)}$, resulting in a total oxidation number of less than 1.

(c) Adsorption of $\text{Au}(\text{CN})_2^-$ followed by partial degradation to AuCN

Tsuchida *et al.* (1984) observed a molar ratio of adsorbed $\text{Au}(\text{CN})_2^-$ to K^+ of 1.0 on carbon that has been deoxygenated under vacuum at 950 °C. The higher ratio (2.5:1) measured on normal carbon implied that part of the $\text{Au}(\text{CN})_2^-$ was adsorbed as a neutral species. Tsuchida and Muir (1986b) proposed the following dual mechanism for the adsorption of $\text{Au}(\text{CN})_2^-$: The cyanide complex adsorbs onto the carbon by anion exchange with OH^- , followed by the partial oxidation thereof to AuCN by chemisorbed oxygen. The AuCN does not take part in the equilibrium between $\text{Au}(\text{CN})_2^-$ in solution and on the carbon, thus allowing higher gold loading than would be the case on deoxygenated carbon. Further proof for the oxidation-reduction part of the mechanism was obtained by measuring the redox potential of the carbon during the adsorption of metal cyanides (Tsuchida and Muir, 1986a). It was found that the adsorption of CN^- , $\text{Au}(\text{CN})_2^-$ and $\text{Ag}(\text{CN})_2^-$ irreversibly decrease the carbon potential, indicating the reduction of a surface oxidant. A more pronounced decrease in the potential in the presence of $\text{Ag}(\text{CN})_2^-$ than $\text{Au}(\text{CN})_2^-$ suggested less oxidation of $\text{Au}(\text{CN})_2^-$ than $\text{Ag}(\text{CN})_2^-$ on the carbon. The oxidative mechanism appeared to be enhanced by the absence of free cyanide and a pH of 7 rather than a pH of 10.

Cook *et al.* (1989) followed a similar approach to that of Tsuchida (1984), but used "normal" carbon only. They reported loaded Au:K ratios of 1:1 for adsorption from deoxygenated solutions, but much higher ratios (31:1) than Tsuchida from aerated solutions. It was

suggested that AuCN was formed in the presence of oxygen through the oxidation of CN^- .

Yet, other workers (Jones *et al.*, 1988; Adams and Nicol, 1986; Adams and Fleming, 1989) confirmed the absence of any irreversibly adsorbed species like AuCN or Au on their carbons by eluting all of the adsorbed gold with hot sodium hydroxide solutions. This could be achieved for carbons loaded from both alkaline and acidic solutions at room temperature (Adams and Nicol 1986; Adams and Fleming, 1989). These findings led them to reject a mechanism in which it is assumed that AuCN is formed on adsorption.

(d) Adsorption in an electrical double layer

In their studies on the adsorption of silver cyanide onto activated carbon, Cho and Pitt (1979b) found that Na^+ and Ca^{2+} were adsorbed only in the presence of the anionic metal cyanide. They postulated that the cations adsorb onto the silver cyanide anions already adsorbed on the active sites of the carbon surface. Adsorption of these cations promote further silver cyanide adsorption, thus creating an electrical double layer. The theory of anion adsorption is supported by the observation by Dixon *et al.* (1978) that the zeta potential of the carbon becomes more negative as more silver cyanide is adsorbed.

However, the neutral $\text{Hg}(\text{CN})_2$ species is adsorbed onto activated carbon to an extent comparable to that of $\text{Au}(\text{CN})_2^-$ (Tsuchida, 1984). Furthermore, $\text{Hg}(\text{CN})_2$ can displace $\text{Au}(\text{CN})_2^-$ from loaded activated carbon. This implies (Adams *et al.*, 1987b) that these two species compete for the same adsorption sites, thus contradicting a mechanism of anionic adsorption. The effect of perchlorate on the adsorption of gold onto activated carbon provided more evidence against such a mechanism: Whereas ClO_4^- was found to be extremely detrimental to the loading of $\text{Au}(\text{CN})_2^-$ onto an anion-exchange resin, it affected the adsorption onto carbon only slightly (McDougall *et al.*, 1980).

(e) Adsorption in the graphitic structure

According to Jones *et al.* (1988), the $\text{Au}(\text{CN})_2^-$ anion is being adsorbed without change or chemical reaction in its normal linear form ($\text{N}\equiv\text{C}-\text{Au}-\text{C}\equiv\text{N}$) in a symmetrical environment parallel to the graphitic planes of the carbon. A similar theory was published by Groszek (1970) to explain the selective adsorption of organics on graphite. Jones *et al.* (1988) postulated that the gold cyanide adsorption bond is formed by charge transfer of 0.3 to 0.5 electron to the central Au-cation from the delocalized π -electron system of the graphitic structure. At a pH of 10 in the absence of free cyanide the equilibrium adsorption and desorption isotherms for gold on Calgon GRC 22 were identical. It was concluded that $\text{Au}(\text{CN})_2^-$ is being adsorbed without chemical change. As further proof, an Au:N mole ratio of 2 has been measured on the loaded carbon with the use of X-ray photoelectron spectroscopy (XPS).

1.5 THE INTER-RELATIONSHIP BETWEEN ADSORPTION AND ELUTION

Few, if any, desorption processes are possible without being preceded by an adsorption process. This is (unfortunately for Mammon) also true for the elution of gold from activated carbon. The starting-point of the desorption will therefore be determined by whatever has happened in the adsorption step.

With regard to elution, the most important difference between the proposed mechanisms for adsorption concerns the character of the adsorbed species. Possible adsorbed gold species include $\text{KAu}(\text{CN})_2$, $\text{HAu}(\text{CN})_2$, $\text{Au}(\text{CN})_2^-$, AuCN , Au and the sub-stoichiometric species proposed by McDougall *et al.* (1980). The latest investigations of loaded carbon surfaces by direct analysis with X-ray photoelectron spectroscopy (XPS) (Cook *et al.*, 1989; Jones *et al.*, 1988) and Mössbauer spectroscopy (Cashion *et al.*, 1988) show beyond doubt that the gold adsorbed on the carbon is present only in the $\text{Au}^{(I)}$ oxidation state. This leaves only AuCN and $\text{Au}(\text{CN})_2^-$ (adsorbed with or without cations) as possible adsorbed gold species. No evidence of the presence of AuCN could be found by Mössbauer analysis. What is more, this analysis was carried out on a

sample of dry carbon loaded with gold approximately one year before. In the case of the XPS investigations, Jones *et al.* (1988) found only $\text{Au}(\text{CN})_2^-$ on carbon loaded from alkaline solution, whereas Cook *et al.* (1989) proposed that the gold was present as a combination of $\text{KAu}(\text{CN})_2$ and AuCN , with the latter being the dominant species at high gold loadings.

In studying the elution process, it will also be important to account for the kinetics of adsorption. If the carbon was, for example, loaded with gold over a short period of time from a solution with a high gold concentration, most of the gold would be adsorbed near the external surface or in the macropores of the carbon and might be more readily available for desorption.

1.6 OBJECTIVES OF THIS STUDY

As illustrated above, the adsorption of metal cyanides onto activated carbon has been studied extensively. Although controversy still exists on the mechanism of adsorption, it was shown that the adsorption of gold cyanide from clear solutions can be modelled accurately (Van Deventer, 1984b) without accounting for chemical changes in the adsorbed state. However, if species such as AuCN are formed on the loaded carbon, the leaching thereof might affect the kinetics of elution.

It is believed that cyanide is needed in gold elution processes to "convert the adsorbed gold to a more readily elutable cyanocomplex form" (Brittan, 1988), while others claim that all the adsorbed gold can be eluted with distilled water (Jones *et al.*, 1988). The disagreement on the form of the adsorbed species thus had to be resolved before a study of the elution process could be attempted. The specific objectives were :

To establish whether irreversibly adsorbed metal cyanide species are formed on the loaded carbon and to determine what role oxygen plays in the adsorption reaction thereof.

To determine the most important sub-processes of elution (such as the reactions of cyanide) and to quantify their effects on the elution of gold cyanide.

To investigate the mechanism of the elution of gold cyanide and to determine the associated role of cyanide.

To develop a general model for the elution of gold cyanide by both the AARL and Zadra procedures. Although such a model also had to account for important sub-processes other than the desorption of the gold, it was attempted to keep the model as simple as possible so as to enhance its functionality. It was also to be applicable to different reactor configurations and operating procedures, such as batch and continuous column operations, as well as starting with filled or drained beds.

To evaluate the general model by testing it against gold elution data obtained from experiments on laboratory and pilot plant scale.

To investigate the sensitivity of the model to changes in equilibrium and kinetic parameters.

To use the model for predicting continuous elution profiles so as to show how it can be used to optimize the operation of such a continuous process.

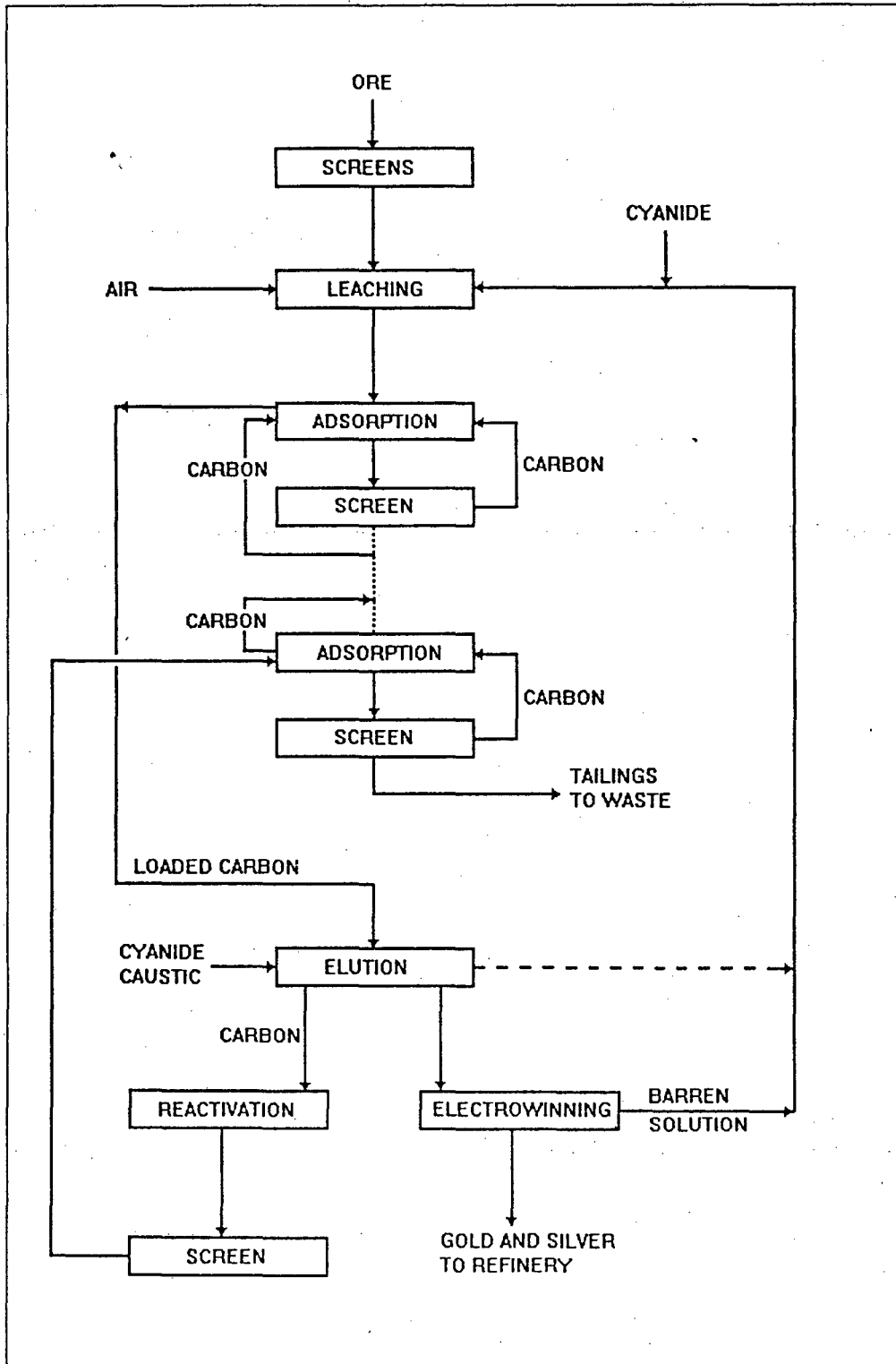


Figure 1.1 Overview of a typical CIP plant. (Fleming, 1983)

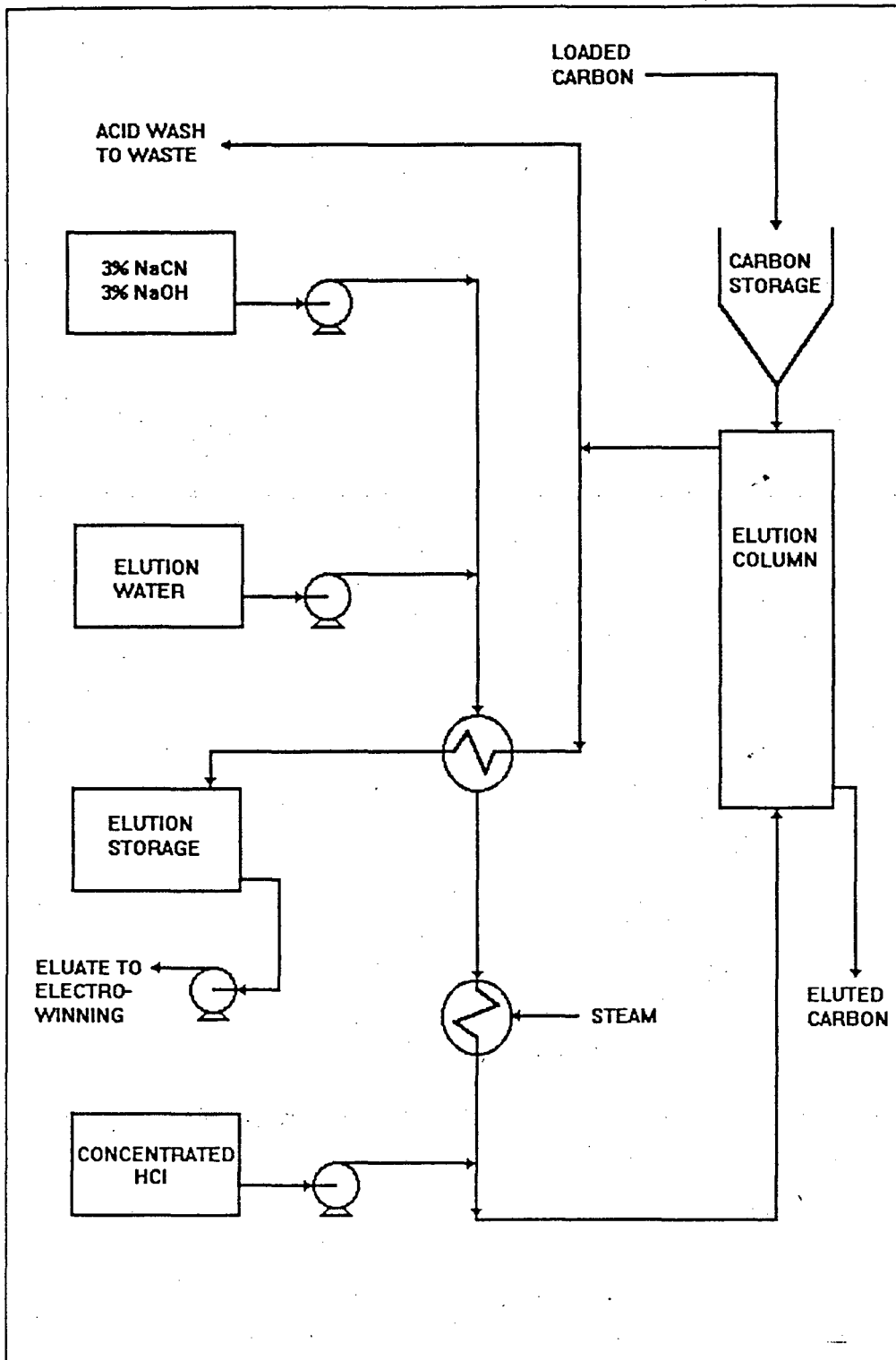


Figure 1.2 Flow diagram of the AARL elution system (Brittan, 1988)

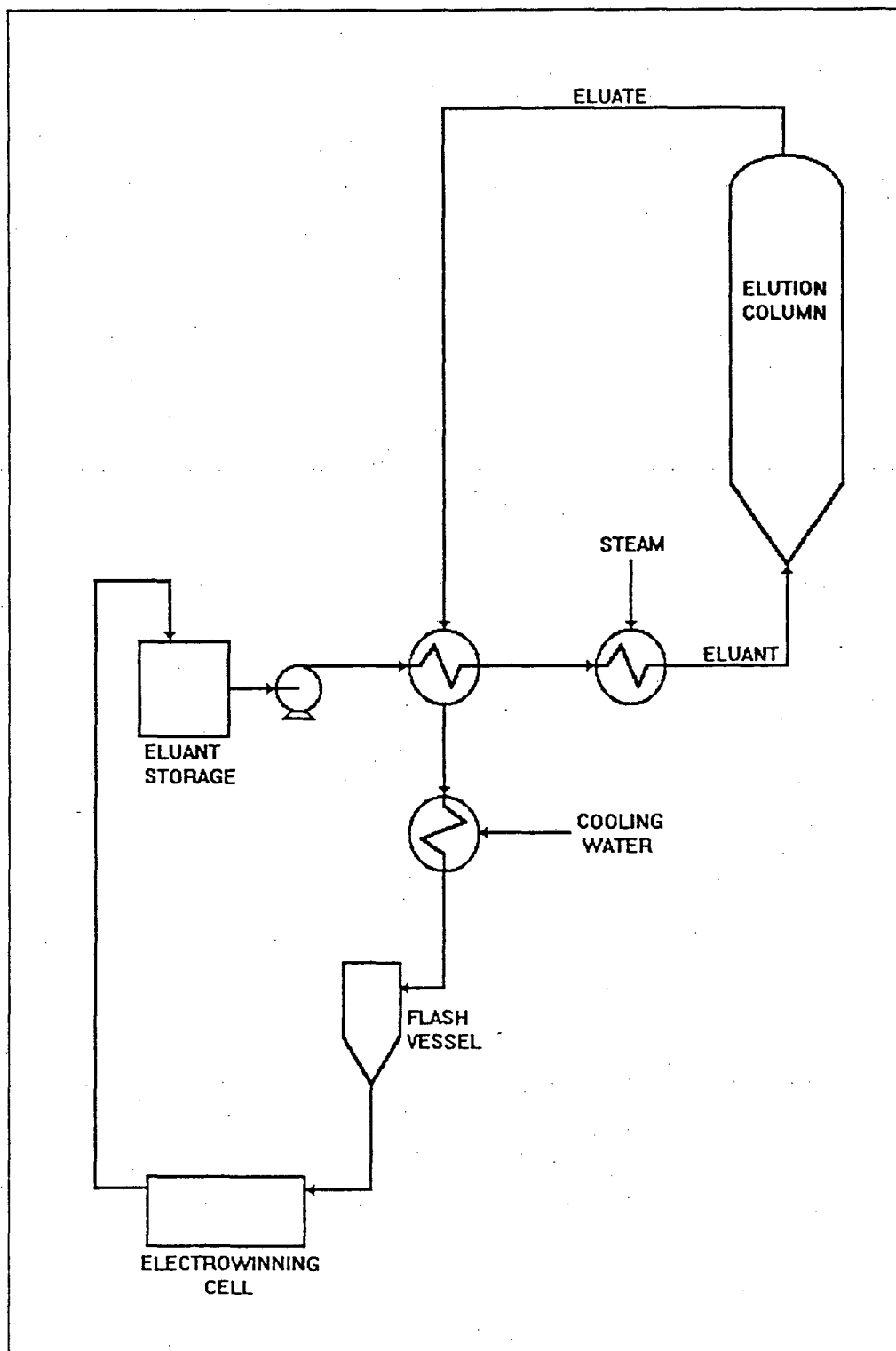


Figure 1.3 Flow diagram of the Zadra elution system (Bailey, 1985)

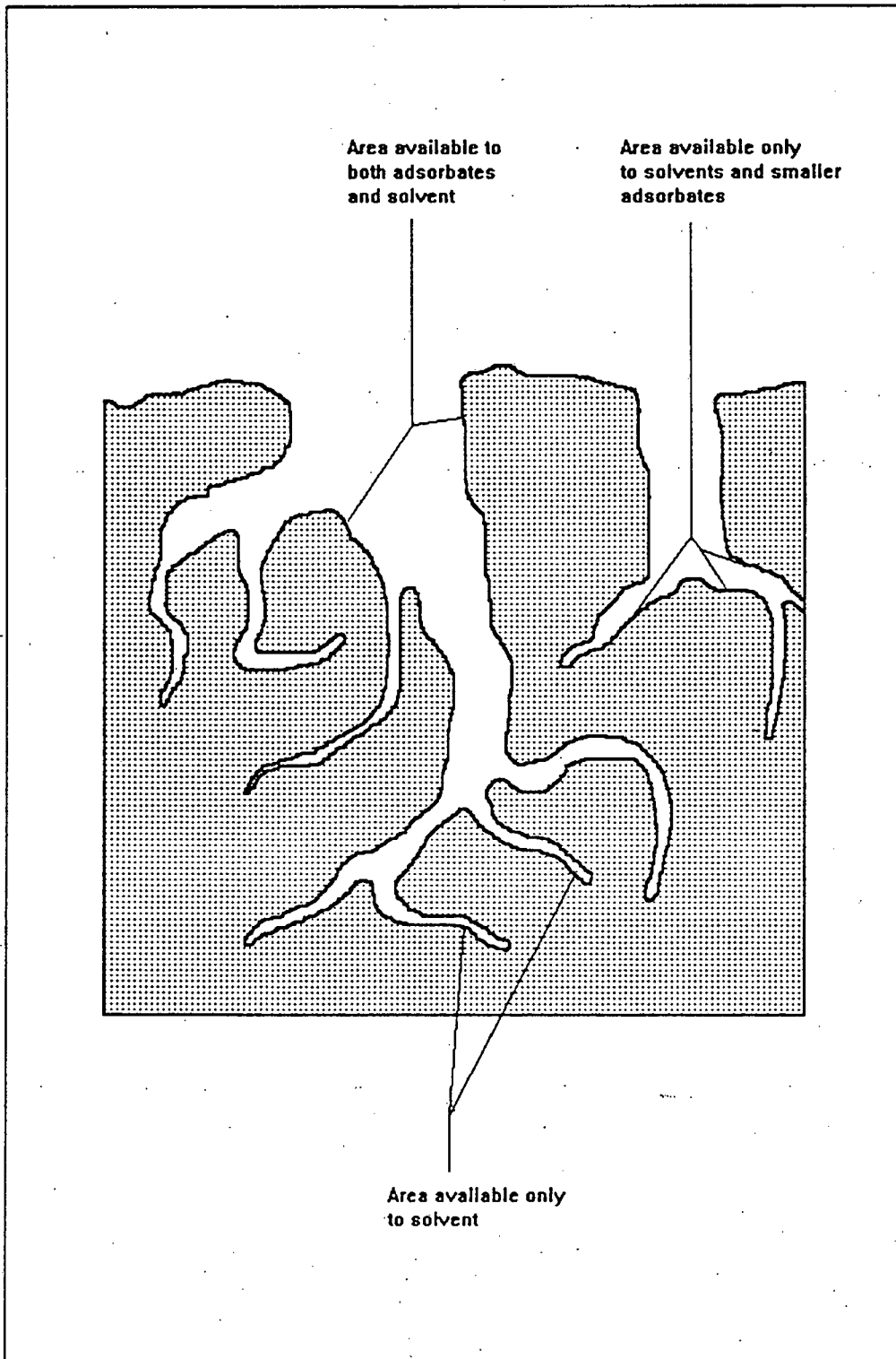


Figure 1.4 Schematic representation of pore structure of activated carbon (Acton, 1982).

2

OXYGEN AND THE NATURE OF THE ADSORBED SPECIES

In order to study the desorption of gold cyanide from activated carbon, it is important to know the initial condition for desorption, which is the same as the final condition for the adsorption process. It is not only necessary to know the concentration of gold on the loaded carbon, but also the form in which it is adsorbed as this will determine the need for cyanide in the elution process. As discussed in Chapter 1, controversy exists on the nature of the adsorbed species and the role which oxygen plays in transforming one species into another. This chapter was therefore devoted to shed more light on these subjects, and to create a better understanding of the starting point of the desorption process.

2.1 EXPERIMENTAL

2.1.1 Chemicals

The gold and silver used in the experimental work were supplied by Barry Colne & Co. in the form of $\text{KAu}(\text{CN})_2$ and AgCN respectively. The AgCN was dissolved in water at $95\text{ }^\circ\text{C}$ by the addition of 10% more than stoichiometric KCN . Despite the excess of cyanide, the solutions had to be filtered to remove grains of undissolved AgCN . It was found that the resulting $\text{Ag}(\text{CN})_2^-$ solutions contained practically no free cyanide. This can be ascribed to the rapid decomposition of cyanide at the high temperature employed to dissolve the AgCN . Mercury in the form of $\text{Hg}(\text{CN})_2$ was used in comparative experiments. Distilled water was used throughout. The pH was adjusted by the addition of small amounts of HCl and KOH . All chemicals were of AR grade.

2.1.2 Carbon

Mainly two types of experimental coconut shell carbon, designated A and B, were used for the experiments in this chapter. Only the 1.7 to 2 mm sieve size fraction was used. Various tests were conducted on the carbons to try and match their characteristics to their interaction with metal cyanides. Figure 2.1 shows their zeta potential versus pH curves determined at 25 °C. Both carbons revealed a point of zero charge at a pH of 1.8, and a natural pH in distilled water of 5.5. The iodine test described by Hassler (1974) was performed on both carbons. Carbon A adsorbed 48% of the available iodine and carbon B 53%. The zeta potential and iodine number proved to be of little value in the prediction of a carbon's adsorption capacity for metal cyanides. Whereas carbons A and B have nearly identical zeta potential versus pH curves, they differ significantly in the adsorption of metal cyanides. The iodine test suggested a difference of 10% in the adsorption behaviour of the two carbons, while their equilibrium metal cyanide loadings at a solution phase concentration of 10 mg/l differed by approximately 58% and 18% for gold and silver respectively.

Carbons A and B had apparent densities of 1080 and 1004 kg.m⁻³ respectively. The apparent densities were calculated by dividing the mass of a known number of oven dried particles (with the same sieve size diameter) by the total volume based on the assumption of spherical particles. The Langmuir surface areas of carbons A and B were determined with a Micromeritics Flowsorb 2300 apparatus as 1070 and 1870 m².g⁻¹. Unless otherwise specified, the carbon was dried at 120 °C for 3 days before being weighed and used in the experiments.

Some of the experiments were conducted with an industrial, eluted carbon from the Beatrix mine in South Africa. The carbon, which will be referred to here as carbon BTX, was acid washed and rinsed with deionised water to remove as many impurities as possible. A BET surface area of 792 m².g⁻¹ and an apparent density of 838.8 kg.m⁻³ was measured for the carbon. Figure 2.2 shows the particle size distribution of carbon BTX. The mean particle size was calculated as 1.42 mm.

2.1.3 Analytical methods

A Beckman Φ 70 meter with a Beckman combination pH electrode was used to measure the pH of the solutions. The dissolved oxygen concentration was monitored with a Schott Geräte model CG867 oxygen meter. The metal concentrations in solution were determined with a Varian AA-1275 atomic absorption (AA) spectrophotometer, and the loadings on the carbon calculated by mass balance. Table 2.1 summarizes the spectrophotometer conditions for the elements in this study that were determined in this way. Samples with solution phase concentrations higher than C_{\max} were diluted prior to analysis.

A AgNO_3 titration was used to test for free cyanide. KI was used as an indicator. Free cyanide reacts with Ag^+ as in Equation 2.1. At the end point of the titration, i.e. when all the cyanide has been reacted, the silver reacts with the iodine (Equation 2.2) and forms a yellow precipitate of AgI .



Zeta potential measurements were conducted with a Rank Brothers Mark II instrument. 50 mg of powdered carbon ($d_c < 125 \mu\text{m}$) was mixed with 1 litre of distilled water and conditioned for 20 minutes at 25 °C before any measurements were made. The zeta potentials presented, are average values of measurements at potential differences of 51.9 and 71.5 mV.

Fourier Transform Infrared (FTIR) scans of the carbons were obtained by using the "DRIFT" technique on a Perkin-Elmer model 1710 infrared spectrophotometer. Owing to the intense background caused by organic groups on the carbon, sufficiently high loadings of gold were required in order to observe the $\nu(\text{CN})$ vibrations of the gold cyanide species. For this purpose 0.5 g of powdered carbon was contacted for 5 days with 0.8 litre of solution containing 200 mg Au/l at a pH of 8.5. This resulted in metal loadings of approximately 60 mg Au/g carbon. At the end of the adsorption period the loaded carbon was filtered and washed with distilled water to remove any dissolved gold present in the liquid layer surrounding the carbon particles. The moist samples were then analysed

in their wet state so as to prevent possible changes in the gold species upon drying. It was found that the spectrum remained unchanged after 80 to 100 scans were performed on a sample. A standard of 100 scans per spectrum was therefore used for all the FTIR work.

A scanning electron microscopy (SEM) study was performed on carbon BTX. The images and accompanying X-ray spectra were recorded on a JEOL JSM-35 scanning electron microscope coupled to an EDAX model 707B energy-dispersion X-ray apparatus.

2.1.4 pH of adsorption

Davidson *et al.* (1979) investigated the effect of pH on the adsorption of gold and silver from gold-plant solutions and recommended the acidification of pregnant solutions before contact with carbon. A pH of 5 or lower resulted in less fouling by calcium carbonate, higher gold adsorption rates and less displacement of adsorbed silver by gold. Although most gold extraction plants still use pH values higher than 10, there is a tendency towards lower pH's with improvements in control systems (Davidson, 1986b).

Unless specified otherwise, all the adsorption experiments were conducted at a pH of 8.5.

2.1.5 Equilibrium adsorption experiments

The equilibrium isotherms were determined by contacting weighed, oven dried samples of carbon with 1 litre solutions of gold or silver cyanide with known initial concentrations for 21 days. In earlier investigations (Cho and Pitt, 1979a) equilibrium was assumed as little as 3 hours after the activated carbon was brought into contact with the metal cyanide solution. Van Deventer (1984), however, showed that even after one week significant loading still takes place. Equilibrium was practically obtained only after 3 weeks. Despite this, most workers still determine equilibrium isotherms over periods ranging from 20 hours (Adams *et al.*, 1987b) to 4 days (Tsuchida *et al.*, 1985) to 1 week (Adams and Fleming, 1989).

After equilibrium was attained, the metal cyanide concentrations in

solution were determined by AA-analysis, and the concentrations of metal cyanide on the carbon calculated as :

$$Q_e = \frac{(v_i \cdot C_i - v_e \cdot C_e)}{m_c} , \quad [2.3]$$

with v_e the volume of solution at equilibrium. v_e was generally smaller than v_i (the initial volume), because of evaporation during the adsorption period.

Part of this study was devoted to the contacting of carbon with solutions at different levels of dissolved oxygen. For the experiments at 0 mg O₂/l the solutions were depleted of oxygen by purging with nitrogen for approximately 1 hour before adding the carbon. The bottles were then tightly sealed and rolled end over end. After the 3 week adsorption period, the oxygen concentrations were measured and found to be zero. The equilibrium experiments at oxygen concentrations other than 0 mg/l were conducted in stirred reactors with loose fitting lids. Constant dissolved oxygen levels were maintained by a continuous supply of air-oxygen or air-nitrogen mixtures to the surface of the solutions via plastic tubes through the lids.

All the equilibrium isotherms in this chapter were determined at a room temperature of 17 to 22 °C.

2.1.6 General

More detail of the individual experiments are supplied in the tabulation of the experimental results in Appendix K.

2.2 EFFECT OF OXYGEN ON ADSORPTION OF METAL CYANIDES

2.2.1 Equilibrium studies

The gold loading capacity of activated carbon was reported to decrease when the adsorption was conducted under a nitrogen instead of an air atmosphere (Dixon *et al.*, 1978). No difference in adsorption could be observed between runs in which air or pure oxygen was present. It was postulated that the exclusion of oxygen reduces the amount of active

sites available for adsorption. From the above observations the question arises whether the concentration of oxygen, or just the availability thereof, is important.

A series of experiments was then carried out to determine the effect of the concentration of dissolved oxygen on the equilibrium loadings of gold and silver cyanide. Figures 2.3 to 2.5 show the isotherms determined for carbon A, and Figures 2.6 and 2.7 those for carbon B. From these figures it is clear that characteristic gold and silver isotherms exist at different dissolved oxygen levels. It was found that the Freundlich equation (Eq. 2.4) could be fitted to each set of experimental data. The values of the equilibrium constants are summarized in Tables 2.2 and 2.3.

$$Q_e = A C_e^n \quad [2.4]$$

The equilibrium metal loadings calculated from these isotherms at a C_e of 10 mg/l are plotted in Figure 2.8 as a function of the oxygen concentration. For both carbons there existed oxygen levels above which the equilibrium loadings showed no further increase. For carbon A this point for both gold and silver was approximately 9 mg O_2 /l. Oxygen concentrations higher than 9 mg/l caused a decreased silver loading on carbon A. The maximum loading of gold on carbon B had already been reached at an oxygen concentration of 4.2 mg/l, while this point appeared to be slightly higher for silver.

The detrimental effect of oxygen concentrations higher than 9 mg/l was further investigated by comparing the rates of adsorption from solutions in contact with air and solutions in contact with pure oxygen. The oxygen concentrations for these two cases were measured as 9 and 40 mg/l respectively. Figure 2.9 shows that purging with pure oxygen instead of air decreased the rate of adsorption of $Au(CN)_2^-$ from an alkaline solution. However, at a pH of 3.5, the higher oxygen concentration led to a slightly higher rate of adsorption (Figure 2.10).

From the equilibrium experiments at 0 mg O_2 /l, it follows that significant loadings of gold and silver are obtained even in the absence of oxygen. This means that, if oxygen is necessary for the adsorption of metal cyanides, the adsorption in the absence of dissolved oxygen had to

occur via the use of chemisorbed oxygen.

2.2.2 Chemisorbed vs. dissolved oxygen

The following observations led Jones *et al.* (1988) to believe that carbon-oxygen functional groups on activated carbon do not take part in the adsorption reaction :

- (1) Gold can be adsorbed onto carbon up to very high loadings (2 mmol/g) without any apparent restriction. In contrast, the oxygen concentration on the carbon surface has been determined as being smaller than 0.1 mmol/g. This does not agree with theories in which it is assumed that adsorption involves the reaction between equimolar amounts of $\text{Au}(\text{CN})_2^-$ and oxygen.
- (2) Pretreatment of the carbon with MnO_2 , which will oxidize oxygen-functional groups to CO_2 , did not lower the gold capacity of the carbon.

Tsuchida *et al.* (1985) investigated the effect of oxygen by comparing the adsorption onto "normal" and "deoxygenated" carbon. The latter was prepared by heating carbon at 950 °C under vacuum for approximately 10 hours. By this procedure most of the chemisorbed oxygen were removed. As expected, higher loadings of gold were obtained on the normal carbon under an air atmosphere than on the deoxygenated carbon under a nitrogen atmosphere. The loading on the deoxygenated carbon could be increased to that on the normal carbon by exposure of the solution to oxygen. However, no results were presented to enable a comparison of the adsorption on normal and deoxygenated carbon both in the absence of dissolved oxygen. It is thus impossible to determine the relative importance of the chemisorbed and dissolved oxygen from the results of Tsuchida *et al.* (1985). More light is shed on the problem if those results are compared to those of Cook *et al.* (1989). Identical molar ratios (1:1) of loaded Au:K were reported for adsorption onto deoxygenated carbon (Tsuchida *et al.*, 1985) and normal carbon (Cook *et al.*, 1989) from deaerated solutions. (Norit R2020 carbon was used in both studies.) From the arguments of Tsuchida *et al.* (1985), these similar ratios can be interpreted as an indication that the mechanism of gold adsorption is the same in both cases. (It was shown by Tsuchida and

Muir (1986a) that the ratio of adsorbed gold to potassium increased up to 31:1 in aerated solutions.) This implies that the chemisorbed oxygen on normal carbon has a negligible effect on the mechanism of adsorption if compared to the effect of oxygen in solution.

Tsuchida (1984) ascribed the increased adsorption in the presence of oxygen to the oxidation of $\text{Au}(\text{CN})_2^-$ to AuCN . However, although XPS investigations of gold loaded carbons showed an increase in the concentration of oxygen groups on the exterior surface of the carbon, Cook *et al.* (1989) concluded that oxygen is not associated directly with the adsorption mechanism of the gold as the adsorbed Au:CN ratio was found to be homogeneous throughout the carbon particles.

2.2.3 Adsorption of $\text{Hg}(\text{CN})_2$

When $\text{Hg}(\text{CN})_2$ is dissolved in water, it remains in the solution as the neutral $\text{Hg}(\text{CN})_2$ molecule. Although it has no charge, it is adsorbed onto activated carbon to the same extent as $\text{Au}(\text{CN})_2^-$ and $\text{Ag}(\text{CN})_2^-$ (McDougall *et al.*, 1980; Tsuchida, 1984). It has even been reported (Adams *et al.*, 1987b) that $\text{Hg}(\text{CN})_2$ can displace adsorbed $\text{Au}(\text{CN})_2^-$ from carbon. In Experiments 19(a) and (b) the adsorption of $\text{Hg}(\text{CN})_2$ onto carbon A from an aerated solution was compared to its adsorption from a deaerated solution. After an adsorption period of 2 days the mercury concentration in the deaerated solution was slightly lower than that in the aerated solution. To investigate the possibility that pure oxygen may have a detrimental effect on the adsorption of $\text{Hg}(\text{CN})_2$ similar to that observed for $\text{Au}(\text{CN})_2^-$, the adsorption of $\text{Hg}(\text{CN})_2$ from an oxygen saturated solution was compared to that from a solution saturated with air (Experiment 19 (c) and (d)). The adsorption efficiency was exactly the same in both cases.

From these results it follows that the adsorption of $\text{Hg}(\text{CN})_2$ is unaffected by oxygen. This implies that if $\text{Au}(\text{CN})_2^-$ is adsorbed as a neutral species (eg. $\text{KAu}(\text{CN})_2$), the adsorption thereof should be independent of the dissolved oxygen concentration.

2.2.4 Ion-exchange

As a mechanism of ion-exchange for the loading of metal cyanides onto activated carbon cannot be ruled out completely, the effect of oxygen on the adsorption of $\text{Au}(\text{CN})_2^-$ on a weak-base ion exchange resin was investigated in Experiment 20. It was found that the adsorption was unaffected by the presence or absence of oxygen. This suggests that if the adsorption of anionic metal cyanides onto activated carbon can be described by an ion exchange mechanism, oxygen cannot be involved in the adsorption reaction itself, but is used in rendering the surface of the carbon receptive for adsorption.

The change in the zeta potential of carbon A with a change in oxygen concentration was measured in Experiment 21. Although the zeta potential was much less sensitive to changes in $[\text{O}_2]$ than to changes in pH, increased oxygen concentrations led to less negative zeta potentials. However, the higher zeta potential of the carbon in water that was saturated with oxygen instead of air is not reconcilable with the decreased gold adsorption experienced at oxygen levels higher than that in equilibrium with air.

2.2.5 Lowering of $[\text{O}_2]$ during adsorption

Figure 2.11 illustrates the effect of lowering the oxygen concentration during the adsorption of gold cyanide onto carbon A. Although it was possible to increase the loading of gold and silver at 0 mg O_2/l by increasing the level of dissolved oxygen, the adsorption reaction could not be reversed by lowering the oxygen concentration. The step-wise decrease in the oxygen concentration in Figure 2.11 retarded the adsorption, but did not cause the loaded gold to desorb.

Similar behaviour was observed for the elution process. For the experiment in Figure 2.12, three identical samples of carbon A were loaded with gold in open containers (i.e. it was exposed to oxygen during the adsorption reaction.) The loaded carbon was then transferred to vessels containing water at a pH of 12 and oxygen concentrations of 0, 9 and 40 mg/l. The rate of desorption was unaffected by the dissolved oxygen level. Yet, in a similar experiment (Figure 2.13) it was found that oxygen had a small negative effect on the desorption of gold from

loaded carbon onto which the adsorption had taken place in the absence of oxygen.

2.3 CONSUMPTION OF OXYGEN

It is well-known that activated carbon chemically adsorbs oxygen to form carbon-oxygen surface groups (Parentich and Kinsella, 1984). These complexes are believed to have an important effect on the behaviour of the carbon. Besides the adsorption of oxygen by dry carbon, a further quantity of oxygen is adsorbed in the presence of water or other source of hydronium ion.

With a constant feed of dissolved oxygen (as in a packed column) carbon can adsorb oxygen up to levels of $600 \mu\text{mole O}_2/\text{g carbon}$ (or $19.2 \text{ mg O}_2/\text{g carbon}$) over a period of 2 months (Prober et al., 1975). However, only small quantities of oxygen are adsorbed from aerated water in closed containers. From the results for Filtrasorb 400 (Fig.6 of Prober et al., 1975) it can be calculated that over a period of 2 weeks carbon will typically adsorb $0.2 \text{ mg O}_2/\text{g carbon}$ from water in a closed container. Physical adsorption accounted for only 5% of the total adsorption. The rest was attributed to oxidation reactions forming groups such as quinones, carboxylic acids and basic oxides. Oxide groups increase the polarity of activated carbon and, depending on the specific adsorbate-oxide interactions, can enhance or decrease the adsorption of polar adsorbates (Prober et al., 1975). The adsorption of O_2 onto carbon A was investigated in Experiment 25. In this experiment, a sample of carbon A was contacted with distilled water in a tightly sealed bottle for 2 weeks. From the difference between the oxygen concentration in the solution with carbon, and the oxygen concentration of a reference solution without carbon, it was calculated that the carbon adsorbed $0.45 \text{ mg O}_2/\text{g carbon}$.

When the adsorption of gold or silver cyanide onto activated carbon occurs in a closed vessel, a decrease in the oxygen concentration can be monitored as shown in Figure 2.14(a). If it is estimated that the carbon alone adsorbed $0.45 \text{ mg O}_2/\text{g}$, it seems that the adsorption reaction of the metal cyanide must have been responsible for the rest of the oxygen

consumed (1.8 mg O₂/g). No stoichiometric relationship could however be found between the amount of gold adsorbed and the oxygen consumed (Van der Merwe and Van Deventer, 1988). Furthermore, it was found that the results from experiments where the oxygen concentration was measured continuously did not correlate with experiments in which only the initial and final oxygen concentrations were measured. One of the main reasons for the discrepancy was the inability to calibrate the oxygen meter during experiments in which the dissolved oxygen level was monitored continuously over periods of up to 90 hours. The unreliability of the oxygen measurements without frequent calibration is illustrated in Figure 2.14(b) where the same experiment was repeated 4 times. In order to calibrate the meter, it had to be removed from the reactor, and that would have led to breaking the closed system. Further experiments were thus conducted in tightly sealed bottles and the oxygen and metal cyanide concentrations measured only at the start and end of the runs.

The results of the experiments in which only the initial and final concentrations were measured, are summarized in Table 2.4. As a test of the impermeability of the wax sealed tops of the bottles used in these experiments, a bottle was filled with distilled water at an O₂ concentration of 0 mg/l, sealed and rolled for 5 days. At the end of the period it was opened and the oxygen concentration measured as 0.5 mg/l (Experiment 27(a)). Even though this concentration is low in comparison with the 9 mg O₂/l concentration difference between the environment and the solution, the bulk of the oxygen is believed to have entered the solution while measuring the oxygen concentration. Experiments in these bottles were thus regarded as being conducted in completely closed systems.

Experiments 27(i) to 27(l) in Table 2.4 compare the uptake of oxygen from distilled water by carbon A after being dried at different temperatures. The consumption of oxygen increased with an increase in drying temperature of up to 200 °C. The decreased consumption by the sample of carbon that was dried at 300 °C can possibly be ascribed to a change in the intrinsic characteristics of the carbon at the high temperature. The sample of carbon that was used without pre-heating, resulted in a slight increase in the oxygen concentration in solution. Carbon BTX displayed similar behaviour (Experiments 27(n) and 27(o) in Table 2.4). It arises

from these results that the surface oxygen on the carbon is in equilibrium with the oxygen of its surroundings. If this equilibrium has been shifted by, for example, a change in temperature, the carbon will adsorb or desorb oxygen in order to satisfy the new equilibrium. From Experiments 27(d) to 27(f) it follows that the adsorption of oxygen by carbon A is independent of the pH of the water.

The possibility of an increased consumption of oxygen during the adsorption of $\text{Au}(\text{CN})_2^-$ onto carbon A was investigated in Experiment 27(b). To eliminate the contribution of the carbon to the consumption of oxygen, the carbon was soaked in aerated, distilled water for more than 24 hours prior to the experiment. The subsequent adsorption of gold by this carbon in a closed vessel was accompanied by a decrease in oxygen concentration of only 0.2 mg/l. This small decline in oxygen concentration led to an adsorption of gold in the closed system similar to that of a reference solution open to the atmosphere (Experiment 27(c) in Table 2.4). For silver cyanide instead of gold cyanide (Experiments 27(g) and 27(h)) 0.5 mg O_2 /l was consumed during the adsorption reaction. Even though the final oxygen concentration was as high as 8.3 mg/l, compared to the 8.8 mg O_2 /l in the open system, 35 % less silver was adsorbed in the closed than in the open system. As the equilibrium experiments predict a much lower sensitivity of silver adsorption to oxygen concentration, it follows that the difference in silver adsorption had to be caused by another factor, such as the pH of the solution. Both solutions had an initial pH of 8.5, but at the end of the runs the pH in the open system was 7.6 compared to 8.7 in the closed vessel. The drop in pH of the open system was attributed to the availability of CO_2 in air.

The effect of pH on the consumption of oxygen during the adsorption of gold was examined in Experiments 27(o), 27(p) and 27(r). Although the consumption of oxygen was increased by the addition of $\text{Au}(\text{CN})_2^-$, the molar ratio of adsorbed Au to adsorbed O_2 was more than 7:1. The low pH of 3.9 increased the consumption of oxygen only marginally, resulting in much less oxygen consumed per mole of gold adsorbed. This is in contradiction to the mechanism proposed by Tsuchida (1984). The lower pH should have resulted in more $\text{Au}(\text{CN})_2^-$ being converted to AuCN , i.e. a higher demand for oxygen per mole of gold adsorbed.

In the mechanism of Tsuchida (1984) the CN^- that is released during the adsorption of the $\text{Au}(\text{CN})_2^-$ is oxidized to CO_3^{2-} and NH_3 . The first step in the oxidation of cyanide occurs via the following reaction :



A comparison of the results of Experiments 27(q) and 27(o) in Table 2.4 confirms the increased demand for oxygen in a cyanide solution containing carbon BTX. The molar ratio of CN^- consumed to O_2 consumed was however 6:1. If the stoichiometry in Equation 2.5 is accounted for, it implies that only 33% of the cyanide was oxidized and the rest adsorbed. For carbon A (Experiment 27(m)) even less oxygen was consumed for a similar cyanide consumption. By applying the same argument to this experiment, it follows that 95% of the CN^- was adsorbed onto carbon A, while only 5% was oxidized.

To model the adsorption of silver cyanide in packed beds of activated carbon, Jansen van Rensburg and Van Deventer (1985) used equilibrium isotherms determined in sealed bottles. Equilibrium isotherms determined in open vessels predicted higher adsorption efficiencies than were measured experimentally. This was attributed to low oxygen concentrations in the column, resulting from co-adsorption of O_2 with $\text{Ag}(\text{CN})_2^-$. As the results in Experiment 27 do not suggest a large consumption of oxygen, the oxygen concentration during the adsorption of gold in a column of carbon was monitored and plotted in Figure 2.15. Because of the low flow rate in the column, the readings on the oxygen meter were adjusted with a predetermined calibration curve. The details of the procedure are summarized in Experiment 28. From Figure 2.15 it follows that the oxygen concentration did not change through the column. The following points must however be stressed :

- (a) $\text{Au}(\text{CN})_2^-$, and not $\text{Ag}(\text{CN})_2^-$, was used in Figure 2.15. The adsorption of silver cyanide may result in higher oxygen consumptions.
- (b) No free cyanide was present in this experiment. The oxidation of cyanide in the presence of activated carbon consumes large quantities of oxygen (see Experiment 27) and will result in lower oxygen concentrations in the column.

- (c) To minimize the interaction between the dissolved oxygen and the functional groups on the surface of the carbon, the carbon was soaked over night in aerated, distilled water prior to the experiment.

2.4 REVERSIBILITY OF ADSORPTION IN AN ALKALINE MEDIUM

The reversibility of the adsorption of gold onto activated carbon is a function of the nature of the adsorbed species. Whereas $\text{Au}(\text{CN})_2^-$ and $\text{M}^{n+}(\text{Au}(\text{CN})_2^-)_n$ are soluble in distilled water, AuCN or Au would require the addition of cyanide to form $\text{Au}(\text{CN})_2^-$ before it can enter the solution phase. Reversible adsorption is therefore defined here as desorption without the addition of cyanide. As it was proved beyond doubt that no metallic gold is formed upon adsorption of gold cyanide on activated carbon in alkaline solutions (Adams *et al.*, 1987b; Cook *et al.*, 1989; Cashion *et al.*, 1988), it leaves AuCN as the only known, irreversible species.

Fleming (1988) investigated the reversibility of adsorption of gold cyanide by mixing small, unloaded carbon particles with large, gold loaded carbon particles in distilled water. When the particles were mixed intimately in a rolling bottle, it was found that an equal distribution of gold between the particles was reached in less than 24 hours, regardless of the concentration of free cyanide in solution. The same result could be achieved even after heating the gold loaded carbon at 200 °C for 24 hours before the experiment. This was interpreted as proof that no chemical change occurred in the adsorption-desorption mechanism as a result of heating, and that the adsorption of gold cyanide was fully reversible. If, however, the particles were separated by a glass frit, very little migration took place from the loaded to the unloaded particles. Most of the $\text{Au}(\text{CN})_2^-$ is therefore transferred upon contact between particles across the liquid film surrounding the particles without entering the bulk of the solution.

McDougall *et al.* (1980) found however that a new equilibrium was not established upon contact of gold loaded carbon with distilled water and

criticized the adsorption models of workers who assumed that the adsorption process was reversible.

2.4.1 Desorption with distilled water

It was decided to make use of the difference in solubility of $\text{Au}(\text{CN})_2^-$ and AuCN in order to determine the fraction of gold loaded onto activated carbon as AuCN . While AuCN is practically insoluble in the absence of free cyanide (Weast, 1985), the $\text{Au}(\text{CN})_2^-$ could be eluted with distilled water, and the difference between the eluted and remaining gold accounted for as AuCN . The pH of the distilled water was raised to approximately 12 by the addition of KOH. The presence of KOH enhances the desorption of $\text{Au}(\text{CN})_2^-$, but does not form a complex with AuCN .

Proper mass balances could not be obtained using conventional desorption methods (i.e. temperatures $> 90^\circ\text{C}$ and $\text{pH} > 12$) without the addition of free cyanide. In the absence of cyanide a yellow precipitate was observed in the solutions and on the carbon. The precipitate on the carbon had the same appearance as that of metallic gold on carbon loaded from AuCl_4^- solutions. To prevent the possible decomposition of the $\text{Au}(\text{CN})_2^-$ species at high temperature, further determinations of AuCN were conducted at room temperature. The results of these tests (Experiments 29 to 33) are summarized in Table 2.5. In Experiment 29 all the gold loaded onto carbon A under alkaline conditions and at an oxygen concentration of 9 mg/l could be recovered without the addition of cyanide. This means that even after a loading period of 3 weeks no $\text{Au}(\text{CN})_2^-$ changed to AuCN . Under the same adsorption conditions 62% of the adsorbed silver was reduced to AgCN (Experiment 30). The silver cyanide complex, $\text{Ag}(\text{CN})_2^-$, is therefore less stable than the corresponding gold complex. The formation of AuCN on carbon B was tested in Experiment 31. Only 79% of the gold adsorbed onto carbon B from an alkaline, aerated solution could be recovered with distilled water through which N_2 was purged. After adsorption from a solution depleted of oxygen, 75% of the gold could be eluted as above. This means that about 20% of the gold on carbon B was present as AuCN and that the formation of AuCN is independent of the dissolved oxygen concentration. Experiment 32 shows that, as for carbon A, no decomposition of $\text{Au}(\text{CN})_2^-$ took place on carbon BTX.

The formation of AuCN on carbons A and B was investigated in three more independent tests :

2.4.2 Fourier Transform Infrared scans

Fourier Transform Infrared (FTIR) scans of $\text{KAu}(\text{CN})_2$ powder and gold loaded carbons A and B are presented in Figures 2.16 to 2.18. The $\nu(\text{CN})$ vibrations of the two gold cyanide species have been published (Adams, 1967) as follows :

$\text{Au}(\text{CN})_2^-$ in aqueous solution : 2147 cm^{-1} , and
AuCN in the solid state : 2239 cm^{-1} .

The FTIR scan of $\text{KAu}(\text{CN})_2$ in the solid state showed a peak at 2154 cm^{-1} and not at 2147 cm^{-1} . The $\nu(\text{CN})$ vibration of $\text{Au}(\text{CN})_2^-$ can thus be shifted depending on the spectator cation and the state of the species. Therefore, the peaks within 2 cm^{-1} from the published values were marked in Figures 2.17 and 2.18. Only the $\text{Au}(\text{CN})_2^-$ peak was observed for carbon A, while both the $\text{Au}(\text{CN})_2^-$ and AuCN peaks appeared in the case of carbon B.

2.4.3 Equilibrium isotherms

The fraction of the adsorbed $\text{Au}(\text{CN})_2^-$ that is converted to AuCN no longer participates in the equilibrium between $\text{Au}(\text{CN})_2^-$ in solution and $\text{Au}(\text{CN})_2^-$ in the adsorbed phase. This is illustrated in Figure 2.19 where the equilibrium isotherm for adsorption of gold onto carbon B was compared with the isotherm determined for desorption under the same conditions. As 20% of the adsorbed gold is present as AuCN, the isotherm for desorption is approximately 20% higher than that for adsorption. As expected, there is no difference between the isotherms for adsorption and desorption of gold in contact with carbon A (Figure 2.20). From Figure 2.21 it follows that the same applies for carbon BTX.

2.4.4 X-ray photoelectron scans

X-ray photoelectron scans (XPS) of gold loaded samples of carbon A and B were carried out by the Division of Mineral Products, CSIRO, Curtin University, Western Australia. From measurements of the Au 4f and N 1s

signals it was possible to determine the ratio of CN to Au on the gold loaded carbon. The results of the tests are plotted in Figure 2.22. Carbon A showed an average CN:Au ratio of 2, which corresponds to $\text{Au}(\text{CN})_2^-$, whereas the ratio on carbon B was of the order of 1.3:1, indicating a mixture of $\text{Au}(\text{CN})_2^-$ and AuCN.

2.5 EFFECT OF TEMPERATURE AND pH ON THE NATURE OF ADSORBED SPECIES

As discussed previously, if an irreversibly adsorbed gold cyanide species is formed on carbon loaded under "normal" CIP conditions, most researchers (Tsuchida, 1984; Adams *et al.*, 1987b; Cook *et al.*, 1989; Baily, 1987) agree that that species will be AuCN. Much controversy exists, however, on the nature of the adsorbed species in the presence of acids, high temperatures or high alkalinity. An example of these extreme conditions can be found in the hot acid wash step recommended for the AARL elution process (Davidson, 1986a).

A precipitate of AgCN will form in acidified $\text{Ag}(\text{CN})_2^-$ solutions at room temperature even in the absence of activated carbon (McDougall *et al.*, 1987; Davidson *et al.*, 1979). $\text{Au}(\text{CN})_2^-$ is more stable in an acid medium, as it was found that no precipitation of gold occurred over a period of 24 hours at a pH as low as 1 (Davidson *et al.*, 1979). Degradation to AuCN took place only if the acidified gold solutions were heated to 60 °C (McDougall *et al.*, 1987). However, when hydrophobic polymeric adsorbents were present in these solutions, AuCN precipitation also occurred in the cold solutions (Adams *et al.*, 1987a). It was postulated that a hydrophobic surface catalyses the reaction :



Similar behaviour was observed when the equilibrium gold loading on various resins was tested (Adams *et al.*, 1987a) for hysteresis following heating to 100 °C. Even though the adsorption on most resins was fully reversible, hysteresis did occur in the case of a chelating resin. This was seen as an indication that AuCN was formed at the elevated temperature. As this resin was in the protonated form, the H^+ required in the above reaction was readily available. In the case of activated

carbon (Adams et al., 1987b), no hysteresis could be detected on reheating. In the presence of excess acid, however, significant degradation of $\text{Au}(\text{CN})_2^-$ occurred at elevated temperatures.

Davidson (1974) showed that when loaded carbon was exposed to an acid wash at room temperature, a pretreatment with KOH was necessary to ensure a gold recovery of more than 90%. This led him to believe that at the low pH prevailing during an acid wash, part of the gold is adsorbed as the more firmly held $\text{HAu}(\text{CN})_2$ and the rest (less than 11%) is reduced to the metallic state.

Adams and Fleming (1989) investigated the effect of boiling acid followed by treatment with hot sodium hydroxide in more detail. They proposed that boiling acid converts the aurocyanide on the loaded carbon to AuCN. Nevertheless, it was found that even after extended periods of acid treatment, a minimum of 50% of the adsorbed gold could be eluted with hot sodium hydroxide (0.1 M). It was suggested that under these conditions AuCN is reduced by the carbon as follows :



The fact that this reaction occurs only in alkaline solution and not after treatment with boiling acid, was explained by the possible formation of a more mobile intermediate species such as AuCNOH^- .

From the results of Experiments 29 and 33(a) in Table 2.5 it follows that approximately 15% of the $\text{Au}(\text{CN})_2^-$ adsorbed onto carbon A from a solution with a pH of 3.5 was decomposed to an irreversibly adsorbed species. Interestingly, the formation of the irreversible species was not increased by an increase in oxygen concentration (Experiment 33(b)). FTIR scans of carbons A and B loaded from acidified gold cyanide solutions are presented in Figures 2.23 and 2.24. While no AuCN could be found on carbon A loaded from alkaline solutions (Figure 2.17), the AuCN peak shows clearly on the scan in Figure 2.23 of carbon A after exposure to an acidified gold solution. The presence of the $\text{Au}(\text{CN})_2^-$ peak in both Figures 2.23 and 2.24 indicates that not all of the $\text{Au}(\text{CN})_2^-$ was decomposed to AuCN.

The effect of high temperature on the transformation of $\text{Au}(\text{CN})_2^-$ to an irreversible species was investigated in Experiment 38. A sample of carbon BTX was loaded from an alkaline gold solution and then oven dried at 150 °C for 18 hours. In subsequent elutions with distilled water, only 60% of the gold could be recovered. This means that the $\text{Au}(\text{CN})_2^-$ species is susceptible to degradation at higher temperatures even without the addition of acids or other chemicals. Espiell et al. (1987) reported that at temperatures of higher than 300 °C, metallic gold was formed on the carbon.

The results of Adams and Fleming (1989) presented above led to the possibility that the determination of AuCN by elution of $\text{Au}(\text{CN})_2^-$ with cold, distilled water at a pH of 12 could be inaccurate. This led to an SEM study of gold loaded carbon BTX exposed to HCl and KOH solutions at different temperatures.

Figure 2.25, an SEM photograph of carbon BTX loaded from a AuCl_4^- solution, was used as a basis for this study. The gold adsorbed from such a solution is reduced to the $\text{Au}^{(0)}$ state on the carbon and can be seen clearly as white spots on electron microscope photographs. Under a reflected light microscope the gold shows as bright, golden metallic particles. Thus, from Figure 2.26 it follows that exposure of carbon BTX to a cold 0.1 M KOH solution, after it was loaded with gold from a $\text{Au}(\text{CN})_2^-$ solution, did not result in reduction of $\text{Au}(\text{CN})_2^-$ to Au. After boiling the loaded carbon in the hydroxide solution, some bright spots were observed with the electron microscope (Figure 2.27(a)). Microanalysis of the particles (Figure 2.27(b)) revealed the M-line for Au and the K-lines for potassium and chloride. No bright spots could be seen under an optical microscope. As the AuCN determinations with distilled water were conducted at room temperature and a KOH concentration of 10 times lower than in these experiments, it can be safely assumed that no reduction of $\text{Au}(\text{CN})_2^-$ or AuCN to Au would have taken place.

The sample of gold loaded carbon in Figure 2.28 was boiled in distilled water without adjusting the pH. From this photograph and the result of Experiment 38 above, it follows that a portion of the adsorbed $\text{Au}(\text{CN})_2^-$ was decomposed to AuCN by exposure to temperatures between 100 °C and

150 °C, but that further reduction to Au will only take place under more extreme conditions. Figures 2.29(a) and (b) represent such a condition. In this case a sample of gold loaded carbon BTX was boiled in distilled water containing 3 vol % of a 33 mass % HCl solution. The large crystals that formed under these conditions (compare Figure 2.29(b) to Figure 2.27(a)) contained mainly Au as can be seen from the X-ray analysis thereof (Figure 2.29(c)). Under an optical microscope it appeared similar to the gold adsorbed from a AuCl_4^- solution.

The effect of $\text{Au}^{(0)}$ on the $\text{Au}(\text{CN})_2^-$ equilibrium was investigated in Experiment 39. A sample of carbon BTX was loaded with gold cyanide and then boiled in a HCl solution to decompose the adsorbed gold to $\text{Au}^{(0)}$ as above. This gold loaded sample of carbon was then contacted with an alkaline $\text{Au}(\text{CN})_2^-$ solution for three weeks and its adsorption capacity compared to that of a fresh sample of carbon BTX. The adsorption capacities of the two samples of carbon for $\text{Au}(\text{CN})_2^-$ were nearly identical. This means that the irreversibly adsorbed metallic gold did not take part in the $\text{Au}(\text{CN})_2^-$ equilibrium. However, in the presence of free cyanide, some of the Au would have been dissolved, and this would have resulted in a decreased adsorption of $\text{Au}(\text{CN})_2^-$.

2.6 SUMMARY OF RESULTS

Dissolved oxygen was found to play a vital role in the adsorption of anionic metal cyanides onto activated carbon. Although the gold loading capacities of the tested carbons were directly related to the dissolved oxygen concentration, the small oxygen consumptions during the adsorption of the metal cyanides indicate that oxygen does not take part in the adsorption reaction. Furthermore, if oxygen did take part in the adsorption reaction of metal cyanides, concentrations higher than 9 mg O_2/l would have led to increased adsorption capacities, which was not the case. It was illustrated that chemisorbed oxygen on the surface of the carbon plays a minor role in comparison to oxygen in solution. It is postulated that physically adsorbed oxygen, which is in equilibrium with the oxygen in solution, acts as a surfactant which renders the carbon surface more or less receptive to the adsorption of anionic species. It

is possible that an increase in the dissolved oxygen concentration not only increases the zeta potential of the carbon, but also screens off the carbon surface for adsorption of solutes. These two opposing effects will result in an increase in the adsorptivity up to a point where the block-out effect exceeds the effect of the higher zeta potential and therefore results in lower adsorption of anionic metal cyanides with a further increase in oxygen concentration.

In solutions where free cyanide was present, the consumption of oxygen was increased because of the oxidation of CN^- to CO_3^{2-} and NH_3 . Although the formation of AuCN can increase the consumption of oxygen, oxygen did not promote the decomposition of $\text{Au}(\text{CN})_2^-$ to AuCN . In closed systems where no free cyanide was present, the carbon itself was the main consumer of oxygen. The uptake of oxygen by activated carbon in such a closed system reduces the dissolved oxygen concentration and thereby lowers the adsorption capacity of the carbon for anionic metal cyanides.

The fraction of adsorbed $\text{Au}(\text{CN})_2^-$ that will be decomposed to AuCN was found to be a function of the pH and temperature of the solution, and the type of activated carbon used. Under "normal" CIP conditions, but with no free cyanide present, 20% of the gold adsorbed onto carbon B was present as AuCN , whereas no decomposition took place on carbons A and BTX. The formation of AuCN was enhanced by lowering the pH at room temperature. However, a combination of low pH and high temperature, as would be found in the hot acid wash step of an AARL elution, led to the reduction of both $\text{Au}^{(1)}$ species to metallic gold, $\text{Au}^{(0)}$.

The finding that no AuCN is formed on carbon BTX under normal CIP conditions will have a significant bearing on investigating the effect of a cyanide pretreatment on the elution of the adsorbed gold. If cyanide is found to enhance the elution of gold from carbon BTX, the increased desorption cannot be ascribed to the transformation of AuCN to $\text{Au}(\text{CN})_2^-$.

Table 2.1

AA settings for determination of various elements.

Element	Mode	Wavelength [nm]	Slit Width [nm]	C _{max} [ppm]
Au	Absorption	242.8	1.0	30
Ag	Absorption	328.1	0.5	20
K	Emission	776.5	0.2	2000

Table 2.2

Freundlich isotherm constants for adsorption onto carbon A.

Oxygen level [mg/l]	Gold		Silver	
	A	n	A	n
0.0	7.302	0.339	2.192	0.530
4.4	13.478	0.264	8.920	0.409
9.0(atm.)	18.970	0.219	13.620	0.398
14.5	18.470	0.226	7.603	0.482

Table 2.3

Freundlich isotherm constants for adsorption onto carbon B.

Oxygen level [mg/l]	Gold		Silver	
	A	n	A	n
0.0	22.020	0.168	9.206	0.194
4.2	35.370	0.159	18.134	0.286
9.0(atm.)	38.646	0.131	25.374	0.223

Table 2.4

The consumption of oxygen by activated carbon in the presence and absence of metal cyanides.

Experiment 27	(b)	(c)	(d)	(e)	(f)
Carbon	A	A	A	A	A
Carbon pretreatment*	D,S	D,S	D	D	D
Drying temp. [°C]	110	110	110	110	110
Open/Closed bottle	C	O	C	C	C
pH	8.5	8.5	11.2	9.1	3.2
Metal cyanide (M)	Au	Au			
$C_i(M)$ [g/m ³]	22.8	19.7			
$C_f(M)/C_i(M)$	0.478	0.487			
$[O_2]_{diff.}$ [mg/l]	0.2		1.4	1.2	1.4

Experiment 27	(g)	(h)	(i)	(j)	(k)	(l)
Carbon	A	A	A	A	A	A
Carbon pretreatment*	D,S	D,S		D	D	D
Drying temp. [°C]	110	110		110	200	300
Open/Closed bottle	C	O	C	C	C	C
pH	8.5	8.5				
Metal cyanide (M)	Ag	Ag				
$C_i(M)$ [g/m ³]	23.2	23.2				
$C_f(M)/C_i(M)$	0.634	0.440				
$[O_2]_{diff.}$ [mg/l]	0.5		-0.2	1.3	1.8	0.3

Experiment 27	(m)	(n)	(o)	(p)	(q)	(r)
Carbon	A	BTX	BTX	BTX	BTX	BTX
Carbon pretreatment*		D				
Drying temp. [°C]		110				
Open/Closed bottle	C	C	C	C	C	C
pH				8.8		3.9
Metal cyanide (M)	CN			Au	CN	Au
$C_i(M)$ [g/m ³]	409			70.5	409	70.5
$C_f(M)/C_i(M)$	0.941			0.400	0.954	0.148
$[O_2]_{diff.}$ [mg/l]	0.6	0.2	-0.5	0.5	3.2	0.7

*Carbon pretreatment :

D = Oven dried at specified temperature for 24 hrs

S = Soaked in aerated, distilled water for 24 hrs

Table 2.5

Determination of adsorbed species by elution with distilled water.

Exp. no.	29	30	31a	31b	32	33a	33b
ADSORPTION							
Carbon	A	A	B	B	BTX	A	A
Metal (M)	Au	Ag	Au	Au	Au	Au	Au
mg O ₂ /l	9.0	9.0	9.0	0.0	9.0	9.0	40
pH	8.5	8.5	8.5	8.5	8.5	3.5	3.5
t [days]	21	21	1	1	3	2	2
Q _M [mg/g]	36.6	33.6	19.2	13.6	26.2	22.6	22.6
ELUTION							
% Eluted	100	38	79	75	100	84	89
MCN/M(CN) ₂ ⁻	0.0	1.63	0.27	0.33	0.00	0.19	0.12

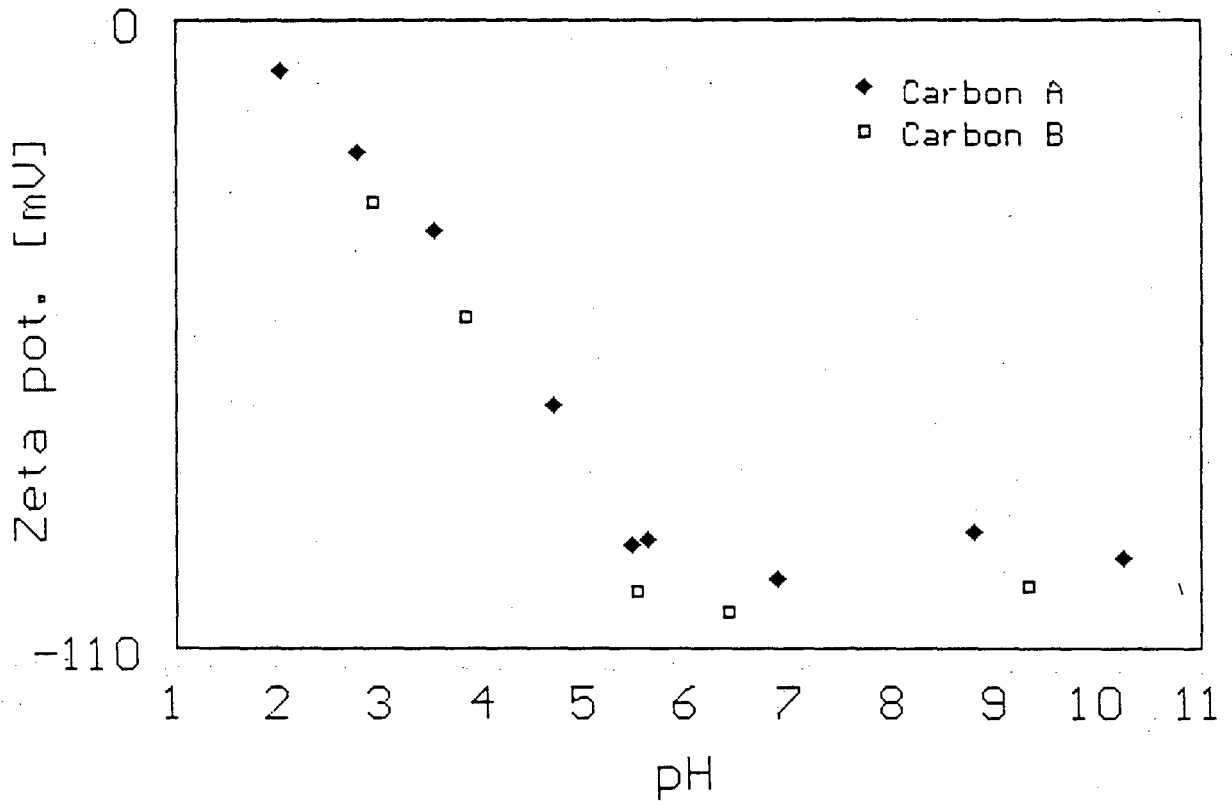


Figure 2.1 Zeta potential of carbons A and B as a function of solution pH. (Exp.1)

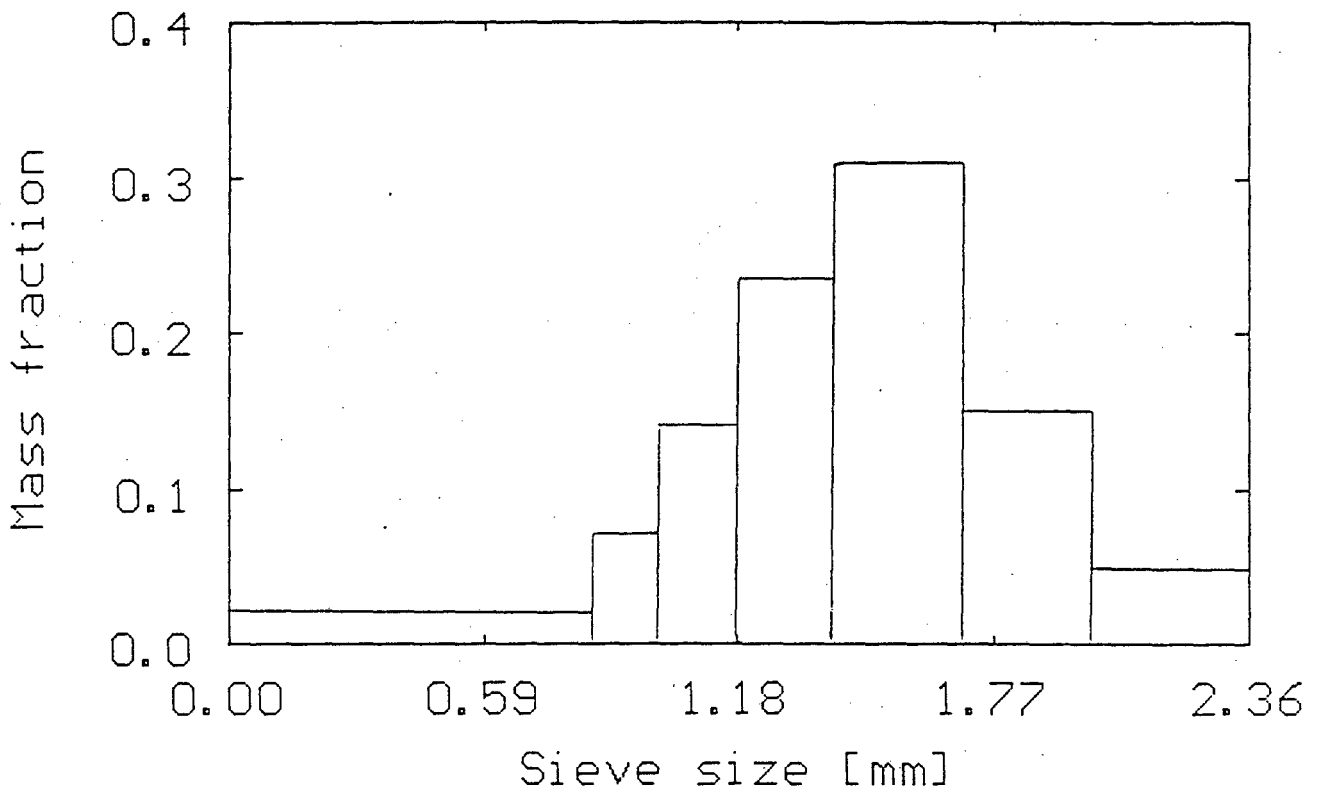


Figure 2.2 Particle size distribution of carbon BTX. (Exp.2)

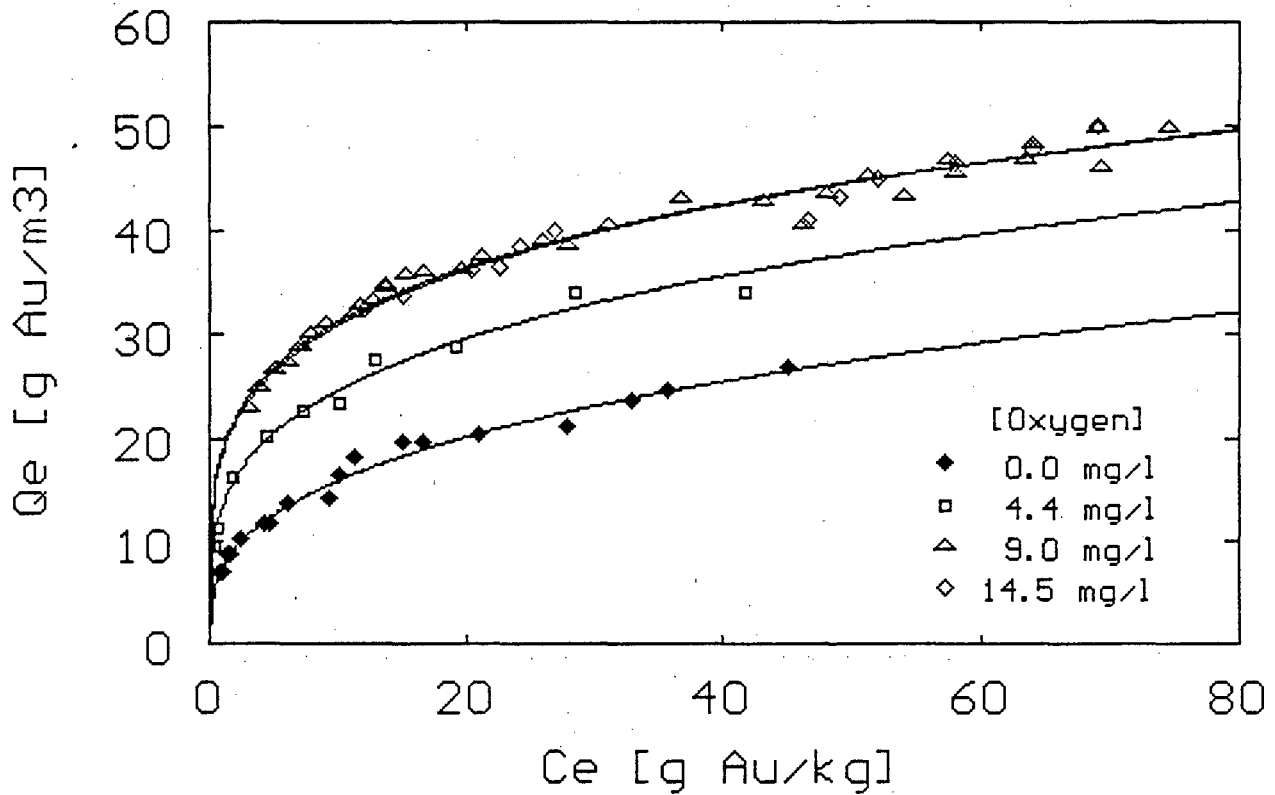


Figure 2.3 Equilibrium adsorption of $\text{Au}(\text{CN})_2^-$ on carbon A at different constant oxygen concentrations. (Exp. 3,4,5 and 6)

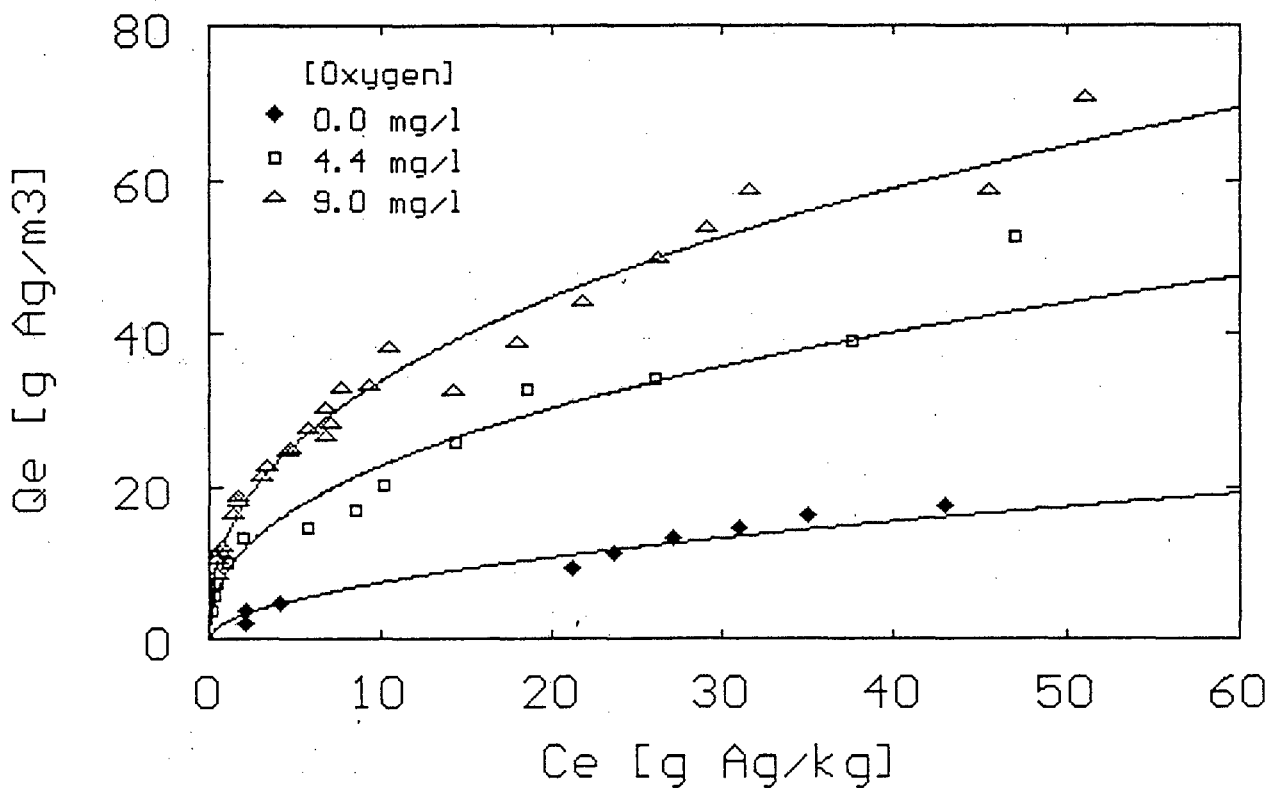


Figure 2.4 Equilibrium adsorption of $\text{Ag}(\text{CN})_2^-$ on carbon A at different constant oxygen concentrations. (Exp. 7,8 and 9)

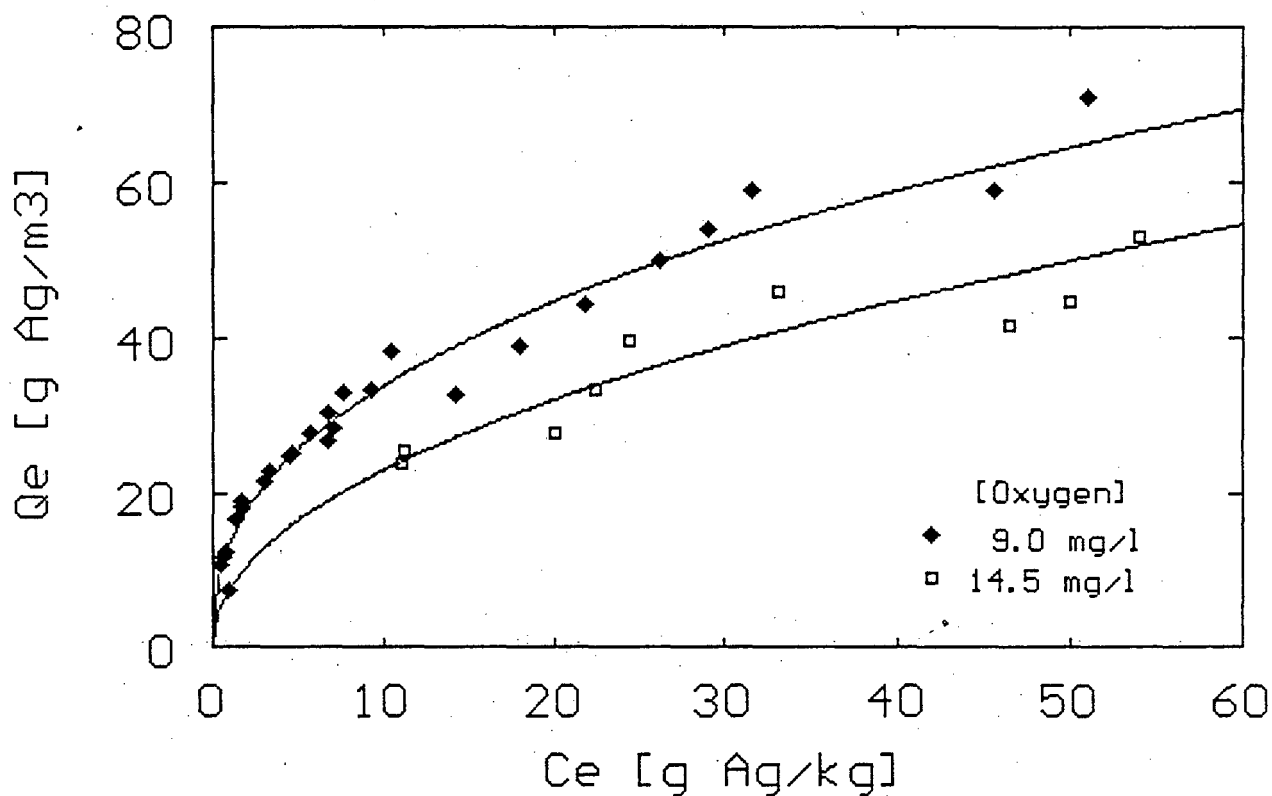


Figure 2.5 The detrimental effect of oxygen concentrations higher than 9 mg/l on the equilibrium adsorption of $\text{Ag}(\text{CN})_2^-$ on carbon A. (Exp. 7 and 10)

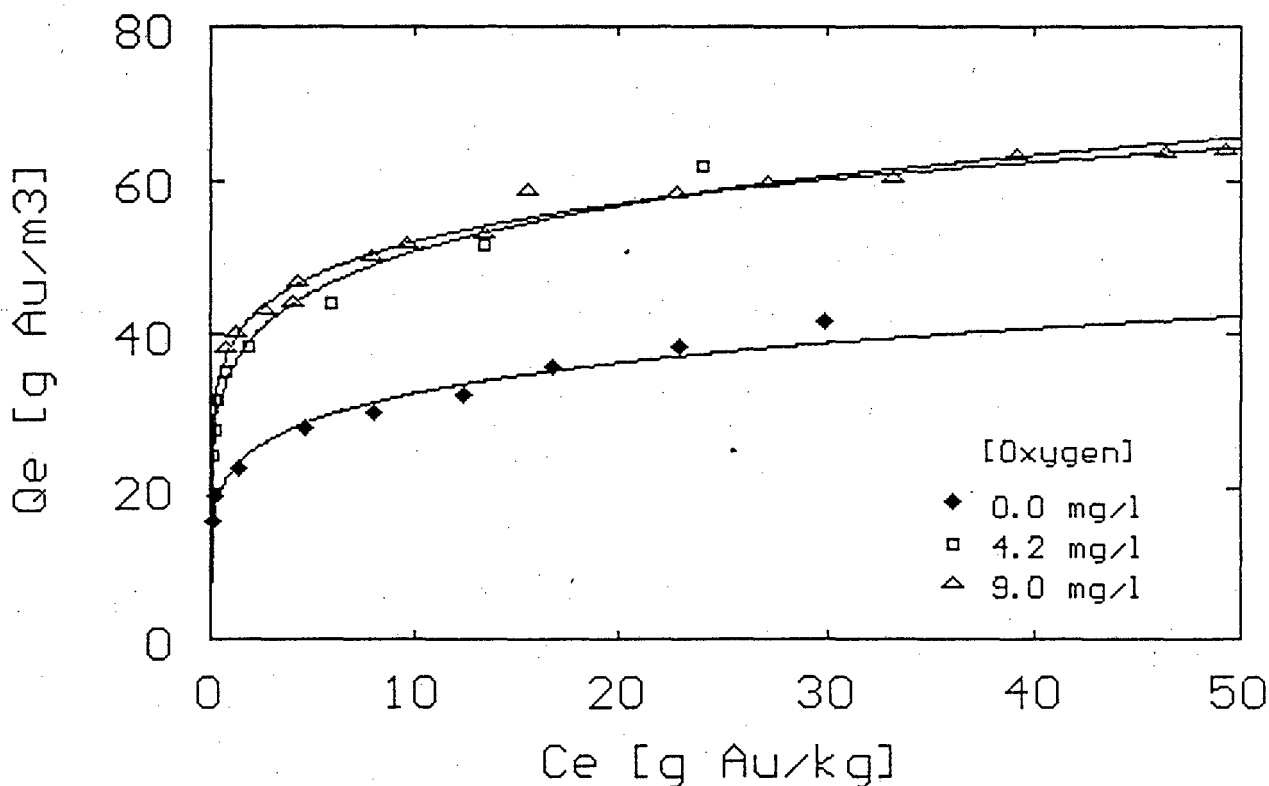


Figure 2.6 Equilibrium adsorption of $\text{Au}(\text{CN})_2^-$ on carbon B at different constant oxygen concentrations. (Exp. 11, 12 and 13)

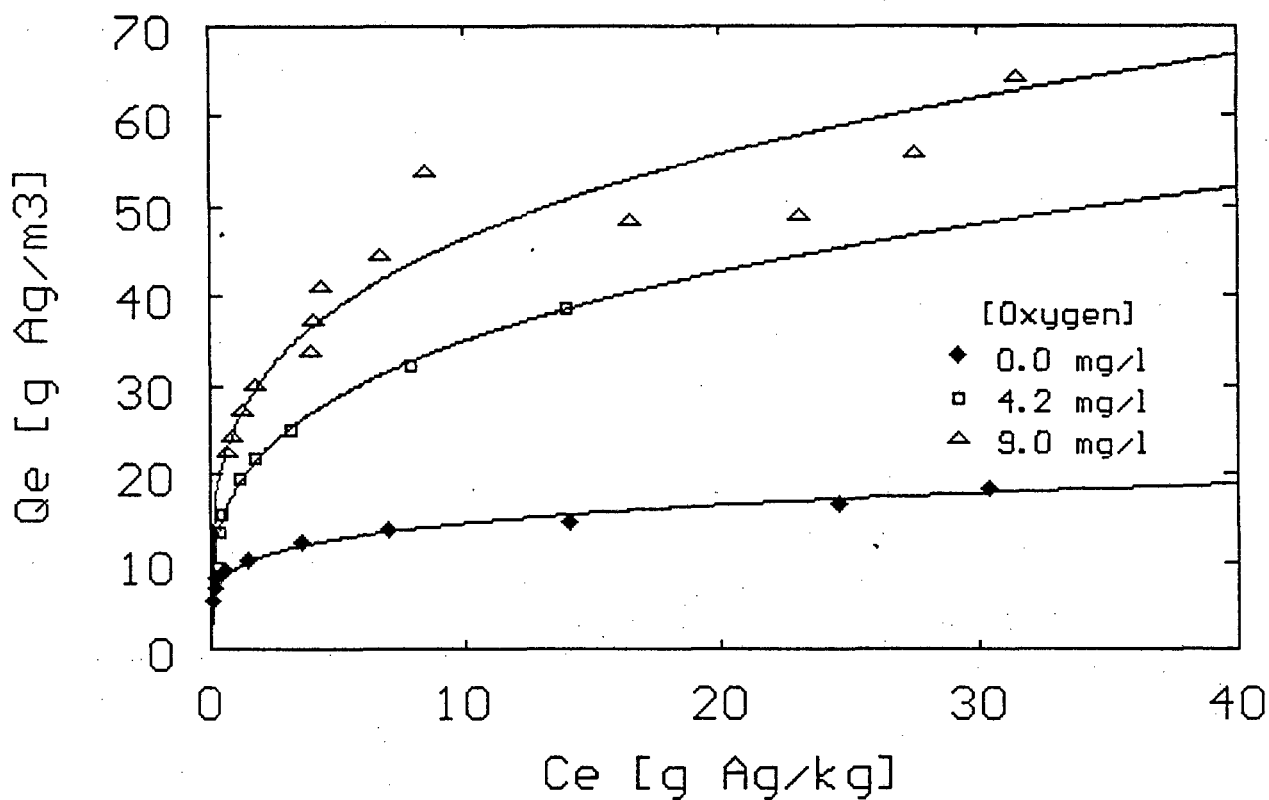


Figure 2.7 Equilibrium adsorption of $\text{Ag}(\text{CN})_2^-$ on carbon B at different constant oxygen concentrations. (Exp. 14, 15 and 16)

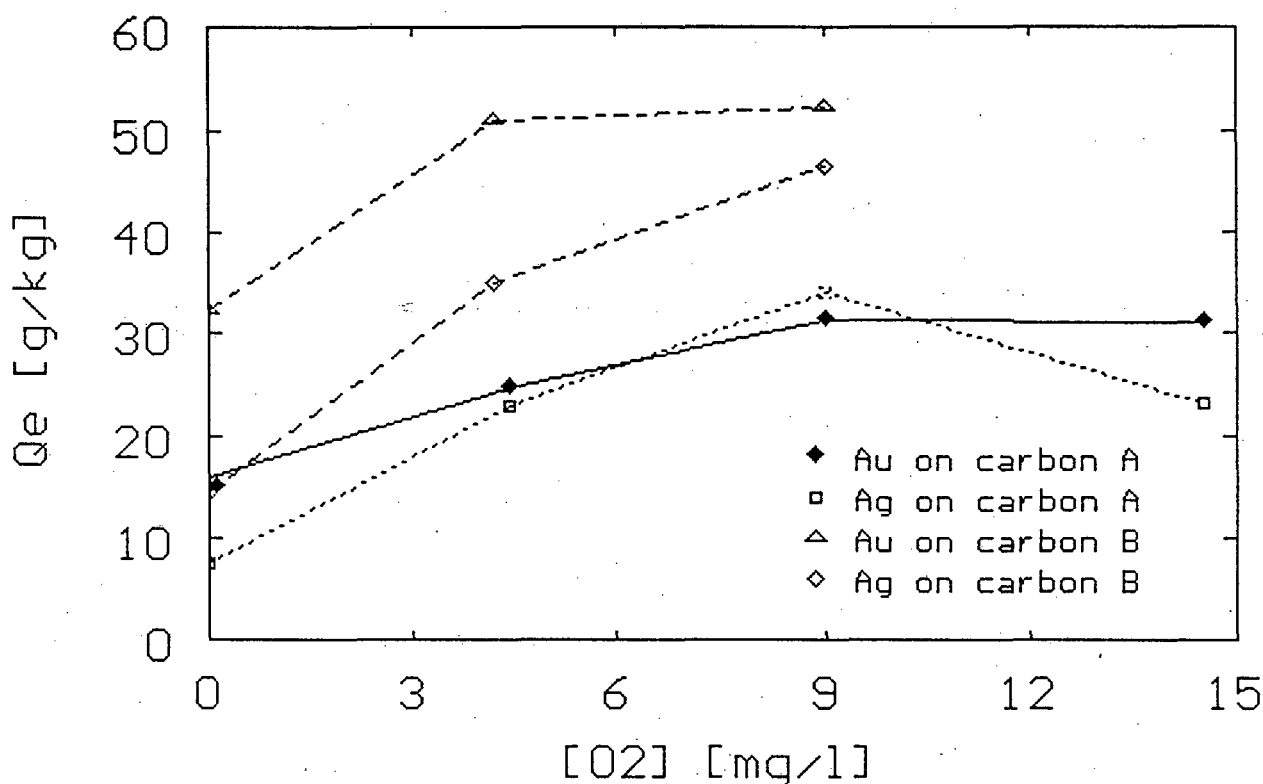


Figure 2.8 The effect of the dissolved oxygen level on the equilibrium adsorption of $\text{Au}(\text{CN})_2^-$ and $\text{Ag}(\text{CN})_2^-$ on carbons A and B at a constant liquid phase metal concentration of $C_e = 10 \text{ g.m}^{-3}$.

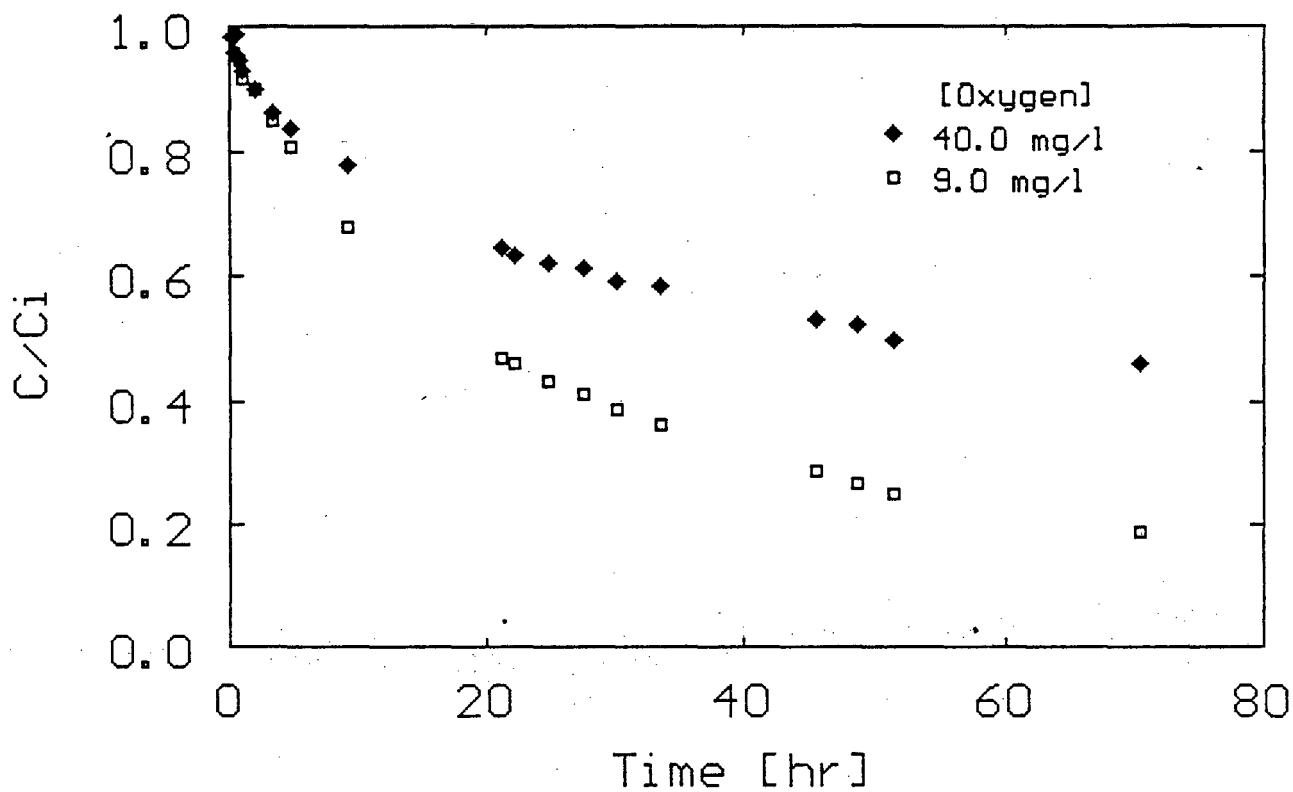


Figure 2.9 The detrimental effect of purging with pure oxygen on the adsorption of $Au(CN)_2^-$ onto carbon A. (Exp.17)

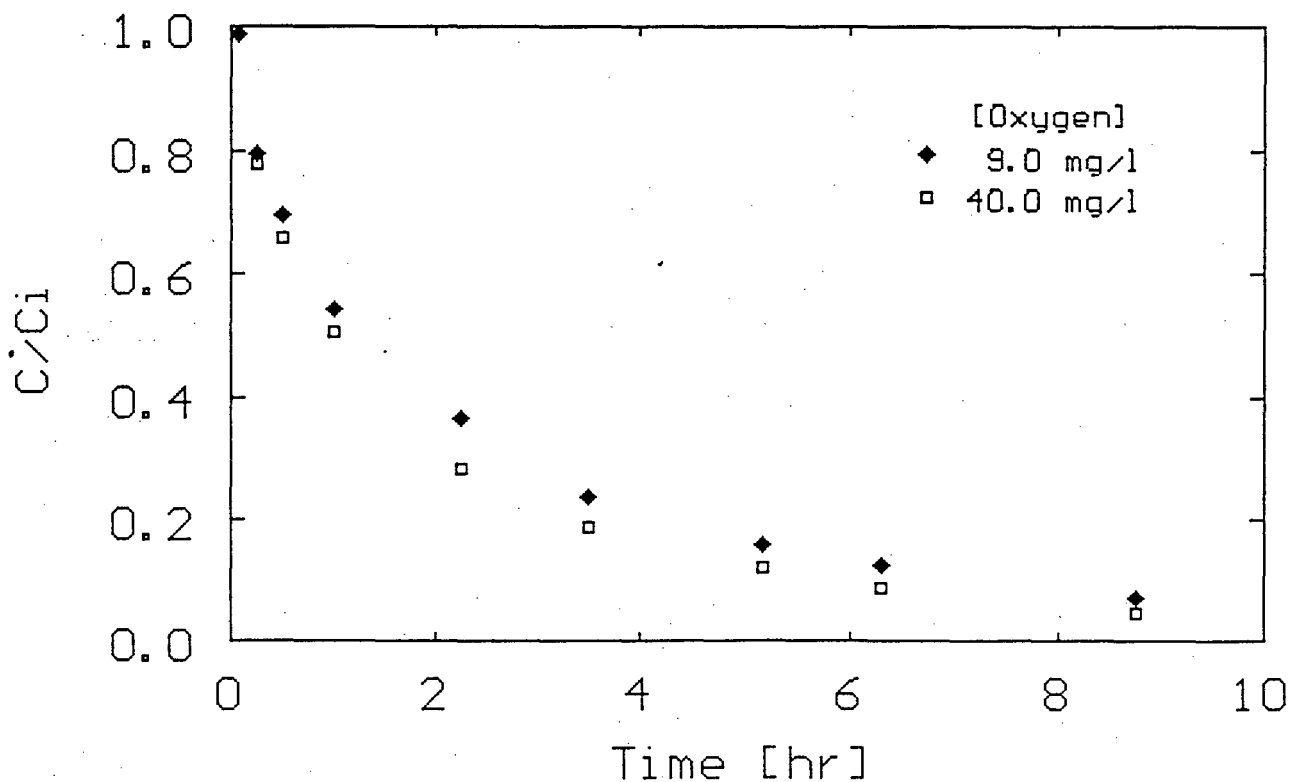


Figure 2.10 The effect of pure oxygen on the adsorption of $Au(CN)_2^-$ onto carbon A from a solution with a pH = 3.5. (Exp.18)

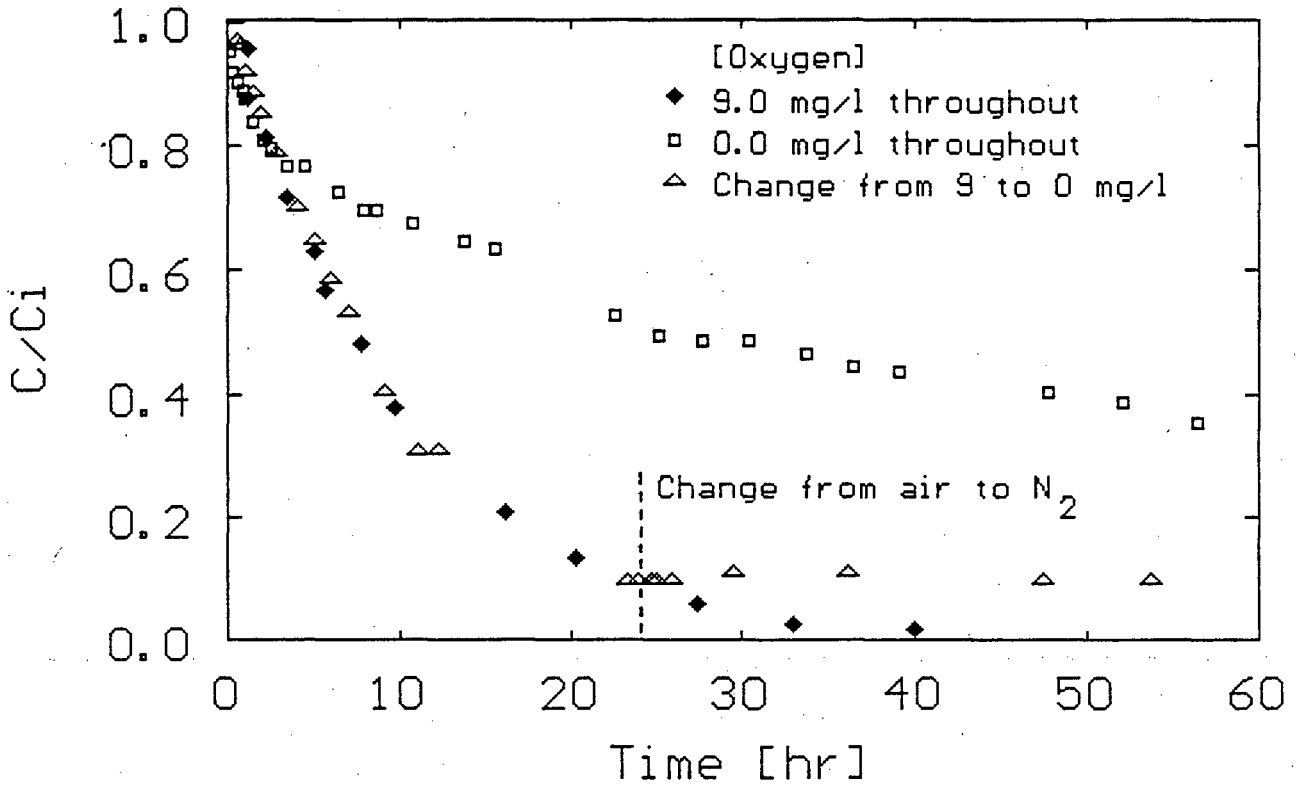


Figure 2.11 Lowering of the oxygen concentration during the adsorption of $Au(CN)_2^-$ from an aerated solution. (Exp.22)

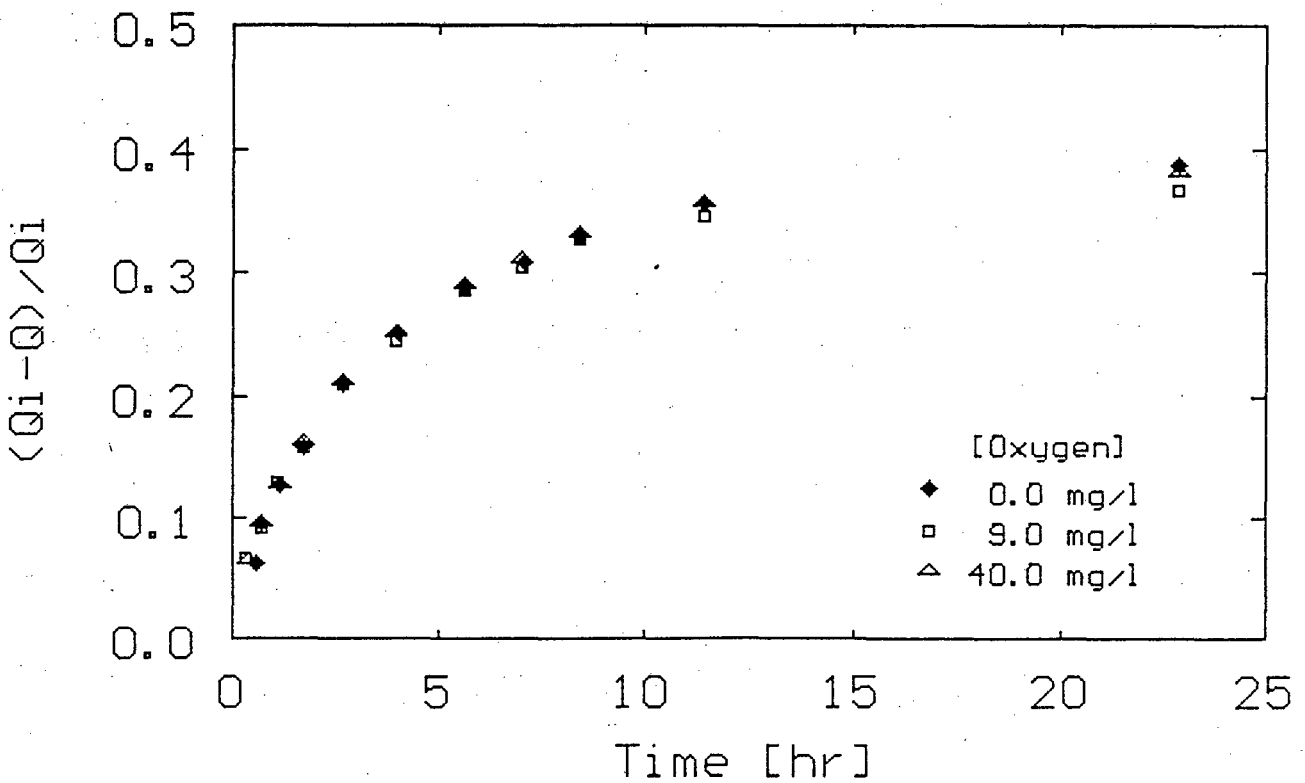


Figure 2.12 Desorption of $Au(CN)_2^-$ at different constant oxygen concentrations after adsorption from aerated solutions. (Exp.23)

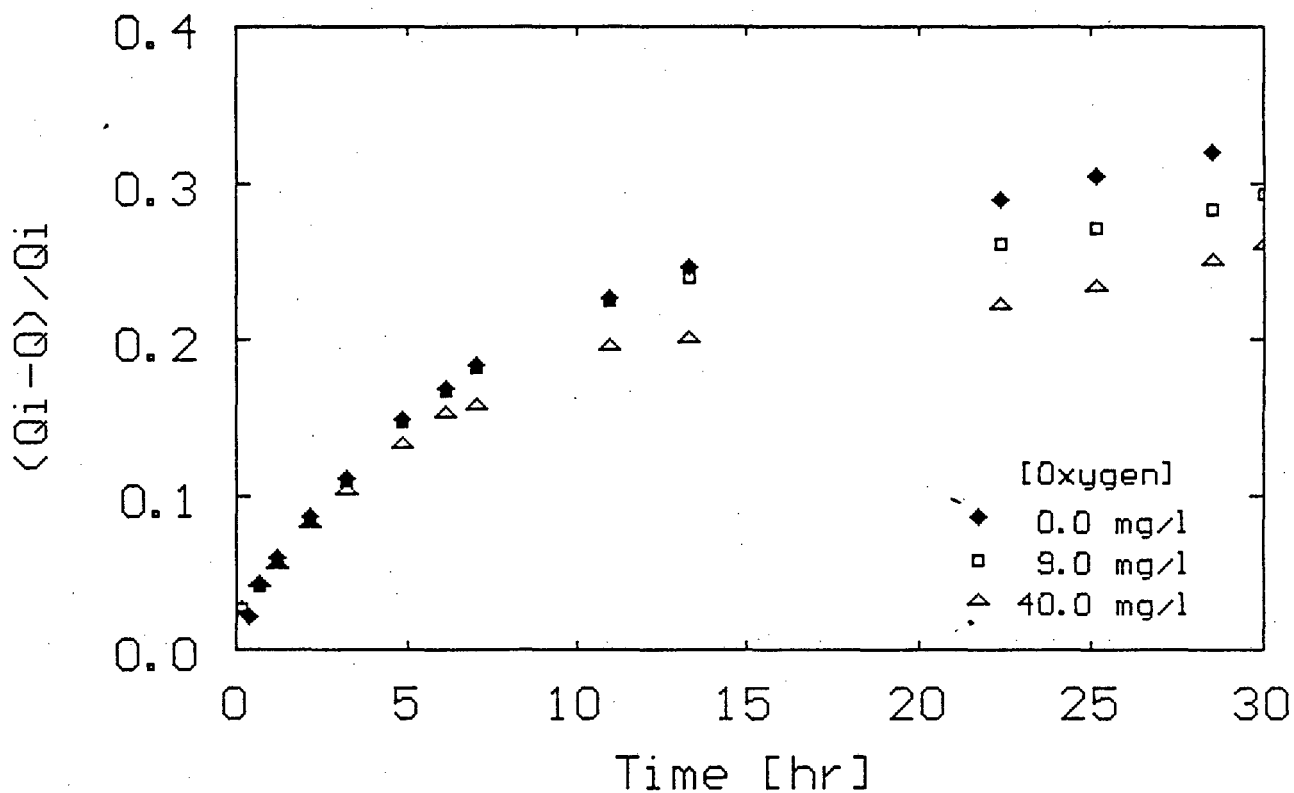


Figure 2.13 Desorption of $\text{Au}(\text{CN})_2^-$ at different constant oxygen concentrations after adsorption from deaerated solutions. (Exp.24)

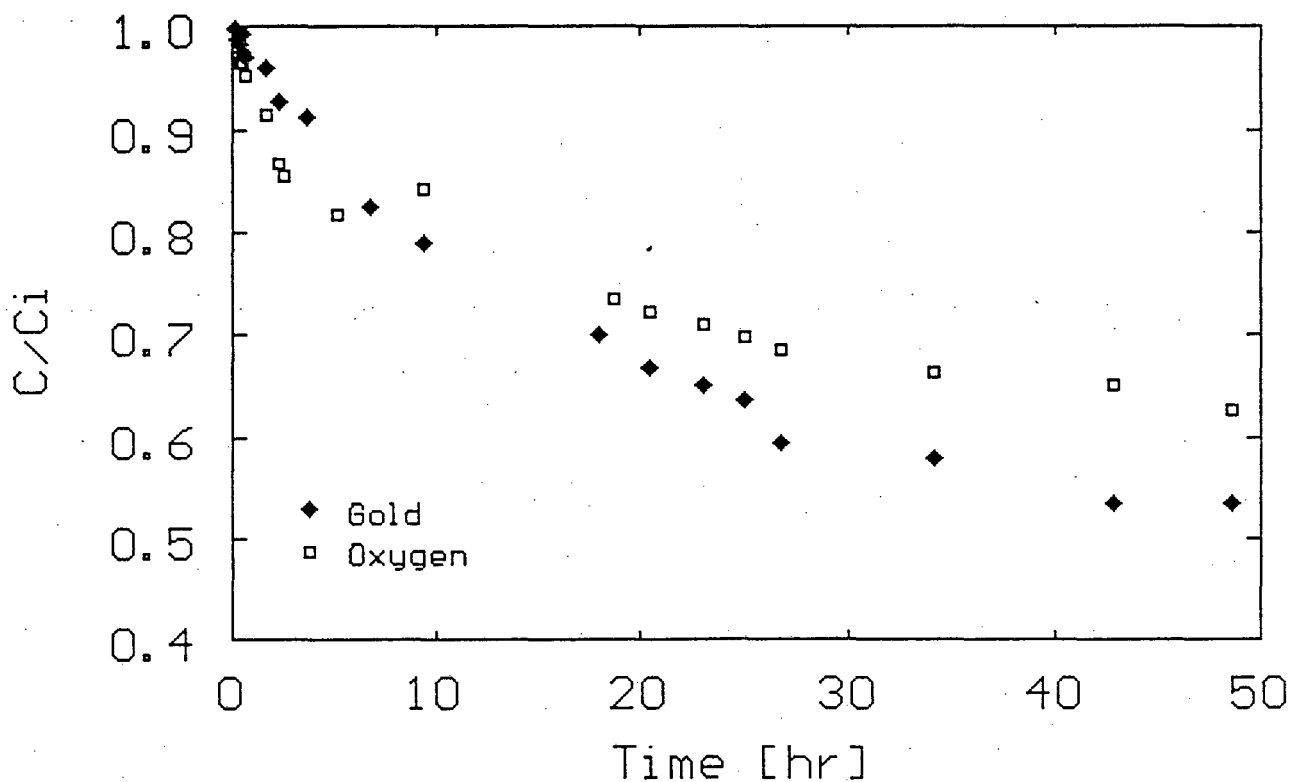


Figure 2.14(a) Measurement of the consumption of oxygen during the adsorption of $\text{Au}(\text{CN})_2^-$ onto carbon A in a closed vessel. (Exp.26)

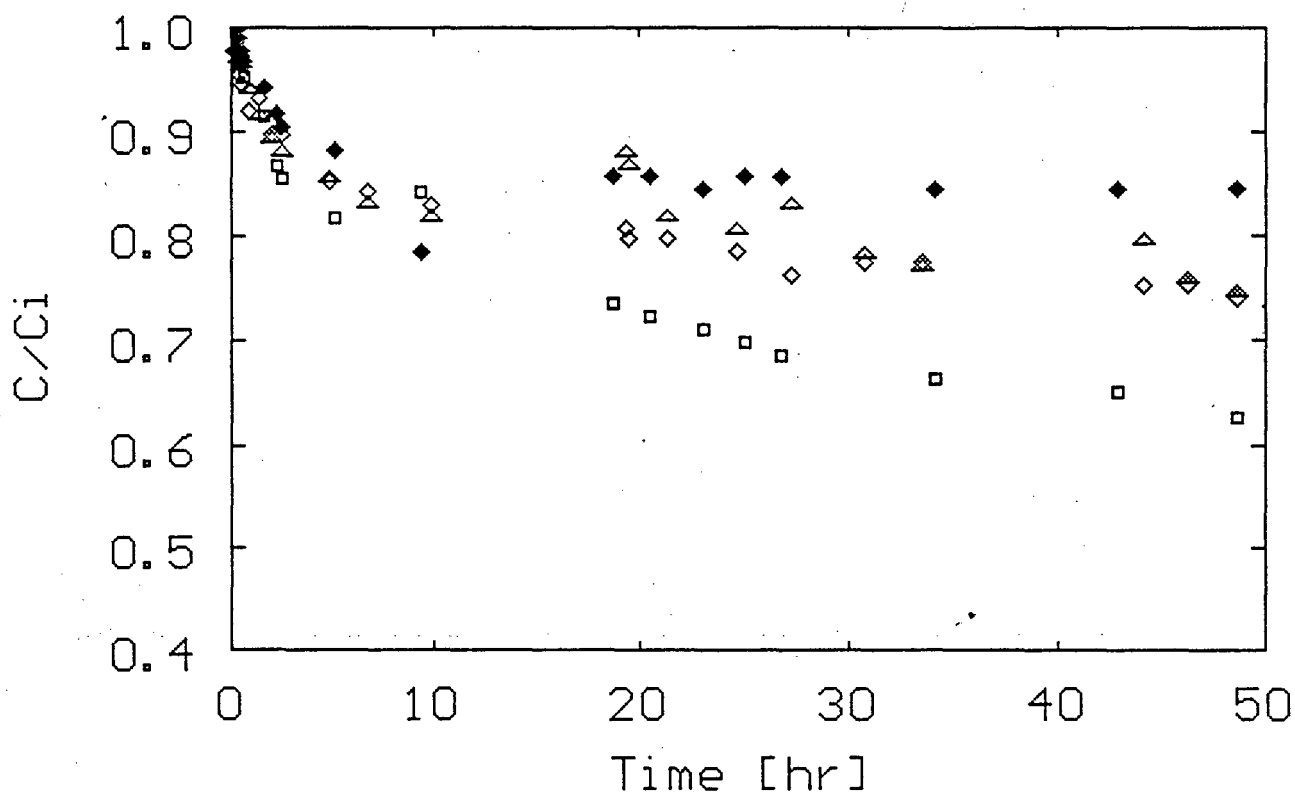


Figure 2.14(b) The reproducibility of the continuous monitoring of the dissolved O_2 level during the adsorption of $Au(CN)_2^-$ in a closed vessel. (Exp.26)

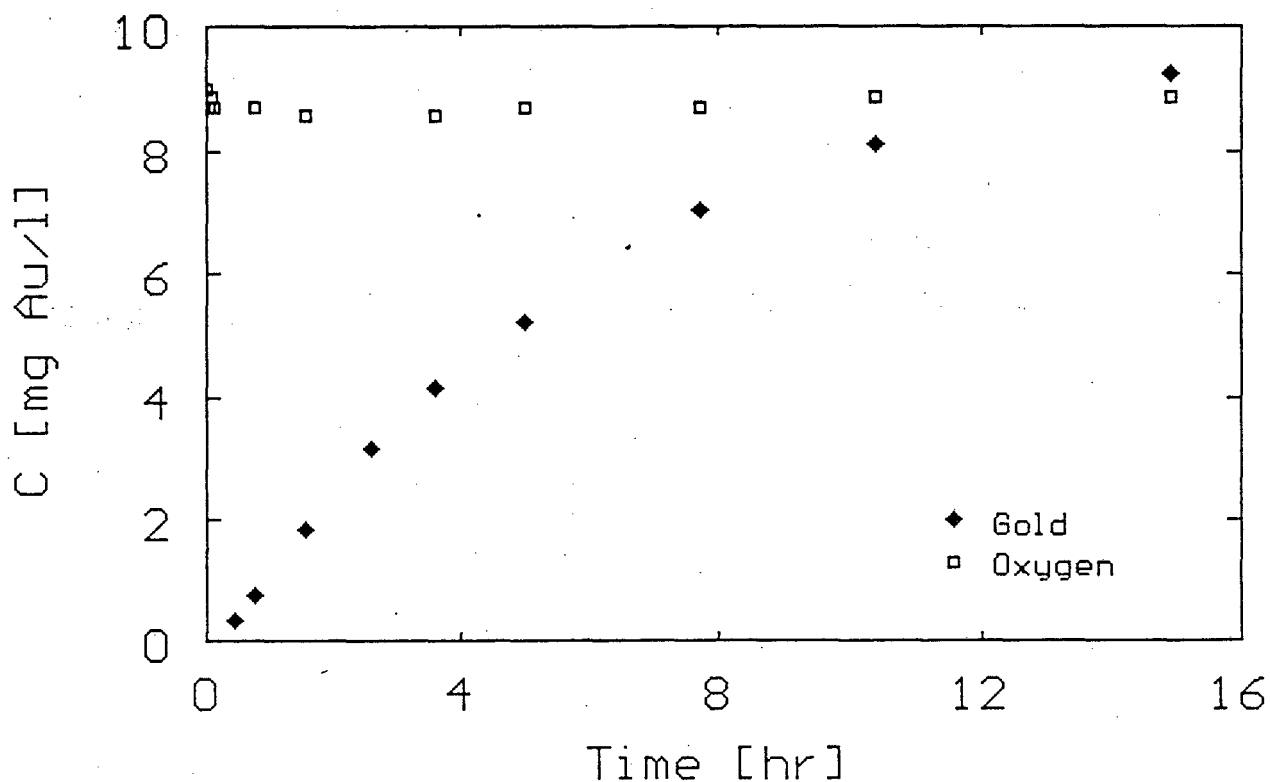


Figure 2.15 Measurement of the dissolved oxygen concentration during the adsorption of $Au(CN)_2^-$ in a packed bed of carbon A. (Exp. 28)

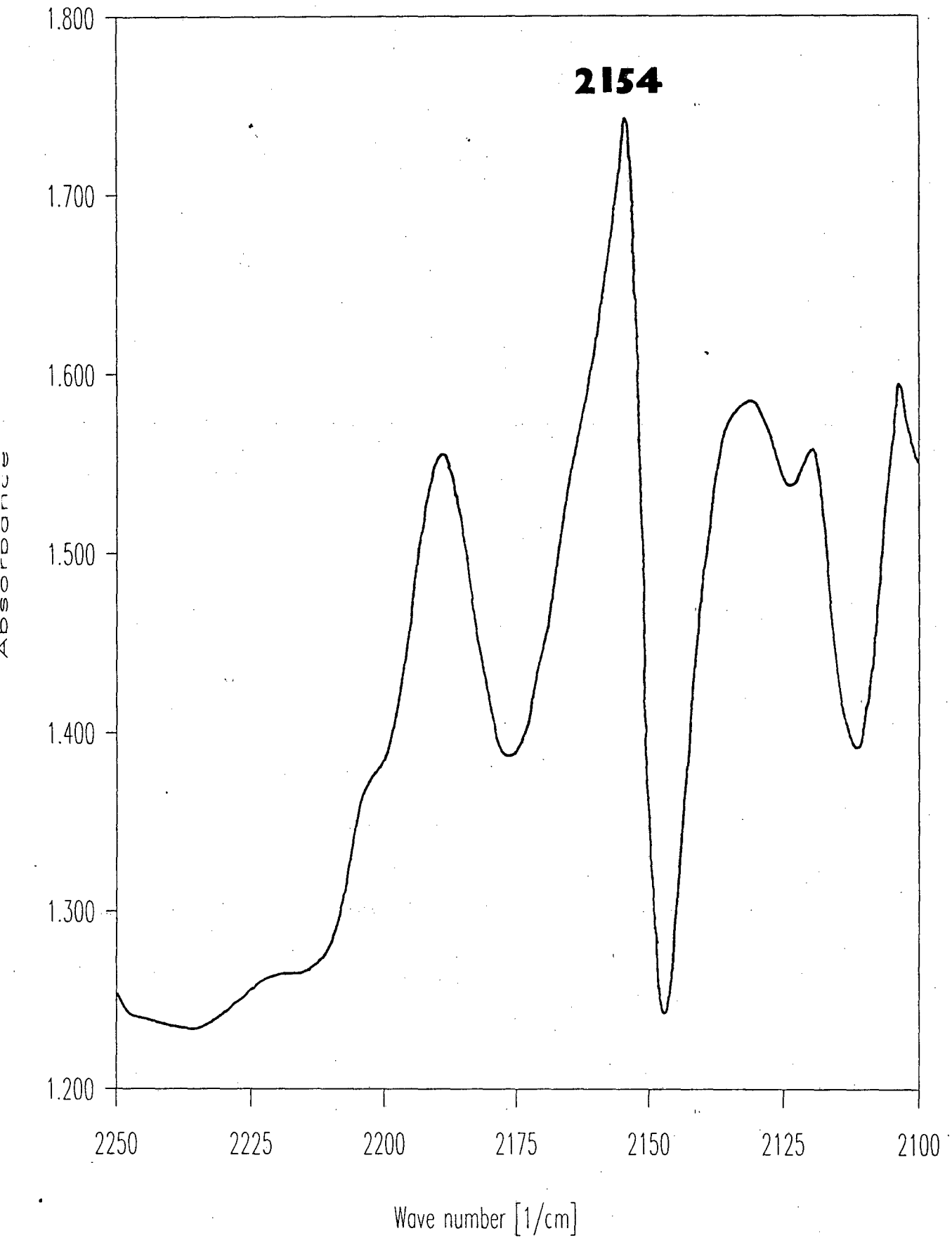


Figure 2.16 FTIR scan of $\text{KAu}(\text{CN})_2$ powder.

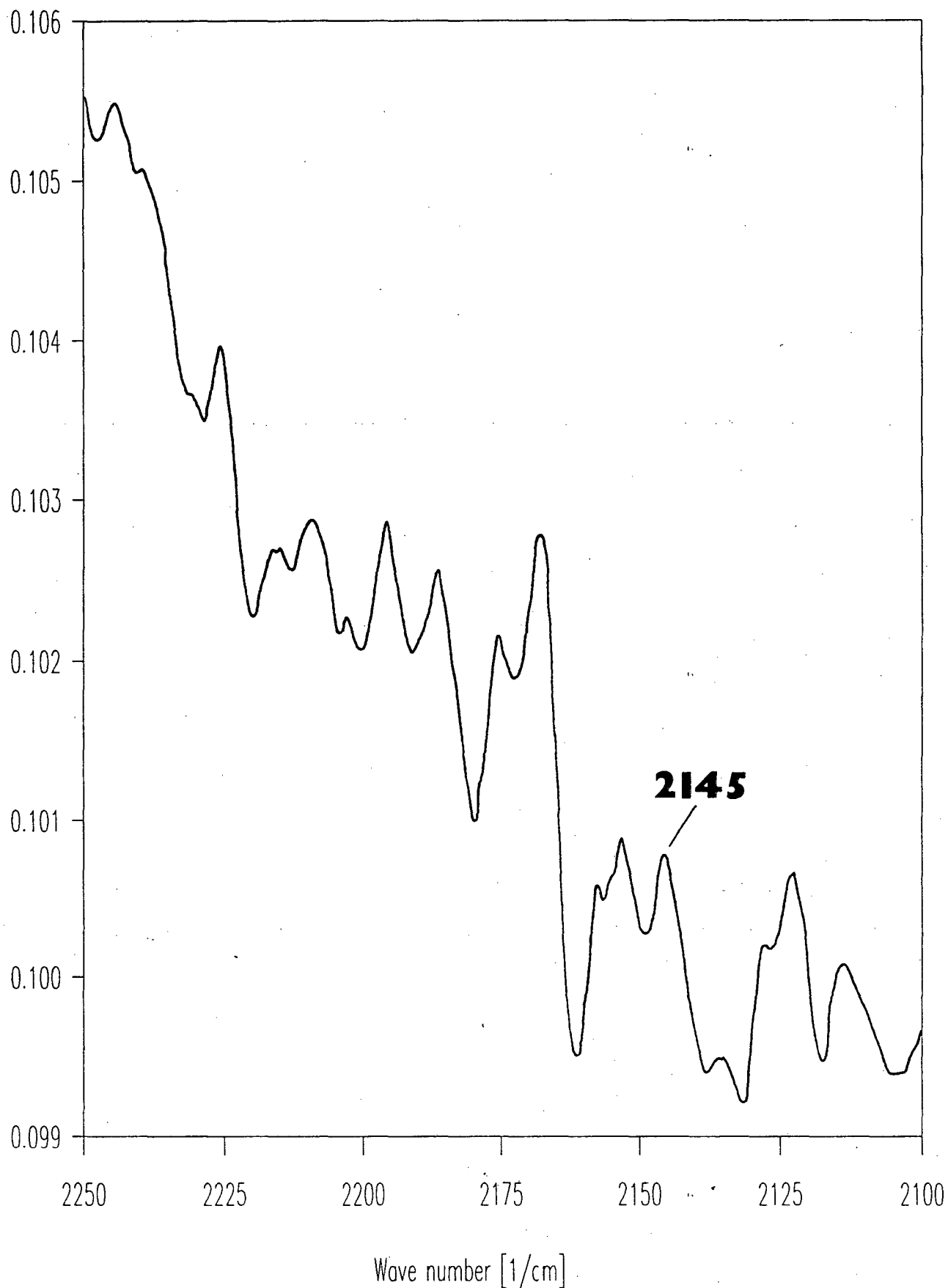


Figure 2.17 FTIR scan of carbon A loaded with gold cyanide from an aerated alkaline solution.

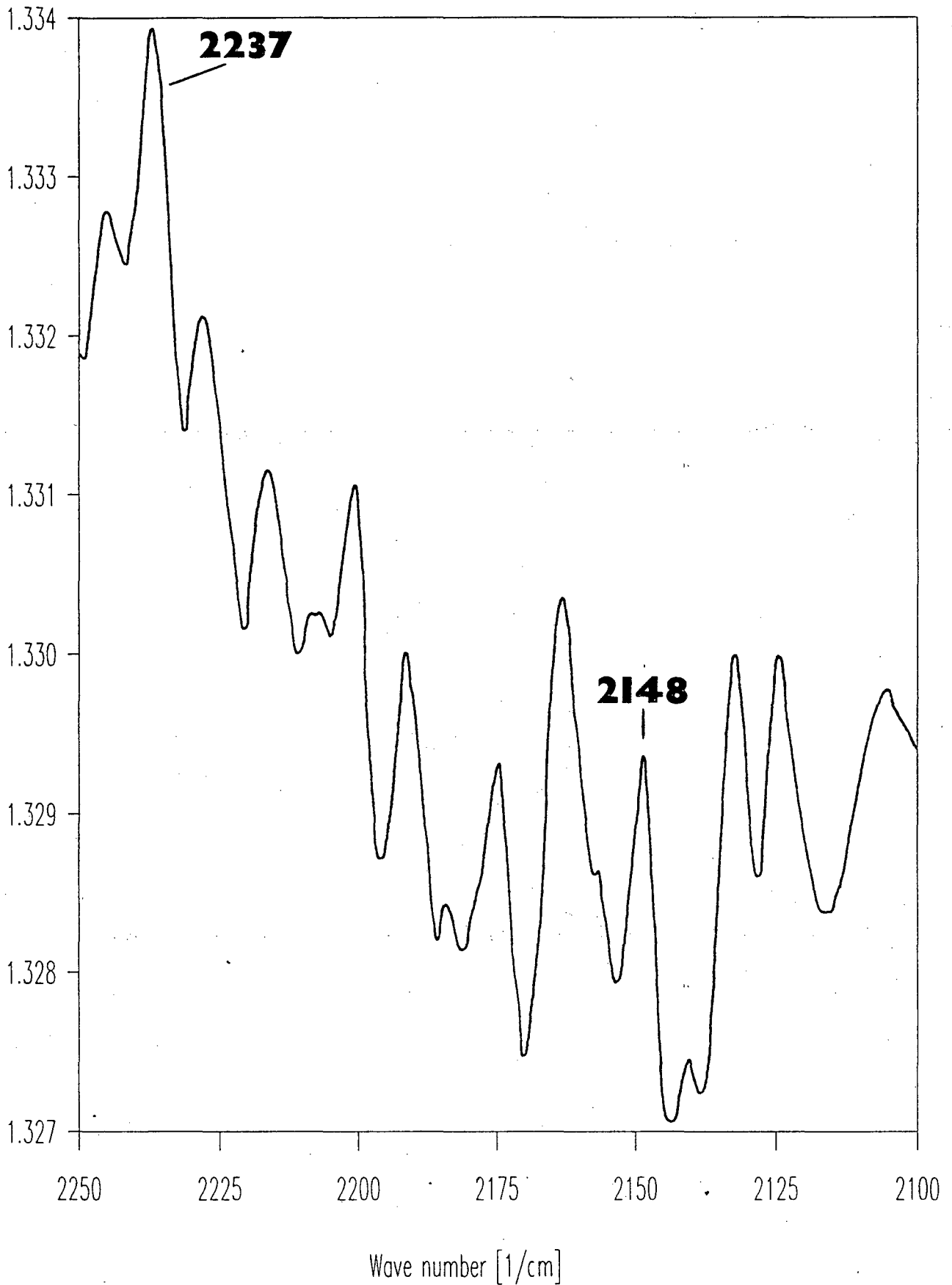


Figure 2.18 FTIR scan of carbon B loaded with gold cyanide from an aerated alkaline solution.

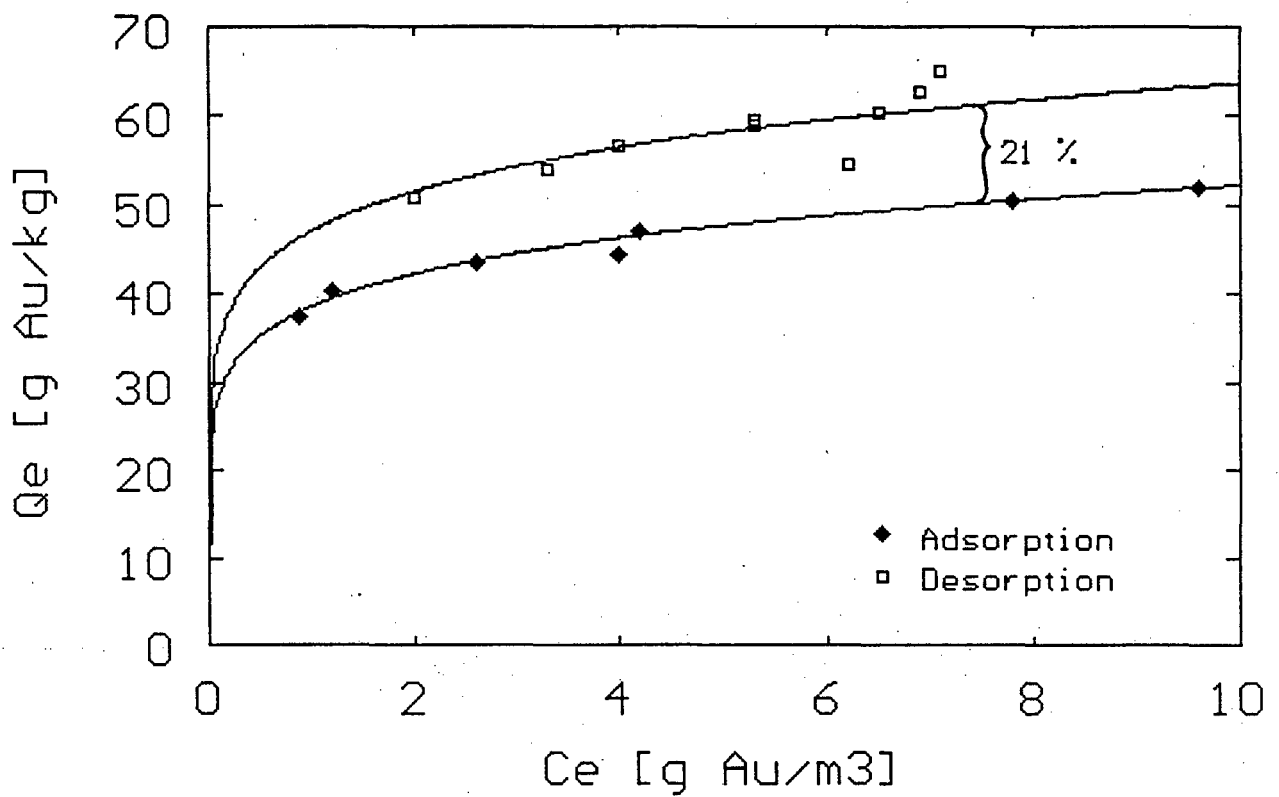


Figure 2.19 Equilibrium isotherms for gold cyanide on carbon B as determined by adsorption and desorption. (Exp. 11 and 34)

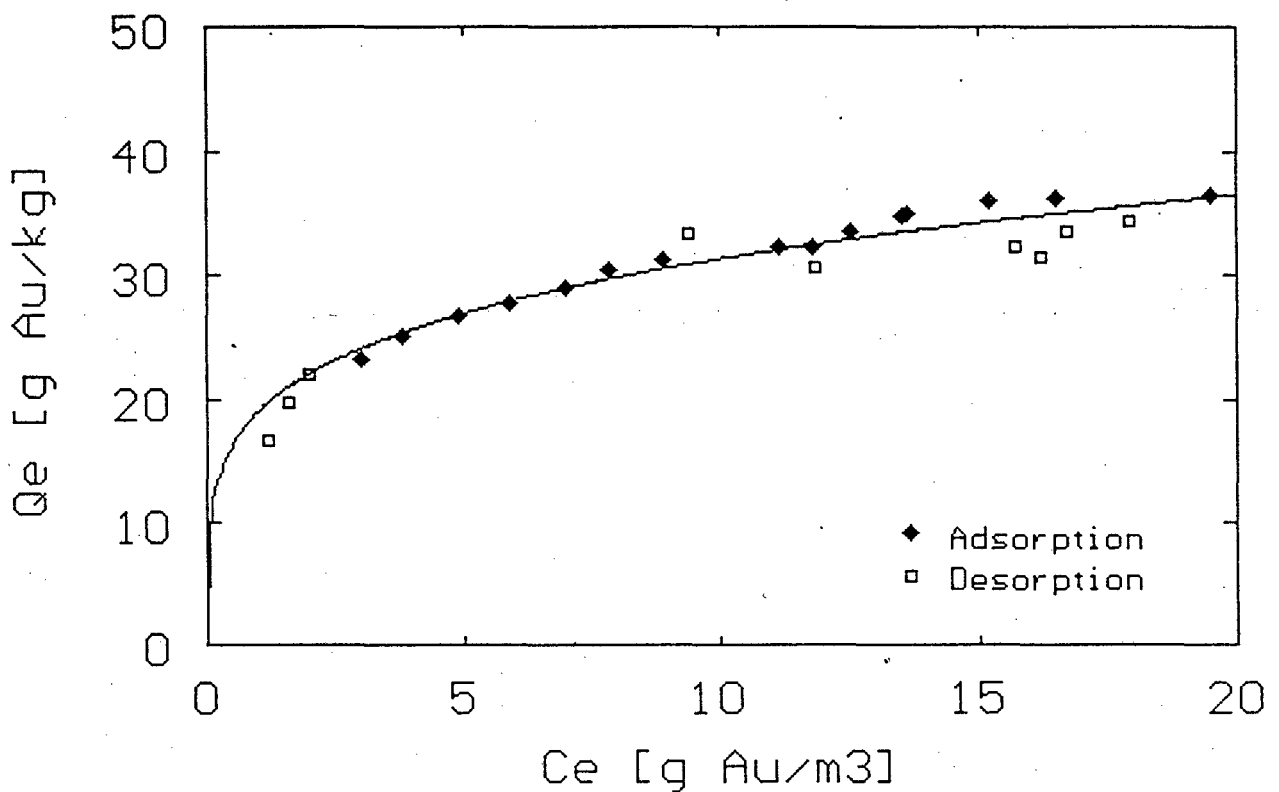


Figure 2.20 Equilibrium isotherms for gold cyanide on carbon A as determined by adsorption and desorption. (Exp. 3 and 35)

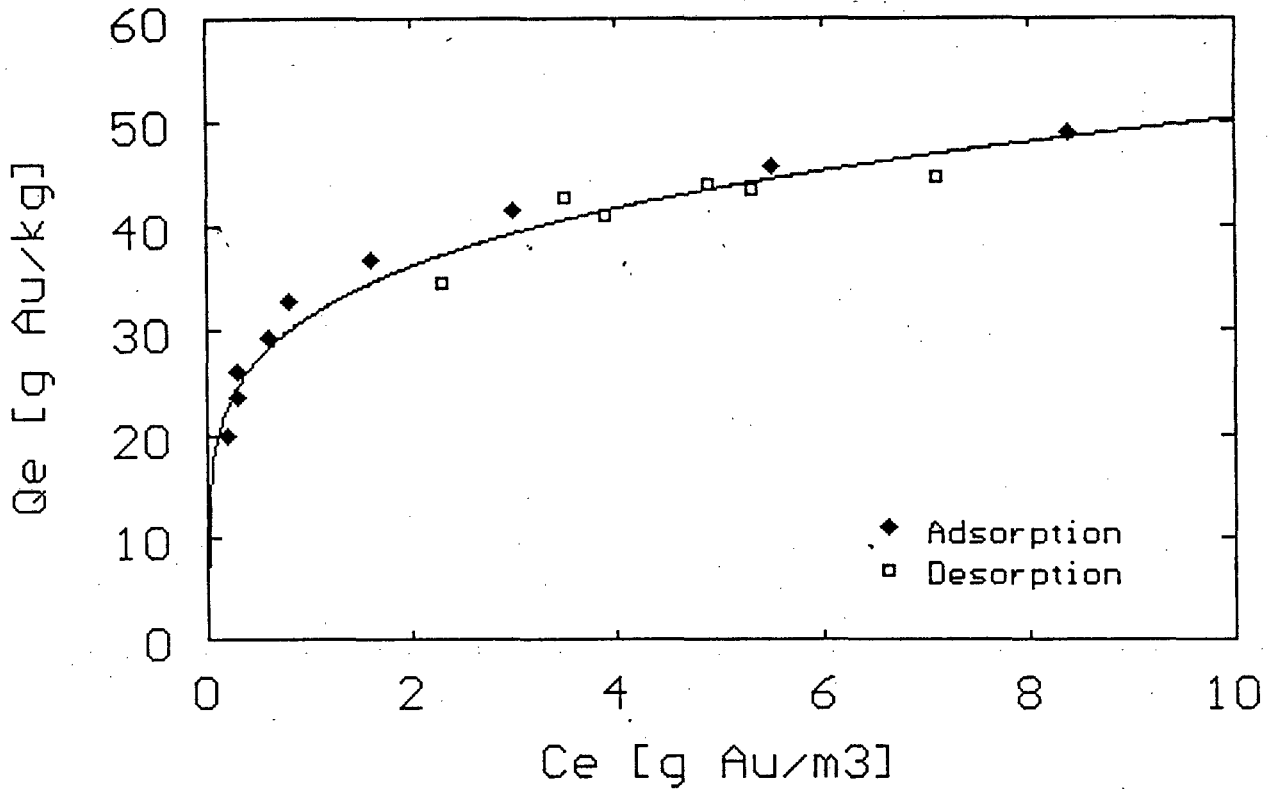


Figure 2.21 Equilibrium isotherms for gold cyanide on carbon BTX as determined by adsorption and desorption. (Exp. 36 and 37)

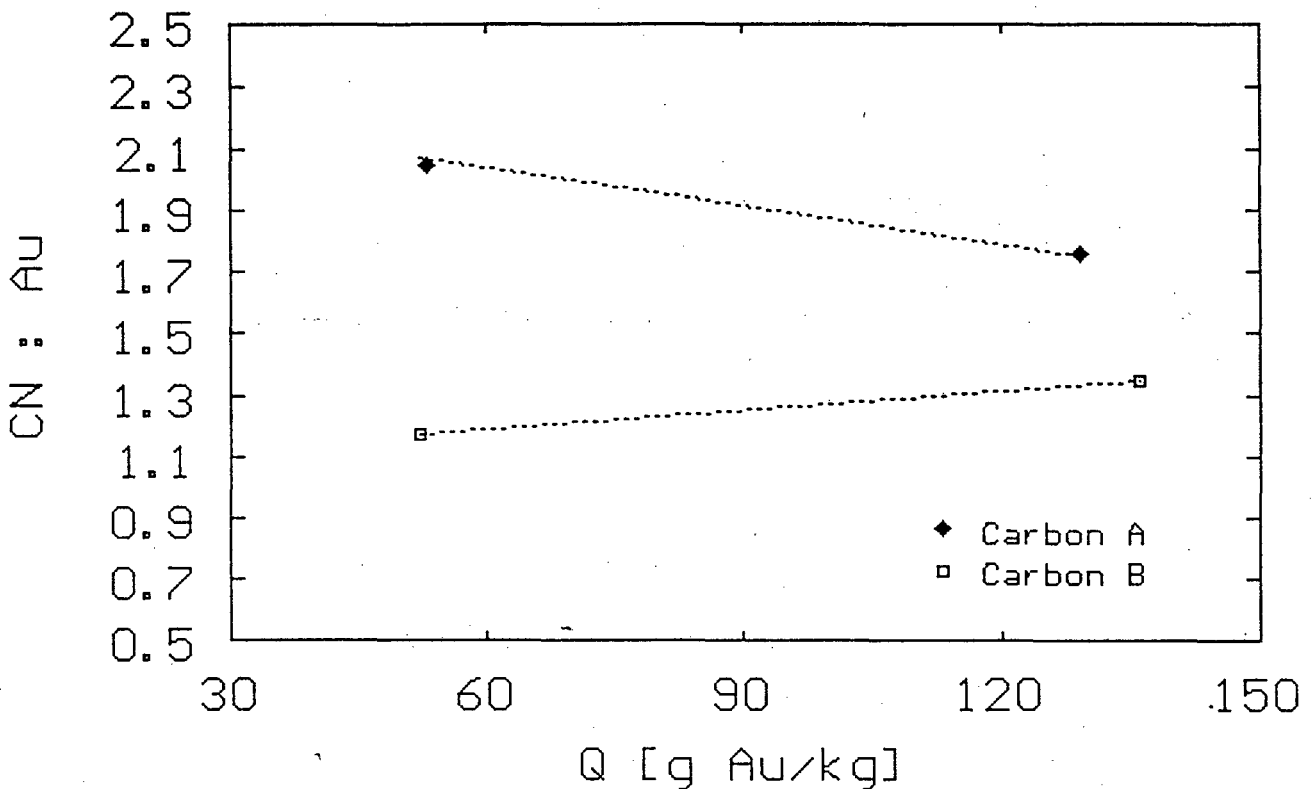


Figure 2.22 Molar ratio of CN : Au on carbons A and B as determined by XPS measurement.



Figure 2.23 FTIR scan of carbon A loaded with gold cyanide from an acidic solution.

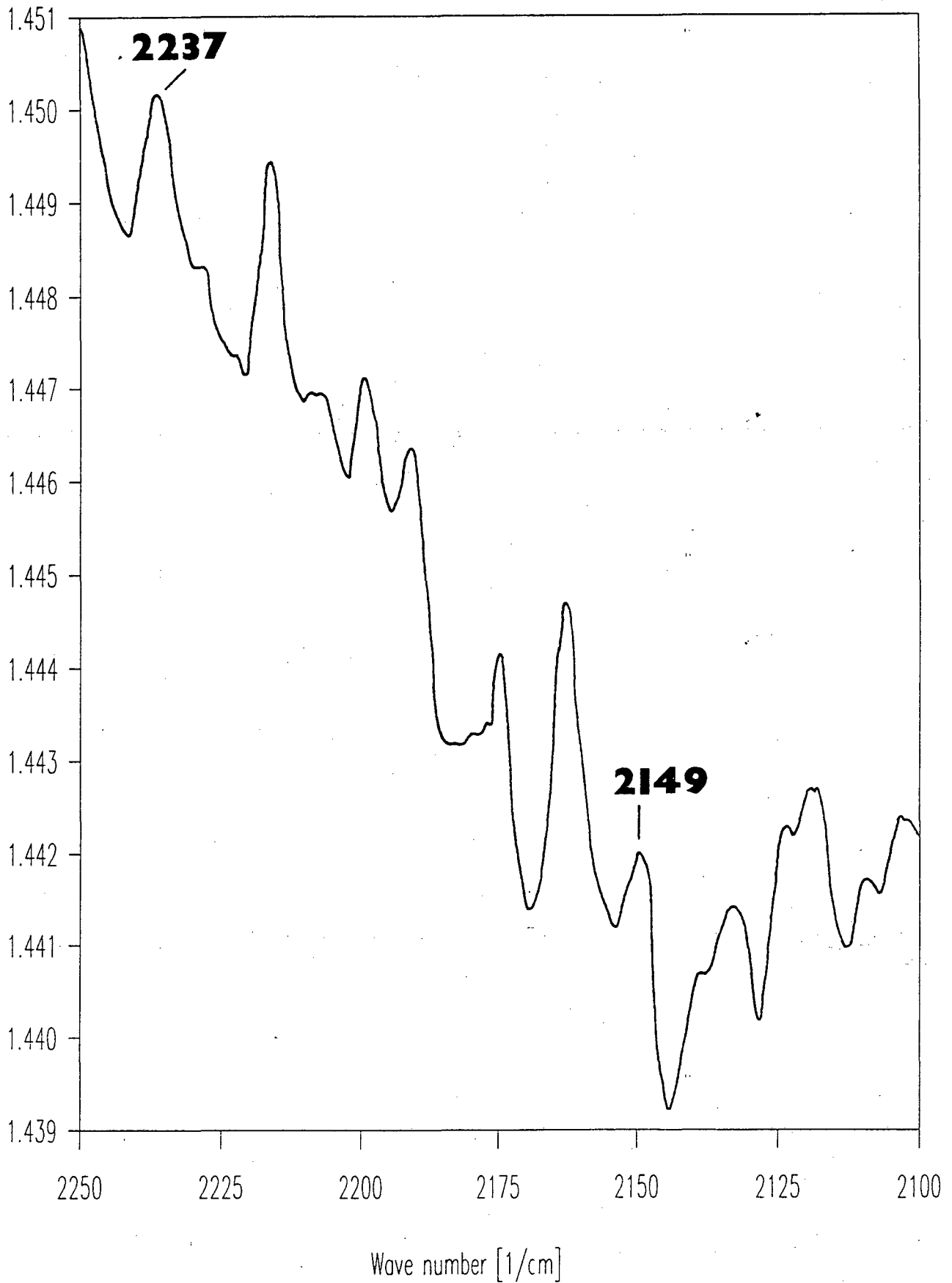


Figure 2.24 FTIR scan of carbon B loaded with gold cyanide from an acidic solution.

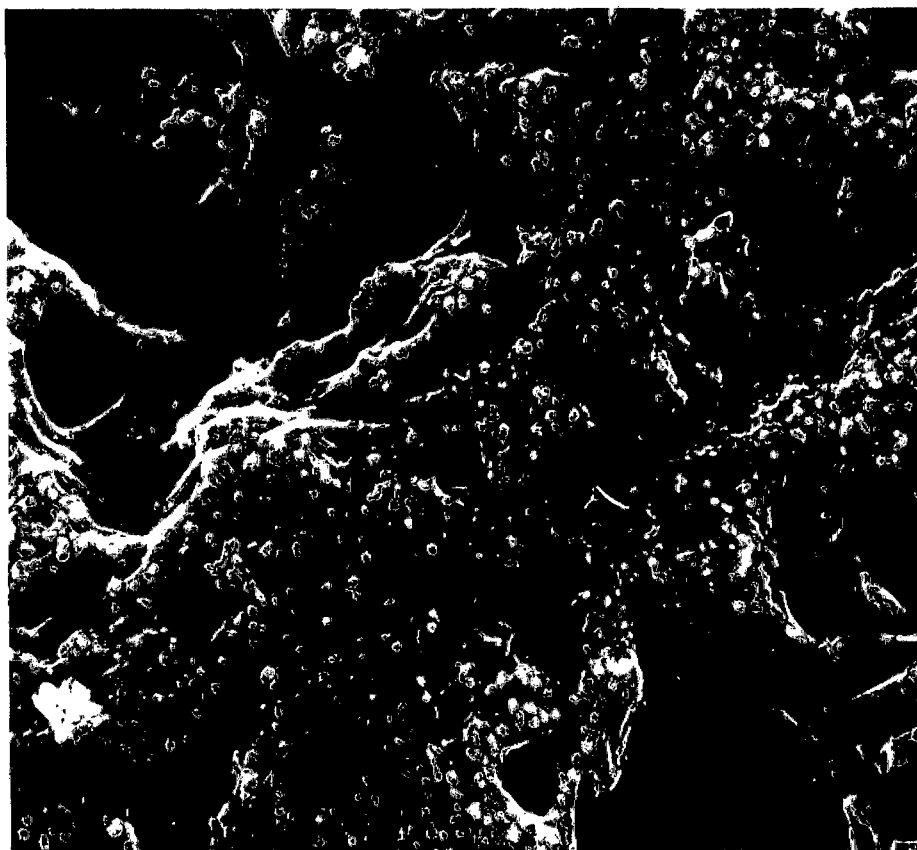


Figure 2.25 SEM photograph of surface of carbon BTX loaded with Au⁽⁰⁾ from an AuCl solution. (Magnified 2000 x)

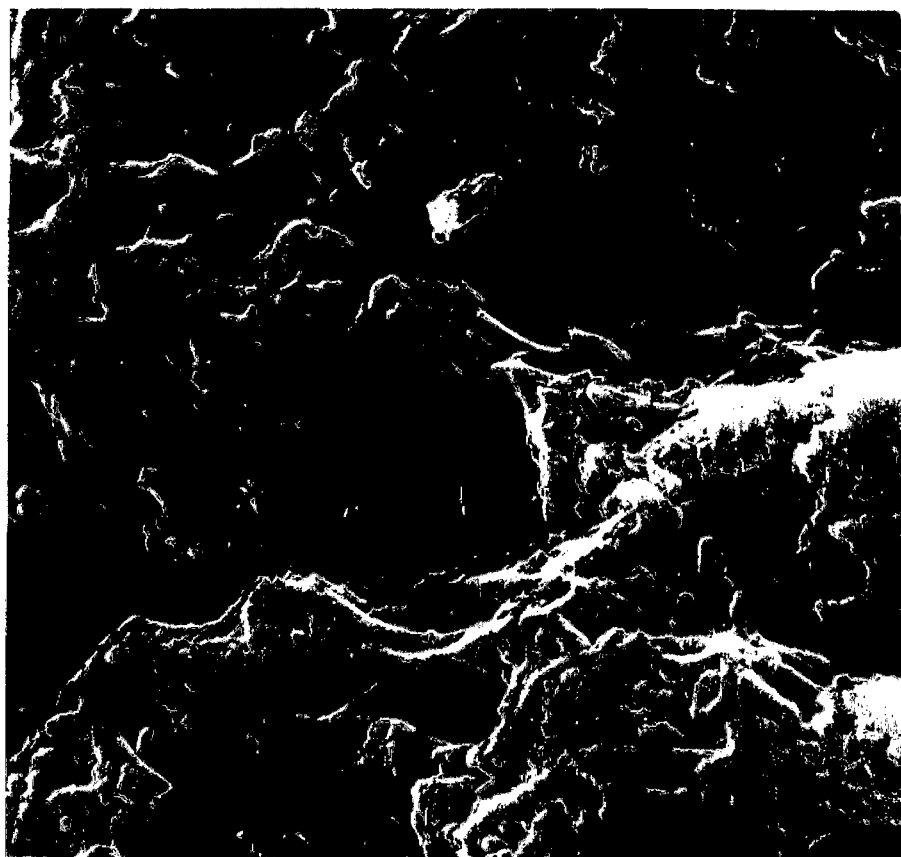


Figure 2.26 SEM photograph of surface of carbon BTX loaded with gold cyanide from an Au(CN)₂⁻ solution. (1 g of carbon stirred for 7 h in a solution with C₁₆ = 200 g.m⁻³). Soaked loaded carbon in a cold 0.1 M KOH solution for 5 h. (Magnified 2000 x)

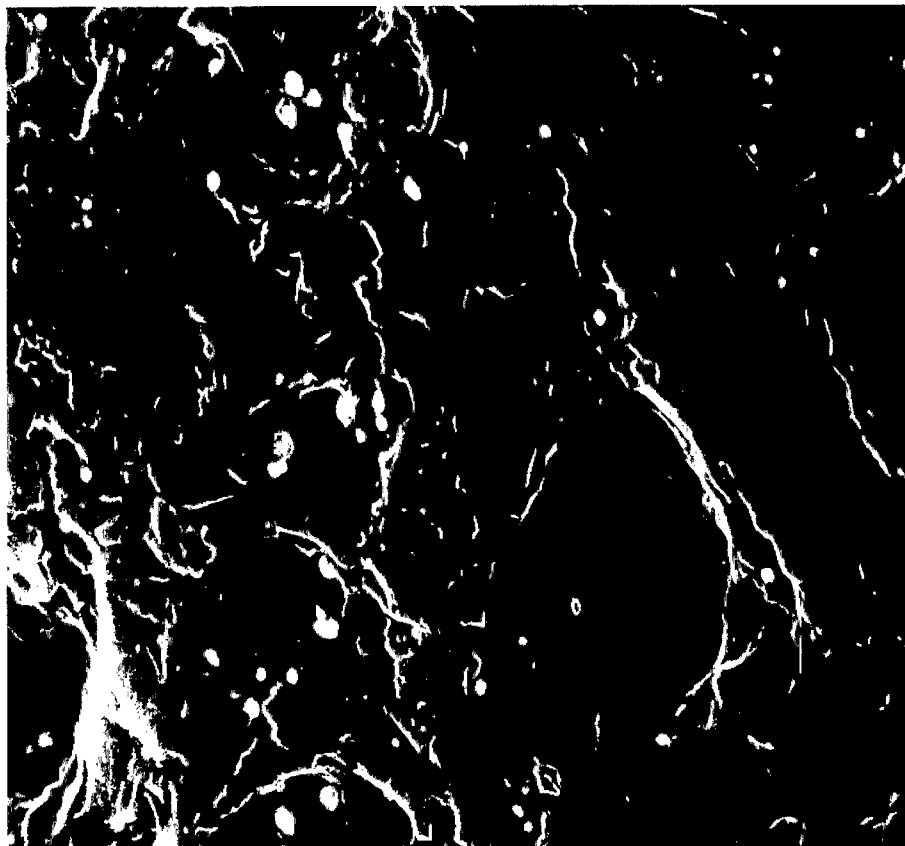


Figure 2.27(a) SEM photograph of surface of carbon BTX loaded with gold cyanide from an $\text{Au}(\text{CN})_2^-$ solution. (1 g of carbon stirred for 7 h in a solution with $C_{iG} = 200 \text{ g}\cdot\text{m}^{-3}$). Boiled loaded carbon in a 0.1 M KOH solution for 5 h. (Magnified 2000 x)

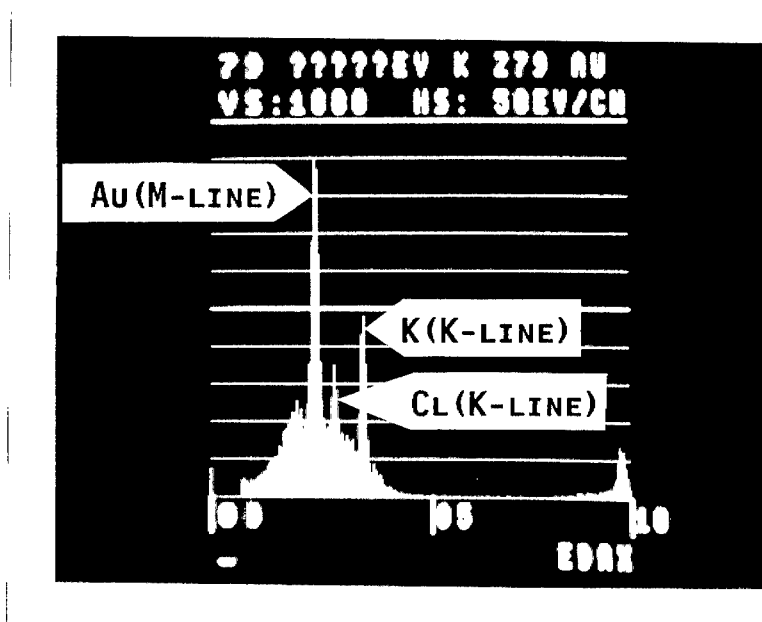


Figure 2.27(b) X-ray scan of sample of carbon used in Figure 2.27(a).

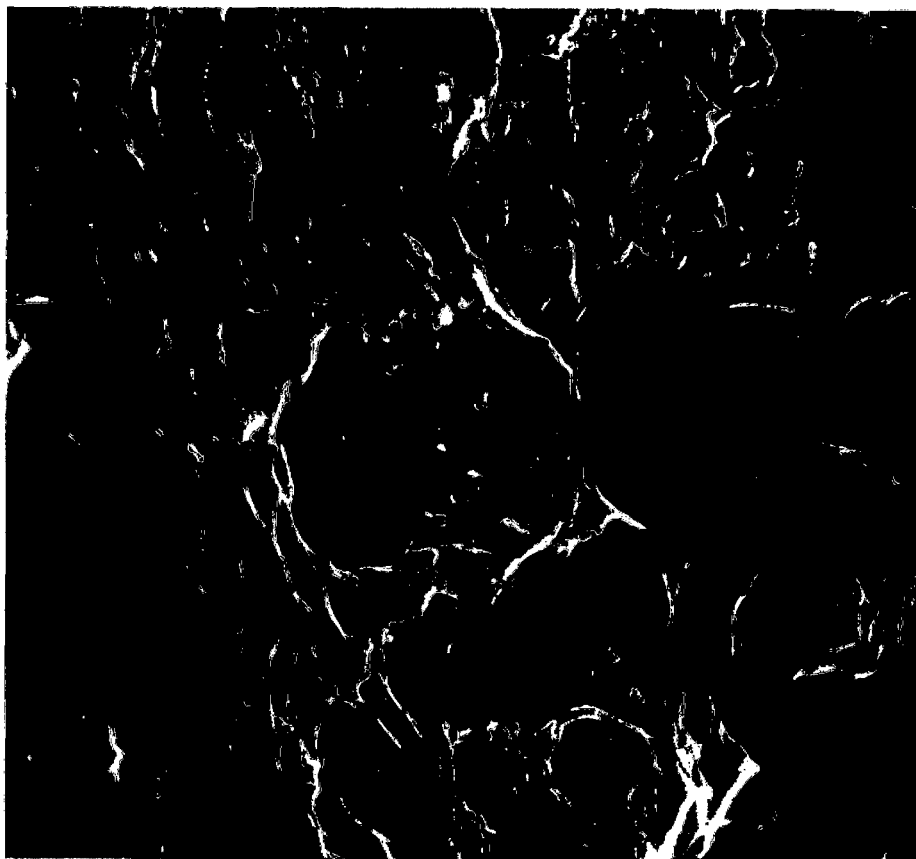


Figure 2.28 SEM photograph of surface of carbon BTX loaded with gold cyanide from an $\text{Au}(\text{CN})_2^-$ solution. (1 g of carbon stirred for 7 h in a solution with $C_{\text{ig}} = 200 \text{ g.m}^{-3}$). Boiled loaded carbon in distilled water for 5 h. (Magnified 2000 x)

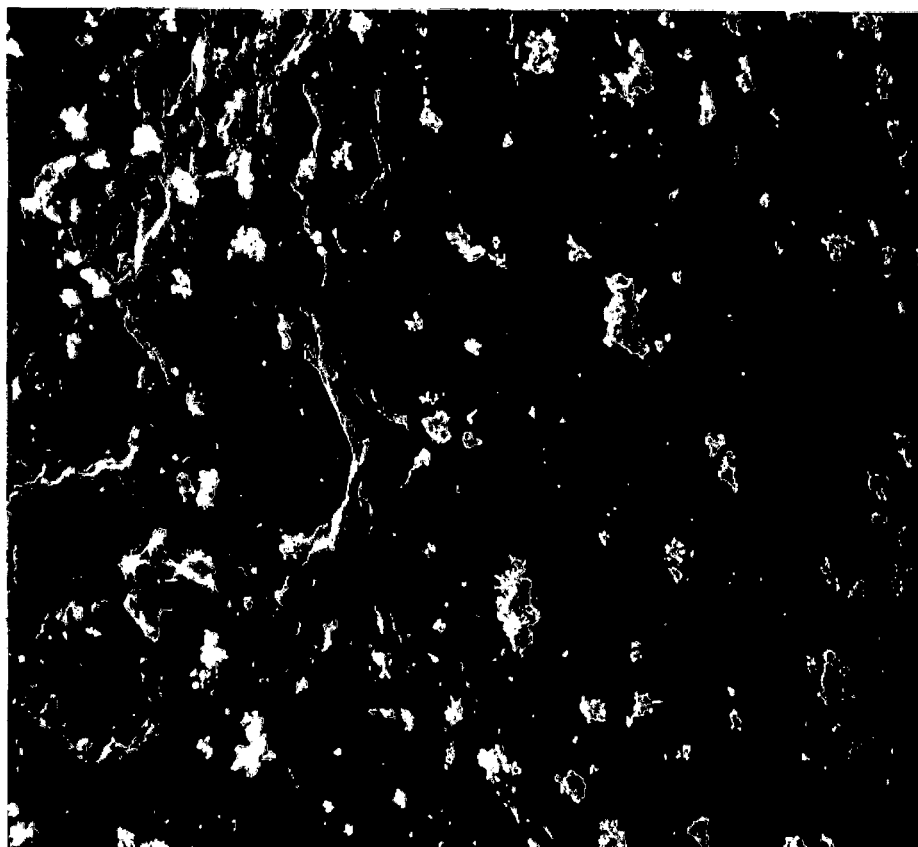


Figure 2.29(a) SEM photograph of surface of carbon BTX loaded with gold cyanide from an $\text{Au}(\text{CN})_2^-$ solution. (1 g of carbon stirred for 7 h in a solution with $C_{\text{ig}} = 200 \text{ g.m}^{-3}$). Boiled loaded carbon in 3 vol.% of a 33 mass % HCl solution for 5 h. (Magnified 200 x)

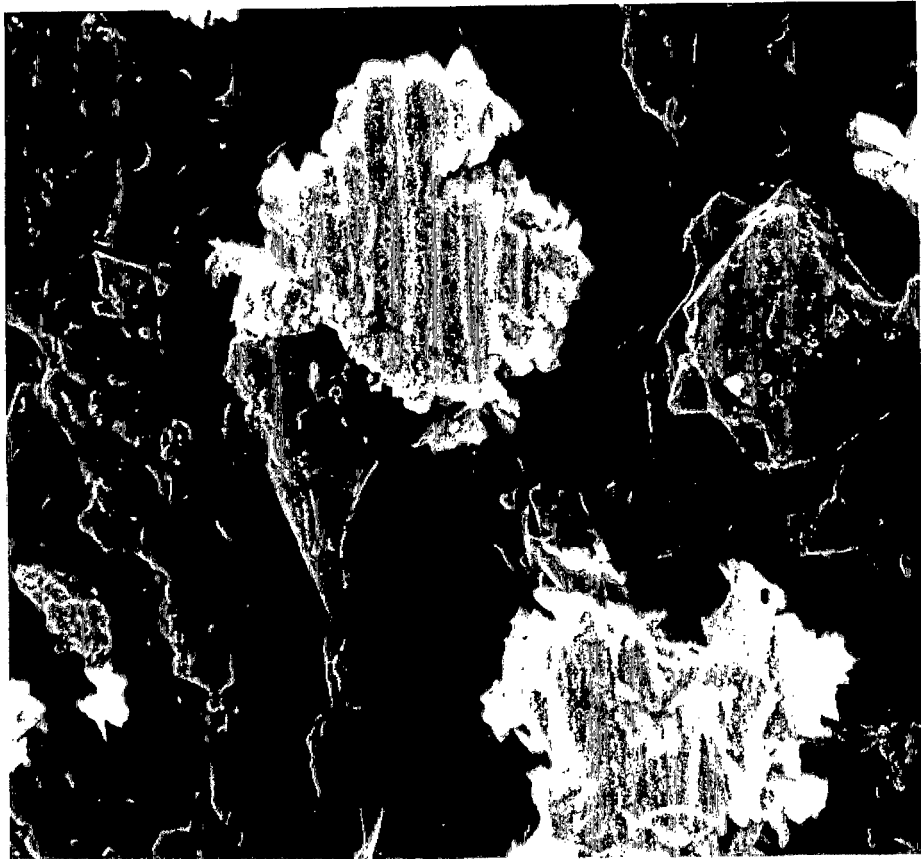


Figure 2.29(b) SEM photograph of sample of carbon in Figure 2.29(a) (Magnified 2000 x)

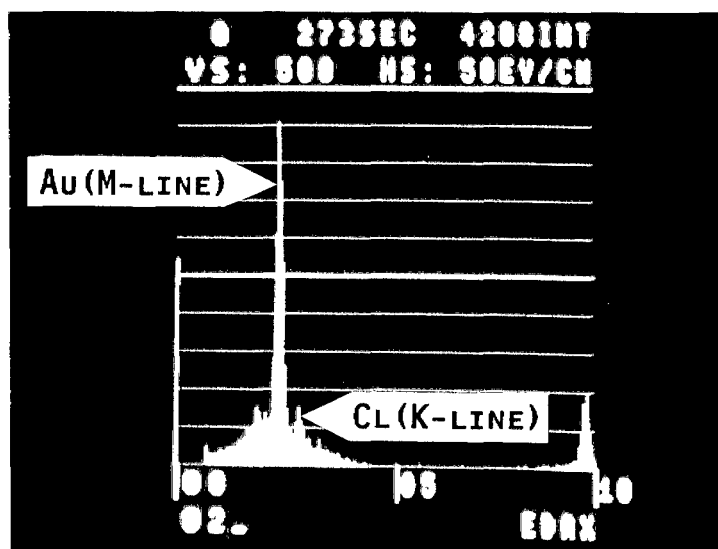


Figure 2.29(c) X-ray scan of sample of carbon used in Figure 2.29(a)

3

SUB-PROCESSES OF ELUTION

Cyanide and hydroxide salts are added during both the AARL and Zadra elution procedures to enhance the elution of the gold cyanide. The concentrations of the additives change continuously during the elution process because of dilution, adsorption and decomposition thereof. As the equilibrium between the adsorbed gold cyanide and the gold cyanide in solution is affected by these concentrations and other physical conditions, it was important to quantify the effects of such influences on the elution of gold.

Adams and Nicol (1986) listed the most significant influences on elution, in order of decreasing importance, as follows : temperature, cyanide and hydroxide concentrations, and the ionic strength of the eluant. Likewise, Davidson (1986a) considered the temperature and reagent cyanide addition to be the most important factors affecting gold elution. In cases where the loaded carbon contained large amounts of calcium carbonate, the temperature and acid washing of the carbon were considered to be most important for efficient elution (Davidson and Veronese, 1979).

Although it is believed (Davidson, 1986a) that the effects of temperature, reagent cyanide addition and ionic strength gradient are confounded to such extent that it is "not possible to quantify each parameter in isolation", an attempt was made in this chapter to quantify the effects of the most important influences on the gold cyanide equilibrium.

An important factor which was overlooked by most workers is the effect of adsorption on the desorption process. The adsorption process will determine (a) the form in which the gold is adsorbed, and (b) the radial distribution thereof through the carbon particles. It was shown in Chapter 2 that the gold can be loaded on the carbon as $\text{Au}(\text{CN})_2^-$ or AuCN

and that the ratio between these species will determine the extent of elution in the absence of cyanide. Although the form in which the gold is adsorbed will have little or no effect on the elution efficiency if a cyanide pretreatment is conducted, it is important when studying the pretreatment process to know which adsorbed species are present.

The kinetics of the adsorption process will determine the radial distribution of the adsorbed gold. The depth to which the gold has penetrated into the porous structure of the carbon might determine the ease with which it will desorb. This was touched upon by Van Deventer (1986) in his study of the kinetics of the adsorption of gold cyanide.

3.1 EXPERIMENTAL

3.1.1 Activated carbon

All the experimental data on the elution of gold cyanide have been collected by using carbon BTX. The carbon was tested for the formation of AuCN as described in Chapter 2. It was found that no AuCN was formed on the carbon during adsorption from alkaline solutions at room temperature. An apparent density of 838.8 kg.m^{-3} was measured for the carbon. The pore volume of the carbon was determined as $6.34 \times 10^{-4} \text{ m}^3.\text{kg}^{-1}$ by measuring the mass loss upon oven drying of a sample of carbon saturated with water. The average particle size was 1.42 mm (Experiment 2) and provided a void fraction of 0.292 in a packed column.

3.1.2 Columns

The AARL elution column is usually constructed of rubber-lined mild steel to permit the acid treatment to be carried out in the same vessel as the elution (Brittan, 1988). The choice of a column lining will be most important as this will determine the maximum temperature at which the column can be operated (Davidson, 1986a). Butyl rubber linings should be adequately vulcanised and not used at temperatures higher than $110 \text{ }^\circ\text{C}$. Other possible linings include Hastalloy C and PDVF (polydivinylidene fluoride). Costello *et al.* (1988) solved the problem of elution at higher temperatures by performing the acid wash in a separate rubber

lined vessel and the elution at 130 °C in a stainless steel column.

The objective of this study was to investigate the fundamentals of elution and not to achieve the highest possible elution efficiencies. A "comfortable" temperature of 70 °C was therefore selected for most of the elution runs. These investigative runs were conducted in a glass column with a temperature controlled water jacket. A drawing of the experimental setup is provided in Figure 3.1. Unless otherwise specified, the pretreatment steps were conducted outside the column in 50 ml glass beakers. After the pretreatment, the carbon was separated from the solution with a tea strainer, and excessive pretreatment solution removed by blotting with filter paper. The carbon was then dropped into the glass column containing half a bed volume of eluant at the elution temperature. The starting time for the elution was taken as the moment when flow of eluant was introduced. The eluant passed through the column in a downward direction under gravitation. The flow rate was periodically measured with a measuring flask and stop watch. Adjustments to the flow rate were made with the valve on the outlet of the column. Preheating of the feed was accomplished by keeping the section of the column above the carbon bed filled with eluant.

A stainless steel column with a hot oil jacket was used for comparative tests on a larger scale and for runs at higher temperatures than were possible with the glass column. A graphical presentation of the column and its utilities is shown in Figure 3.2. The eluant was pumped upwards through the column with a positive displacement pump. A single pass shell and tube exchanger was used to preheat the feed to the operating temperature of the column. By using a high flow rate of oil and more than 2 meters of tube in the preheater it was possible to obtain a temperature difference of less than 2 °C between the eluant and oil leaving the preheater. The oil from the preheater could therefore be fed directly to the jacket of the column to control the operating temperature of the carbon bed within 2 °C of the feed temperature of the eluant. The outlet temperature of the eluant from the preheater was controlled by a feed back controller that was connected to the electrical heating elements of the oil heater. At temperatures higher than 90 °C the column was pressurized by the use of a valve on the outlet of the column. The eluate was cooled by passing it through a coil that was submerged in cold

water. Four thermocouples were inserted into the carbon bed to monitor the temperature at different heights in the column.

The dimensions of the columns are summarized in Table 3.1. A bed volume (BV) is defined here as the empty volume of the reactor that is occupied by the packed bed of carbon, i.e. 1 BV = a.h. One bed volume of the glass column contained 9.4 g of dry carbon BTX, and the stainless steel column 3500 g.

3.1.3 Chemicals

To simplify the investigation it was decided to use mainly the potassium salts of aurocyanide, cyanide and hydroxide. In more complex systems other cations, or combinations thereof, can be treated similarly to K^+ . Unless otherwise specified, the pretreatment step for AARL type of elutions in the glass column involved soaking of the carbon for 30 min. in 20 ml of a 20 g KCN/l solution at room temperature. As no acid treatments were conducted, no KOH was added to the pretreatment solutions. The high concentration of cyanide in the pretreatment ensured sufficiently high pH values in the pretreatment step as well as the subsequent elutions. The pH of the distilled water used as eluant was also not adjusted.

3.1.4 Equilibrium tests

Batch experiments were conducted in 1000 ml stirred reactors with loose fitting lids to minimize evaporation at temperatures higher than room temperature and to prevent contamination with oil from the overhead stirrers. Equilibrium experiments at higher temperatures were conducted in a temperature controlled water bath. The equilibrium conditions were measured after a period of 3 weeks. The values of the pH and concentrations of reagents used in the quantification of the influences were measured at the same time as the equilibrium gold concentrations. As it was proved earlier that the equilibrium isotherms for adsorption and desorption of gold in contact with carbon BTX are the same, all the equilibrium data presented here were determined for adsorption. Furthermore, the determination of equilibrium data by adsorption involves only the adsorption step, whereas measuring desorption equilibria requires an adsorption and desorption step. As the concentrations of

gold have to be measured after each step, less errors are possible in the case of determining the equilibria by adsorption than desorption.

3.2 SUB-PROCESSES

The continuous change in the conditions during the elution step of the AARL procedure is the result of mainly three important sub-processes occurring simultaneously. The most obvious of these is the desorption of the gold, followed by the diffusion thereof out of the carbon into the interparticle solution. The other two sub-processes involve the removal of the pretreatment reagents from the carbon bed. These two processes are defined as, firstly, the diffusion of cations from the pores of the carbon, and, secondly, the decomposition and diffusion of the cyanide from the carbon pores.

Figure 3.3 shows a typical elution profile obtained at 70 °C. The concentrations of the gold, cyanide and potassium have been normalized for comparative reasons. Note the sharp decline in the cyanide and potassium concentrations within the first two bed volumes. The tailing effect is because of the reagents being trapped in the pores of the carbon. The peak in the gold profile only appears once the bulk of the pretreatment reagents have been removed. The pH remains high for the whole duration of the run, even though the pH of the water supply has not been adjusted.

As discussed earlier, the gold cyanide equilibrium is affected by the above mentioned factors. Because these factors change continuously throughout the elution, the gold cyanide equilibrium will also change continuously. It is therefore important to know the equilibrium isotherm at all possible combinations of these factors. Furthermore, it will only be possible to model the elution of the gold cyanide once models have been developed to describe the changes in the concentrations of the cyanide and the potassium.

3.3 MODIFIED FREUNDLICH ISOTHERM

At each possible combination of factors, such as pH, temperature and cyanide concentration, a unique Freundlich isotherm can be measured for the equilibrium adsorption of aurocyanide onto a specific activated carbon. To determine the two parameters, A and n, in the isotherm, at least 3 to 4 combinations of equilibrium gold loadings and concentrations were required. It is clear that it would have been impossible to establish the gold cyanide equilibrium at enough combinations of conditions to enable extrapolation to other combinations.

In an attempt to minimize the parameters in the Freundlich isotherm, Equation 2.4, it was decided to investigate a possible relationship between A and n. From the work of Cho and Pitt (1979a) it seemed that lowering of the equilibrium constant, A, is usually accompanied by an increase in the value of the exponent. The values of A and n determined (Van Deventer, 1984) for more than ten different carbons under different adsorption conditions were then plotted in Figure 3.4. From this plot it is clear that n decreases linearly with an increase in A, and that the Freundlich isotherm for the adsorption of gold cyanide onto activated carbon can be modified to :

$$Q_{eG} = A C_{eG}^{bA+B} \quad [3.1]$$

where b and B are constants that can be determined from Figure 3.4 or by measuring the Freundlich isotherms for a specific carbon at different conditions. With only the one unknown, A, in the isotherm expression, it was now possible to describe the equilibrium at a certain combination of factors with only one value of Q_{eG} and C_{eG} . By keeping all factors constant and changing only one factor at a time it was thus possible to quantify the effect of each factor on the value of A, and therefore its effect on the gold cyanide equilibrium.

3.4 FACTORS INFLUENCING THE ELUTION OF AUROCYANIDE

3.4.1 Temperature

The adsorption of gold onto activated carbon is an exothermic process (Nicol, 1986; Davidson, 1974) and an increase in temperature will shift the equilibrium to favour desorption. Temperature is considered (Davidson, 1986a; Adams and Nicol, 1986; Nicol, 1986) to be the most important factor in the efficient elution of gold and other metal cyanides from activated carbon. It was found that an increase in elution temperature from 90 °C to 110 °C significantly improved the elution efficiency and maximum eluate concentration for all carbons tested (Davidson and Veronese, 1979). McDougall *et al.* (1980) related the need for high elution temperatures to the more than 14 times higher solubility of $\text{KAu}(\text{CN})_2$ in hot than cold water. They further reported that plots of the logarithm of the equilibrium solution phase concentration versus the reciprocal of the absolute temperature in Kelvin gave a set of straight lines. From these plots an average value for the isosteric heat of adsorption was calculated as $42 \text{ kJ}\cdot\text{mol}^{-1}$. Similar linear relationships were found by plotting the distribution of gold between the liquid and solid phases at equilibrium ($K = Q_e/C_e$) versus $1/T$ for two sets of data with different initial gold concentrations (Adams *et al.*, 1987b).

Figure 3.5 presents equilibrium isotherms determined for gold cyanide adsorption onto carbon BTX at temperatures of 22 °C, 30 °C, 40 °C and 60 °C. Higher temperatures would have necessitated the addition of cyanide to prevent the formation of AuCN. As cyanide is readily hydrolysed at high temperatures, it would have been impossible to determine all equilibria at the same cyanide concentration. The A and n values, determined by fitting the Freundlich equation to the 4 sets of experimental data in Figure 3.5, are summarized in Table 3.2. A least squares regression on the data in Table 3.2 provided the following correlation between A and n for carbon BTX :

$$n = -0.002688.A + 0.2902 \quad [3.2]$$

The predicted exponents (n_{pred}) in Table 3.2 were calculated with Equation 3.2. Further proof for the validity of Equation 3.2 was obtained by

using the correlation for n on the experimental data in Figure 3.5 to determine an average A -value for each temperature. The curves in Figure 3.6 were calculated with these average A -values as follows :

$$Q_{eG} = A \cdot C_{eG}^{-0.002688 \cdot A + 0.2902} \quad [3.3]$$

Whereas the lines in Figure 3.5 were calculated by fitting the Freundlich isotherm (Equation 2.4) to the experimental data, the lines in Figure 3.6 were calculated with the modified isotherm (Equation 3.3). The main advantage of using Equation 3.3 is that it contains only one parameter (A), which makes it easier to quantify the effect of a factor, such as temperature, on the gold cyanide equilibrium. Therefore, all of the A -values presented from here onwards, were calculated with Equation 3.3.

To test the validity of an Arrhenius relationship between temperature and the equilibrium gold loading on carbon BTX, the logarithm of A was plotted in Figure 3.7 against the reciprocal of the absolute temperature in Kelvin. The straight line through the data represents the following relationship :

$$A = 0.019 \exp(2190/T) \quad [3.4]$$

3.4.2 pH of solution

Davidson (1974) related the effect of pH on the adsorption of metal cyanide complexes to the strong adsorption of both hydroxide and hydronium ions, whereas Adams *et al.* (1987b) and Adams and Fleming (1989) favoured a mechanism in which OH^- reacts with the functional groups on the surface of the carbon. Table 3.3 summarizes the relationships between the equilibrium metal loading and pH as calculated from the results of previous workers. It was found that log-log plots of the data resulted in straight lines in all 4 cases.

The A values for gold cyanide in contact with carbon A at different pH values are plotted in Figure 3.8. To eliminate the effects of other influences on the equilibrium, all the experiments in Figure 3.8 were conducted at room temperature, a $[\text{CN}^-] = 0 \text{ g/m}^3$, and a $[\text{K}^+] = 1100 \text{ g/m}^3$. The same potassium concentrations were achieved by the addition of KCl.

It was shown (McDougall, 1982) that the chloride ion has a negligible effect on the interaction between gold cyanide and activated carbon. From the straight line obtained in Figure 3.8, the following relationship was found to describe the effect of pH on the value of A :

$$A = 113 \exp(-0.16 \text{ pH}) \quad [3.5]$$

Figure 3.9 shows a repetition of the above experiment at a temperature of 40 °C, a $[\text{CN}^-] = 0 \text{ g/m}^3$, and a $[\text{K}^+] = 1500 \text{ g/m}^3$. Although the constants in Equation 3.6 at 40 °C differed from those determined at room temperature, the function remained the same :

$$A = 138 \exp(-0.21 \text{ pH}) \quad [3.6]$$

3.4.3 Cyanide concentration

It was found (Adams and Nicol, 1986) that the rate of desorption in a Zadra type of elution reached a maximum at a cyanide concentration of 0.2 M. The decrease in elution rate at higher concentrations was ascribed to the opposing effect of cyanide and ionic strength. It was illustrated that, at a constant ionic strength (achieved by the addition of NaCl), an increase in cyanide and hydroxide concentrations resulted in faster desorption kinetics. The effect of cyanide on the equilibrium adsorption of gold cyanide on carbon BTX (see Figure 3.10) was thus determined at a constant potassium concentration of 1200 g/m^3 . As in the case of the determination of the effect of pH, KCl was added to the solutions to achieve the same $[\text{K}^+]$'s. Even though the initial pH's were all adjusted to the same value by the addition of KOH, the pH-values at equilibrium ranged between 8.6 and 10.5 because of the different cyanide concentrations. In spite of the variation in pH values, a log-log plot of A vs. $([\text{CN}^-]+1)$ produced a perfect straight line (Figure 3.10). The value of 1 was added to the cyanide concentration to prevent taking the log of 0. From Figure 3.10, it followed that A can be written as a function of the free cyanide concentration in solution as follows :

$$A = 32 (C_N + 1)^{-0.155} \quad [3.7]$$

3.4.4 Cation concentration

The gold loading capacity of carbon increases with an increase in cation concentration. The beneficial effect of cations on gold adsorption is reported (Costello *et al.*, 1988) to be in the order $\text{Ca}^{2+} > \text{Mg}^{2+} > \text{H}^+ > \text{Na}^+ > \text{K}^+$. Thus, a low ionic strength and the absence of Ca^{2+} and Mg^{2+} will favour desorption. Nicol (1986) presented equilibrium data to illustrate the increase in gold loading capacity with an increase in ionic strength from 0.005 to 1.0 M. The loading capacities have been given at a fixed solution phase concentration and will therefore be representative of the constant A in the Freundlich isotherm. A least squares regression on his data showed $\ln(A)$ to be a linear function of $\ln(\text{ionic strength})$.

The equilibrium capacity under elution conditions will not only be a function of the concentration of cations in the liquid phase, but also of the cations adsorbed on the carbon (Davidson, 1974). Table 3.4 shows typical metal loadings of carbon loaded from a gold plant effluent. It can be seen that during an acid wash, most of these elements are removed. Furthermore, it was shown (Davidson, 1974) that during the pretreatment step the aurocyanide anion will be preferably linked to the spectator cation introduced with the pretreatment reagents. From these observations it can safely be assumed that after an acid wash and a cyanide or hydroxide pretreatment the main cation to be considered in the elution step will be the cation introduced with the pretreatment reagents.

Because different cations, even with the same charge, have different effects on the adsorption and desorption of $\text{Au}(\text{CN})_2^-$, it was decided to treat each cation separately and not to study the ionic strength as such. Furthermore, it is unlikely that an ion such as CN^- , which has a positive effect on desorption, will contribute to the negative effect of the ionic strength. As discussed earlier, mainly potassium was studied here. Even though other cations will affect the adsorption of gold to different degrees, the trends will be similar to that observed for potassium. This is illustrated in Figure 3.11 where $\ln(A)$ was plotted as a function of the concentration of potassium and calcium respectively. The

relationship between A and the cation concentration was the same for both cations :

$$A = 24 (C_K + 1)^{0.069} \quad [3.8]$$

$$A = 26 (C_{Ca} + 1)^{0.127} \quad [3.9]$$

The stronger dependence on the calcium concentration than the potassium concentration can be seen clearly from Figure 3.11 and Equations 3.8 and 3.9. Although inconceivable, a nil cation concentration was provided for in the $(C_{cat} + 1)$ -term.

The effect of using NaCN instead of KCN as pretreatment reagent in an AARL elution was investigated in Figure 3.12. Little or no difference could be observed in the resulting gold elution profiles.

The H^+ cation was not treated here as another cation, because it was already accounted for in the effect of the solution pH.

3.4.5 Cyanide pretreatment in an AARL elution

It was shown (Davidson and Duncanson, 1977) that more than 99% of the gold loaded onto Le Carbone G210 could be recovered with deionized water after a pretreatment with potassium carbonate. A nearly identical gold elution profile was obtained with an equimolar sodium carbonate pretreatment. The carbonate pretreatment led, however, to poor elution of silver and other base metals as well as the build-up of calcium carbonate on the carbon. The poor elution of the metals, other than gold, was blamed on the instability of these complexes under high pH pretreatment conditions. Further tests indicated that it was the higher hydroxide concentration associated with the addition of carbonate, and not the carbonate itself, that was responsible for the efficient elution of gold. The carbonate in the pretreatment was then replaced with sodium hydroxide and sodium cyanide. The sodium cyanide was added in order to increase the stability of the metal cyanide complexes. Further investigations revealed that the elution of all the metal cyanide species (including gold) could in fact be improved by adding less hydroxide to the pretreatment. Hydroxide is still added to the pretreatment, but mainly to stabilize the cyanide, (for safety reasons).

The relative insignificance of hydroxide compared to cyanide in the pretreatment is illustrated in Figure 3.13. Identical elutions were carried out with identical samples of gold loaded carbon. The only difference was that the one sample was pretreated with a KCN solution and the other with a KOH solution with the same pH and potassium concentration as the cyanide solution. In the case of the cyanide pretreatment the maximum gold concentration in the elution was more than 10 times higher than for the hydroxide pretreatment.

As discussed previously, the effect of cyanide in the above experiment cannot be linked to the dissolution of an irreversibly adsorbed gold species. Furthermore, if CN^- displaces $\text{Au}(\text{CN})_2^-$ from loaded activated carbon by a mechanism of competitive adsorption, it would have been expected that more desorption of gold would have occurred during the pretreatment step. What is even more peculiar, is that the peak in the gold elution profile appeared only after most of the cyanide was already washed out of the carbon bed. An experiment, (see Figure 3.14), was then devised to investigate the necessity for cyanide in the eluant. To ensure the lowest possible carry over of cyanide from the pretreatment to the elution stage, the carbon was boiled in the pretreatment reagent to decompose most of the cyanide. At the end of the pretreatment, the cyanide concentration was measured as 80 mg CN^-/l (compared to the initial concentration of 8000 mg CN^-/l). The elution step of this experiment consisted out of two stages. During the first stage an eluant containing 2000 ppm potassium (as KCl) was pumped through the carbon bed. The high cation concentration suppressed the elution of the gold and provided 4 bed volumes of eluant to rinse the carbon of cyanide that was carried over from the pretreatment step. For the second stage of the elution the potassium rich eluant was replaced with distilled water. Even though the cyanide concentration in the solution was practically zero at this stage, a peak in the gold concentration appeared almost instantaneously. Moreover, the maximum gold concentration was more than 60 % higher than that measured in a similar elution without the initial high cation stage (Experiment 50). This can be ascribed, however, to the more "intense" pretreatment that was carried out here.

From the above experiment it follows that the free cyanide that is present during the elution step of the AARL procedure is of secondary

importance to that in the pretreatment. This means that it is the effect of the cyanide that was present in the pretreatment step and not the carry-over of pretreatment reagents to the eluant that enhances the elution of the gold. Because of the high ionic strength in the pretreatment step, the bulk of the gold desorption occurs only during the elution stage once the cation concentration is lowered. The horizontal position of the gold peak will therefore be a function of the kinetics of the removal of the cations carried over from the pretreatment stage.

The deactivation of activated carbon by cyanide was investigated by comparing the gold adsorption ability of fresh carbon to that of carbon that was pretreated in a strong cyanide solution. When this test was done initially, the carbon that was treated with cyanide was boiled in distilled water before the adsorption test to decompose all the free cyanide occluded in its pores. No difference could be detected in the subsequent behaviour of the two samples of carbon towards gold cyanide. The test was then repeated, but instead of boiling the cyanide treated carbon, the remaining cyanide was eluted with distilled water in a glass column at room temperature. The carbon was then removed from the column and the adsorption of gold cyanide onto the pretreated carbon (in a batch stirred tank reactor) was compared to the adsorption onto a similar sample of fresh carbon in Figure 3.15. The lower adsorption capacity of the pretreated sample proves that the surface of the carbon was changed in such a way that its affinity for the aurocyanide anion was reduced. This deactivation can however be reversed easily by exposure of the carbon to high temperature.

The effect of cyanide in solution and the effect of cyanide that was decomposed or adsorbed on the carbon, will be referred to here as the effect of cyanide and the effect of cyanide-age respectively. The cyanide-age of the carbon, Q_N , is defined as the amount of cyanide, in g CN^- /kg carbon, that was previously adsorbed or oxidized on the carbon. Experiment 55 represents an attempt to quantify the effect of cyanide-age on the desorption of gold cyanide. For this experiment, 5 samples of carbon BTX were loaded with gold to the same level. These gold loaded samples of carbon were then treated with solutions of different cyanide concentrations, before they were transferred to distilled water and the gold concentrations monitored. The elution parts of the experiments were

conducted in small quantities of water at 70 °C to resemble the high carbon concentration in an elution column. Samples of the solutions were taken after 22, 52 and 94 hours. As it was found that the gold concentration in solution declined with time, it was decided to take the concentrations at 94 hours as representative of the effect of the cyanide-age on the gold equilibrium. To account for the different pH values measured for the 5 samples, the calculated A-values were "normalized" for pH by dividing them by $\exp(-0.2 \text{ pH})$ as determined earlier. These normalized A-values were plotted in Figure 3.16 as a function of the cyanide-age of the carbon. The A-value was found to be related to the cyanide-age, Q_N , as in Equation 3.10 :

$$A = \text{const}/(0.06 Q_N + 1) \quad [3.10]$$

The value of the constant in Equation 3.10 was determined as 10.2 at a solution pH of 10.

The decline in the concentration of gold in solution during the elutions in Experiment 55 can be attributed to two possible factors :

- (1) The carbon was loaded with gold over a period of less than 2 days. This would have resulted in a concentration gradient of adsorbed gold through the carbon particles. Further diffusion into the finer pores of the carbon during the elution step could thus lead to the re-adsorption of gold that was eluted from the surface of the particles during the initial stage of the experiment.
- (2) As discussed earlier, the activity of the activated carbon towards gold cyanide can be easily restored after a cyanide pretreatment if the carbon is exposed to higher temperatures. The elution temperature of 70 °C employed here could therefore be responsible for the gradual recovery of the activity of the carbon. This would have resulted in the re-adsorption of the gold that was initially desorbed.

The occurrence of re-activation of the carbon after a cyanide pretreatment was further investigated by measuring the elution of gold from carbon that was loaded over a period of three weeks. Sufficient time was thus allowed during the adsorption stage to ensure a homogeneous

distribution of gold throughout the carbon particles, and thereby eliminating factor (1) above. The elution profile determined in a batch reactor, after a cyanide pretreatment in a separate container, is presented in Figure 3.17. Desorption occurred for the initial 3 hours of the experiment, whereafter the concentration of gold in solution started to decrease. In this case the re-adsorption of the gold could only be ascribed to the deterioration of the effect of the cyanide pretreatment in the elution step. This re-activation of the carbon makes it difficult to accurately quantify the effect of the cyanide pretreatment, or cyanide-age, on the gold cyanide equilibrium. By the time that sufficient time has elapsed to reach equilibrium, the effect of the cyanide-age has already been destroyed.

3.4.6 Presence of irreversibly adsorbed species

Davidson and Veronese (1979) reported nearly identical gold elution profiles for loaded carbon that has been air-dried, oven-dried at 110 °C or used as is. All of these carbons, however, have been acid washed and pretreated with cyanide before the elution. As discussed earlier, the oven drying of loaded carbon can lead to the formation of AuCN or Au⁽⁰⁾ and care should be taken in the cyanide pretreatment of such carbons to ensure the "leaching" of any irreversibly adsorbed species before the elution.

From Figure 3.18 it becomes evident that the leaching of AuCN or Au during the elution step will slow down the process and affect its efficiency. Although the experiments in Figure 3.18 were conducted in batch, the same detrimental effect of an irreversibly adsorbed species is expected for the Zadra elution process in which no cyanide pretreatment is conducted. Under such circumstances the reaction of AuCN or Au with CN⁻ can become rate controlling. The batch elution profiles presented in Figure 3.19 are of acid washed carbon in cyanide solutions at room temperature. The one sample of carbon was powdered before the elution and the other used as is. Although the same equilibrium seems to apply in both cases, the rate of elution was much higher where contact between the cyanide and the gold species was increased by reducing the particle size of the carbon. It is thus expected that particle size will have a

significant effect on the rate of Zadra type elutions if the carbon contains irreversibly adsorbed species.

3.4.7 h/d Ratio

Menne (1987) presented elution profiles obtained from laboratory scale columns with h/d ratios ranging from 1.5:1 to 12:1. No apparent effect could be observed. Variations due to different h/d ratios on large columns were attributed mainly to deviations from plug flow. Davidson (1986a), on the other hand, supported a chromatographic mechanism for the process and expected (more so than proved) the resolution of the elution profile to be strongly dependent on the h/d ratio. Both workers stressed, however, that care should be taken in the design of proper distributors for large columns so as to avoid the eluant from bypassing portions of the carbon bed.

The effect of the geometry of the elution column was investigated in Figure 3.20. The gold elution profiles presented, were obtained by performing identical elutions in the glass column and the more than 300 times larger stainless steel column discussed earlier. These columns had h/d ratios of 11.3 and 7.5 respectively. The same flow rate of eluant, expressed as number of bed volumes per hour, was used. Nearly identical elution profiles were measured for both cases, with only a slightly sharper profile for the glass column, which had the higher h/d ratio. The relative insensitivity to column geometry, at the same space-time, can be seen as an indication that little deviation from plug flow occurred.

3.4.8 Flow rate

Davidson (1974) investigated the effect of flow rate on the elution of gold after a 3 % potassium carbonate/ 1 % potassium hydroxide pretreatment and found that sharper elution profiles were obtained at lower flow rates. However, in a later publication (Davidson, 1986a) he reported that in a column with an h/d ratio of 10, the elution of gold was independent of flow rate in the region of 1 to 5 bed volumes per hour. (A pretreatment solution of 2 % sodium cyanide/ 2 % sodium hydroxide was used in the latter study.) The insensitivity of elution towards flow rate was interpreted as an indication that the elution

mechanism was not intraparticle controlled under the specified conditions. Davidson (1986a) stated that the choice of a suitable flow rate would depend largely on a compromise between peak power demand and elution time. Flow rates of 2-3 BV/h are usually employed in order to fit the elution into an 8 hour shift. At such low flow rates the pressure drop over the column becomes insignificant.

Figure 3.21 contains elution profiles obtained from the glass column at identical conditions, except for different flow rates of eluant. Nearly identical profiles were measured for flow rates of 2.89 and 5.89 bed volumes per hour. Even at a flow rate of 37 BV/h, the elution of the gold was still comparable to elutions in the range of 2 to 6 BV/h.

The breakthrough curves in Figures 3.22 and 3.23 were calculated from data for the adsorption of silver cyanide onto activated carbon in columns (Jansen Van Rensburg, 1986). From the curves in Figure 3.22, it is clear that adsorption is more sensitive to variations in flow rate than is the case for elution. When the conditions are less favourable for adsorption, as in the case of Figure 3.23 where a higher pH was used, the sensitivity towards flow rate decreases. This implies that even though adsorption onto activated carbon is widely accepted to be diffusion controlled (Jansen van Rensburg and Van Deventer, 1985; Cho et al., 1979; Fritz et al., 1981), it is not necessarily the case for desorption.

3.4.9 Distribution of adsorbed gold

The distribution of gold cyanide through gold loaded carbon particles will depend on the initial concentration of gold in solution and the duration of contact between the solution and the carbon. The higher the initial concentration and the shorter the time of adsorption, the more gold will be adsorbed closer to the particle surface and in the macropores. If more time for diffusion of the gold is allowed, it will be distributed more evenly through the particle and more gold would have diffused from the macropores to the micropores. The effect of the distribution of adsorbed gold on the desorption thereof at room temperature was investigated in Figure 3.24. It was found that the rate of elution was higher for carbons that were loaded with gold over shorter

periods of time, i.e. where steeper adsorbed gold concentration gradients were present on the carbon.

As with the effect of flow rate, it was found that the elution was less sensitive to the distribution of the adsorbed gold under conditions that were more favourable for desorption. The gold elution profiles in Figure 3.25 were obtained for carbons that were loaded with gold for 22 and 72 hours respectively. These elutions were conducted at 70 °C after a cyanide pretreatment.

3.4.10 Organic solvents

Various solvents have been investigated in published efforts to improve the elution of gold with the use of pure organic solvents or organic solvent/water mixtures (Espiel *et al.*, 1988; Muir *et al.*, 1985a,b). These included ethanol (EOH), methanol (MOH), acetone (AC), isopropanol (POH), acetonitrile (AN), dimethylformamide (DMF), methyl ethyl ketone (MEK), acrylonitrile (AcN) and ethylene glycol (EG).

Muir *et al.* (1985b) studied the effect of using organic solvent/water mixtures as eluant in the conventional AARL and Zadra elutions. They reported the effectiveness of the organic solvents in promoting gold elution in the order AN > MEK > AC > DMF > EOH. The best results were obtained using eluants comprising of 40% (vol/vol) AN/water containing 5 to 40 g/l NaCN. It was found that organic solvents increase the kinetics of desorption, but that they do not cause desorption of gold in the absence of cyanide. Furthermore, the addition of organic solvents to the pretreatment reagents of the AARL elution was shown (La Brooy and Ariti, 1988) to have little or no effect upon the subsequent elution with water.

In elutions with organic solvent/water mixtures, the concentration of the solvent remains unchanged for the duration of the run. It can therefore be assumed that the equilibrium or kinetic parameters for such an elution will differ from the parameters for an elution with water with a factor that will remain constant during the course of the process.

3.4.11 Acid washing

The use of an acid wash step is advocated mainly for increasing the efficiency of the AARL elution (Davidson, 1986a). It was shown that the AARL elution process was less sensitive to the ionic strength of the eluant after an acid wash. This was especially the case when the gold loaded carbon contained large amounts of calcium. Most of the calcium was found to be eluted during the acid wash. It was speculated that the gold that is loaded from calcium containing solutions is present on the carbon as the $\text{Ca}(\text{Au}(\text{CN})_2)_2$ ion pair. During the acid wash the Ca is eluted and the gold cyanide decomposed to AuCN. In the subsequent cyanide treatment step the AuCN reacts with cyanide and the cation (eg. Na^+) introduced with the pretreatment reagent to form the $\text{NaAu}(\text{CN})_2$ species. The $\text{NaAu}(\text{CN})_2$ is adsorbed less strongly than the $\text{Ca}(\text{Au}(\text{CN})_2)_2$ ion pair and is therefore less sensitive to the water quality (ionic strength) of the eluant.

The effect of an acid wash where no calcium is present, was investigated in Figure 3.26. The carbon used in the experiments was loaded from gold cyanide solutions and treated in acid and cyanide solutions containing H^+ and K^+ as the only cations. Much lower gold elution was measured where the carbon was acid washed prior to the cyanide pretreatment. This can be attributed to mainly two factors : (a) Even though the acid washed carbon was washed with distilled water before it was added to the cyanide solution, enough acid was left on the carbon to destroy a large percentage of the cyanide that would have been utilized for the desorption of the gold, and (b) the acid lowered the pH of the eluant from approximately 10 for the non-acid washed carbon to 9 for the acid washed carbon. It is therefore not advisable to perform an acid wash in cases where the cation that is co-adsorbed with the gold is the same as that introduced with the pretreatment reagents.

As discussed, it is presumed that a large percentage of the cyanide requirement in the pretreatment is for the neutralization of residual acid from the acid wash. It is anticipated that the hydroxide in the pretreatment step can be utilized better if the pretreatment step is split into a separate hydroxide pretreatment (to neutralize the acid), followed by a cyanide pretreatment (to solubility the gold). The carbon

used in the elution experiments in this study was loaded from gold solutions containing no calcium. No acid treatments were thus conducted and no hydroxide was added to the pretreatment solutions.

3.5 INTER-RELATIONSHIP OF EFFECTS ON GOLD EQUILIBRIUM

If the effects of cyanide, temperature, cation concentration and pH on the equilibrium adsorption of gold cyanide are independent of each other, it follows from the law of mass action that the value of A in the Freundlich expression can be written as a product of functions (f_1 to f_5) as follows :

$$A = A_0 \cdot f_1(Q_N) \cdot f_2(C_N) \cdot f_3(\text{pH}) \cdot f_4(C_K) \cdot f_5(T) \quad [3.11]$$

(A_0 is a constant if all other possible effects are kept constant.) If all variables except one are kept constant in equation 3.11, those constant influences can all be combined in the value of A_0 and the functional form of the relationship between A and the one variable can be determined as was done in the previous section. However, if equations 3.5 and 3.6 are compared, it is clear that the dependency of A on the pH is a function of the temperature. Although the functional relationship between A and pH was the same at different temperatures, the parameters had to be changed. It can thus be expected that more of the effects will be dependent on temperature and that Equation 3.11 cannot be used to extrapolate from one temperature to another, except if all the other variables remain the same.

By combining equations 3.5, 3.7, 3.8 and 3.11 for a constant temperature and cyanide-age, equation 3.11 changes to :

$$A = A_0 (C_N+1)^f (C_K+1)^p \exp(p_h \cdot \text{pH}) \quad [3.12]$$

In equation 3.12 the value of A_0 accounts for all the other effects that are kept constant. To investigate the inter-relationship between the concentration of cyanide, potassium and pH, equation 3.12 was fitted to all the data from experiments 45, 47 and 48 collected at room

temperature. The values of the constants in equation 3.12 were calculated as :

$$A_o = 87.66, \quad f = -0.104, \quad p = 0.0455, \quad \text{and} \quad p_h = -0.1636.$$

Table 3.5 compares the values of the measured A-values to those predicted by equation 3.5 with the above parameters. The average error was calculated as 3 % and the maximum error as 7 %. If the effects of CN^- , K^+ and pH were totally independent of each other, the values of the parameters would have remained the same as those determined previously. It therefore appears that interaction between the different effects does exist. This interaction is however small enough to permit the use of equation 3.12 within acceptable limits of error. Because of the temperature dependency of, for example, the pH, the values of the parameters will not be the same at other temperatures.

3.6 DECOMPOSITION OF CYANIDE

For the AARL elution process, most of the adsorption and reaction of cyanide occurs in the pretreatment step, whereas for the Zadra process, the cyanide is decomposed simultaneously with the elution of the gold. Yet, in both processes, both the presence and the reactions of cyanide are used to enhance the elution of the gold. It was thus important to investigate the decomposition of cyanide and some of the factors influencing it.

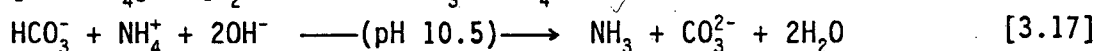
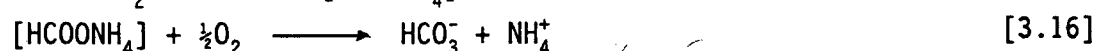
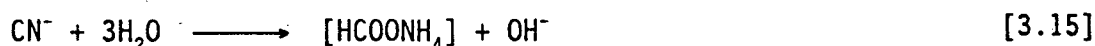
When Bernardin (1970) tried to measure the equilibrium adsorption of cyanide onto activated carbon under atmospheric conditions, he established that the adsorbed cyanide is oxidized by oxygen in solution and on the carbon. His isotherm results showed that in the presence of air or oxygen, the capacity of carbon for cyanide was respectively 3 and 6 times higher than in the presence of nitrogen. This is in contrast with the findings of the developers of the Kamyr C.I.L.O. process (Elmore *et al.*, 1988) in which pure oxygen is injected into a carbon-in-leach operation. They reported the consumption of cyanide to be lower than that of a conventional, aerated C.I.L. operation. This was accredited to shorter treatment time and the exclusion of CO_2 from the solutions in a

C.I.L.O. operation. The CO_2 content of air is believed to increase the consumption of cyanide by the evolution of prussic acid :



The last reaction will also account for a large portion of the cyanide consumption in the pretreatment step of the AARL elution process if it is preceded by an acid wash (Davidson, 1986a). Under normal, alkaline gold elution conditions, cyanide is decomposed via several reactions (Hoecker and Muir, 1987). Of these, the following reactions are considered (Nicol, 1986) to be the most important :

(a) Hydrolysis



(b) Oxidation



The oxidation reaction, equations 3.18 and 3.19, is catalyzed by the presence of activated carbon. Nicol (1986) showed that at room temperature, the decomposition of cyanide was very slow unless carbon was present. He further observed that the effect of the presence of carbon decreased with an increase in temperature. This suggests that the hydrolysis reaction is dominant at high temperatures, whereas the catalytic oxidation reaction is more significant at low temperatures. This shift in reaction mechanism occurs because of the decreased rate of the oxidation reaction at the very low dissolved oxygen concentrations (Muir *et al.*, 1988) at high temperatures. Muir *et al.* (1988) regarded the hydrolysis reaction as the main cause for the loss of cyanide during Zadra or AARL elution procedures. They found the rate of hydrolysis to be more temperature sensitive than the rate of oxidation, but independent of pH higher than 10.5. Measurement of the decomposition rate of cyanide revealed first order kinetics for both the hydrolysis and oxidation reactions (Hoecker and Muir, 1987). Table 3.6 summarizes the rate

constants and activation energies (E_a) determined (Muir et al., 1988) for these reactions in the absence of carbon at a pH of 10.5.

Figure 3.27 shows the effect of temperature on the decomposition of cyanide in the absence of carbon. The first order rate constants determined from these curves were plotted in Figure 3.28. As it is impossible to isolate the oxidation and hydrolysis reactions, the plots in Figures 3.27 and 3.28 represent combinations of these two reactions. The rate equation was calculated as :

$$k_N = 4.17 \times 10^7 \cdot \exp(-87143/R_o T) \quad [3.20]$$

The activation energy of 87143 J/mol compares favourably with the activation energy for the hydrolysis reaction as reported (Muir et al., 1988) in Table 3.6. This implies that mainly the hydrolysis reaction occurred in the above experiments which were all conducted at temperatures of higher than 50 °C.

In the presence of carbon, the rate constant of the oxidation reaction was found to be a direct function of the carbon concentration (Muir et al., 1988). No distinction was however made between adsorption and oxidation of the cyanide. It is expected that adsorption would have accounted for a large percentage of the "reacted" cyanide, because the experiments have been conducted at room temperature to minimize hydrolysis of the cyanide. The carbon concentration and particle size were reported to have the largest influence on the oxidation of cyanide. Although the concentration of carbon proved to be just as important in the case of carbon BTX, Figure 3.29 shows that the oxidation of cyanide was insensitive to the particle size of the carbon. The mixing speed in batch reactors had a much more prominent effect on the decomposition of cyanide in contact with carbon BTX (see Figure 3.30). The results of Figures 3.29 and 3.30 imply (Levenspiel, 1972) that resistance to film diffusion is the rate controlling step and that resistance to pore diffusion can be neglected.

Controversy seems to exist on the relative contributions of the adsorption and the decomposition of cyanide on activated carbon to the total consumption thereof. Hughes et al. (1984) reported the adsorption

of different anions to be in the order $F^- < Cl^- < Br^- < I^- < CO_3^{2-} < CN^- < Ag(CN)_2^- < Au(CN)_2^-$. It follows that the adsorption of cyanide should be comparable to that of $Ag(CN)_2^-$. No mention was however made of the decomposition of cyanide and it is doubted if it was taken into account. Muir *et al.* (1988) claim that the "poor" adsorption of CN^- at room temperature (0.1 mg/g) is in accordance with the adsorption of other simple anions like OH^- and Cl^- . Adams (1990b), however, attributes 35% of the cyanide loss, under the same conditions, to adsorption onto the carbon (2 mg/g). At high cyanide concentrations, as will be the case in the AARL pretreatment, he expects that the relative importance of the adsorption reaction will be reduced. Much of the disagreement on the ratio of adsorption to reaction of cyanide that is in contact with carbon can be attributed to the variation in the characteristics of activated carbons. As illustrated in Chapter 2 under the "Consumption of oxygen", carbons A and BTX consumed different amounts of oxygen in achieving identical cyanide-ages. As O_2 is directly involved in the oxidation reaction of cyanide, it follows that large variations in the ratio of adsorbed to oxidized cyanide will occur on different carbons. However, it can be assumed that the adsorption of cyanide, like $Au(CN)_2^-$, will decrease with an increase in temperature and that it will become negligible under typical elution conditions.

Another factor that can lead to an apparent increase in the "consumption" of cyanide in the pretreatment step of an AARL elution process, is dilution. Even though the carbon bed is drained before the pretreatment reagents are pumped into the bed, a large volume of liquid is retained in the pores of the carbon. By using the physical properties of carbon BTX, it was calculated that for pretreatment with 1 bed volume of reagent (Davidson, 1986a), the pore liquid will dilute the pretreatment reagents to 65 % of their original concentrations.

The concentration profile of cyanide in the eluate of a Zadra elution was plotted in Figure 3.31. As no electrowinning of the recovered gold was performed, the eluant was not recycled and the carbon was therefore supplied with an eluant with a constant cyanide concentration. It is evident from the profile in Figure 3.31 that the conversion of the cyanide declined with time (constant conversion of a reactant in a plug flow reactor results in a constant concentration of the reactant in the

solution leaving the reactor, Levenspiel, 1972). This means that the activity of the carbon towards cyanide was decreased as a result of the reaction of the cyanide. The effect of the cyanide-age of carbon on its activity towards cyanide was further investigated in Figure 3.32 where one sample of carbon was repeatedly contacted (Runs no.1 to 5) with "fresh" solutions with the same initial cyanide concentrations. The reaction rate constant and initial cyanide-age were calculated for each run from the initial and final cyanide concentrations. These reaction rate constants were plotted against the cumulative cyanide-age in Figure 3.33. As expected from Figure 3.32, the rate of the decomposition of the cyanide decreased with an increase in the cyanide-age of the carbon. The following relationship was found to describe the change in the rate constant :

$$k_N = c_1 / (Q_N + 1)^{c_2} \quad [3.21]$$

where c_1 and c_2 are constants that will depend on temperature and other influences.

3.7 ADSORPTION AND DESORPTION OF CATIONS

From Experiment 50 it followed that the concentration of potassium in the pretreatment solution decreased from 12300 to 7380 g K⁺/m³ after it was added to the gold loaded carbon. The carbon was however only blotted with filter paper after it was removed from the adsorption solution and the residual water in the pores could be responsible for the dilution of the pretreatment reagents.

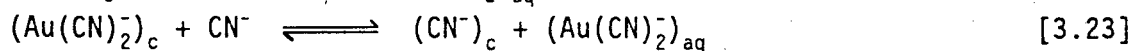
In Experiment 71 a sample of dry carbon BTX was added to a KCl solution with the same initial potassium concentration as above. This led to a slight increase in the concentration of potassium in the solution. The increase in the potassium concentration was attributed to the fact that the carbon must have contained some adsorbed potassium that was desorbed when it was brought into contact with water. When the pretreatment step of Experiment 50 was repeated with dry carbon BTX (Experiment 72a), it was found that the potassium concentration decreased from 12481 to 10213 g K⁺/m³ and the cyanide concentration from 7435 to 5841 g CN⁻/m³.

The observation that more potassium is adsorbed from a KCN than a KCl solution indicates that K^+ is co-adsorbed with anions and does not adsorb on its own. (It was shown (Tsuchida, 1984) that the adsorption capacity of carbon for cyanide is much higher than for chloride.) The molar ratio of potassium to cyanide consumed in the above experiment was calculated as 1 : 1.03. When the pretreatment was conducted at a higher temperature (Experiment 72b), this ratio decreased to 1 : 1.37. This agrees with the finding that more decomposition and less adsorption of cyanide occurs at higher temperatures.

Figure 3.34 shows elution profiles for K^+ at different flow rates and temperatures, but identical KCN pretreatment conditions. It follows that the elution of potassium is independent of temperature and flow rates up to 37 bed volumes per hour. As expected from the adsorption experiments with K^+ , the elution of potassium is affected, however, by the nature of the anion in the pretreatment reagents. This can be seen in Figure 3.35 where the elution profiles of K^+ after a KCl and KCN pretreatment were compared. The concentration of K^+ in the eluate was higher for KCN than for KCl for most of the run, because of the lower adsorption of K^+ from KCl than KCN solutions.

3.8 MECHANISM OF GOLD ELUTION

Nicol (1986) mentioned that the desorption of gold is thought to involve the competitive adsorption of cyanide and aurocyanide on activated carbon. Likewise, Tsuchida (1984) assumed that the desorption of gold from carbon can be expressed by the following equilibria :



Measurements (Tsuchida, 1984) of the activity coefficients of CN^- and $Au(CN)_2^-$ revealed that in an organic rich environment the activities of CN^- and $Au(CN)_2^-$ were respectively $10^2 - 10^4$ and 20 times higher than in water. It was claimed that in organic solvent/water mixtures the much higher increase in activity of the CN^- than the $Au(CN)_2^-$ will shift the above equilibria to favour the desorption of the gold. The decreased

kinetic activity of eluted carbon was attributed to -CN being a poor leaving group, as well as to the deactivation of the active sites by the oxidation of cyanide by chemisorbed O_2 to CO_3^{2-} and NH_4^+ (Tsuchida, Ruane and Muir, 1985). In testing the effect of various anions on the elution of gold, it was found that anions with higher nucleophilicities were more capable of desorbing gold. This was interpreted as an indication that the active sites are able to undergo nucleophilic substitution reactions.

Adams et al. (1987) and Adams and Fleming (1989) explained the desorption of $Au(CN)_2^-$ from activated carbon at high pH on a similar basis to the elution from a polymeric adsorbent with phenolic hydroxyl functional groups. According to them, the weakly acidic functional groups, such as phenolic hydroxyl, are deprotonated by OH^- , leaving the surface more negatively charged and hydrophilic :



Such a surface will be less compatible with the aurocyanide ion-pair, thus favouring desorption. This mechanism is supported by the observation (Cho and Pitt, 1979) that an increase in pH results in a more negative zeta potential of the activated carbon.

From the above findings and the results presented in this chapter, it is evident that cyanide can promote the elution of gold by 3 different mechanisms. These are (1) competitive adsorption (which is regarded here as being similar to ion-exchange), (2) reaction with the adsorbed gold cyanide species and (3) reaction with the carbon functional groups. As discussed previously, the reaction of cyanide with adsorbed AuCN or Au is necessary for the desorption of these irreversibly adsorbed species. However, in the case of carbon BTX it was proved that all the gold was present as $Au(CN)_2^-$. In order to determine the relative importance of mechanisms (1) and (3), elution runs were carried out on 2 samples of carbon with equal cyanide-ages, but with different ratios of adsorbed to decomposed cyanide. The cyanide-age of carbon that was exposed to a cyanide solution will increase with increases in time of contact, the initial concentration of cyanide and the temperature of the solution. An increase in temperature will, however, result in a decrease in the adsorption and an increase in the decomposition of cyanide. By

performing pretreatments at different temperatures, the ratio of adsorption to decomposition of cyanide could thus be varied. Even though the carbon samples used in Figure 3.36 had identical cyanide-ages of 7 mg CN⁻/g, the pretreatments were conducted at 20 °C and 100 °C respectively. It is clear that much better elution of gold was obtained after the pretreatment at the higher temperature, where very little adsorption of cyanide would have occurred. A mechanism of displacement of aurocyanide by cyanide during conventional cyanide pretreatment at elution temperatures can thus be ruled out to a large degree. As it was proved that the cyanide in the pretreatment step does not displace or alter the gold cyanide species, it was postulated that the cyanide that is decomposed on the surface of the carbon during the pretreatment stage changes the functional groups on the surface in such a way that the surface becomes less receptive for adsorption. Adams and Fleming (1989) presented the following examples of possible reactions that can occur between cyanide and the functional groups present on the surface of the carbon :



($K \approx 11000$)



The above reactions would increase the negative charge density on the surface and render it less receptive for Au(CN)₂⁻. Even though this change in the carbon surface would already occur during the pretreatment step, the high concentration of cations (Mⁿ⁺) would favour the formation of Mⁿ⁺(Au(CN)₂⁻)_n ion-pairs on the carbon surface and thereby restrict the desorption of gold during this stage. Once less cations are available during the elution stage, the Au(CN)₂⁻ will be desorbed from the deactivated carbon surface.

Because of the high cyanide concentration in the pretreatment reagent of an AARL elution, the carbon is expected to be deactivated towards cyanide

to such a high degree that little more cyanide will be decomposed on the carbon during the elution step. Furthermore, this will lead to a low sensitivity of the gold towards variations in the cyanide concentration in the elution step. This ties in with the observation by Davidson (1986a) that an increase in the cyanide concentration from 3% to 10% in the pretreatment had little effect on the gold elution efficiency. At cyanide concentrations below 3% the gold elution profile was much more sensitive to the pretreatment cyanide additions. The carbon had therefore reached its maximum deactivation at a cyanide concentration of 3% in the pretreatment and was unaffected by higher cyanide concentrations. A similar result was obtained by Laxen et al. (1982) who found that a reduction in pretreatment time from 8 hr to 2 hr plus a 4 times weaker pretreatment solution had no detrimental effect on the elution.

3.9 SUMMARY OF FINDINGS

Functional relationships were found between the more important effects on elution and the gold cyanide equilibrium. Even though the parameters in these functionalities might differ under different conditions, the nature of the relationships would remain unchanged.

Cyanide was found to be involved in the gold elution reaction as follows :

- (1) If an irreversibly adsorbed species like $\text{Au}^{(0)}$ or AuCN is present on the carbon, the cyanide in the pretreatment step will convert this species to the soluble $\text{Au}(\text{CN})_2^-$ species.
- (2) Competitive adsorption of cyanide with aurocyanide will increase the elution of the gold, but this was found to play a minor role at elevated temperatures.
- (3) The most important effect of cyanide is the reaction thereof with the functional groups on the carbon surface to passivate the surface for the adsorption of anionic metal cyanides and thereby promote the elution of the gold cyanide.
- (4) Free cyanide in the elution step of an AARL elution is of lesser importance than the cyanide in the pretreatment step. During a

Zadra elution, however, the passivation of the carbon by cyanide occurs during the elution and will have to be accounted for when modelling the process.

The elution of gold cyanide is suppressed by the presence of cations (M^{n+}) through the formation of $M^{n+}(Au(CN)_2^-)_n$ on the carbon. The horizontal position of the gold peak in an AARL elution profile was found to be a function of the elution of the cations from the carbon bed.

High temperatures and cyanide pretreatments, i.e. conditions favourable for desorption, decreased the sensitivity of the elution of gold cyanide to flow rate and the radial distribution of the gold through the carbon particles. This implies that the resistance to mass transfer was less profound under strong elution conditions.

The three most important sub-processes of the gold elution process were defined as the changes in cyanide, potassium and gold concentrations. As the changes in cyanide and potassium concentrations directly affect the elution of the gold cyanide, a kinetic model for the elution of the gold also has to account for the other two sub-processes. The next three chapters are therefore devoted to the development of mathematical models to describe each of these sub-processes.

Table 3.1
Dimensions of columns.

Column	Glass	Steel
Height [m]	0.170	0.825
Bed height [m]	0.143	0.749
h/d ratio	11.57	7.49
Flow area [m ²]	1.2x10 ⁻⁴	7.854x10 ⁻³
Bed volume [cm ³]	17.16	5883

Table 3.2
Accuracy of predicted Freundlich isotherm exponents for equilibrium gold adsorption on carbon BTX.

$$n_{\text{pred}} = -0.002688.A + 0.2902$$

T [°C]	A	n	n _{pred}	% error
22	31.49	0.204	0.206	1.0
30	25.79	0.210	0.221	5.2
40	21.84	0.251	0.232	-7.5
60	13.43	0.247	0.254	2.9

Table 3.3
Relationships between A and pH determined from published data.

Investigators	Metal	pH range	Linear relationship between
Cho & Pitt (1979)	Ag	8-11	ln(Q _e) vs. ln(pH) or Q _e vs. pH
Davidson (1974)	Au	4-11	ln(A) vs. ln(pH)
McDougall et al. ('80)	Au	1-12	ln(Q _e) vs. ln(pH)
Adams et al. (1987)	Au	2-14	ln(K) vs. ln(pH)

Table 3.4

Typical metal loadings encountered on activated carbon in different stages of the CIP circuit (Davidson, 1974). (All values in ppm).

Element	Original carbon	Loaded carbon	Acid-washed loaded carb.
Na	18500	4500	-
K	10400	1900	-
Ca	640	4800	410
Mg	300	100	-
Au	0	3300	3500
Ag	<10	45	25
Fe	1500	1500	1600
Ni	10	2500	290
Cu	20	240	170
Co	4	2	-
Zn	120	380	80

Table 3.5

Determination of accuracy of predictions of A-values with Equation 3.12.

Exp.no.	A Measured	A Calc.	% Error
45	15.59	15.16	2.8
	20.60	21.04	2.1
	31.55	31.63	0.3
	34.23	34.90	1.9
	38.05	39.13	2.8
47	20.63	22.03	6.8
	18.16	18.75	3.3
	15.70	16.06	2.3
	14.41	14.79	2.6
	14.01	13.77	1.7
	13.58	13.04	4.0
	12.99	12.26	5.7
	12.62	12.17	3.6
	12.05	11.81	2.0
11.84	11.22	5.2	
48	29.03	28.13	3.1
	31.52	31.29	0.7
	33.16	34.19	3.1
	37.98	37.46	1.4
	42.09	40.08	4.8

Table 3.6

Rate constants and activation energies (E_a) for the hydrolysis and oxidation reactions of cyanide in the absence of carbon at a pH of 10.5 (Muir et al., 1988).

T (°C)	Rate constants [$10^{-6}/s$]	
	Hydrolysis	Oxidation
50	0.30	1.10
60	1.81	1.51
80	4.81	4.70
103	32.80	
E_a [kJ/mol]	87	37

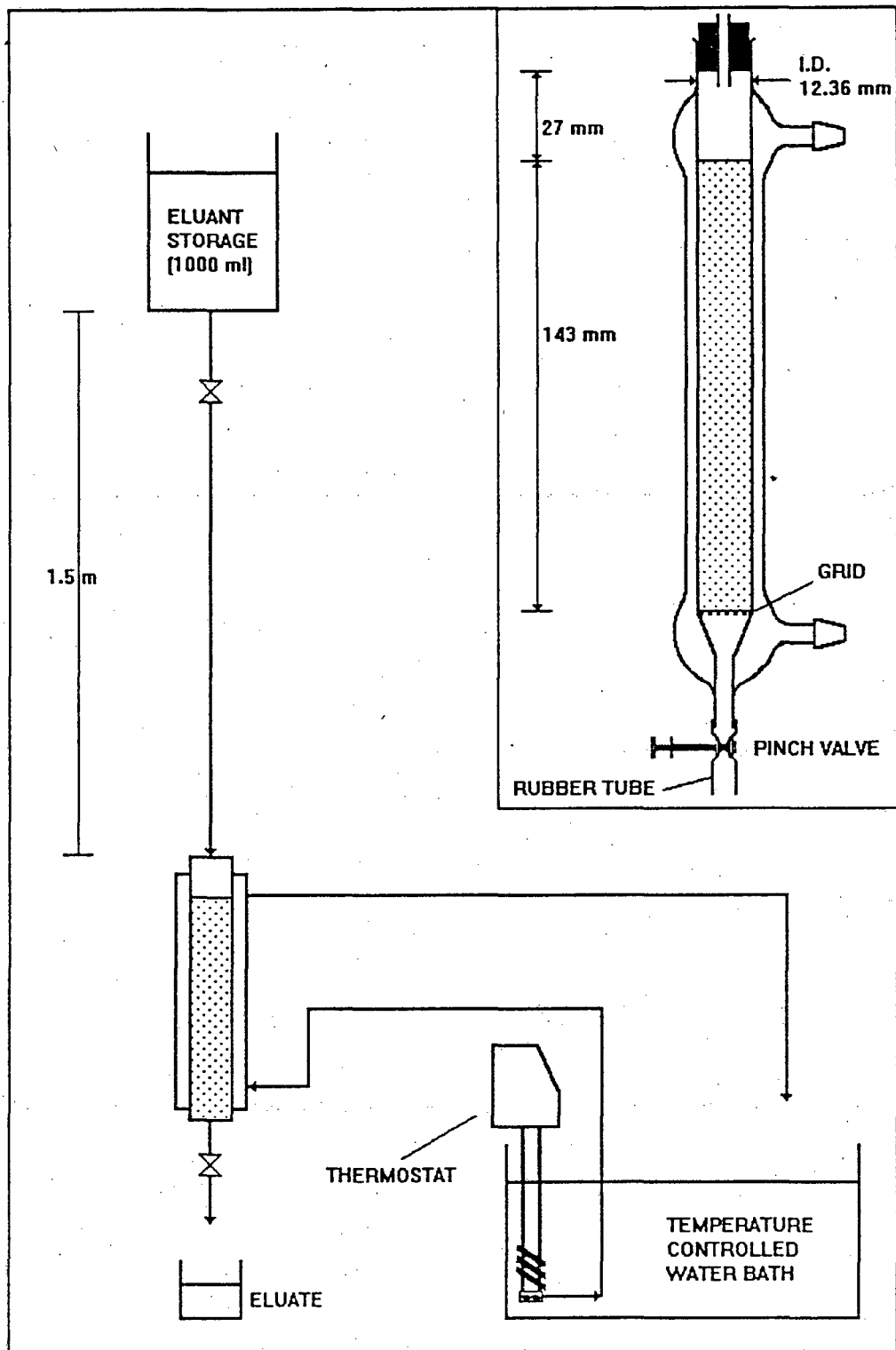


Figure 3.1 Experimental arrangement for elutions in glass column.

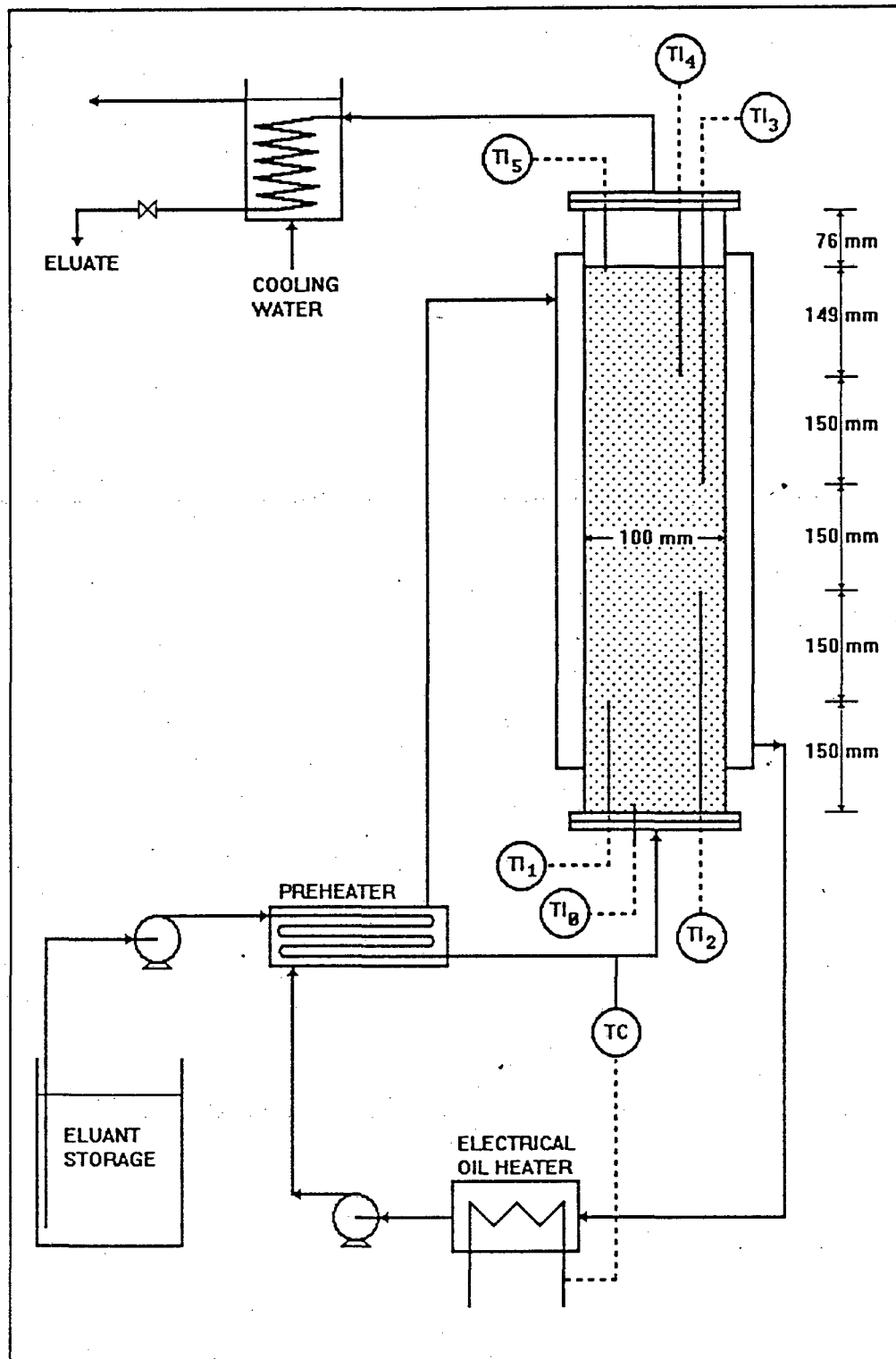


Figure 3.2
column.

Experimental arrangement for elutions in stainless steel

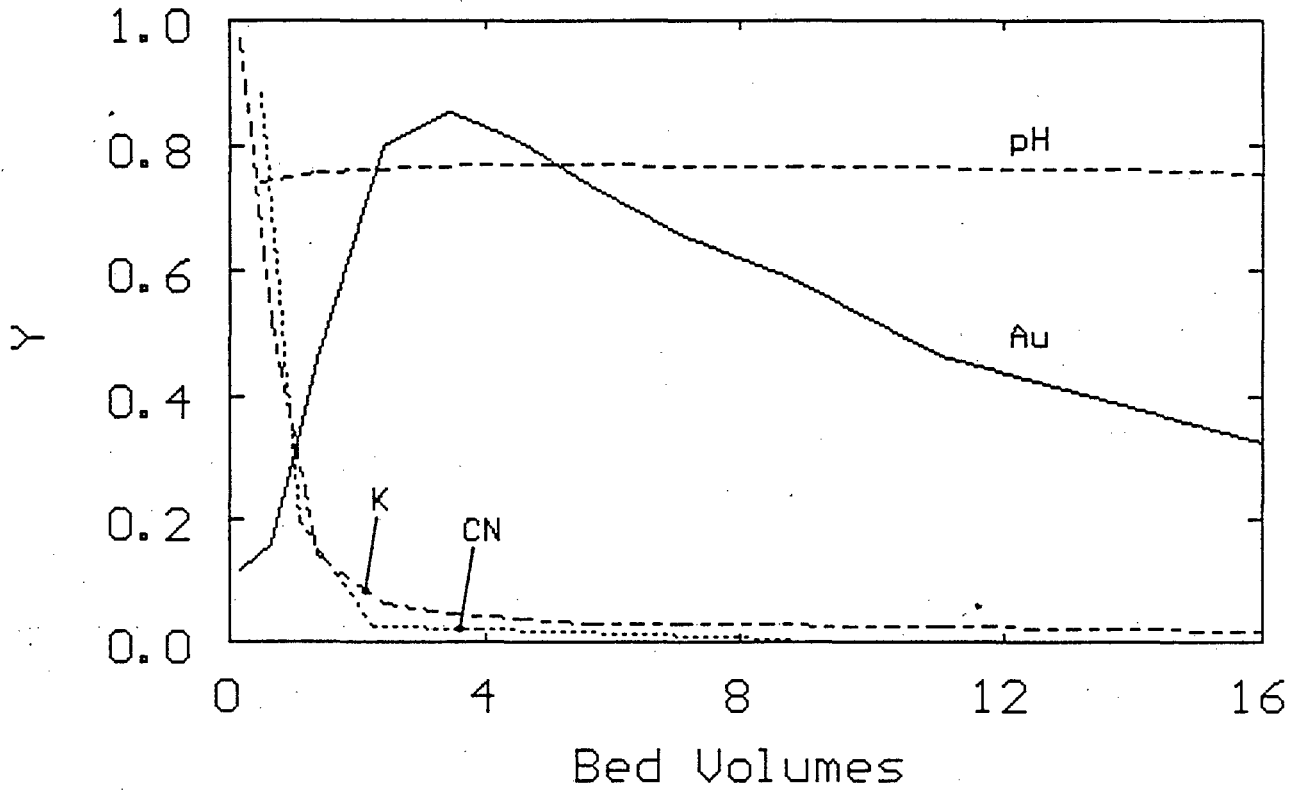


Figure 3.3 Normalized AARL elution profiles. $C_G = 140. \text{Y g.m}^{-3}$, $C_K = 3500. \text{Y g.m}^{-3}$, $C_N = 1500. \text{Y g.m}^{-3}$, $\text{pH} = 14. \text{Y}$. (Exp.40)

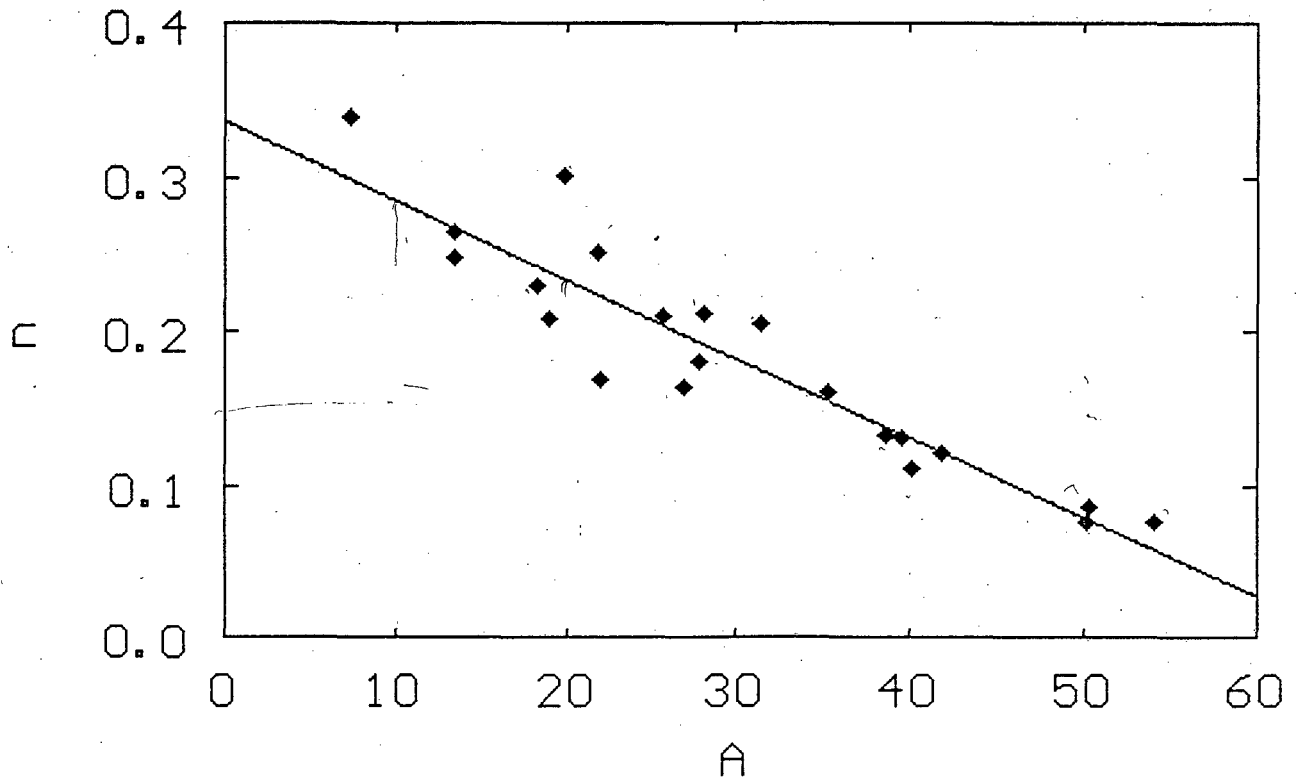


Figure 3.4 Freundlich isotherm parameters for the equilibrium adsorption of $\text{Au}(\text{CN})_2^-$ onto various carbons. (Exp.41)

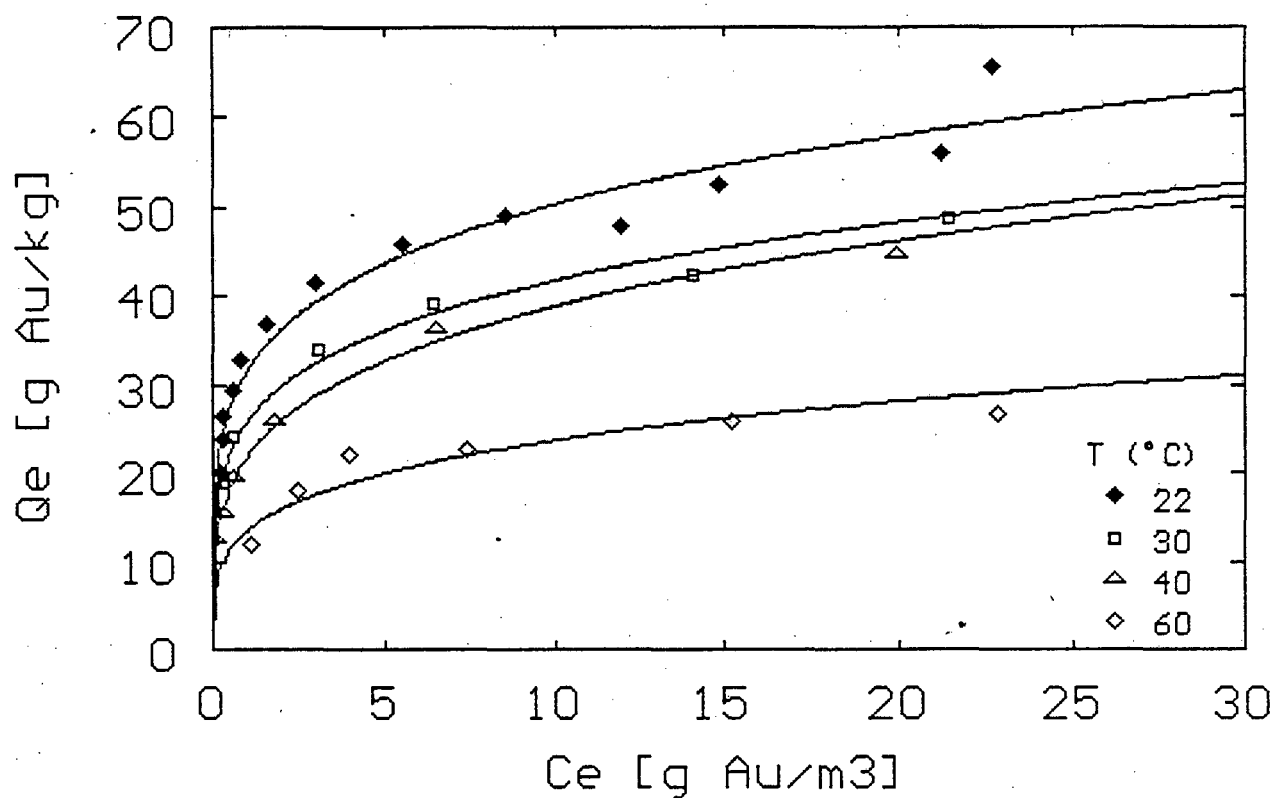


Figure 3.5 Equilibrium adsorption of $\text{Au}(\text{CN})_2^-$ onto carbon BTX at different temperatures. (Exp. 36, 42, 43 and 44)

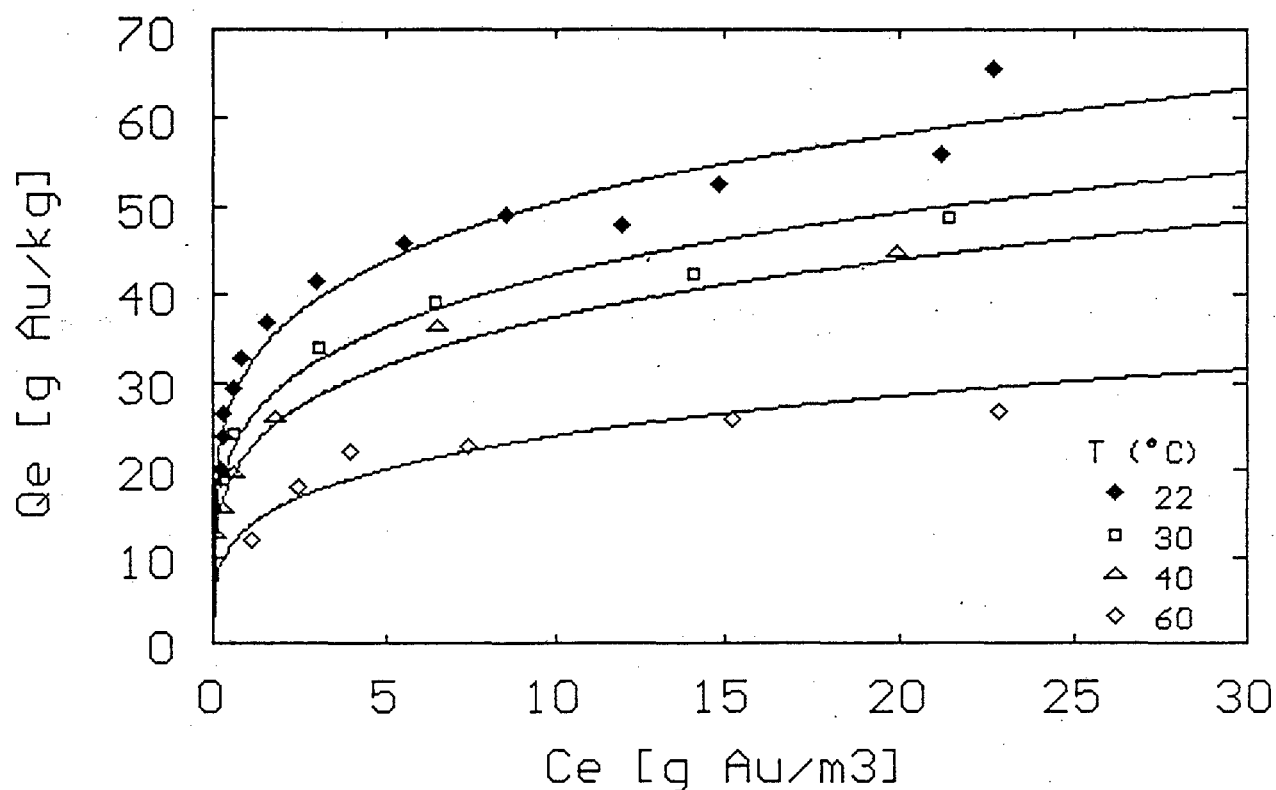


Figure 3.6 Equilibrium isotherms for the adsorption of $\text{Au}(\text{CN})_2^-$ onto carbon BTX. Curves calculated from average A-values with $n = -0.002688.A + 0.2902$. (Exp. 36, 42, 43 and 44)

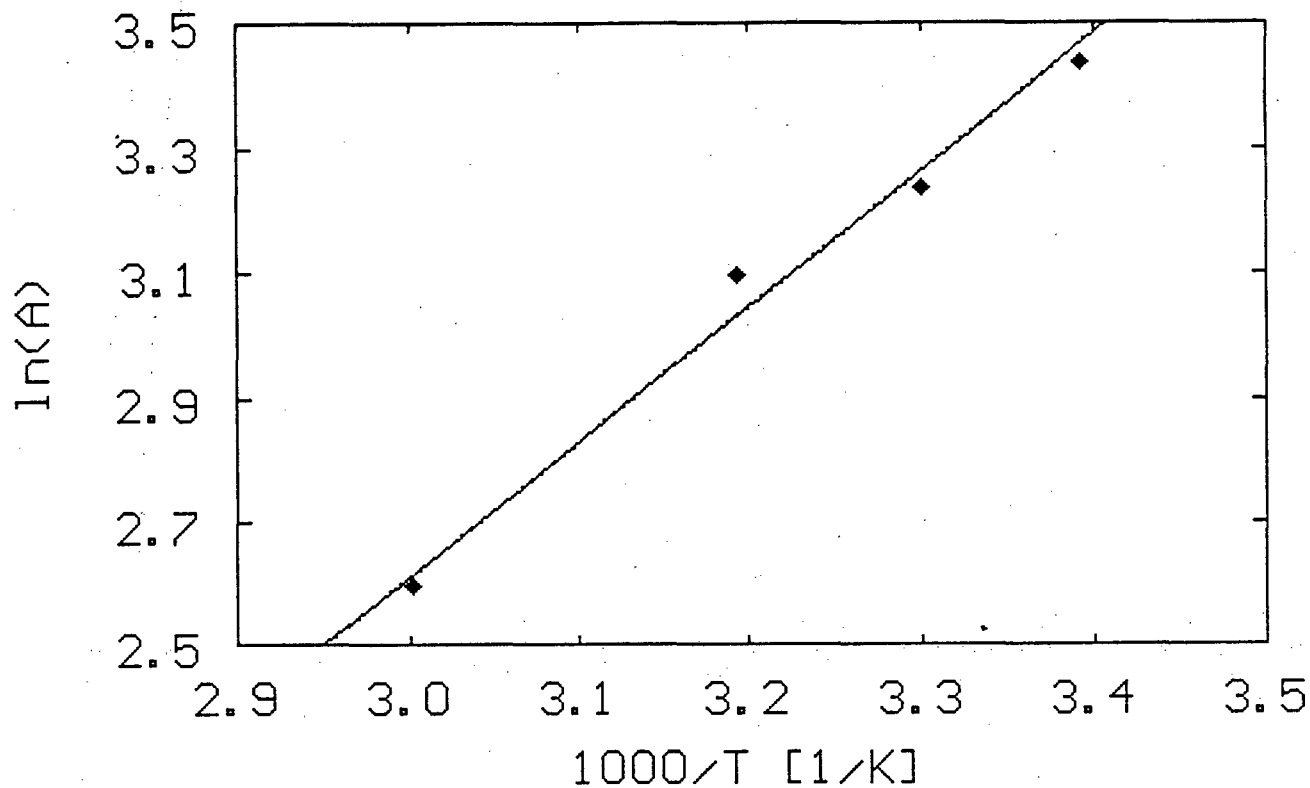


Figure 3.7 Effect of temperature on the Freundlich constant, A, for adsorption of $\text{Au}(\text{CN})_2^-$ onto carbon BTX. (Exp. 36, 42, 43 and 44)

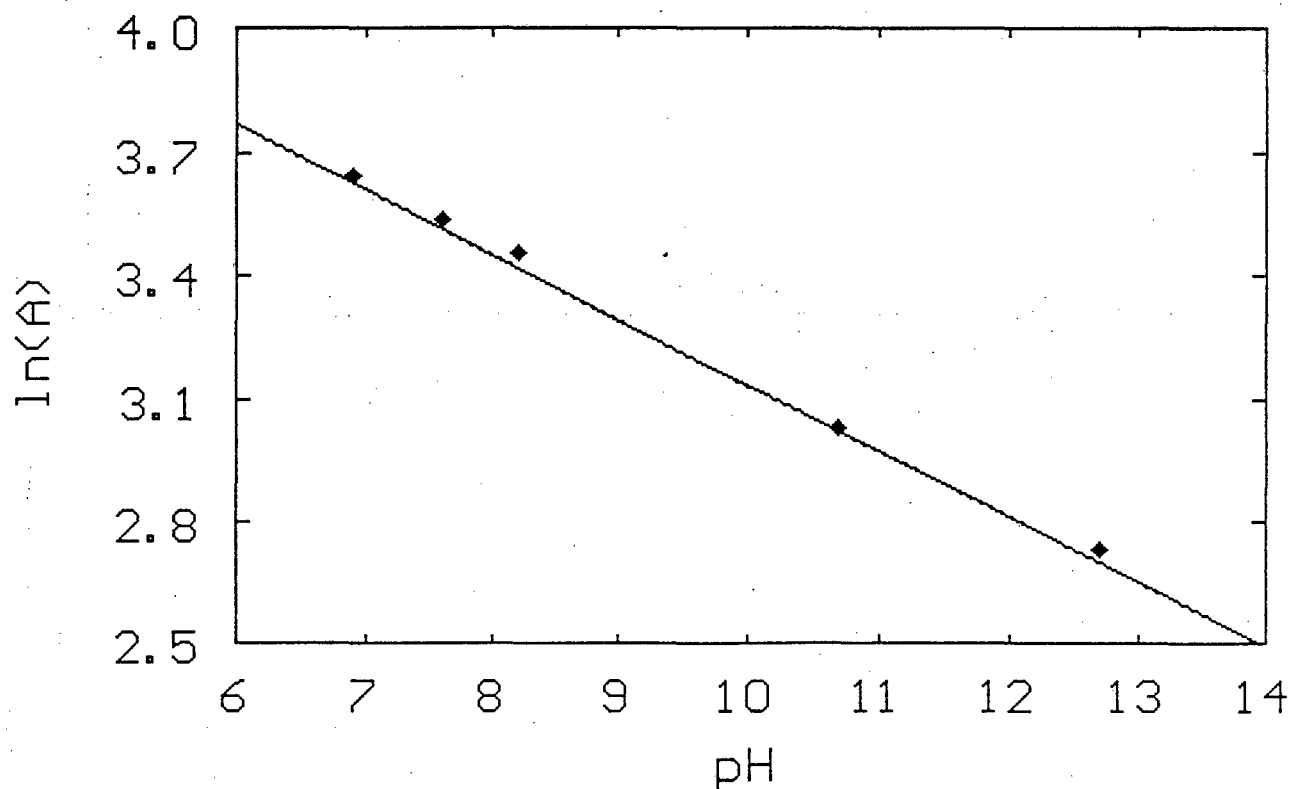


Figure 3.8 Effect of pH on equilibrium adsorption of $\text{Au}(\text{CN})_2^-$ onto carbon BTX at room temperature. (Exp. 45)

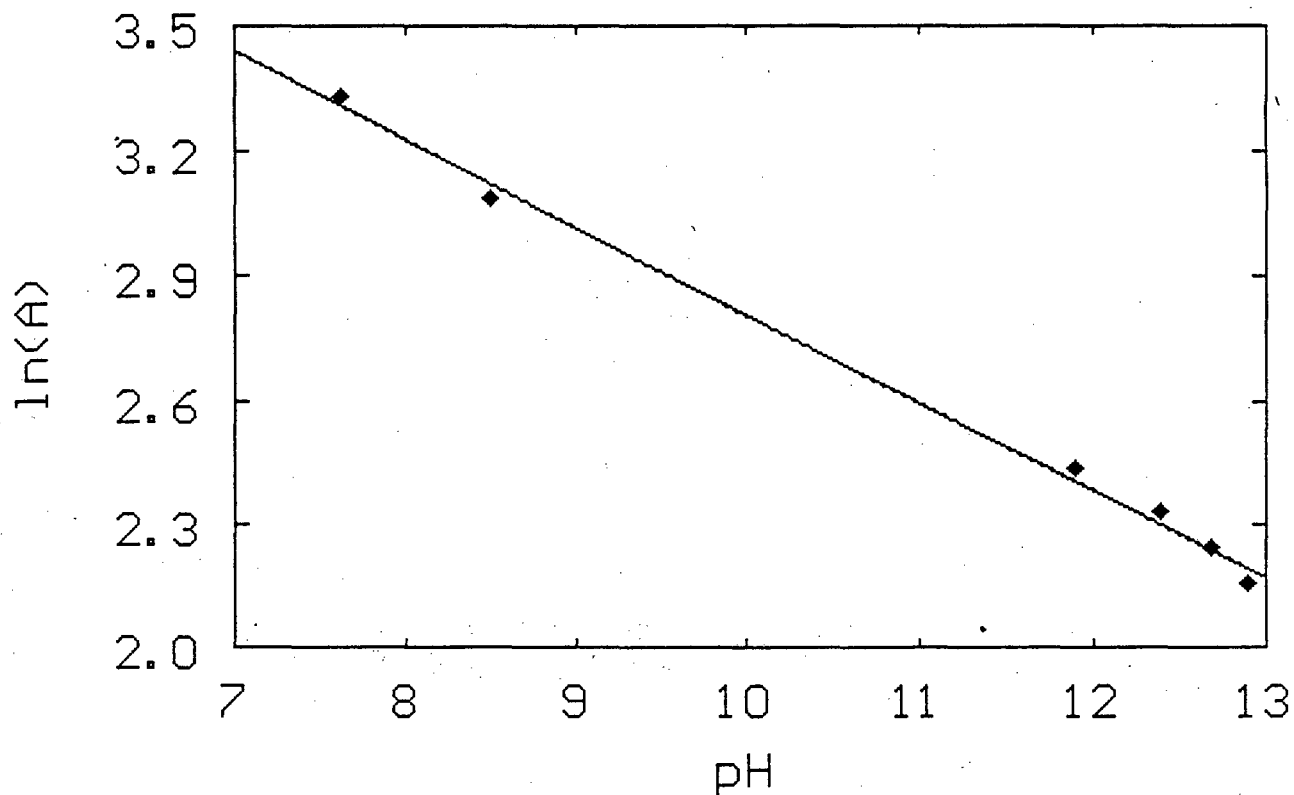


Figure 3.9 Effect of pH on equilibrium adsorption of $\text{Au}(\text{CN})_2^-$ onto carbon BTX at 40 °C. (Exp. 46)

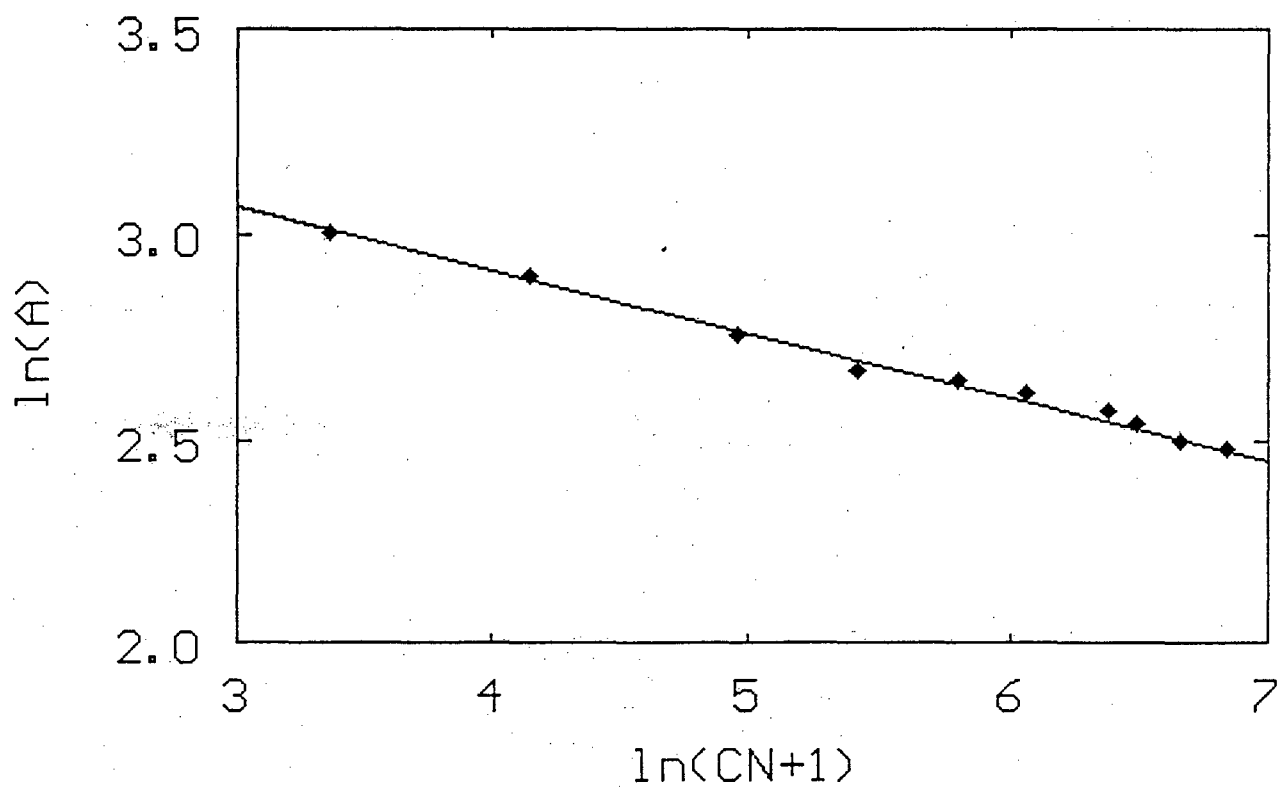


Figure 3.10 Effect of cyanide concentration on the equilibrium adsorption of $\text{Au}(\text{CN})_2^-$ onto carbon BTX. (Exp. 47)

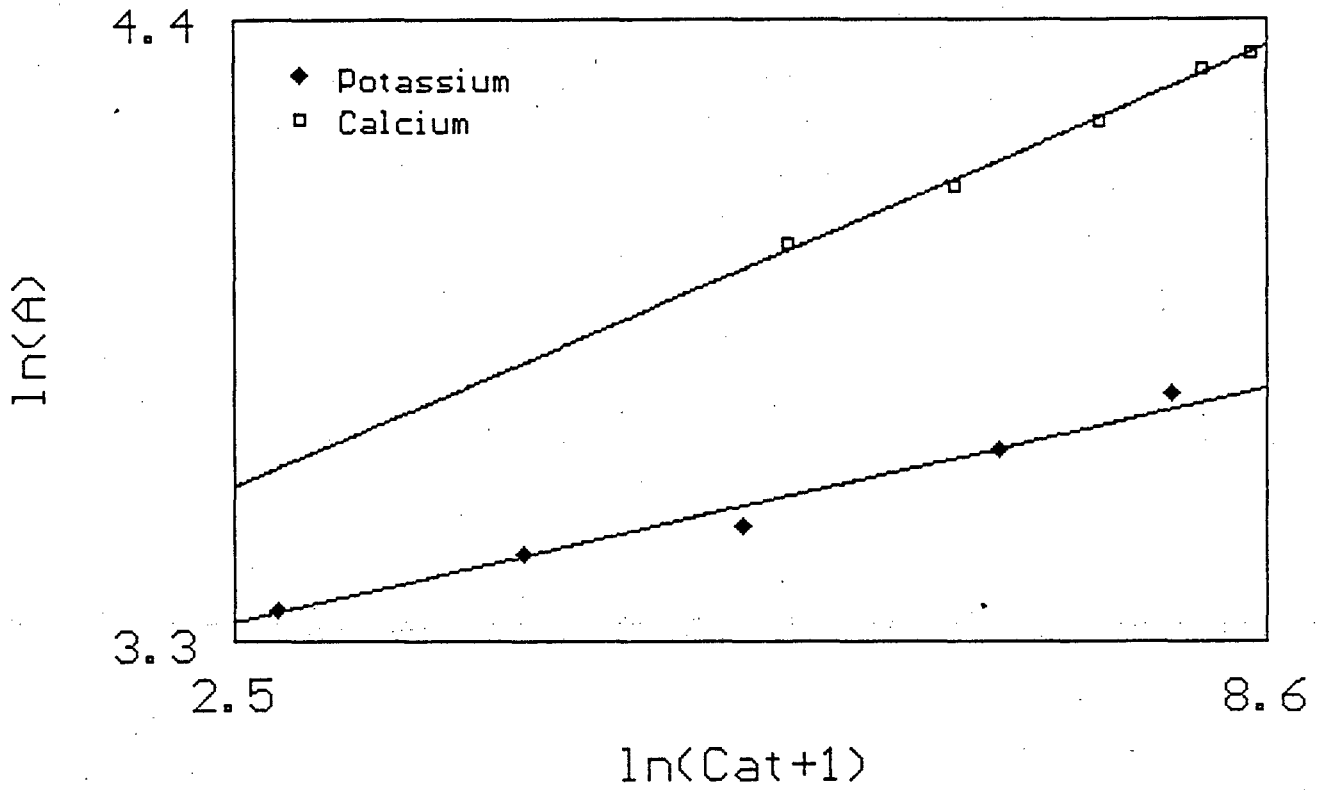


Figure 3.11 The effect of cations (Cat) on the equilibrium adsorption of $\text{Au}(\text{CN})_2^-$ onto carbon BTX. (Exp. 48 and 49)

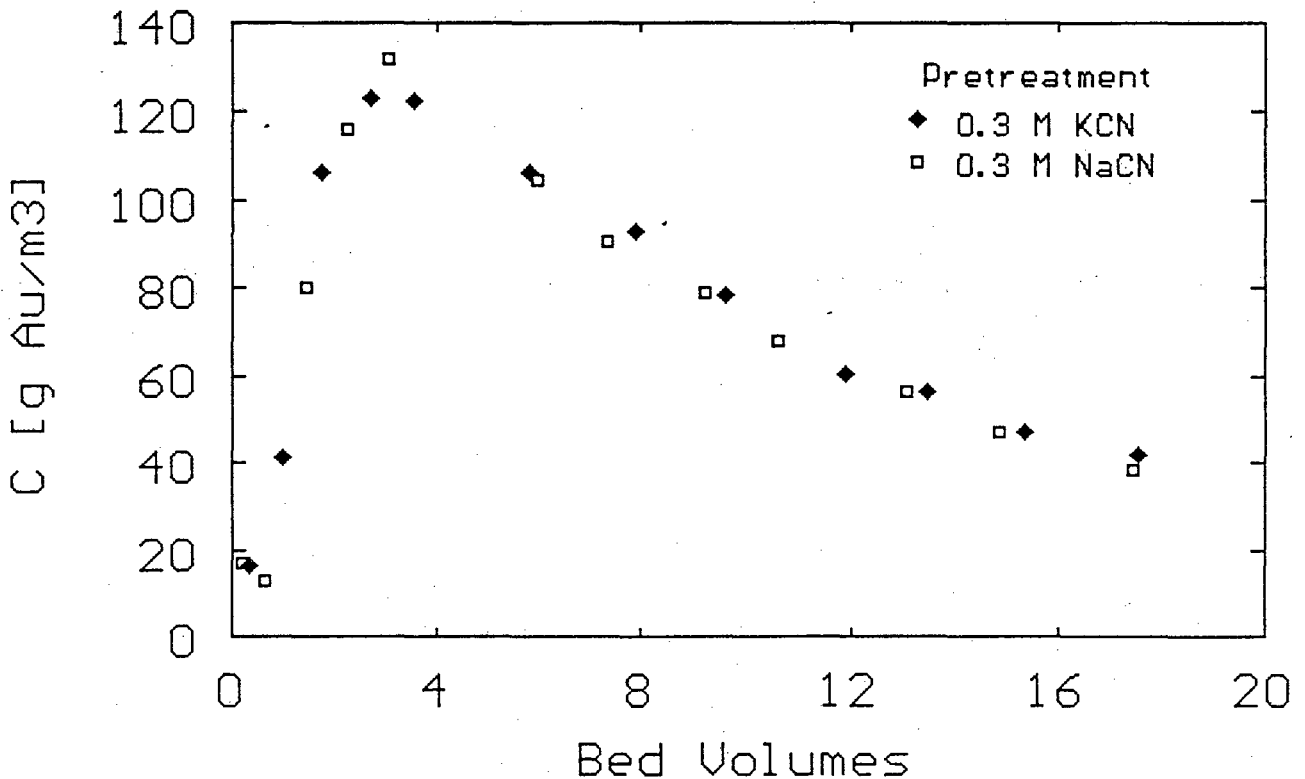


Figure 3.12 Gold elution profiles after pretreatments with equimolar NaCN and KCN solutions. (Exp. 50 and 51)

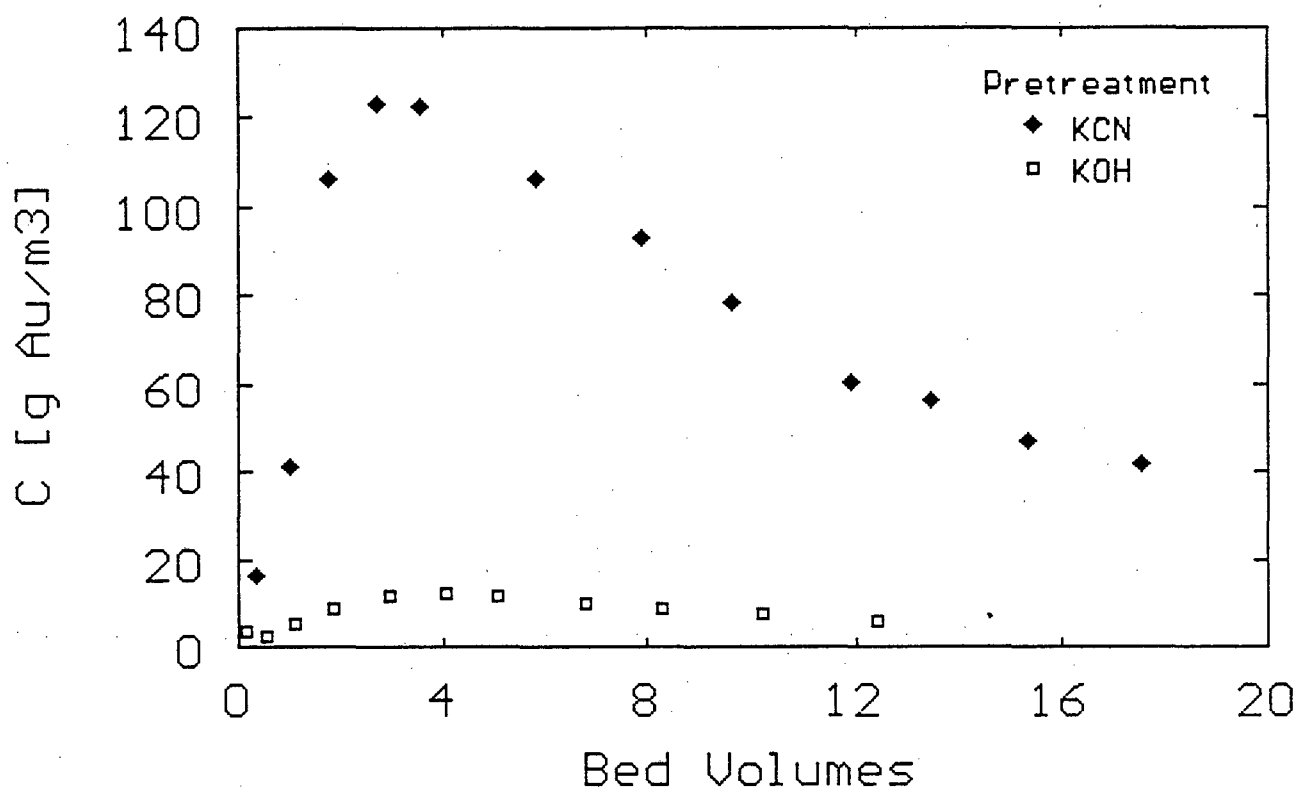


Figure 3.13 Gold elution profiles after pretreatments with KCN and KOH solutions with the same pH and potassium concentration. (Exp.50 and 52)

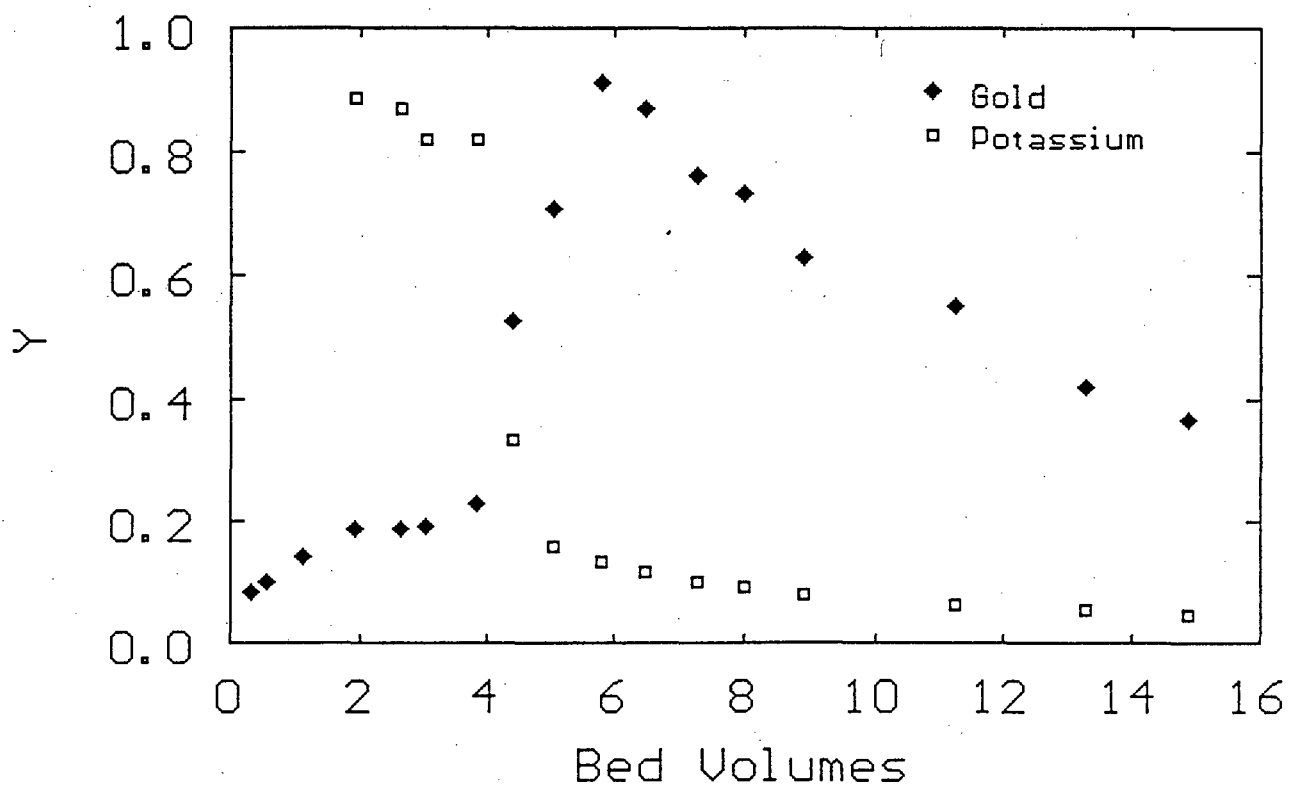


Figure 3.14 The prolonged effect of a cyanide pretreatment on the elution of gold cyanide. $C_G = 220.Y \text{ g.m}^{-3}$, $C_K = 2500.Y \text{ g.m}^{-3}$. (Exp.53)

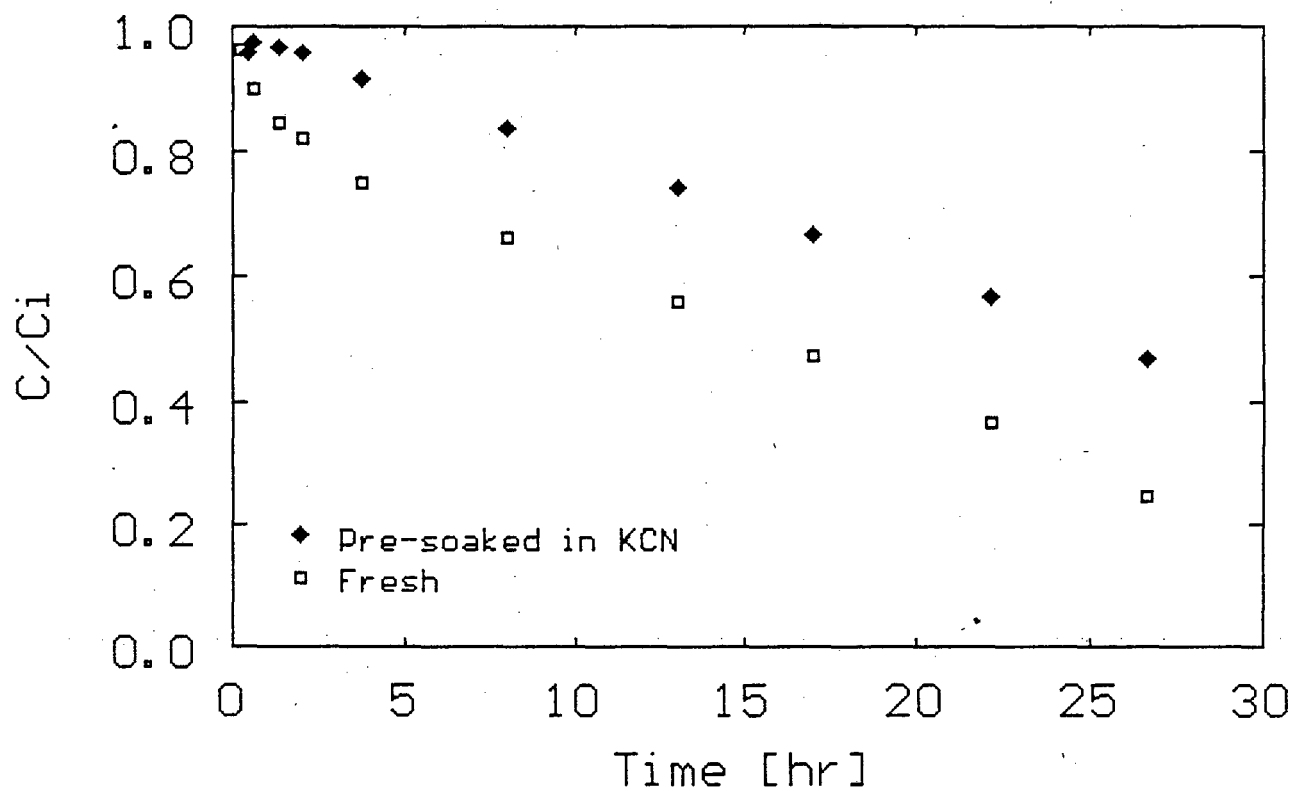


Figure 3.15 Illustration of the effect of the deactivation of carbon towards aurocyanide by cyanide. (Exp.54)

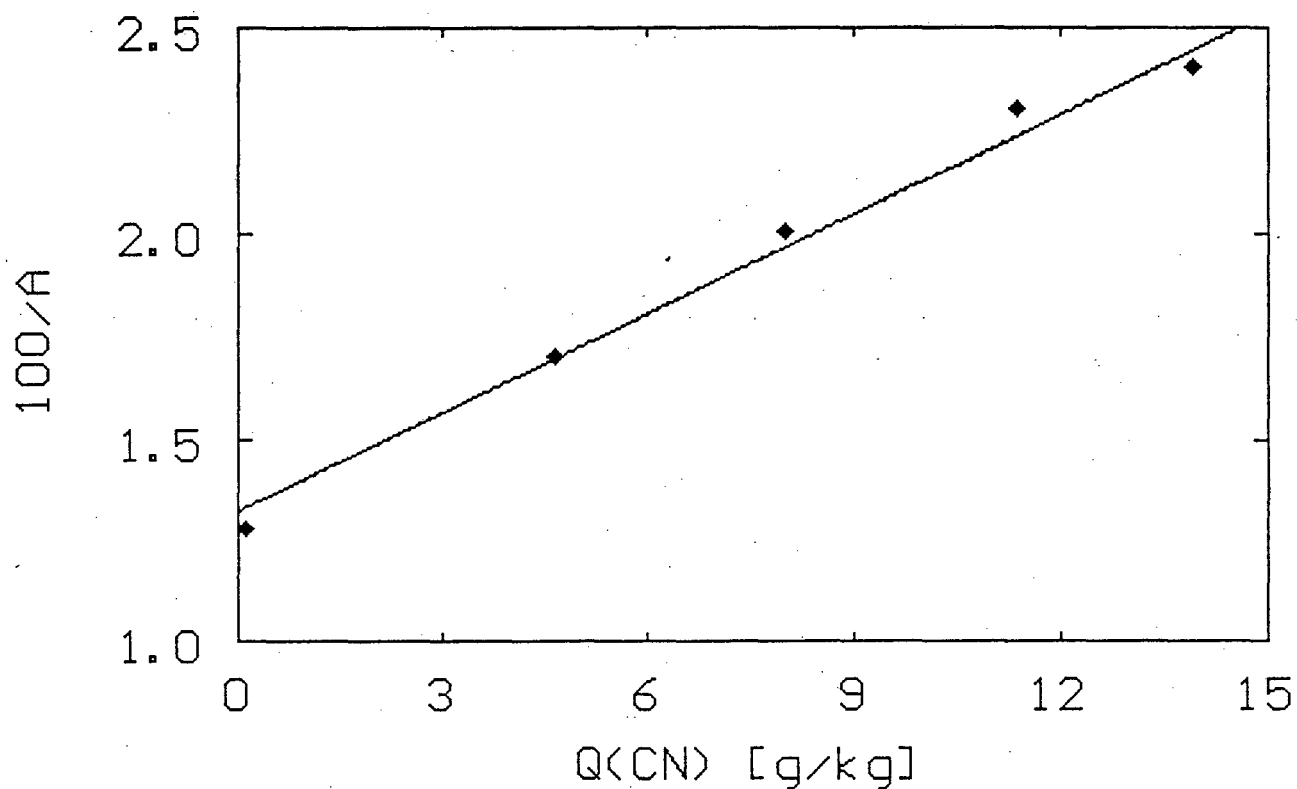


Figure 3.16 The effect of cyanide age on the gold cyanide equilibrium on carbon BTX at 70 °C. (Exp.55)

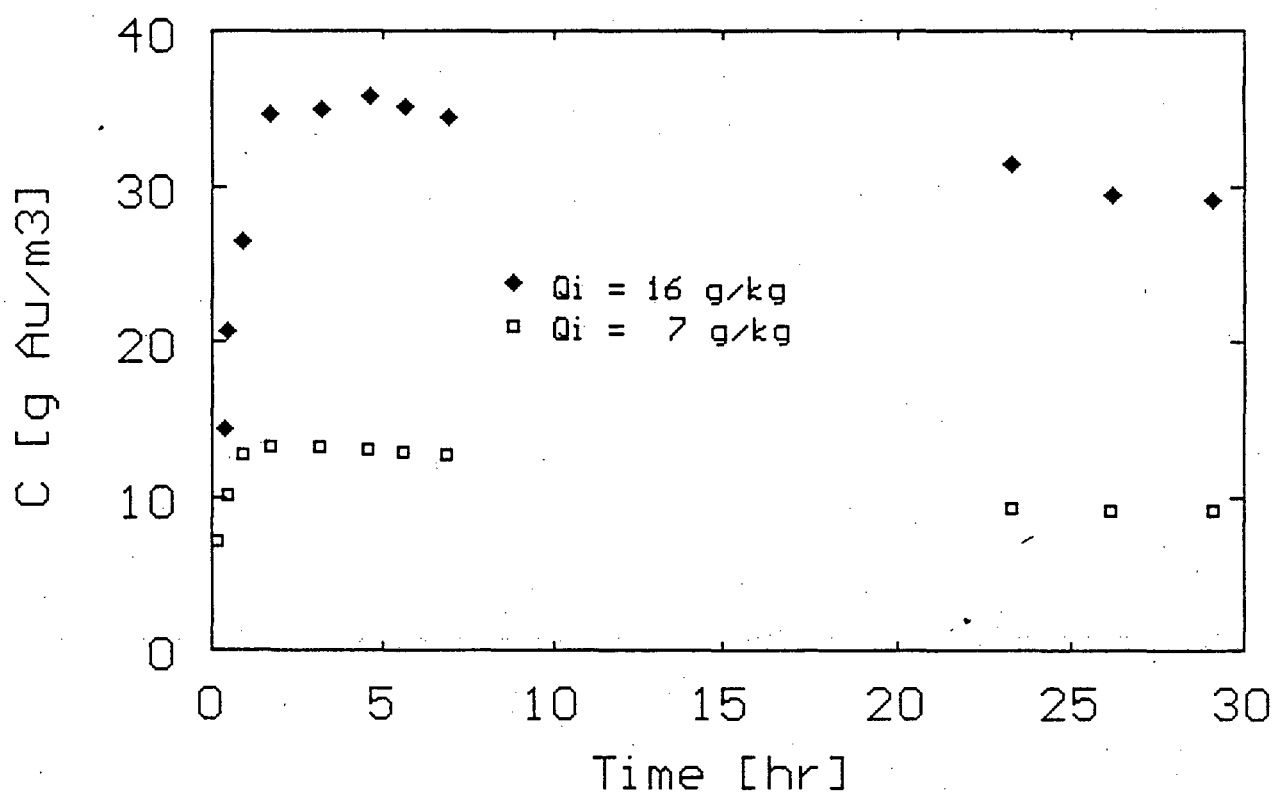


Figure 3.17 Reactivation of carbon BTX towards aurocyanide after a cyanide pretreatment. (Exp.56)

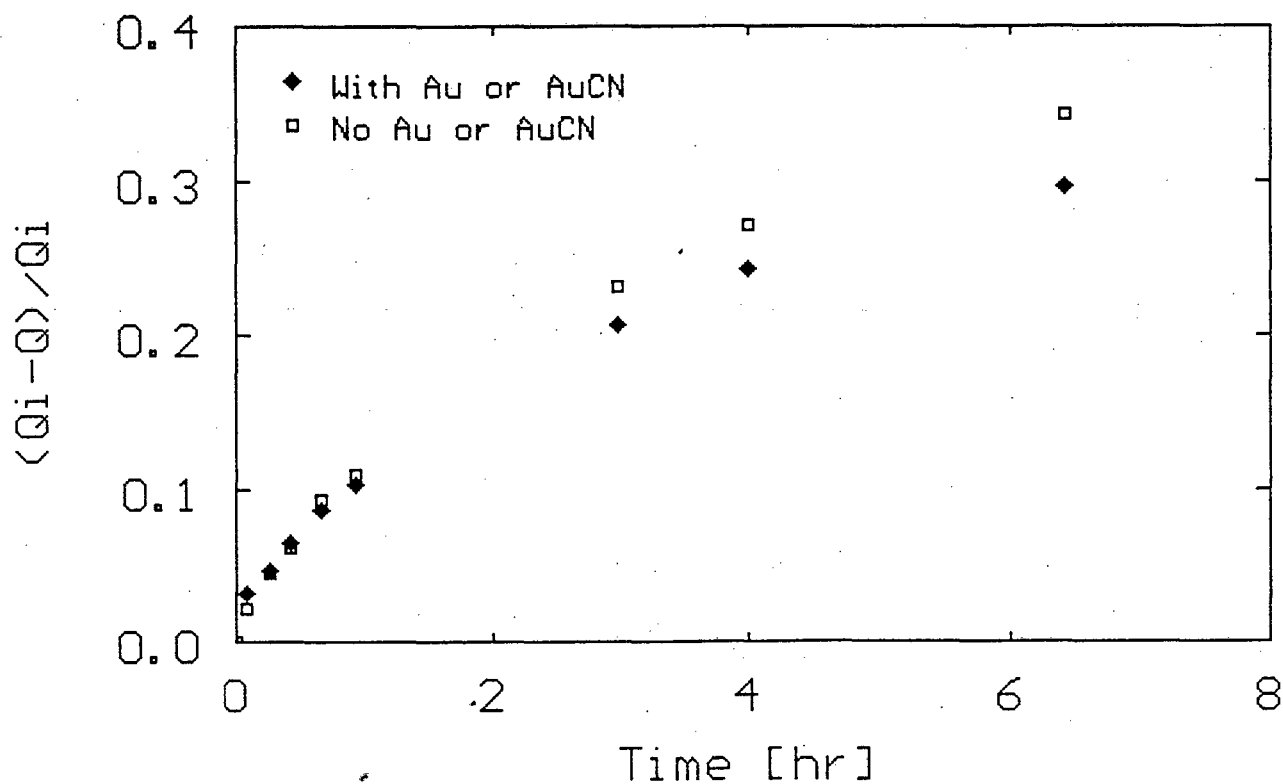


Figure 3.18 The effect of an irreversibly adsorbed gold species on elution with cyanide, but without a cyanide pretreatment. (Exp.57)

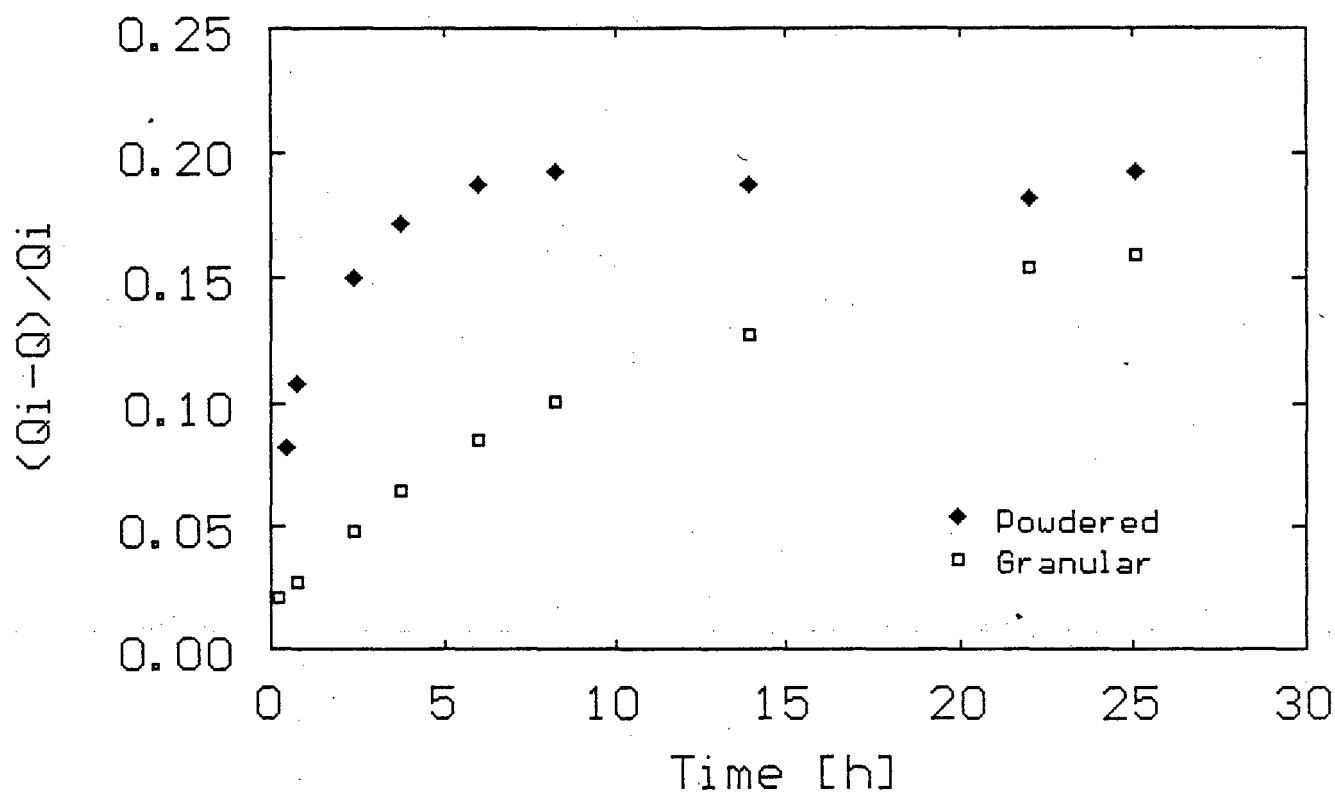


Figure 3.19 Effect of particle size on elution in batch with $\text{Au}^{(0)}$ or AuCN present on the carbon. (Exp.58)

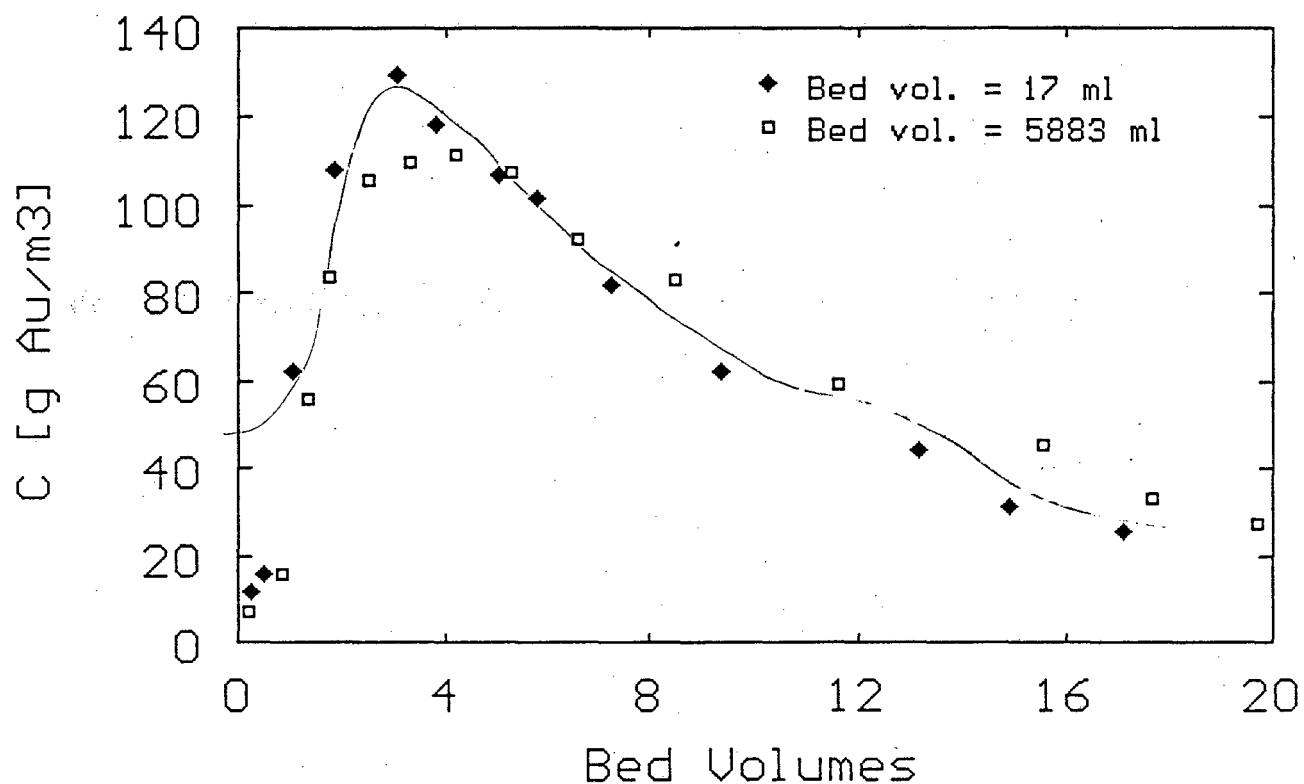


Figure 3.20 Gold elution profiles from columns with different geometry and size. (Exp.59,60)

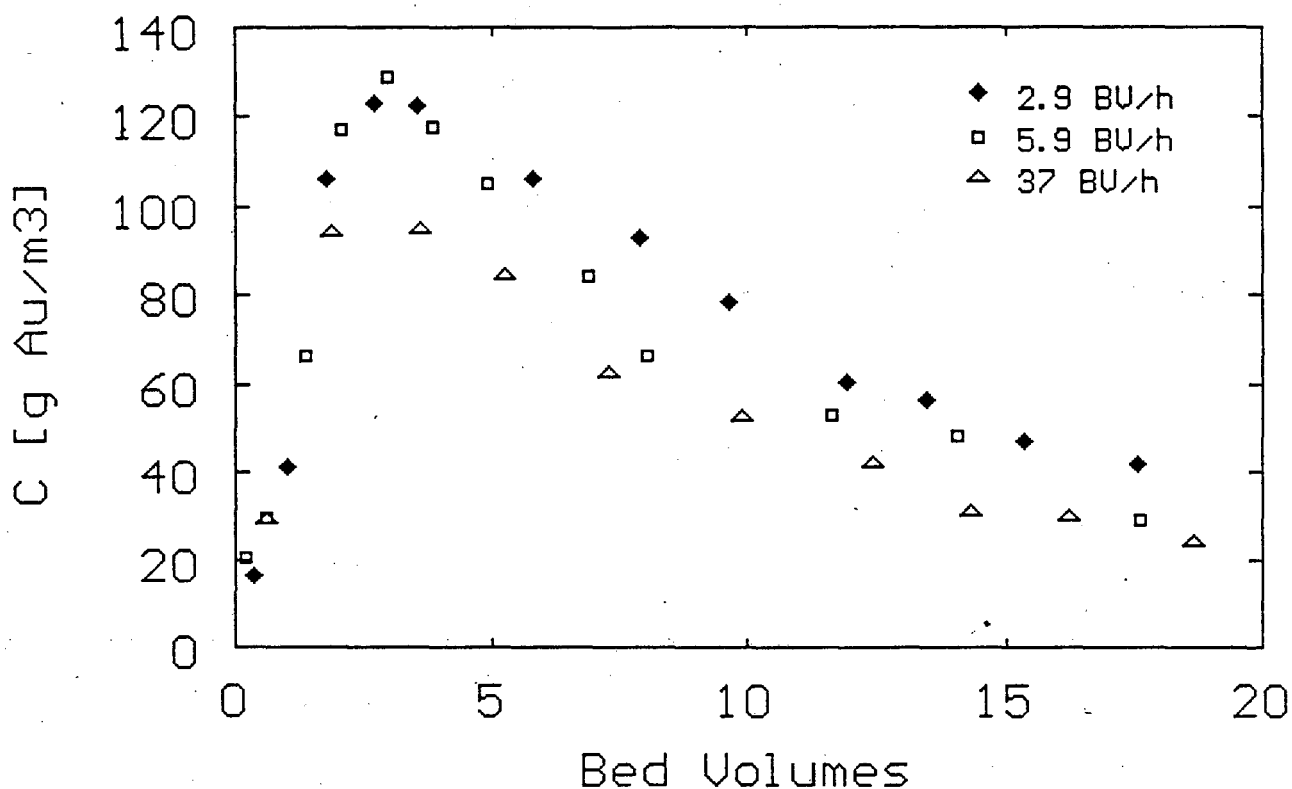


Figure 3.21 The elution of gold cyanide from carbon BTX at different flow rates. (Exp. 50, 61 and 62)

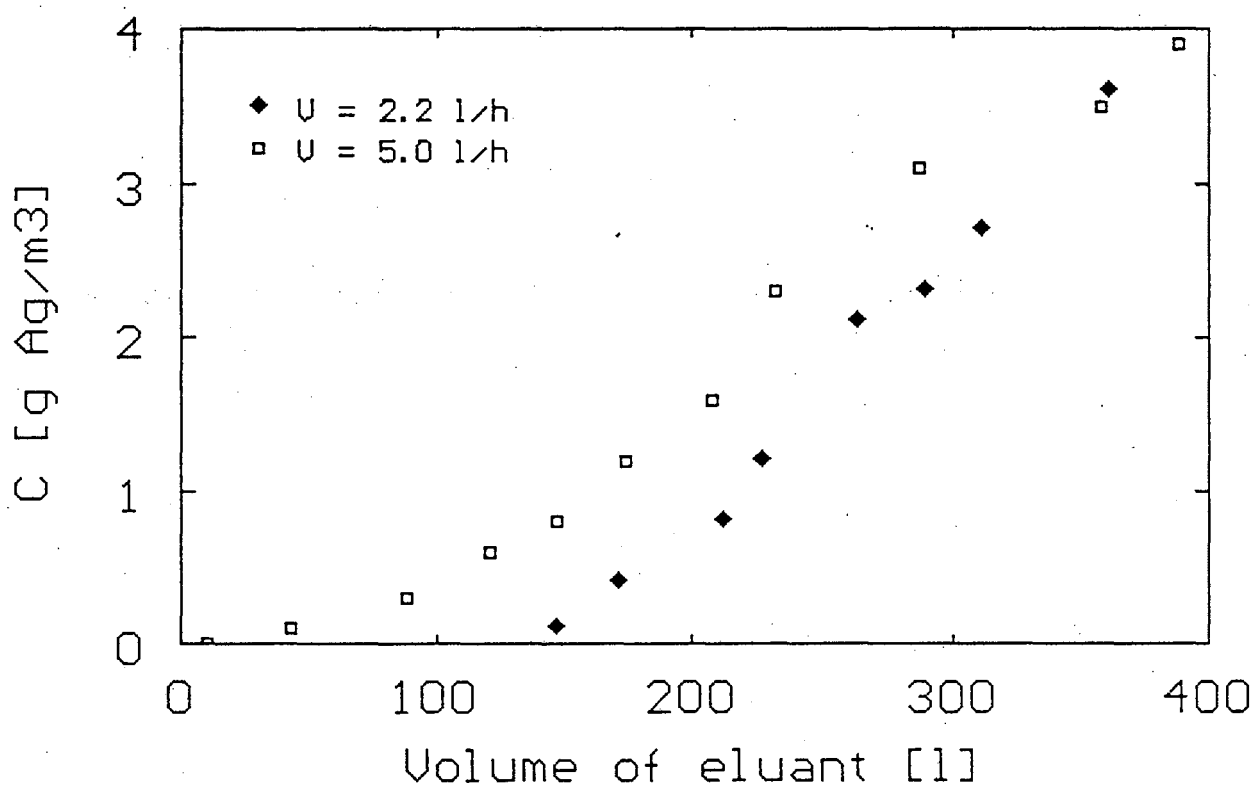


Figure 3.22 Effect of flow rate on the adsorption of $\text{Ag}(\text{CN})_2^-$. pH = 8.5, $d = 0.031$ m, $h = 0.25$ m, $C_{\text{FG}} = 4.5$ g.m⁻³. (Exp. 25 and 27 of Jansen, van Rensburg, 1986)

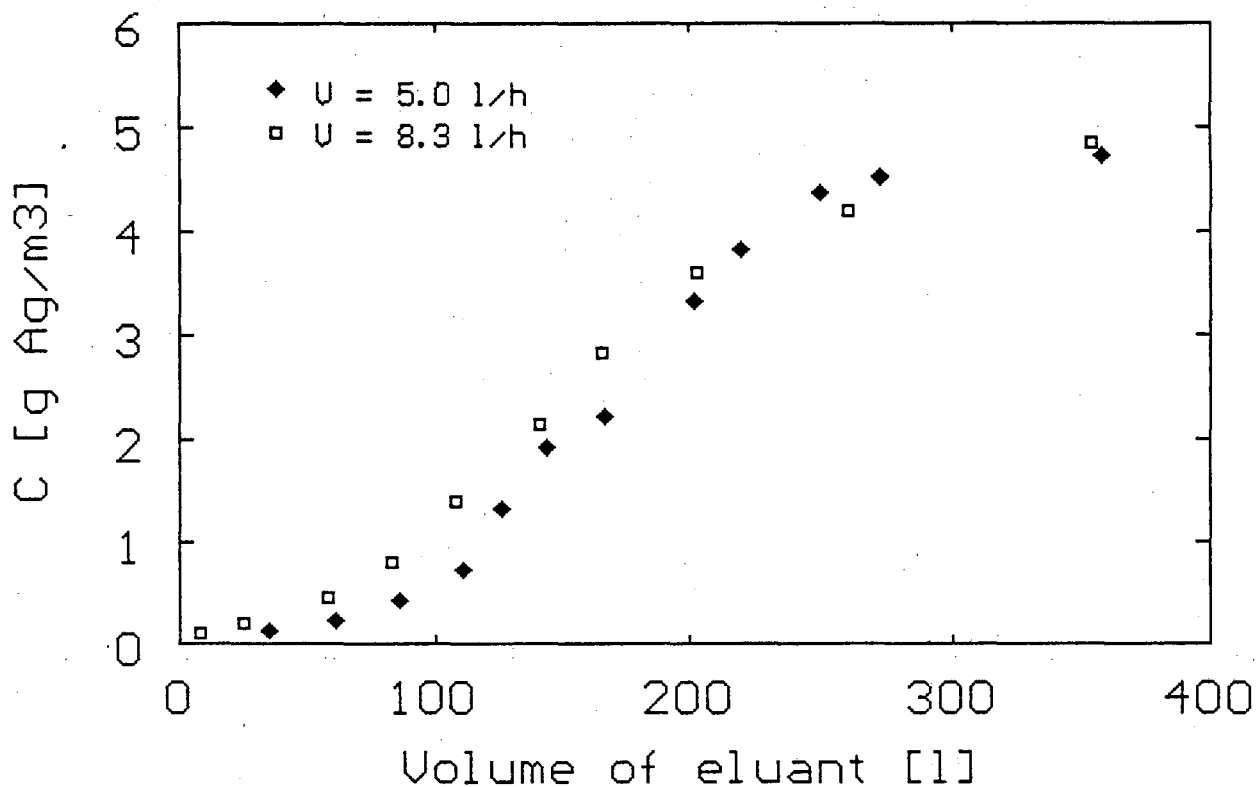


Figure 3.23 Effect of flow rate on the adsorption of $\text{Ag}(\text{CN})_2^-$. pH = 11.5, $d = 0.031$ m, $h = 0.4$ m, $C_{\text{FG}} = 5.1$ g.m⁻³. (Exp. 28 and 30 of Jansen van Rensburg, 1986)

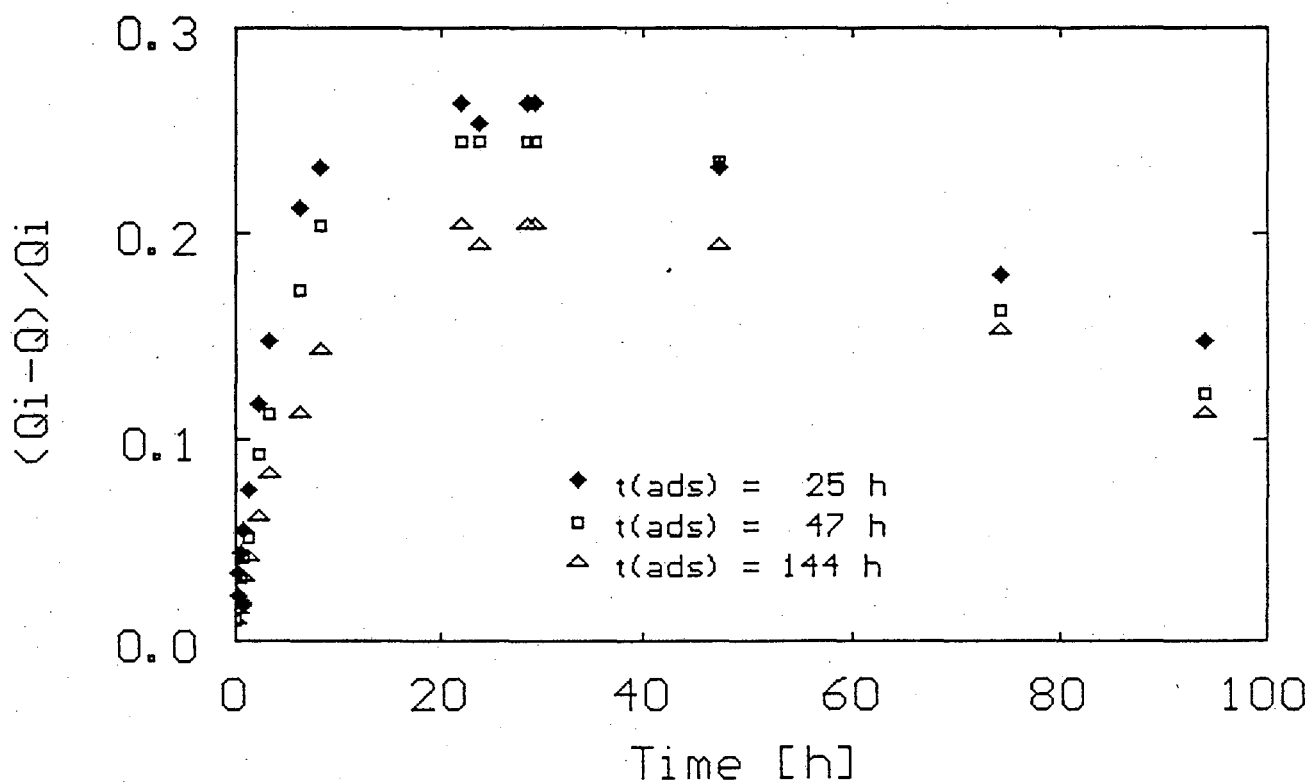


Figure 3.24 Effect of radial distribution of adsorbed gold cyanide on the kinetics of elution in batch. (Exp.63)

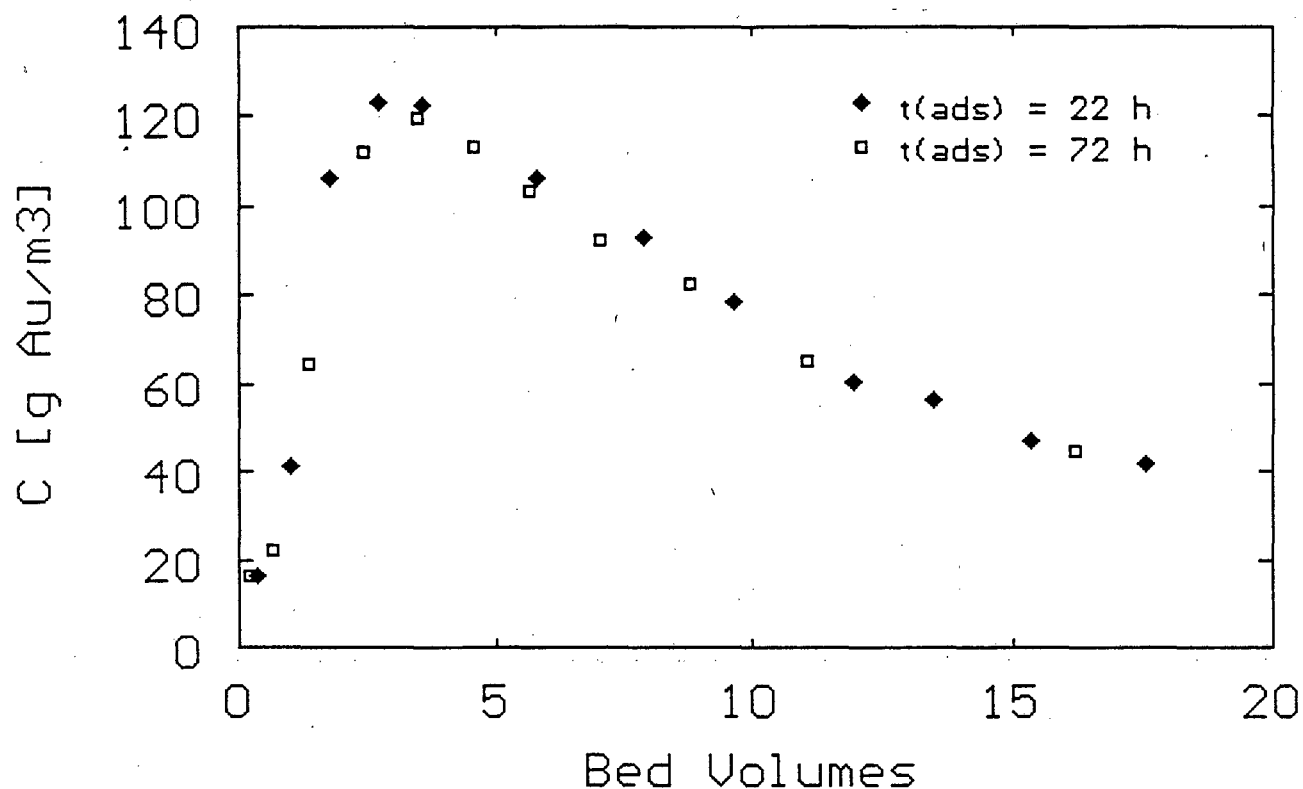


Figure 3.25 The insensitivity of elution to the radial distribution of the adsorbed gold under conditions of strong desorption. (Exp. 40 and 50)

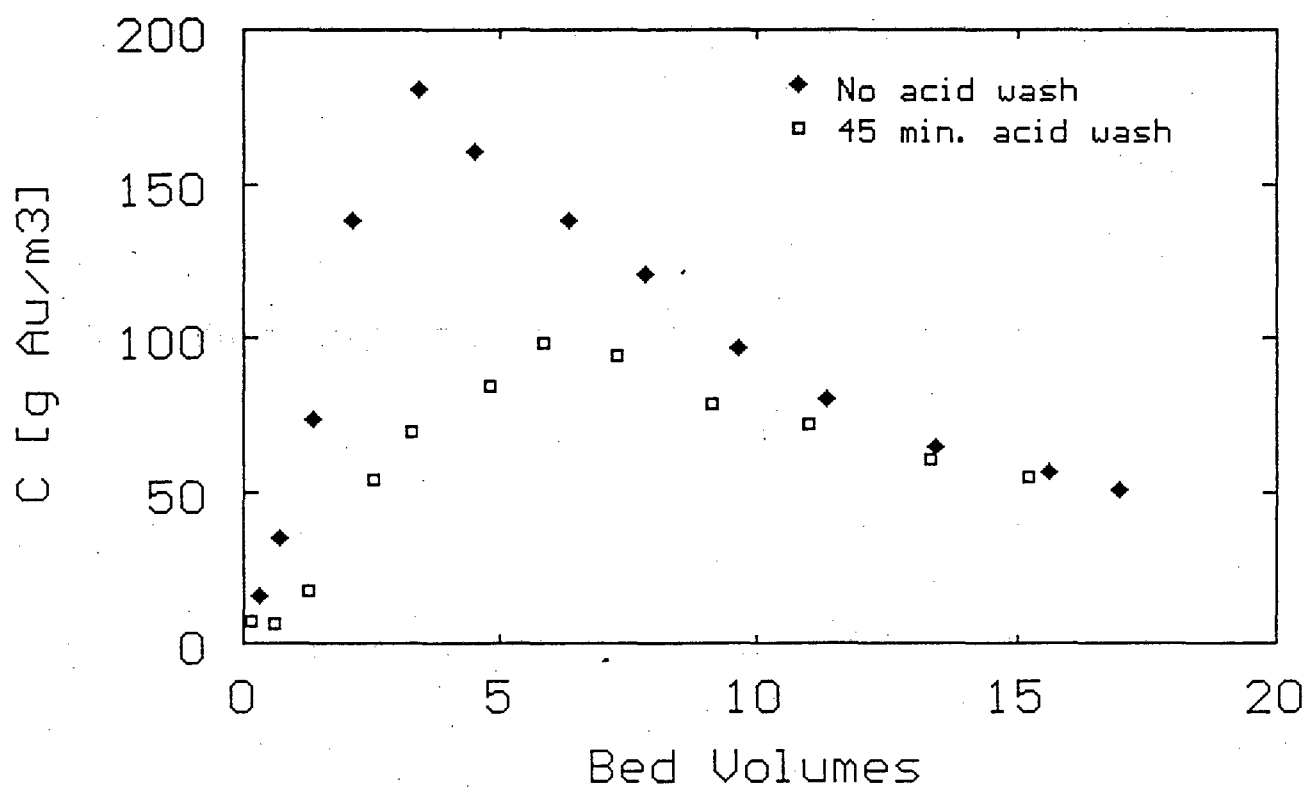


Figure 3.26 The detrimental effect of an acid wash on the elution of gold adsorbed from solutions without Mg and Ca. (Exp. 64 and 65)

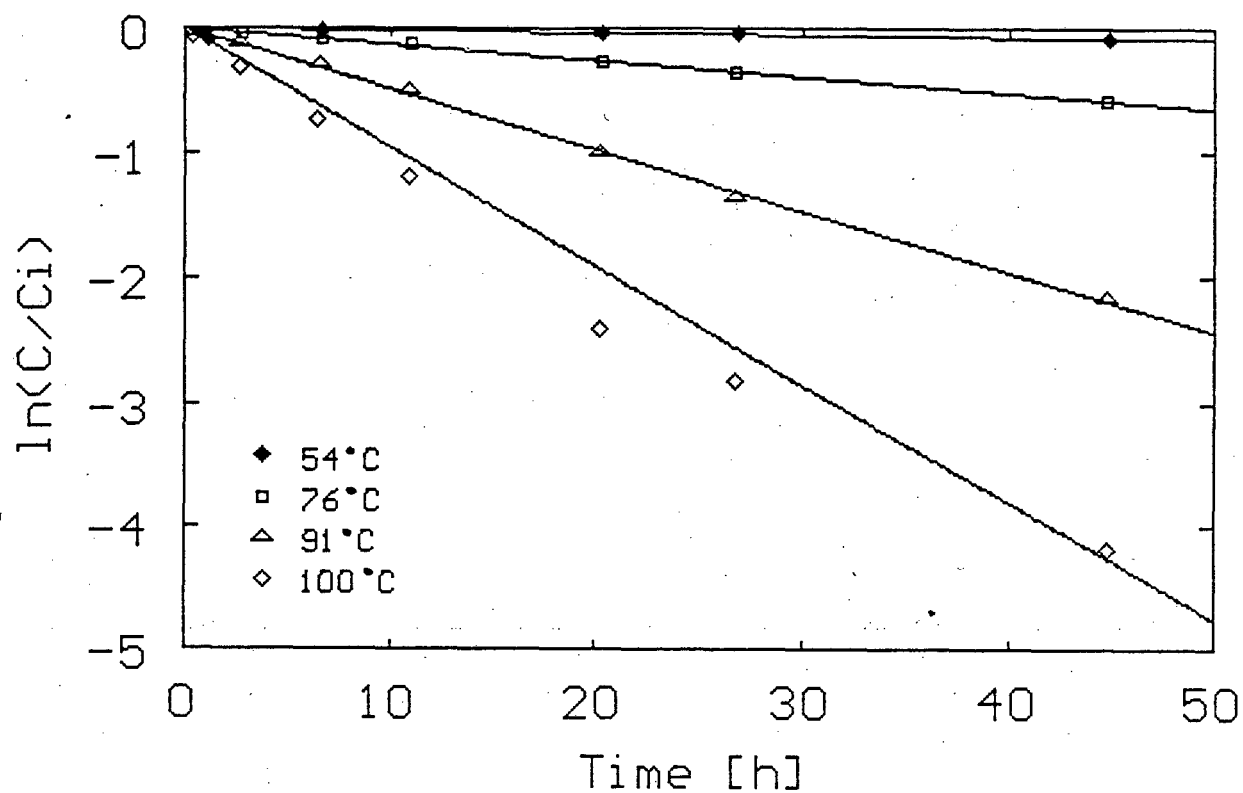


Figure 3.27 The decomposition of cyanide at different temperatures in the absence of carbon. (Exp. 66)

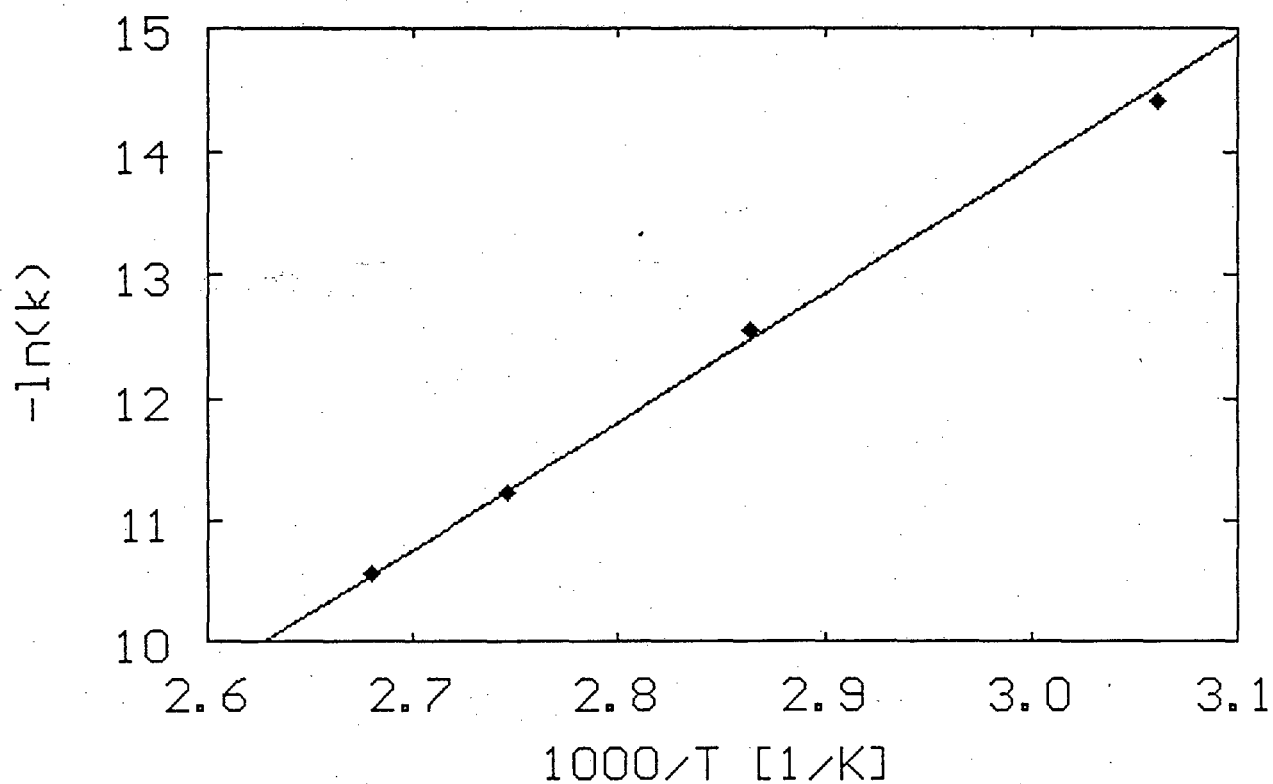


Figure 3.28 Arrhenius plot of the rate constant for the decomposition of cyanide in the absence of carbon. (Exp.66)

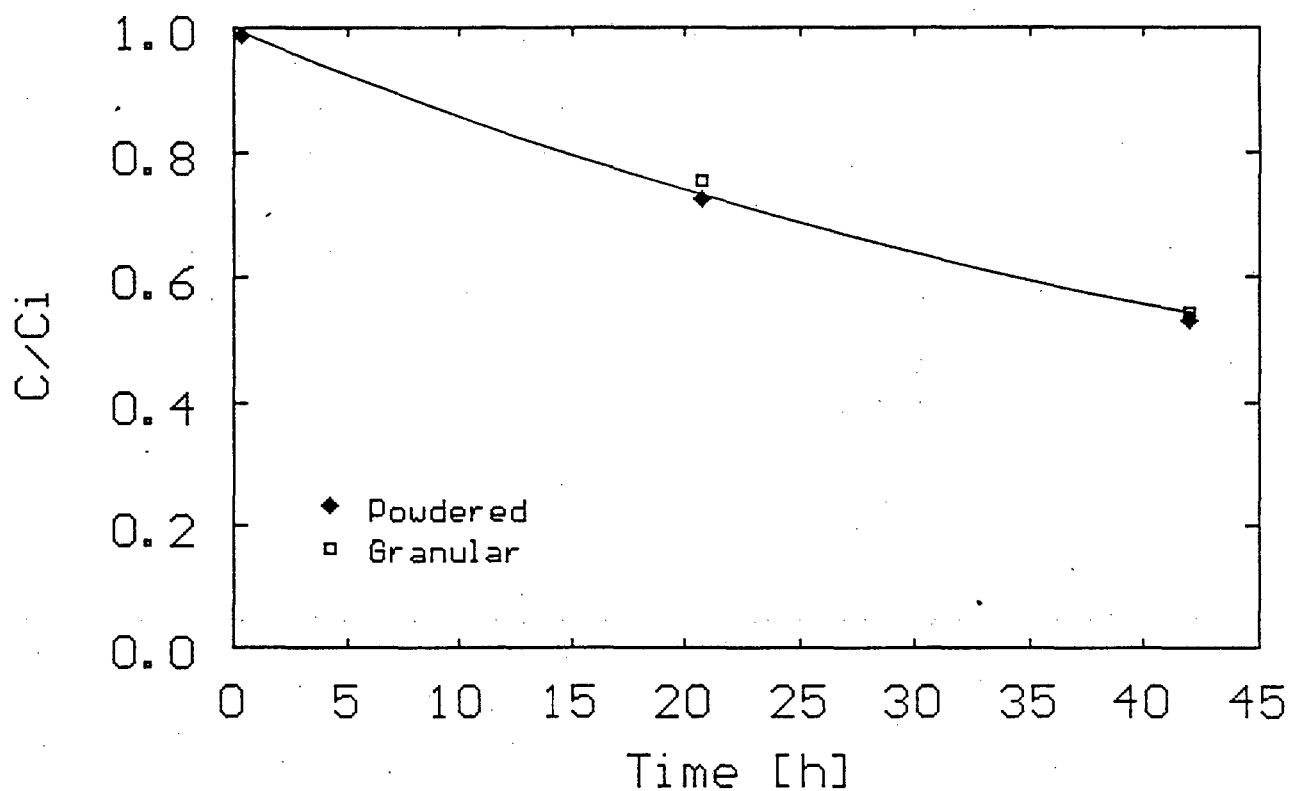


Figure 3.29 The sensitivity of the adsorption and decomposition of cyanide on the particle size of carbon BTX. (Exp.67)

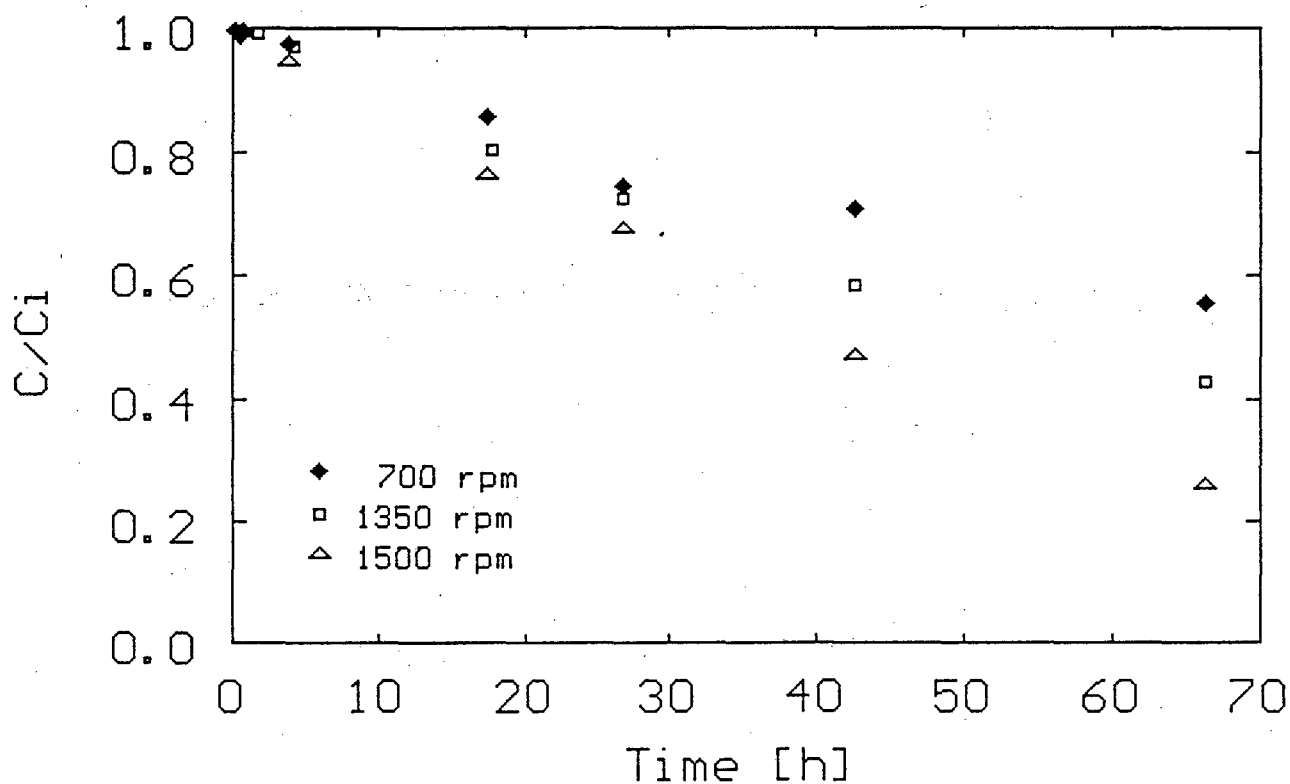


Figure 3.30 The sensitivity of the adsorption and decomposition of cyanide on carbon BTX to mixing speed. (Exp.68)

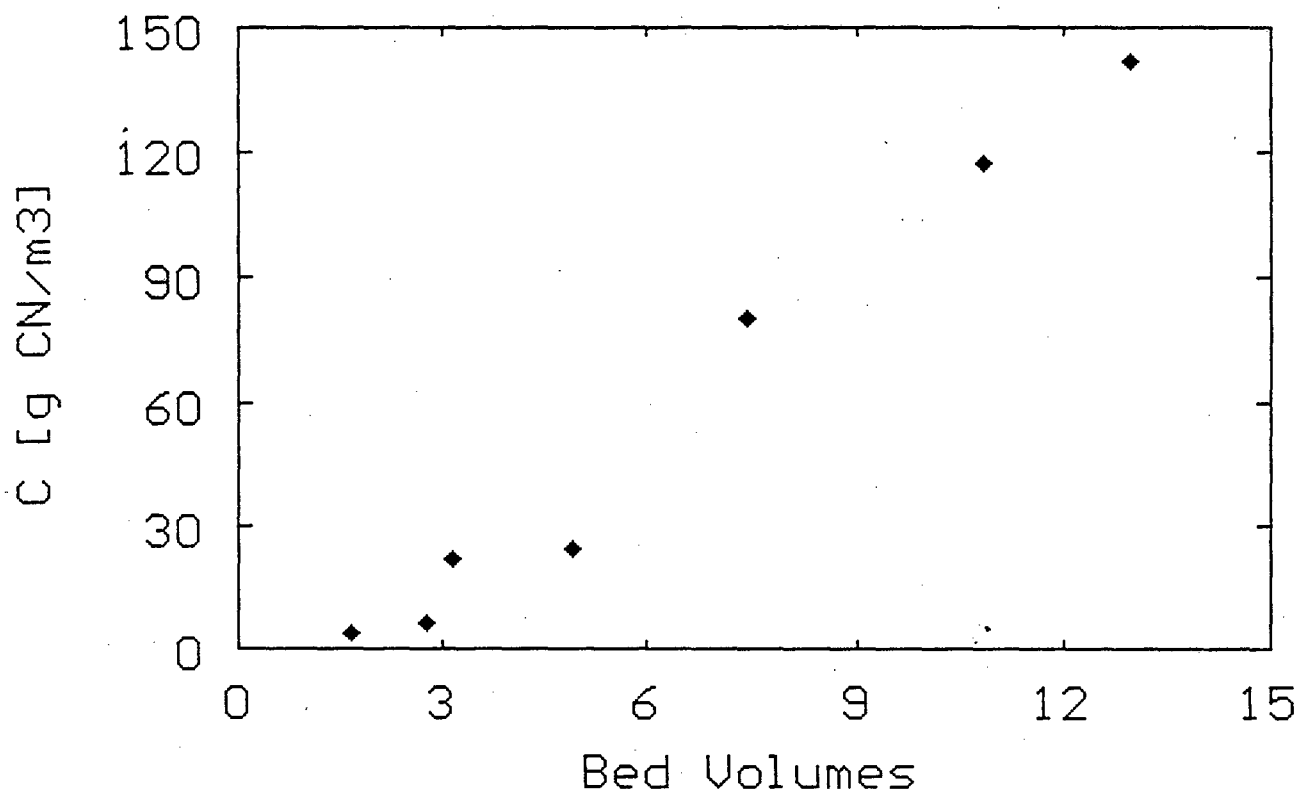


Figure 3.31 Profile of cyanide concentration in eluate of a Zadra elution. (Exp.69)

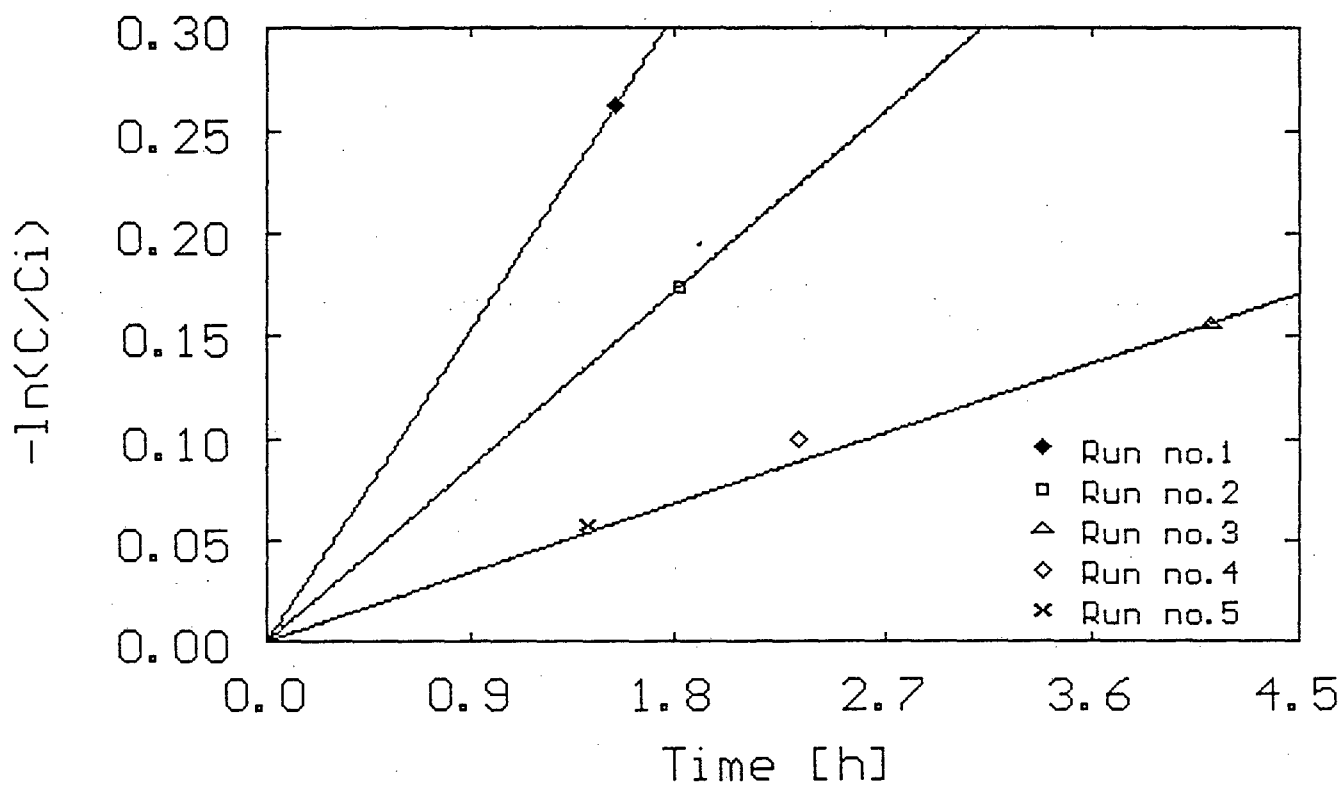


Figure 3.32 The deactivation of carbon BTX towards cyanide by cyanide. (Exp.70)

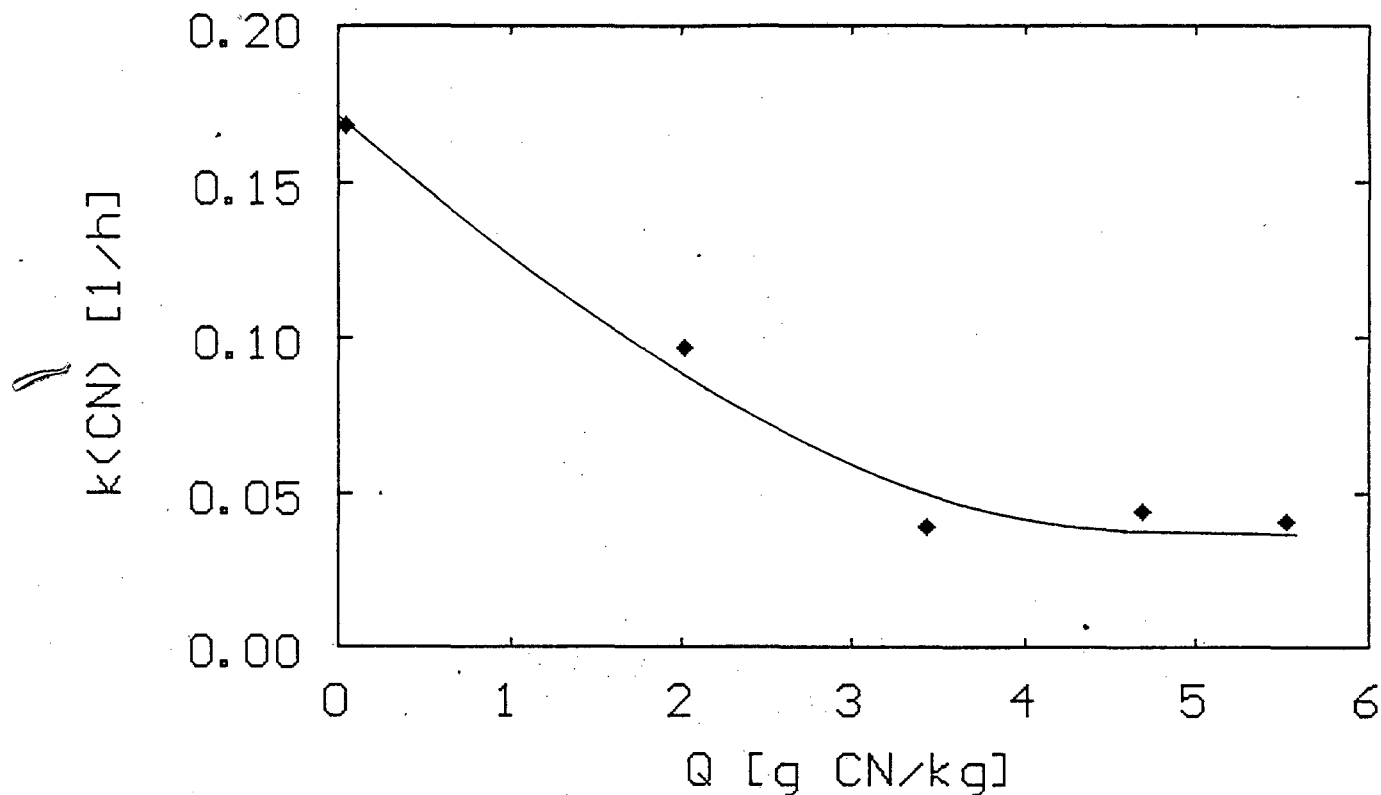


Figure 3.33 The decrease in the kinetics of the decomposition of cyanide with an increase in cyanide age of carbon BTX. (Exp.70)

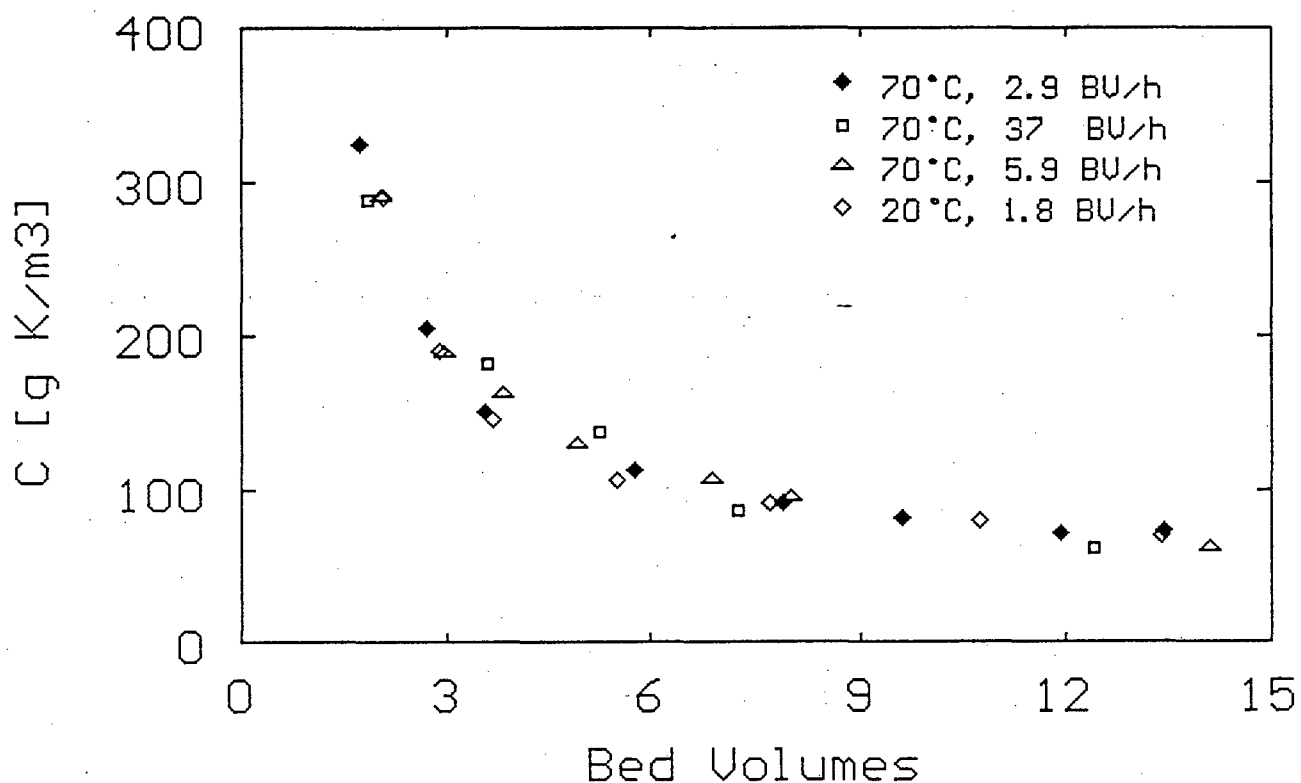


Figure 3.34 The insensitivity of the elution of potassium to temperature and flow rate. (Exp.50, 61, 62 and 73)

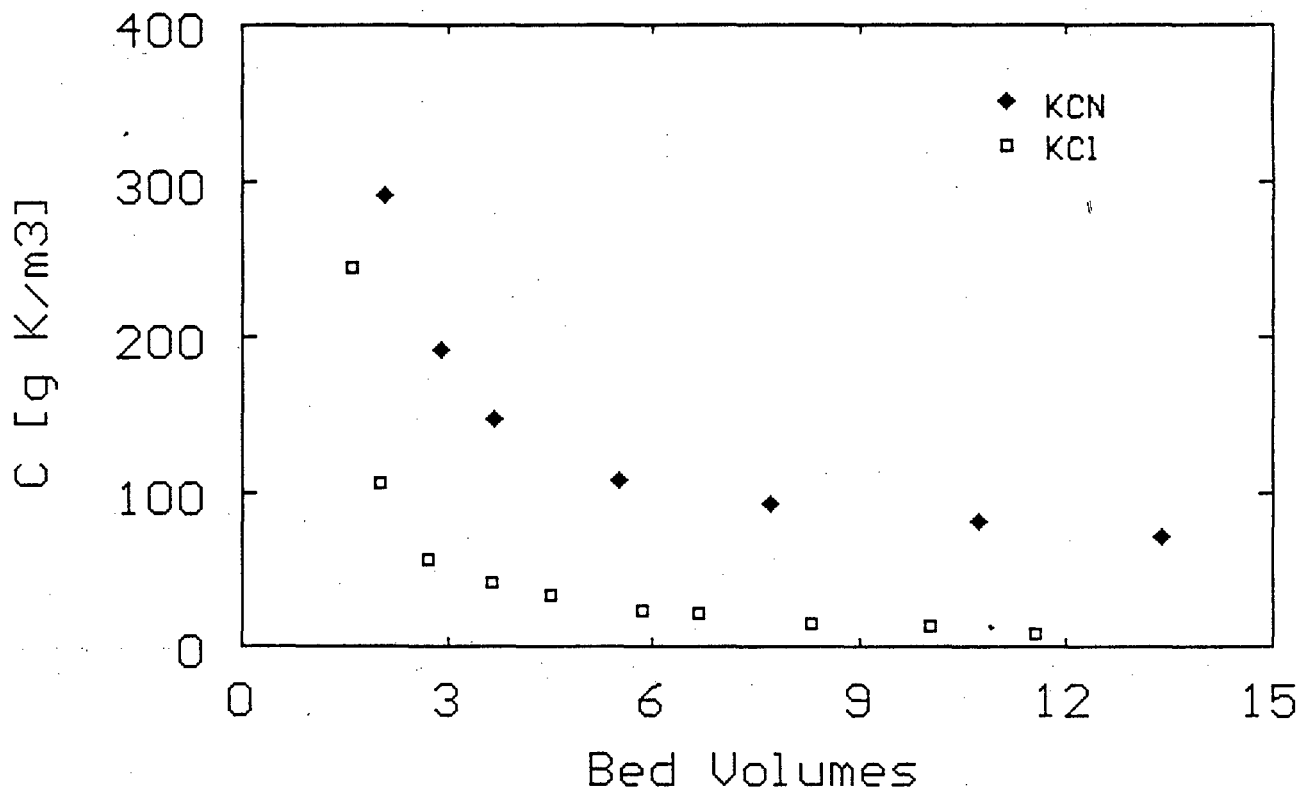


Figure 3.35 The influence of the counter anion on the elution of potassium from carbon BTX. (Exp.71 and 73)

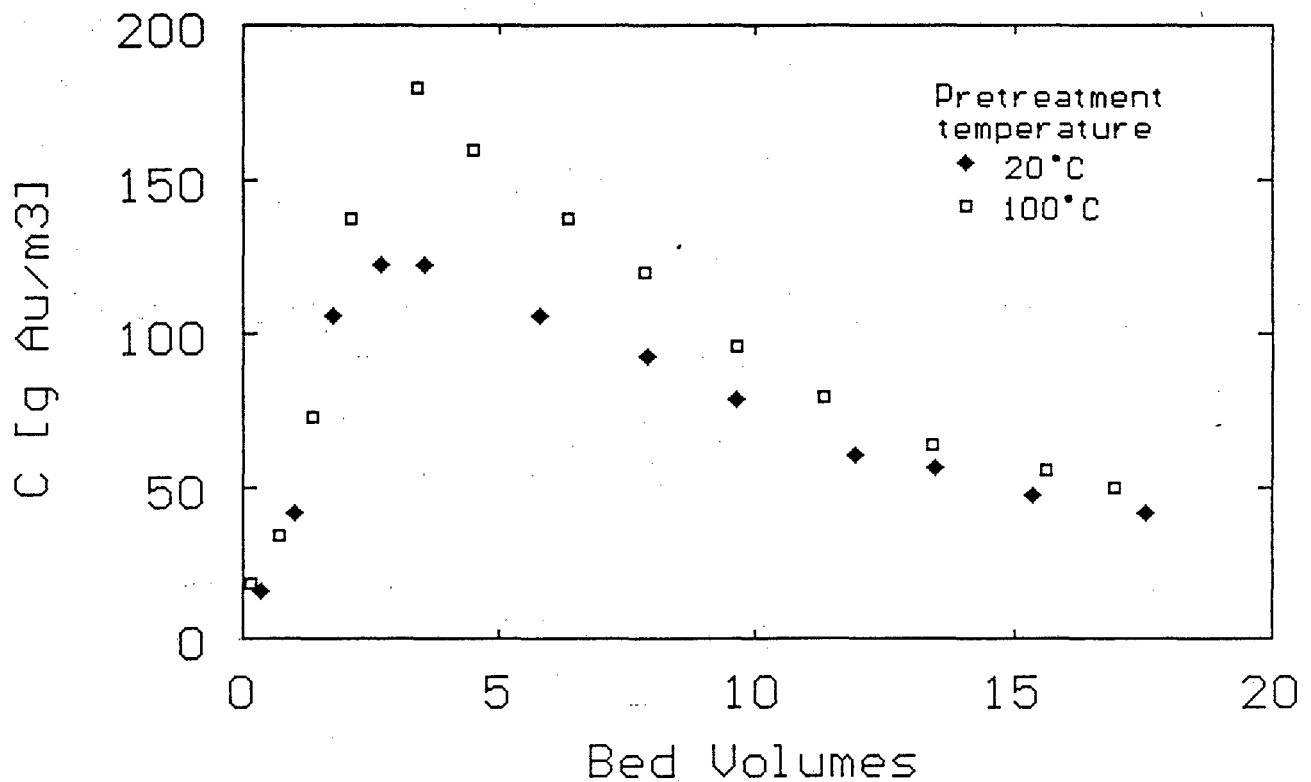


Figure 3.36 The effect of the temperature of the cyanide pretreatment on the elution of gold cyanide from carbon BTX. (Exp.50 and 64)

4

MODELLING OF CYANIDE PROFILES DURING GOLD ELUTION

It was illustrated in Chapter 3 that cyanide can undergo at least 3 reactions in a gold elution environment. These are :

1. Oxidation,
2. Hydrolysis, and
3. Adsorption.

Furthermore, it was shown that the uptake of cyanide was independent of carbon particle size, but sensitive to mixing speed. This means that the mass transfer between the bulk solution and the carbon particles will be the rate determining factor and that intraparticle diffusion will be of minor importance. A fundamentally correct mathematical model for the change in cyanide concentration during the elution of gold will therefore have to account for oxidation and hydrolysis in the bulk solution, film diffusion transfer between the solution and carbon particles, and oxidation, hydrolysis and adsorption in the pores of the carbon. As the oxidation reaction is catalyzed by activated carbon, the reaction rate in the pore liquid will differ from that in the surrounding liquid. Furthermore, the reaction rate of the oxidation reaction inside the pores will be a function of the cyanide-age of the carbon, because of the deactivation effect of cyanide on activated carbon. From Equation 3.18 it follows that the oxidation reaction rate will also be a function of the oxygen concentration.

The use of such a model will be complicated further by factors such as :

- (1) the difficulty to distinguish between the different reactions,
- (2) measurement of the oxygen concentration on the carbon surface, and

- (3) the influence of other factors, such as pH, which will have to be quantified.

A model that would account for all the above factors will contain at least 5 unknown parameters that will have to be determined by fitting the model to experimental data. This will make the use of such a model highly impractical. Furthermore, in the case of an AARL elution it was illustrated that the effect of cyanide in the elution step is of minor importance and a fundamentally correct model for the cyanide would unnecessarily complicate the overall modelling of the process. To keep the model for the cyanide as practical as possible, it was thus decided to simplify the model significantly.

4.1 ASSUMPTIONS

The following assumptions were made to enable the development of a simple mathematical model for the change in cyanide concentration :

- (1) The oxidation and hydrolysis reactions of the cyanide in the bulk solution can be combined and described by a single first-order reaction,
- (2) Adsorption of cyanide at gold elution temperatures is negligible,
- (3) The oxidation and hydrolysis reactions of the cyanide in the carbon pores can be combined and described by a single first-order reaction,
- (4) The cyanide concentration inside the carbon particles is homogeneous,
- (5) Mass transfer between the bulk solution and the pore liquid occurs via diffusion through a liquid layer surrounding the carbon particles, and
- (6) The combined reaction rate in the pores of the carbon will change with the cyanide-age of the carbon as described by equation 3.21.

4.2 FORMULATION OF MODEL

The model for the change in cyanide concentration is presented graphically in Figure 4.1. It is also shown how the column is subdivided into sections with heights of Δh . Each of these sections is assumed to behave as a perfect mixed reactor. It is clear that an ideal plug flow reactor is obtained with Δh approaching zero. An imaginary 0'th section was added at the inlet to the column to simplify the solution of the model. The concentration in the 0'th section remains equal to the eluant concentration for the whole duration of the run.

A mass balance of cyanide in the pore liquid is given by :

$$\rho \cdot V_p \frac{\partial C_{Np}}{\partial t} = \bar{n} \cdot a_c - k_{Np} \cdot C_{Np} \cdot \rho \cdot V_p, \quad [4.1]$$

where \bar{n} , the flux of cyanide through the liquid film surrounding the particles, can be written as :

$$\bar{n} = k_s \cdot (C_N - C_{Np}). \quad [4.2]$$

With the assumption of spherical carbon particles, the specific external area of the carbon becomes :

$$a_c = 6/d_c. \quad [4.3]$$

Substitution of Eq.4.2 and Eq.4.3 in Eq.4.1 yields :

$$\frac{\partial C_{Np}}{\partial t} = \frac{6k_s}{\rho \cdot V_p \cdot d_c} (C_N - C_{Np}) - k_{Np} \cdot C_{Np} \quad [4.4]$$

A mass balance of cyanide in the interparticle solution of a section (j+1) of the elution column is :

$$V \cdot C_N^{(j)} - V \cdot C_N^{(j+1)} - \bar{n} \cdot (1-\epsilon) \cdot a \cdot \Delta h \cdot a_c - \epsilon \cdot a \cdot \Delta h \cdot k_N \cdot C_N^{(j+1)} = \epsilon \cdot a \cdot \Delta h \cdot (dC_N^{(j+1)}/dt) \quad [4.5]$$

By substituting Eq.4.2 and Eq.4.3 in Eq.4.5, and dividing Eq.4.5 by Δh

and letting $\Delta h \rightarrow 0$, Eq.4.5 becomes :

$$\frac{\partial C_N}{\partial t} = -\frac{V}{a\epsilon} \frac{\partial C_N}{\partial h} - \frac{6k_s(1-\epsilon)}{\epsilon \cdot d_c} (C_N - C_{Np}) - k_N \cdot C_N \quad [4.6]$$

k_N was calculated as in Equation 3.20 and k_{Np} assumed to change with the cyanide age of the carbon at a given temperature as in Equation 3.21 :

$$k_{Np} = \frac{c_1}{(Q_N + 1)^{c_2}} \quad [4.7]$$

The change in the cyanide age of the carbon was calculated from the amount of decomposition of cyanide in the pores of the carbon as follows :

$$\frac{\partial Q_N}{\partial t} = V_p \cdot k_{Np} \cdot C_{Np} \quad [4.8]$$

c_1 , c_2 and k_s were unknown parameters that had to be determined by fitting the model to experimental data.

4.3 NUMERICAL SOLUTION PROCEDURE

Equations 4.4, 4.6 and 4.8 were solved simultaneously by discretizing with backward differences in time and column height. This involved the following substitutions in Equations 4.4, 4.6 and 4.8 :

$$\frac{\partial C}{\partial t} = \frac{C^{(j,t)} - C^{(j,t-1)}}{\Delta t} \quad [4.9]$$

$$\frac{\partial C}{\partial h} = \frac{C^{(j,t)} - C^{(j-1,t)}}{\Delta h} \quad [4.10]$$

where C in Equations 4.9 and 4.10 could be C_N , C_{Np} or Q_N .

The equations resulting from the above substitutions in Equations 4.4 and 4.6 were combined to yield :

$$C_N^{(j,t)} = \frac{C_N^{(j,t-1)} + S_4 \cdot C_N^{(j-1,t)} + S_1 \cdot S_3 \cdot C_{Np}^{(j,t-1)}}{S_5} \quad [4.11]$$

where the constants S_0 to S_5 were defined as :

$$S_0 = \frac{6k_s \cdot \Delta t}{\rho \cdot V_p \cdot d_c} + k_{Np} \cdot \Delta t + 1 \quad [4.12]$$

$$S_1 = 1/S_0 \quad [4.13]$$

$$S_2 = \frac{6k_s \cdot \Delta t}{\rho \cdot V_p \cdot d_c \cdot S_0} \quad [4.14]$$

$$S_3 = \frac{6k_s \cdot (1-\epsilon) \cdot \Delta t}{\epsilon \cdot d_c} \quad [4.15]$$

$$S_4 = \frac{V \cdot \Delta t}{a \cdot \epsilon \cdot \Delta h} \quad [4.16]$$

$$S_5 = 1 + S_4 + k_N \cdot \Delta t + S_3(1-S_2) \quad [4.17]$$

Discretizing Equation 4.8 yielded :

$$Q_N^{(j,t)} = Q_N^{(j,t-1)} + V_p \cdot k_{Np} \cdot \Delta t \cdot C_{Np}^{(j,t)} \quad [4.18]$$

The following boundary conditions were defined for use with Equation 4.10 :

- (1) For a Zadra elution : $C_{Np}^{(j,0)} = 0$, $C_N^{(j,0)} = 0$, $Q_N^{(j,0)} = 0$, $C_N^{(0,t)} = C_N$ in eluant
- (2) For an AARL elution where the pretreatment was conducted in a separate vessel : $C_{Np}^{(j,0)} = \psi_N \cdot C_{Nf}$ of pretreatment step, $Q_N^{(j,0)} = Q_{Nf}$ of pretreatment step, $C_N^{(j,0)} = 0$, $C_N^{(0,t)} = C_N$ in eluant
- (3) For an AARL elution where the pretreatment was conducted in the column : $C_{Np}^{(j,0)} = \psi_N \cdot C_{Nf}$ of pretreatment step, $Q_N^{(j,0)} = Q_{Nf}$ of pretreatment step, $C_N^{(j,0)} = C_{Nf}$ of pretreatment step, $C_N^{(0,t)} = C_N$ in eluant

As the decomposition of cyanide was shown to be catalysed by activated carbon, it was assumed that the concentration of cyanide in the pore liquid would be lower than the concentration in the interparticle solution at the end of a cyanide pretreatment. The factor ψ_N was

therefore introduced above to account for the concentration gradient between the bulk solution and the solution in the carbon pores.

A Turbo Pascal procedure was written to calculate the change in the cyanide concentration as discussed above. This procedure forms part of the program for the elution of gold cyanide and can be found in Appendix I as "procedure mod_cn".

4.4 EVALUATION OF MODEL

The experimental data used in the evaluation of the above model were obtained with the same techniques as those described in Chapters 2 and 3. The values of the parameters and conditions used in the simulations are summarized in Table 4.1.

Figure 4.2 shows a simulation of the cyanide profile as measured during the Zadra elution in Experiment 69. By continuously calculating the cyanide-age of the carbon, it was possible to account for the passivation of the carbon towards the decomposition of the cyanide. The simulation in Figure 4.3 differs from that in Figure 4.2 in that the carbon was soaked in a cyanide pretreatment solution before the introduction of the feed. This case represents a combination of a Zadra and an AARL procedure. To prevent the calculation of a false cyanide-age because of dilution, the initial cyanide-age of the carbon was calculated from the result of Experiment 73(a) where an identical pretreatment was conducted with dry carbon BTX.

It is illustrated in Figure 4.4 that the same parameters used for the simulation of the cyanide profiles during the Zadra process can be used for the AARL profiles. Figure 4.4 contains the plots of results from 3 different elutions which were identical as far as cyanide is concerned. The poor reproducibility is partly because of the tricky end-point of the AgNO_3 titration used for the determination of the cyanide concentration.

The above 3 simulations illustrate the applicability of the model to describe the cyanide profiles during AARL as well as Zadra elutions. All the data shown in these figures have been collected from elutions at

70 °C. The simulation in Figure 4.2 has been repeated in Figure 4.5 with $k_{Np} = 0$ and $k_s = 0$ to show the contribution of the decomposition of cyanide in the bulk solution at different temperatures. From this simulation it follows that decomposition in the bulk solution is negligible at 70 °C and only becomes significant at 120 °C. Although it was not done here, the effect of temperature on k_{Np} can thus be determined by repeating Experiment 69 at different temperatures below 100 °C.

A similar simulation as in Figure 4.4, but with $k_{Np} = k_N = 0$, gave the same curve as in Figure 4.4. This implies that little further decomposition of cyanide occurred during the elution step at 70 °C after the cyanide pretreatment. The effect of temperature on the cyanide profiles during an AARL elution was investigated in Figure 4.6. For these simulations it was assumed that the deactivation of the carbon is independent of temperature and that the activation energy of the combined reactions inside the carbon pores is equal to the activation energy of 36000 J/mol as determined by Hoecker and Muir (1987) for the oxidation reaction.

From the simulations of the experimental data in Figures 4.2 to 4.4, it is clear that satisfactory predictions of cyanide profiles during AARL and Zadra elutions can be made with the model presented here. This model could thus be incorporated in the model for the elution of gold cyanide to assist in the prediction of the gold equilibrium conditions during the elution process.

4.5 SUMMARY

A simplified model was derived to describe the change in the cyanide concentration during the elution of gold cyanide from activated carbon. It was illustrated that this model is applicable to both the AARL and Zadra elution processes.

Table 4.1

Parameters and conditions used in simulations of cyanide profiles.

	Fig.4.2	Fig.4.3	Fig.4.4 Fig.4.6	Fig.4.6	Fig.4.6
C_{Npi}	0	4100	4100	4100	4100
C_{Nbi}	191	7726	0	0	0
C_{NF}	191	7726	0	0	0
c_1	0.07	0.07	0.07	0.26	0.76
Q_{Ni}	0	3.39	3.39	3.39	3.39
T (K)	343	343	343	383	423
$V \times 10^8$ m ³ /s	1.315	1.356	1.367	1.367	1.367

$h = 0.143$ m, $a = 1.2 \times 10^{-4}$ m², $d_c = 0.00142$ m, $\rho = 838.8$ kg.m⁻³, $V_p = 6.34 \times 10^{-4}$ m³.kg⁻¹, $\epsilon = 0.292$, $N = 10$, $\Delta t = 20$ s, $k_N = 4.17 \times 10^7 \exp(-87143/R_o T)$ s⁻¹,
 $k_s = 2 \times 10^{-6}$ m.s⁻¹, $c_2 = 3.5$, $\psi_N = 0.9$

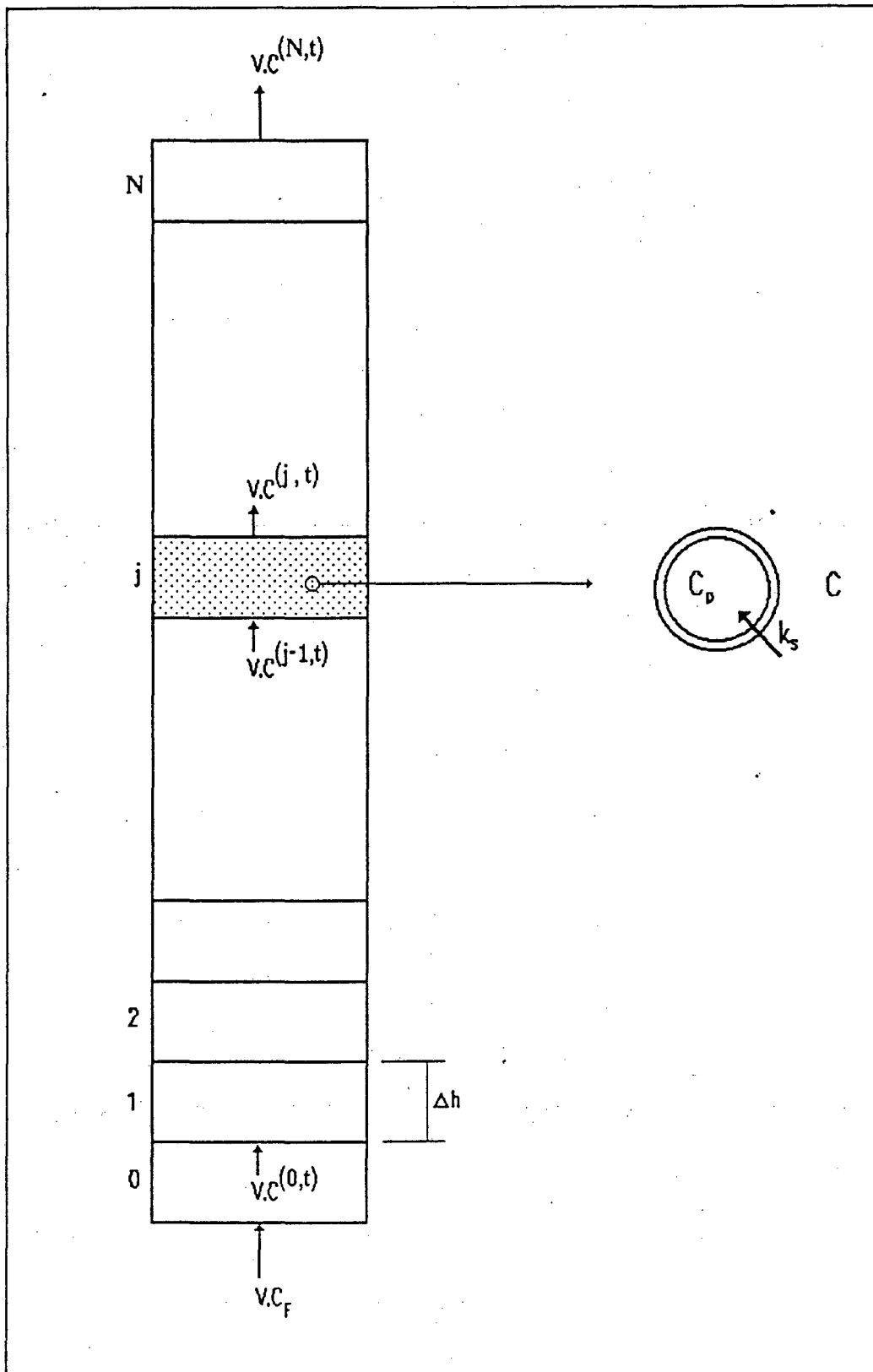


Figure 4.1 Definition of column and graphical presentation of elution model for cyanide.

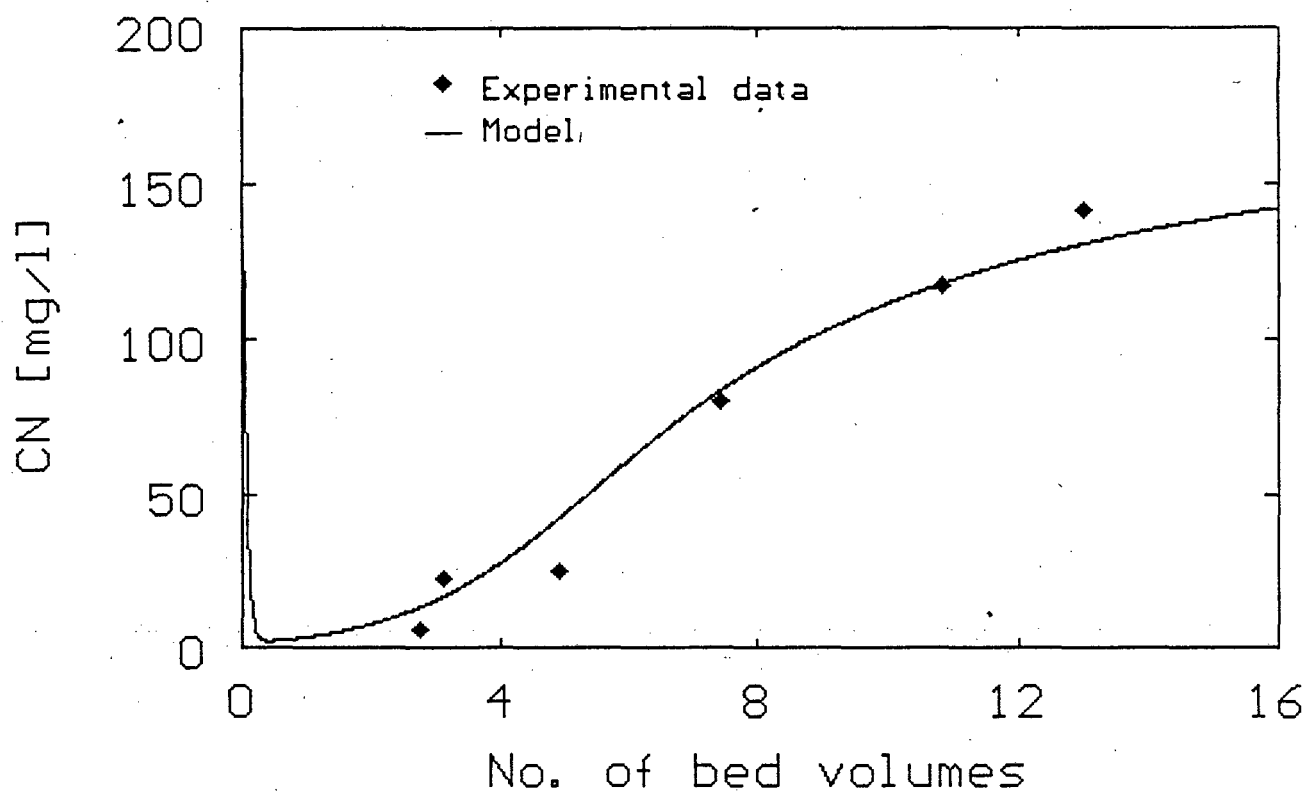


Figure 4.2 Simulation of the cyanide profile in the eluate of a Zadra elution. (Exp.69)

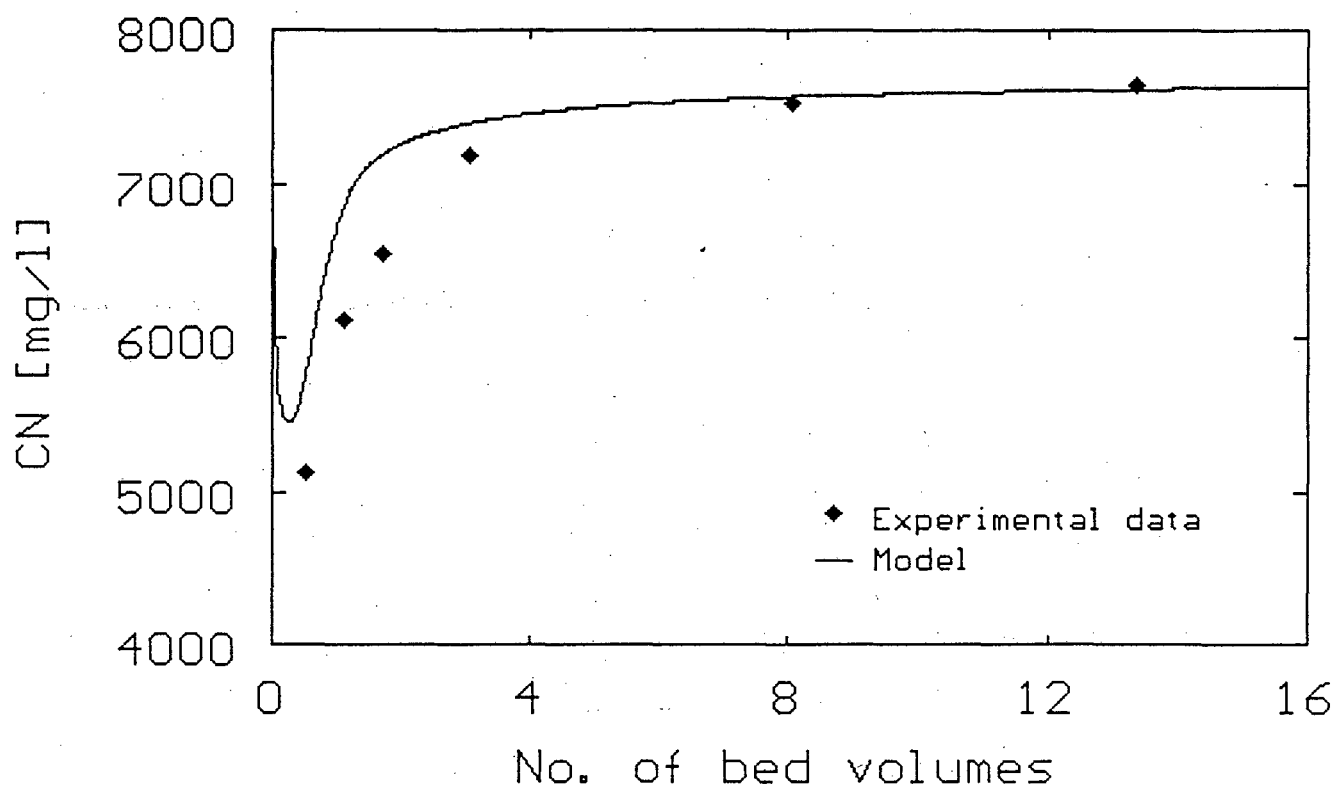


Figure 4.3 Simulation of the cyanide profile in the eluate of a Zadra elution with a cyanide pretreatment. (Exp.74)

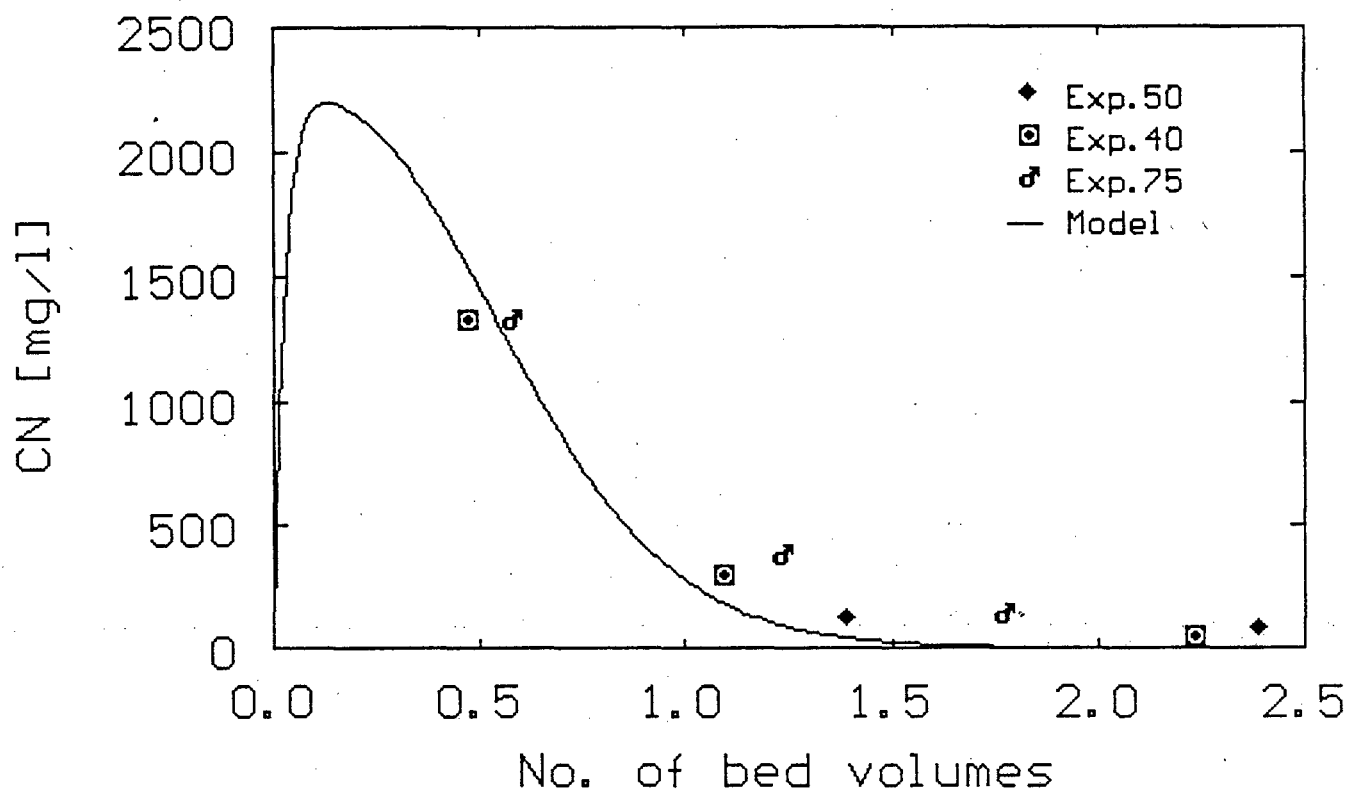


Figure 4.4 Simulation of the cyanide profile in the eluate of an AARL elution. (Exp.40, 50 and 75)

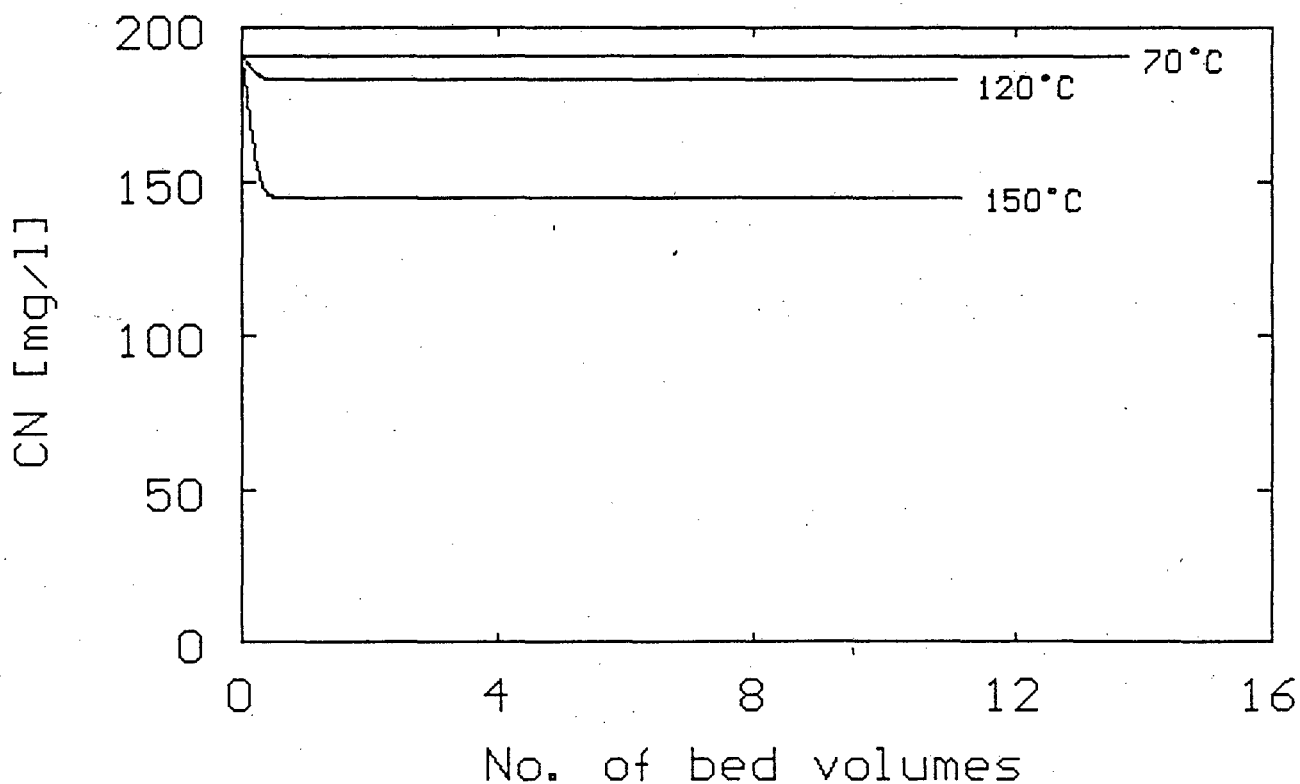


Figure 4.5 Predictions of the contribution of the decomposition of cyanide in the interparticle solution.

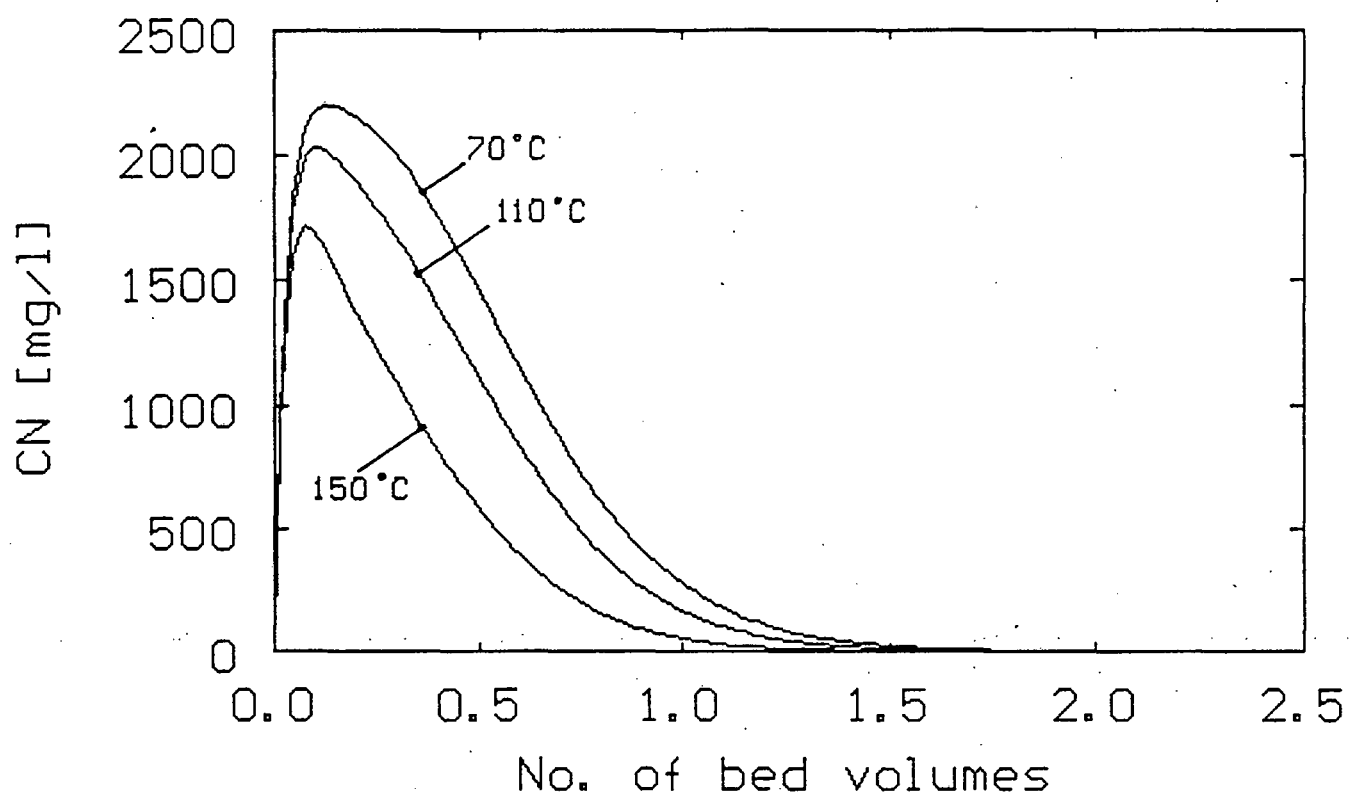


Figure 4.6 Predictions of cyanide profiles during ARL elutions at different temperatures.

5

MODELLING OF POTASSIUM PROFILES DURING GOLD ELUTION

The section on the adsorption and desorption of cations in Chapter 3 revealed the following points that had to be considered in the choice of a model for the simulation of the potassium profiles during the elution of gold cyanide :

- (1) Potassium from the pretreatment step of an AARL elution is introduced to the elution step through its presence in the pore liquid as well as through adsorption on the carbon,
- (2) The profiles for the elution of the potassium proved to be independent of flow rate and temperature, and
- (3) A long tail of potassium was evident in all of the experiments.

Several models were tested in the search for a suitable model for the potassium. Some of these models are presented in Appendices A to C. The main characteristics of the different models are discussed below on the basis of simulation experiences with them. The experimental data were collected as described in Chapters 2 and 3, and in the tabulation of each individual experiment in Appendix K.

5.1 LEVENSPIEL'S DISPERSION MODEL (APPENDIX A)

Levenspiel (1972) derived a model for dispersed plug flow specifically for high degrees of dispersion. The dispersion coefficient and mean residence time were treated here as unknown parameters and varied to determine the applicability of the model. The parameters and conditions used for the simulation in Figure 5.1 are presented in Appendix A.

Figure 5.1(a) shows that the model could be fitted to the experimental profile for the first 4 bed volumes of eluant. Because of the large variation in the potassium concentration, the section of Figure 5.1(a) lower than 500 mg K⁺/l was redrawn in Figure 5.1(b). Most of the profiles in this chapter were split as in Figure 5.1 to show both the high initial concentrations and the tail sections of the profiles.

It follows from Figure 5.1(b) that the main disadvantage of the model is its inability to simulate the long tail of the potassium profile. This implies that the tailing effect of the potassium profile could not be attributed to dispersion alone and that the contribution of the stagnant regions such as the carbon pores had to be taken into account.

5.2 "STAGNANT REGION" MODEL (APPENDIX B)

Wakeman (1976) developed a rigorous model for the "diffusional extraction from hydrodynamically stagnant regions in porous media". All of the liquid remaining in a bed of porous particles after draining was considered as stagnant. This included the liquid in the pores and in the contact areas between the particles. The model is only applicable to a bed of porous particles that was drained before the introduction of the eluant. Although this was not true for most of the experiments in this thesis, the model was tested to observe its behaviour at especially the later stages of the elution runs. It follows from the profile in Figure 5.2 that it was impossible to fit the model to the experimental data. Except for the model's inability to simulate the tail sections of the profiles, it was inflexible and could not be adopted to beds that were initially filled with eluant. The values of the parameters and conditions for the simulation in Figure 5.2 are given in Appendix B.

5.3 PORE DIFFUSION MODEL (APPENDIX C)

Leyva (1981) studied the adsorption of KCl on activated carbon and showed that the intraparticle diffusion was controlled by pore liquid diffusion and that the resistance to external mass transfer was negligible. A

similar model was developed here, but with the difference that 2 types of pores were considered which presented different resistances to mass transfer. Furthermore, the model presented in Appendix C does not account for adsorption.

The initial pore concentration was calculated with Equation 5.1 by assuming that all of the adsorbed potassium was present in the pore liquid :

$$C_{pK} = (Q_k/V_p) + C_{fK} \quad [5.1]$$

C_{fK} was taken here as the end concentration of potassium in the pretreatment solution and Q_k , the concentration of potassium adsorbed on the carbon surface, as determined in Experiment 72(a). The adsorption of potassium was not accounted for separately as this would have complicated the model and would have necessitated the determination of equilibrium isotherms for potassium at different cyanide concentrations and cyanide-ages of the carbon.

The behaviour of a model with one type of pore could be simulated by setting the fraction of pores which is regarded as macropores equal to 99.9%. Such a profile is shown in Figure 5.3. A sensitivity analysis of the model showed that it would be impossible to simulate the potassium profiles with a one parameter model.

However, by accounting for a mixture of macropores and micropores, it was possible to fit the model to the experimental data as in Figure 5.4. The first part of the simulated profile represents mainly the diffusion from the easily accessible macropores, whereas the tail section is the result of diffusion from the micropores. Except for the fact that the model fits the experimental data, it has a number of advantages that need to be mentioned :

- (1) Provision is made for accumulation in the porous structure of the carbon,
- (2) It is possible to adapt the model to beds that are initially filled or drained,
- (3) Different initial concentrations can be specified for the inter- and intraparticle solution, and

- (4) The potassium concentration is calculated throughout the bed and not only at the outlet as with the previous models.

Nevertheless, it does have a major disadvantage : While the elution of potassium was found to be insensitive to flow rate, the model is not. This is illustrated in Figure 5.5 where the same simulation as in Figure 5.4 was repeated, but at a higher flow rate. Even though the potassium can only be transported from the inside of the particles by a mechanism of diffusion, all diffusion models are sensitive to flow rate. This made it necessary to simulate the potassium profiles with a less fundamental type of model as used for nonideal flow reactors.

5.4 NONIDEAL FLOW MODEL

Levenspiel (1972) presented several models specifically for "small deviations from plug flow and long tails". The long tails were explained as being the result of adsorption on the solid surface and liquid trapped in the pores and stagnant regions at the contact points of the solid.

The model sketched in Figure 5.6(a) represented the concept of interaction between a porous structure and the surrounding fluid. The tanks A in the main stream can be visualized as the interparticle solution and the tanks M in the cross flow as the pore volume of the carbon. Closer inspection of the model indicates that it is identical to the pore diffusion model with one type of pore. The nonideal flow model, however, permits concepts and configurations that would not have been justifiable with a more fundamental model. One such a concept is the cross flow ratio which is defined here as :

$$X = V_{\text{cross}}/V \quad [5.2]$$

where V_{cross} is the flow rate to and from the deadwater regions. If X is assumed to be constant for the reactor that is being studied, the model becomes independent of flow rate. Three parameters were specified for the model, namely the number of stages, the cross flow ratio and the fraction of the volume which is not active.

As it was illustrated before that the profiles for the potassium cannot be simulated with a model with one resistance to mass transfer, the model in Figure 5.6(a) was expanded to a model with two interconnected deadwater regions as in Figure 5.6(b). These two deadwater regions will be referred to here as the macropores and the micropores of the carbon. The model in Figure 5.6(a) could be simulated with the model in Figure 5.6(b) by letting the volumes of the second deadwater regions (i.e. tanks B) approach zero.

5.4.1 Material balance equations

The cross flow ratios for the tanks in Figure 5.6(b) are defined as :

$$X_m = V_m/V \quad [5.3]$$

and

$$X_b = V_b/V_m \quad [5.4]$$

By dividing the column in sections with equal heights of Δh , and assuming the volume of each tank A to be equal to the interparticle solution in each section, the volume of these tanks becomes :

$$v_A = a \cdot \epsilon \cdot \Delta h \quad [5.5]$$

With the tanks M and B taken as the macro and micropores of the carbon, their volumes are written as :

$$v_M = \beta_K \cdot a \cdot (1 - \epsilon) \cdot \Delta h \cdot \rho \cdot V_p \quad [5.6]$$

and

$$v_B = (1 - \beta_K) \cdot a \cdot (1 - \epsilon) \cdot \Delta h \cdot \rho \cdot V_p \quad [5.7]$$

A mass balance for potassium over the j 'th tank A in the main stream is :

$$a \cdot \epsilon \cdot \Delta h \cdot (dC_K^{(j)}/dt) = V(C_K^{(j-1)} - C_K^{(j)}) + X_m V(C_{K_m}^{(j)} - C_K^{(j)}) \quad [5.8]$$

or

$$(dC_K^{(j)}/dt) = k_1(C_K^{(j-1)} - C_K^{(j)}) + k_1 X_m (C_{K_m}^{(j)} - C_K^{(j)}) \quad [5.9]$$

with

$$k_1 = V/(a \cdot \epsilon \cdot \Delta h) \quad [5.10]$$

Similarly, mass balances over the j 'th tanks M and B are :

$$(dC_{K_m}^{(j)}/dt) = k_2(C_K^{(j)} - C_{K_m}^{(j)}) + k_2 X_b (C_{K_b}^{(j)} - C_{K_m}^{(j)}) \quad [5.11]$$

and

$$(dC_{K_b}^{(j)}/dt) = k_3(C_{K_m}^{(j)} - C_{K_b}^{(j)}) \quad [5.12]$$

with

$$k_2 = \frac{X_m V}{\beta_K \cdot a \cdot (1-\epsilon) \cdot \Delta h \cdot \rho \cdot V_p} \quad [5.13]$$

and

$$k_3 = \frac{X_b X_m V}{(1-\beta_K) \cdot a \cdot (1-\epsilon) \cdot \Delta h \cdot \rho \cdot V_p} \quad [5.14]$$

5.4.2 Numerical solution procedure

The three ordinary differential equations 5.9, 5.11 and 5.12 were solved simultaneously by the use of the 4th order Runge Kutta method. An example of this procedure is presented in Appendix D.

The boundary conditions for the variables C_K , C_{K_m} and C_{K_b} were defined as :

1. For an AARL elution where the pretreatment was conducted in a separate vessel : $C_{K_m}^{(j,0)} = C_{K_b}^{(j,0)} = C_{K_p}^{(j,0)}$, where $C_{K_p}^{(j,0)}$ was calculated as in Equation 5.1, and $C_K^{(j,0)} = C_K^{(0,t)} = C_K$ in eluant
2. For an AARL elution where the pretreatment was conducted in the column : $C_{K_m}^{(j,0)} = C_{K_b}^{(j,0)} = C_{K_p}^{(j,0)}$ as above, $C_K^{(j,0)} = C_{K_f}$ of pretreatment step, and $C_K^{(0,t)} = C_K$ in eluant.
3. For a Zadra elution : $C_{K_m}^{(j,0)} = C_{K_b}^{(j,0)} = C_{K_p}^{(j,0)} = 0$,
 $C_K^{(j,0)} = C_K^{(0,t)} = C_K$ in eluant

A Turbo Pascal routine for the solution of the model is included in Appendix I in the sub-routine designated "procedure mod_cat".

5.4.3 Evaluation of nonideal flow model

The nonideal flow model was used in Figure 5.7 to simulate the elution of potassium from a bed of carbon after a KCN pretreatment. As expected from the results of the pore diffusion model, it was possible to fit the nonideal flow model to the experimental data. (The only significant difference between these two models is the flow rate dependency of the "mass transfer coefficients" of the nonideal flow model.) The values of the parameters and conditions used in Figure 5.7 were :

$$N = 10$$

$$X_m = 0.05$$

$$X_b = 0.025$$

$$\beta_K = 0.57$$

$$h = 0.143 \text{ m}$$

$$a = 1.2 \times 10^{-4} \text{ m}^2$$

$$d_c = 0.00142 \text{ m}$$

$$\rho = 838.8 \text{ kg.m}^{-3}$$

$$V_p = 6.34 \times 10^{-4} \text{ m}^3.\text{kg}^{-1}$$

$$\epsilon = 0.292$$

$$\Delta t = 20 \text{ s}$$

Unless stated otherwise, the same parameters were used in all of the following simulations of potassium profiles.

The effect of the number of height increments, N , was investigated in Figures 5.8 and 5.9. It is clear from Figure 5.8 that the model is very sensitive to variations in N . The profile for a certain number of increments can however be closely imitated with less increments by changes to the other parameters. The two nearly identical profiles in Figure 5.9 were obtained for (N, X_m) equal to $(50, 0.05)$ and $(10, 0.3)$ respectively. It was thus decided to choose $N = 10$ for all further simulations of potassium profiles obtained from the glass column described earlier.

The possibility of using the nonideal flow model with one deadwater region per stage was tested in Figure 5.10. All the simulated profiles were either too high for the initial bed volumes or too high for the tail

section. This confirmed the assumption that the potassium profiles had to be simulated with a model with accumulation in two separate regions in the porous structure.

Figure 5.11 proves the model's insensitivity to flow rate. The model prediction in Figure 5.11 was calculated with the same parameters as in Figure 5.7, but at a flow rate of twice that in Figure 5.7. Very high flow rates (in the order of 40 bed volumes per hour) do appear to affect the elution of potassium slightly, but with the evidence presented in Figure 3.34, it is safe to assume that the elution of potassium from packed beds of activated carbon is insensitive to flow rate within the range of flow rates employed for the elution of gold cyanide.

Furthermore, the model predicts identical concentration versus throughput profiles irrespective of the geometry of the column, provided that the same number of height increments are used. This is illustrated in Figure 5.12 where the same profile was obtained for the elution of potassium from the glass column and the much bigger stainless steel column. The fact that the same number of height increments had to be used in both cases implies that the extent of deviation from plug flow was the same in both columns. The following two sets of conditions resulted in the same simulated profile given in Figure 5.12 :

$$h = 0.139 \text{ m}$$

$$a = 1.2 \times 10^{-4} \text{ m}^2$$

$$V = 1.45 \times 10^{-8} \text{ m}^3 \cdot \text{s}^{-1}$$

$$N = 10$$

$$C_{K_{pi}} = 14000 \text{ g} \cdot \text{m}^{-3}$$

$$C_{K_{bi}} = 4000 \text{ g} \cdot \text{m}^{-3}$$

$$C_{KF} = 0 \text{ g} \cdot \text{m}^{-3}$$

$$h = 0.749 \text{ m}$$

$$a = 78.54 \times 10^{-4} \text{ m}^2$$

$$V = 508 \times 10^{-8} \text{ m}^3 \cdot \text{s}^{-1}$$

$$N = 10$$

$$C_{K_{pi}} = 14000 \text{ g} \cdot \text{m}^{-3}$$

$$C_{K_{bi}} = 4000 \text{ g} \cdot \text{m}^{-3}$$

$$C_{KF} = 0 \text{ g} \cdot \text{m}^{-3}$$

The rest of the parameters were the same as before.

The model also performs satisfactorily with a constant concentration of potassium in the feed to the column as would be the case with water of lower quality. The profile in Figure 5.13 was obtained by using an eluant with a potassium concentration of $559 \text{ g} \cdot \text{m}^{-3}$ through the addition of KCl.

However, when KCl was present in the pretreatment step, the parameters had to be changed to account for the lower adsorptivity of potassium in a KCl than a KCN environment. The profile in Figure 5.14 was measured after soaking the carbon in water containing only KCl. The model was fitted to the experimental data with the following set of parameters :

$$\begin{aligned} N &= 10, \\ X_m &= 0.3, \\ X_b &= 0.0025, \text{ and} \\ \beta_K &= 0.92. \end{aligned}$$

As little or no adsorption of potassium could be detected from KCl solutions, the initial pore concentration for the elution was taken as being equal to the end concentration measured in the pretreatment solution. By comparing this set of parameters to that used for elutions after KCN pretreatments, it becomes clear that the model approaches the model of Figure 5.6(a) in the case of poorer adsorption of the cation. The "micropore concept" thus seems to be accounting mainly for that portion of the potassium that is adsorbed on the carbon.

Because of the co-adsorption of potassium with cyanide, the model does not apply to the initial stages of Zadra elutions as illustrated in Figure 5.15. Fortunately, the elution of gold cyanide is much less sensitive to the cation concentration in Zadra elutions than AARL elutions and it will be illustrated that the poorer prediction as in Figure 5.15 will not markedly affect the simulation of the Zadra gold elution profiles.

5.5 SUMMARY

Most of the models tested in this Chapter failed in describing the long tail of potassium observed in the elution experiments. This was attributed to the diffusion of potassium into the micropore structure of the carbon and to the omission of adsorption of potassium in these models. A pore diffusion model which accounted for accumulation of potassium in the macropores as well as the micropores of the carbon was found to describe the potassium profile effectively, but unlike the

experimental data, this model was sensitive to the flow rate of the eluant. The sensitivity to flow rate was overcome by employing a tanks-in-series nonideal flow model with two deadwater regions per stage. This model is similar to the pore diffusion model, except that it is insensitive to flow rate in the interparticle solution.

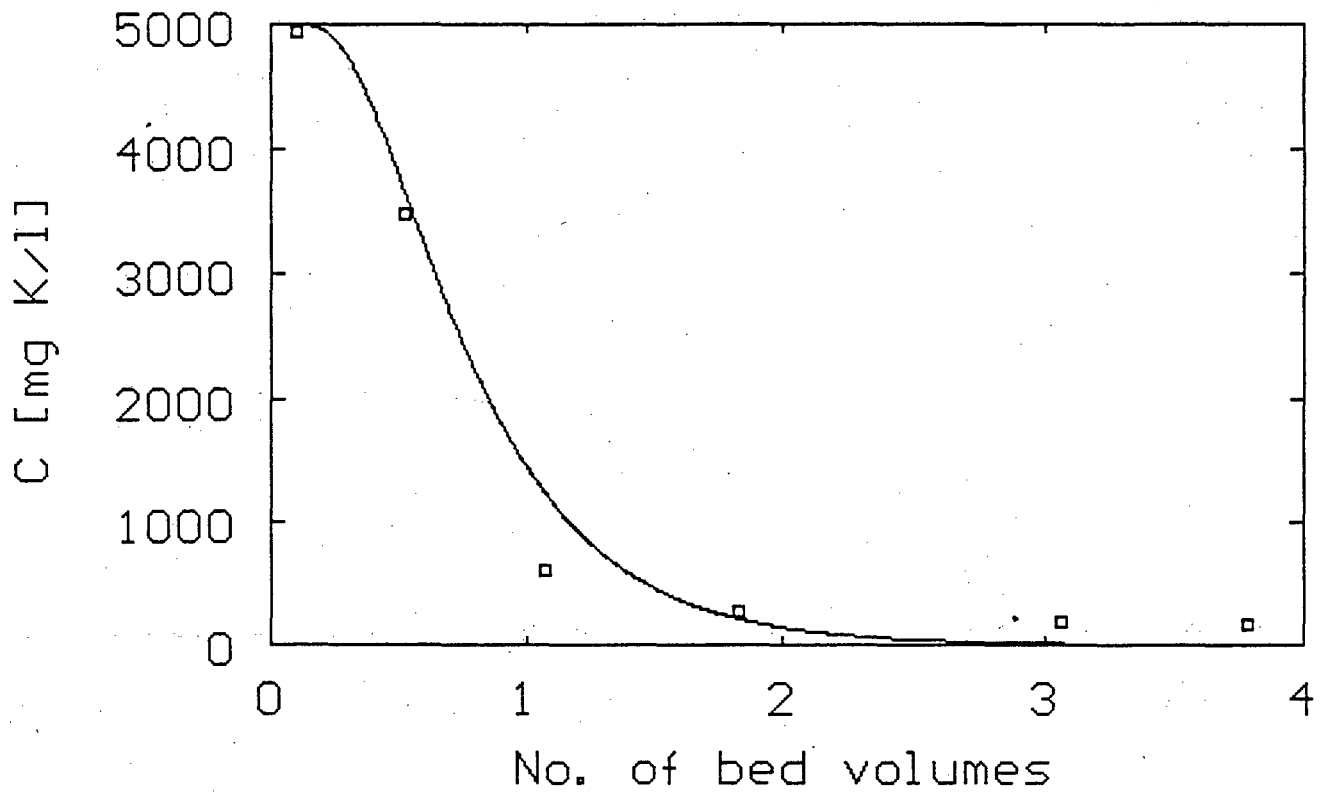


Figure 5.1(a) Fit of Levenspiel's dispersion model to the potassium profile of an AARL elution. (Exp.59)

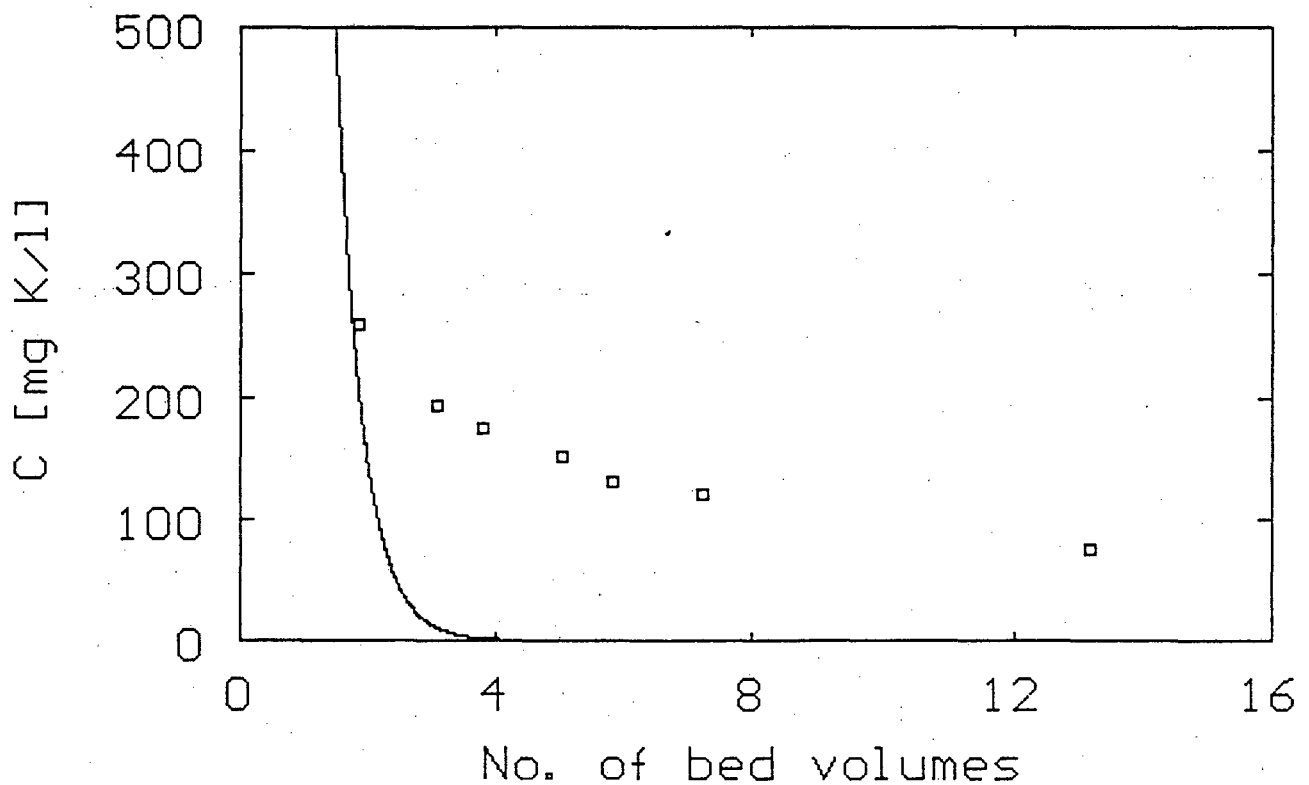


Figure 5.1(b) Tail section of potassium profile shown in Figure 5.1(a).

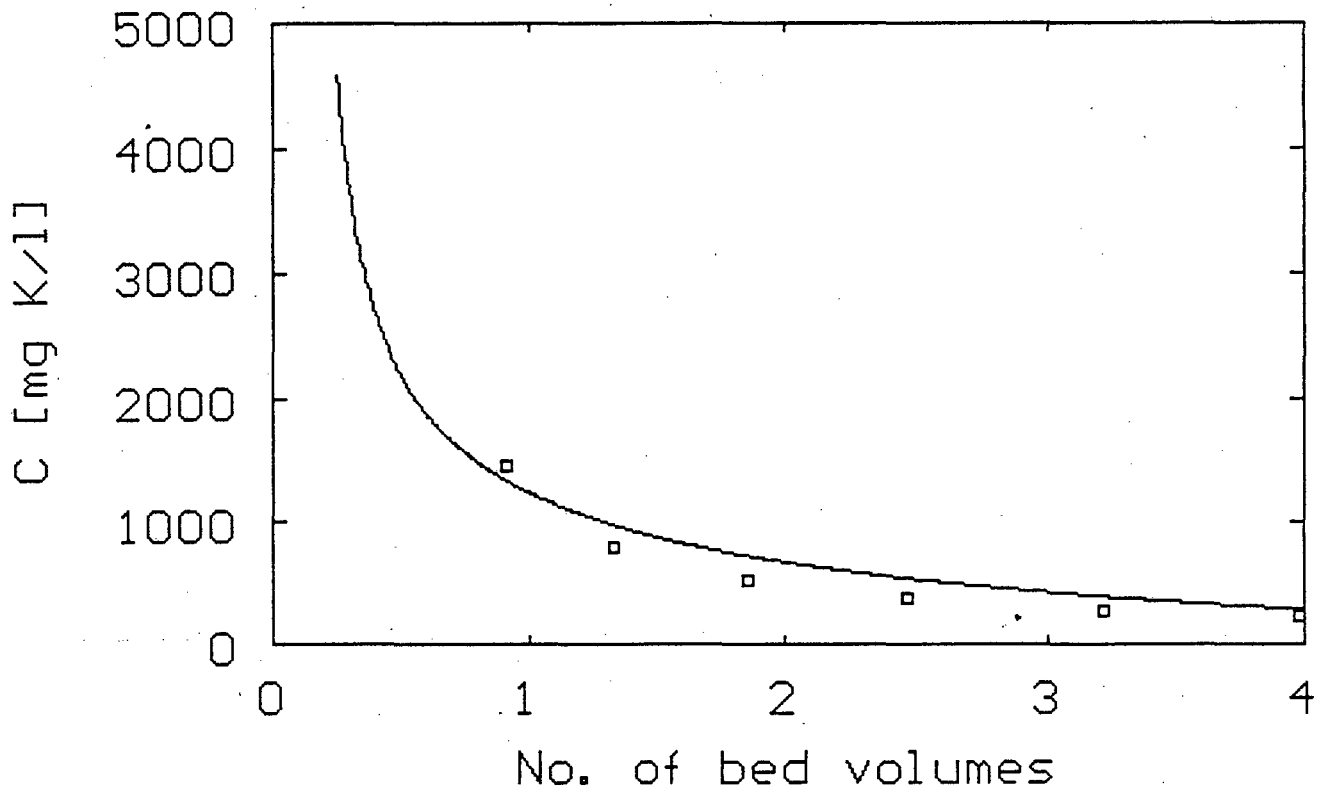


Figure 5.2(a) Fit of the Stagnant region model to the potassium profile of an AARL elution. (Exp.76)

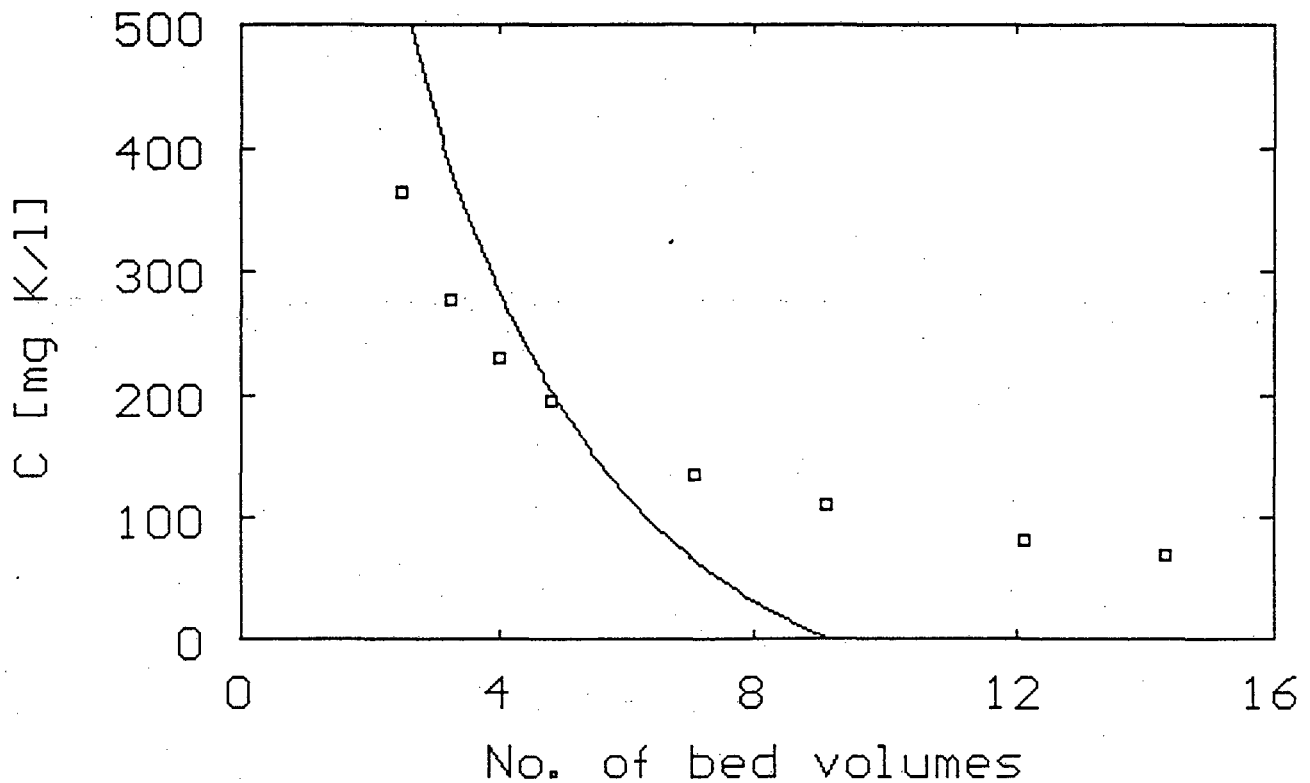


Figure 5.2(b) Tail section of potassium profile shown in Figure 5.2(a).

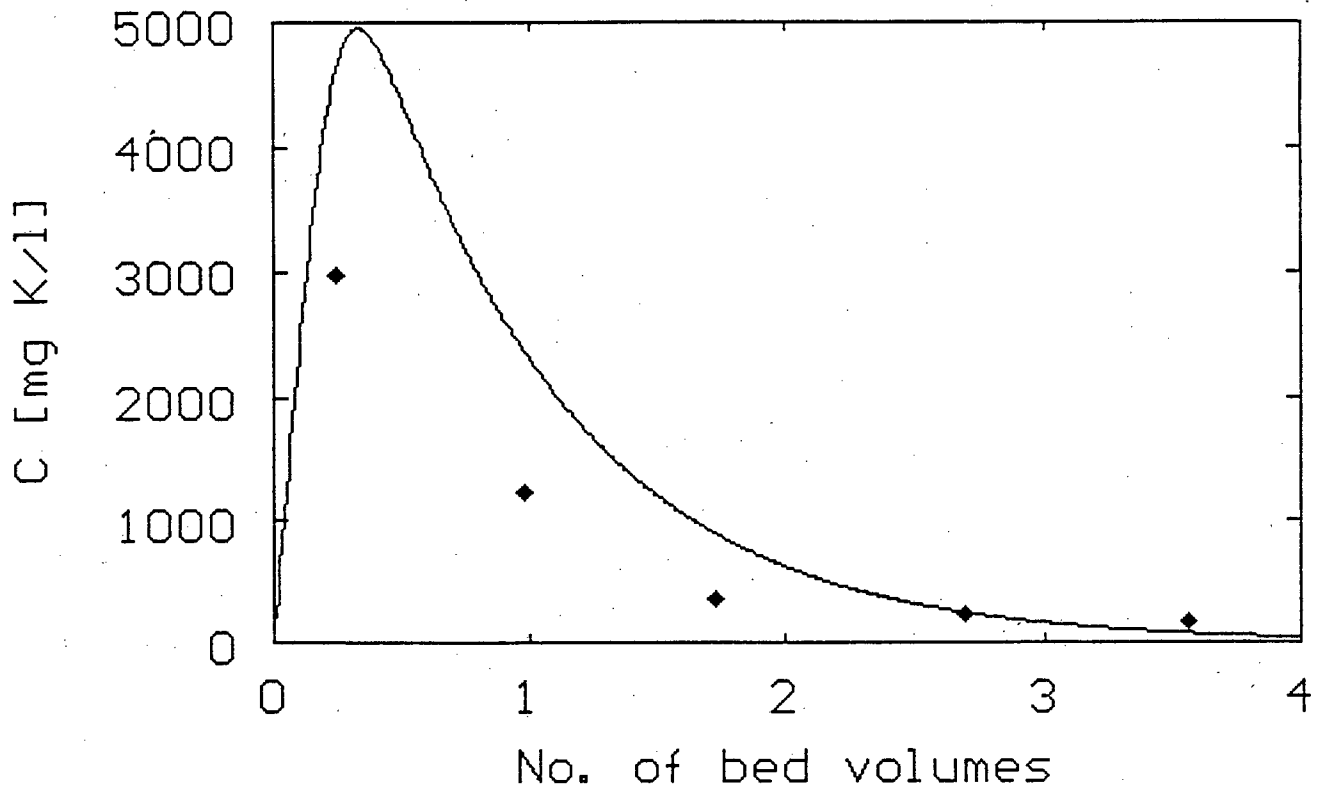


Figure 5.3(a) Fit of the Pore diffusion model to the potassium profile of an AARL elution. Accounted for one type of pore only. (Exp.50)

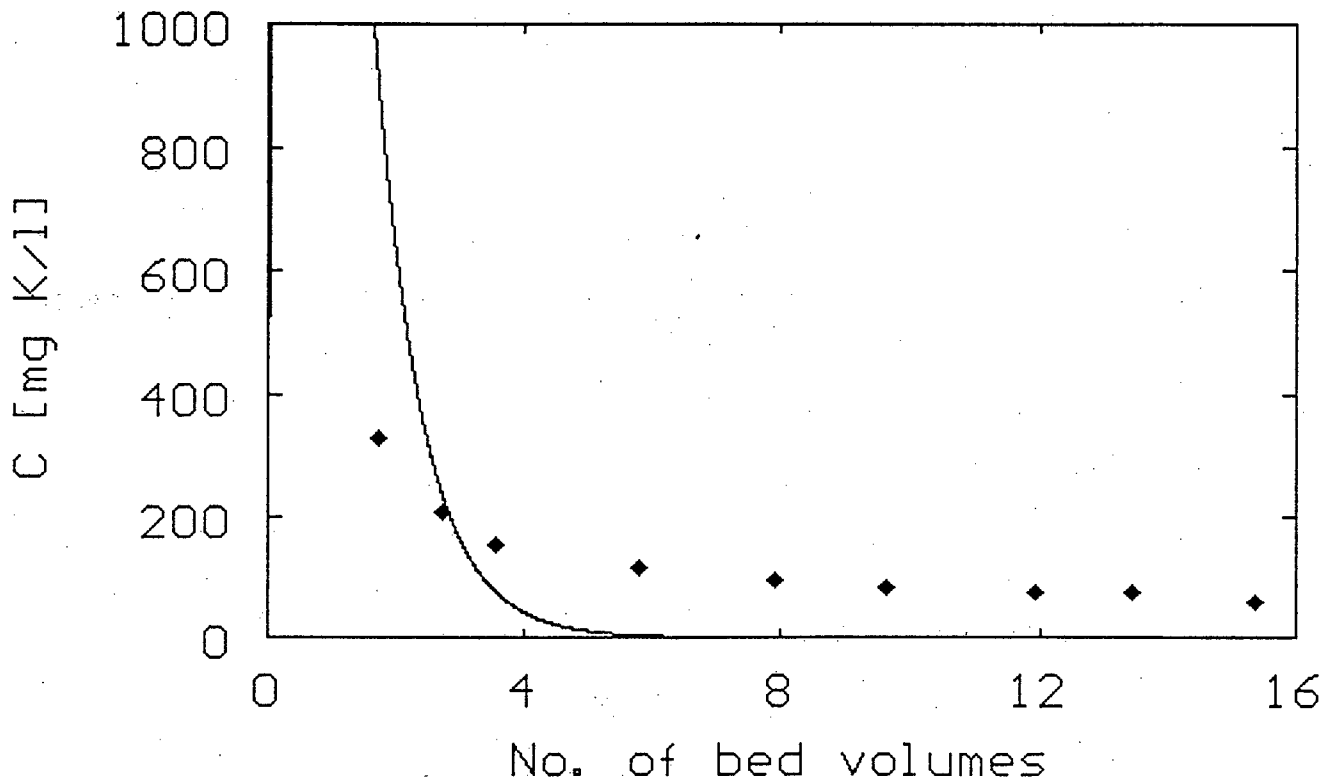


Figure 5.3(b) Tail section of potassium profile shown in Figure 5.3(a).

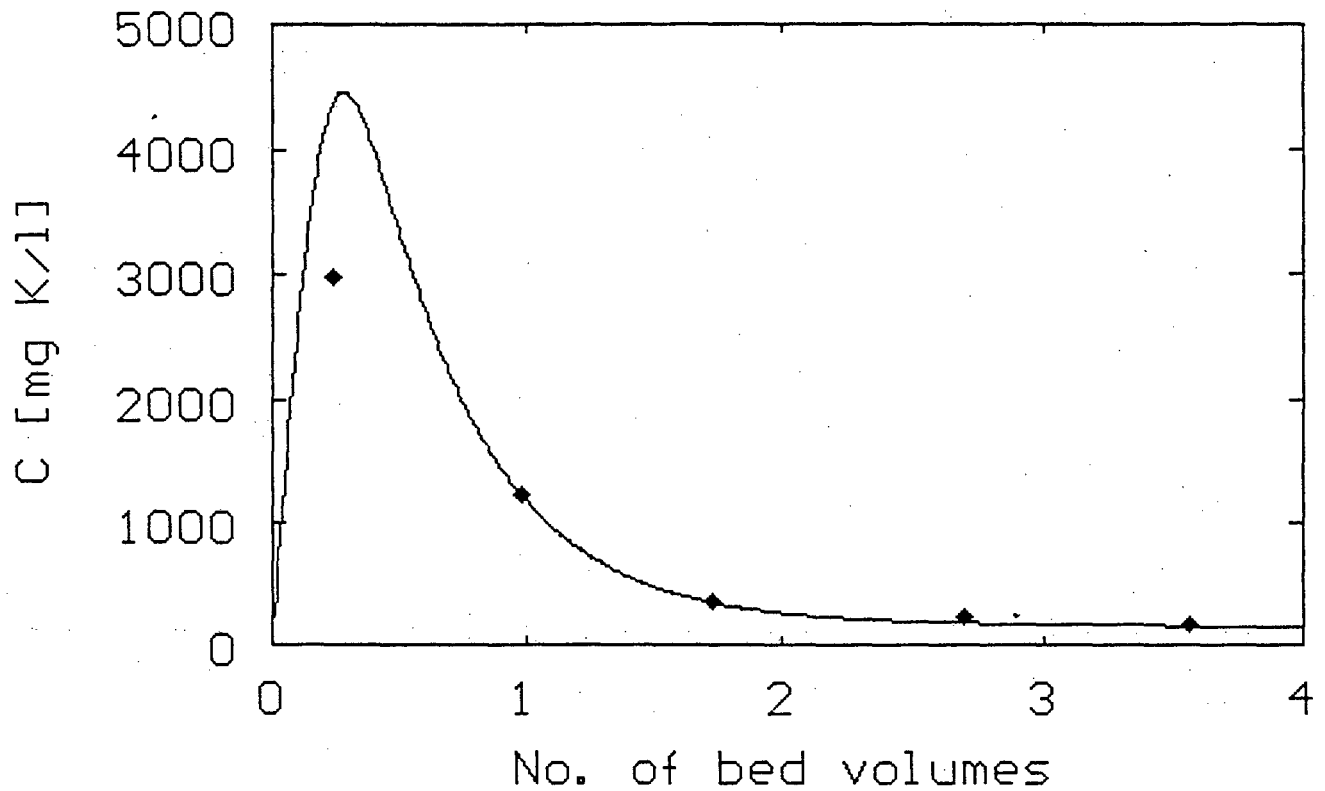


Figure 5.4(a) Fit of the Pore diffusion model to the potassium profile of an AARL elution. Accounted for macropores and micropores. (Exp.50)

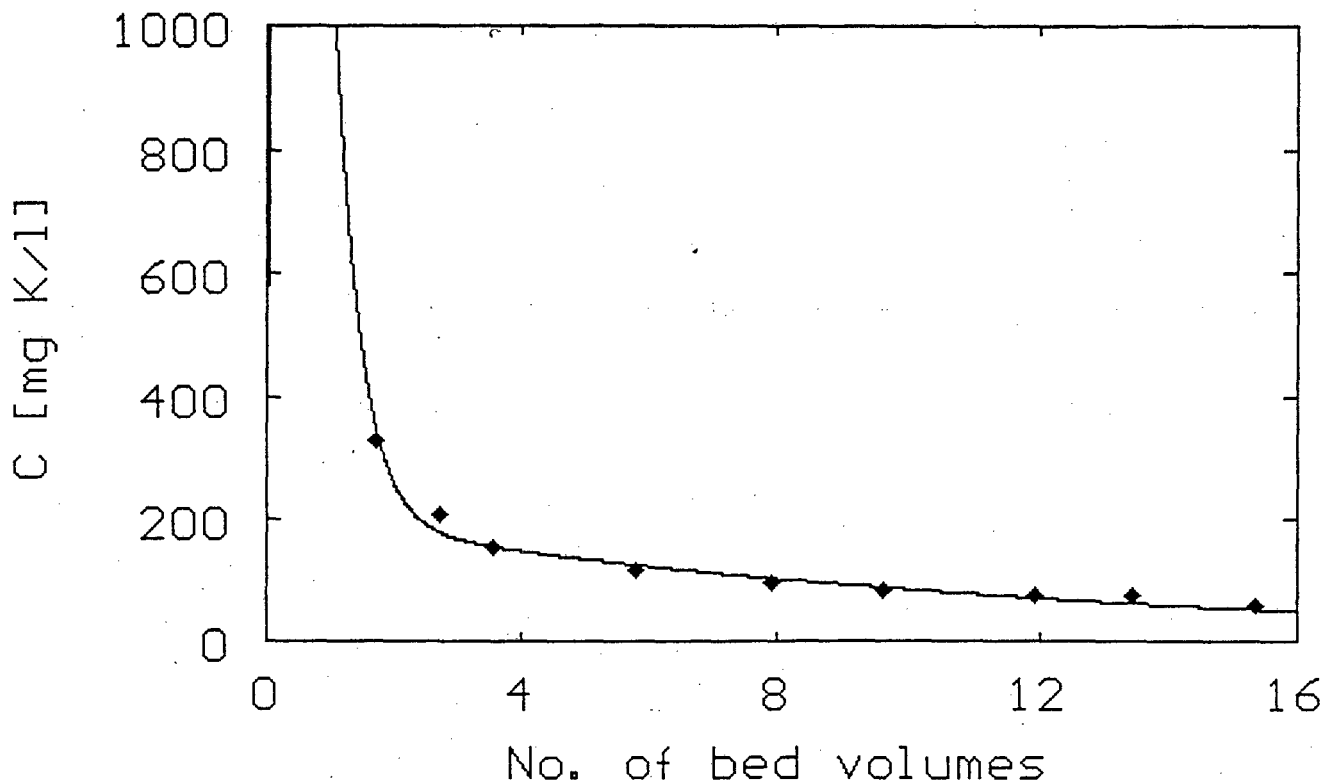


Figure 5.4(b) Tail section of potassium profile shown in Figure 5.4(a).

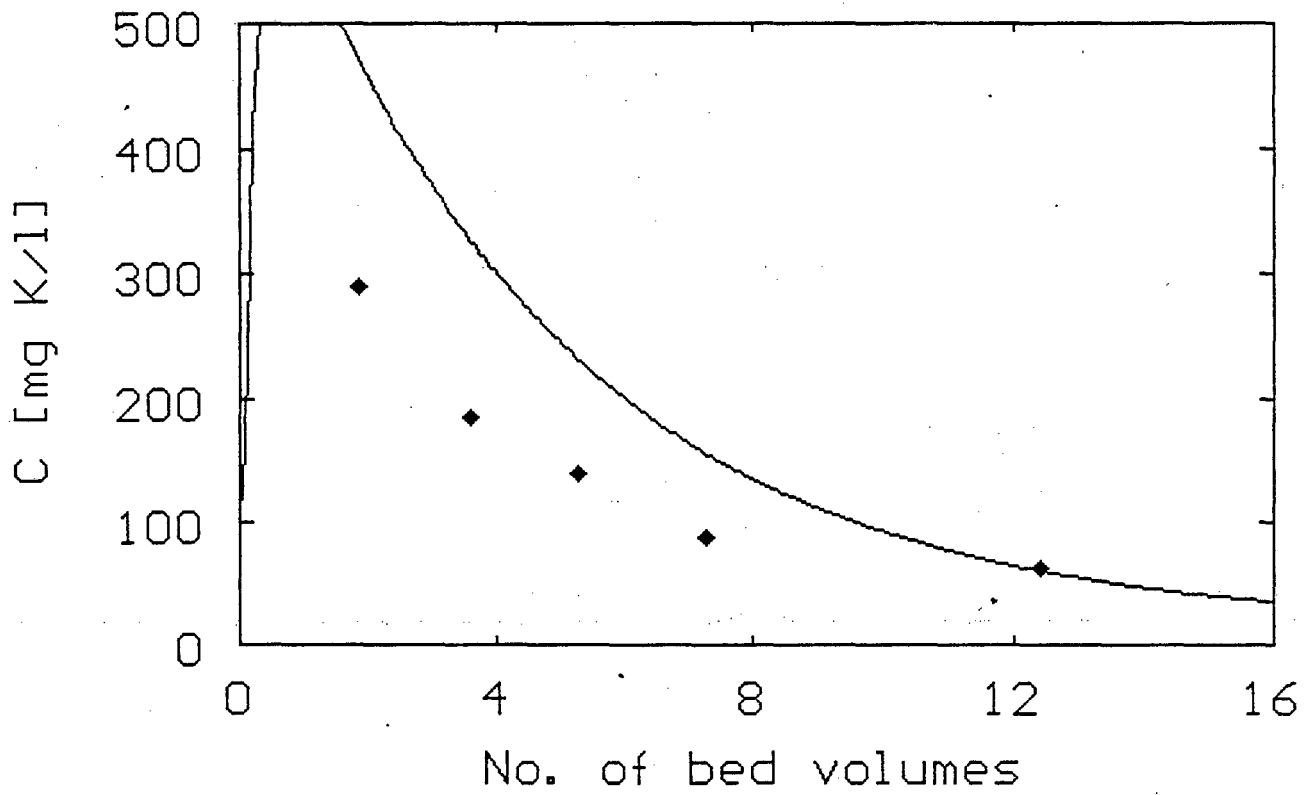


Figure 5.5 Fit of the Pore diffusion model to the potassium profile of an AARL elution at a flow rate of 37 bed volumes per hour. (Exp.62)

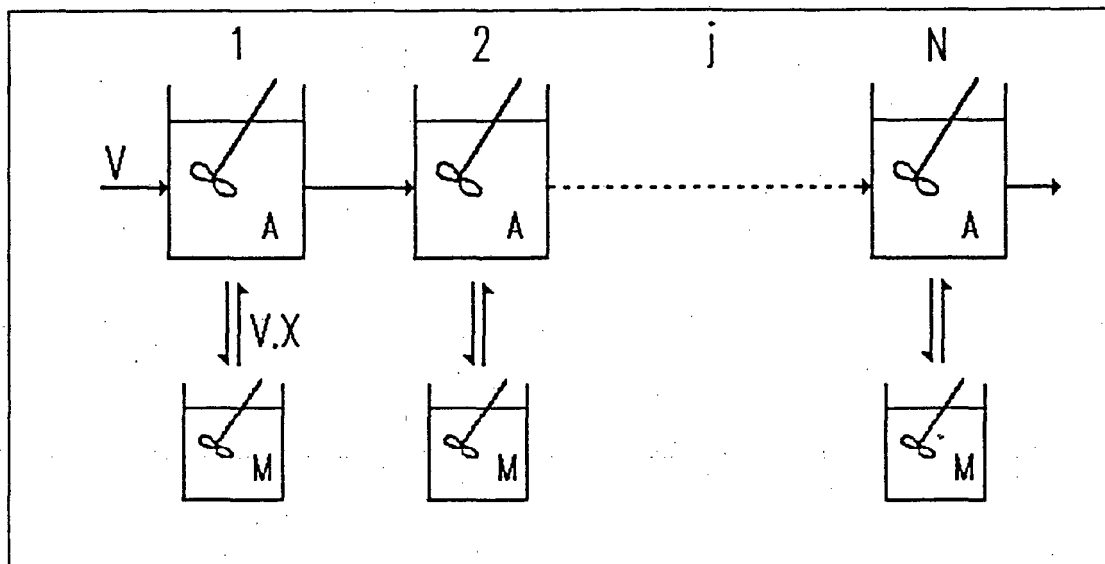


Figure 5.6(a) Levenspiel's nonideal flow model for long tails.

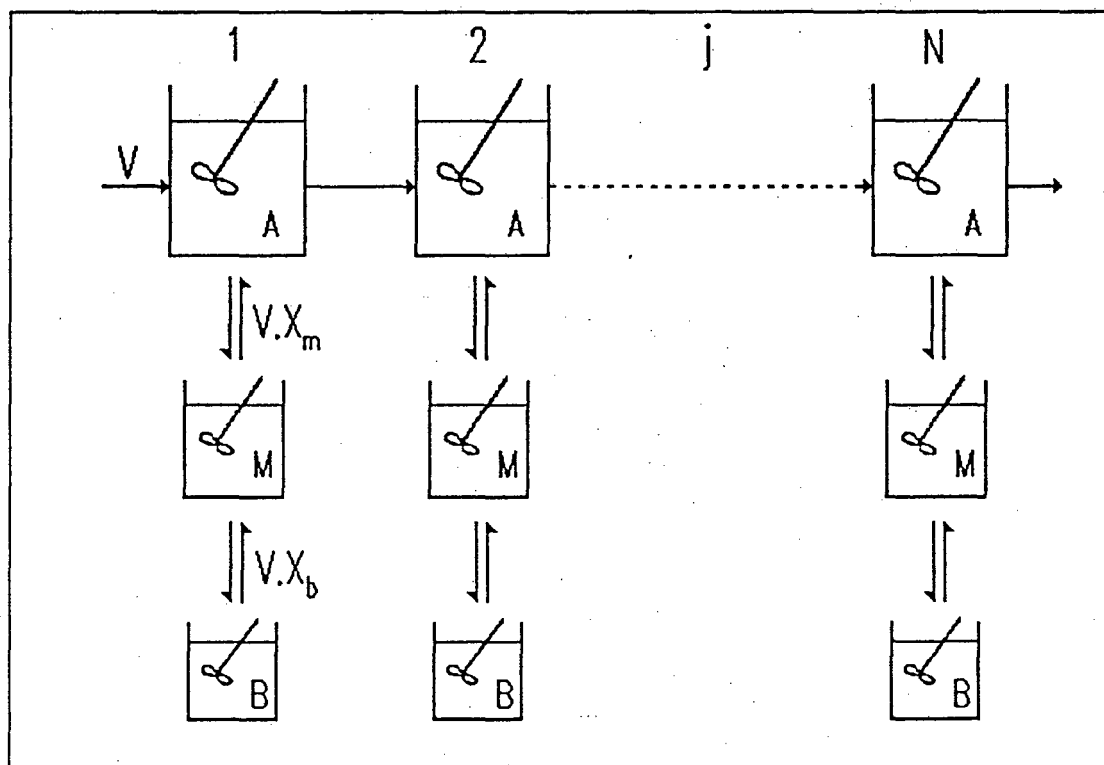


Figure 5.6(b) Adapted nonideal flow model with two deadwater regions per stage.

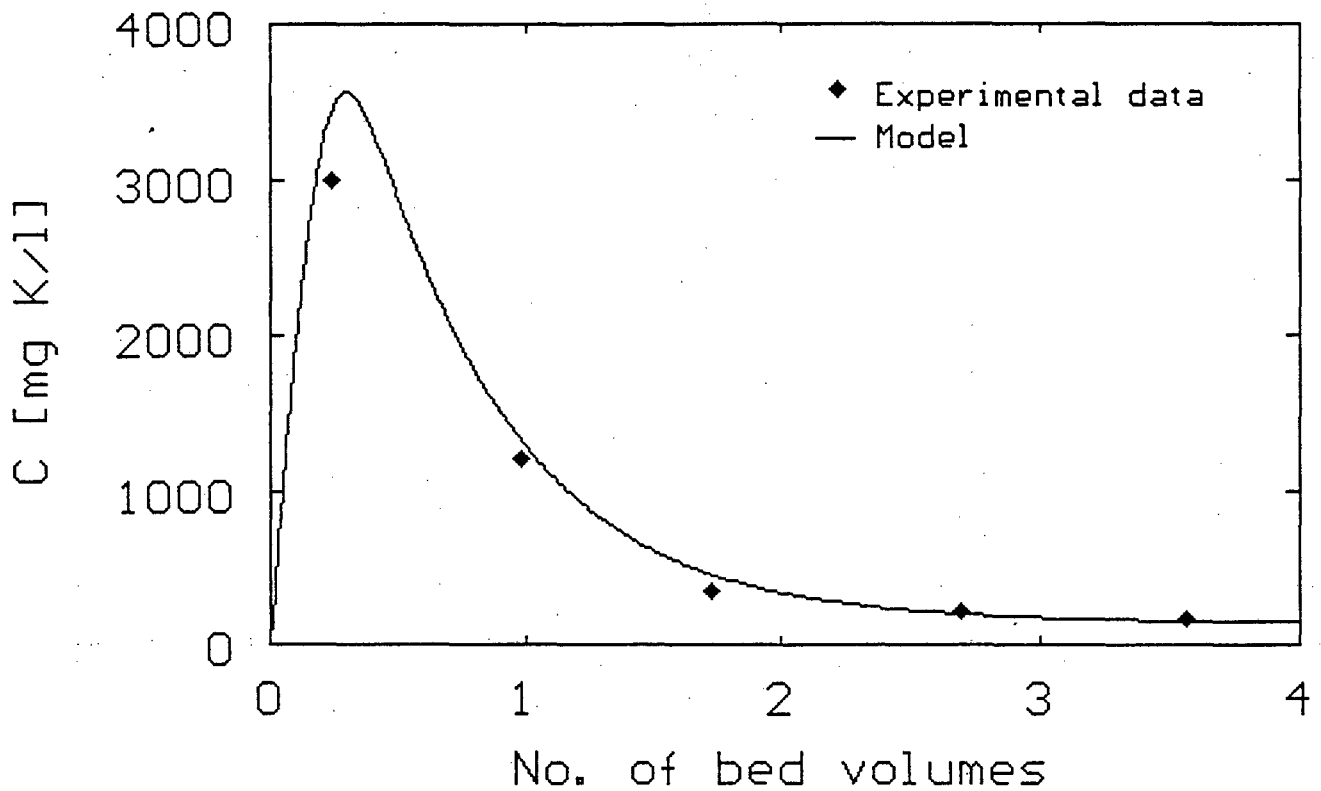


Figure 5.7(a) Fit of the Nonideal flow model to the potassium profile of an AARL elution. Accounted for two deadwater regions. $V = 1.367 \times 10^{-8} \text{ m}^3 \cdot \text{s}^{-1}$, $C_{Kpi} = 14000 \text{ g} \cdot \text{m}^{-3}$, $C_{Kbi} = 0 \text{ g} \cdot \text{m}^{-3}$, $C_{KF} = 0 \text{ g} \cdot \text{m}^{-3}$. (Exp.50)

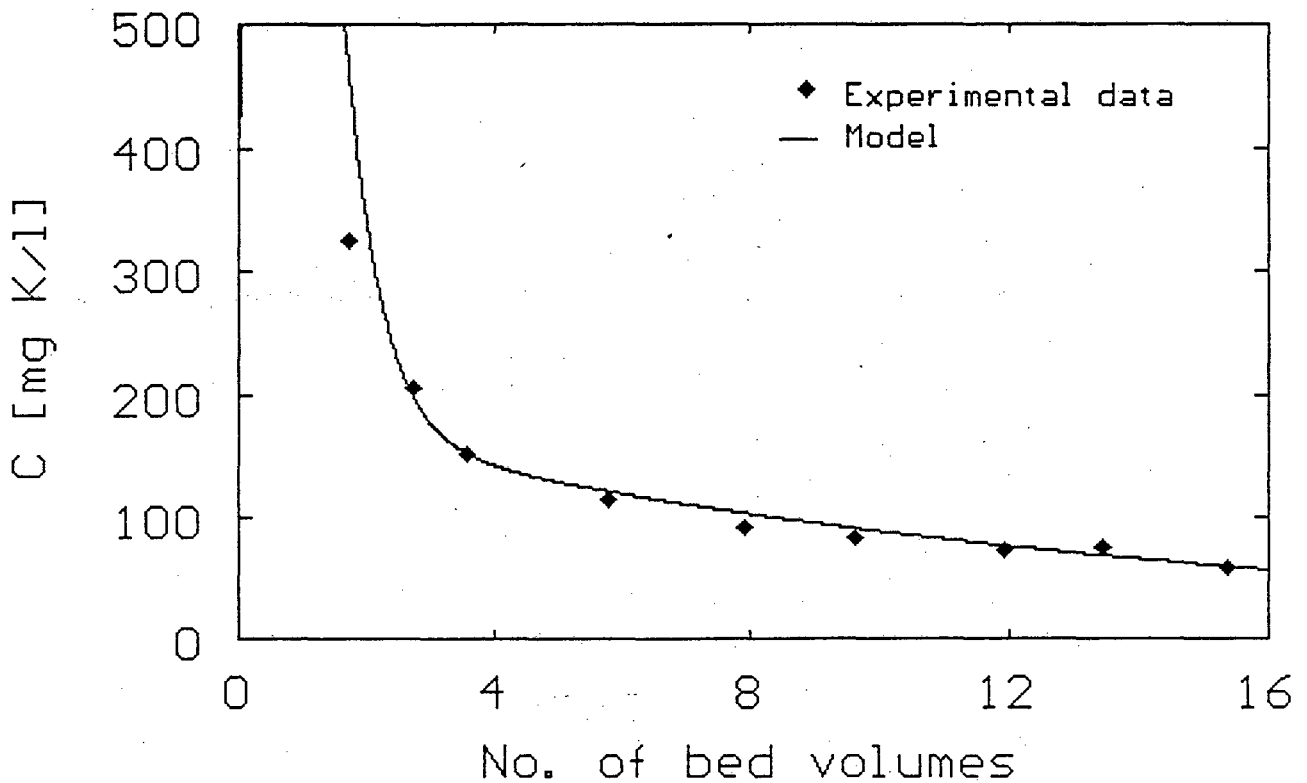


Figure 5.7(b) Tail section of potassium profile shown in Figure 5.7(a).

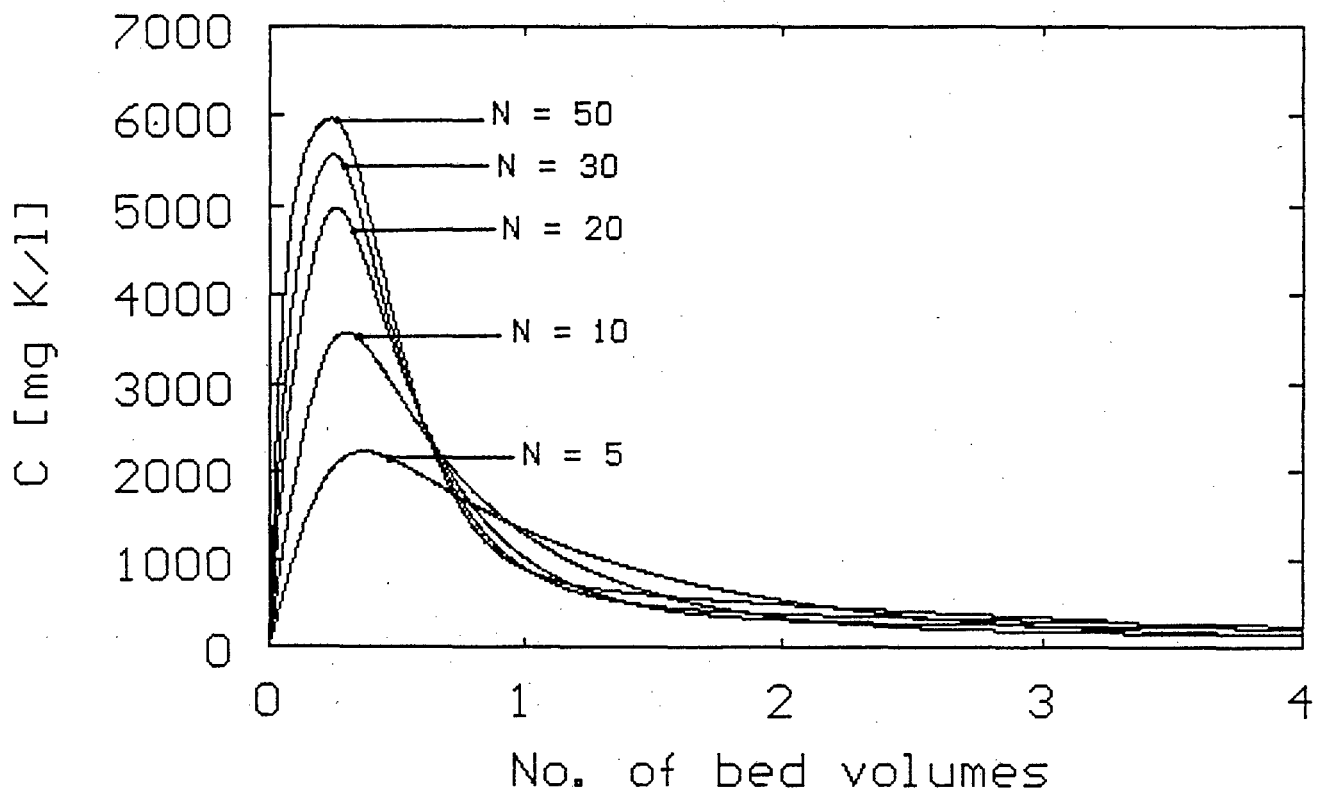


Figure 5.8 Sensitivity of the nonideal model for the elution of potassium to the number of mixed reactor sections. $V = 1.367 \times 10^{-8} \text{ m}^3 \cdot \text{s}^{-1}$, $C_{K_{pi}} = 14000 \text{ g} \cdot \text{m}^{-3}$, $C_{K_{bi}} = 0 \text{ g} \cdot \text{m}^{-3}$, $C_{K_F} = 0 \text{ g} \cdot \text{m}^{-3}$, $\Delta t = 5 \text{ s}$.

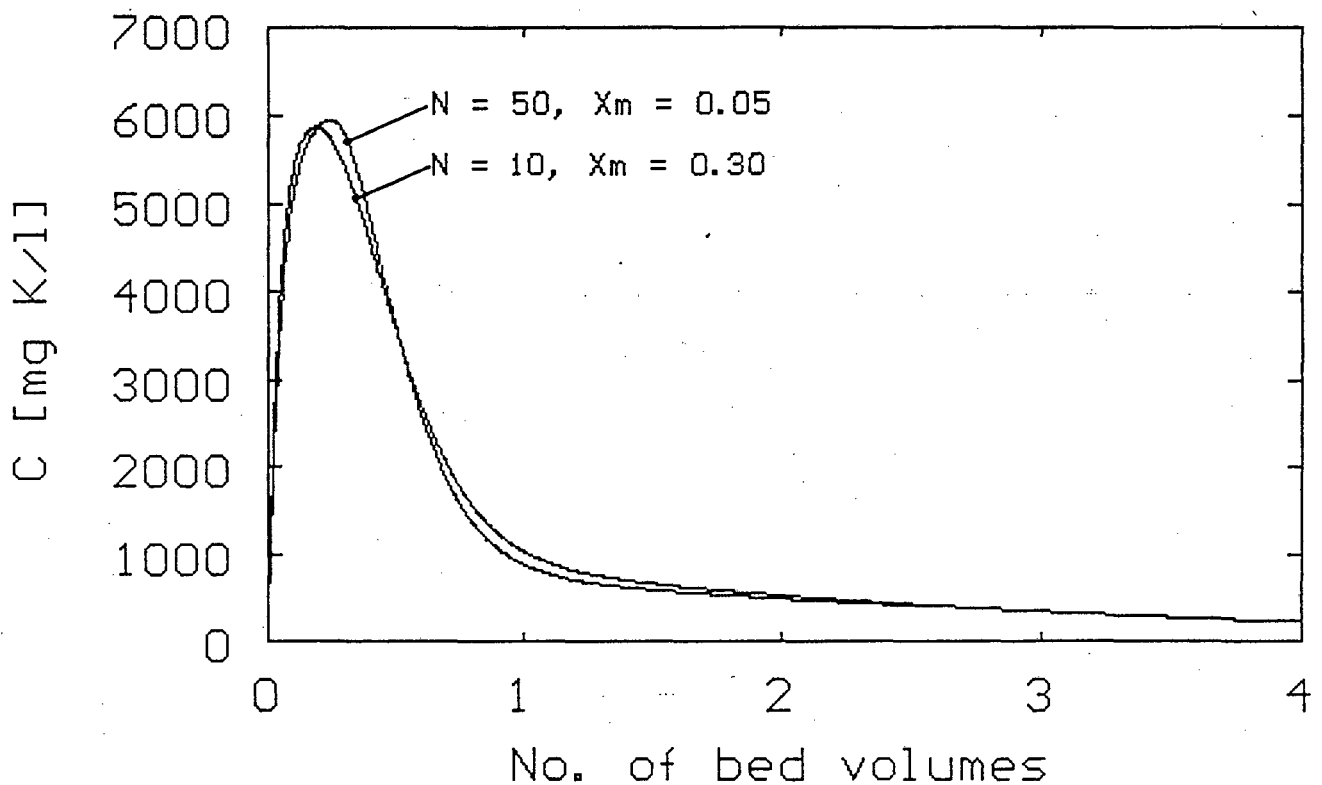


Figure 5.9 Simulation of potassium profiles with nonideal flow model with different cross flow parameters. $V = 1.367 \times 10^{-8} \text{ m}^3 \cdot \text{s}^{-1}$, $C_{K_{pi}} = 14000 \text{ g} \cdot \text{m}^{-3}$, $C_{K_{bi}} = 0 \text{ g} \cdot \text{m}^{-3}$, $C_{K_F} = 0 \text{ g} \cdot \text{m}^{-3}$, $\Delta t = 5 \text{ s}$.

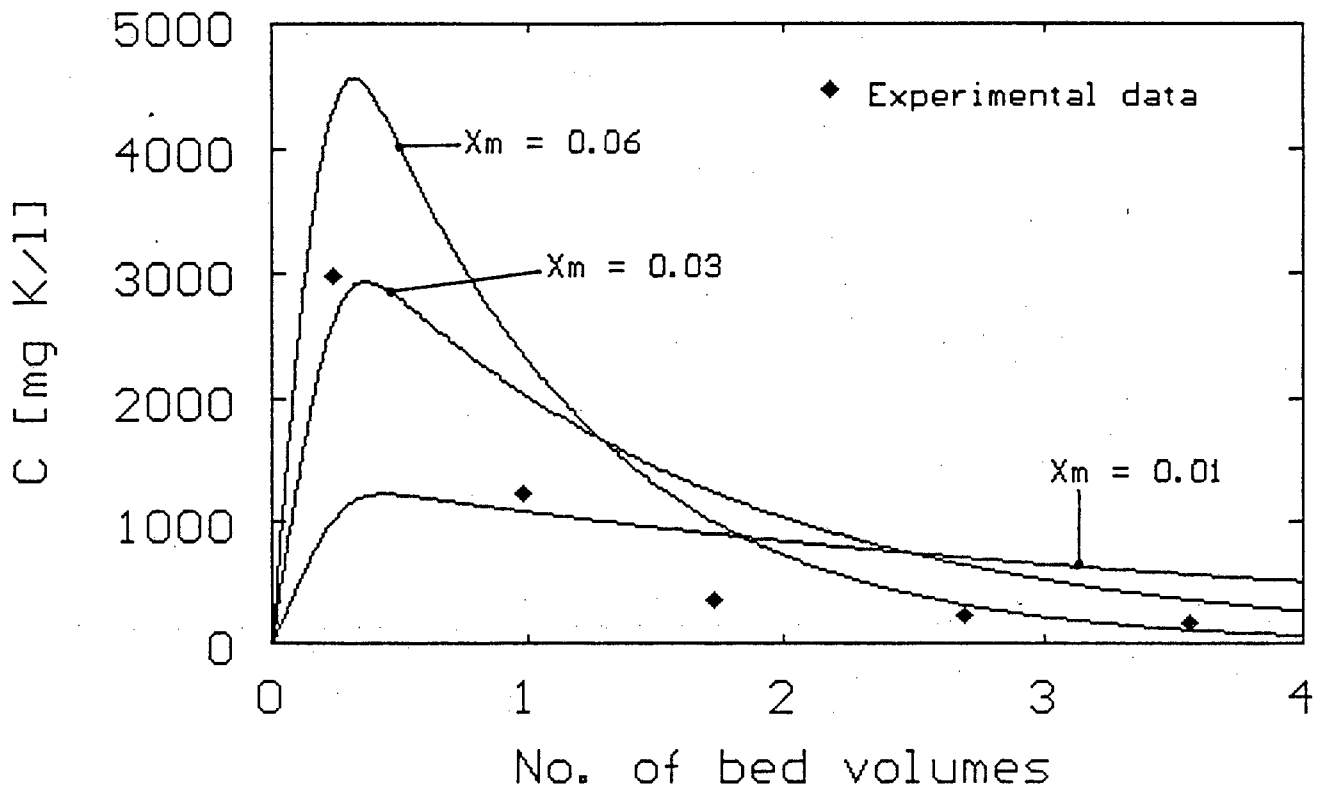


Figure 5.10 Simulations with Levenspiel's nonideal flow model with one stagnant region per stage. $V = 1.367 \times 10^{-8} \text{ m}^3 \cdot \text{s}^{-1}$, $C_{K0j} = 14000 \text{ g} \cdot \text{m}^{-3}$, $C_{Kbi} = 0 \text{ g} \cdot \text{m}^{-3}$, $C_{KF} = 0 \text{ g} \cdot \text{m}^{-3}$, $X_b = 0$, $\beta_K = 0.999$. (Exp.50)

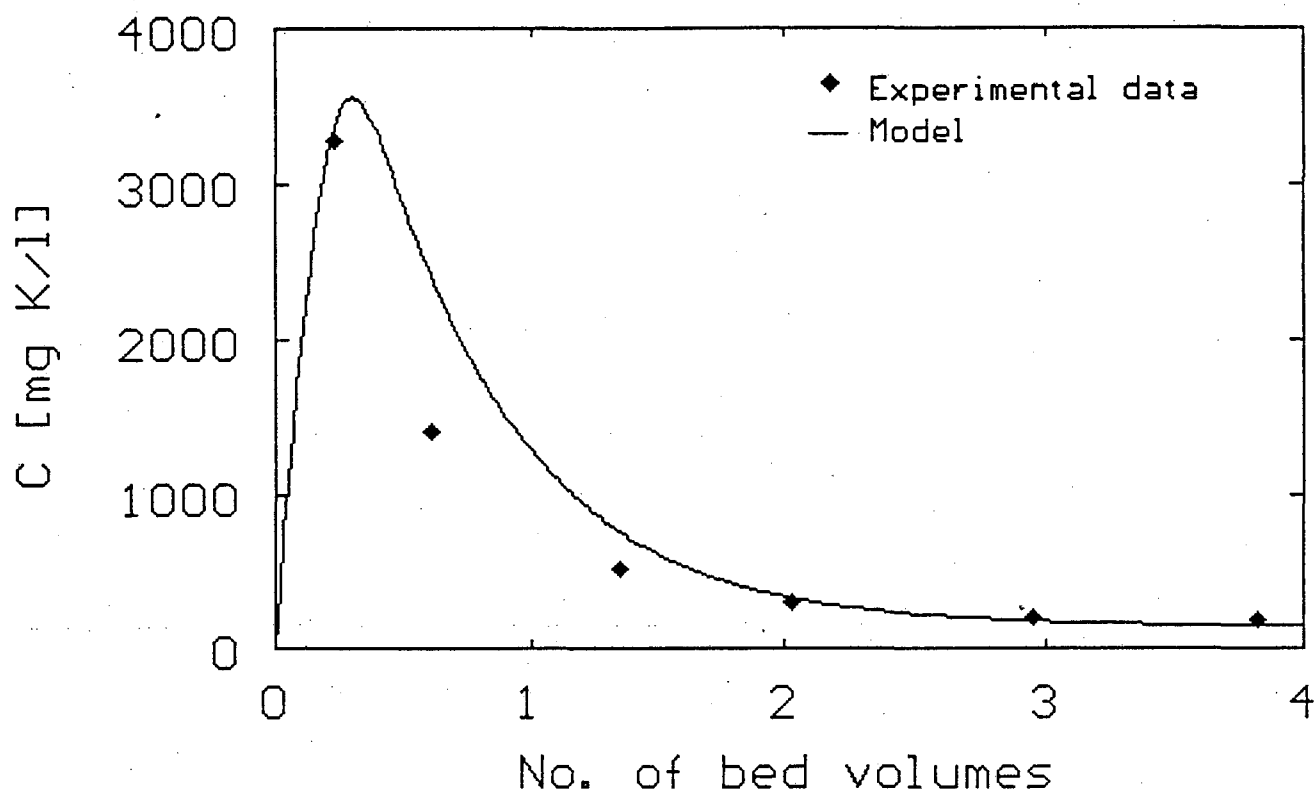


Figure 5.11(a) Fit of the nonideal flow model to the potassium profile of an AARL elution at a flow rate of 5.9 bed volumes per hour. $V = 2.89 \times 10^{-8} \text{ m}^3 \cdot \text{s}^{-1}$, $C_{Kpi} = 14000 \text{ g} \cdot \text{m}^{-3}$, $C_{Kbi} = 0 \text{ g} \cdot \text{m}^{-3}$, $C_{KF} = 0 \text{ g} \cdot \text{m}^{-3}$. (Exp.61)

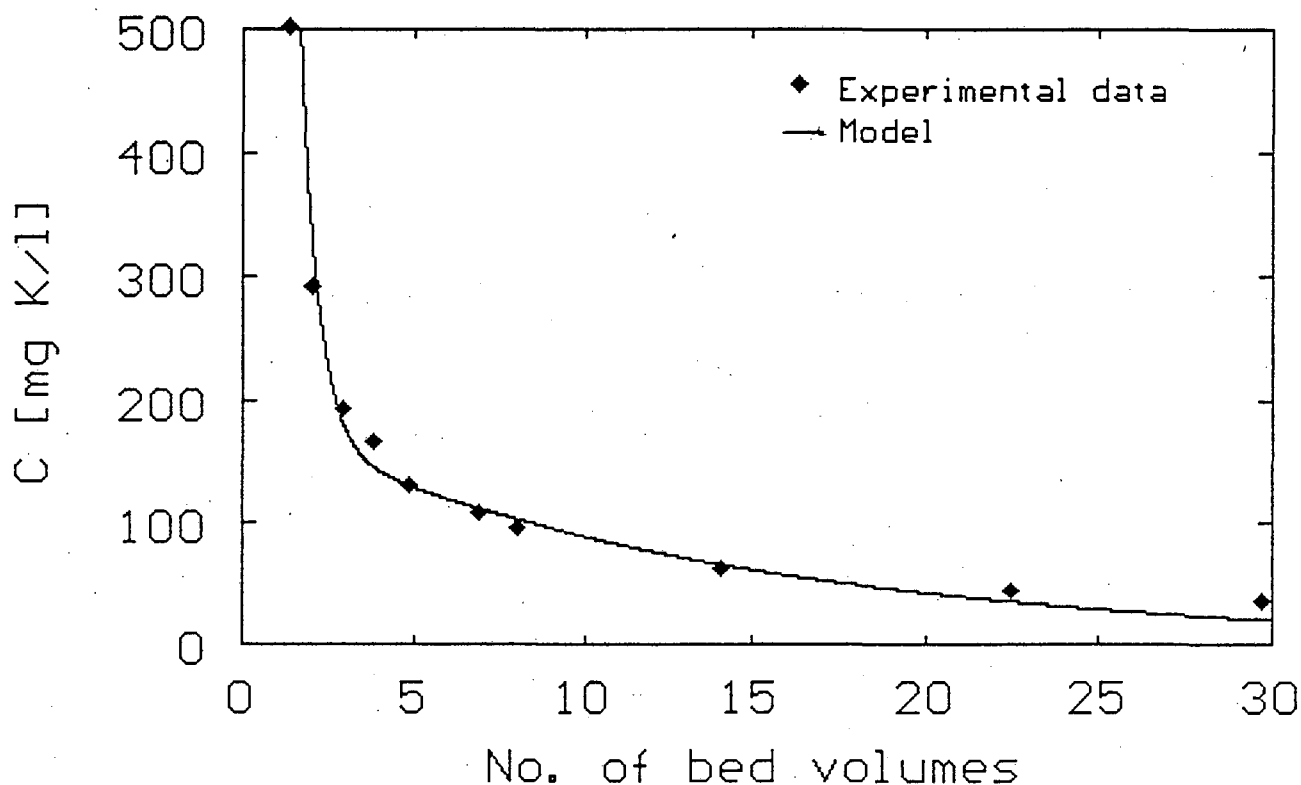


Figure 5.11(b) Tail section of potassium profile shown in Figure 5.11(a).

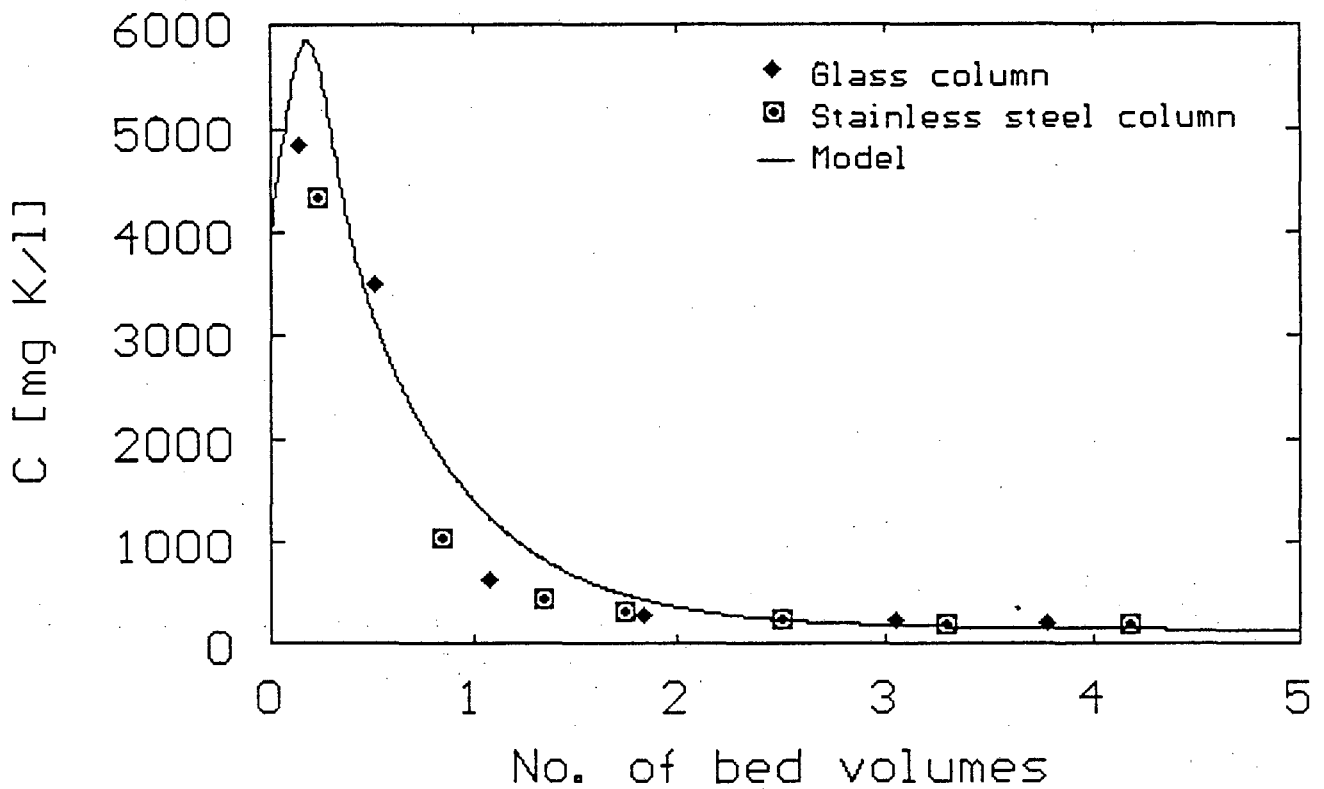


Figure 5.12 Insensitivity of the nonideal flow model for the elution of potassium to the geometry of the elution column. (Exp.59 and 60)

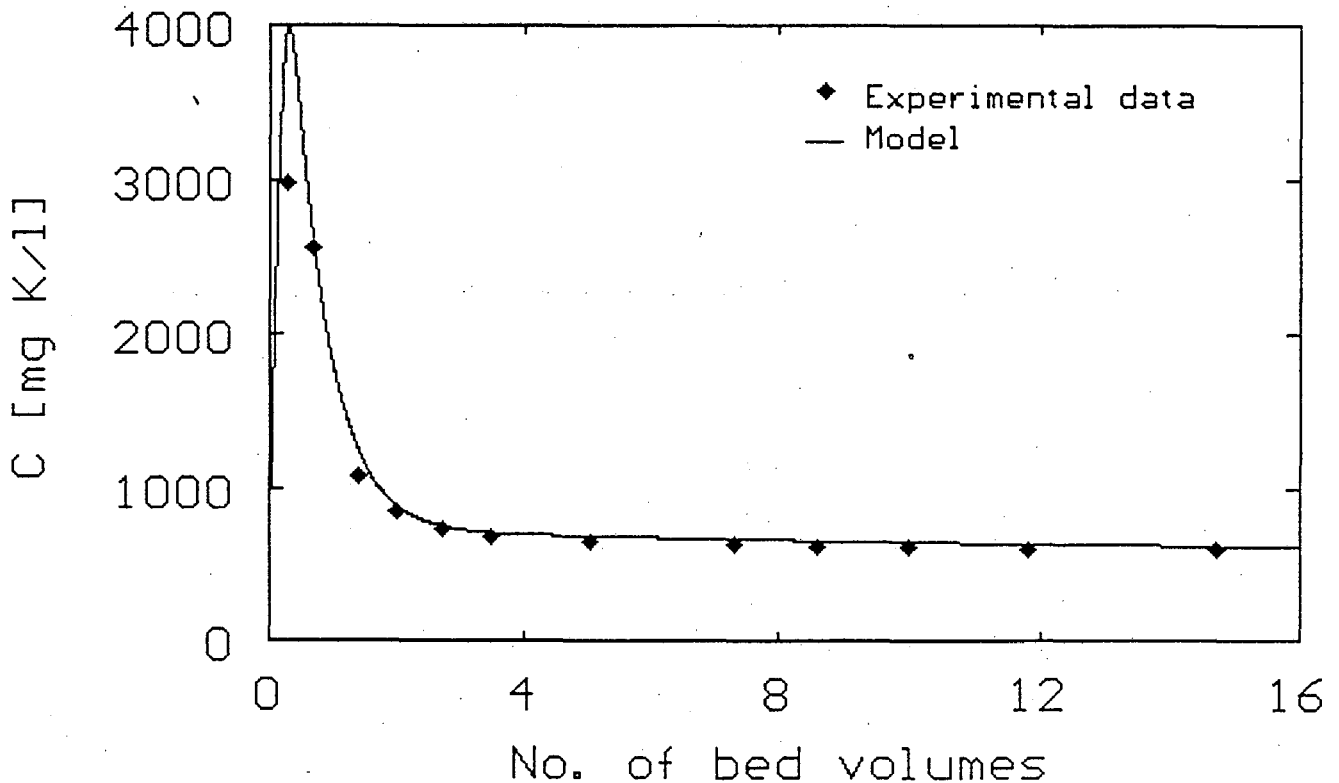


Figure 5.13 Simulation of the potassium profile during an AARL elution with a constant concentration of potassium in the feed. $V = 1.376 \times 10^{-8} \text{ m}^3 \cdot \text{s}^{-1}$, $C_{Kpi} = 14000 \text{ g} \cdot \text{m}^{-3}$, $C_{Kbi} = 559 \text{ g} \cdot \text{m}^{-3}$, $C_{KF} = 559 \text{ g} \cdot \text{m}^{-3}$ (Exp.75)

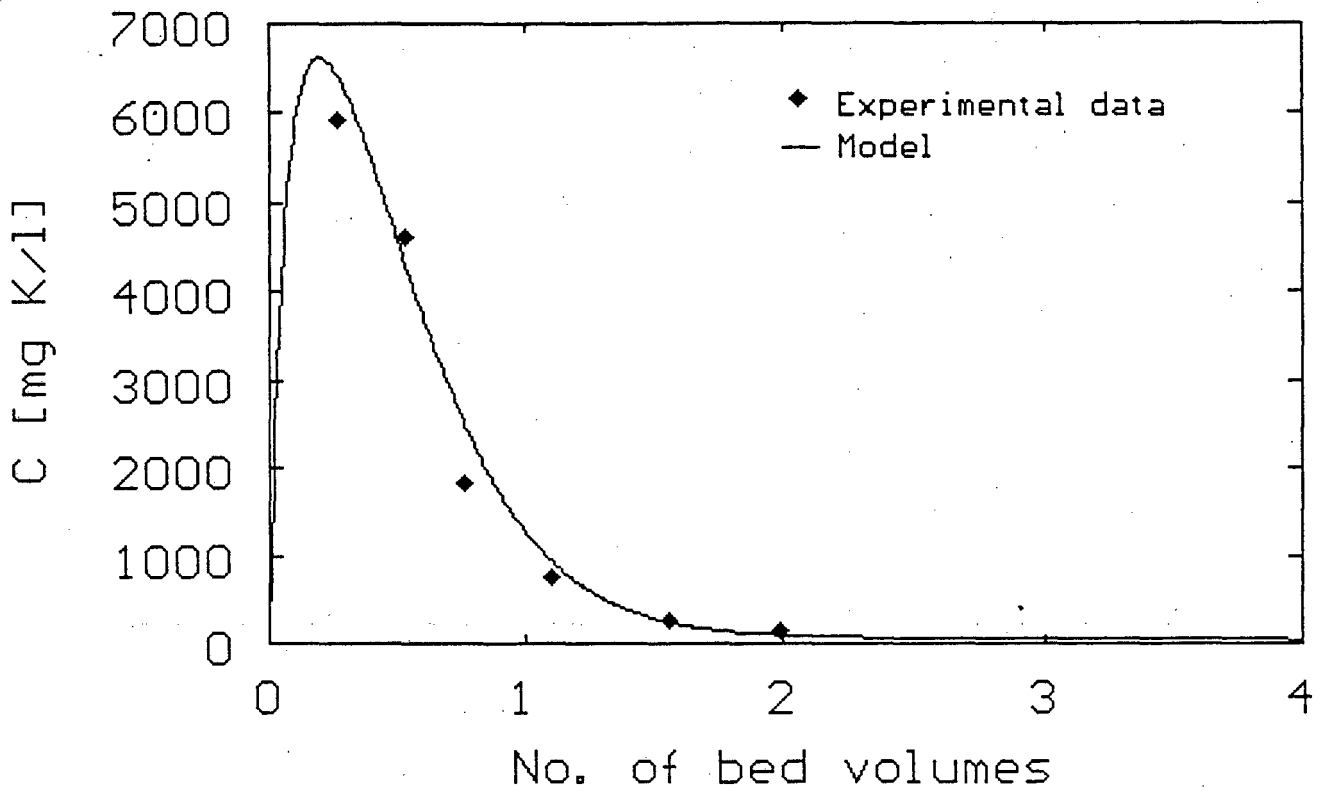


Figure 5.14(a) Fit of the nonideal flow model to the profile of potassium eluted from carbon that was soaked in a KCl solution. $V = 1.361 \times 10^{-8} \text{ m}^3 \cdot \text{s}^{-1}$, $C_{Kpi} = 12740 \text{ g} \cdot \text{m}^{-3}$, $C_{Kbi} = 0 \text{ g} \cdot \text{m}^{-3}$, $C_{KF} = 0 \text{ g} \cdot \text{m}^{-3}$ (Exp.71)

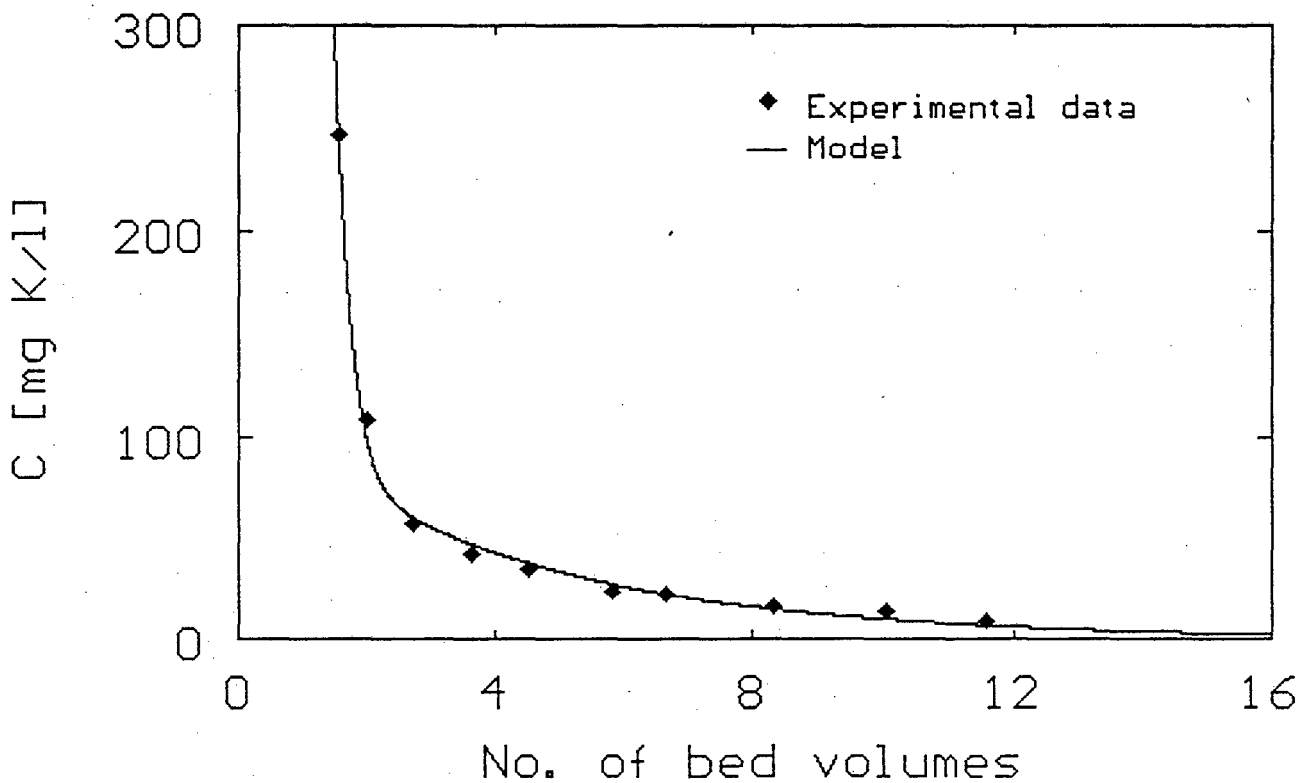


Figure 5.14(b) Tail section of potassium profile shown in Figure 5.14(a).

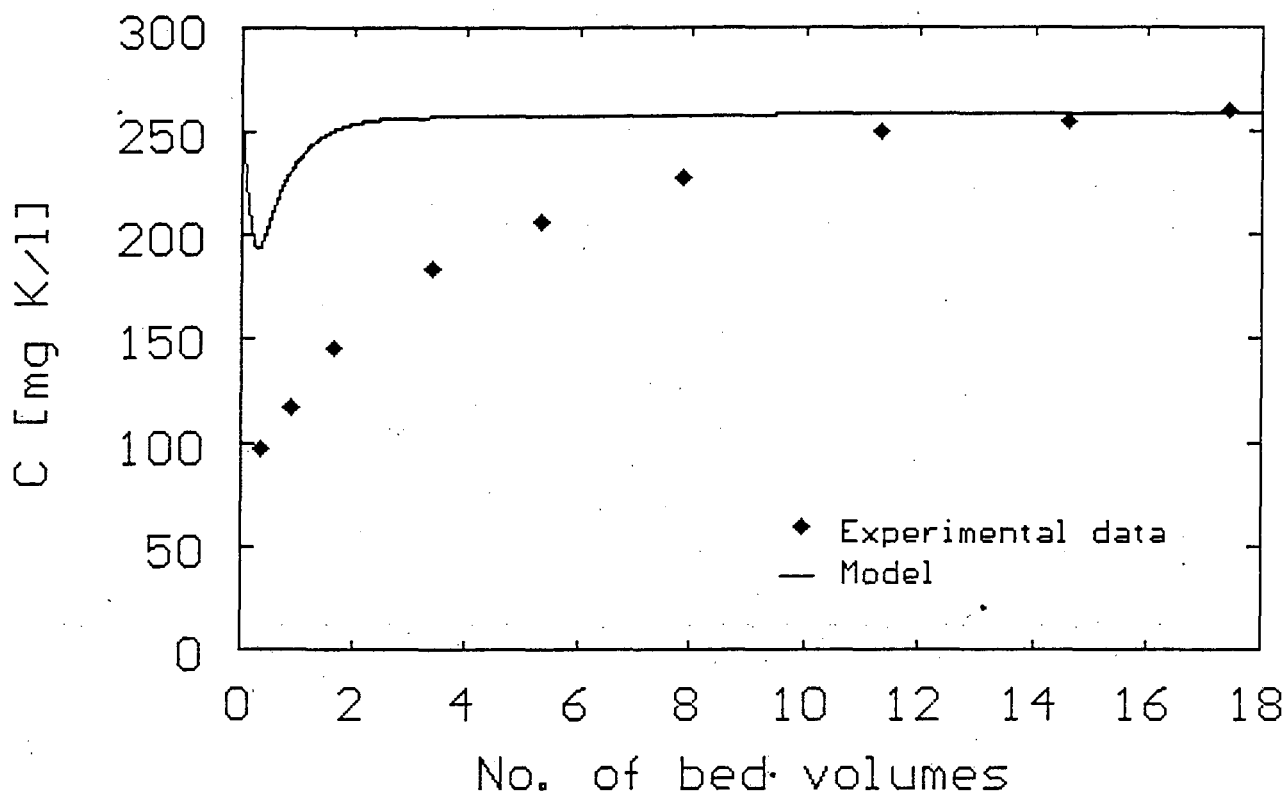


Figure 5.15 Simulation of the potassium profile during a Zadra elution. $V = 1.315 \times 10^{-8} \text{ m}^3 \cdot \text{s}^{-1}$, $C_{Kpi} = 0 \text{ g} \cdot \text{m}^{-3}$, $C_{Kbi} = 260 \text{ g} \cdot \text{m}^{-3}$, $C_{KF} = 260 \text{ g} \cdot \text{m}^{-3}$ (Exp.69)

6

MATHEMATICAL MODELS FOR ELUTION OF GOLD CYANIDE

A few attempts have been published to model the elution of gold cyanide from activated carbon by the use of the Zadra elution process (Adams and Nicol, 1986; Adams, 1990a), the AARL elution process (Stange, 1990; Stange and King, 1990) and organic solvents (Vegter and Sandenbergh, 1990). Each of these models was developed for a specific elution process. Only one general model was proposed which was claimed to describe all of these processes (Van der Merwe and Van Deventer, 1990). This model was further refined and elaborated on in this chapter.

6.1 DISCUSSION OF EXISTING GOLD ELUTION MODELS

The earliest attempt to model the elution of gold cyanide from activated carbon was the modelling of the Zadra process by Adams and Nicol (1986).

The authors assumed that the adsorption and desorption of gold in the presence of cyanide do not involve any slow chemical reactions and that the slow steps in these processes can be associated with mass transfer in the solid and liquid phases. They considered the carbon as a homogeneous phase through which the aurocyanide diffuses to an interface where instantaneous equilibrium with the liquid exists. A linear isotherm was used to describe this equilibrium. From the interface the gold diffuses through a liquid film to the surrounding liquid. To keep the model as simple as possible, the intraparticle diffusion was described by a single mass transfer coefficient.

The assumption of a linear isotherm will only be applicable under conditions of low solution phase concentrations as was the case for the

continuous stirred tank reactor in which they had performed their tests. Even though they have included an extension of their model to describe the elution in a column, no experimental evidence for the applicability thereof was provided. It was supposed that the conditions during the course of a Zadra elution remain constant and that the process could therefore be modelled with a single, fixed equilibrium isotherm. As demonstrated in Experiments 69 and 74, the conditions during the Zadra elution of a column of loaded carbon do not remain constant and it is therefore unlikely that the model of Adams and Nicol (1986) will be of use in practice.

This was illustrated in a later publication by Adams (1990a) where it was shown that the model applies to very short columns operated at high flow rates. (A column with a 5 ml carbon bed was used for an elution at 14.9 bed volumes per hour.) Such an experimental setup approaches that of a mixed reactor to which all of the above arguments apply. The inability of the model to describe the elution of gold from a 25 ml carbon bed at a flow rate of 2.3 BV/h was attributed to the fact that not enough time was allowed for the eluant to diffuse into the carbon. The experiments were then changed to fit the model by allowing a "pre-equilibration period" during which the carbon was soaked in the eluant for 2 hours before starting the elution. The experimental elution profiles obtained after this "pre-equilibration" corresponded more closely to the model predictions. This can be explained from the results from Chapter 3. The cyanide pretreatment reduced the carbon's activity towards cyanide and resulted in a low degree of cyanide decomposition during the elution. This ensured a fairly constant cyanide-age and free cyanide concentration during the elution. Moreover, the potassium concentration does not change much during a Zadra elution, so that the aurocyanide equilibrium would have remained constant and would thus have enabled fitting a model which utilizes a constant equilibrium. In practice, however, Zadra elutions are performed without cyanide pretreatments.

From the results obtained for an AARL-elution in a CSTR it appeared that the rate of elution increased during the course of the experiment (Adams and Nicol, 1986). This was attributed to the continuous change of the ionic strength of the eluate. Nicol(1986) stated that "this phenomenon makes simulation of the AARL very difficult, and it is not surprising

that there" were at that stage "no published reports of attempts to do so."

The first attempt to model the AARL elution process was published by Van der Merwe and Van Deventer (1990) who showed that it was possible to model elutions from AARL and Zadra columns with the same fundamental model. This model was essentially the same as that used for the simulation of the adsorption of gold onto activated carbon (Van Deventer, 1984, 1985). A shifting equilibrium isotherm was used for the first time to account for the changes in cation and cyanide concentrations during the elution process. This model is also the only published gold elution model accounting for an initial non-uniform distribution of gold through the carbon particles. A copy of this publication is attached in Appendix M.

The concept of a changing equilibrium isotherm was also used in publications by Stange and King (1990) and Stange (1990). They used the rate expression of Adams and Nicol (1986) in conjunction with a changing linear isotherm to describe an AARL gold elution profile. The process was considered as a binary system containing gold cyanide and sodium. The change in the sodium concentration was modelled with the same rate expression used for the gold cyanide, but with a constant linear equilibrium isotherm. Resistance to film diffusion was assumed to be the only rate limiting process for the elution of both Na^+ and $\text{Au}(\text{CN})_2^-$. A good fit of their model to experimental data measured for a single run was presented. An exponential relationship between the sodium concentration and the gold cyanide equilibrium was assumed, but no experimental evidence was provided.

Vegter and Sandenbergh (1990) also used a one parameter model, similar to that of Adams and Nicol (1986), to simulate the elution of gold cyanide with organic solutions in batch reactors. The equations were however solved for a Freundlich isotherm expression instead of a linear isotherm. As no cyanide or cyanide pretreatments were used, the equilibrium conditions during an elution run were assumed to remain constant.

The above observations again emphasize that it is impossible to model the elution of gold cyanide without considering the sub-processes which have

an influence on the gold cyanide equilibrium. Another important aspect which needs to be taken into account in the modelling of any adsorption or desorption process, is the mechanism of intraparticle mass transport. This is discussed in the next section.

6.2 PORE AND SURFACE DIFFUSION MODELS

The diffusion of an adsorbing solute through the fluid-filled pores of a porous solid is generally accepted (Cussler, 1984) to occur via 2 mechanisms that can act simultaneously. These mechanisms are described as follows :

- (a) Pore diffusion : This type of transfer involves the diffusion of a solute through the pore liquid. Because the pores are tortuous, the diffusion effectively takes place over a longer distance than it would have in a homogeneous medium. The effective diffusion coefficient in the pores (D_p) can be approximated (Furusawa and Smith, 1973) as :

$$D_p = \frac{D \epsilon_c}{\delta}, \quad [6.1]$$

where D is the molecular diffusivity, ϵ_c the particle porosity and δ the tortuosity factor.

- (b) Surface diffusion : The concept of surface or solid-phase diffusion is generally used to explain higher diffusion rates than would be expected if only pore diffusion is considered, and therefore remains difficult to interpret physically (Cussler, 1984). It is defined (Vermeulen, 1958) to include "diffusion through a homogeneous, permeable (*i.e.* absorbing), non-porous solid; diffusion in a mobile, adsorbed phase covering the pore surfaces of a porous solid whose crystalline portion is impermeable; or diffusion in an absorbing liquid held in the spaces of a solid."

All the comparisons of pore and solid diffusion mechanisms have been based on the adsorption process. According to Hall et al. (1966), the

same particle can show either pore or solid diffusion behaviour. Pore diffusion will be dominant under conditions of high pore fluid concentration, and conversely for surface diffusion. Because the two mechanisms act in parallel, the fastest one of them will control.

Weber and Chakravorti (1974) studied the adsorption mechanism by defining four types of equilibrium isotherms. These isotherms are (in order of increasing adsorptivity) : unfavourable, linear, favourable and irreversible. Of these, the unfavourable isotherm will be the most representative of the conditions prevailing during an elution. Although their study was concerned mainly with the more favourable isotherms, breakthrough curves for an unfavourable isotherm were presented. The breakthrough curves calculated with a pore or surface diffusion model for the unfavourable isotherm showed little difference. No values for the diffusivities were, however, provided.

Mansour *et al.* (1984) studied the simultaneous adsorption of butanol-2 and 1-amyl alcohol in a stirred finite bath. Their model consisted of equations for film transfer, pore liquid diffusion and pore surface diffusion. Pore diffusion coefficients of 59 times higher than the surface diffusion coefficients were used for both components. The main object of their paper was to introduce a general multicomponent adsorption model, but no discussion of the values of the diffusion coefficients was presented.

For the simulation of the adsorption of benzene onto activated carbon, Furusawa and Smith (1973) had to use a total, effective diffusivity of ten times greater than the molecular diffusivity of benzene in water. The diffusion coefficient in the pore volume should however be lower than the molecular value, because of tortuosity and a void fraction smaller than one. They calculated the pore volume diffusivity (D_p) as in Equation 6.1 with $\delta = 4$. This calculated pore diffusivity was found to be two orders of magnitude smaller than the observed total diffusivity. From these results it was concluded that the intraparticle diffusion occurs mainly via a mechanism of surface diffusion and that the contribution of pore volume diffusion can be neglected. The same approach was used in a study of the adsorption of benzaldehyde on polymeric, porous particles from both methanol and aqueous solutions

(Komiyama and Smith, 1974a). It was found that the poor adsorption of benzaldehyde from methanol solutions could be simulated by a pore diffusion model. For adsorption from aqueous solution (in which the adsorption capacity was much higher), surface diffusion had to be included in the simulation.

Leyva (1981) used a model that included both pore and surface diffusion. The pore diffusion coefficient was estimated as above, and the resulting one parameter model fitted to the experimental data to determine the value of the surface diffusivity.

Hashimoto et al. (1975) used the pore and surface diffusion mechanisms separately in the simulation of the adsorption of phenol and DBS. In the case of the pore diffusion mechanism, the diffusivity was calculated as above and compared to the observed diffusivity. If the difference between these two diffusivities was too large, a surface diffusion mechanism was assumed. To achieve similar results with the pore and surface diffusion models, pore diffusivities of more than 2000 times the surface diffusivities had to be used.

The following important conclusions could be drawn from the above literature study :

- (1) Pore diffusion is more prevalent at conditions of low adsorption equilibria as would be the case for desorption,
- (2) The values used for pore diffusion coefficients were usually higher than for surface diffusion coefficients.
- (3) A mechanism of surface diffusion is usually assumed when the rate of diffusion is higher than that described by pore diffusion alone.

6.3 FORMULATION OF COMBINATION MODEL

Van Deventer (1984) modelled the adsorption of gold cyanide onto activated carbon with a surface diffusion model in which the porous structure of the carbon particles was artificially divided into macropores and micropores. Although this model gave excellent results for the adsorption process, it was shown in the above section that the

role of pore diffusion needs to be considered during a desorption process. This led to the development of a similar model to that of Van Deventer (1984), but with the difference that diffusion in the macropores was assumed to occur via both pore and surface diffusion.

The following assumptions were made in the development of the model :

- (1) The pores of the carbon can be divided artificially into micropores and macropores. Micropores are defined as pores of which the diameter is comparable to that of the diffusing solute.
- (2) Mass transfer in the macropores occurs via pore liquid diffusion as well as pore surface diffusion.
- (3) Because of the steric interaction between the walls of the micropores and the solute, it is impossible to differentiate between pore and surface diffusion, so that it can be assumed that mass transfer between the macropores and the micropores can be described adequately by a mechanism of surface diffusion.
- (4) The macropores and micropores are uniformly distributed throughout the carbon particles, and the pore radius distribution does not change from the outside to the inside of the particles.
- (5) Mass transfer between the bulk solution and the particle occurs through film diffusion through the liquid film surrounding the particles.
- (6) There is no accumulation of solute on the particle surface.
- (7) The adsorption or desorption reaction is instantaneous and equilibrium exists between the solute in the liquid phase and in the adsorbed phase throughout the macropores.
- (8) The carbon particles are spherical.

6.3.1 Macropore mass balance

A mass balance over the macropores in a spherical shell of thickness Δr at a distance r from the centre of a particle is :

$$\alpha \frac{\partial Q_m}{\partial t} 4\pi r^2 \cdot \Delta r \cdot \rho + \beta \frac{\partial C_m}{\partial t} 4\pi r^2 \cdot \Delta r \cdot \rho \cdot V_p = 4\pi (r^2 \tilde{n}_s)_{r+\Delta r} - 4\pi (r^2 \tilde{n}_s)_r + 4\pi (r^2 \tilde{n}_p)_{r+\Delta r} - 4\pi (r^2 \tilde{n}_p)_r - 4\pi r^2 \cdot \Delta r \cdot \rho \cdot k_b (Q_m - Q_b), \quad [6.2]$$

where α and β are the fractions of the total surface area and total pore

volume of the carbon available as macropores. Although the subscript G was not used in this chapter, all variables refer to gold cyanide.

By dividing by Δr and letting Δr approach zero, Equation 6.2 changes to :

$$\alpha \frac{\partial Q_m}{\partial t} r^2 + \beta \frac{\partial C_m}{\partial t} r^2 \cdot V_p = \frac{1}{\rho} \frac{\partial(r^2 \bar{n}_s)}{\partial r} + \frac{1}{\rho} \frac{\partial(r^2 \bar{n}_p)}{\partial r} - r^2 \cdot k_b (Q_m - Q_b) \quad [6.3]$$

It follows from Fick's law that the mass fluxes, \bar{n}_s and \bar{n}_p , can be written as :

$$\bar{n}_p = \beta \cdot D_p \cdot \rho \cdot V_p \frac{\partial C_m}{\partial r} \quad \text{and} \quad [6.4]$$

$$\bar{n}_s = \alpha \cdot D_s \cdot \rho \frac{\partial Q_m}{\partial r} \quad [6.5]$$

The combination of Equations 6.3, 6.4 and 6.5 yields :

$$\alpha \frac{\partial Q_m}{\partial t} + \beta V_p \frac{\partial C_m}{\partial t} = \alpha D_s \frac{\partial^2 Q_m}{\partial r^2} + \frac{2\alpha D_s}{r} \frac{\partial Q_m}{\partial r} - k_b (Q_m - Q_b) + \frac{\partial^2 C_m}{\partial r^2} \beta D_p V_p + \frac{2\beta D_p V_p}{r} \frac{\partial C_m}{\partial r} \quad [6.6]$$

6.3.2 Micropore mass balance

The micropore mass balance is written as :

$$(1-\alpha) \frac{\partial Q_b}{\partial t} = k_b (Q_m - Q_b) \quad [6.7]$$

6.3.3 Mass balance at external particle surface

It follows from the assumption that no accumulation of solute occurs at the external particle surface that :

$$\bar{n}_L = (\bar{n}_p + \bar{n}_s)_{r=R} \quad [6.8]$$

where \bar{n}_L is the mass flux through the liquid layer surrounding the

particle :

$$\bar{n}_L = k_s (C - C_s) \quad [6.9]$$

Substitution of Equations 6.4, 6.5, 6.9 in Equation 6.8 yields :

$$k_s(C - C_{m \text{ } r=R}) = \alpha D_s \rho \left. \frac{\partial Q_m}{\partial r} \right|_{r=R} + \beta D_p \rho V_p \left. \frac{\partial C_m}{\partial r} \right|_{r=R} \quad [6.10]$$

6.3.4 Combination model with linear isotherm

The general model developed above consists of the three Equations 6.6, 6.7 and 6.10 with the 4 variables C , C_m , Q_m and Q_b . By assuming that Q_m is in equilibrium with C_m , the model can be written as a system of 3 equations with 3 variables. If the equilibrium is described by a Freundlich isotherm, the resulting system of equations becomes highly non-linear and difficult to solve. It was therefore decided to first test the model with a constant, linear isotherm so as to investigate the possibility of simplifying the model. The mathematical formulation and numerical solution procedure are presented in Appendix E. A Turbo Pascal computer program was written to solve the model. This program is supplied in Appendix G.

Table 6.1 shows the results of simulations with the combination model with a linear isotherm. The values of the parameters that are not presented in Table 6.1, are summarized in Appendix E. It was calculated in Appendix F that for an α -value of 0.4, β will range between 0.87 and 0.999.

It follows from simulations no.1 and 2 in Table 6.1 that a pore diffusion coefficient of smaller than or equal to the surface diffusion coefficient makes little or no difference to the resulting elution profile. Although it would be expected from a comparison of these profiles that very little elution would be possible with a surface diffusion coefficient of zero, simulation no.3 shows that this is not true. The results of these 3 simulations agree with the observations by Hall *et al.* (1966) that, because the two diffusion mechanisms act in parallel, the largest of them will control.

A comparison of the results of simulations no.1, 2 and 4 in Table 6.1 show that exactly the same profile can be obtained with a pore diffusion model, a surface diffusion model, and a model accounting for both mechanisms of diffusion by changing the values of the diffusion coefficients. In order to achieve similar results with a pore diffusion model and a surface diffusion model, the pore diffusion coefficient had to be 7 times higher than the surface diffusion coefficient. However, simulations no.5 and 6 show that with a 50 times higher equilibrium isotherm, the pore diffusion coefficient had to be 200 times higher than the corresponding surface diffusion coefficient in order to achieve the same elution profile.

Although it was shown that the contribution of pore diffusion increases with a decrease in adsorptivity, it was decided to model the elution of the gold by accounting for surface diffusion only. The following reasons are presented for this decision :

- (1) Exactly the same results can be obtained with a pore or surface diffusion model.
- (2) Including both pore and surface diffusion complicates the model unnecessarily.
- (3) It is not the purpose of this thesis to study the values of the diffusion coefficients, and it is therefore acceptable to use a single diffusion coefficient accounting for more than one mechanism of diffusion.
- (4) The surface diffusion model can be simplified more conveniently than the pore diffusion model and therefore uses less computing time.

6.4 SURFACE DIFFUSION MODEL

6.4.1 Formulation of model

If only surface diffusion is considered, the assumptions made for the combination model are still applicable except for assumptions no.'s 2 and

7 which change as follows :

- (2) Mass transfer in the macropores occur via surface diffusion only.
- (7) The adsorption or desorption reaction is instantaneous and equilibrium exists between the solute in the liquid phase and in the adsorbed phase on the external carbon surface.

Another assumption is added here, namely :

- (9) All the gold inside the porous structure is in the adsorbed state and only desorbs once it reaches the carbon surface. Accumulation in the pore liquid is thus assumed to be negligible.

With these assumptions Equation 6.6 changes to :

$$\frac{\partial Q_m}{\partial t} = \frac{D_s}{r^2} \frac{\partial}{\partial r} r^2 \frac{\partial Q_m}{\partial r} - \frac{k_b}{\alpha} (Q_m - Q_b) \quad [6.11]$$

Equation 6.7 remains the same, while Equation 6.10 changes to :

$$k_s(C - C_s) = \alpha D_s \rho \left. \frac{\partial Q_m}{\partial r} \right|_{r=R} \quad [6.12]$$

with $C_s = C_m$ $r=R$.

The above equations can be simplified by introducing average values for the loading of the solute in the macropores and micropores as in Equations 6.13 and 6.14. The simplifications used here are similar to those used in Appendix C and the same as those used by Van Deventer (1984).

$$Q_{m,ave} = \frac{3}{R^3} \int_0^R Q_m \cdot r^2 \cdot dr \quad \text{and} \quad [6.13]$$

$$Q_{b,ave} = \frac{3}{R^3} \int_0^R Q_b \cdot r^2 \cdot dr \quad [6.14]$$

Integration of Equation 6.10 from $r=0$ to R and substitution with

Equations 6.13 and 6.14 yield :

$$\frac{dQ_{m,ave}}{dt} = \frac{3D_s}{R} \left. \frac{\partial Q_m}{\partial r} \right|_{r=R} - \frac{k_b}{\alpha} (Q_{m,ave} - Q_{b,ave}) \quad [6.15]$$

By approximating the derivative of the macropore loading at the particle surface by a quadratic driving force (Van Deventer, 1984; Peel and Benedek, 1981) :

$$\left. \frac{\partial Q_m}{\partial r} \right|_{r=R} = \frac{5\psi}{R} \frac{(Q_s^2 - Q_{m,ave}^2)}{2Q_{m,ave}} \quad [6.16]$$

Equation 6.15 can be written as :

$$\frac{dQ_{m,ave}}{dt} = \frac{60\Gamma_s}{d_c^2} \frac{(Q_s^2 - Q_{m,ave}^2)}{2Q_{m,ave}} - \frac{k_b}{\alpha} (Q_{m,ave} - Q_{b,ave}) \quad [6.17]$$

$$\text{where } \Gamma_s = \psi \cdot D_s \quad [6.18]$$

The following substitution is introduced to enable the calculation of Equation 6.17 at a zero macropore loading :

$$\text{Let } q_m = Q_{m,ave}^2 \quad [6.19]$$

Equation 6.17 then changes to :

$$\frac{dq_m}{dt} = \frac{60\Gamma_s}{d_c^2} (Q_s^2 - q_m) - \frac{2k_b}{\alpha} (q_m - Q_{b,ave} \cdot q_m^{\frac{1}{2}}) \quad [6.20]$$

By performing similar manipulations as above on Equation 6.7, it becomes :

$$(1-\alpha) \frac{dQ_b}{dt} = k_b (q_m^{\frac{1}{2}} - Q_b) \quad [6.21]$$

A combination of Equations 6.12, 6.16 and 6.19 yields :

$$k_s (C - C_s) q_m^{\frac{1}{2}} = \frac{5\alpha\Gamma_s \rho}{d_c} (Q_s^2 - q_m) \quad [6.22]$$

The relationship between C_s and Q_s follows from the assumption that local equilibrium exists at the external particle surface, namely :

$$Q_s = A.C_s^n \quad [6.23]$$

where n was substituted here by a linear function of A as shown in Chapter 3.

The set of four Equations 6.20 to 6.22 can be solved together with a reactor mass balance equation. Van Deventer (1984) solved the model for batch, stirred tanks and a periodic countercurrent cascade of CSTR's for the adsorption of gold. However, all processes for the elution of gold from loaded carbon employ packed beds of carbon in plug flow reactors. The above model was therefore solved with the assumption that the elution would be carried out in a column.

A mass balance over an incremental section, Δh , of the column is given in Equation 6.24. The contents of each incremental section are considered to be perfectly mixed. By dividing the column into an infinite number of these sections, Equation 6.24 describes the flow through a perfect plug flow reactor (Levenspiel, 1972).

$$\epsilon.a.\Delta h \frac{dC}{dt} = V(C^{(j-1)}-C) - \bar{n}_L.a_c.(1-\epsilon).a.\Delta h \quad [6.24]$$

C and $C^{(j-1)}$ are the concentrations in the j 'th and $(j-1)$ 'th sections respectively.

By assuming the carbon particles to be spherical and substituting the flux, \bar{n}_L , with Equation 6.9, Equation 6.24 becomes :

$$\frac{dC}{dt} = \frac{V}{\epsilon.a.\Delta h} (C^{(j-1)}-C) + \frac{6k_s(1-\epsilon)}{d_c\epsilon} (C_s-C) \quad [6.25]$$

For the first section, $j=1$, at the inlet to the column, $C^{(j-1)}$ is equal to the concentration of gold in the eluant.

6.4.2 Numerical solution

Equations 6.20, 6.21 and 6.25 can be solved at $(t+\Delta t)$ for each height increment of the carbon bed by the Runge Kutta procedure as described in Appendix D. These equations are however functions of C_s . As C_s cannot be isolated in Equation 6.22, an initial guess of C_s is made at each time step and height by linear extrapolation of the change over the previous time steps. The value of $C_s^{(t+\frac{1}{2}\Delta t)}$ needed for the Runge Kutta procedure is taken as the average of the value at the previous time step and the estimate at $(t+\Delta t)$. A linear change in the surface concentration was assumed to be justifiable over small time steps. With C , q_m and Q_b calculated with the estimated value of C_s , an improved value for C_s can be obtained with Equation 6.22 and the calculation repeated until the difference between the estimated and calculated values of C_s becomes insignificant. This iteration is repeated for each section of the column at each step in time.

A Turbo Pascal program was written to solve the above model together with the models for the elution of the cation and the cyanide. This program is presented in Appendix H. The algorithm for the gold elution model can be found in procedure "mod_au" of the program. As the value of A in Equation 6.23 is a function of the cation and cyanide concentrations, the values of these concentrations throughout the column are first determined at each time step. The value of A is then calculated for each section of the column and the model for the elution of the gold solved as described above.

6.5 EQUILIBRIUM MODEL

Edeskuty and Amundson (1952) measured the pore liquid diffusivity of phenol between 25 °C and 48 °C and showed that the logarithm of the diffusivity varied linearly with the reciprocal of the absolute temperature in Kelvin. The same relationship was found to describe the temperature dependency of the surface diffusivity of benzaldehyde on Amberlite particles (Komiya and Smith, 1974a,b). By increasing the methanol : water ratio of the solvent, the capacity of Amberlite for benzaldehyde could be decreased more than one order of magnitude at the

same temperature. The decrease in adsorption capacity resulted in a ten fold increase in the value of the surface diffusivity and was attributed to the decrease in bonding energy between benzaldehyde and the carbon surface.

It was shown in Chapter 3 that the elution of gold is independent of flow rate under certain conditions. This implies that the mass transport under these conditions is so fast that the system can be regarded as being in equilibrium at each point in time.

6.5.1 Formulation of model

The following assumptions are made for this special case of the general model derived earlier :

- (1) The adsorption or desorption reaction is instantaneous and equilibrium exists between the solute in the liquid phase and that in the adsorbed phase.
- (2) The concentration in the pore liquid is equal to that in the bulk solution.
- (3) No concentration gradient exists within the liquid or adsorbed phases.

A mass balance over the j 'th section of the column is :

$$a \cdot \Delta h \cdot \rho \cdot (1-\epsilon) \frac{dQ}{dt} + \{a \cdot \Delta h \cdot \rho \cdot V_p (1-\epsilon) + a \cdot \Delta h \cdot \epsilon\} \frac{dC}{dt} = V(C^{(j-1)} - C) \quad [6.26]$$

where all of the variables refer to the j 'th section, except for $C^{(j-1)}$ which refers to the section directly below section j . It follows from the assumption that equilibrium exists between the adsorbed and liquid phases that :

$$Q = A \cdot C^n \quad [6.27]$$

As the equilibrium changes continuously during the elution, both A and n

are functions of time and the time derivative of Equation 6.27 thus is :

$$\frac{dQ}{dt} = A \cdot C^n \left[\frac{n}{C} \frac{dC}{dt} + \frac{dn}{dt} \ln C \right] + C^n \frac{dA}{dt} \quad [6.28]$$

It was shown in Chapter 3 that n is a linear function of A :

$$n = b \cdot A + B \quad [6.29]$$

thus,

$$\frac{dn}{dt} = b \frac{dA}{dt} \quad [6.30]$$

By substituting with Equations 6.28 and 6.30, Equation 6.26 becomes :

$$\frac{dC}{dt} = \frac{m_2(C^{(j-1)} - C) - C^n(A \cdot b \cdot \ln(C) + 1)(dA/dt)}{m_1 + A \cdot n \cdot C^{n-1}} \quad [6.31]$$

where

$$m_1 = \frac{\epsilon}{(1-\epsilon)\rho} + V_p \quad [6.32]$$

and

$$m_2 = \frac{V}{(1-\epsilon)a \cdot \Delta h \cdot \rho} \quad [6.33]$$

6.5.2 Numerical solution

As before, the cation and cyanide concentration profiles through the column are determined first in each time step. A is then calculated in each section as a function of these concentrations. With A known, it is then possible to determine n and (dA/dt) with Equations 6.29 and 6.34 respectively.

$$\frac{dA}{dt} = \frac{A^{(t)} - A^{(t-\Delta t)}}{\Delta t} \quad [6.34]$$

Equation 6.31 is then solved by the Runge Kutta routine, where the values of A and $C^{(j-1)}$ at $(t+\frac{1}{2}\Delta t)$ are estimated with the average of the values at (t) and $(t+\Delta t)$. The value of (dA/dt) is assumed to be constant over the time step so that the value at $(t+\frac{1}{2}\Delta t)$ is the same as in Equation 6.34.

The initial concentrations of gold in the eluant (C_i) and on the carbon (Q_i) are not in equilibrium. The initial A -value is therefore calculated from the cation and cyanide concentrations in the eluant and the equilibrated, initial gold concentration (C) calculated with the following mass balance :

$$AC^n + m_1C = Q_i + (m_1 - V_p)C_i + V_p C_{pi} \quad [6.35]$$

The initial pore concentration (C_{pi}) is normally assumed to be zero.

Appendix I contains a Turbo Pascal program for the solution of the equilibrium model. Except for the gold elution procedure, the rest of the program is similar to the program for the surface diffusion model.

6.6 REACTOR CONFIGURATIONS

6.6.1 Definition of column

The column is defined as a series of N CSTR's as shown in Figure 4.1. An imaginary 0'th section at the inlet to the column was added to enable reference to the $(j-1)$ 'th section at $j=1$. The concentrations in the 0'th section are equal to the concentrations in the eluant. For all column runs, the starting time of elution, $t=0$, is defined as that moment when flow of the eluant is started.

6.6.2 Batch reactor

The computer programs for the surface diffusion and equilibrium models can also be used to describe the kinetics in a batch stirred reactor containing a volume of liquid, v , and a mass of carbon, m_c .

For this purpose the values of a , h , Δh , ϵ and V in Equation 6.25 should be chosen so that :

$$a.h = v \quad [6.36]$$

$$\epsilon = 1 - \frac{m_c}{a.h.\rho} \quad [6.37]$$

$$\Delta h = h \quad [6.38]$$

and

$$V = 0 \quad [6.39]$$

With these adjustments, Equation 6.25 reduces to the mass balance over a batch stirred tank reactor :

$$\frac{dC}{dt} = \frac{6k_s(1-\epsilon)}{d_c\epsilon} (C_s - C) \quad [6.40]$$

6.6.3 CSTR

The same principles apply to a continuous stirred tank reactor as to a batch reactor, except for Equation 6.39. For a CSTR, V is equal to the volumetric flow rate through the reactor. By substituting with Equations 6.36 and 6.38, Equation 6.25 becomes :

$$\frac{dC}{dt} = \frac{V}{\epsilon.v} (C_{\text{feed}} - C) + \frac{6k_s(1-\epsilon)}{d_c\epsilon} (C_s - C) \quad [6.41]$$

6.6.4 Drained carbon beds

Because of the difficulties in quantifying the interparticle solution remaining in a drained bed, most of the experimental runs in this thesis were conducted with carbon beds that were initially filled with eluant. On an industrial scale however, it is easier to conduct the pretreatment and elution in the same vessel and to drain the bed between the two stages. The programs in Appendices H and I make provision for elutions

from beds which first have to be filled. The time to fill the bed is calculated as :

$$t_{fill} = (1-s) \cdot \epsilon \cdot a \frac{h}{V} \quad [6.42]$$

where s is the fraction of the voids external to the particles which is initially filled with retained liquid. The time increment for the fill procedure is chosen so that one height section of the column is filled per time increment :

$$\Delta t_{fill} = \frac{t_{fill}}{N} \quad [6.43]$$

The concentration in the section that is being filled is calculated as the weighted average of the concentrations in the retained liquid and the liquid from the previous section. The intraparticle concentrations are assumed to remain unchanged for that increment in time. The concentrations in the sections below the one that is being filled are calculated as usual with the models for the gold, potassium and cyanide.

6.6.5 Continuous elution

The need for a process capable of stripping large quantities of carbon led to the development of the "Atmospheric Continuous Elution System" (Paterson, 1987). The apparatus is claimed to be suitable for adoption to both the AARL and Zadra method of elution. It comprises of a single column incorporating a preheating, a presoak and an elution section, as shown in Figure 6.1. Loaded carbon is fed by gravity from a vessel mounted on the top of the column. Whenever eluted carbon is withdrawn from the base of the column, the bed moves down and the top section is filled with carbon from the soaking section. The eluant flows in counter-current with the carbon.

Provision has been made for modelling of a continuous elution process with the programs in Appendixes H and I. A start-up period is allowed before the first transfer of carbon occurs. This prevents the discharge of carbon with high gold loadings. The rest of the run is divided into equal periods between transfers. Removal of an integer number of the bottom sections of the bed is allowed.

The following nomenclature is defined to explain the changes that occur with a carbon discharge :

N Total number of height sections

N_d Number of sections in bottom of column to be discharged

At the moment that the discharge of carbon occurs, the carbon loadings and pore concentrations in sections $j=1$ to $j=(N-N_d)$ are changed to those in sections $(j+N_d)$. The sections $j=(N-N_d+1)$ to $j=N$ are filled with carbon from the pretreatment stage and the loadings and pore concentrations of these sections are set equal to the values in the pretreatment stage. As it is assumed that only carbon is removed, the interparticle concentrations remain unchanged.

6.7 SUMMARY

It was shown that a model accounting for both pore diffusion and surface diffusion in the porous structure of the carbon would unnecessarily complicate the use of such a model, and that it is justified to simplify the model by assuming intraparticle mass transfer by surface diffusion only. A second model was derived in which resistance to mass transfer was considered to be negligible. The use of this model requires the gold in the adsorbed and liquid phases to be in equilibrium at any point of time. The applicability of these two models will be investigated in the next chapter.

Table 6.1

Simulations of gold elution profiles in a batch stirred tank reactor with the combination model and a linear isotherm.

No.	1	2	3	4	5	6
A	0.01	0.01	0.01	0.01	0.5	0.5
$D_s \times 10^{-10}$	1.0	1.0	0.0	0.0	1.0	0.0
$D_p \times 10^{-10}$	1.0	0.0	1.0	7.0	0.0	200
t [h]	$(Q-Q_i)/Q_i$					
0.00	0.000	0.000	0.000	0.000	0.000	0.000
0.25	0.349	0.349	0.233	0.349	0.064	0.064
0.50	0.389	0.389	0.280	0.389	0.097	0.097
1.00	0.411	0.411	0.338	0.411	0.125	0.125
1.50	0.425	0.425	0.371	0.425	0.133	0.133
2.00	0.440	0.440	0.400	0.440	0.137	0.137
2.50	0.455	0.455	0.424	0.455	0.139	0.139
3.00	0.469	0.469	0.440	0.469	0.141	0.141

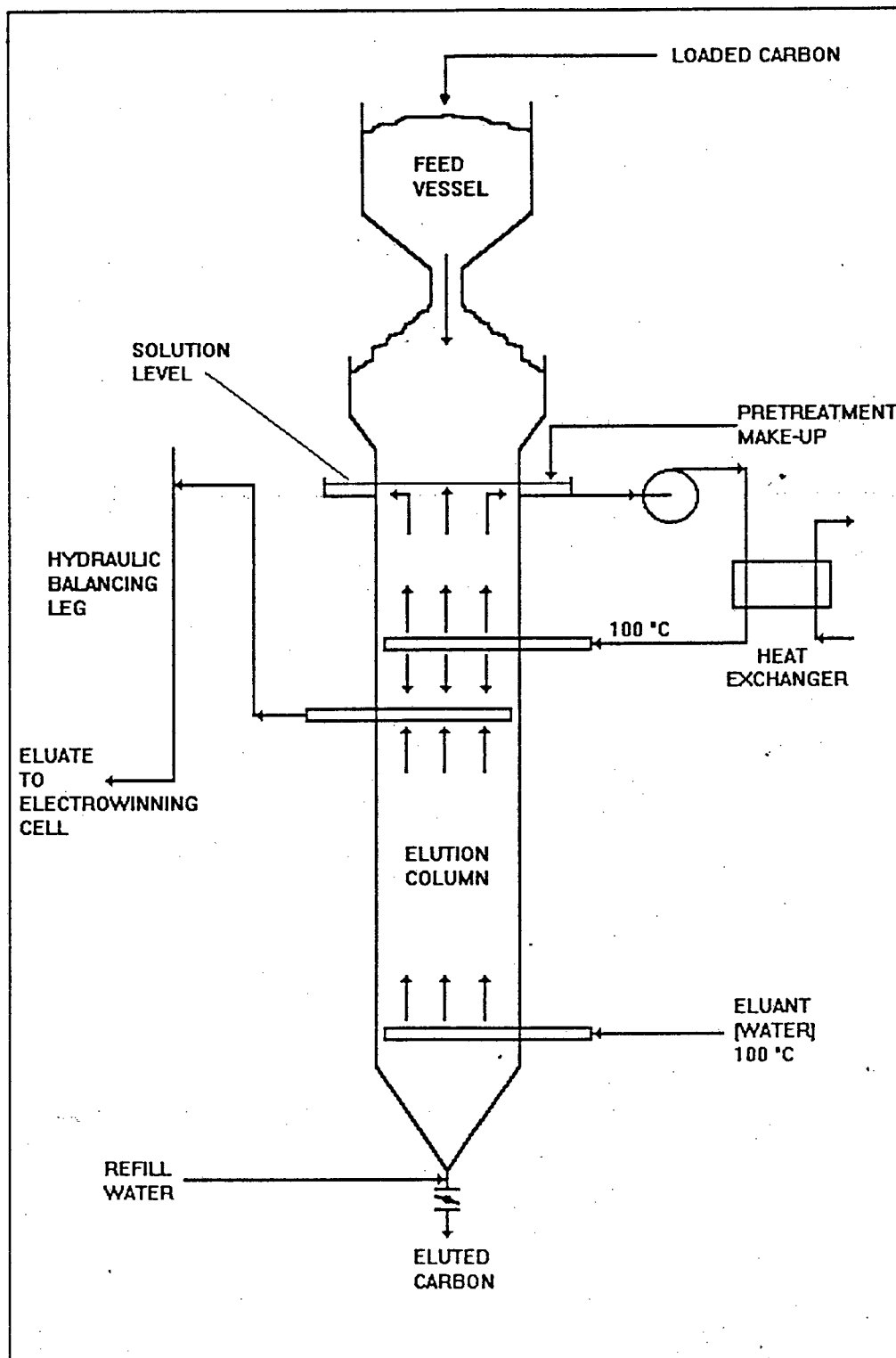


Figure 6.1 The continuous atmospheric elution column (Paterson, 1987).

7

EVALUATION OF GOLD ELUTION MODELS

The mathematical models of Chapter 6 are evaluated in this chapter by fitting them to experimental gold elution profiles measured under different operating conditions. Because it is inconceivable that diffusion control can be eliminated completely, the diffusion model would be fundamentally more correct than the equilibrium model. The second model, however, is favoured for its simplicity and was therefore used whenever possible. It will be shown that the choice between the models depends on the extent to which the isotherm favours elution.

The potassium and cyanide profiles of the elution runs in this chapter have been simulated with the parameters as determined in Chapters 4 and 5. Therefore, only the gold profiles are shown here. The experimental data were collected as discussed in Chapters 2 and 3 and Appendix K.

7.1 BATCH KINETIC STUDIES

A number of adsorption and elution runs were conducted in batch stirred tank reactors to investigate the difference in mass transfer parameters under adsorption and elution conditions. The gold elution equilibrium isotherm was assumed here to remain constant for the duration of the run. This was justified by adjusting the pH of the solutions during the experiments and by using low concentrations of carbon at room temperature to minimize the decomposition of cyanide. Furthermore, the concentration of cations remained constant and very low during the runs, because no pretreatments were conducted for these elutions.

Figures 7.1 to 7.4 show the adsorption of gold cyanide onto carbon BTX at various gold and carbon concentrations. The model predictions were obtained with the surface diffusion model in "batch mode" as explained in

Chapter 6. Table 7.1 shows that all four adsorption runs could be simulated with the same set of kinetic parameters. As the conditions during these adsorption runs were similar to those in Experiment 36, the same equilibrium constant that was determined in Experiment 36 was used here. The finding that all four runs could be simulated with the same set of kinetic parameters proved that the surface diffusion model applies to the adsorption of gold cyanide onto carbon BTX. If the different conditions used to promote adsorption and desorption of gold cyanide affect only the gold cyanide equilibrium, the kinetics of adsorption and desorption would be the same and the kinetic parameters in Table 7.1 also would apply to the desorption process. This was investigated below.

The desorption data associated with the above adsorption runs are plotted in Figures 7.5 to 7.9 and the parameters used in the simulations thereof are summarized in Table 7.2(a). It can be seen from the experimental data in Figure 7.5 that equilibrium of desorption was practically reached within 30 hours. As illustrated in Chapter 3, re-adsorption of gold can take place in batch elutions when the effects of, for example, cyanide and cyanide-age are declining. It is thus impractical to determine gold elution equilibria over long periods of time as was done in Chapter 3. For the purpose of the mathematical simulations of the batch elution runs, the equilibrium constants were therefore calculated from the gold concentrations at the end of each run. The equilibrium data in Chapter 3 are, however, still useful in providing the functional relationships between the Freundlich isotherm constant and the different effects that were investigated.

The equilibrium constant for the elution in Figure 7.5 was calculated as $A = 10.6$ from the gold concentration measured at 46 h. Except for the isotherm constants, the kinetic parameters used in the simulations in Figure 7.5 were equal to those determined for adsorption. It can be seen that it was impossible to fit the model to the experimental data with these parameters. The possibility that the isotherm constant of 10.6 was incorrect, was investigated by repeating the simulation with two and ten times lower A-values in Figure 7.5. It is clear from these model predictions that it is impossible to predict the desorption of gold with the same mass transfer coefficients as for adsorption by varying only the equilibrium isotherm. A good fit of the model to the experimental data

was possible, however, with the calculated isotherm constant of 10.6 and with intraparticle diffusion coefficients of 20 times higher than for adsorption (see Figure 7.6). The ratio of initial gold loading in the micropores to the loading in the macropores, m_{mb} , was calculated from the final pore surface concentrations obtained from the adsorption simulations. Figure 7.7 shows the elution of gold under similar conditions as in Figure 7.6, but at a higher concentration of carbon. As expected, the same parameters could be used for both runs.

Unlike the previous 2 runs, the experimental data presented in Figures 7.8 and 7.9 have been obtained in the presence of $380 \text{ g CN}^- \cdot \text{m}^{-3}$. This resulted in a nearly 2 times lower equilibrium isotherm constant as well as a higher macropore diffusivity.

Figures 7.6 to 7.9 also illustrate that it would be impossible to simulate the experimentally measured gold profiles with the equilibrium model developed in Chapter 6. As the equilibrium isotherm remains constant for the whole run, the equilibrium model predicts an instant increase in the gold concentration at $t=0$ to the equilibrium value, and a constant concentration for the rest of the run.

The samples of carbon used in the experiments in Figures 7.10 to 7.13 were loaded with gold over a period of 3 weeks. This provided enough time to reach equilibrium, and therefore an even distribution of gold between the macropores and the micropores could be assumed. An initial value of $m_{mb} = 1.0$ was therefore used in the model predictions of the elutions with these carbons. The parameters and elution conditions for Figures 7.10 to 7.13 can be found in Table 7.2(b).

The film transfer coefficient could not be determined separately as in the case of adsorption (Van Deventer, 1984), and was treated as one of the set of unknown parameters which were determined by fitting the model to the experimental data. It follows from the parameters presented in Table 7.2(b) that a higher value of the film transfer coefficient had to be used for the runs at temperatures higher than ambient temperature. Not enough runs were conducted, however, to establish a trend.

The following conclusions could be drawn from the experimental data and

simulations presented in Figures 7.5 to 7.13 :

- (a) The experimentally measured batch elution profiles could not be described with the equilibrium model,
- (b) The kinetics of desorption were found to be higher than the kinetics of adsorption,
- (c) It was possible to describe all the batch elution runs conducted under different conditions with the surface diffusion model,
- (d) Both the equilibrium and kinetics of desorption changed with a change in the elution conditions,
- (e) The kinetics of desorption seemed to increase with a decrease in the value of the equilibrium constant, A , and
- (f) The shape of the curves presented in Figures 7.5 to 7.13 is exactly the same as those measured for the elution of gold cyanide with organic solvents, with and without the addition of cyanide (Vegter and Sandenbergh, 1990; Espiell et al., 1988). Although it was not formally proved here, it can be assumed with confidence that the surface diffusion model with a constant equilibrium would also be applicable to the elution of gold cyanide with organic solvents.

The values of the macropore diffusivities of both the adsorption and desorption experiments at room temperature were plotted in Figure 7.14 versus the equilibrium isotherm constants. A sharp increase in the intraparticle mass transfer coefficient occurred with a decrease in the adsorption capacity. This complies with the findings of workers on the adsorption of organic substances (Edeskuty and Amundson, 1952; Komiyama and Smith, 1974a) where it was found that the value of the surface diffusivity increased with a decrease in the adsorptivity. Vegter and Sandenbergh (1990) reported a ten fold increase in the rate of desorption of gold cyanide from activated carbon in a water-acetone solution when the equilibrium was reduced 4 times by raising the temperature from 20 °C to 50 °C.

7.2 ELUTION FROM PACKED BEDS OF CARBON

7.2.1 Constant equilibrium

Figures 7.15(a) and 7.15(b) show the elution of gold from a bed of carbon at 70 °C in the absence of cyanide and without a cyanide pretreatment. As with the batch elution runs presented above, the pH and potassium concentration remained constant and a constant equilibrium isotherm had to be used. It can be seen from Figure 7.15(b) that it was not possible to simulate the profile with the equilibrium model with a constant equilibrium isotherm. This can be ascribed to the fairly high value of the Freundlich isotherm constant, which implies low intraparticle diffusivities and thus the need to account for a diffusion control mechanism. The macropore diffusivity used in the simulation with the surface diffusion model in Figure 7.15(a) corresponds to that predicted by the batch elution runs (refer Figure 7.14). The value of m_{mb} was calculated as before by the use of the surface diffusion model in "adsorption mode". Table 7.3 summarizes the parameters used in the simulations of column operations with the surface diffusion model.

7.2.2 AARL elution

The data in Figure 7.16 were obtained by performing an elution at 70 °C after soaking the loaded carbon in a potassium cyanide solution for 30 minutes. As shown before, the potassium cyanide pretreatment resulted in changing cyanide and potassium concentrations during the elution step. To account for the effect of the potassium concentration on the gold elution equilibrium, the generalized isotherm was written as :

$$Q_e = A.C_e^{-0.002688.A + 0.2902}, \text{ with} \quad [7.1]$$

$$A = A_0.(C_K + 50)^p. \quad [7.2]$$

The constant value of 50 was added in Equation 7.2 to lower the sensitivity of the gold equilibrium to potassium at low concentrations of potassium. This modification made it possible to tolerate deviations in the predicted potassium profile from the measured profile at low concentrations. A_0 and p were treated as parameters which were determined by fitting the model to the experimental data.

The "peak" in the model simulation at $t=0$ appeared because the gold equilibrium was written as a function of the potassium concentration in the interparticle solution and not the pore solution. When distilled water is used as an eluant, the interparticle potassium concentration is specified as zero at $t=0$. This results in an initially low value of the gold equilibrium while little potassium has yet diffused out of the carbon. The situation is however corrected within less than the first bed volume. Although it would be more correct to write the gold equilibrium as a function of the intraparticle potassium concentration, it is easier to verify the interparticle than the intraparticle concentration.

It was shown in Chapter 3 that the effect of free cyanide carried over from the pretreatment stage was of little importance and was thus omitted in the modelling here.

Although it was possible to fit the surface diffusion model to the experimental data in Figure 7.16, macropore and micropore diffusivities of 170 and 50 times higher than those for adsorption had to be used. The validity of such high diffusivities is however illustrated in Figure 7.17 where the same parameters have been used to predict the elution profile at a higher flow rate. Although a relatively poor fit was obtained, the peak height and the trend were the same as for the measured profile. (The higher flow rate led to a slightly sharper decrease in the gold profile after the maximum concentration was reached.) The high values of the kinetic parameters that had to be used in the simulations in Figures 7.16 and 7.17 indicate that resistance to mass transfer became negligible under these conditions and that these elutions could possibly be described with the equilibrium model.

The relationship between the surface diffusion and equilibrium models is illustrated in Figure 7.18. (Most of the parameters used in Figure 7.18 are given in Table 7.3.) It was assumed for the purpose of this illustration that the carbon contained only macropores. For values of Γ_m larger than or equal to $1 \times 10^{-10} \text{ m}^2 \cdot \text{s}^{-1}$ the elution profile predicted with the surface diffusion model approached that of the equilibrium model. As the equilibrium model is easier to use and entails less unknown parameters to be estimated, it was decided to first use the equilibrium

model from here onwards before resorting to the more complex surface diffusion model.

7.2.2.1 Estimation of equilibrium isotherm parameters

It was illustrated earlier that, unlike the functional forms of the various effects on the gold elution isotherm, the parameters used in these functions vary under different conditions. These parameters would therefore be different for different modes of cyanide pretreatment. Furthermore, as the effect of cyanide-age was shown to wear off with time, it was necessary to devise a method to estimate the equilibrium after a cyanide pretreatment, but during the subsequent elution run. The following approach was used to estimate the change in the equilibrium isotherm parameter A during an AARL elution in a packed bed of carbon :

If it is assumed that resistance to mass transfer becomes negligible after the pretreatment step, equilibrium between the metal cyanide loading on the carbon surface and in the interparticle solution will pertain during the elution step at every position in the column, including the outlet. As the concentration of gold in solution is measured at the outlet, the equilibrium at the outlet will be known if the loading on the carbon is known. The latter can be estimated by assuming that, at any stage, the loading at the outlet will be lower than or equal to Q_{Gi} and higher than the average loading in the column. The average loading at time t can be calculated from a mass balance by integration of the area under the gold elution profile from $t=0$ to $t=t$. With the maximum and minimum loadings at the outlet known, the minimum and maximum values of A at the outlet can thus be calculated from Equation 7.1. (With C_e known, the maximum and minimum values of A would be determined by, respectively, the maximum and minimum values of Q_e .)

Figure 7.19 shows the result of applying the above method to the experimental data of Experiment 50. The values of A varied between 0.8 and 2.1. While the initial gold loading, Q_{iG} , is a constant value, the average loading in the column decreases with an increase in the volume of eluant passed through the column. The difference between the maximum and minimum Q_e -values, and therefore also the difference between the maximum and minimum A -values, increased with time (or bed volumes). However,

during the initial two to three bed volumes when little gold had yet been eluted, the values of A were more exact. These A-values were plotted in Figure 7.20 as a function of the potassium concentration. The exponential relationship between A and the potassium concentration in Figure 7.20 serves as further proof of the validity of an equilibrium approach, as it was shown before that such a relationship exists at true equilibrium. The value of $p = 0.24$ determined from Figure 7.20 corresponds reasonably with the value of 0.2 derived from fitting the model to the experimental data.

7.2.2.2 Reactivation after cyanide pretreatment

It follows from the above that, if the concentration of potassium is kept unchanged during an AARL elution, the value of A should also be constant if all other factors remain constant. This was examined in Figure 7.21 where the calculated minimum and maximum A values were plotted as a function of the number of bed volumes passed through the column. Because of the high potassium concentration, little elution of gold occurred and this led to a very small difference in the minimum and maximum estimates of A.

Figure 7.21 shows that the A-value did not stay constant, but increased with an increase in the volume of eluant passed through the bed. The increase in A was ascribed to the reactivation of the carbon surface towards gold cyanide after a cyanide pretreatment (refer Figure 3.17). The reactivation in Figure 7.21 was empirically accounted for by expressing the value of A as a function of the number of bed volumes as follows :

$$A = 2.16 (V_B + 1)^{0.117} \quad [7.3]$$

The reactivation of the carbon would probably be a function of the removal of the decomposition products of the cyanide from the carbon pores, but this would be very difficult to quantify or to investigate as an isolated process. The volume of eluant with which the carbon had been washed, was thus taken as being representative of the degree of reactivation of the carbon.

To account for the reactivation of the carbon, the general formula for A

in Equation 7.2 was extended to :

$$A = A_o \cdot (C_k + 50)^p \cdot (V_b + 1)^q \quad [7.4]$$

As shown in Table 7.3, the reactivation term is not included in the case of the surface diffusion model, because the effect is accounted for in the values of the intraparticle mass transfer coefficients.

7.2.2.3 Modelling of elution at different cation concentrations

Figure 7.22 shows the equilibrium model fitted to the same data as presented in Figure 7.16. This experiment involved a cyanide pretreatment followed by an elution with distilled water at 70 °C. The parameters used with the equilibrium model are summarized in Table 7.4. Values of $p = 0.2$ and $q = 0.1$ were used here. It can be seen that a reasonable fit could be obtained with the equilibrium model that is much simpler than the surface diffusion model.

As with the surface diffusion model, the equilibrium model also predicts higher than measured gold concentrations during the initial stages of the elution. This is ascribed to the use of the interparticle potassium concentration in the gold cyanide equilibrium as discussed before.

The fits presented in Figures 7.22 to 7.25 represent similar gold elution runs with different constant potassium concentrations in the eluant feeds of 0, 559, 2100 and 6300 ppm K^+ . The fact that all of these runs could be simulated with the same values of p and q further proves the validity of the values of these parameters. The experimental data in Figure 7.25 are the same as those in Figure 7.21 where it was illustrated that the value of A increased as the elution progressed. A simulation with a constant equilibrium and with $q = 0$ was thus included in Figure 7.25 to show the necessity to account for the reactivation of the carbon.

Table 7.4(a) shows that the values of A_o in Figures 7.22 to 7.25 differ with a maximum of 6.7% although the same temperatures and modes of pretreatment were used. The small adjustment in A_o is justified, however, if the experimental error in the determination of the initial gold loading is taken into account. Even with analytical techniques much more sophisticated than the AA-spectroscopy employed here, mass balance

errors of 8% are not uncommon (Vegter and Sandenbergh, 1990).

7.2.2.4 Elution after different modes of adsorption

The equilibrium model for the elution of gold cyanide does not account for an initial radial distribution of gold in the carbon particle. Therefore, if diffusion does play a role, this should become evident when trying to fit the model to elutions from carbons with different values of m_{mb} . Such runs are presented in Figures 7.22, 7.26 and 7.27. The carbons used for these elutions were loaded from identical gold solutions over periods of 22 h, 7 h and 72 h respectively. By using the same adsorption parameters as given in Table 7.1, the values of m_{mb} at the end of the adsorption periods were calculated as 0.437, 0.123 and 0.940 (in the same order as above). As can be seen from the above Figures and Table 7.4, these runs could all be simulated with the equilibrium model, using the same parameters as before, except for minor changes to the value of A_0 . This further proves the assumption that resistance to mass transfer becomes negligible under low equilibrium conditions.

It was investigated in Figure 7.28 whether the same parameters can also be used for the elution from carbon with a higher initial gold loading. Although a very good fit could be obtained, the value of A_0 used in Figure 7.28 was more than 85% higher than the value used in Figure 7.22. As all the conditions, except the initial gold loadings, were the same for the two runs, the same set of equilibrium parameters were expected to apply to both experiments. The apparently higher equilibrium in Figure 7.28 might have been the result of intraparticle diffusion or an inefficient cyanide pretreatment.

The former of these explanations was investigated by attempting to fit the surface diffusion model to the experimental data in Figure 7.28 by using the same parameters as for Figure 7.16, except for the values of $Q_{Gi} = 12.16 \text{ g.kg}^{-1}$ and $m_{mb} = 0.783$. This gave a calculated profile of more than double the height of the experimental profile. Even with drastic changes to the mass transfer coefficients, it was impossible to fit the surface diffusion model to the experimental data without increasing the equilibrium. As with the equilibrium model, the surface diffusion model could only be fitted to the data by increasing the value

of A_0 . The lower than expected elution profile of Figure 7.28 can therefore not be attributed to diffusion.

The higher equilibrium condition applying to Figure 7.28 remains unexplained. It is possible, however, that the relatively short pretreatment of 30 minutes at room temperature was insufficient to ensure homogeneous deactivation of the carbon surface throughout the particles, and that the effect thereof is more profound at higher gold loadings. This will have to be investigated by repeating Experiments 50 and 89 with a more drastic pretreatment, for example at a higher temperature.

7.2.2.5 Elutions with different modes of pretreatment

Because of the problems of quantifying the effect of the cyanide pretreatment on the gold elution equilibrium, it was assumed here that the main difference between elutions after different modes of pretreatment would be a shift in the equilibrium. The experimental data presented in Figures 7.22, 7.29 and 7.30 were collected at the same elution conditions except for different modes of pretreatment. The pretreatment conditions and A_0 -values for these runs can be summarized as follows :

<u>Figure</u>	<u>7.22</u>	<u>7.29</u>	<u>7.30</u>
A_0	0.375	0.60	
C_{iN} [$\text{g}\cdot\text{m}^{-3}$]	7886	1593	7733
v [ml]	20	25	10
T [$^{\circ}\text{C}$]	20	20	100
t [h]	0.5	65	0.5

From the values of A_0 for Figures 7.22 and 7.29, it follows that the gold cyanide equilibrium decreases with an increase in the cyanide concentration employed in the pretreatment. The duration of the pretreatment was of little importance. As the extent of reactivation in Figure 7.30 ($q = 0$) was different from the value of $q = 0.1$ in Figure 7.22, the A_0 values of these Figures cannot be compared directly. It can be seen, however, that the maximum gold concentration in Figure 7.30 was 47% higher than in Figure 7.22, even though only half the quantity of cyanide for Figure 7.29 was available for Figure 7.30. This is

attributed to the higher temperature in the pretreatment of Figure 7.30 and strengthens the argument in Chapter 3 that the decomposition of cyanide on the carbon surface reduces the activity of the carbon towards aurocyanide to a larger extent than does the adsorption of cyanide.

As discussed above, the extent of reactivation, q , of the carbon differed for the different modes of pretreatment in Figures 7.22 and 7.30. This can also be explained on the basis of the difference between adsorption and decomposition of cyanide in the pretreatment: Where mainly adsorption of cyanide occurred in the pretreatment (as in the case of a pretreatment at room temperature), higher degrees of reactivation, q , had to be used in the simulations of the elutions. These higher degrees of "reactivation" can be ascribed to the elution of physically adsorbed cyanide from the carbon surface. As the cyanide is desorbed from the carbon surface, more adsorption sites become available for the adsorption of aurocyanide, and the carbon recovers its activity towards the latter species. The little or no reactivation of the carbon after a cyanide pretreatment at high temperature ($q = 0$ in the simulation in Figure 7.30), is explained as follows: At higher temperatures it was shown that more decomposition than adsorption of cyanide occurs, and that the decomposition reactions (as shown in Equations 3.25 and 3.26) are irreversible or have high equilibrium constants. Because of the irreversible nature of these reactions, the carbon's activity towards aurocyanide is not recovered as easily as when mostly adsorption of cyanide occurred.

The simulation of the effect of a step change in potassium concentration was included in Figure 7.31 to further illustrate the validity of the equilibrium model and the dependency on the potassium concentration ($p = 0.2$). If the value of p was incorrect, it would have been possible to simulate the gold elution profiles before or after the step change in the potassium concentration, but not both, as was done in Figure 7.31. No reactivation was needed in the gold equilibrium function because of the higher temperature employed in the pretreatment.

7.2.2.6 Elutions at different temperatures

The ability of the equilibrium model to simulate gold elution profiles at different temperatures is reflected in Figures 7.22, 7.32 and 7.33. These elutions were conducted at temperatures of 70 °C, 50 °C and 80 °C respectively. Except for the temperatures, all the other conditions were the same. This is reflected in the ability of the model to simulate all three runs with the same set of parameters by changing only the value of A_0 .

Figure 7.34 shows the elution of gold at 130 °C as measured with the use of the stainless steel column described in Chapter 3. Table 7.4 shows that an A_0 value as low as 0.065 had to be used in the simulation. The gold elution also seemed to be more sensitive to the cation concentration at this high temperature. As before, no reactivation had to be included in the simulation, because the pretreatment was conducted at an elevated temperature. Furthermore, different potassium parameters had to be used because of the long soaking period before the elution (see Experiment 93).

The gold elution run shown in Figure 7.35 was conducted at room temperature after a cyanide pretreatment similar to that used for Figures 7.32 and 7.33. It was however impossible to fit the equilibrium model to the data in Figure 7.35. The model simulation in Figure 7.35 was achieved with the surface diffusion model. This can be explained in view of the relatively high value of $A_0 = 3.8$ (see Table 7.3), which resulted in a shift to mass transfer control and hence the need for the diffusion model.

The effect of temperature on the elution equilibrium after a cyanide pretreatment as used for Figures 7.22, 7.32 and 7.33 was quantified in Figure 7.36 by plotting these three A_0 values as a function of the temperature. It follows from Figure 7.36 that the generalized equilibrium isotherm for these runs can be written as :

$$Q_e = A \cdot C_e^{-0.002688 \cdot A + 0.2902}, \text{ where} \quad [7.5]$$

$$A = 0.016636 \cdot \exp \frac{1060.8}{T} (C_K + 50)^{0.2} \cdot (V_B + 1)^{0.1} \quad [7.6]$$

If the parameters in Equation 7.6 are compared to the values measured in Chapter 3, it can be seen that the gold equilibrium became less sensitive to temperature and more sensitive to the potassium concentration after the cyanide pretreatment employed here (E_a/R_0 changed from 2190 K to 1060.8 K, and p changed from 0.069 to 0.2).

7.2.3 Zadra elution

Figure 7.15(a) shows a gold elution profile obtained under conditions of a constant equilibrium. It is clear that this profile differs completely from the Zadra elution profiles shown in Figures 7.37 and 7.38. Whereas the gold cyanide profile with a constant equilibrium decreases from its maximum value at $V_B = 0$, the gold cyanide concentrations in Figures 7.37 and 7.38 both increase with the volume of eluant passed through the bed. A model with a constant equilibrium as proposed by Adams and Nicol (1986) and Adams (1990a) will therefore be incapable of simulating a true Zadra elution where the carbon has not been previously equilibrated with the eluant in order to obtain a constant equilibrium.

Unlike an AARL elution, the cation concentration remains fairly constant during a Zadra elution. However, as all of the cyanide reactions take place during the elution stage of a Zadra elution, the change in cyanide concentration and cyanide-age, and the effect thereof on the gold elution, have to be accounted for in the modelling of the process.

The cyanide profiles associated with Figures 7.37 and 7.38 were already modelled in Figures 4.2 and 4.3 and will not be repeated here. The cyanide-age of the carbon at any position of the column was calculated from the cumulative amount of cyanide previously decomposed on the carbon. The potassium concentrations were assumed to remain unchanged for the duration of the run.

It followed from the work in Chapter 3 that the following form of the

generalized gold elution equilibrium would be applicable here :

$$Q_e = A.C_e^{-0.002688.A + 0.2902} \text{ with} \quad [7.7]$$

$$A = \frac{A_o.(C_K + 50)^p.(C_N + 1)^f}{c.Q_N + 1} \quad [7.8]$$

Although the potassium concentration was assumed to remain constant, the dependency on potassium was included in Equation 7.8 to extrapolate between runs at different potassium levels.

The elution in Figure 7.37 was conducted with a constant feed of a 0.5 g KCN/l eluant, whereas the profile in Figure 7.38 was measured during an elution with 20 g KCN/l after a cyanide pretreatment. Figure 7.37 therefore represents a Zadra elution and Figure 7.38 a combination of a Zadra and an AARL elution. Both runs were conducted at 70 °C.

The equilibrium model with the following set of parameters was found to apply to both elutions, in spite of the big difference in operating conditions :

$$A_o = 2.82$$

$$p = 0.088$$

$$f = -0.11$$

$$c = 0.05$$

Constant potassium concentrations of 200 g.m⁻³ and 11000 g.m⁻³ were used in the simulations of Figures 7.37 and 7.38 respectively. The values of the flow rates and initial gold loadings are given in Experiments 69 and 74. The values of h , a , d_c , ρ , V_p , ϵ , Δt and N were the same as those in Table 7.4(a).

7.3 SUMMARY

The surface diffusion and equilibrium gold elution models derived in Chapter 6 were shown to be suitable for simulating the elution of gold cyanide under a variety of different conditions. While the surface diffusion model applied mainly to conditions of poor desorption, the equilibrium model was applicable to conditions strongly favouring elution. Although it followed from the derivation of these models that

the equilibrium model is only a simplification of the surface diffusion model, this was further proved by illustrating that the difference between the profiles predicted by the two models decreases with an increase in the values of the mass transfer coefficients used in the surface diffusion model.

It is expected that the equilibrium model will be applicable to most industrial AARL and Zadra elutions, because of the higher temperatures and better pretreatments than were employed here. This will simplify the simulation of industrial scale AARL elutions to a large extent, as it was found that the shape of the gold profile after a hot cyanide pretreatment is determined only by the elution of the cations.

Because of the difficulties in analyzing and isolating the reactions that cyanide undergoes, and quantifying the effect thereof on the elution of gold cyanide, it was found that it was in fact more difficult to simulate a Zadra than an AARL elution. Previous attempts to model the Zadra process have failed owing to an oversimplification of the system by assuming that the aurocyanide equilibrium remains constant during the elution.

Table 7.1

Parameters used in simulations of gold adsorption profiles in batch reactors.

Figure	7.1	7.2	7.3	7.4
ϵ	0.999594	0.999203	0.999441	0.998805
C_{Gi}	20.10	20.10	11.4	11.4

$h = 0.190985$ m, $a = 0.007854$ m², $d_c = 0.00142$ m, $\rho = 838.8$ kg.m⁻³, $V_p = 0.000634$ m³.kg⁻¹, $Q_{Gi} = 0$, $\alpha_G = 0.4$, $k_s = 1.0 \times 10^{-5}$ m.s⁻¹, $\Gamma_s = 2.9 \times 10^{-13}$ m².s⁻¹, $k_b = 3.5 \times 10^{-6}$ s⁻¹, $A = 31.485$, $V = 0$ m³.s⁻¹, $\Delta t = 20$ s and $N = 1$ in all cases.

Table 7.2(a)

Parameters used in simulations of gold elution profiles in batch reactors.

Figure	7.5	7.6	7.7	7.8	7.9
ϵ	0.999594	0.999594	0.999203	0.999441	0.998805
Q_{Gi}	23.796	23.796	21.832	17.072	10.872
m_{mb}	0.490	0.490	0.510	0.555	0.696
$k^s \times 10^5$	1.0	1.0	1.0	1.0	1.0
$\Gamma^s \times 10^{12}$	0.29	6.0	6.0	8.0	8.0
$k_b^s \times 10^5$	0.35	6.0	6.0	6.0	6.0
A	see Fig.	10.6	10.6	5.46	5.46

$h = 0.190985$ m, $a = 0.007854$ m², $d_c = 0.00142$ m, $\rho = 838.8$ kg.m⁻³, $V_p = 0.000634$ m³.kg⁻¹, $\alpha_G = 0.4$, $V = 0$ m³.s⁻¹, $C_{Gi} = 0$ g.m⁻³, $\Delta t = 20$ s and $N = 1$ in all cases.

Table 7.2(b)

Parameters used in simulations of gold elution profiles in batch reactors.

Figure	7.10	7.11	7.12	7.13
T [°C]	20	20	52	91
pH	12.6	11.1	6.6	6.6
C_N	0	300	0	0
C_K	1940	700	10	10
ϵ	0.999214	0.999046	0.998088	0.997837
Q_{Gi}	55.71	53.84	30.98	27.45
$k \times 10^5$	1.0	1.0	5.0	5.0
$\Gamma^s \times 10^{12}$	3.0	4.0	4.0	6.0
$k_b \times 10^5$	4.0	4.0	3.0	6.0
A	20.9	14.0	24.21	11.0

$h = 0.127324$ m, $a = 0.007854$ m², $d_c = 0.00142$ m, $\rho = 838.8$ kg.m⁻³, $V_p = 0.000634$ m³.kg⁻¹, $\alpha_G = 0.4$, $V = 0$ m³.s⁻¹, $C_{Gi} = 0$ g.m⁻³, $m_{mb} = 1.0$, $\Delta t = 20$ s and $N = 1$ in all cases.

Table 7.3

Parameters used in surface diffusion model simulations of gold elution profiles from packed bed reactors.

Figure	7.15	7.16	7.17	7.18	7.35
$V \times 10^8$	1.205	1.367	2.809	1.0	3.047
Q_{Gi}	18.18	4.848	4.869	4.0	23.11
m_{mb}	0.353	0.474	0.474	0	0.303
α_G	0.4	0.4	0.4	0.999	0.4
$k \times 10^5$	0.5	1.0	1.0	1.0	0.5
$\Gamma^s \times 10^{12}$	6.0	50	50	10, 100	10
$k_b \times 10^5$	3.0	20	20	0	1.0
A_o	8.5	0.41	0.41	0.31	3.8
p		0.2	0.2	0.2	0.2
C_{Kpi}		14000	14000	14000	14000
C_{Kdi}		0	0	0	0
C_{KF}		0	0	0	0
X^m		0.05	0.05	0.05	0.05
X_b		0.025	0.025	0.025	0.025
α_K		0.57	0.57	0.57	0.57

$h = 0.143$ m, $a = 0.00012$ m², $d_c = 0.00142$ m, $\rho = 838.8$ kg.m⁻³, $V_p = 0.000634$ m³.kg⁻¹, $\epsilon = 0.292$, $\Delta t = 10$ s and $N = 10$ in all cases.

Table 7.4(a)

Parameters used in equilibrium model simulations of gold elution profiles from packed bed reactors.

Figure	7.22	7.23	7.24	7.25	7.26	7.27	7.28
$V \times 10^8$	1.367	1.376	1.239	1.323	1.352	1.386	1.328
Q_{Gi}	4.848	4.70	4.848	4.805	4.189	4.825	12.16
A_o	0.375	0.40	0.40	0.385	0.36	0.375	0.7
p	0.2	0.2	0.2	0.2	0.2	0.2	0.2
q	0.1	0.1	0.1	0.1	0.1	0.1	0.1
C_{Kpi}	14000	14000	14000	6300	14000	14000	14000
C_{Kdi}	0	559	2100	6300	0	0	0
C_{KF}	0	559	2100	6300	0	0	0
X^m	0.05	0.05	0.05	0.05	0.05	0.05	0.05
X_b	0.025	0.025	0.025	0.025	0.025	0.025	0.025
α_K	0.57	0.57	0.57	0.57	0.57	0.57	0.57

$h = 0.143$ m, $a = 0.00012$ m², $d_c = 0.00142$ m, $\rho = 838.8$ kg.m⁻³, $V_p = 0.000634$ m³.kg⁻¹, $\epsilon = 0.292$, $\Delta t = 20$ s and $N = 10$ in all cases.

Table 7.4(b)

Parameters used in equilibrium model simulations of gold elution profiles from packed bed reactors.

Figure	7.29	7.30	7.31	7.32	7.33	7.34
h	0.143	0.143	0.143	0.143	0.143	0.749
$a \times 10^{-4}$	1.2	1.2	1.2	1.2	1.2	78.54
$V \times 10^8$	1.410	1.376	1.36	1.357	1.249	395.8
Q_{Gi}	5.061	4.80	4.98	4.593	4.976	2.46
A_o	0.60	0.42	0.375	0.44	0.33	0.065
p	0.2	0.2	0.2	0.2	0.2	0.25
q	0.11	0	0	0.1	0.1	0
C_{Kpi}	3500	10000	14000	14000	14000	14000
C_{Kdi}	0	0	2000	0	0	7000
C_{KF}	0	0	2000*	0	0	0
X^m	0.05	0.05	0.05	0.05	0.05	0.05
X_b	0.08	0.025	0.1	0.025	0.025	0.03
α_K	0.45	0.57	0.35	0.57	0.57	0.4

$d_c = 0.00142$ m, $\rho = 838.8$ kg.m⁻³, $V_p = 0.000634$ m³.kg⁻¹, $\epsilon = 0.292$, $\Delta t = 20$ s and $N = 10$ in all cases.

*Changed to $C_{KF} = 0$ g.m⁻³ after 1.26 hr.

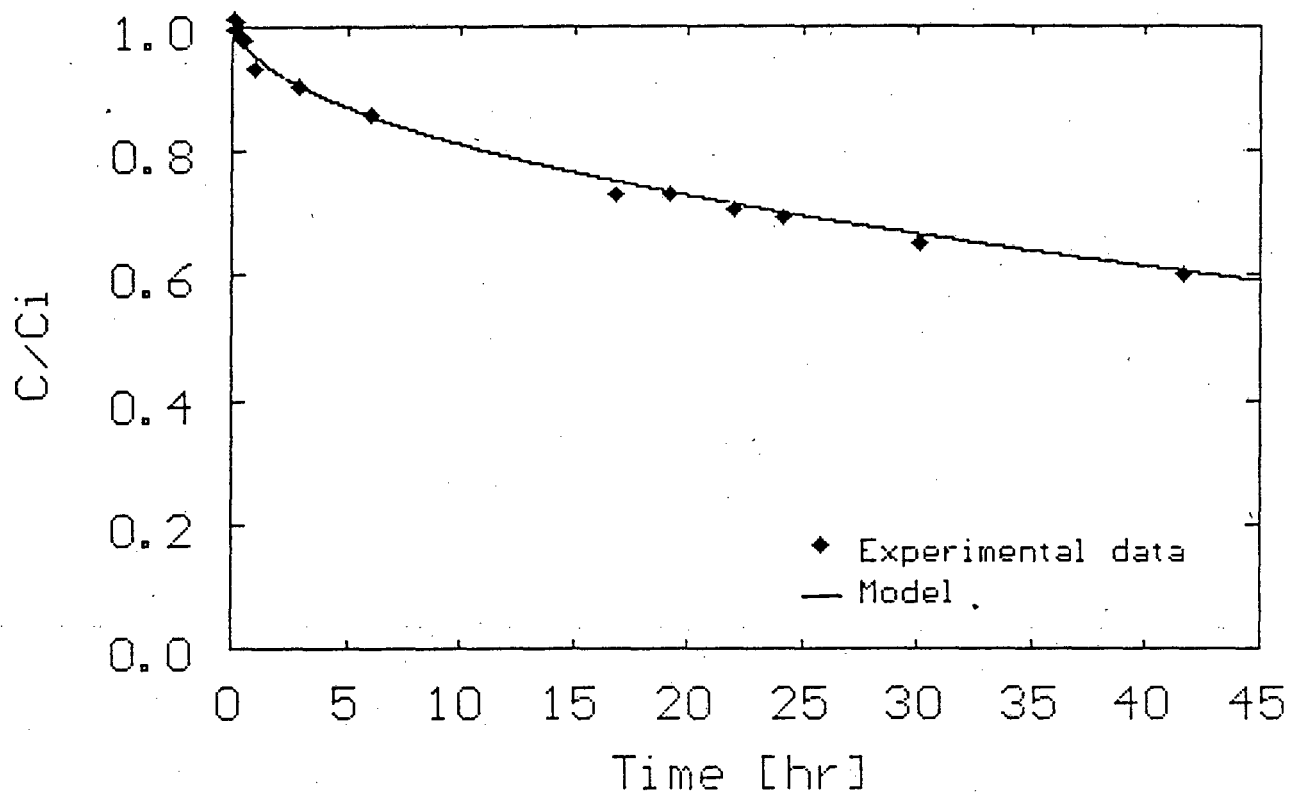


Figure 7.1 Simulation of adsorption of gold in batch with surface diffusion model. (Exp.77)

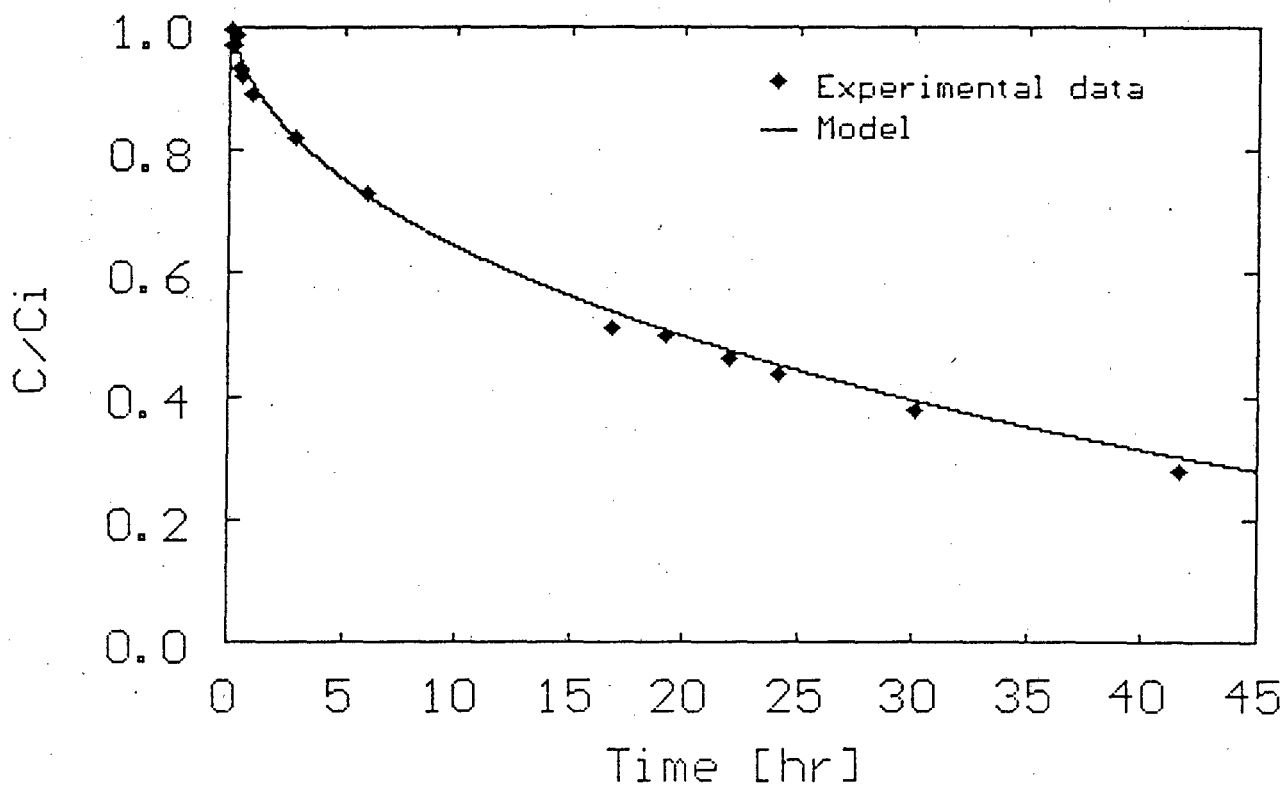


Figure 7.2 Simulation of adsorption of gold in batch with surface diffusion model. (Exp.78)

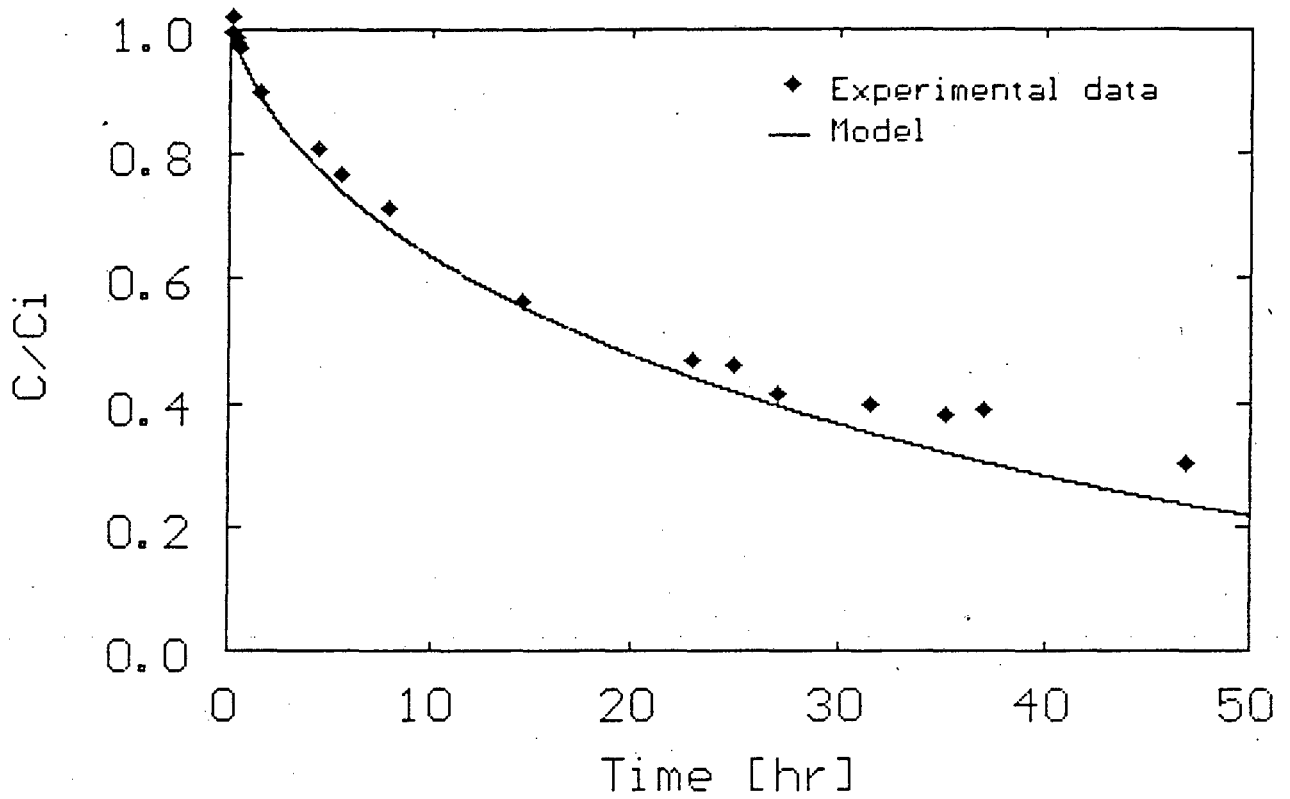


Figure 7.3 Simulation of adsorption of gold in batch with surface diffusion model. (Exp.79)

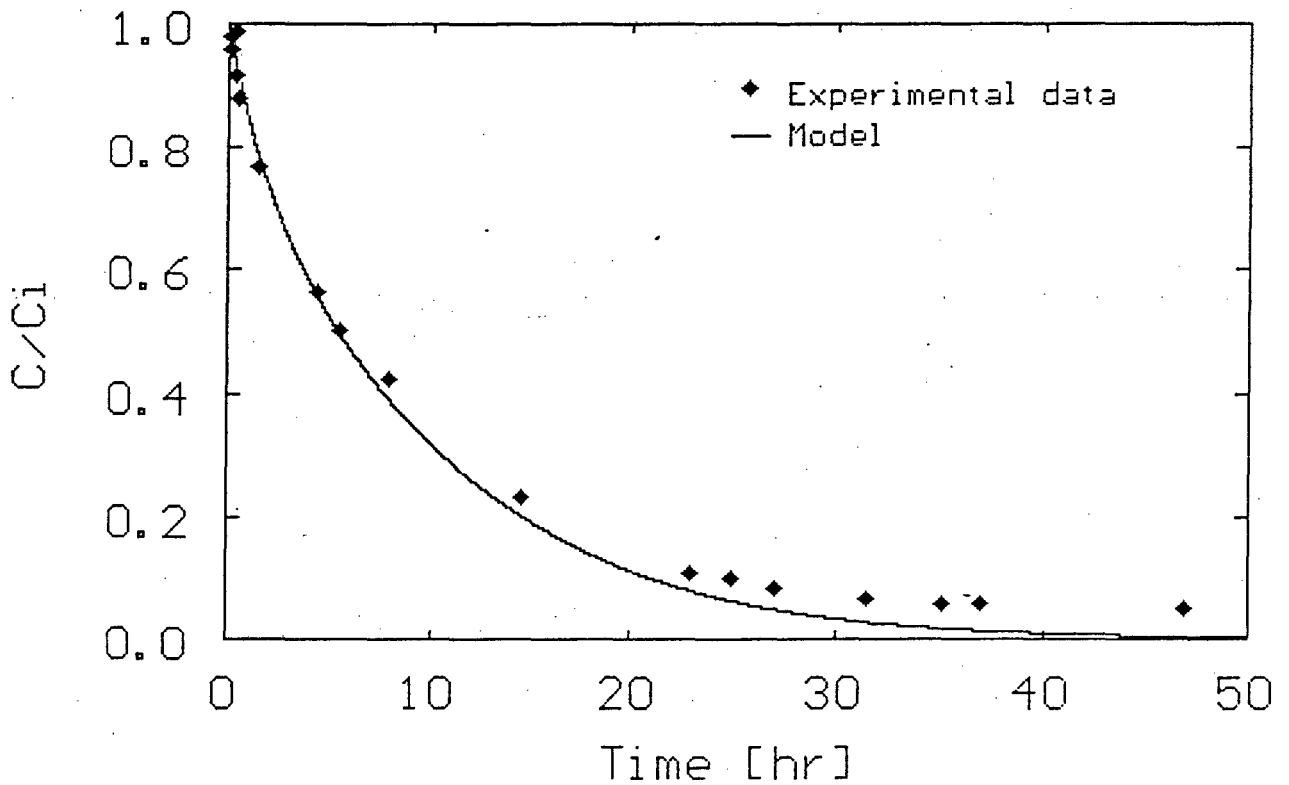


Figure 7.4 Simulation of adsorption of gold in batch with surface diffusion model. (Exp.80)

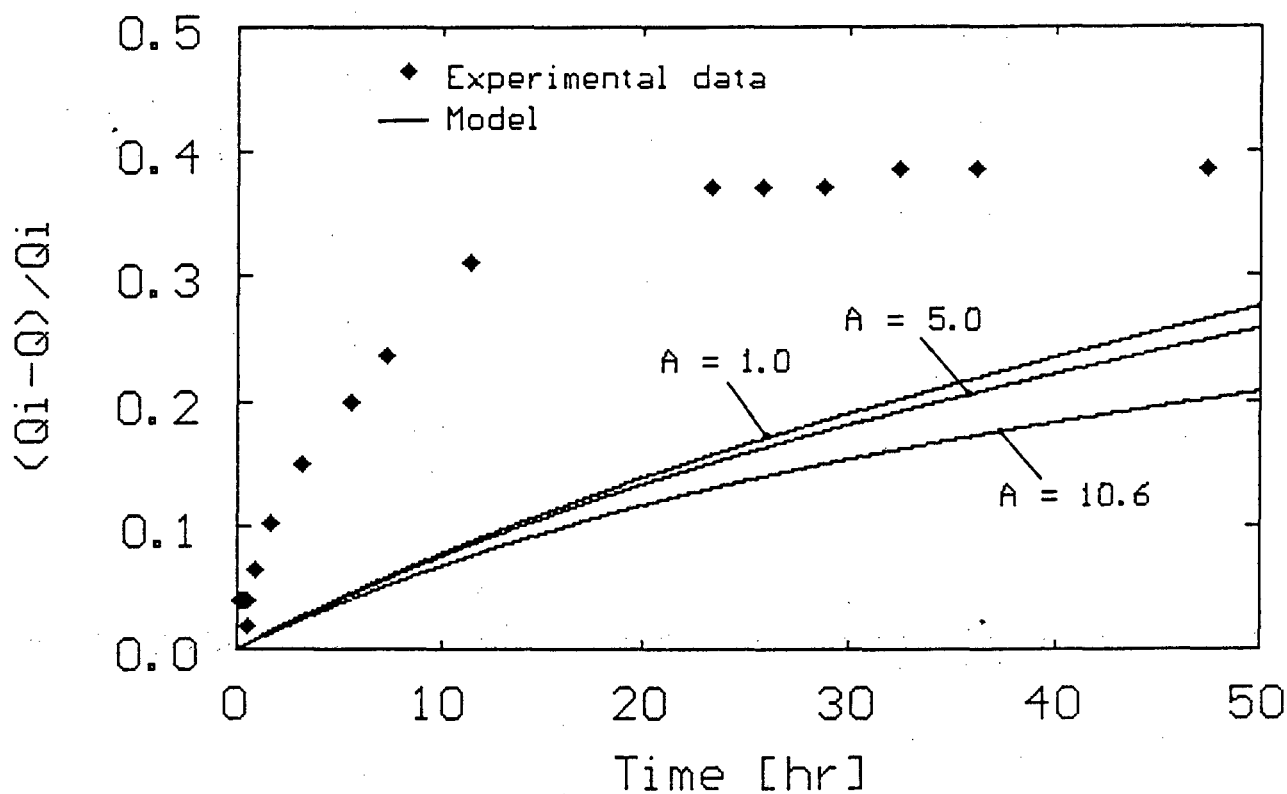


Figure 7.5 Attempt to simulate desorption of gold in batch with kinetic parameters as determined for adsorption. (Exp.77)

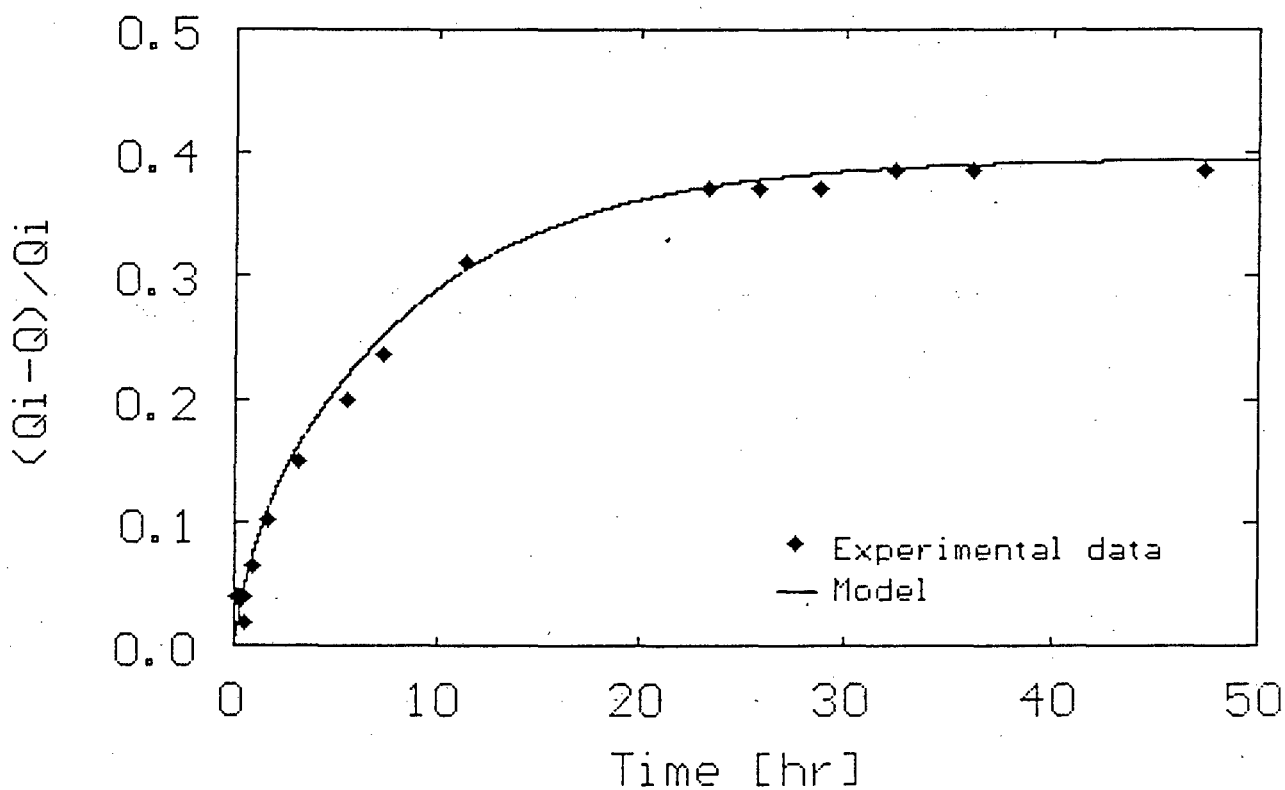


Figure 7.6 Simulation of desorption of gold in batch with surface diffusion model. (Exp.77)

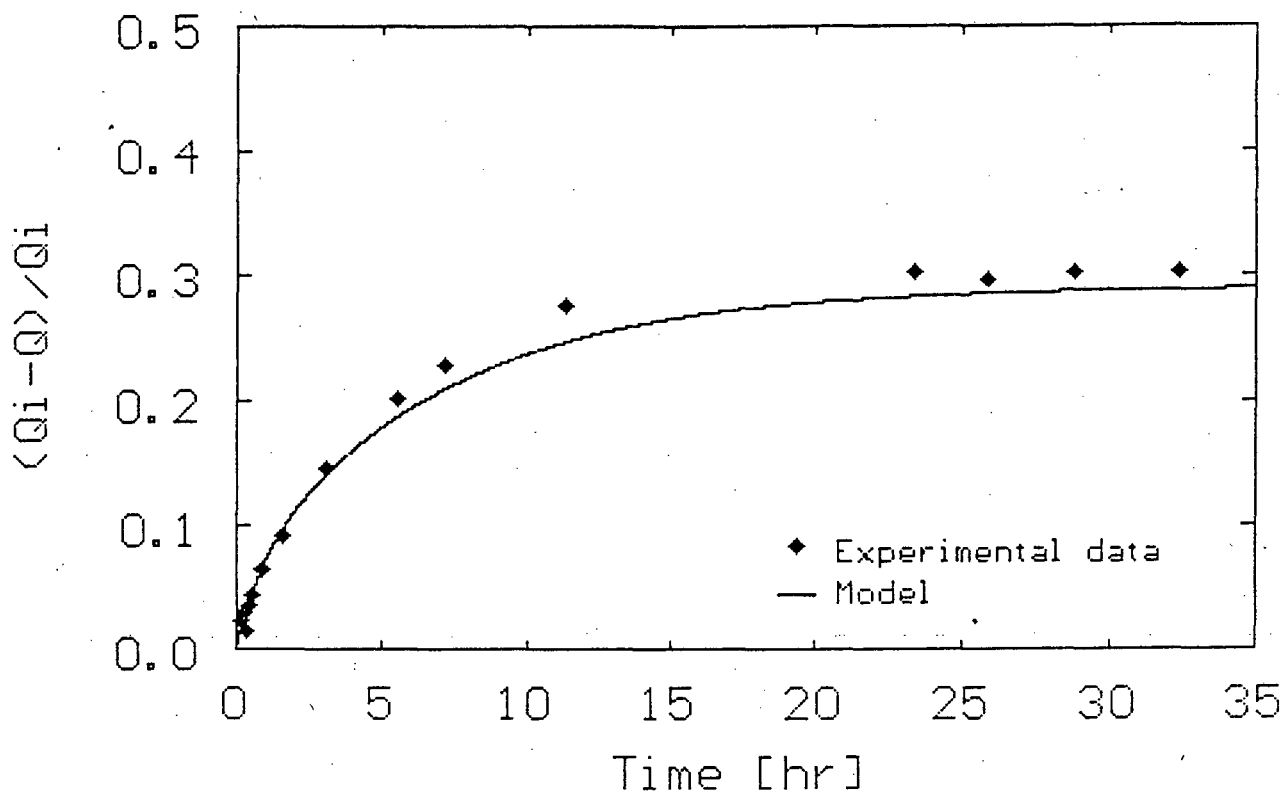


Figure 7.7 Simulation of desorption of gold in batch with surface diffusion model. (Exp.78)

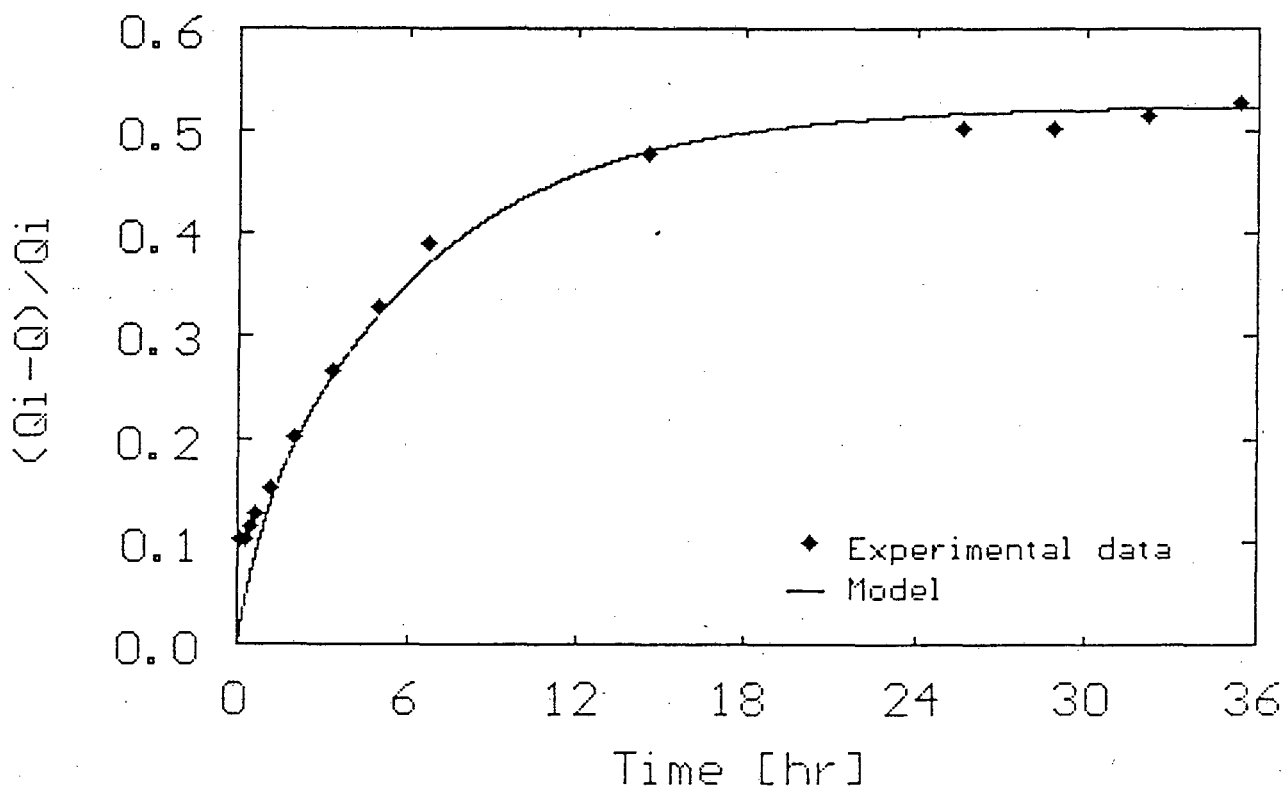


Figure 7.8 Simulation of desorption of gold in batch with surface diffusion model. (Exp.79)

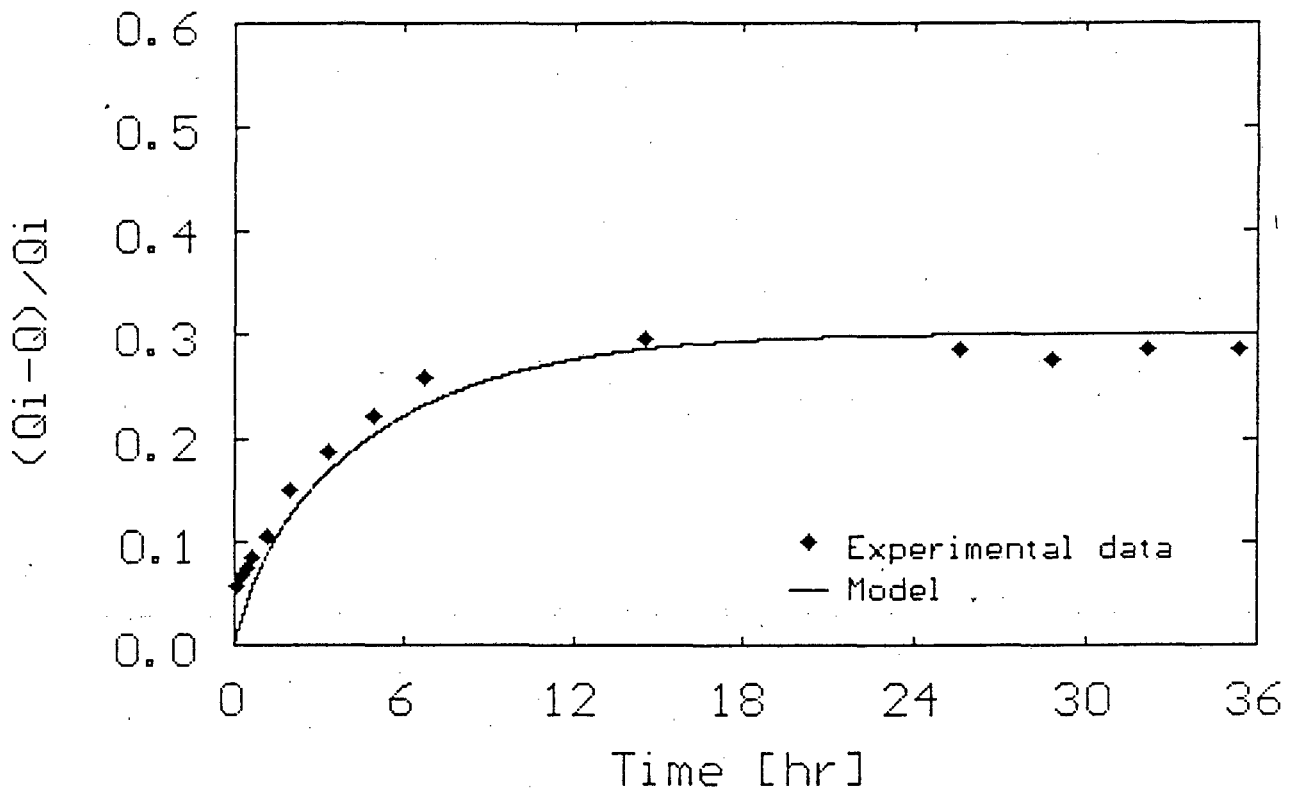


Figure 7.9 Simulation of desorption of gold in batch with surface diffusion model. (Exp.80)

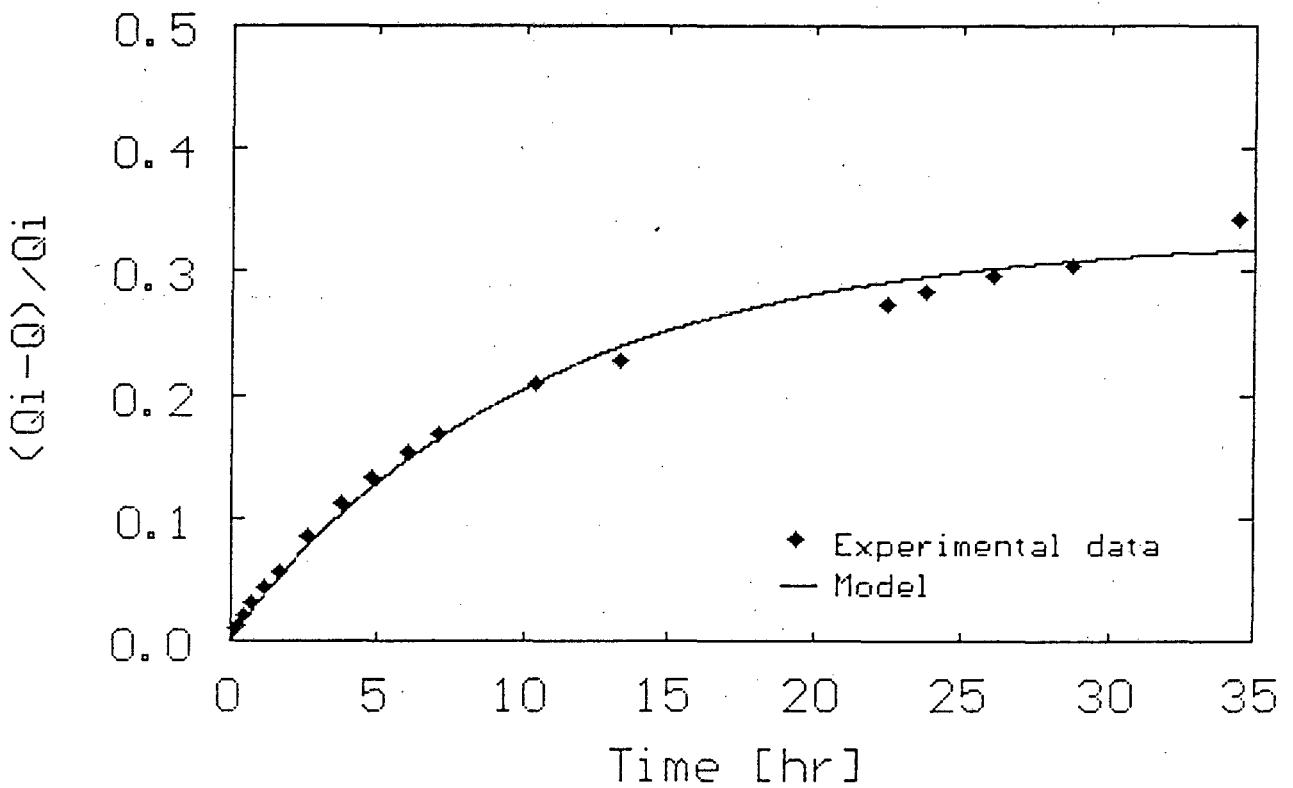


Figure 7.10 Simulation of desorption of gold after adsorption to equilibrium. Modelled in batch with surface diffusion model. (Exp.81)

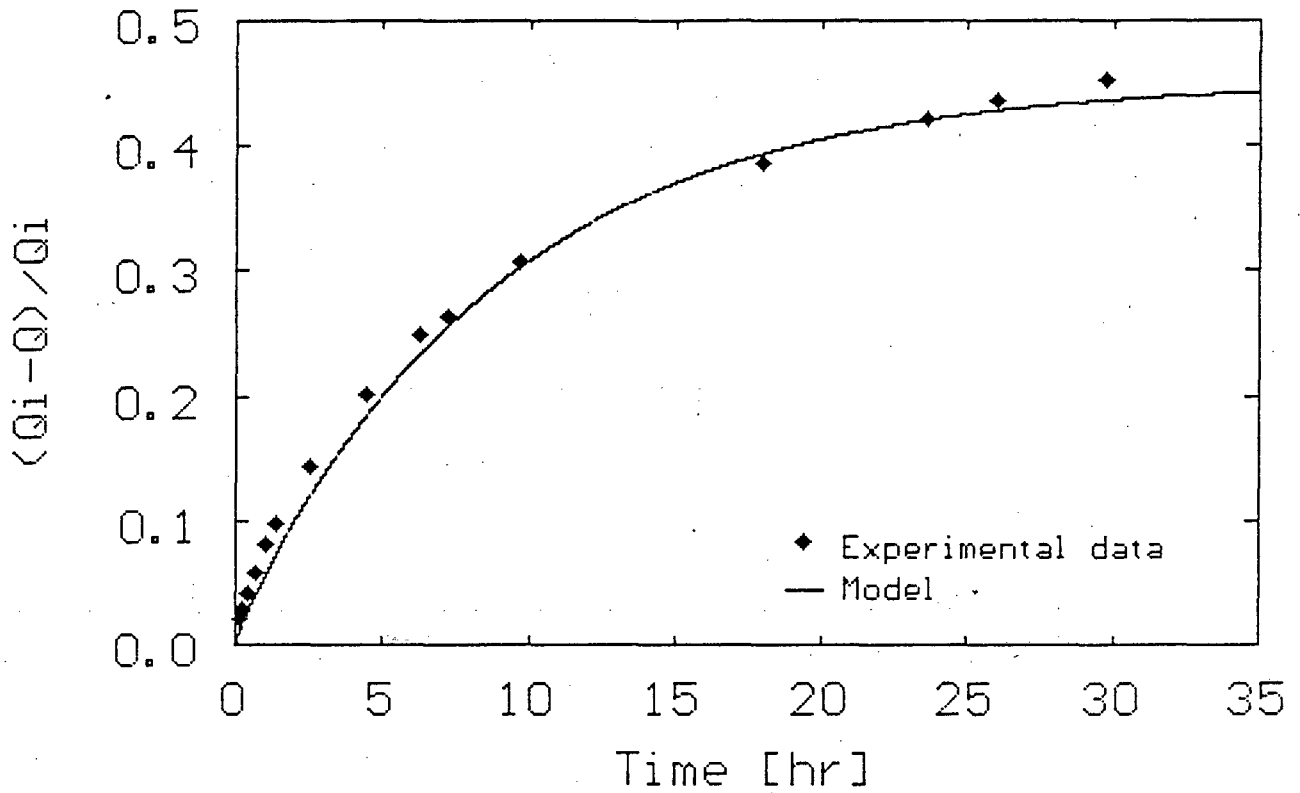


Figure 7.11 Simulation of desorption of gold in the presence of free cyanide. Modelled in batch with surface diffusion model. (Exp.82)

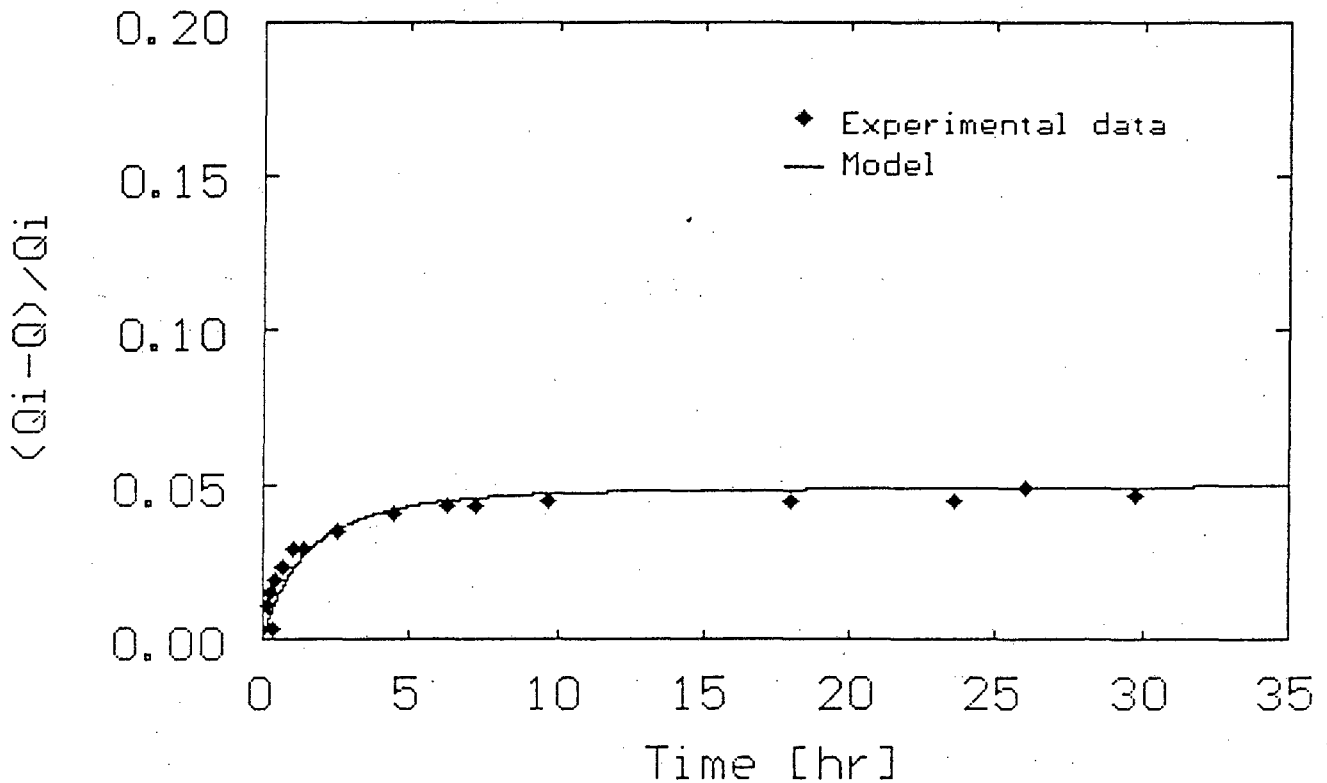


Figure 7.12 Simulation of desorption of gold in batch at 52 °C. Modelled with surface diffusion model. (Exp.83)

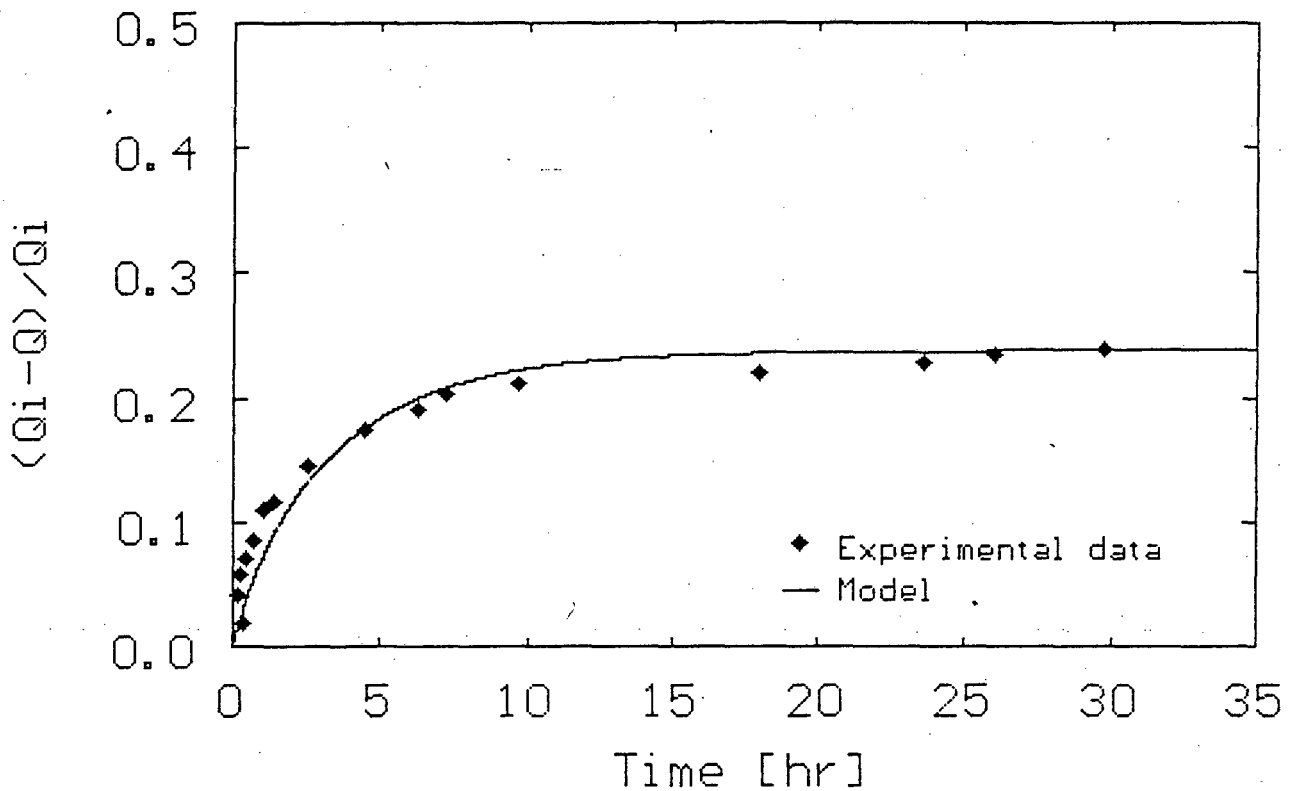


Figure 7.13 Simulation of desorption of gold in batch at 90 °C. Modelled with surface diffusion model. (Exp.84)

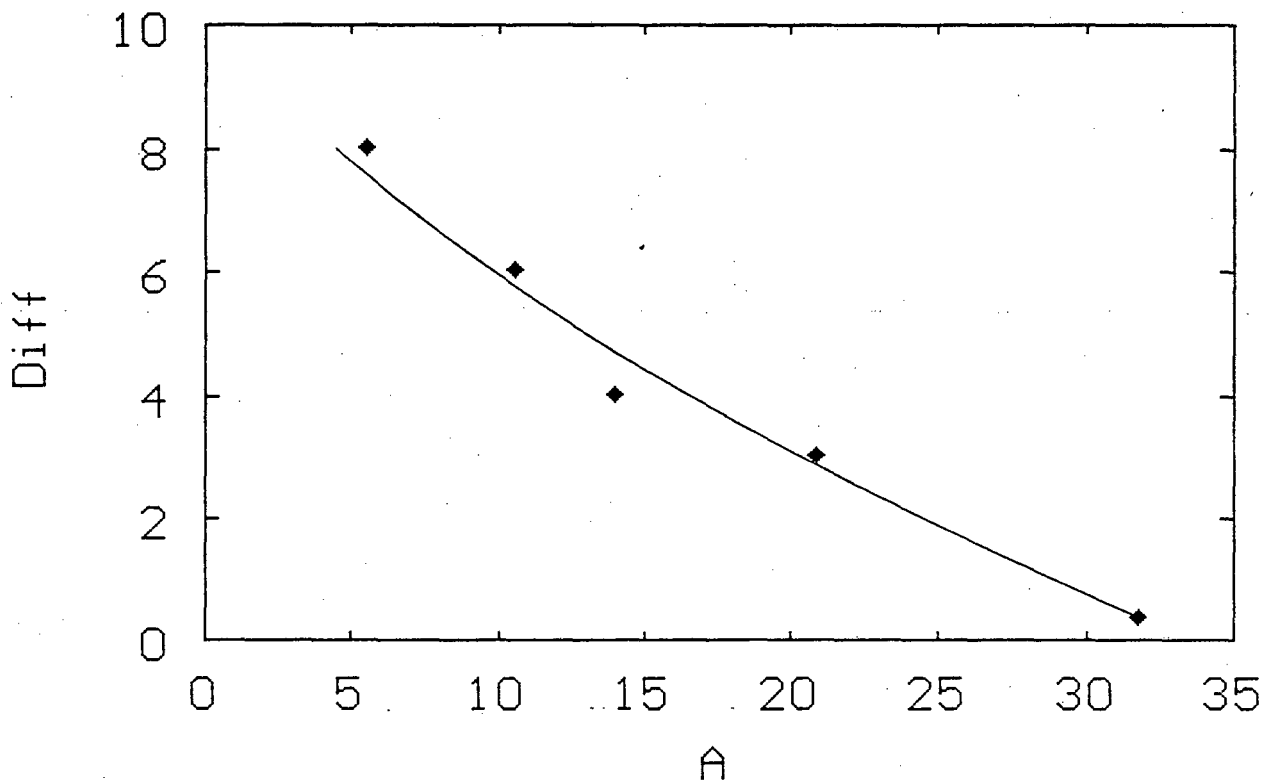


Figure 7.14 The effect of the equilibrium isotherm constant on the value of the combined macropore diffusion coefficient. ($\text{Diff} = \Gamma_m \times 10^{12} \text{ m}^2 \cdot \text{s}^{-1}$) (Exp.77-82)

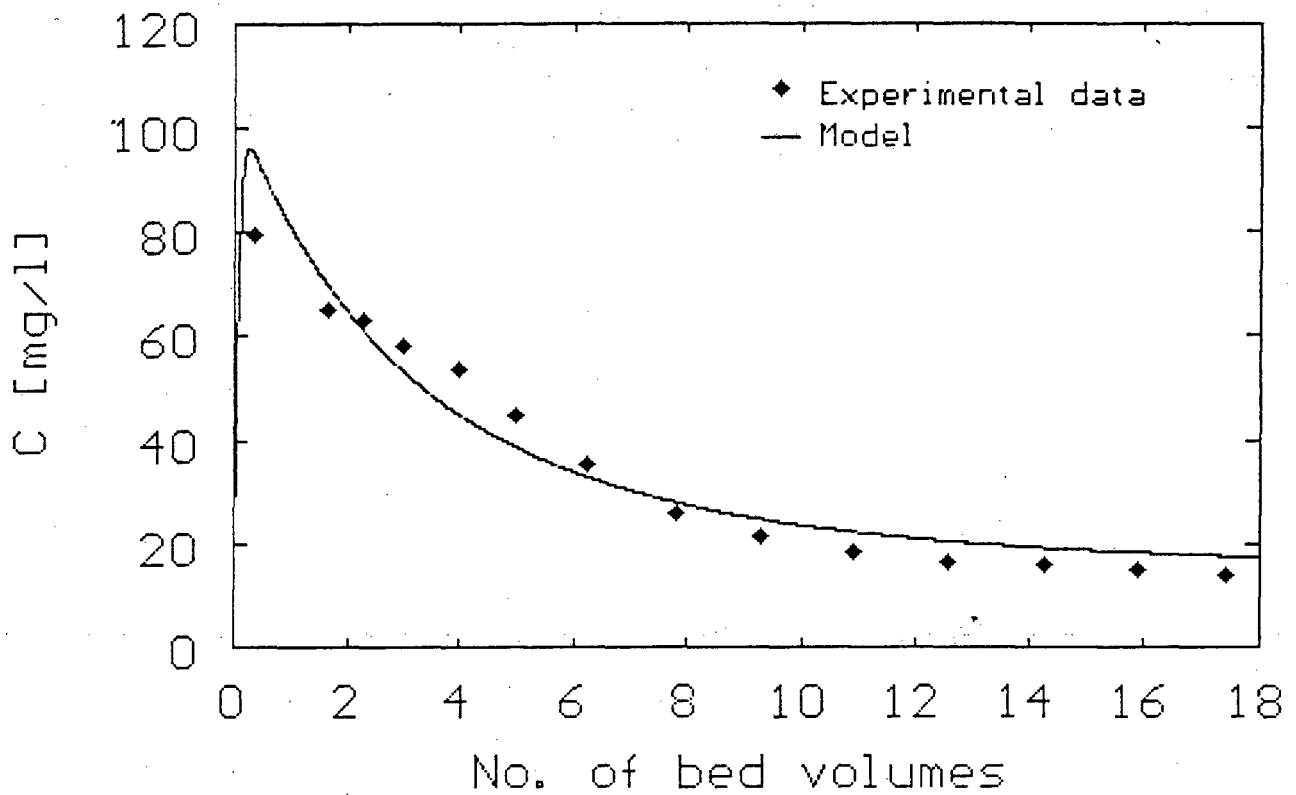


Figure 7.15(a) Simulation of elution of gold from a packed bed of carbon with the surface diffusion model. No pretreatment, constant equilibrium. (Exp.85)

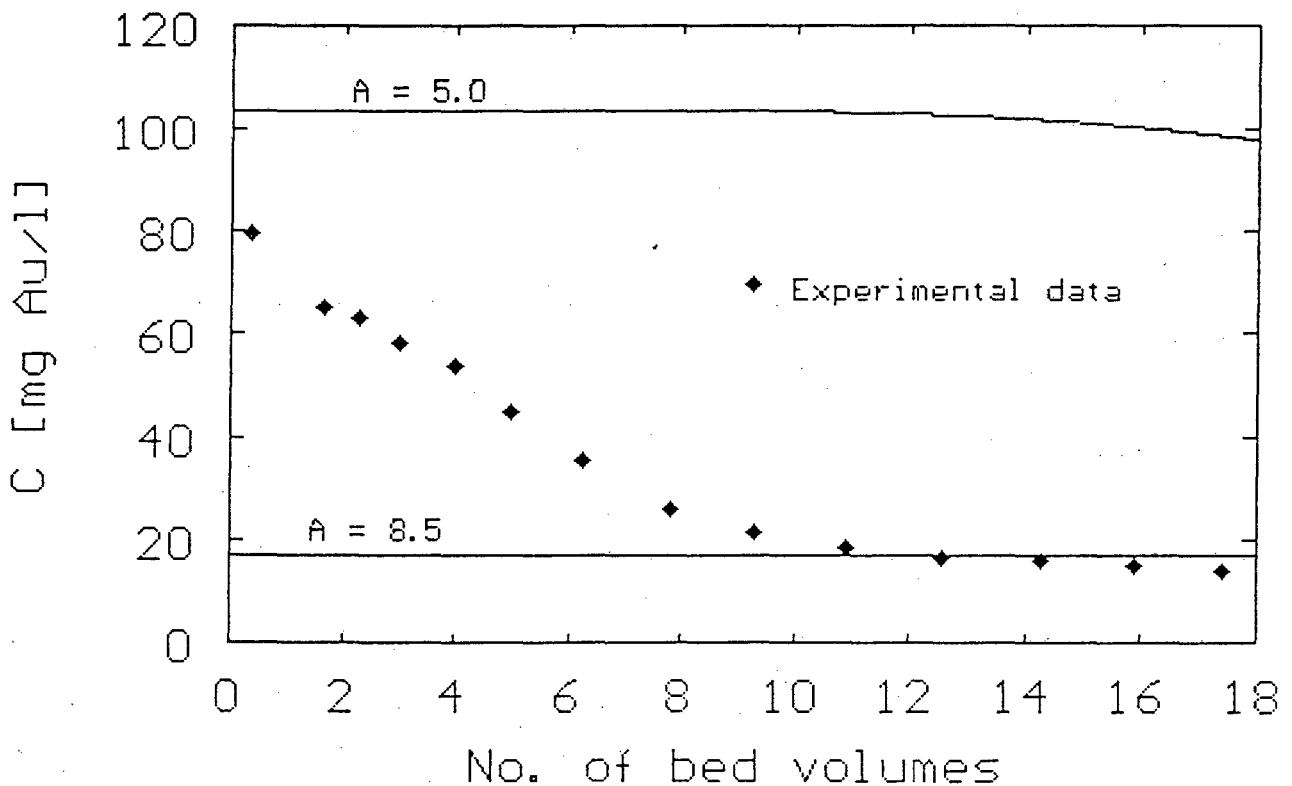


Figure 7.15(b) Attempt to simulate the elution in Fig. 7.15(a) with the equilibrium model. (Exp.85)

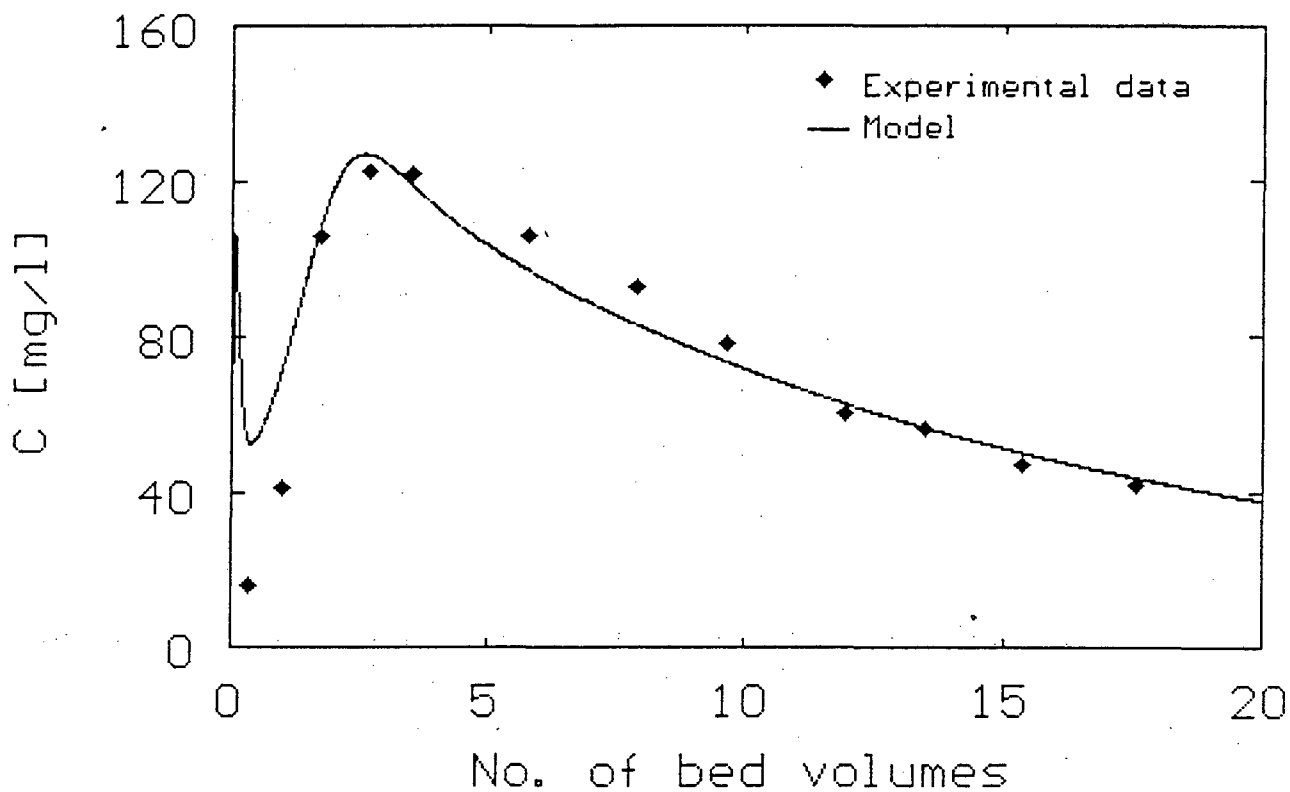


Figure 7.16 Simulation of an AARL elution at a flow rate of 2.9 bed volumes/h with the surface diffusion model. (Exp.50)

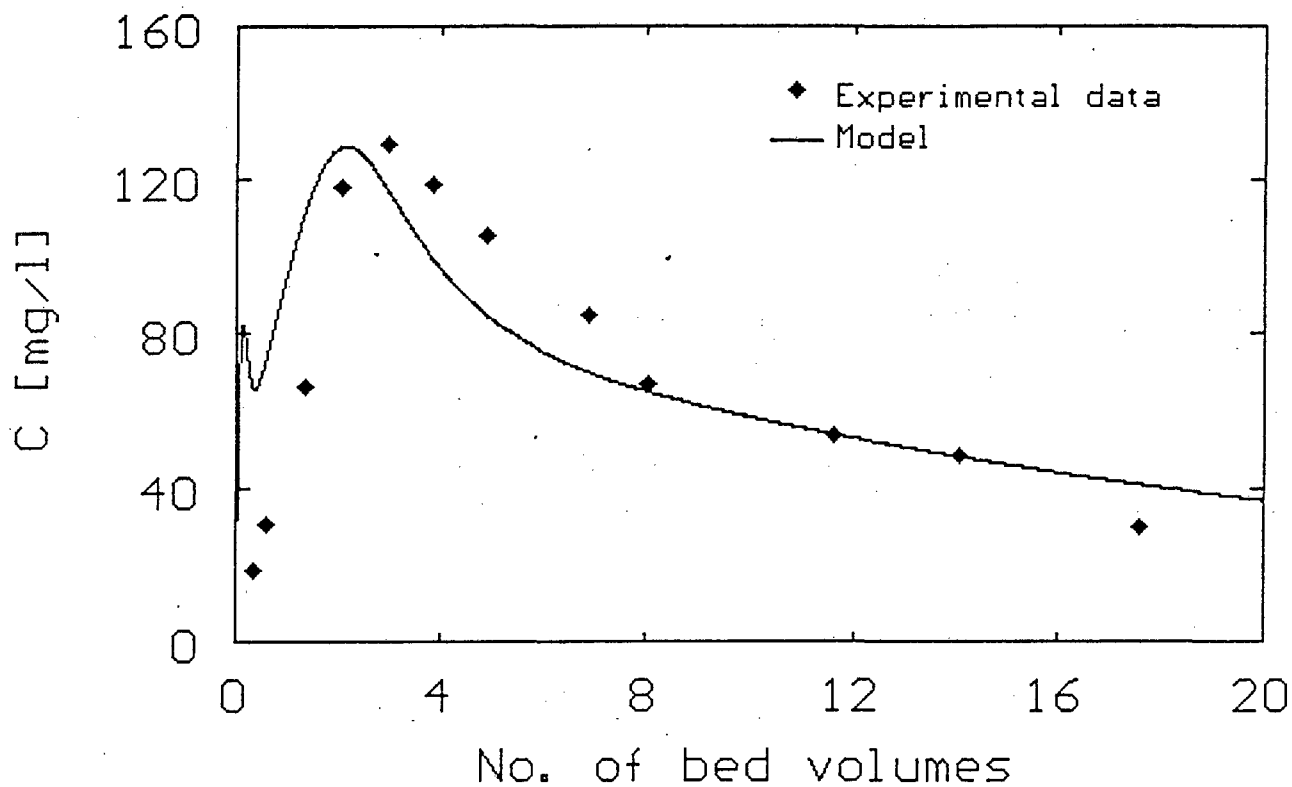


Figure 7.17 Simulation of an AARL elution at a flow rate of 5.9 bed volumes/h with the surface diffusion model. (Exp.61)

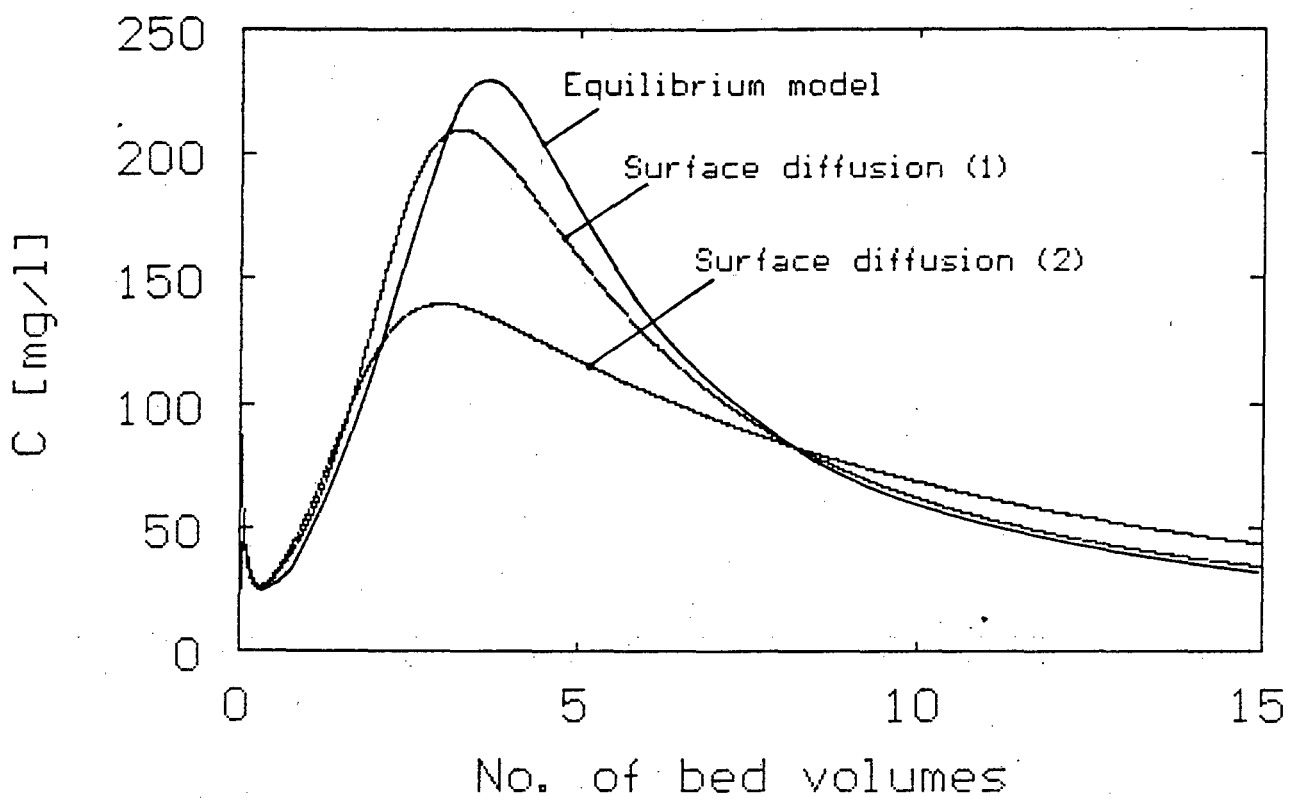


Figure 7.18 The relationship between the surface diffusion and equilibrium models for the elution of gold cyanide. Surface diffusion (1) : $\Gamma_m = 1 \times 10^{-10} \text{ m}^2 \cdot \text{s}^{-1}$, Surface diffusion (2) : $\Gamma_m = 1 \times 10^{-11} \text{ m}^2 \cdot \text{s}^{-1}$

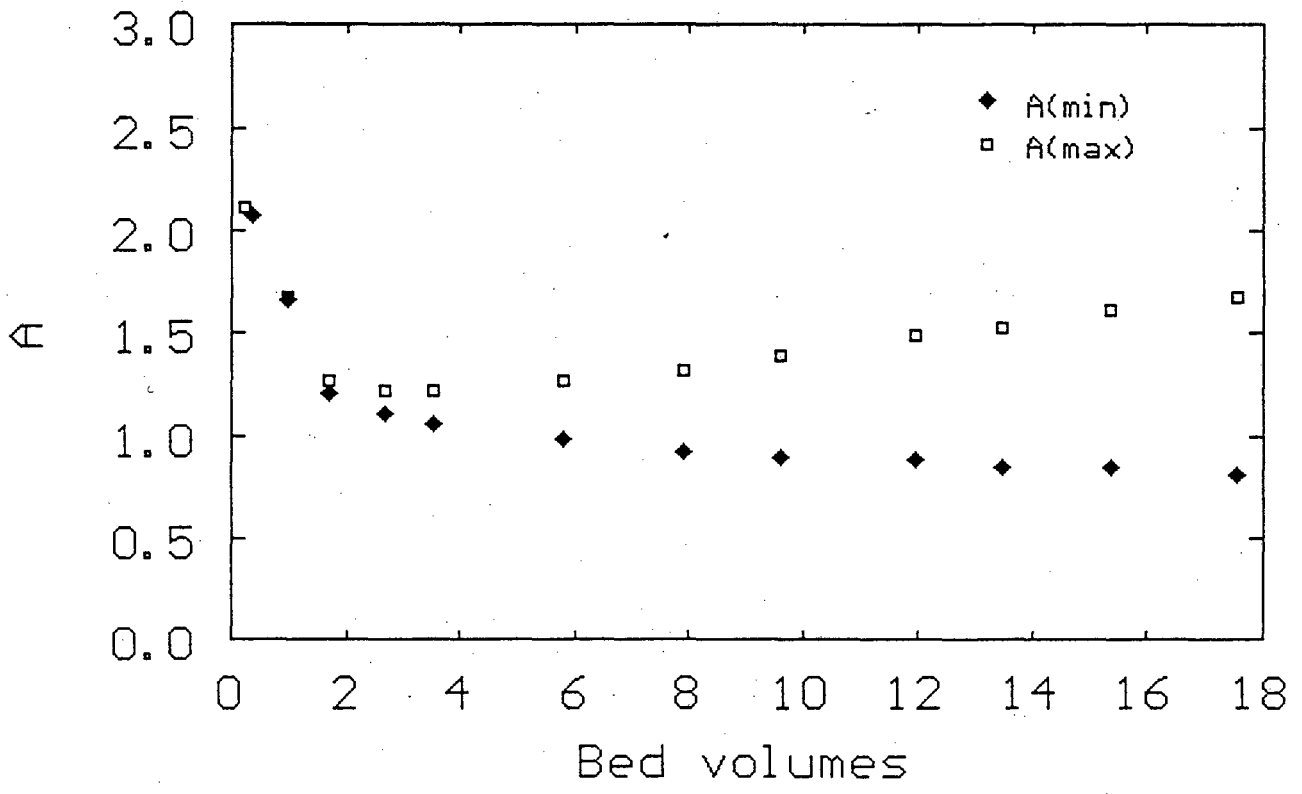


Figure 7.19 Estimation of the A-value in the shifting isotherm during an AARL elution. (Exp.50)

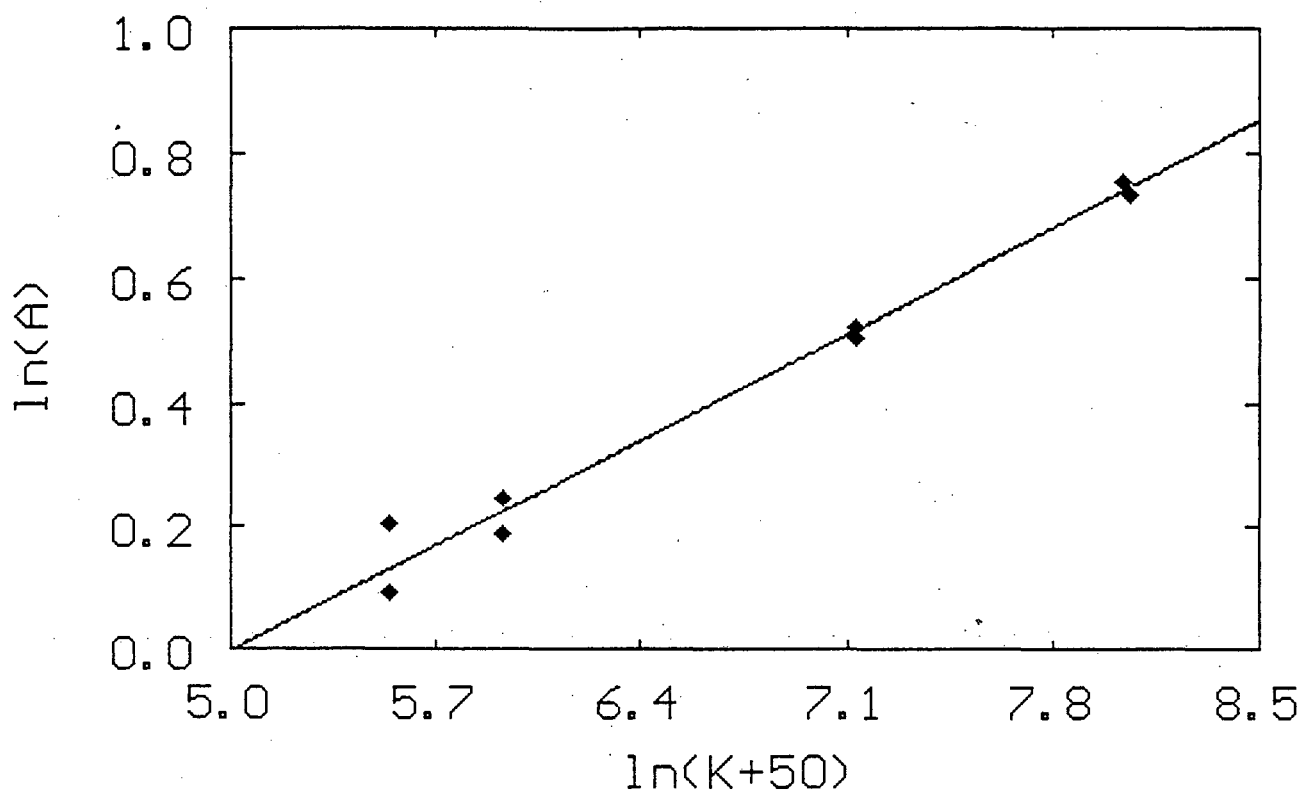


Figure 7.20 Quantification of the effect of potassium on the gold elution equilibrium after a cyanide pretreatment. (Exp.50)

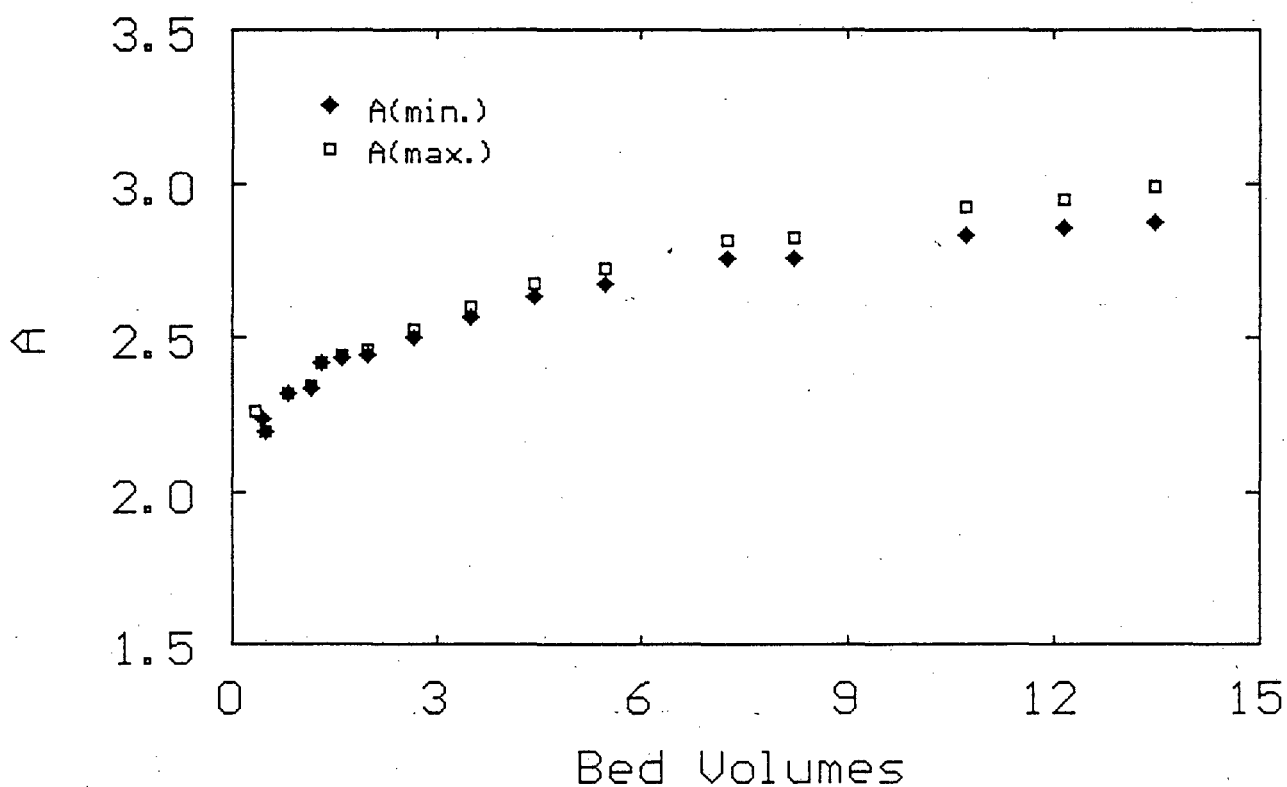


Figure 7.21 Estimation of the A-value for a constant concentration of potassium in the eluant. (Exp.86)

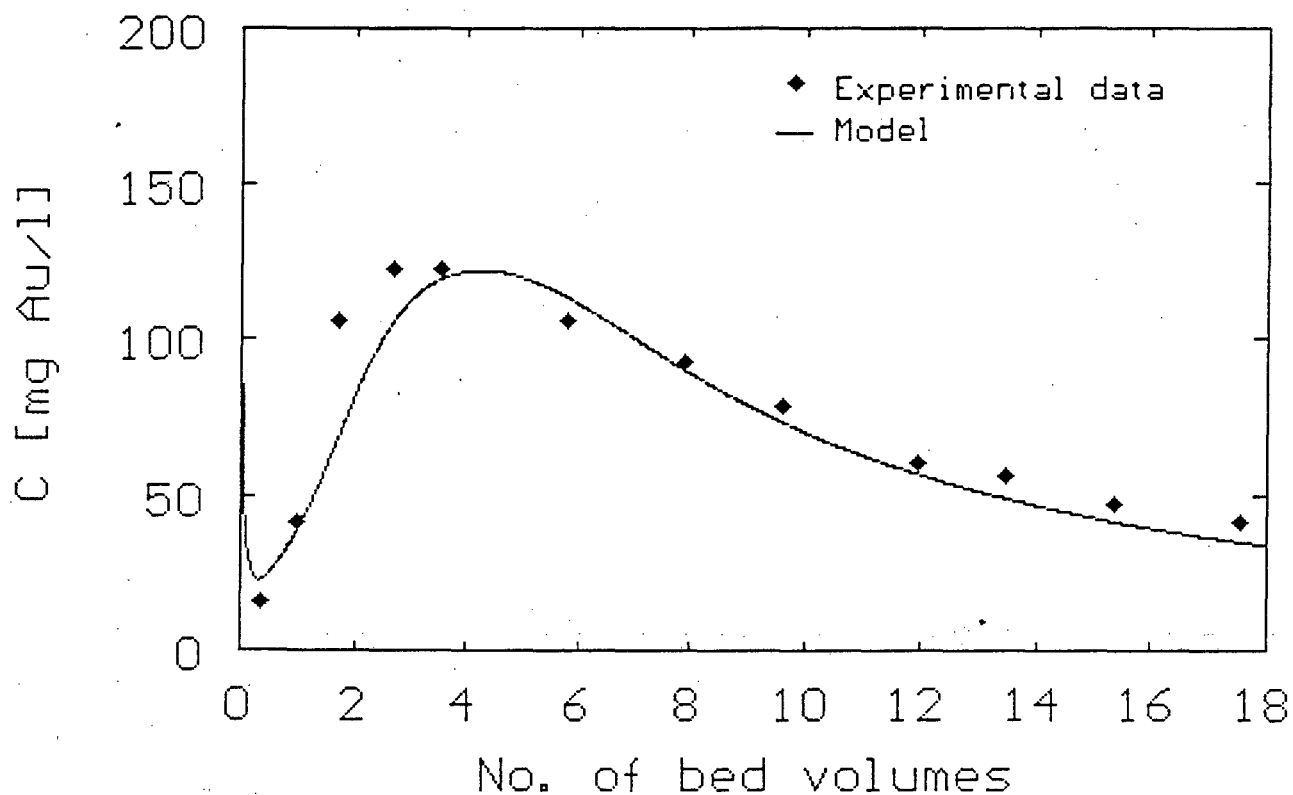


Figure 7.22 Simulation of the AARL elution in Figure 7.16 with the equilibrium model. Potassium concentration in feed = 0 g.m^{-3} , Adsorption period = 22 h, $T = 70 \text{ }^\circ\text{C}$. (Exp.50)

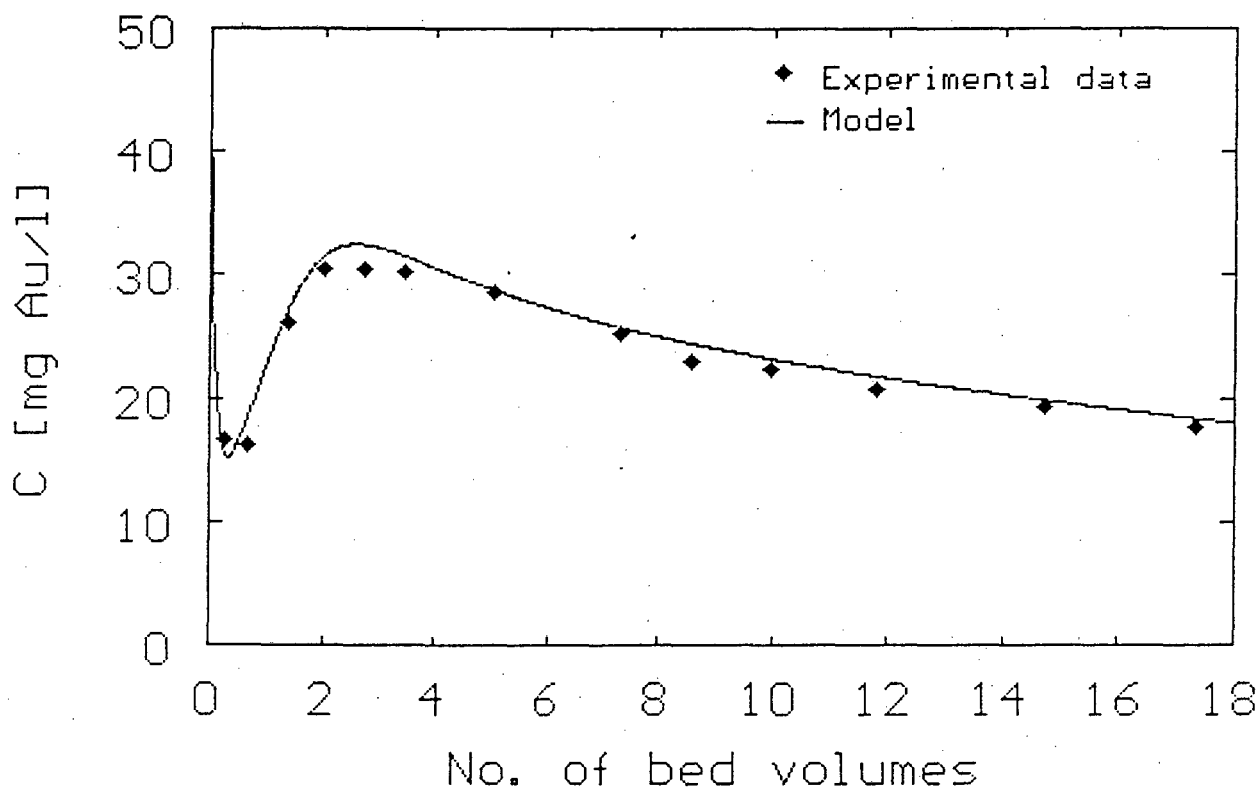


Figure 7.23 Simulation of an AARL elution with the equilibrium model. Potassium concentration in feed = 559 g.m^{-3} . (Exp.75)

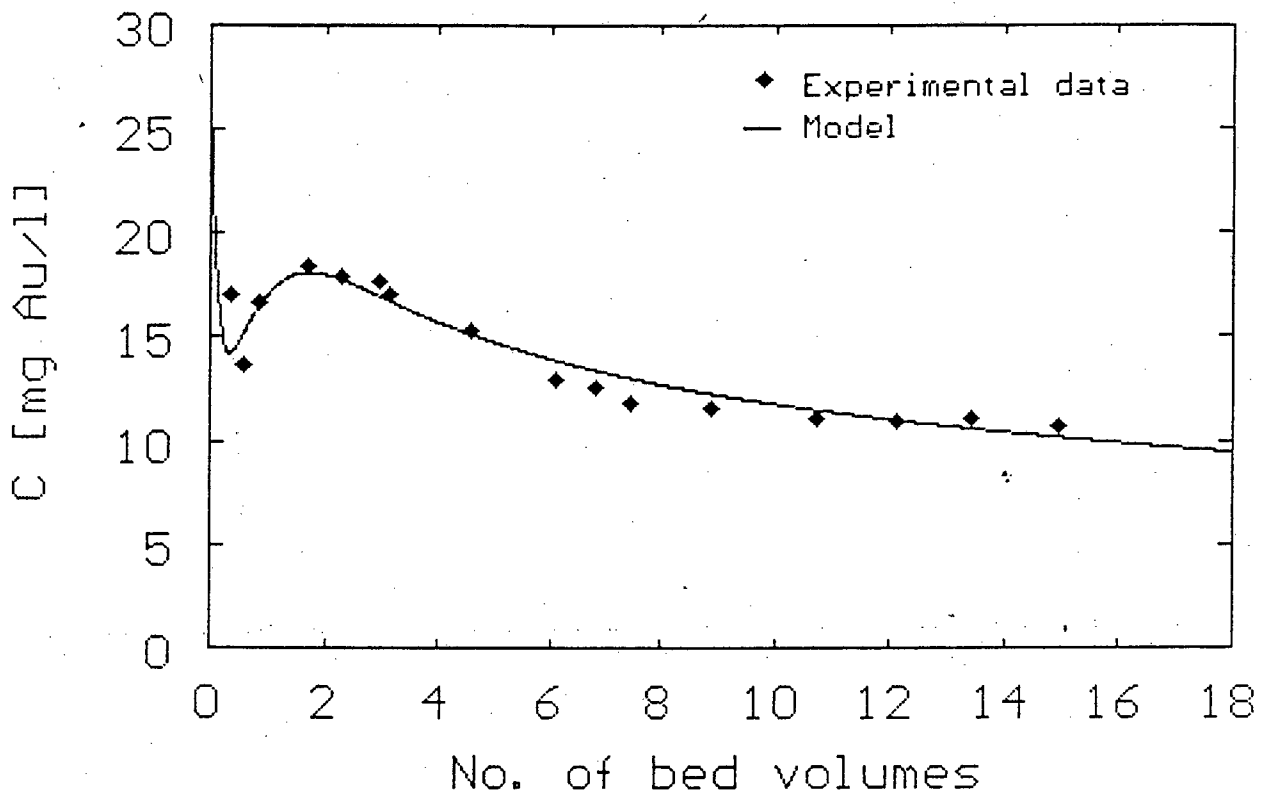


Figure 7.24 Simulation of an AARL elution with the equilibrium model. Potassium concentration in feed = 2100 g.m^{-3} . (Exp.87)

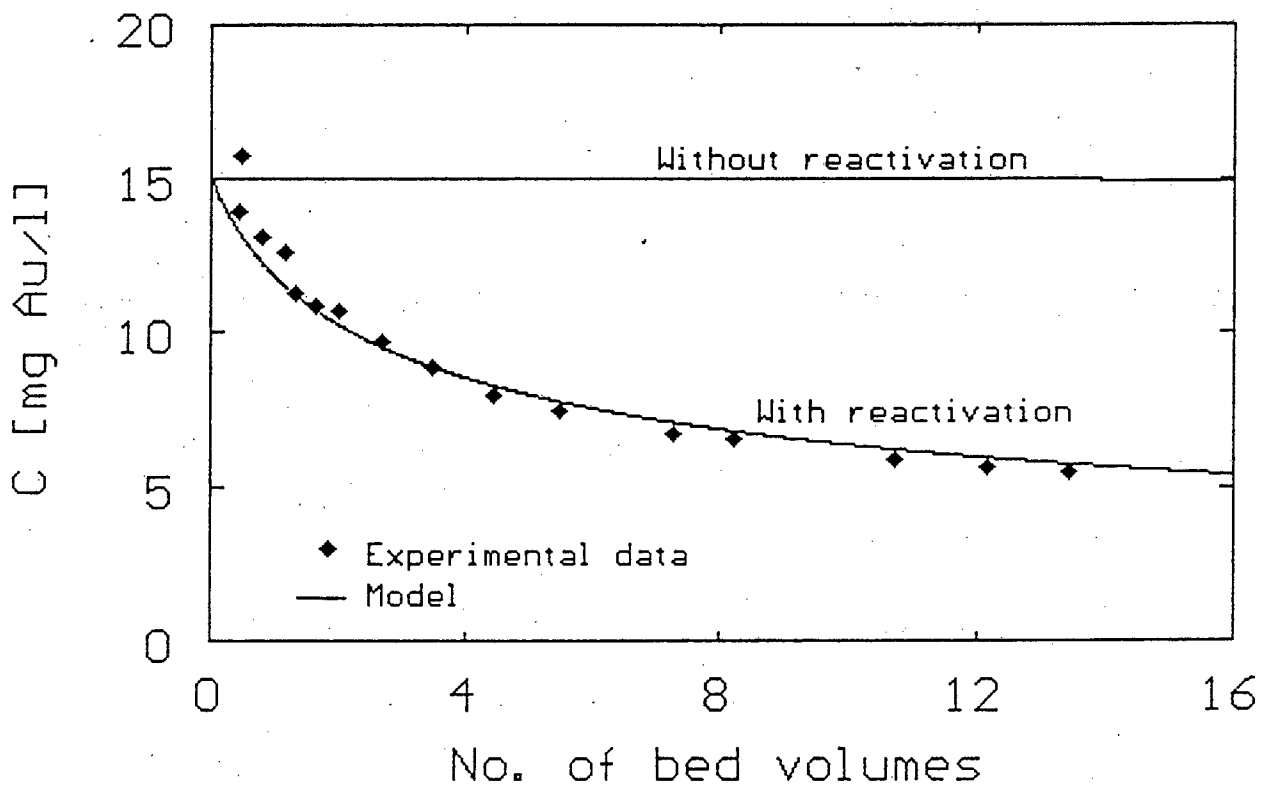


Figure 7.25 Simulation of an AARL elution with the equilibrium model. Potassium concentration in feed = 6300 g.m^{-3} . (Exp.86)

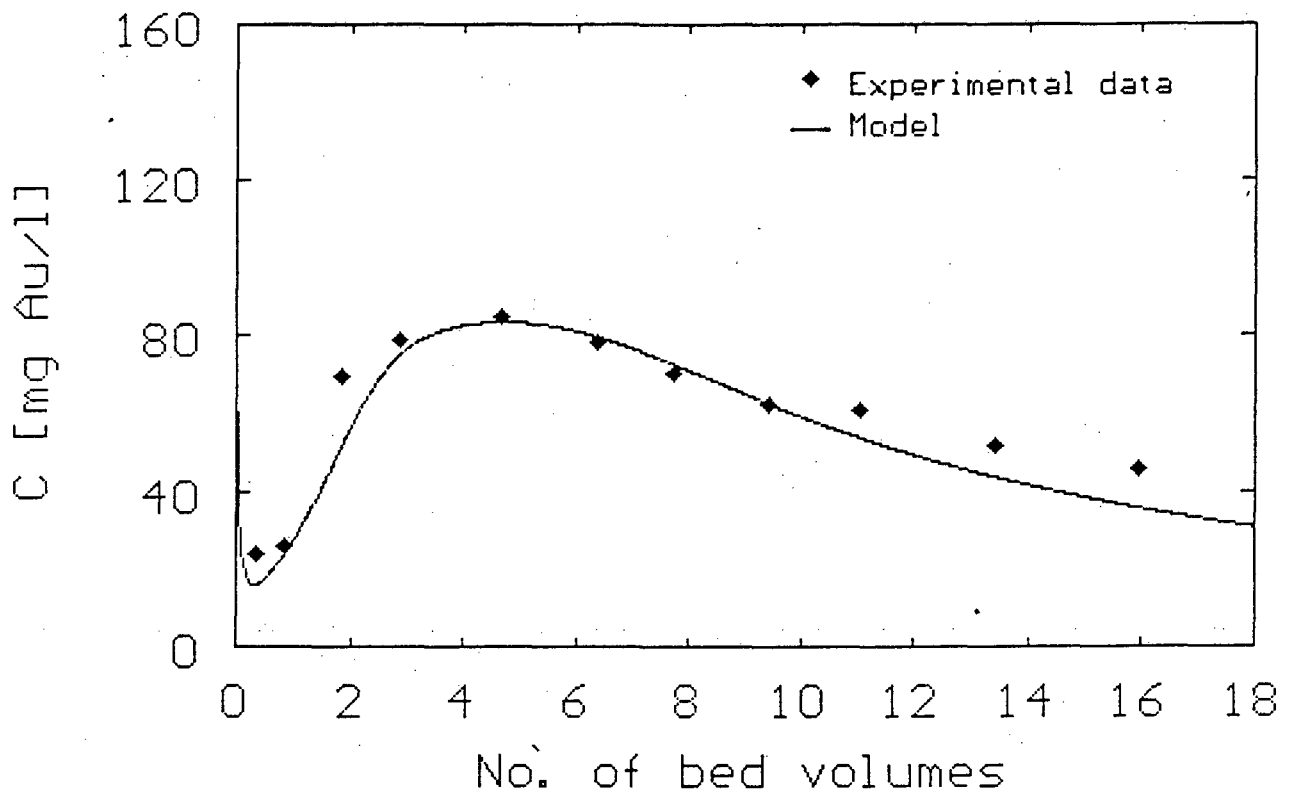


Figure 7.26 Simulation of an AARL elution with the equilibrium model. Adsorption period = 7 h. (Exp.88)

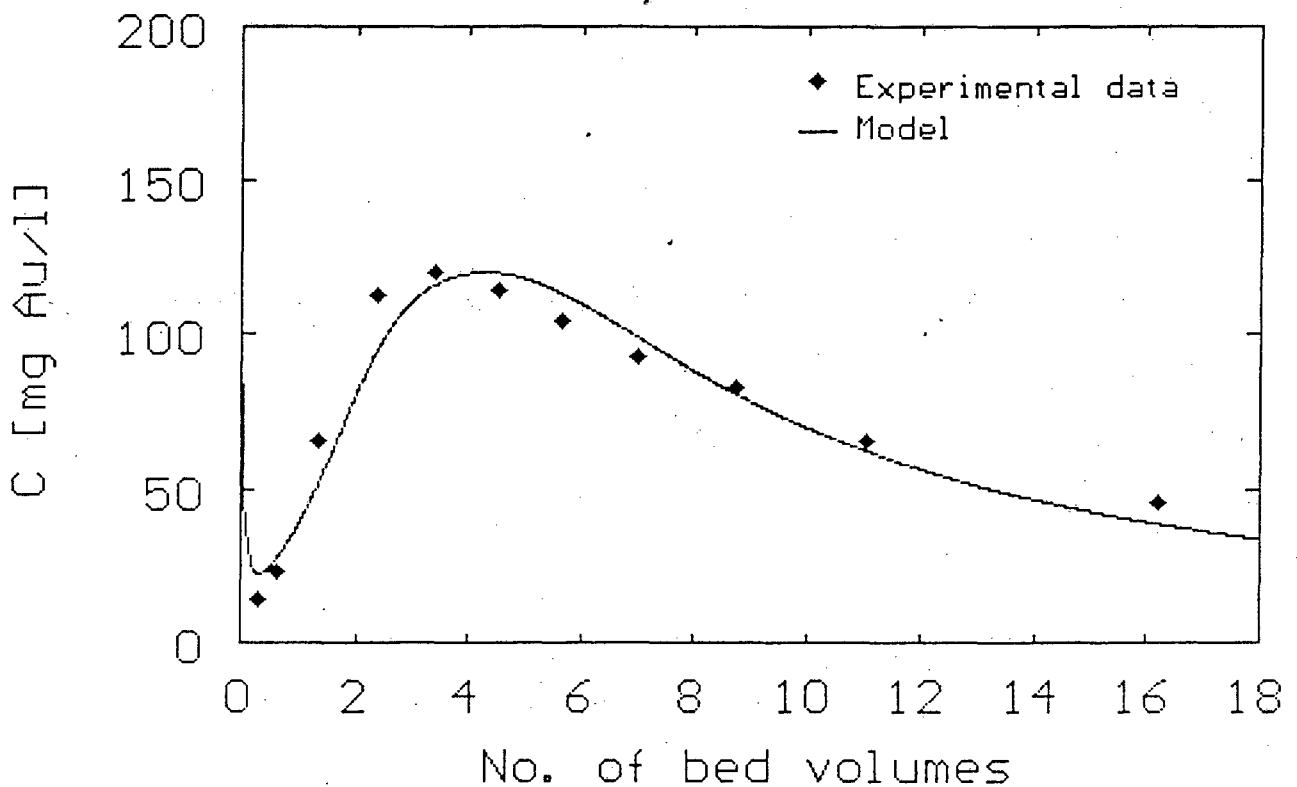


Figure 7.27 Simulation of an AARL elution with the equilibrium model. Adsorption period = 72 h. (Exp.40)

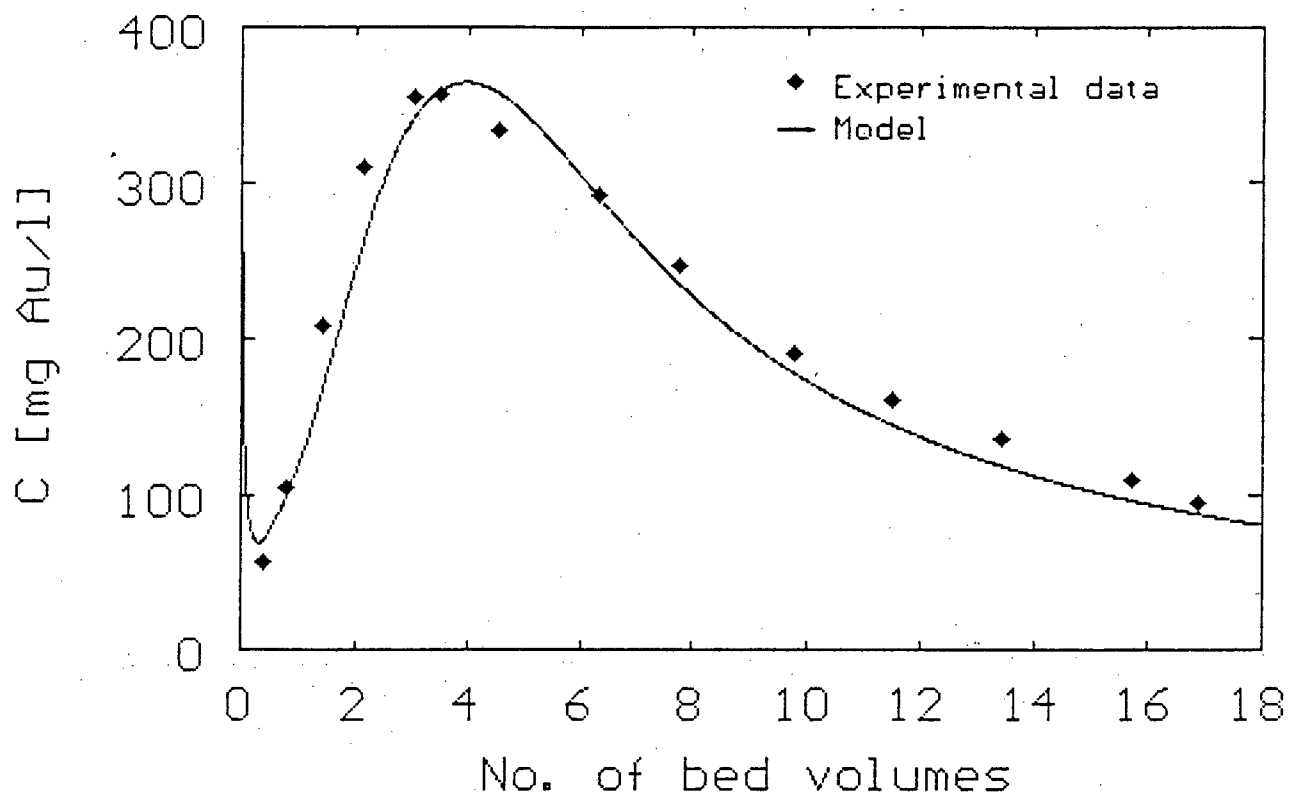


Figure 7.28 Simulation of an AARL elution with the equilibrium model.
 $Q_{Gi} = 12.16 \text{ g.kg}^{-1}$. (Exp.89)

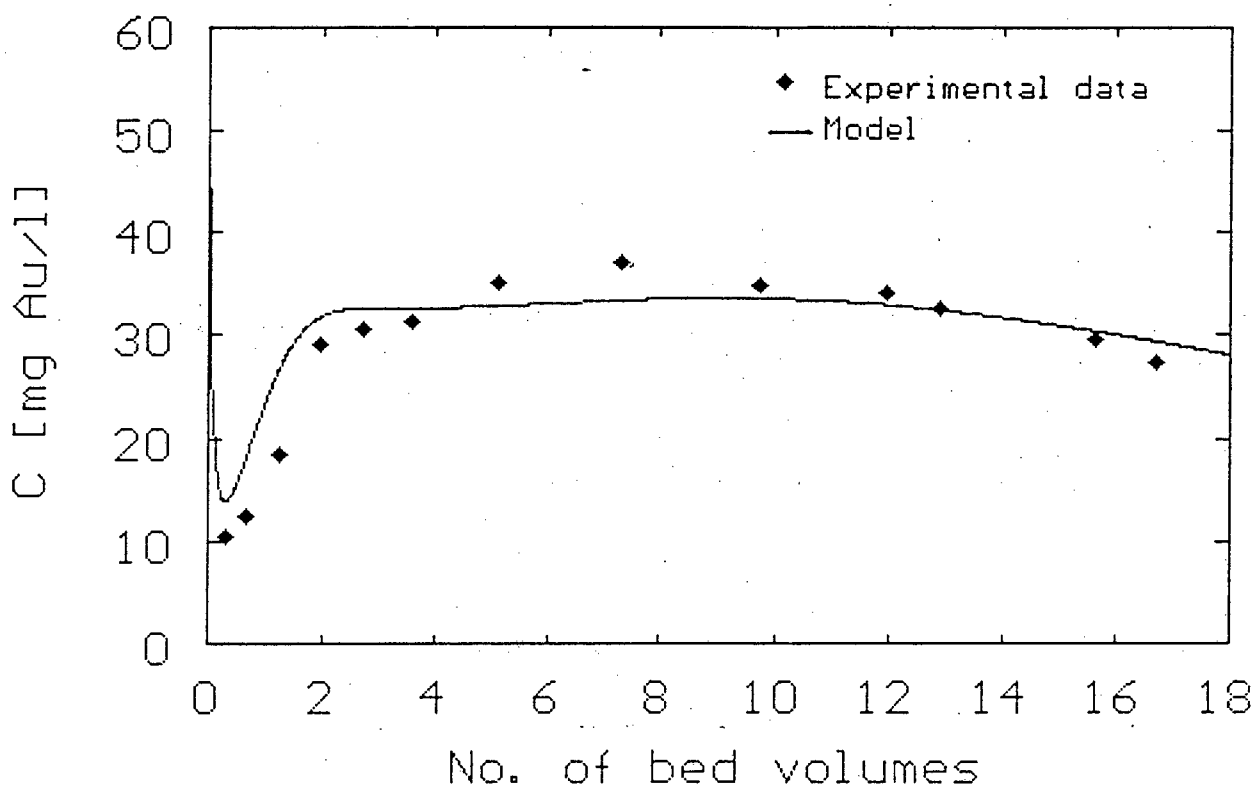


Figure 7.29 Simulation of an AARL elution with the equilibrium model.
Pretreatment with 4 g KCN/l at 20 °C. (Exp.90)

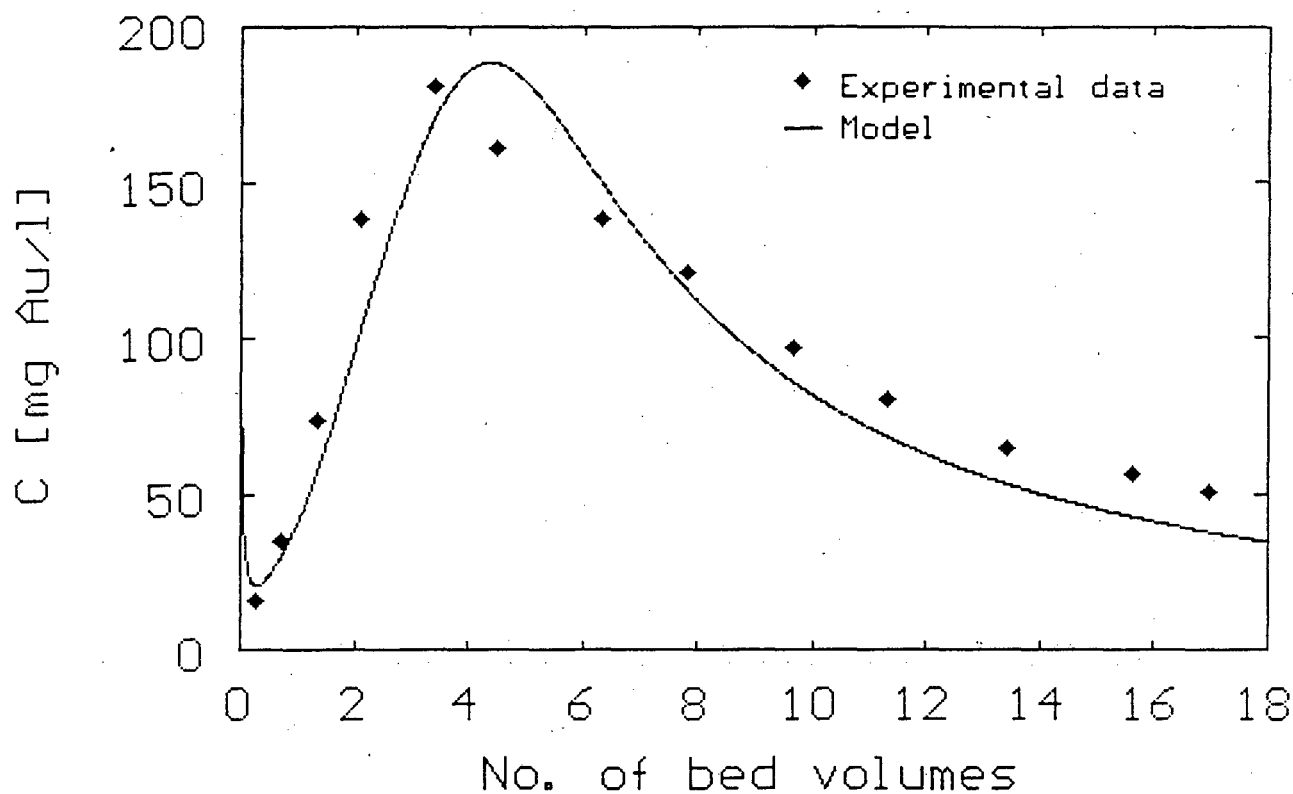


Figure 7.30 Simulation of an AARL elution with the equilibrium model. Pretreatment with 20 g KCN/l at 100 °C. (Exp.64)

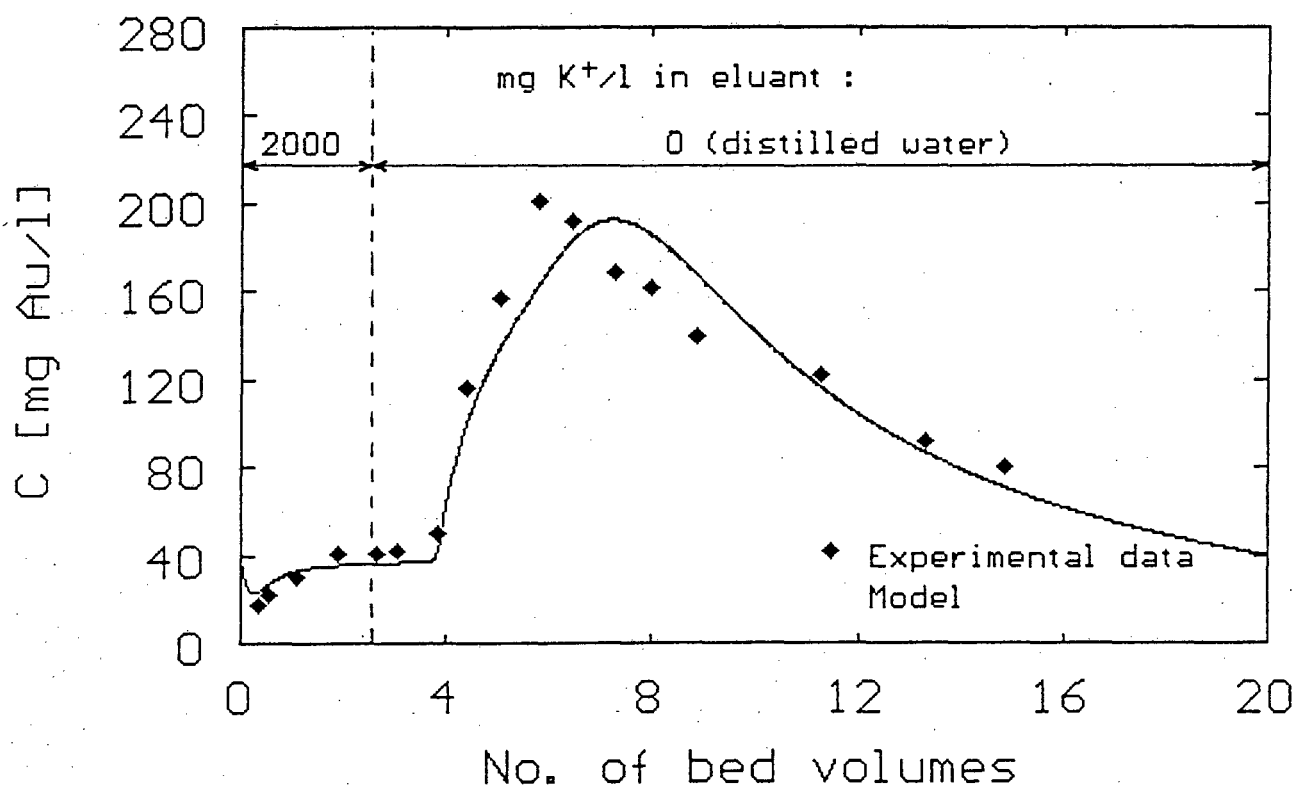


Figure 7.31 Simulation of an AARL elution with the equilibrium model. Step change in potassium concentration in eluant. (Exp.53)

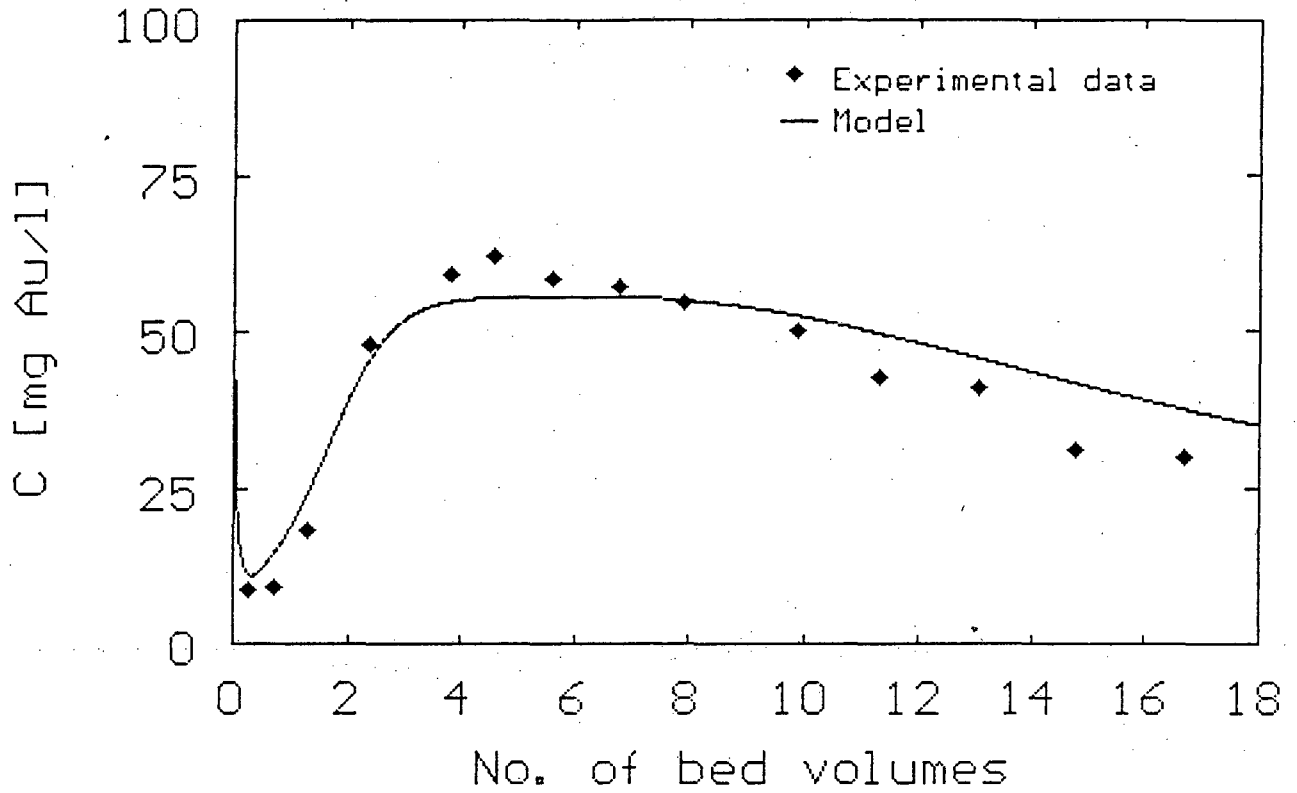


Figure 7.32 Simulation of an AARL elution at 50 °C with the equilibrium model. (Exp.91)

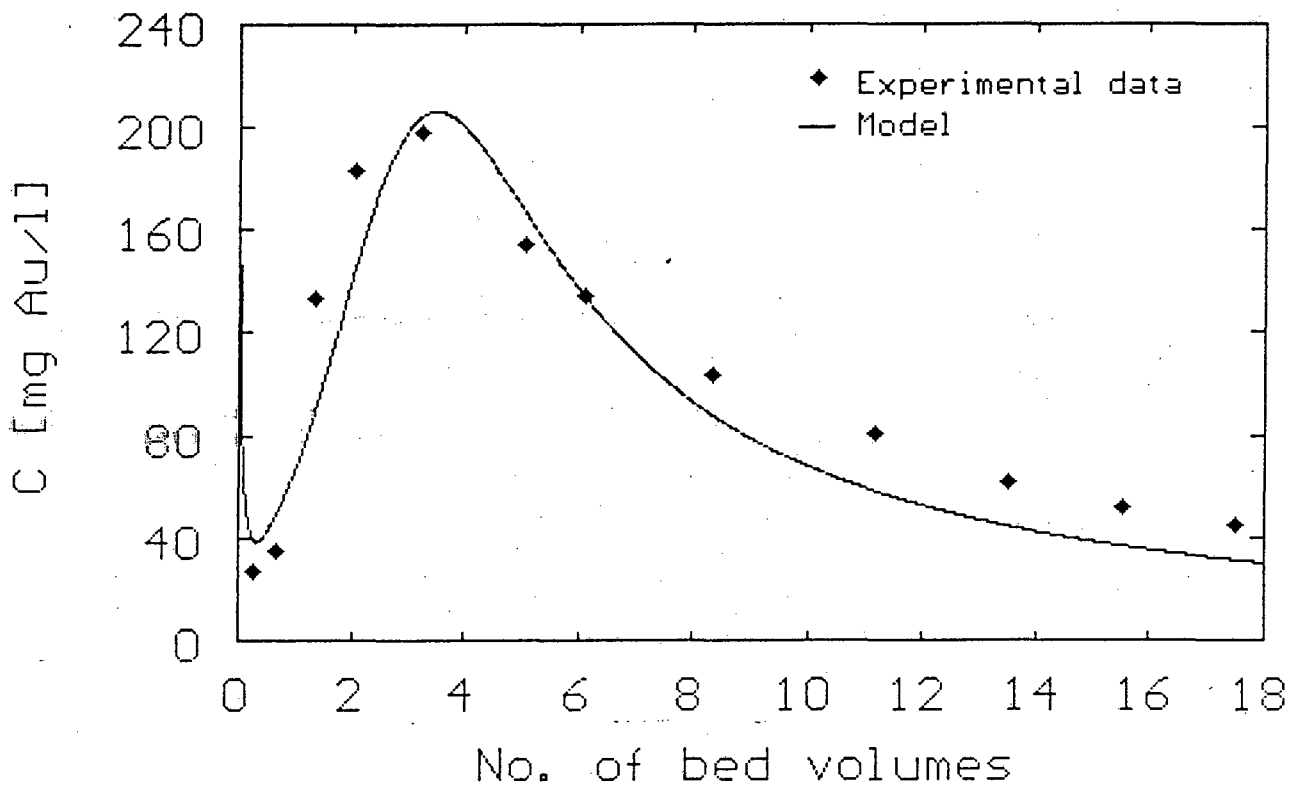


Figure 7.33 Simulation of an AARL elution at 80 °C with the equilibrium model. (Exp.92)

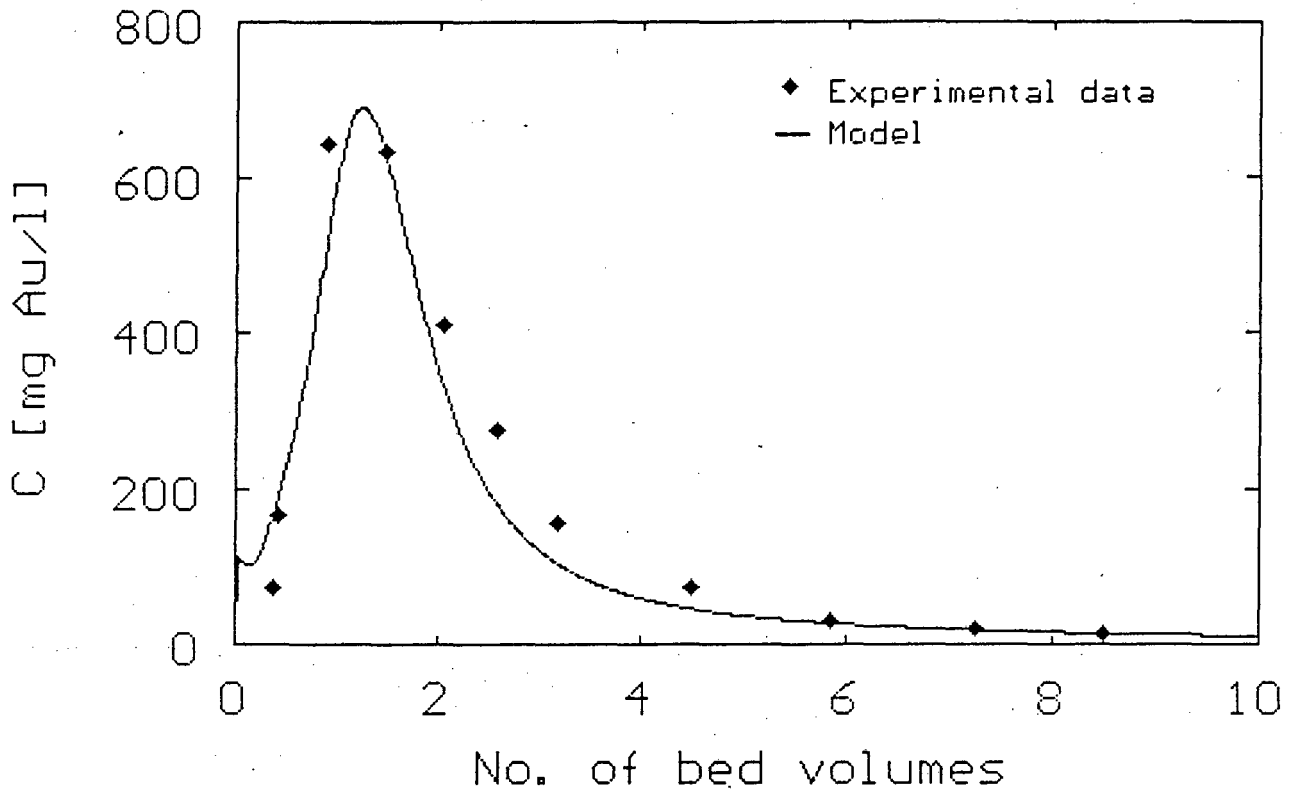


Figure 7.34 Simulation of an AARL elution in the stainless steel column at 130 °C with the equilibrium model. (Exp.93)

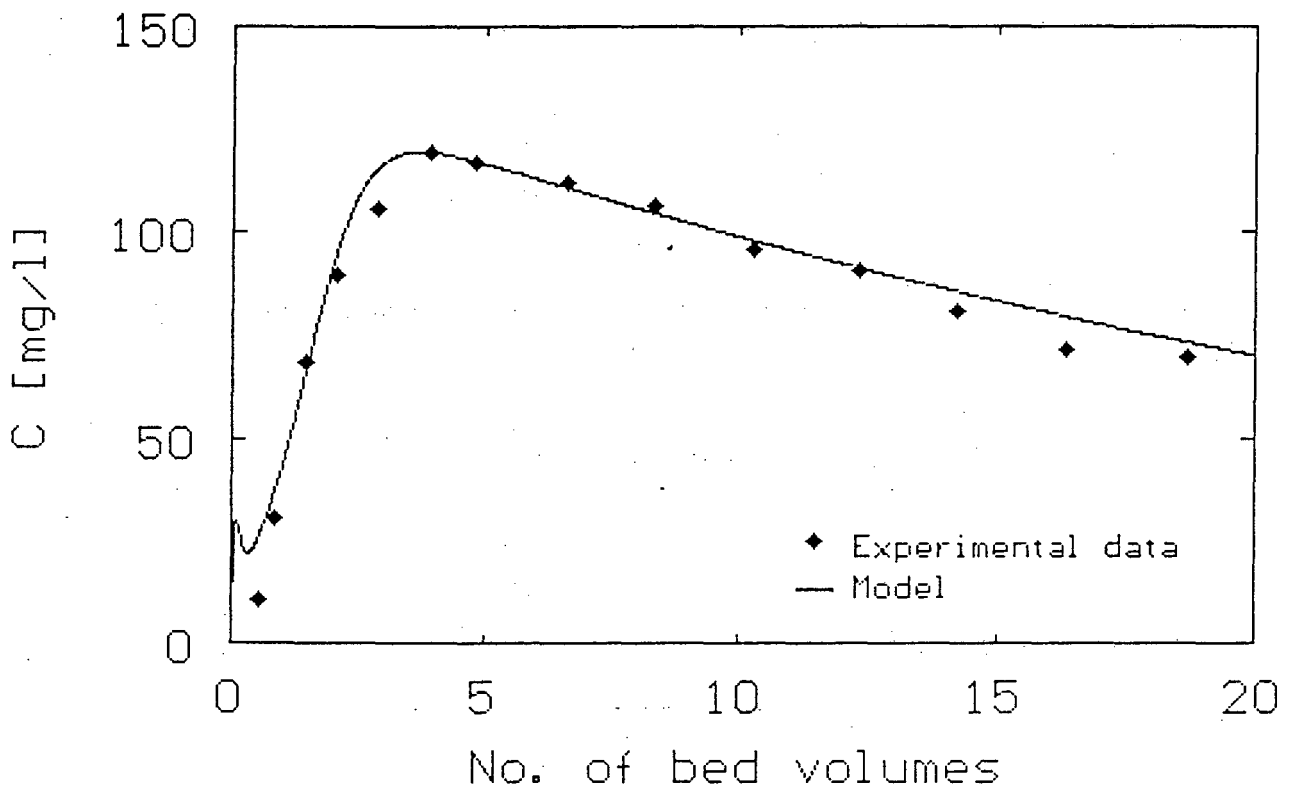


Figure 7.35 Simulation of an AARL elution at 20 °C with the surface diffusion model. (Exp.94)

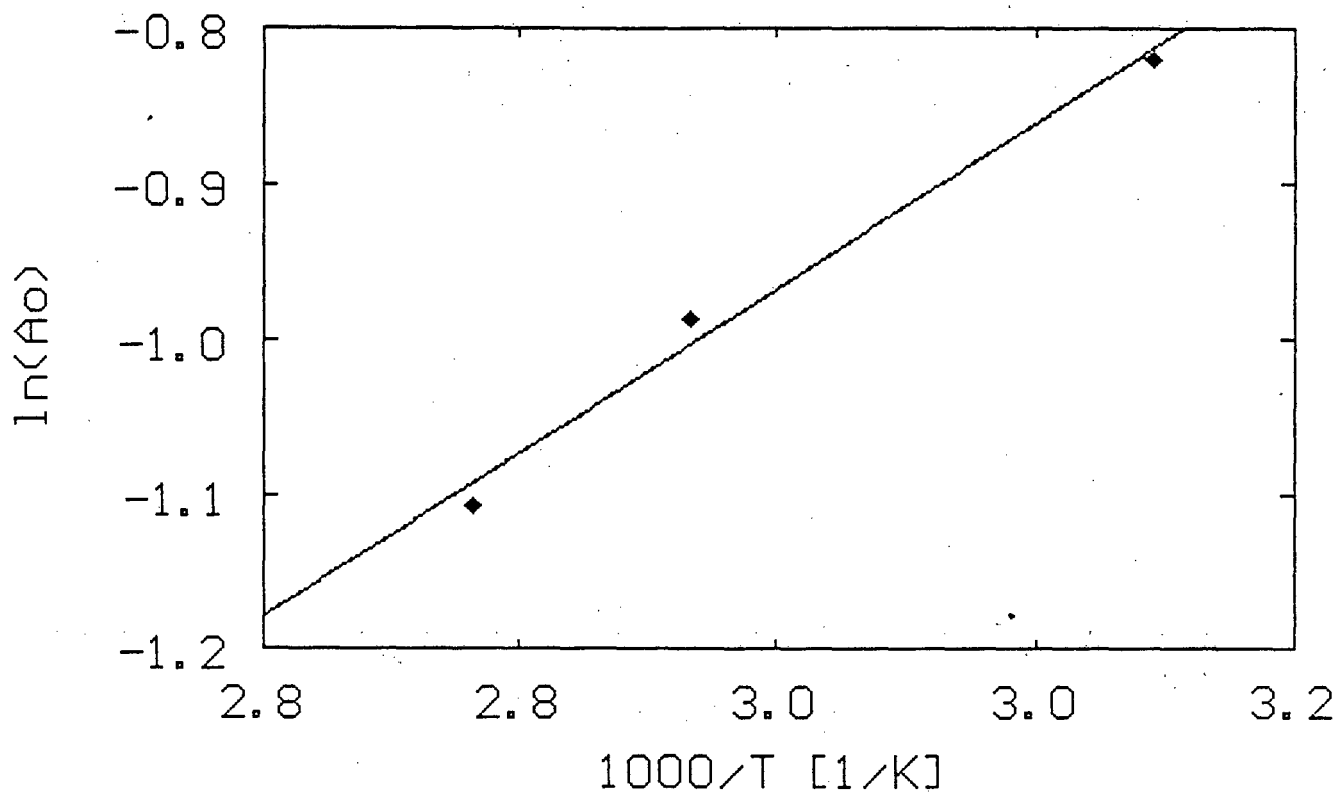


Figure 7.36 Quantification of the effect of temperature on the gold elution equilibrium after a cyanide pretreatment as done in Exp.50, 91 and 92.

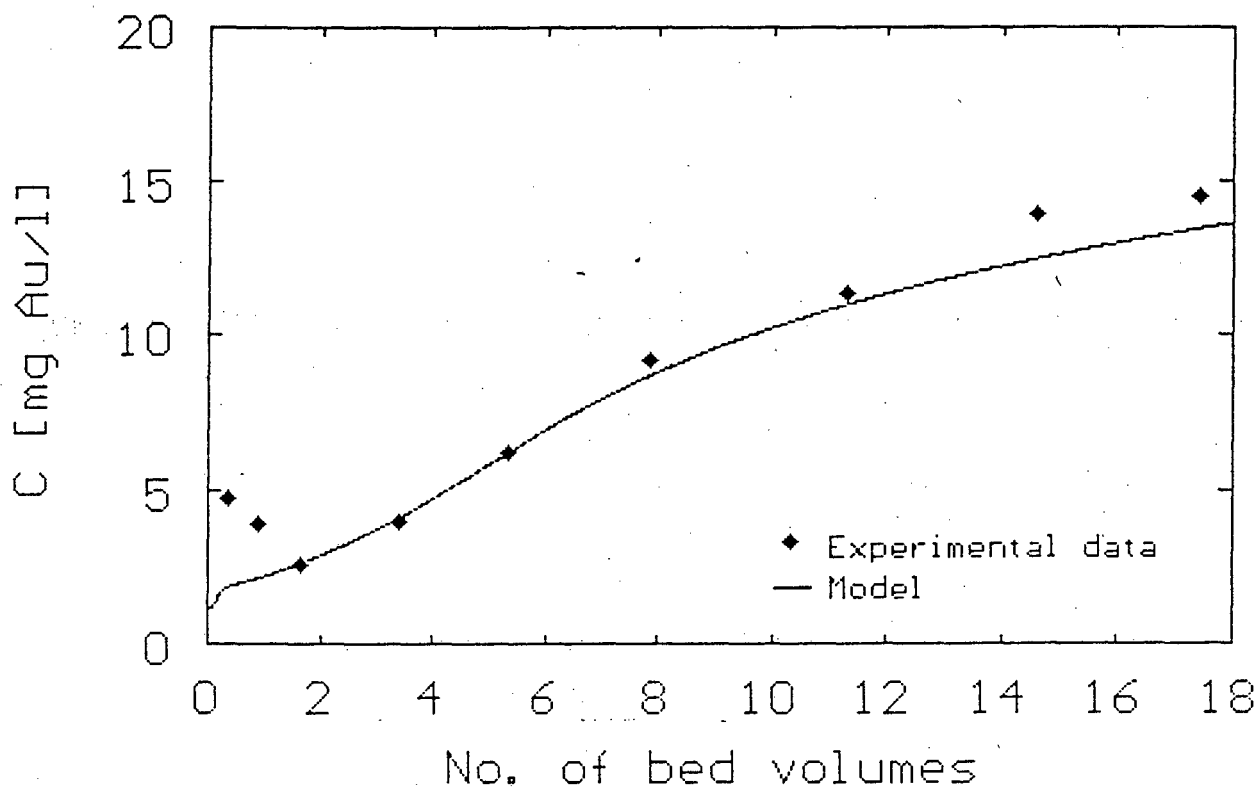


Figure 7.37 Simulation of a Zadra elution with the equilibrium model. (Exp.69)

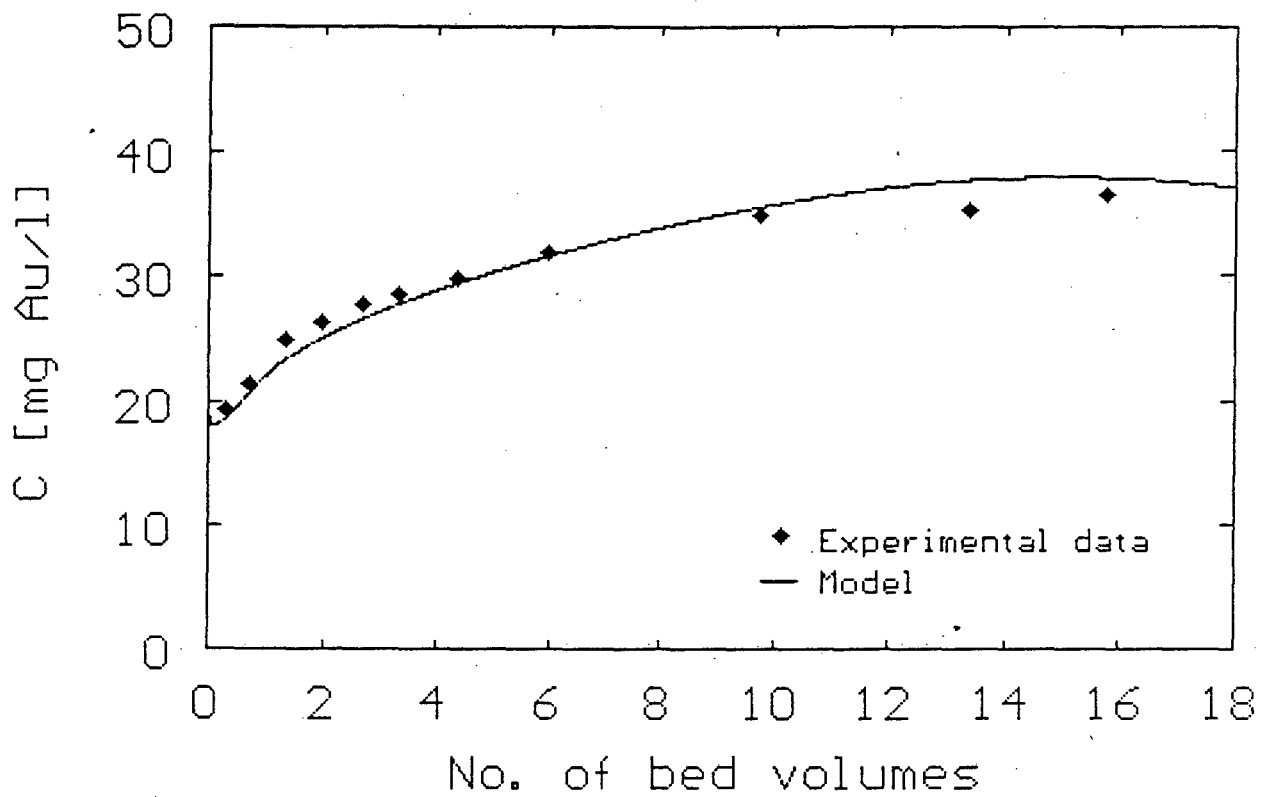


Figure 7.38 Equilibrium model simulation of a Zadra elution with a pretreatment. (Exp.74)

8

SENSITIVITY ANALYSIS

This chapter contains simulations with the surface diffusion and equilibrium models derived in Chapter 6. The sensitivity of these models towards changes in kinetic and equilibrium parameters as well as operating conditions were investigated. A section on reactor configuration was included to illustrate the applicability of the models to reactors other than the batch column operation.

It was illustrated in Chapter 7 that the equilibrium model is only a simplification of the surface diffusion model. These two models will therefore react similarly to changes in equilibrium conditions. For this reason most of the runs in this chapter were conducted with the equilibrium model only. A sensitivity analysis of the surface diffusion model towards changes in diffusion parameters was included in the section on carbon properties.

Unless otherwise specified, the following "Standard" set of conditions and parameters was used in the sensitivity analyses of the surface diffusion and equilibrium models :

Column :	$h = 0.143 \text{ m}$
	$a = 0.00012 \text{ m}^2$
Integration constants :	$N = 10$
	$\Delta t = 10 \text{ s}$
Flow rate :	$V = 1.192 \times 10^{-8} \text{ m}^3 \cdot \text{s}^{-1}$
Carbon properties :	$\epsilon = 0.292$
	$d_c = 0.00142 \text{ m}$
	$\rho = 838.8 \text{ kg} \cdot \text{m}^{-3}$
	$V_p = 0.000634 \text{ m}^3 \cdot \text{kg}^{-1}$
Gold concentrations :	$C_{GF} = 0 \text{ kg} \cdot \text{m}^{-3}$
	$Q_{Gi} = 4 \text{ g} \cdot \text{kg}^{-1}$

Gold equilibrium parameters :	$A_o = 0.3$
	$p = 0.2$
	$q = 0$
	$b = -0.002688$
	$B = 0.2902$
Potassium concentrations :	$C_{Kpi} = 14000 \text{ g.m}^{-3}$
	$C_{Kdi} = 7000 \text{ g.m}^{-3}$
	$C_{KF} = 0 \text{ g.m}^{-3}$
Potassium kinetic parameters :	$X_m = 0.05$
	$X_b = 0.025$
	$\alpha_K = 0.57$

The following additional parameters were applicable to the surface diffusion model only :

$$m_{mb} = 0.5$$

$$\alpha_G = 0.4$$

$$k_s = 1.0 \times 10^{-5} \text{ m.s}^{-1}$$

$$\Gamma_m = 5.0 \times 10^{-11} \text{ m}^2.\text{s}^{-1}$$

$$k_b = 5.0 \times 10^{-5} \text{ s}^{-1}$$

In cases where the sensitivity of the gold elution model had to be tested with a constant equilibrium isotherm, the potassium concentration was assumed to remain constant at 50 g.m^{-3} , i.e. :

$$C_{Kpi} = C_{Kdi} = C_{KF} = 50 \text{ g.m}^{-3}$$

8.1 NUMERICAL INTEGRATION CONSTANTS

Table 8.1 shows the effect of the time step length on the mass balance of gold with the equilibrium model. Even with a $\Delta t = 120 \text{ s}$, the model was still stable and resulted in a mass balance error of only 0.5 %. Little or no difference could be observed in the gold elution profiles calculated with the time step lengths in Table 8.1.

As discussed in Chapter 6, the elution column was modelled as a series of N perfectly mixed CSTR's. A value of $N = 1$ therefore represents a CSTR and a value of $N = \infty$ a plug flow reactor. Values of N between these two extremes describe the reaction kinetics of a non-ideal flow reactor which increasingly deviates from plug flow with a reduction in the value of N (Levenspiel, 1972). The effect of the number of height increments on the gold elution profile is shown in Figure 8.1. A constant concentration of potassium was used to exclude the effect of changes in the potassium profile on the gold equilibrium with a change in N . All the simulations in Chapter 7 were conducted with a value of $N = 10$ and this proved to give satisfactory results. It would be possible to describe deviations from plug flow caused by back-mixing by further decreasing the number of height increments.

It took 3.5 min. with an XT type personal computer, fitted with a math co-processor, to solve the equilibrium model in Appendix I for an elution run of 8 hours with $\Delta t = 30$ s and $N = 10$. The same run took 50 min. with $\Delta t = 10$ s and $N = 50$. Although the computing time can be reduced substantially with the use of the more powerful 386 and 486 PC's now available, the large increase in computing time with smaller time and height increments did not justify the small advantage to be gained by increasing the value of N .

8.2 COLUMN GEOMETRY

In the derivation of the nonideal flow model for the elution of the potassium, as well as the two models for the elution of gold cyanide, the elution column was considered as a series of perfectly mixed CSTR's. All of these models are therefore insensitive to the h/d ratio of the carbon bed, provided that the total bed volume stays constant and that the same number of height increments (or CSTR's) is used. (This finding is not presented graphically, but it was confirmed that there is no difference in the profiles calculated with different h/d ratios.) This is in agreement with the findings in Chapter 3 (Figure 3.20) and Chapter 5 (Figure 5.12) where it was shown that the elution of gold and potassium is unaffected by the geometry of the column.

However, Figures 8.2 and 8.3 show that the potassium and gold profiles are sensitive to the h/d ratio if Δh is kept the same for the different runs. This can be attributed to the change in the number of height increments ($N = h/\Delta h$) with a change in h . The differences in the curves in Figures 8.2 and 8.3 are therefore not caused by varying h/d for the same column volume, but by changing the value of N by keeping Δh constant.

8.3 AUROCYANIDE EQUILIBRIUM

The large sensitivity of the gold elution profile to the equilibrium constant A_0 is illustrated in Figure 8.4. A change in the value of A_0 represents a constant shift in the equilibrium over the whole run. Such a shift can be accomplished by performing elutions at different temperatures, with different modes of pretreatment, or by the addition of organic solvents to the eluant.

Figures 8.5 and 8.6 contain runs at different values of b and B which are parameters in the linear relationship of n with A as shown in Chapter 3 (Equation 3.2) :

$$n = b.A + B \quad [8.1]$$

It follows from Figure 8.5 that, because of the small value of b , the elution profile is relatively insensitive to b for $|b| < 0.01$. However, the value of B has an effect on the height of the gold elution profile similar to that of A_0 (see Figures 8.4 and 8.6).

Figure 8.7 and 8.8 show respectively the effect of varying the values of p , the gold equilibrium dependency on the potassium concentration, and q , the extent to which reactivation of the carbon occurs. It can be seen that the value of q affects only the height of the elution peak, whereas a change in p results in a vertical as well as a horizontal shift in the elution profile. Although the functions describing the effects of p and q in the general equilibrium isotherm (Equation 7.6) are basically the same, the difference in behaviour of the model towards changes in p and q

is ascribed to the difference in the functions describing the change in potassium concentration, C_K , and bed volumes, V_B , with time.

8.4 OPERATING VARIABLES

As discussed in the previous section, changes in operating temperature, pretreatment conditions or organic solvent concentration will result in a singular, constant shift in the equilibrium. Such a shift can be accounted for by changing the value of A_0 as shown in Figure 8.4.

The equilibrium model for the elution of gold cyanide is independent of flow rate if the results are plotted as a function of the volumetric throughput of eluant. The profiles in Figure 8.9, at different volumetric flow rates, are however plotted as a function of time. It can be seen that the heights of the profiles are exactly the same, except that, at lower flow rates, the profiles are more stretched out in the horizontal direction. A shorter time step length of 15 seconds was used for the simulations in Figure 8.9 to assist in the solution of the model at increased rates of change when using higher flow rates.

Figure 8.10 shows the sensitivity of the potassium elution profile to the initial concentration of potassium in the pores of the carbon. The strong effect of these different potassium profiles on the gold elution profile is illustrated in Figure 8.11. However, from Figure 8.12 it follows that the initial concentration of potassium in the interparticle solution has little effect on the gold elution profile. This can be attributed to the relative ease with which the potassium in the interparticle solution is eluted in comparison to the potassium in the intraparticle solution. A slightly higher gold elution peak was obtained with the highest initial concentration of potassium, because of the higher suppression of the desorption of the gold during the initial stages of the elution (Figure 8.12).

The effect of a constant concentration of potassium in the eluant was investigated in Figure 8.13. It can be seen that a potassium concentration as low as 200 g.m^{-3} resulted in a gold profile with a peak of nearly half the height of that for distilled water. The profiles in

Figure 8.13 are also an indication of the effect of water quality on an AARL elution.

Adams and Nicol (1986) showed that the rate of elution reached a maximum with an increase in the concentration of NaCN added to a Zadra elution. This was attributed to the increased ionic strength of the solution. Figure 8.14 shows the Zadra elution profiles predicted with the equilibrium model for KCN concentrations of 1, 5, 10 and 20 g KCN/l. Because of the low sensitivity to the potassium concentration ($p = 0.088$), the elution efficiency increased with an increase in the KCN concentration. If the gold cyanide equilibrium were however more sensitive to the cation concentration, as in Figure 8.15, a similar result to that of Adams and Nicol (1986) was obtained during the initial stages of the elution. This shows that it is difficult to state *a priori* what the effect of [KCN] would be during a Zadra elution.

If the eluate is recycled, as in the case of a Zadra elution or where the "tail" of an AARL elution is recycled (Laxen *et al.*, 1982), the eluant might contain a low concentration of gold cyanide. Because of the large difference in the concentration of gold cyanide in the eluant (typically $< 10 \text{ g Au/m}^3$) and the concentration of gold cyanide in the eluate (typically $> 200 \text{ g/m}^3$), these low concentrations of gold in the feed solution have no effect on the elution profile. Such a constant supply of gold cyanide may, however, affect the eluted carbon loading. This is shown in Figure 8.16 where the gold loading in the first section of the bed (i.e. at the inlet) was plotted as a function of the number of bed volumes of eluant passed through the bed. It can be seen that the sensitivity of the eluted carbon loading to gold in the eluant increased with a decrease in the loading on the carbon towards the end of the elution.

8.5 CARBON PROPERTIES

It was shown in Chapter 7 that both the equilibrium and surface diffusion models are highly sensitive to the initial gold loading on the carbon. This can be seen from Figure 8.17 and by rearranging the equilibrium

expression, Equation 3.3, to give :

$$C_e \approx (Q_e/A)^{3.4} \quad [8.2]$$

It follows from Equation 8.2 that the gold elution profile would be equally sensitive to changes in Q_e than to A and that a 10% change in either of these values results in a change in the value of C_e of between 28% and 43%.

With the surface diffusion model the elution profile is not only sensitive to the initial gold loading, but also to the distribution thereof between the macropores and the micropores. This is demonstrated in Figure 8.18 where values of m_{mb} of 0.3 to 0.7 were used. As expected, the lower values of m_{mb} (i.e. higher loadings of gold in the macropores) resulted in higher initial elution rates. Maximum elution rates would therefore be obtained from carbon that was loaded for short periods from solutions with high gold concentrations.

The equilibrium model is insensitive to changes in the value of the mean carbon particle diameter. The particle size will determine, however, the value of ϵ , the void fraction of the carbon bed. The sensitivity of the equilibrium model to the void fraction of the bed is shown in Figure 8.19.

Figure 8.20 shows that the model used for the elution of the potassium is strongly dependent on the pore volume of the carbon. This is because of the assumption that all the potassium brought over from the pretreatment step is contained in the pore liquid. A variation in the value of the pore liquid therefore results in a change in the initial mass of potassium available for elution.

Because of the sensitivity of the potassium profile for V_p , the effect of the pore volume on the gold elution curve was investigated in Figure 8.21 at a constant concentration of potassium. The value of V_p had the largest effect during the first few bed volumes where an increase in the pore volume resulted in a decrease in the maximum gold concentration. This is attributed to the dilution effect that the pore liquid has on the total volume of liquid in the carbon bed.

The simulations in Figures 8.22 to 8.25 show the sensitivity of the surface diffusion model to the values of the kinetic parameters α_G , k_s , Γ_m and k_b .

It follows from Figure 8.22 that the gold cyanide loaded on a carbon with a large fraction of macropores will be more accessible to elution than would be the case for a carbon with a small value of α_G . This is similar to the results obtained for adsorption (Van Deventer, 1984) where it was shown that a large value of α_G led to faster adsorption kinetics.

The sensitivity of the surface diffusion model for the film transfer coefficient, k_s , was investigated in Figure 8.23. It can be seen that better elution is obtained at higher values of k_s and that film transfer becomes non-controlling at values of k_s higher than $1 \times 10^{-5} \text{ m.s}^{-1}$.

Figure 8.24 explores the effect of varying the value of the combined macropore diffusion coefficient. As Γ_m directly controls the kinetics of the mass transfer through the macropores to the carbon surface, the drastic effect on the elution profile in Figure 8.24 was not unexpected. The profile obtained with $\Gamma_m = 1 \times 10^{-12} \text{ m}^2.\text{s}^{-1}$ again illustrates the need for higher values of the macropore mass transfer coefficient in modelling the elution process.

It was expected that an increase in the value of k_b would, as for Γ_m , result in a higher elution rate. Figure 8.25 indicates that this is, however, not true. Because of the higher initial loading of gold in the macropores than in the micropores, an increase in the value of k_b increased the transfer of gold from the macropores to the micropores. This decreased the value of Q_m and therefore also the values of Q_s and C_s , and eventually the value of the interparticle gold concentration.

If the value of k_b is however further increased, the transfer between the macropores and the micropores becomes so fast that the model eventually approaches a model for particles containing only one type of pore. By also increasing the values of the film transfer and macropore transfer coefficients, the resistance to mass transfer can be decreased to a point where the surface diffusion model matches the equilibrium model as in

Figure 8.26. The following parameters were used in Figure 8.26 which differ from those specified above :

$$N = 1$$

$$\Delta t = 1 \text{ s}$$

$$k_s = 1.0 \times 10^{-5} \text{ m} \cdot \text{s}^{-1}$$

$$\Gamma_m = 1.0 \times 10^{-9} \text{ m}^2 \cdot \text{s}^{-1}$$

$$k_b = 1.0 \times 10^{-2} \text{ s}^{-1}$$

The small incremental time step had to be used to avoid instabilities in the surface diffusion model with these high transfer coefficients. To reduce the computing time, the elution was assumed to occur in a CSTR, (i.e. $N = 1$).

8.6 REACTOR CONFIGURATION

8.6.1 Continuous Stirred Tank reactor

Figures 8.27 and 8.28 compare the potassium and gold cyanide profiles obtained with the equilibrium model for a column, a CSTR with the same volume as one bed volume of the column, and a CSTR holding 10 times that volume. The elution profiles with the column are off-scale in both figures, but these profiles have been calculated with the standard set of parameters and are shown in previous figures. It follows from Figure 8.27 that the potassium profile gets flatter with an increase in the volume of the CSTR and that less potassium is removed in the initial stages of the elution than in the case of a column. The more consistent presence of potassium in the larger CSTR resulted in the corresponding gold elution profile in Figure 8.28 approaching an elution profile with a constant equilibrium.

8.6.2 Batch elution in a column

The elution profiles from a batch wise operated column have been shown in numerous figures, including Figure 8.28. Figure 8.29 however displays the gold loading profile in the column at various points of time during a simulation of an elution run with the standard set of parameters. What

is interesting is that the loading in certain sections of the column increased to values higher than the initial loading during the first stages of the elution. This is because of the higher potassium concentrations and therefore higher equilibrium conditions prevailing in the sections further from the inlet during the early phases of the elution.

All of the profiles shown up to here were obtained from experiments or simulations of runs which were started from columns filled with eluant or pretreatment solution. In practice however, the soaking solution is usually drained before the eluant is pumped into the bed. Figures 8.30 and 8.31 compare the potassium and gold cyanide profiles from full and drained beds. The drained bed was assumed to contain a volume of retained liquid equal to the sum of the pore volume of the carbon plus 10% of the void volume ($s = 0.1$). Figure 8.30 shows that a lower maximum concentration of potassium is predicted for the drained bed, because of the dilution of the interparticle solution with the eluant. Except for the maximum concentrations, the difference between the profiles is negligible. These similar potassium profiles resulted in nearly identical gold elution profiles from the drained and full carbon beds in Figure 8.31. It is clear from Figure 8.31 that draining of the pretreatment solution has little effect on the gold elution profile and that a drained bed can therefore be simulated without accounting for the initial filling of the bed with eluant.

8.6.3 Continuous counter-current elution

Figure 8.32 contains a simulated gold elution profile for a continuous counter-current elution process as shown in Figure 6.1. It can be seen that the first 5 hours of the elution was kept identical to a "normal" AARL elution. The step changes in the gold concentration from 5 hours onwards represent the transfer of carbon. The average gold loading on the carbon in the bottom N_d sections of the column is plotted in Figure 8.33. The minimum loading before each peak is equal to the average gold loading on the eluted carbon which is removed from the column. As discussed before, an initial elution period was allowed before the first transfer of carbon in order to reach an acceptably low loading on the eluted carbon. Figure 8.34 shows the potassium profile during the gold

elution presented in Figures 8.32 and 8.33. The parameters used for the simulations in Figures 8.32 to 8.34 were taken as the "standard" for the sensitivity analysis of the counter-current process. The same values were used as for the batch process, except for the following changes and additions :

$N = 20$ (total number of height sections)
 $N_t = 4 \text{ h}^{-1}$ (frequency of carbon transfers)
 $N_d = 1$ (number of height sections discharged per transfer)
 $Q_{Gi} = 2 \text{ g.kg}^{-1}$
 $A_o = 0.15$

The effect of the frequency with which carbon is extracted from the column, N_t , was investigated in Figures 8.35 and 8.36. The same mass flow rate of carbon as above could be maintained by transferring larger amounts of carbon less frequently. N_t and N_d were changed to :

$N_t = 1 \text{ h}^{-1}$ and
 $N_d = 4$.

This led to a larger fluctuation in the gold concentration in the eluate, but affected the eluted carbon value only marginally. Slightly higher average gold loadings, in comparison with the higher transfer frequency, were calculated on the eluted carbon.

Figures 8.37 and 8.38 show the gold concentrations in the eluate and on the eluted carbon for a carbon mass flow rate of twice that of the standard. The same transfer frequency was used, but the fraction of bed removed per transfer was doubled, i.e. :

$N_d = 2$

Because of the reduced residence time of the carbon in the column, the gold loading on the eluted carbon increased by approximately 60%. It can be seen from Figures 8.35 and 8.37 that larger fluctuations of the eluate gold concentration occurred when larger portions of the carbon bed was shifted during carbon transfers. As could be expected, the higher carbon mass flow rate also increased the average gold concentration in the eluate.

The residence time of the carbon at a fixed carbon flow rate can be increased by increasing the volume of the reactor. This was investigated in Figures 8.39 and 8.40 where a column of twice the height of the standard was used by changing the following values :

$$h = 0.286 \text{ m}$$

$$N = 40$$

The carbon mass flow rate and transfer frequency were kept the same as for the standard. The residence time had no effect on the eluted carbon loading, but the gold concentration in the eluate was slightly higher with the larger column. This means that a higher eluate gold concentration can be obtained for a given eluted carbon loading and carbon flow rate by using a larger column.

8.7 SUMMARY

When comparing predictions of both types of gold elution models for columns of different geometry, it is essential that the number of height sections should be the same and not the heights of the incremental sections. The number of height sections should only be varied to account for smaller or larger deviations from plug flow.

A constant shift in the gold cyanide equilibrium, as would be caused by different operating temperatures or pretreatment conditions, affected mainly the peak height of the gold elution profile. Changes in the sensitivity (p) of the gold equilibrium to the cation concentration, however, resulted in a horizontal as well as a vertical shift in the gold elution profile.

Because of the ease with which the retained liquid in the interparticle solution is washed from the carbon bed, the gold elution profile was found to be much more sensitive to the initial potassium concentration in the intraparticle than the interparticle solution. In a CSTR, however, the solutes in the interparticle solution are not removed as quickly as from a packed bed, and this resulted in flatter cation profiles. As the volume of the CSTR is increased, the change in cation concentration becomes smaller and the gold elution profile approaches a profile with a constant equilibrium isotherm.

An increase in the intraparticle mass transfer coefficients of the surface diffusion model does not necessarily lead to an increase in the kinetics of elution. If the initial gold loading on the carbon is not homogeneously distributed between the macropores and the micropores, an increase in the micro- macro transfer coefficient may result in a lower initial elution rate because of increased diffusion from the macropores to the micropores. A higher initial ratio of gold loaded in the macropores to gold loaded in the micropores, however, leads to a higher rate of elution. Under elution conditions where resistance to mass transfer controls, the rate of elution can therefore be increased by loading of the carbon over short periods of time from solutions with high gold concentrations.

Nearly identical gold elution profiles were obtained for carbon beds that were, and were not, drained of pretreatment solution. The elution of gold from drained carbon beds can thus be approximated adequately with a model that does not contain a filling procedure.

It was found that for a continuous counter-current elution that the frequency of carbon transfer at a constant flow rate of carbon did not affect the gold loading efficiency. However, an increase in the transfer frequency led to less fluctuation of the gold and pretreatment reagent concentrations in the eluate. As expected, a higher flow rate of carbon resulted in higher gold concentrations in the eluate, but also higher eluted carbon gold values. The geometry and size of the elution column had little effect on the elution efficiency and gold concentration in the eluate.

Table 8.1

The effect of Δt on the mass balance of gold cyanide after 15 bed volumes with the equilibrium model and a constant equilibrium.

Δt [s]	10	30	60	120
Au eluted [g]	0.02606	0.02609	0.02613	0.02621
Au remaining [g]	0.01472	0.01472	0.01473	0.01475
Total [g]	0.04078	0.04081	0.04086	0.04095
Initial load [g]	0.04076	0.04076	0.04076	0.04076
% Error	0.049	0.123	0.245	0.466

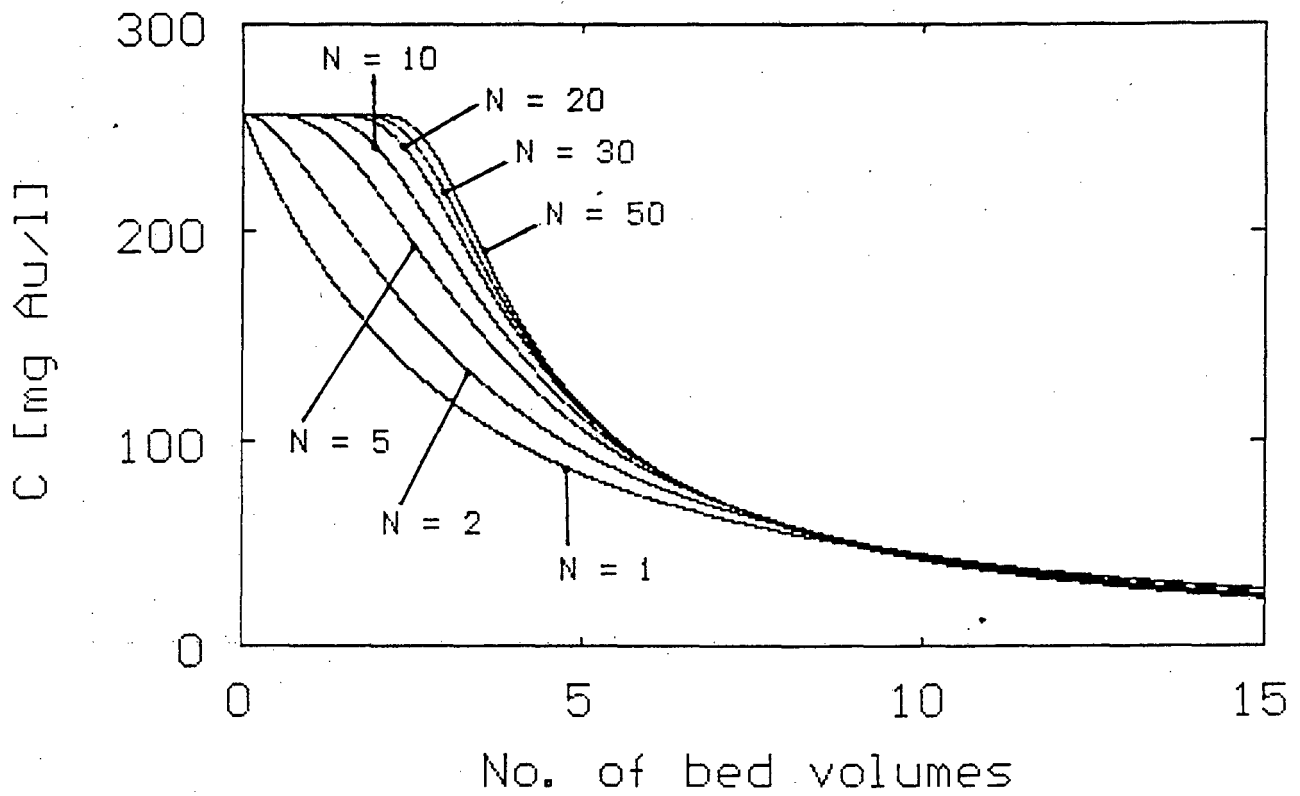


Figure 8.1 Sensitivity of the equilibrium model to changes in the number of height sections in a column operation.

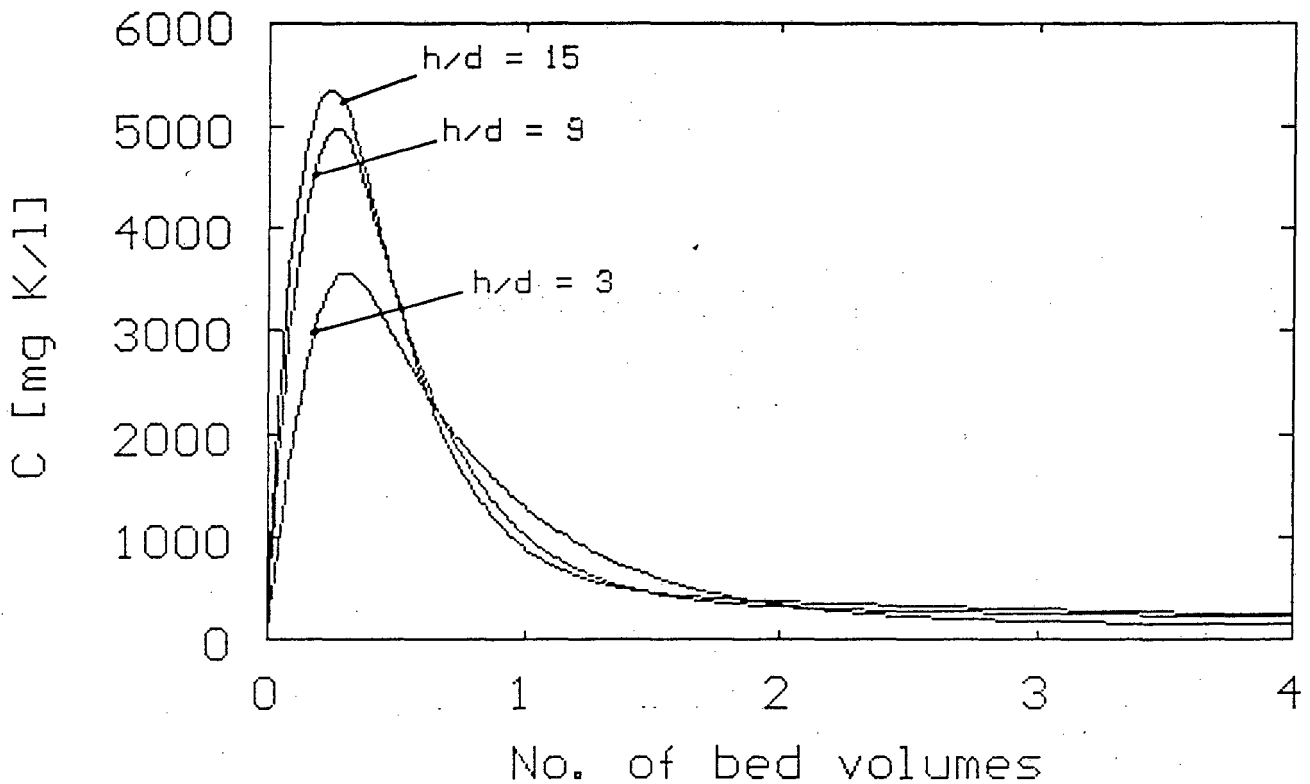


Figure 8.2 Sensitivity of the nonideal flow model for the elution of potassium to column geometry with a constant Δh .

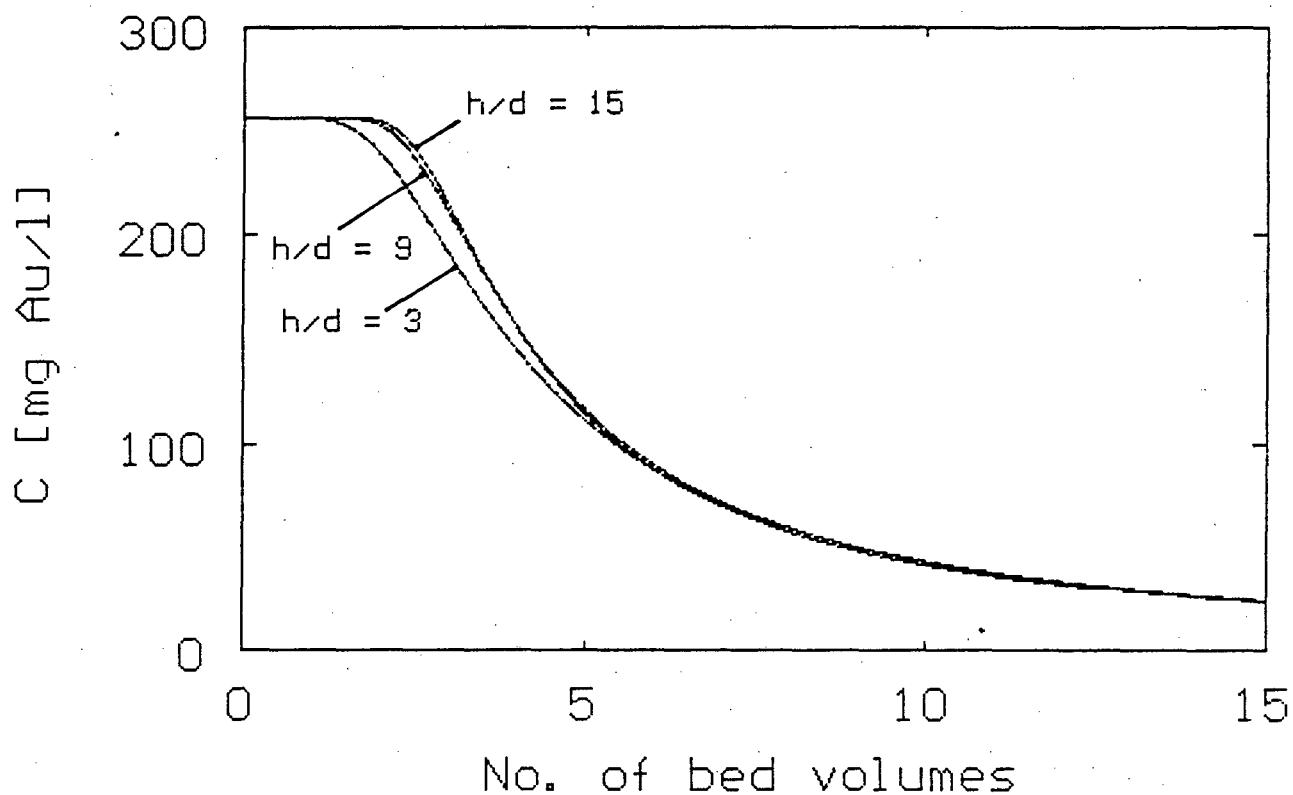


Figure 8.3 Sensitivity of the equilibrium model for the elution of gold cyanide to column geometry with a constant Δh .

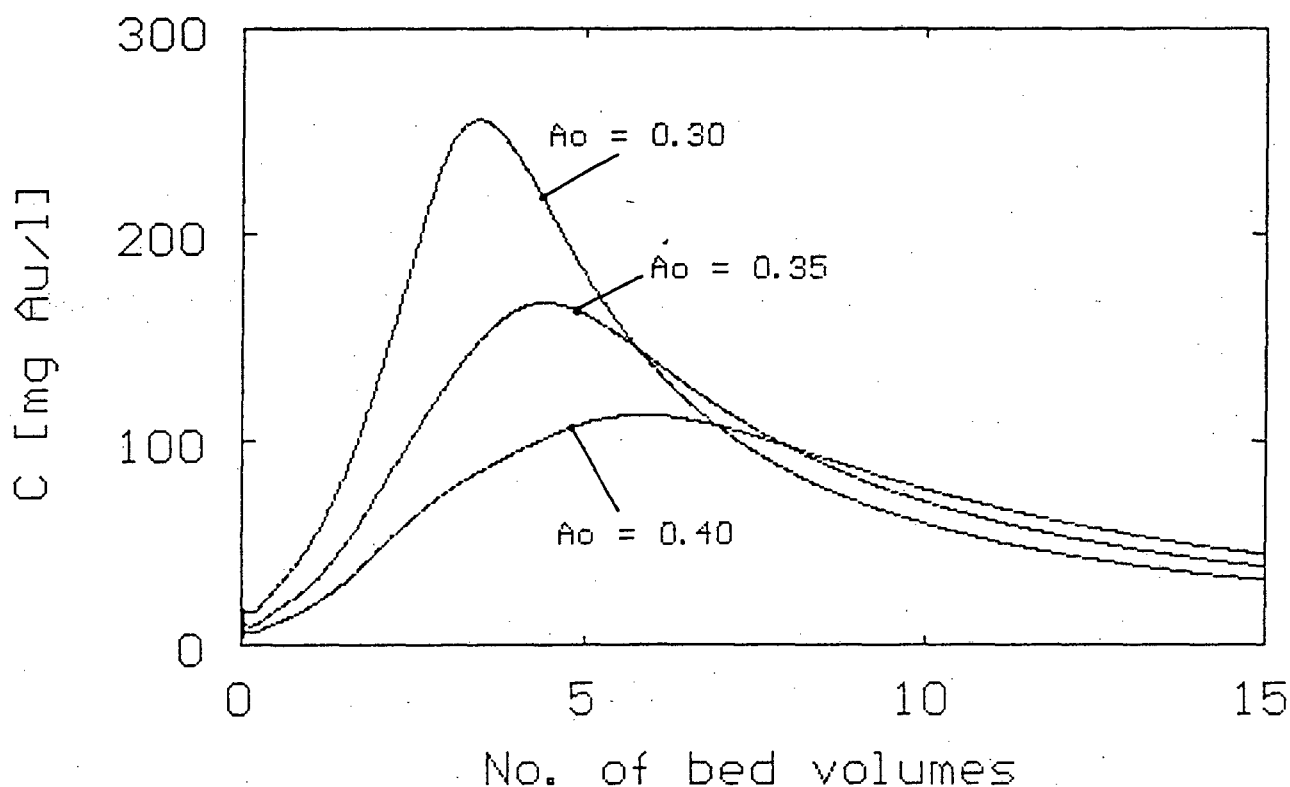


Figure 8.4 Sensitivity of the equilibrium model for the elution of gold cyanide to the equilibrium constant A_0 .

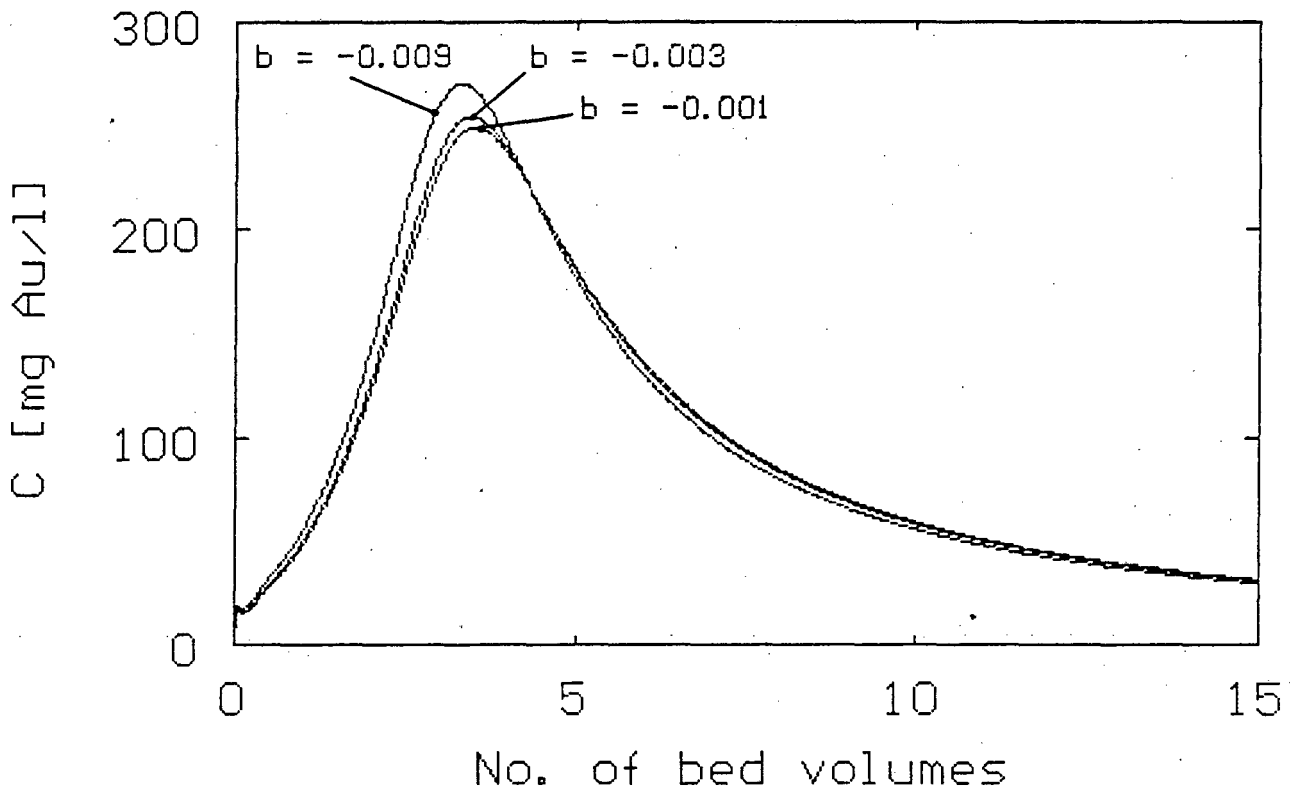


Figure 8.5 Sensitivity of the equilibrium model for the elution of gold cyanide to the equilibrium constant b .

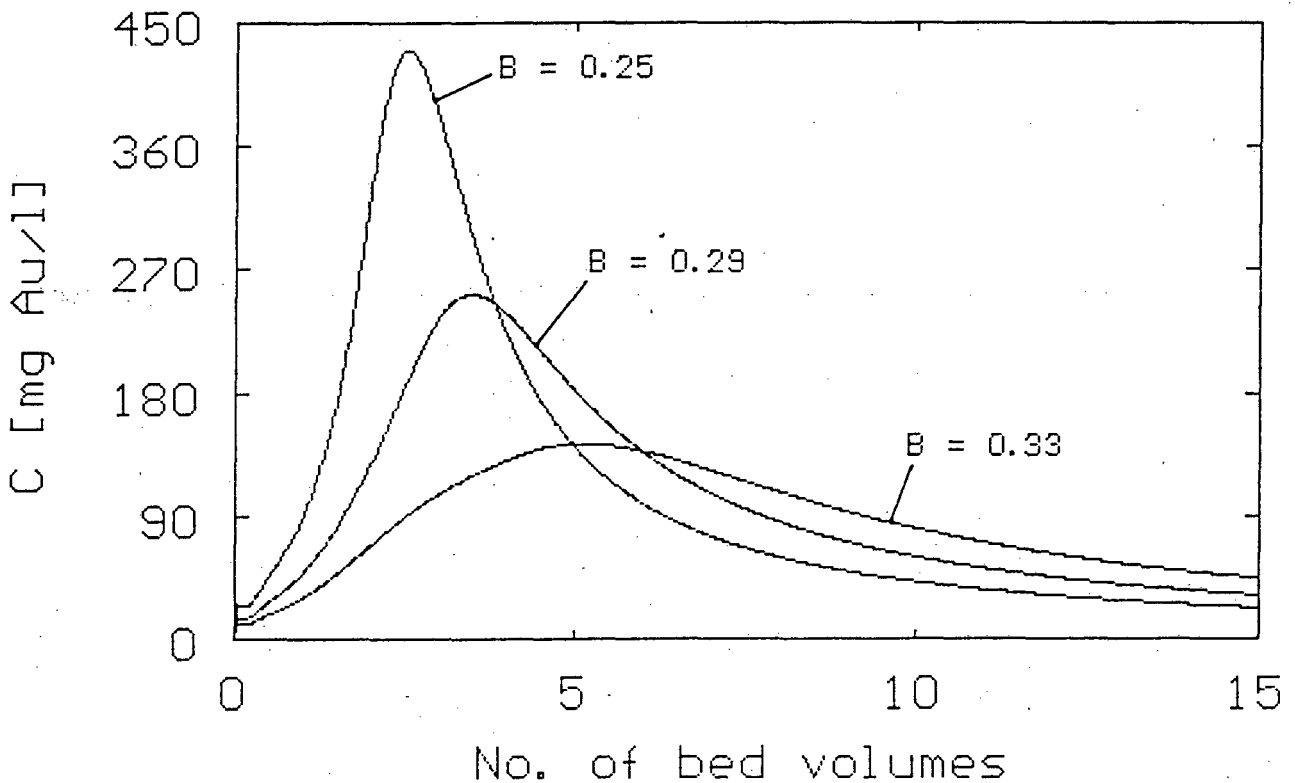


Figure 8.6 Sensitivity of the equilibrium model for the elution of gold cyanide to the equilibrium constant B .

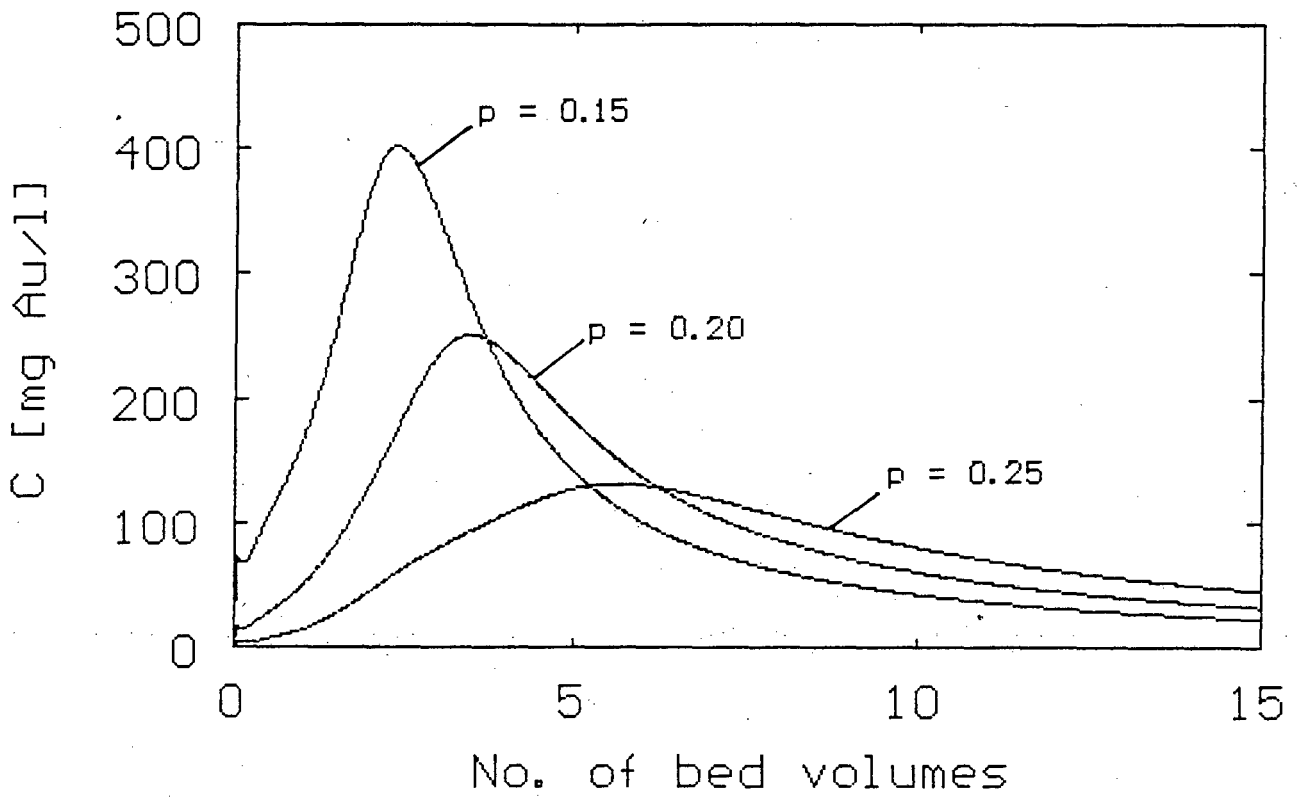


Figure 8.7 Sensitivity of the equilibrium model for the elution of gold cyanide to the equilibrium dependency on the potassium concentration, p .

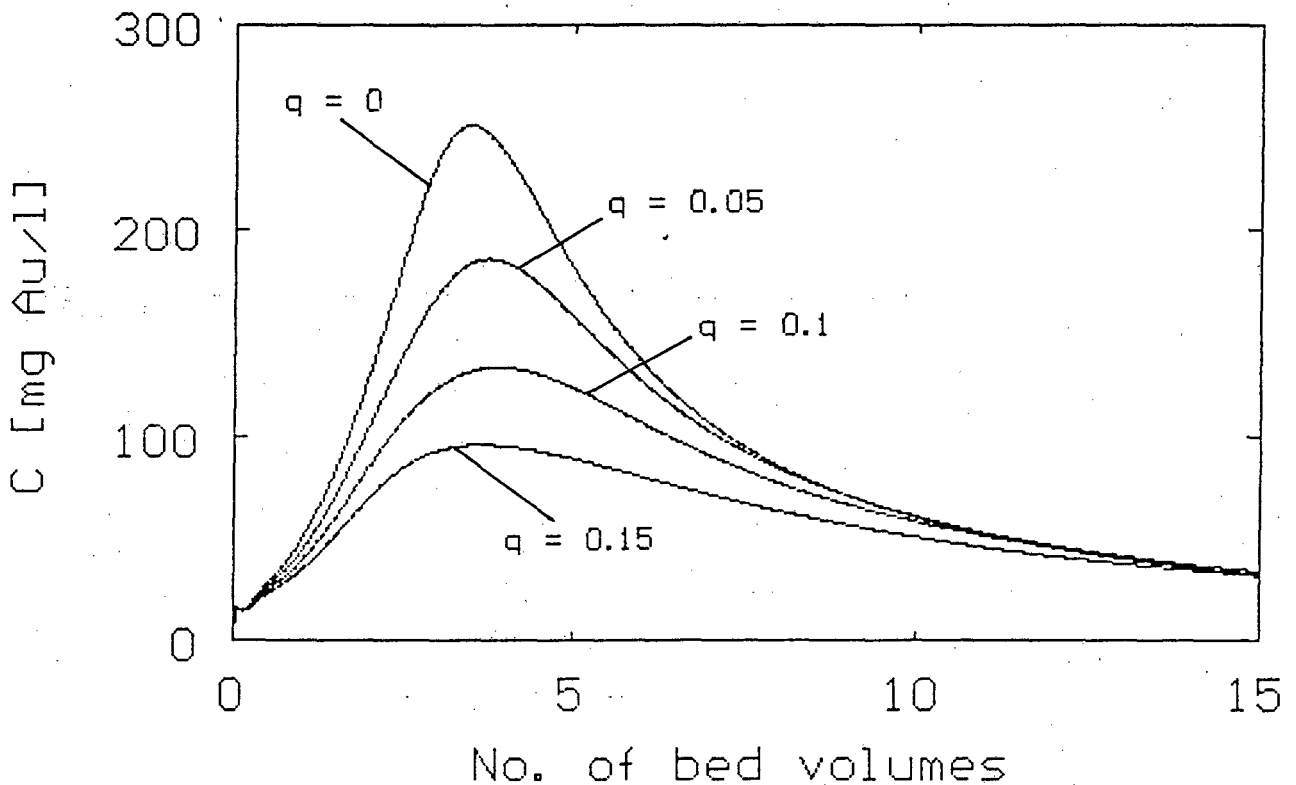


Figure 8.8 Sensitivity of the equilibrium model for the elution of gold cyanide to the extent of reactivation, q .

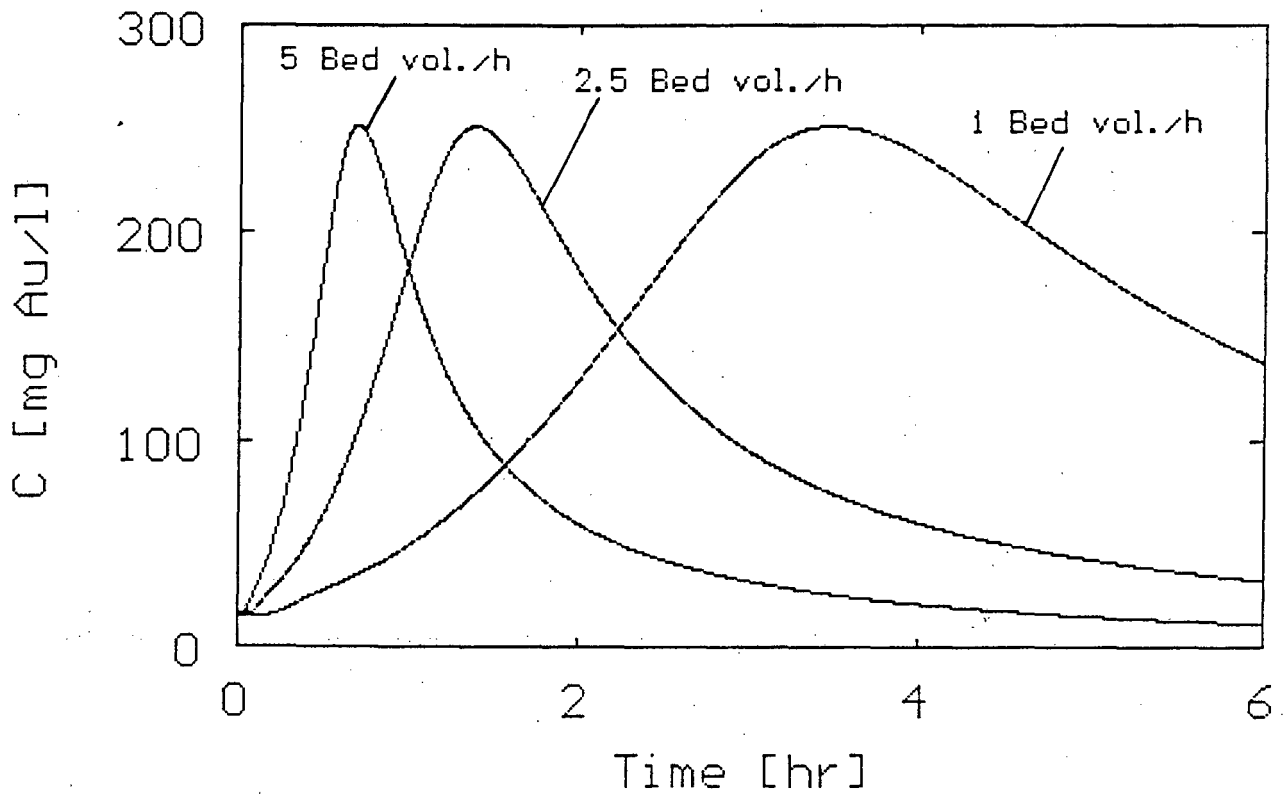


Figure 8.9 Sensitivity of the equilibrium model for the elution of gold cyanide to the flow rate of the eluant.

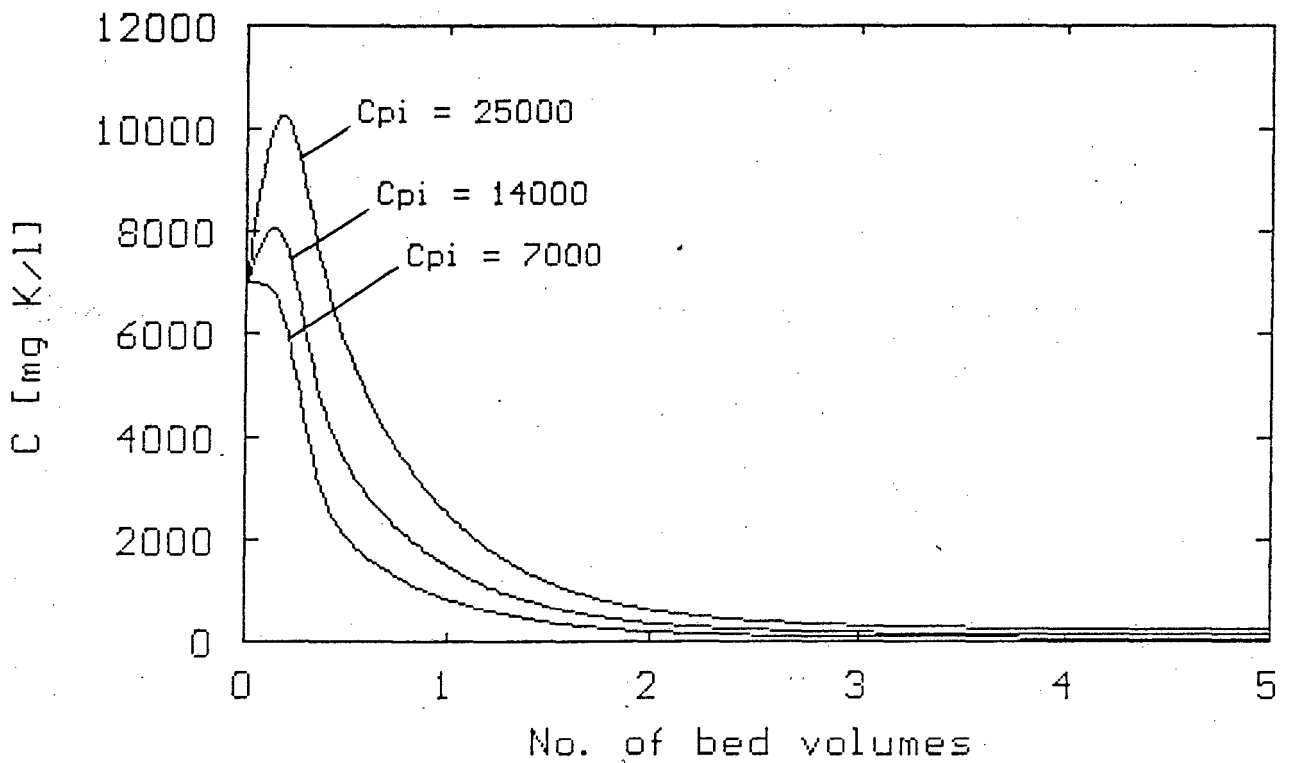


Figure 8.10 Behaviour of the nonideal flow model for the elution of potassium at different initial potassium concentrations in the pore liquid.

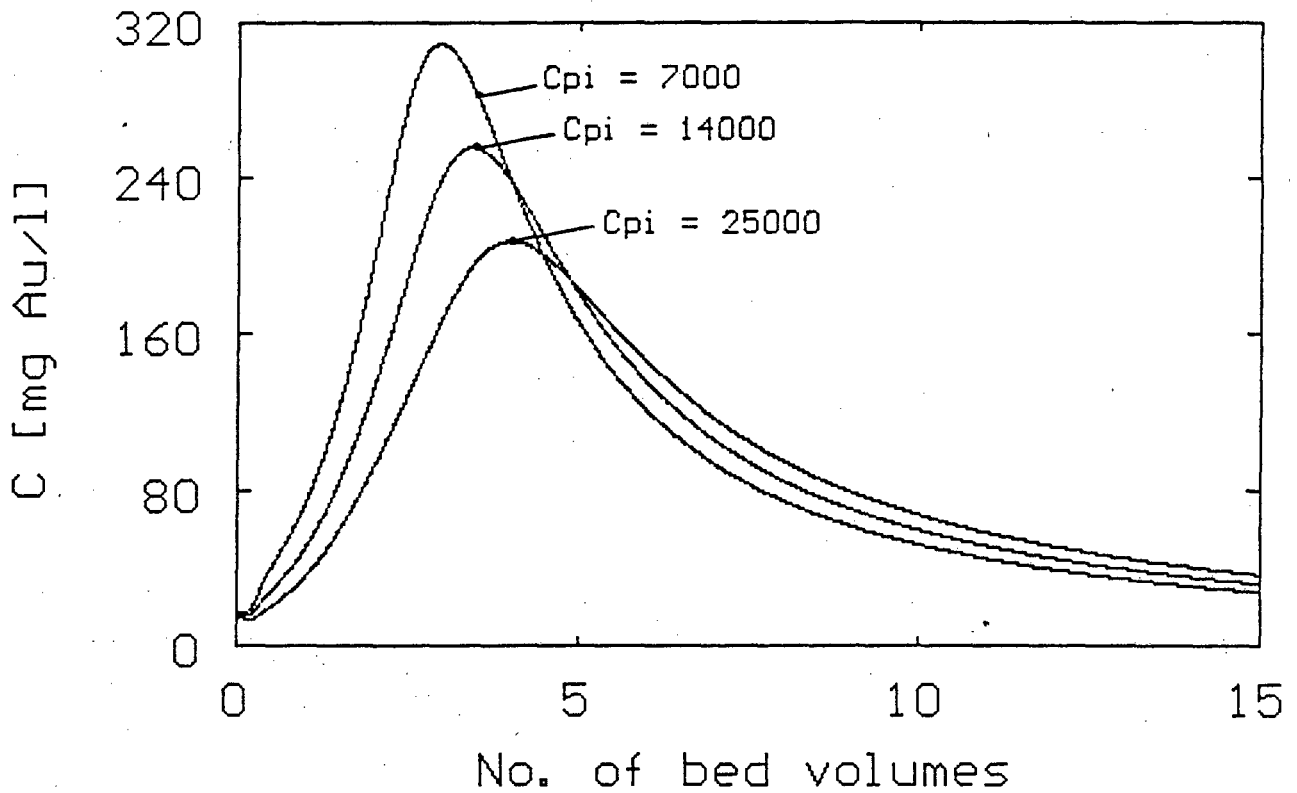


Figure 8.11 Sensitivity of the equilibrium model for the elution of gold cyanide to the initial potassium concentration in the pore liquid.

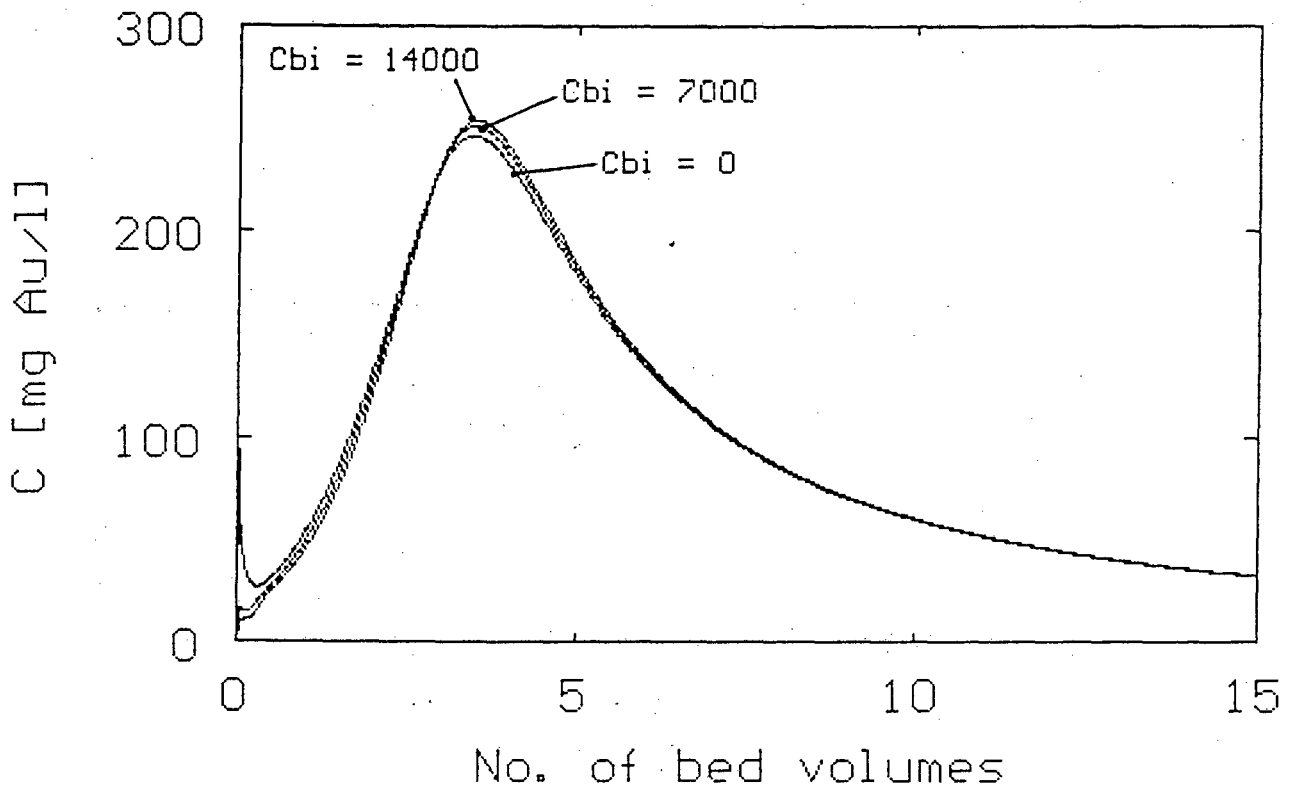


Figure 8.12 Sensitivity of the equilibrium model for the elution of gold cyanide to the initial potassium concentration in the interparticle solution.

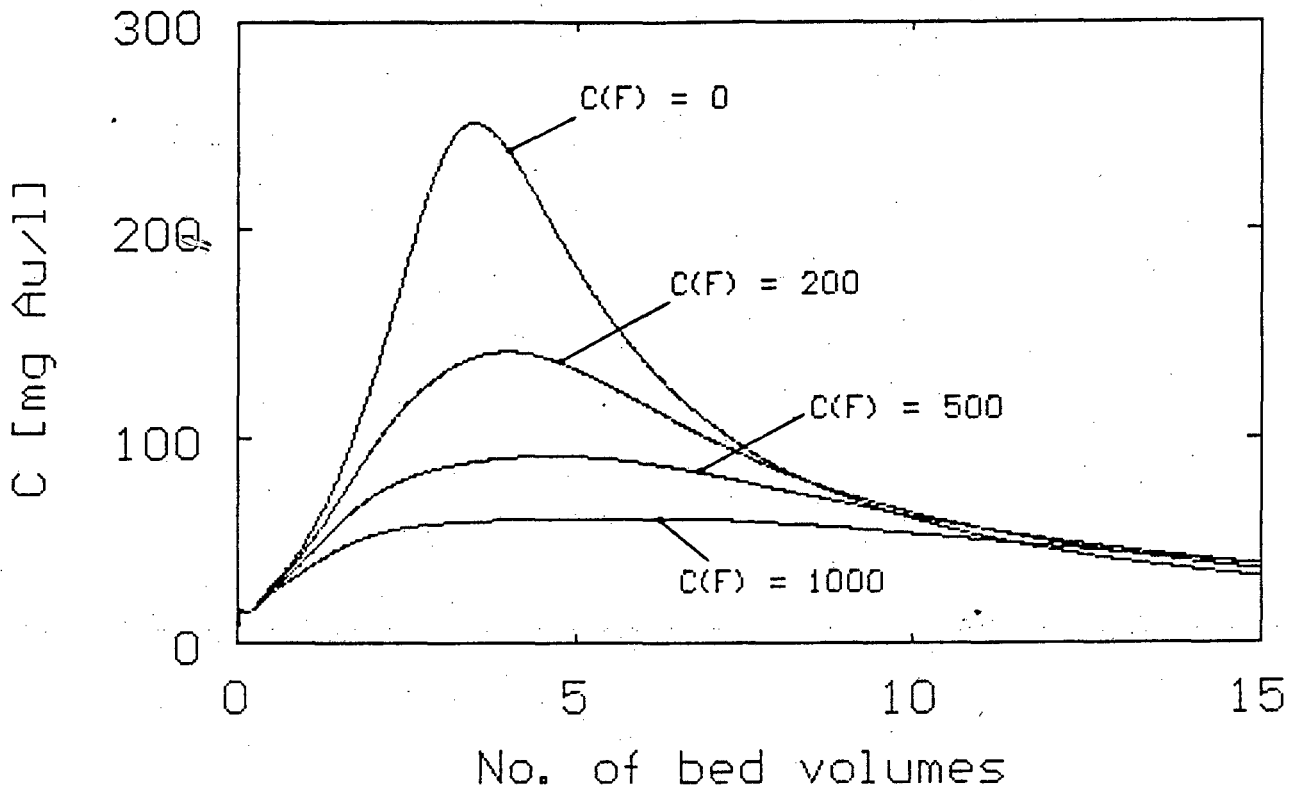


Figure 8.13 Sensitivity of the equilibrium model for the elution of gold cyanide to the potassium concentration in the eluant. $C(F) = C_{KF}$ = feed concentration of potassium.

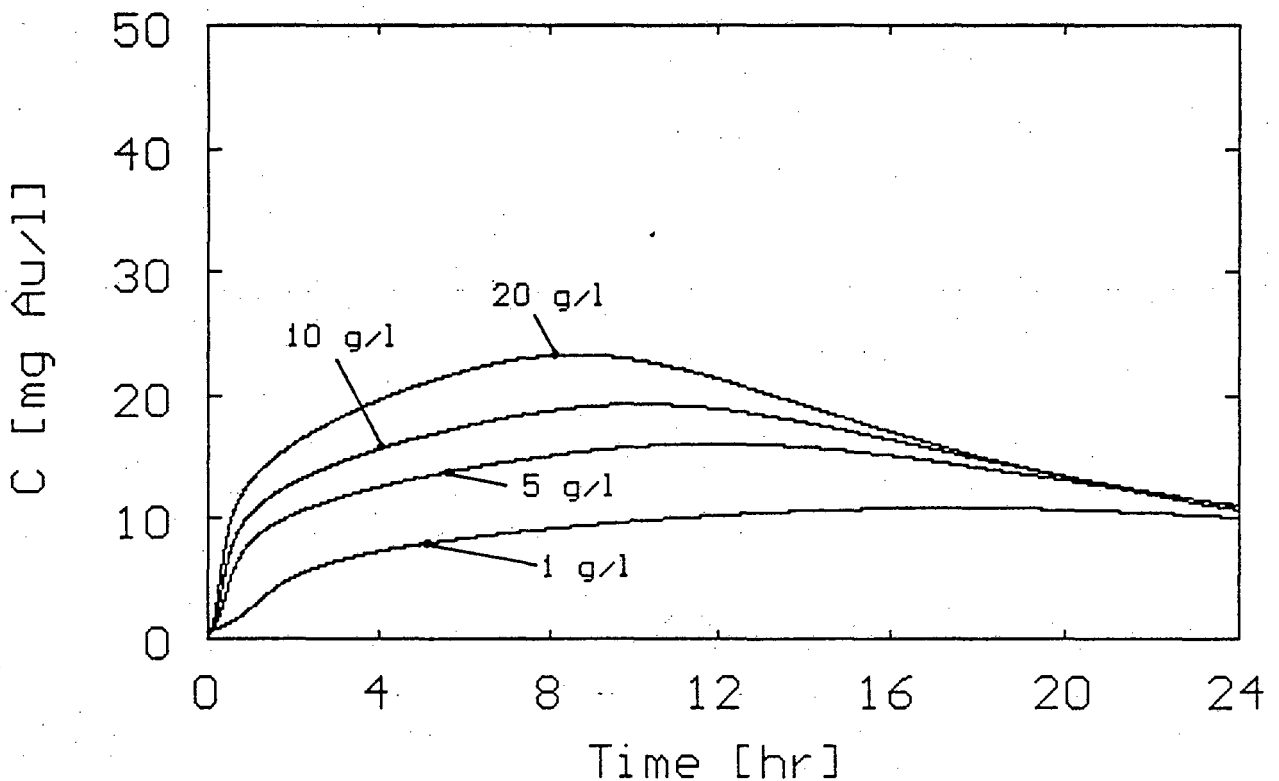


Figure 8.14 The effect of the concentration of KCN on the Zadra elution profiles predicted with the equilibrium model. $A_s = 2.82$, $p = 0.088$, $C_{Kpi} = C_{Kbi} = C_{KF}$, Cyanide parameters as for Fig. 4.2.

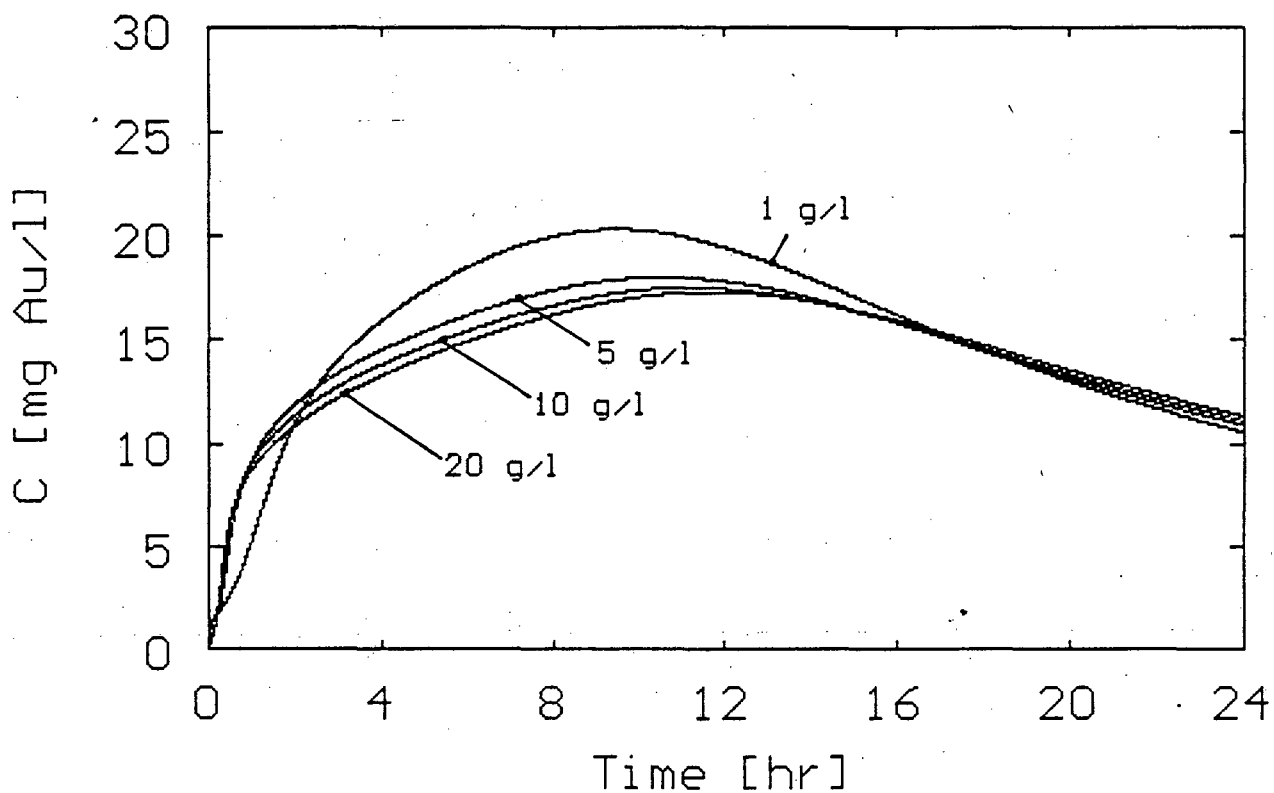


Figure 8.15 The effect of the concentration of KCN on the Zadra elution profiles predicted with the equilibrium model. $A_o = 1.10$, $p = 0.2$, $C_{Kpi} = C_{Kbi} = C_{KF}$, Cyanide parameters as for Fig. 4.2.

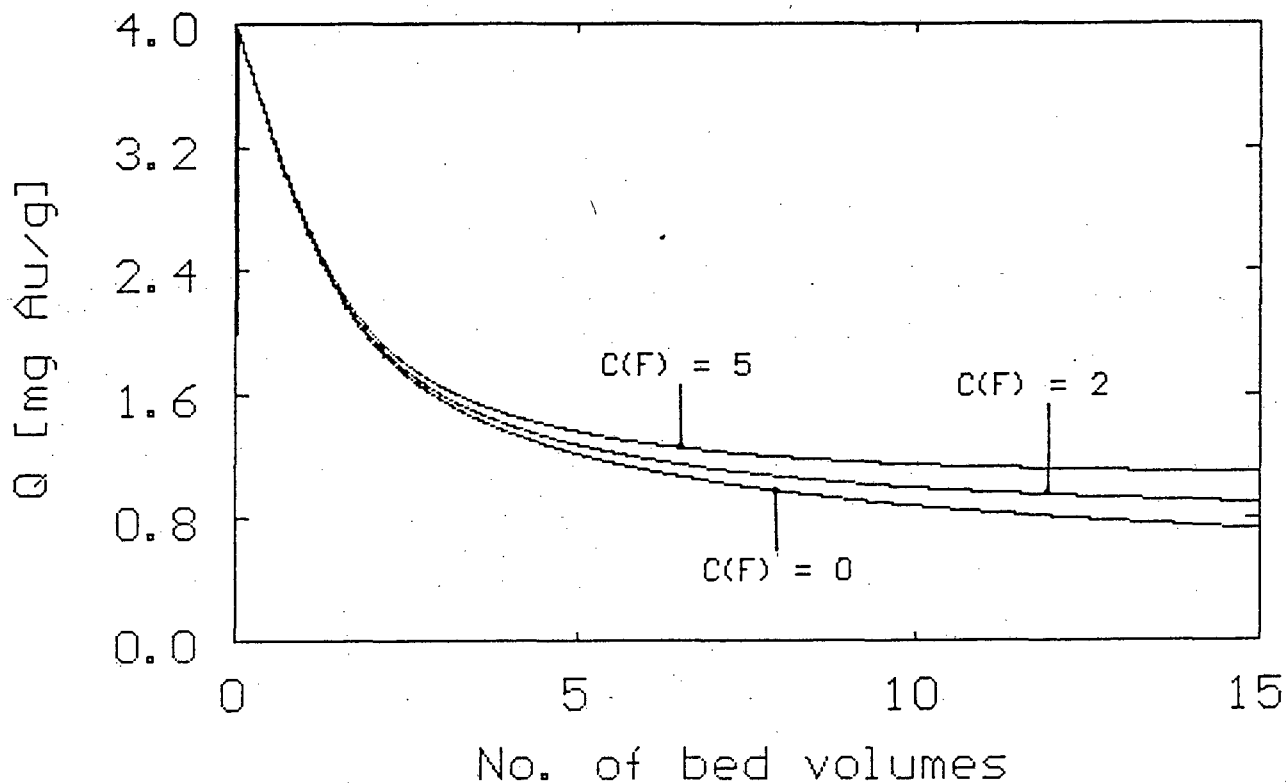


Figure 8.16 Sensitivity of the equilibrium model for the elution of gold cyanide to the gold cyanide concentration in the eluant. $C(F) = C_{GF}$, = feed concentration of gold cyanide.

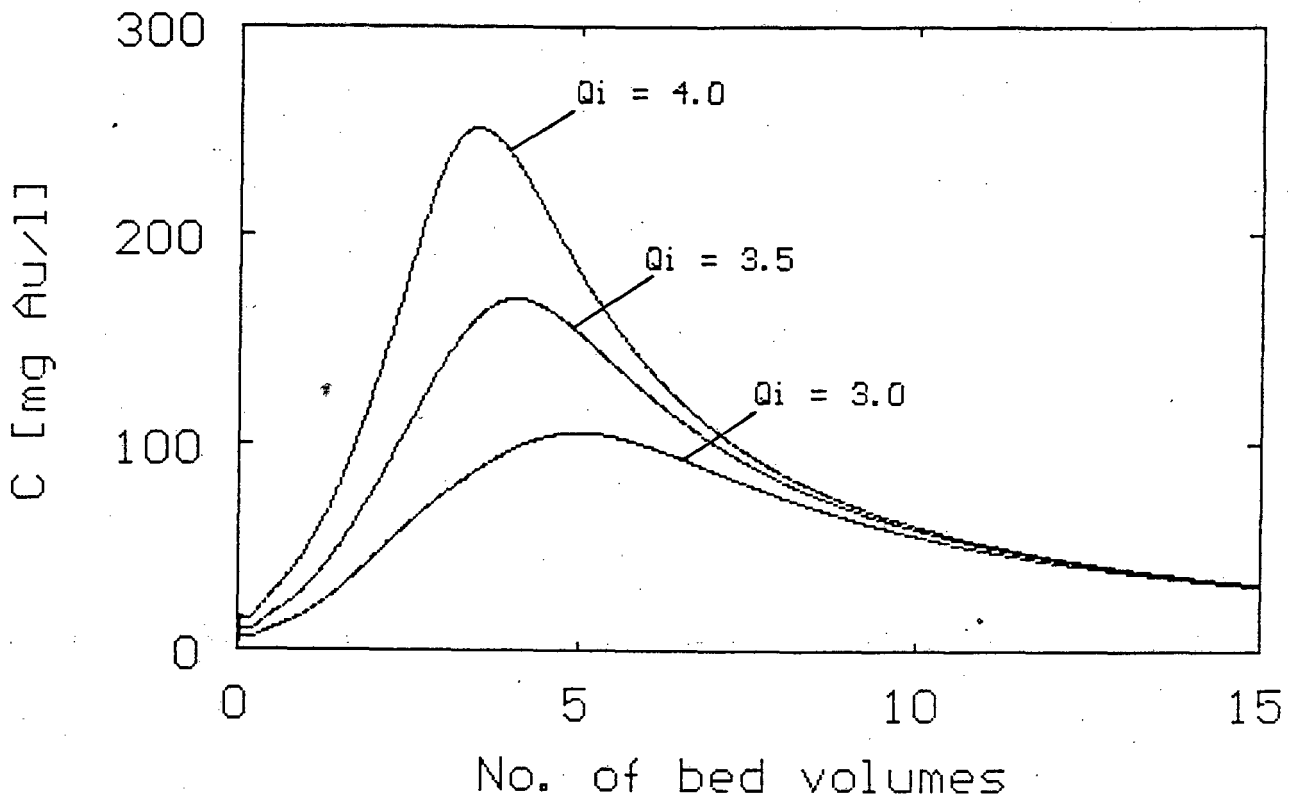


Figure 8.17 Sensitivity of the equilibrium model for the elution of gold cyanide to the initial gold loading on the carbon.

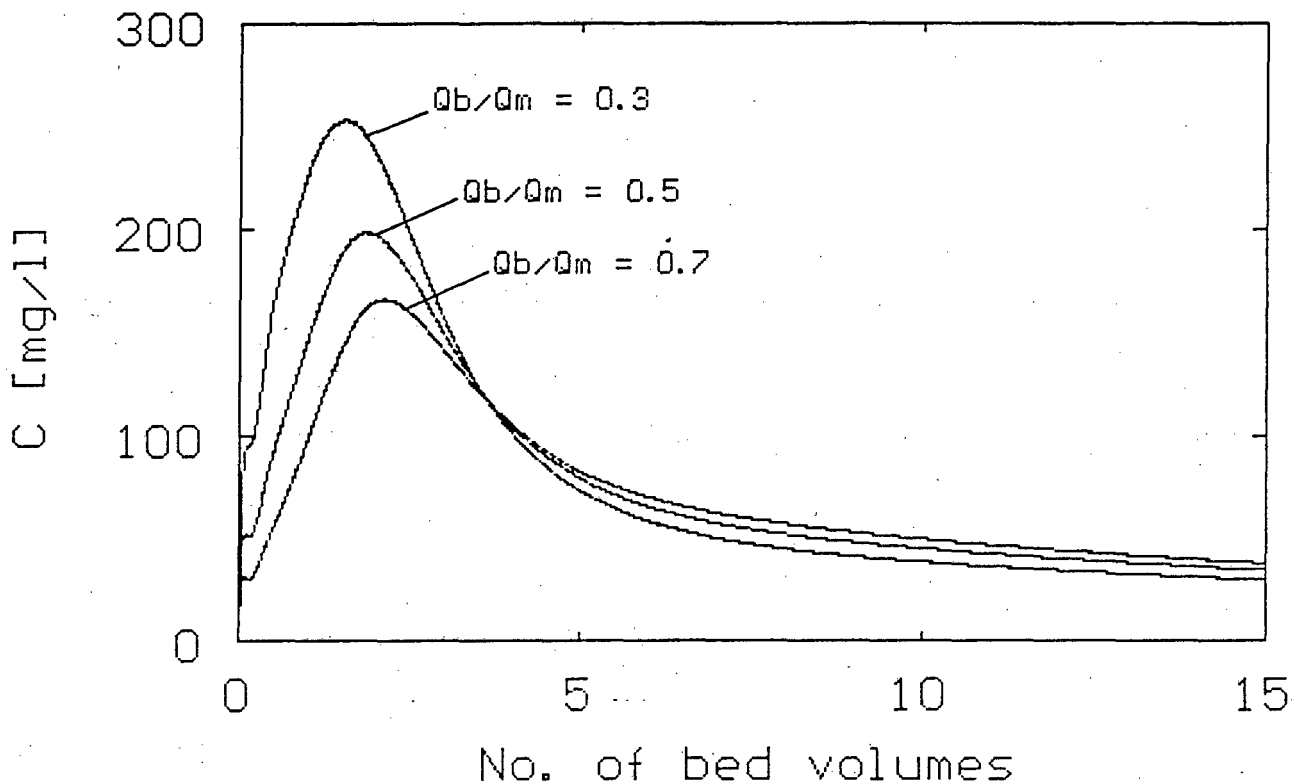


Figure 8.18 Sensitivity of the surface diffusion model for the elution of gold cyanide to the initial distribution of gold between the micropores and the macropores.

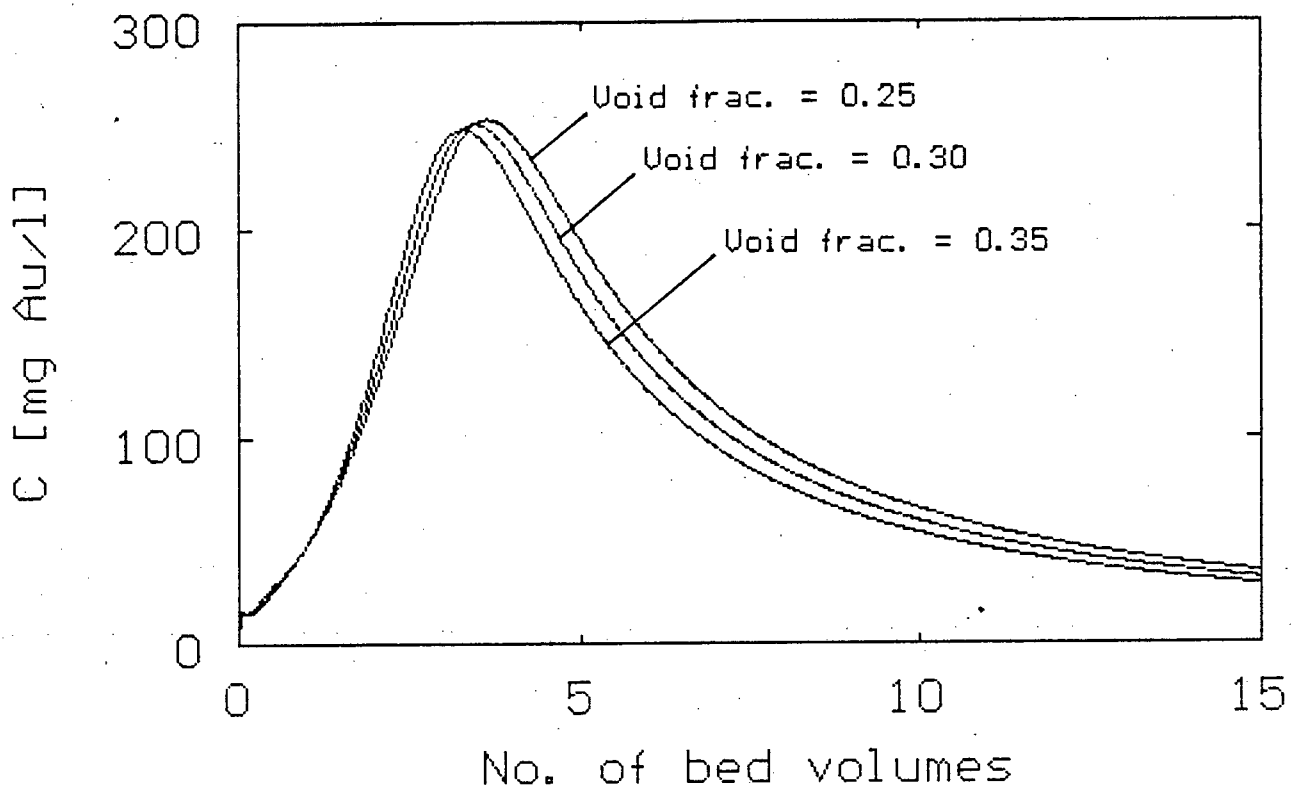


Figure 8.19 Sensitivity of the equilibrium model for the elution of gold cyanide to ϵ , the void fraction of the carbon bed.

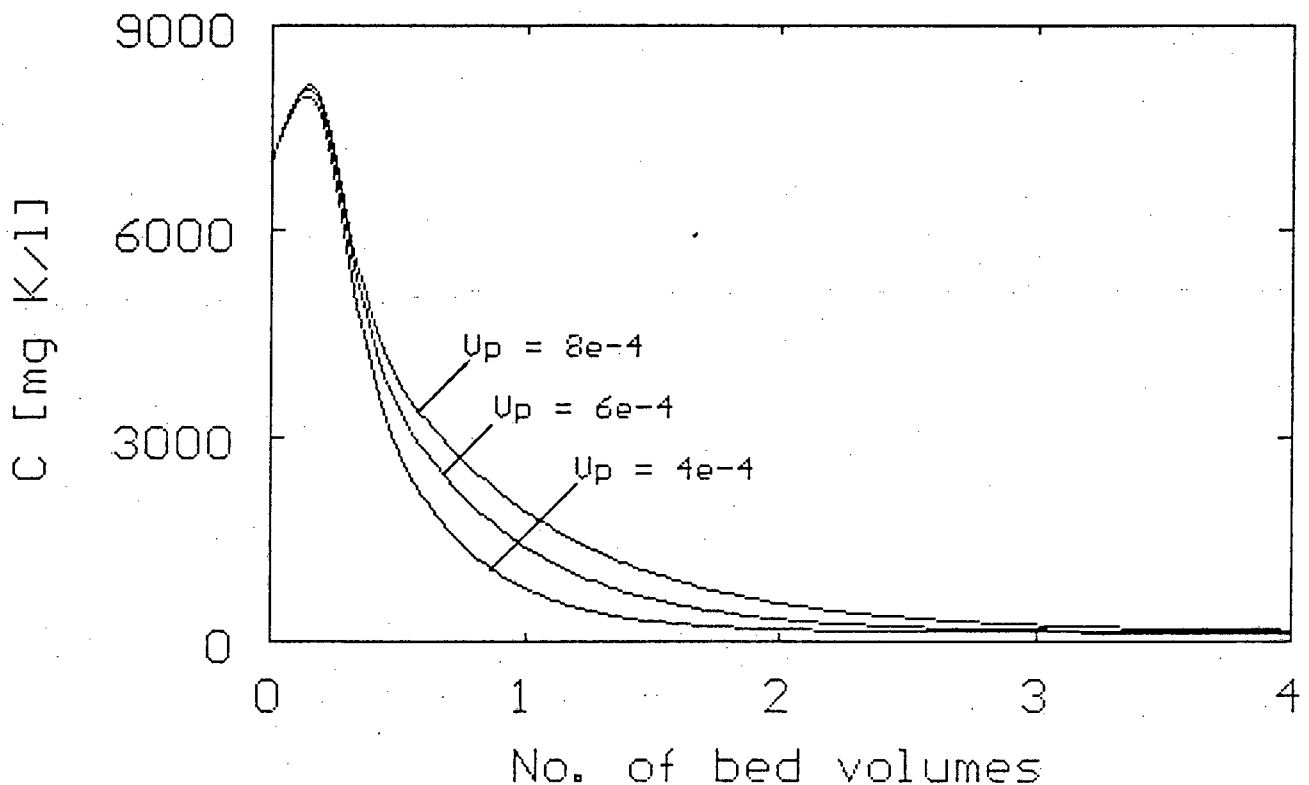


Figure 8.20 Sensitivity of the nonideal flow model for the elution of potassium to V_p , the pore volume of the carbon.

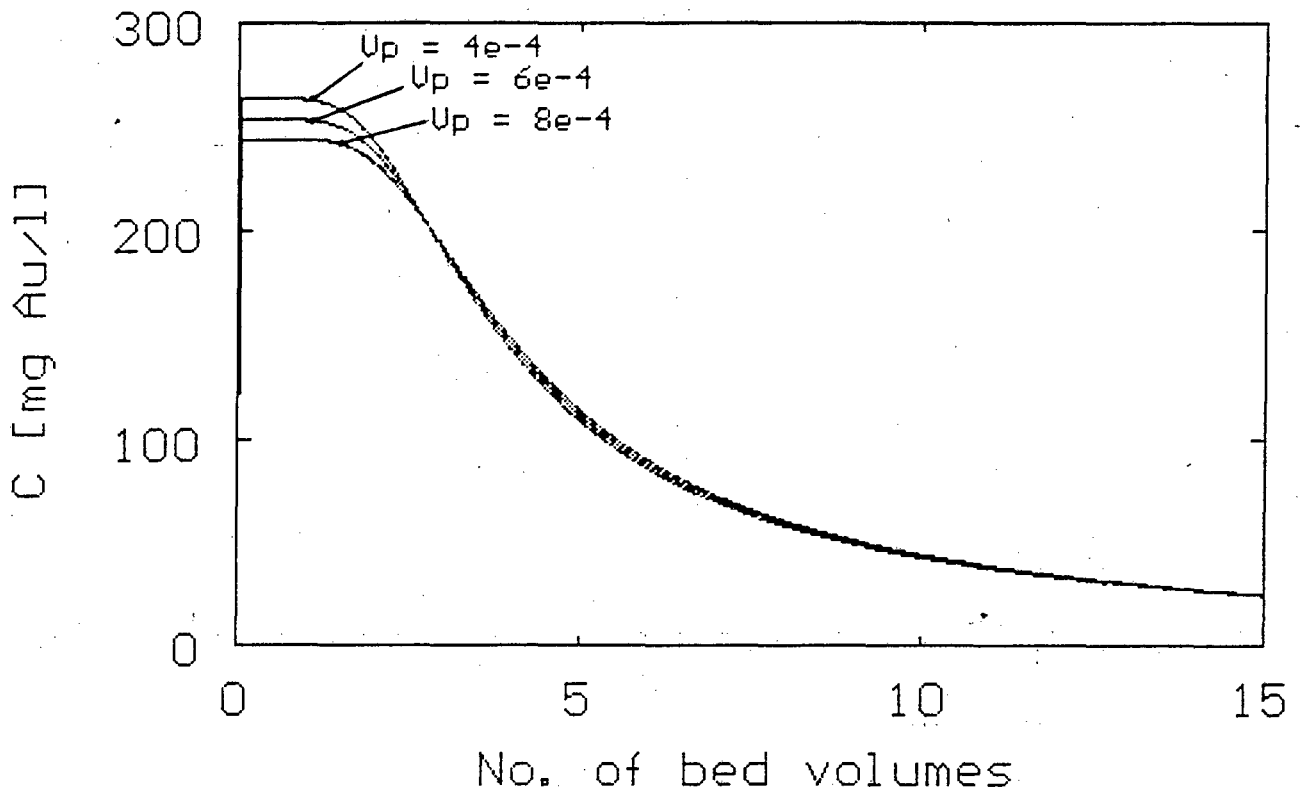


Figure 8.21 Sensitivity of the equilibrium model for the elution of gold cyanide to V_p , the pore volume of the carbon.

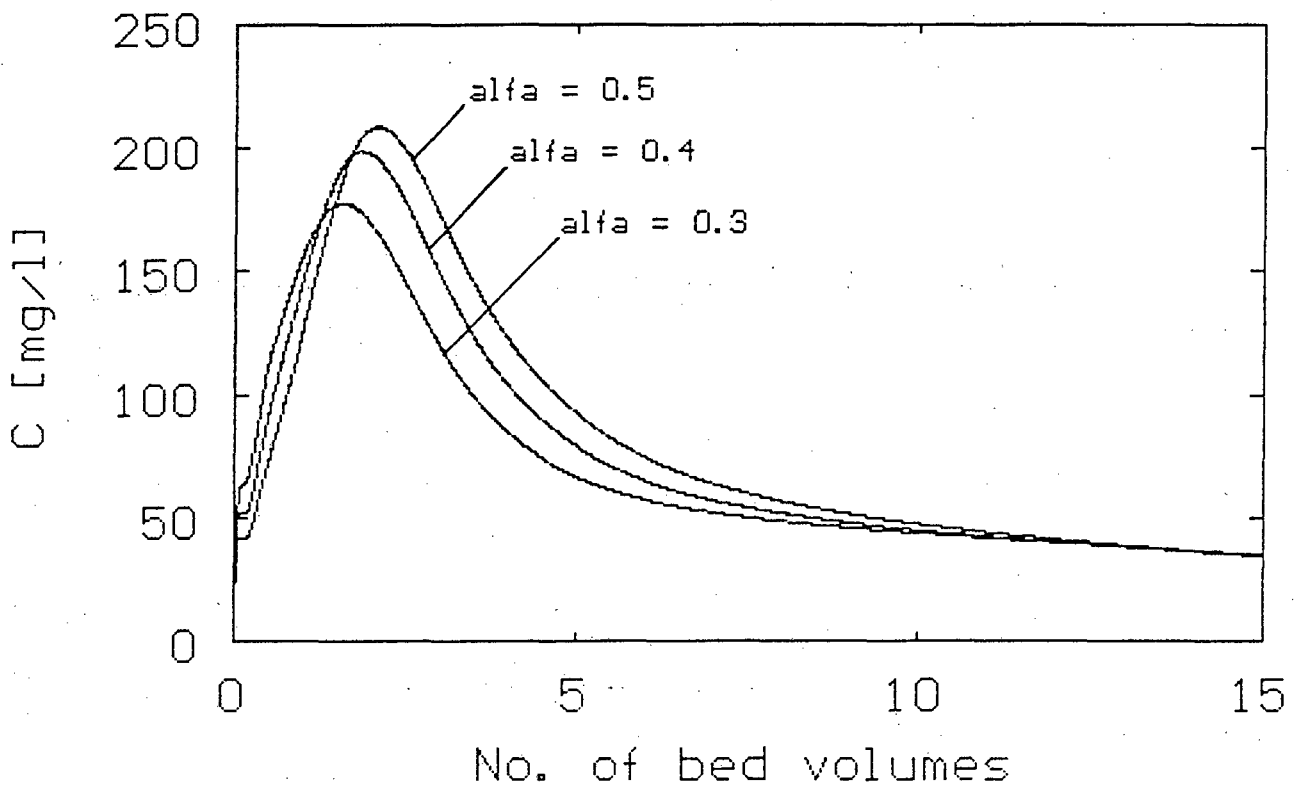


Figure 8.22 Sensitivity of the surface diffusion model for the elution of gold cyanide to α_g (alfa), the fraction of the pores available as macropores.

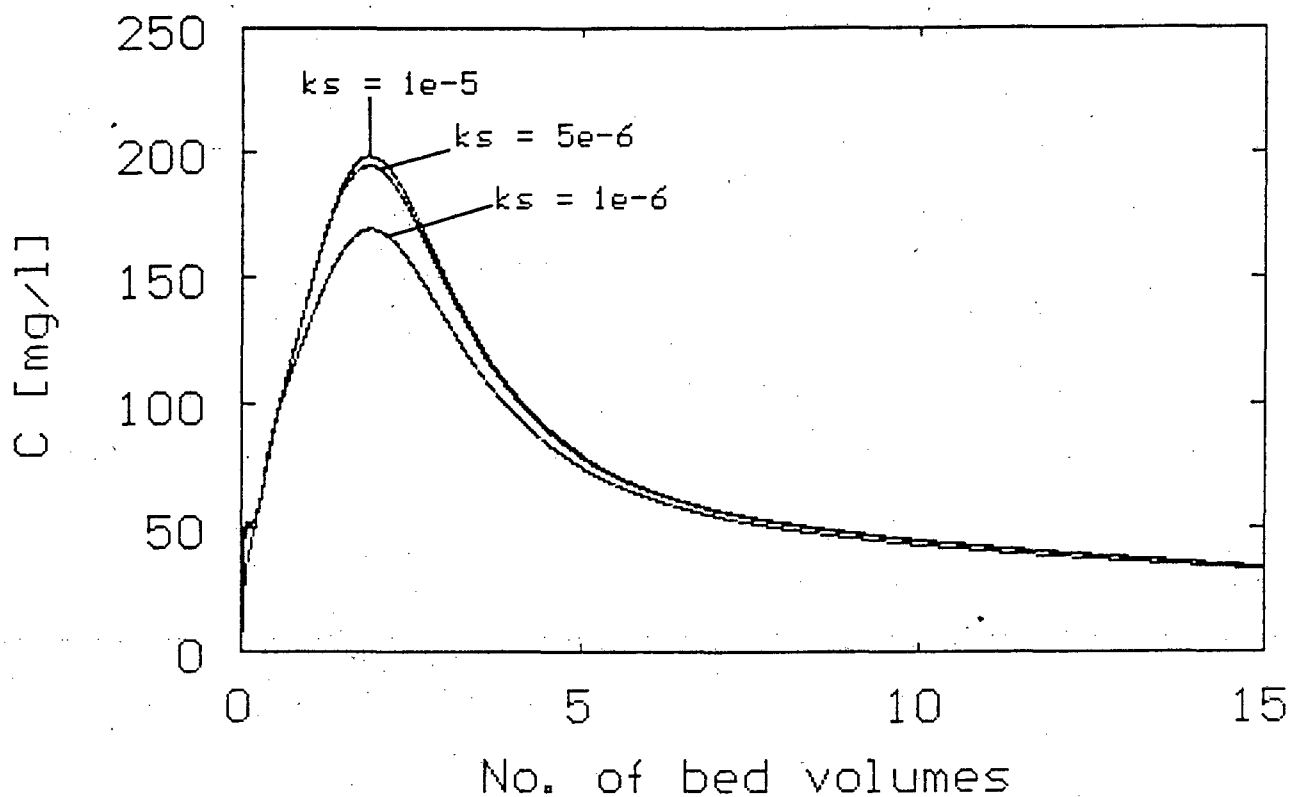


Figure 8.23 Sensitivity of the surface diffusion model for the elution of gold cyanide to k_s , the film diffusion coefficient.

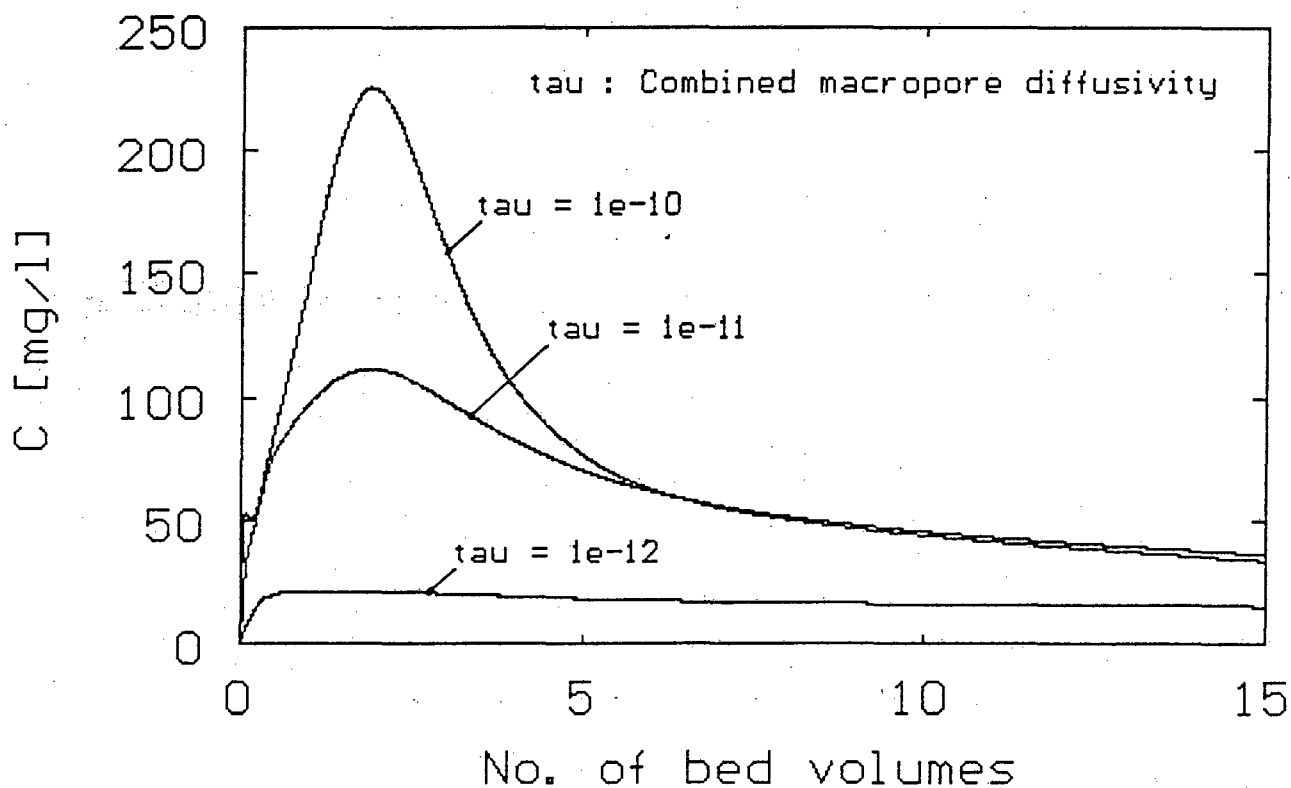


Figure 8.24 Sensitivity of the surface diffusion model for the elution of gold cyanide to Γ_m (τ), the combined macropore diffusivity.

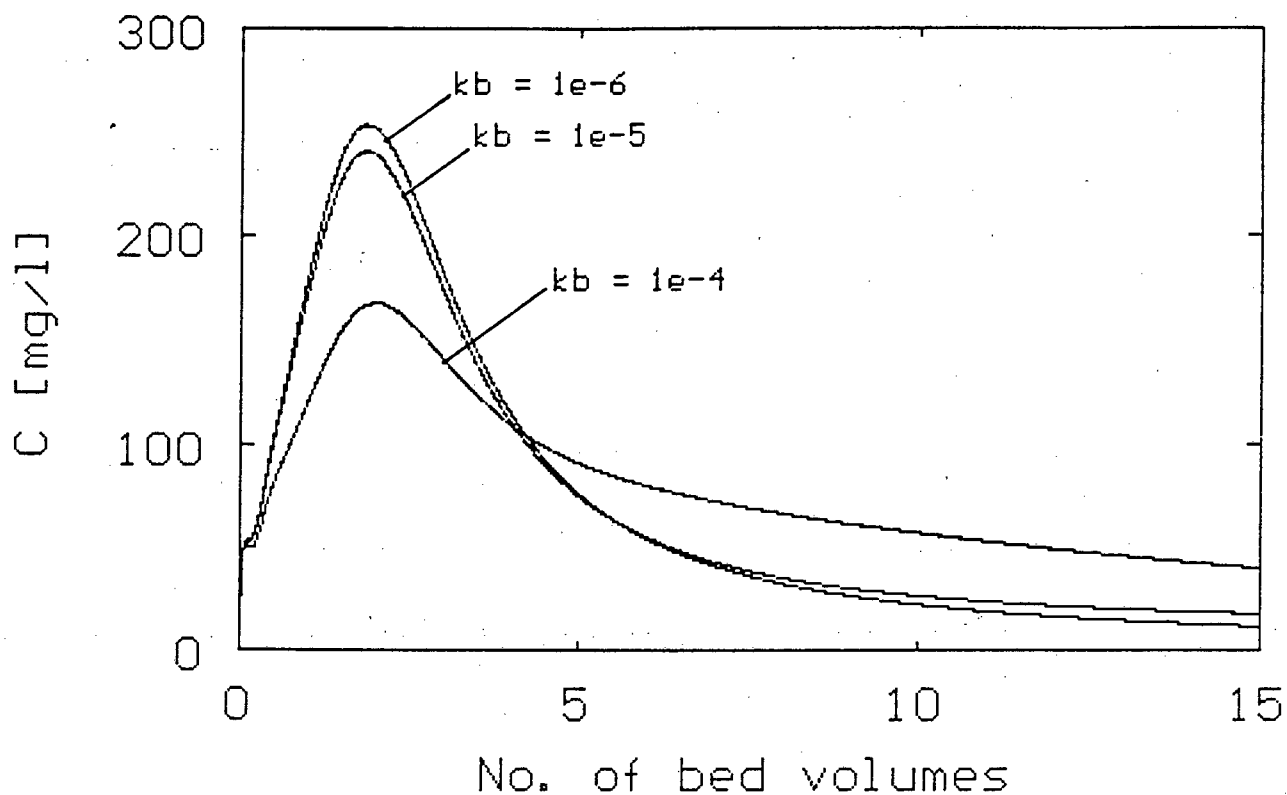


Figure 8.25 Sensitivity of the surface diffusion model for the elution of gold cyanide to k_b , the coefficient for mass transfer between the macropores and the micropores.

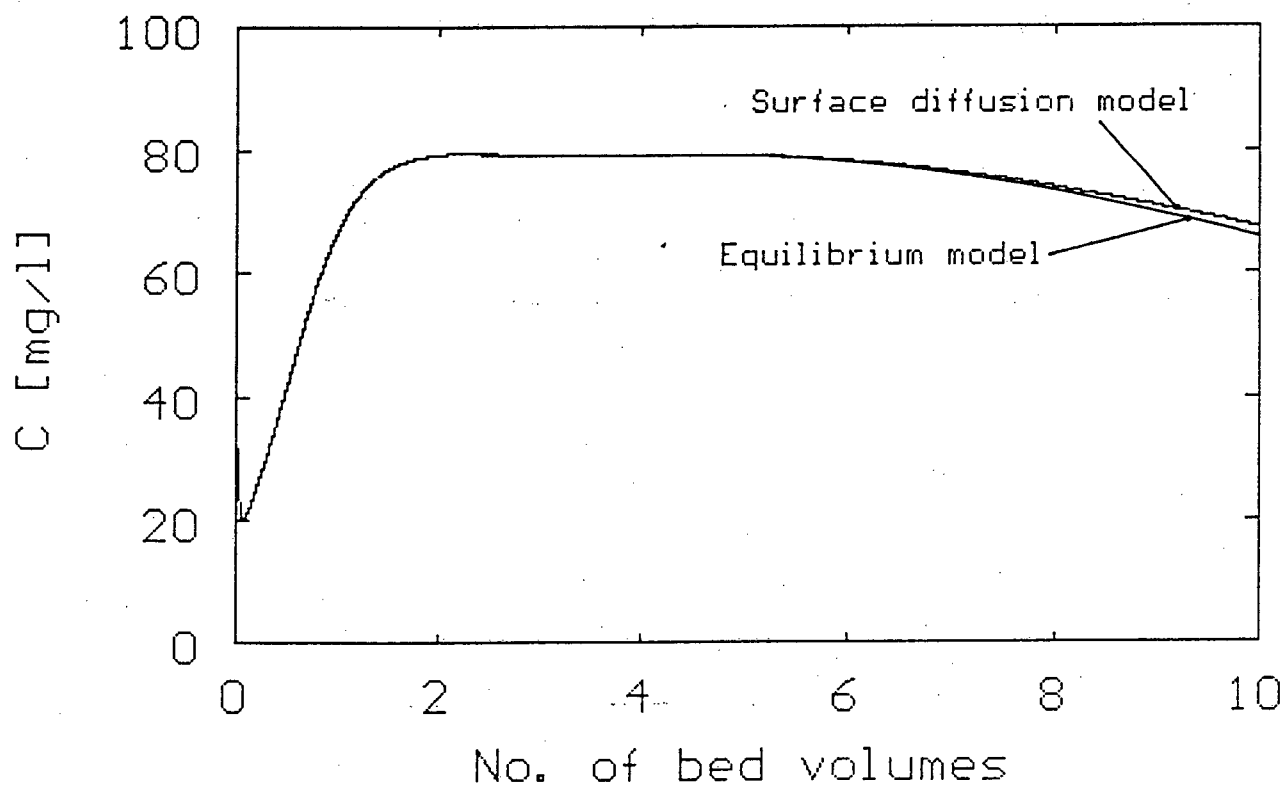


Figure 8.26 Illustration of similarity between equilibrium model and surface diffusion model with high mass transfer coefficients.

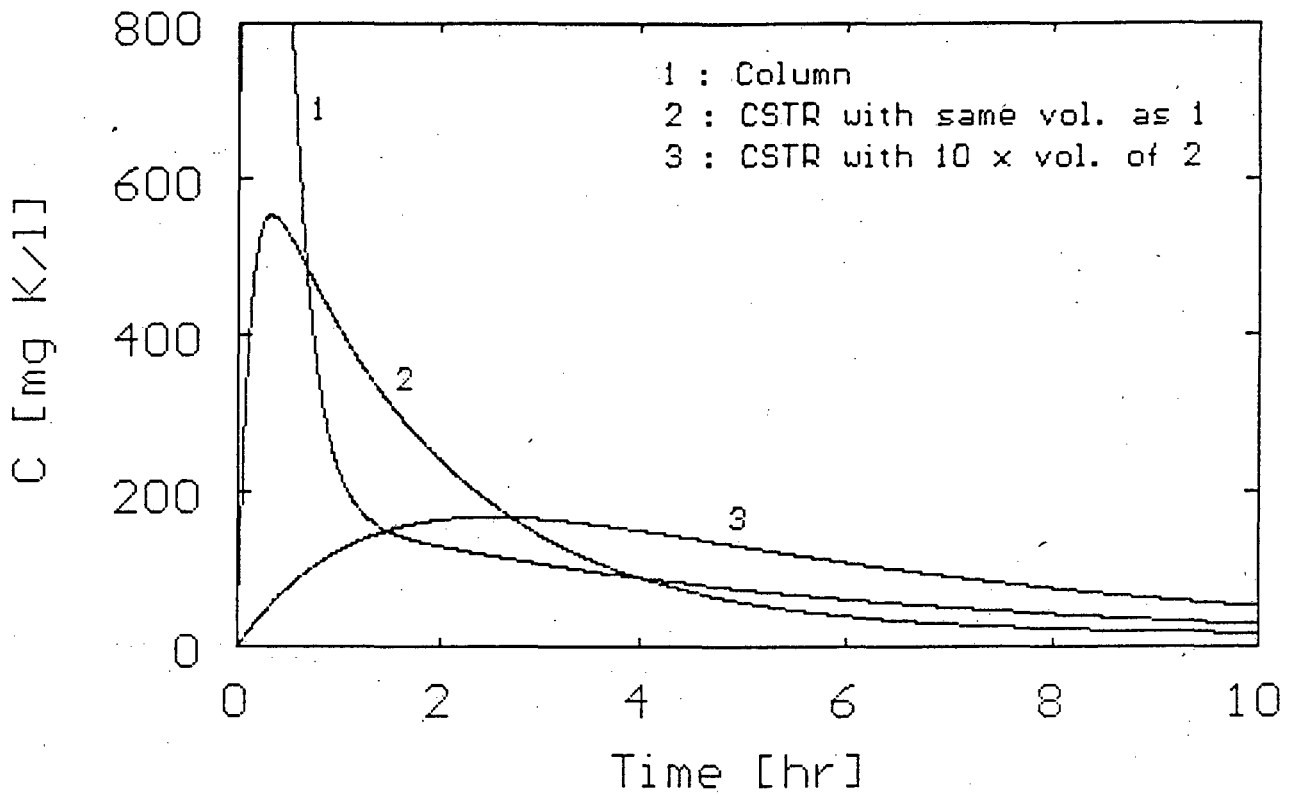


Figure 8.27 Elution profiles for potassium with the nonideal flow model for a column and a CSTR.

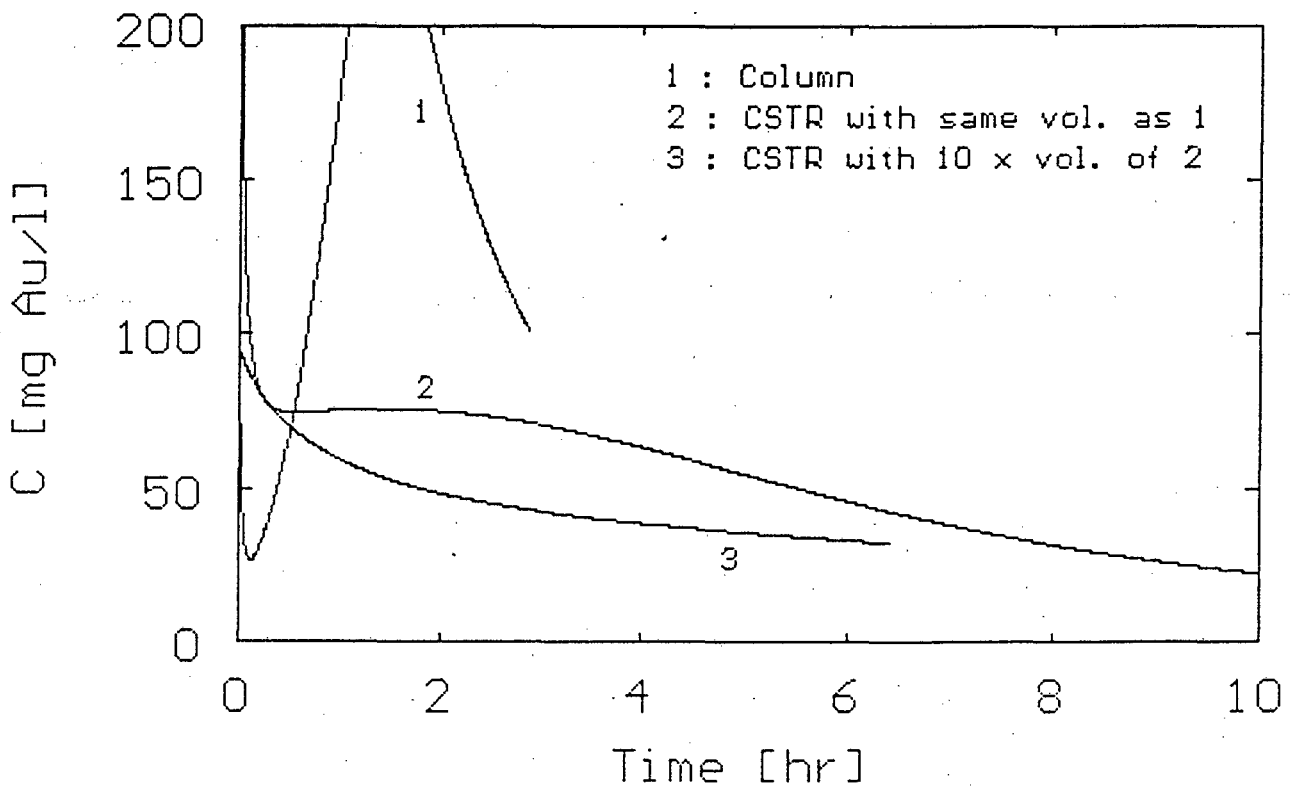


Figure 8.28 Elution profiles for gold cyanide with the equilibrium model for a column and a CSTR.

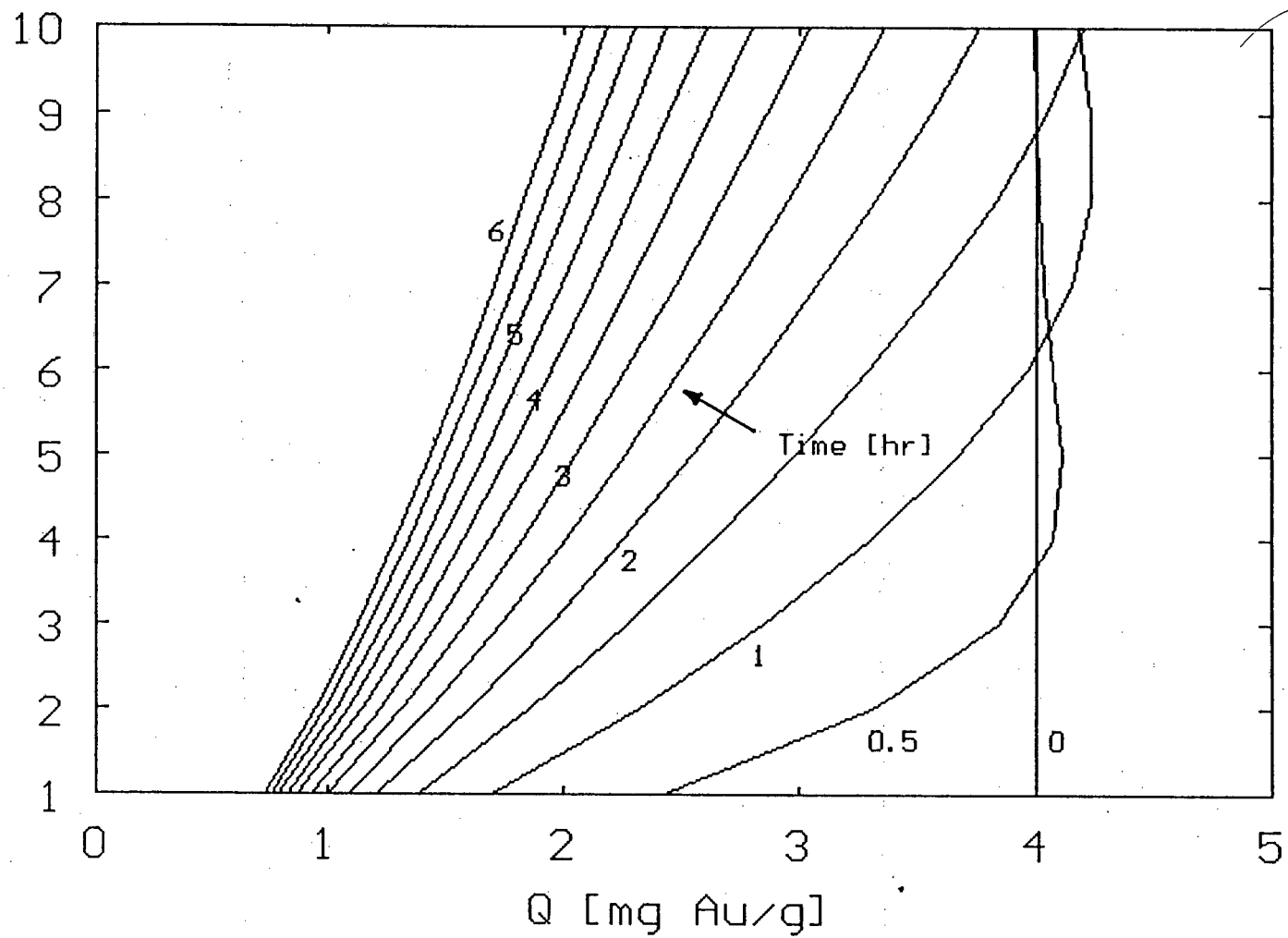


Figure 8.29 Gold loading profile through carbon bed at various points of time as predicted by equilibrium model.

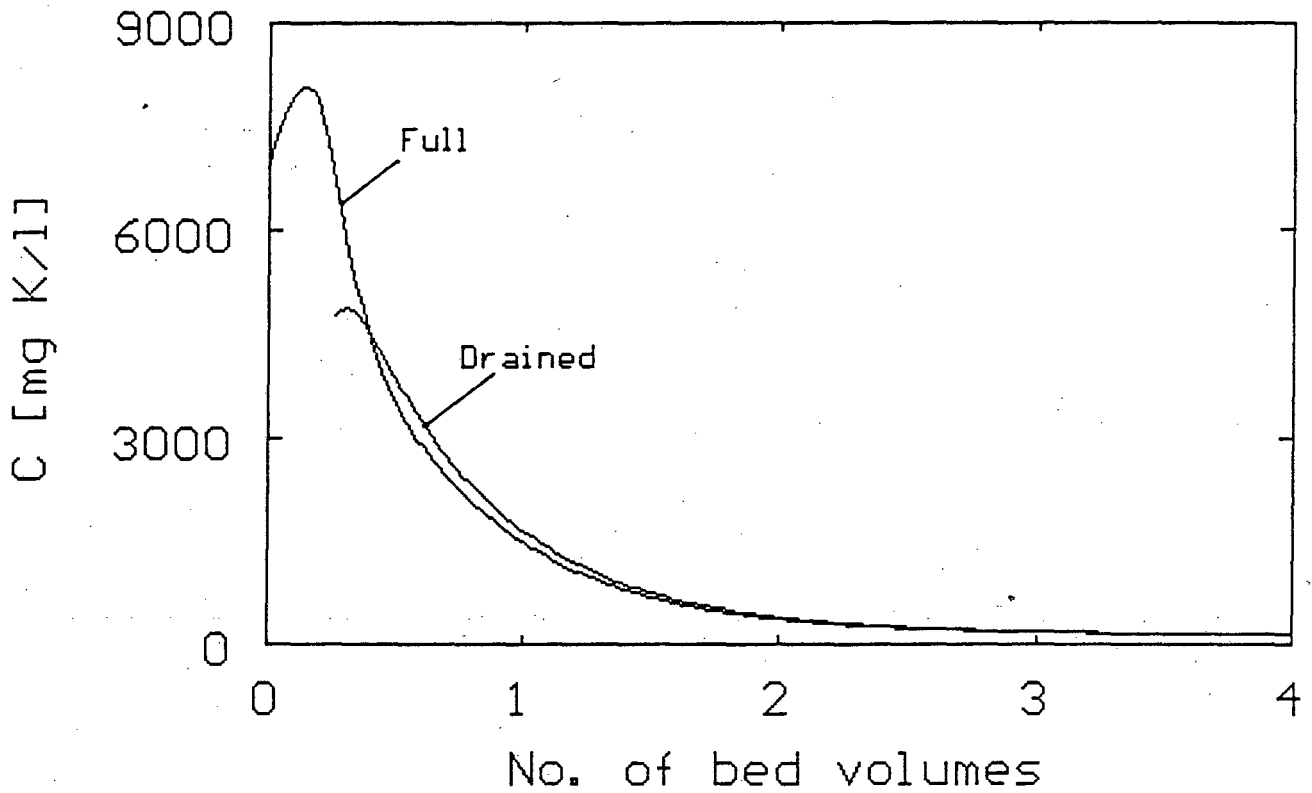


Figure 8.30 Elution profiles of potassium with nonideal flow model for initially full and drained beds of carbon.

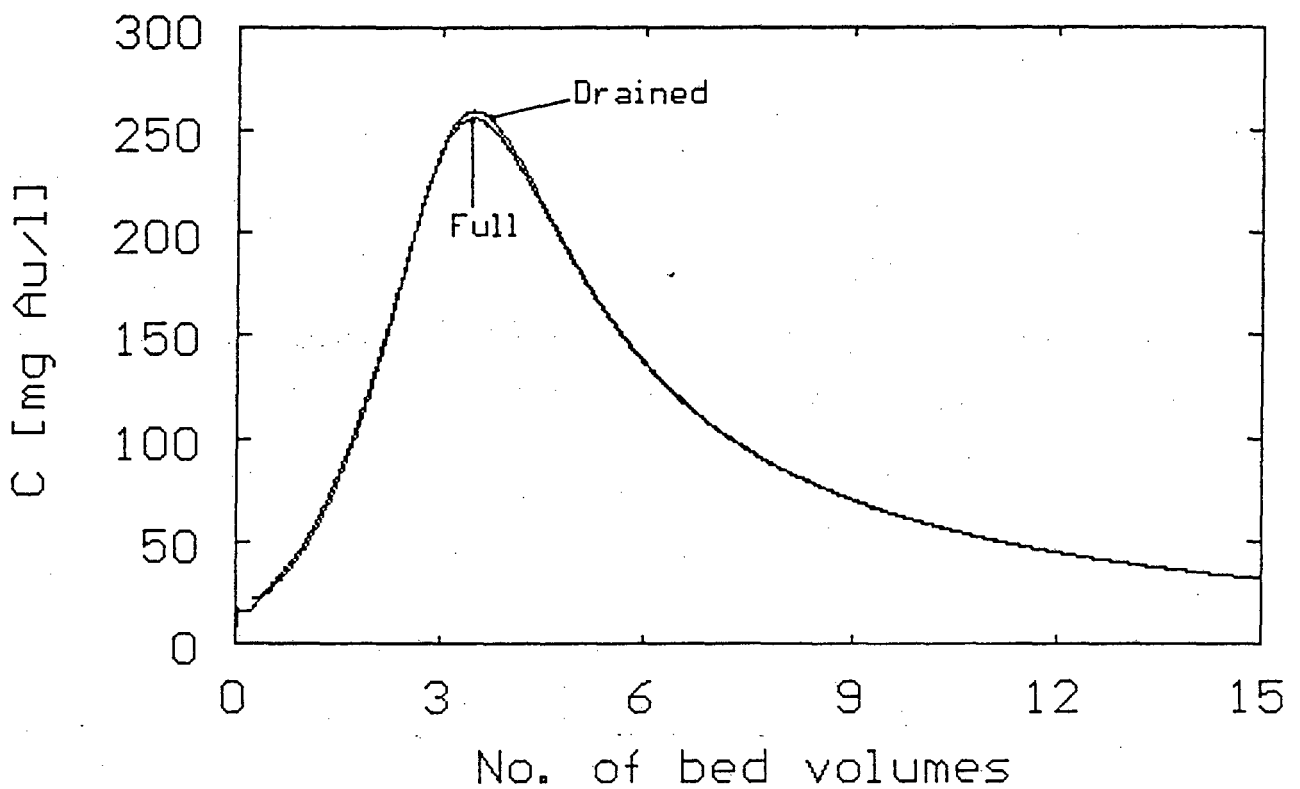


Figure 8.31 Elution profiles of gold cyanide with equilibrium model for initially full and drained beds of carbon.

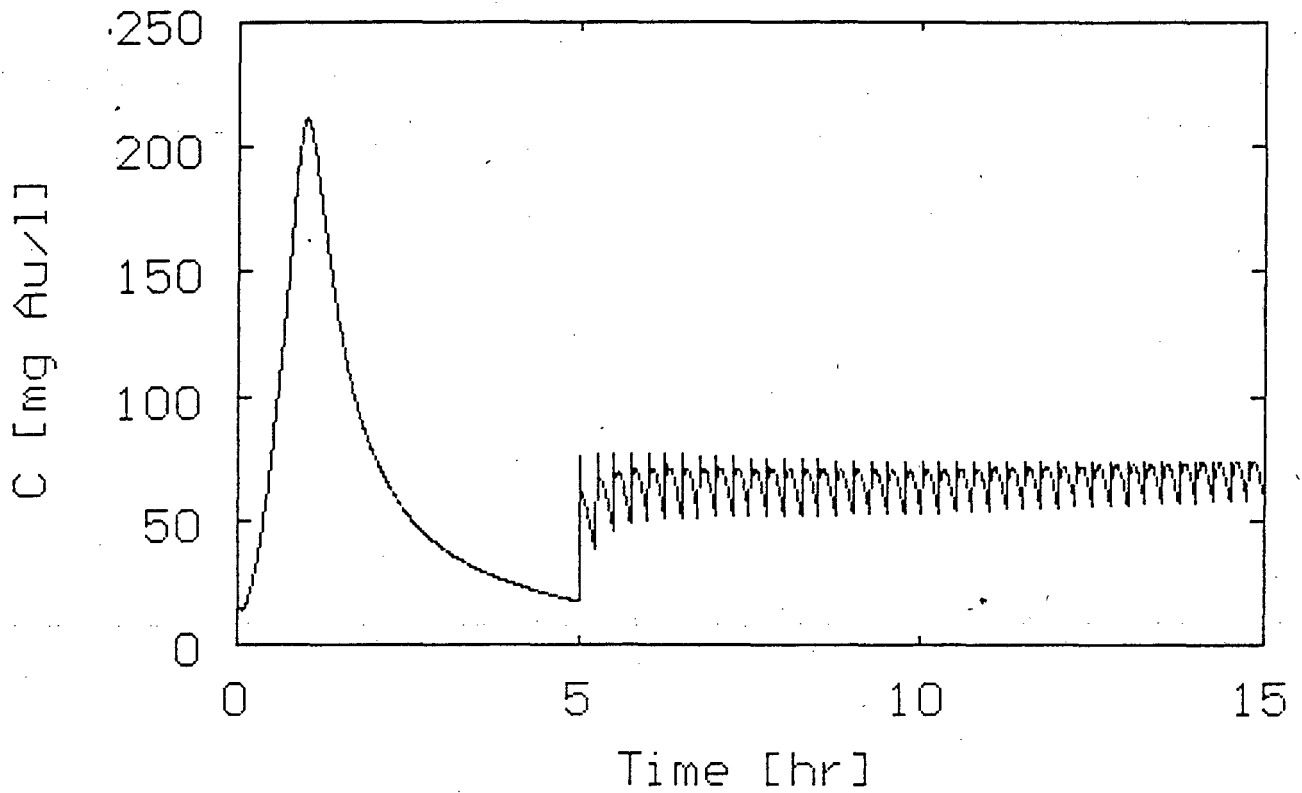


Figure 8.32 Equilibrium model simulation of the gold cyanide profile for a continuous counter-current elution.

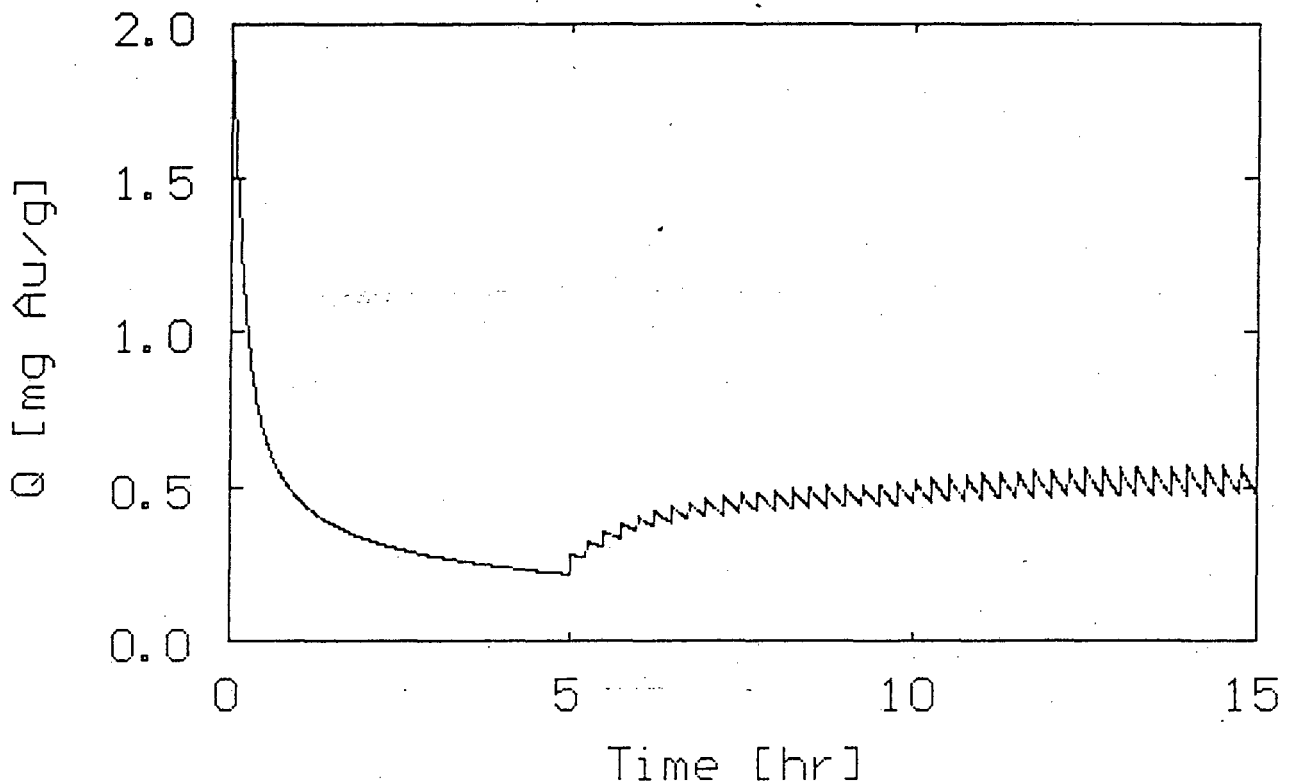


Figure 8.33 Equilibrium model simulation of the eluted carbon loading for a continuous counter-current elution.

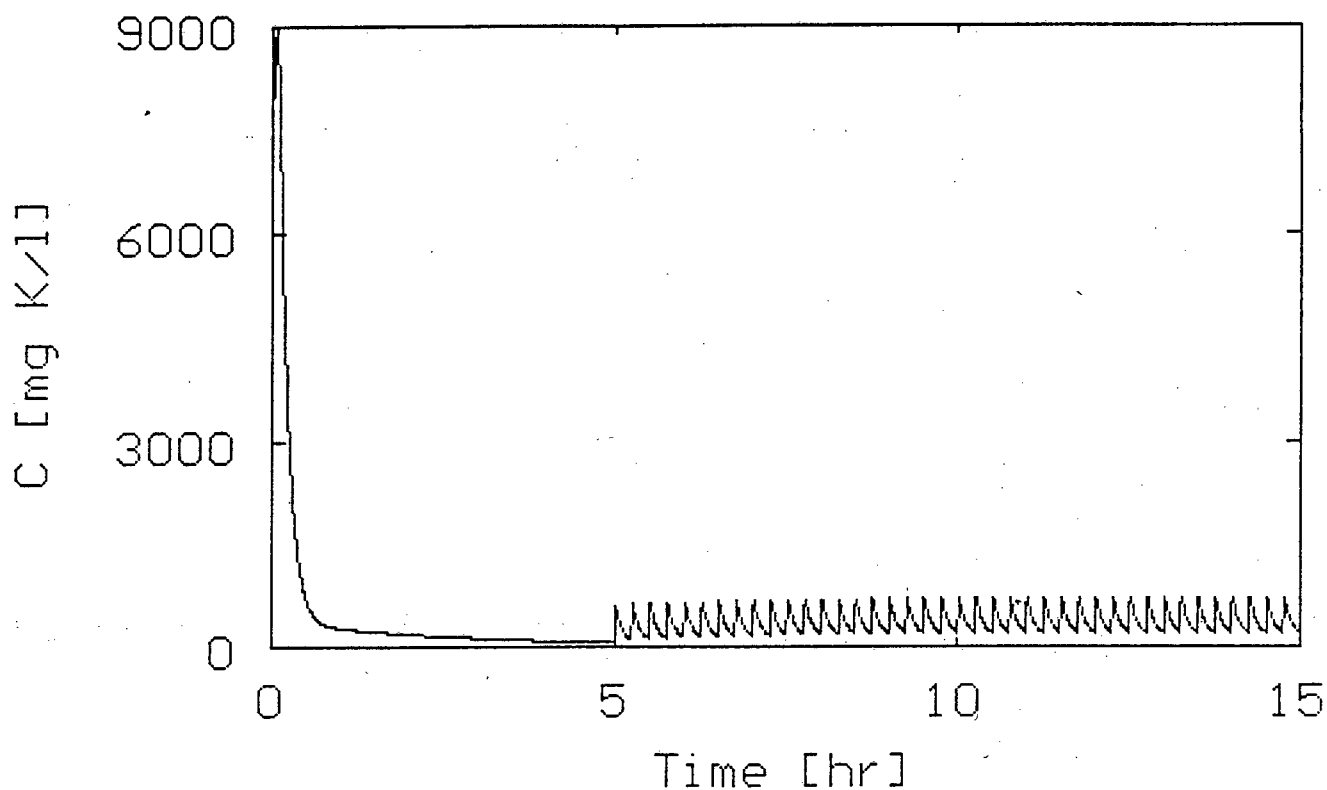


Figure 8.34 Nonideal flow model simulation of the potassium profile for a continuous counter-current elution.

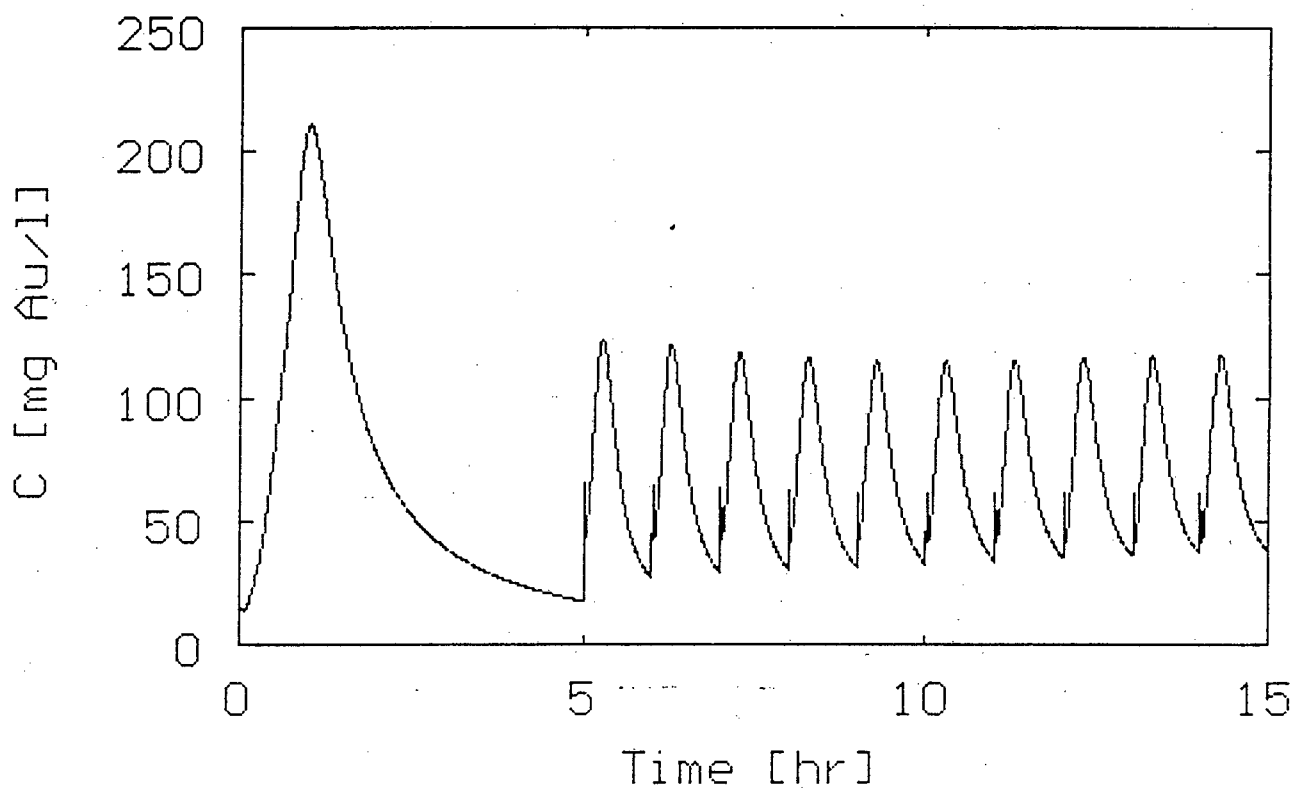


Figure 8.35 Equilibrium model simulation of the gold cyanide profile for a continuous counter-current elution with a lower frequency of carbon transfer than in Figure 8.32.

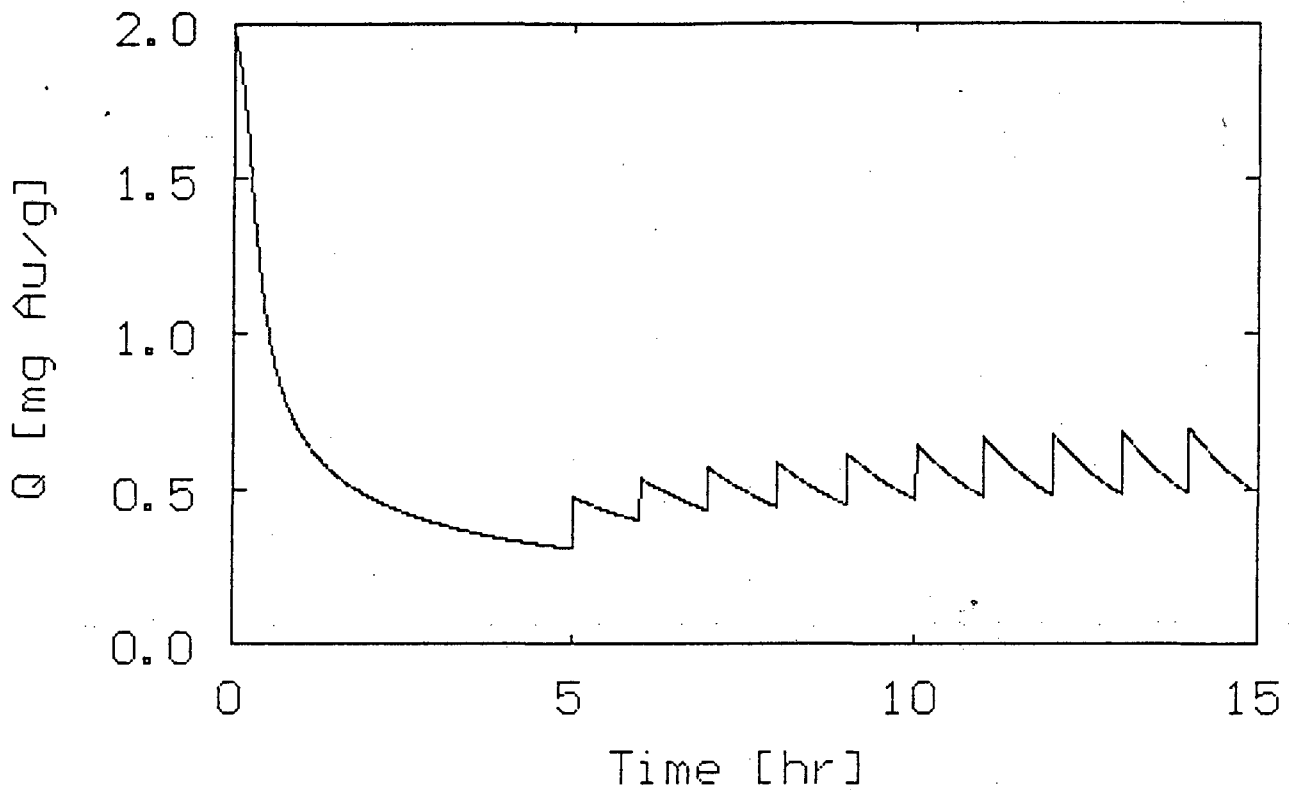


Figure 8.36 Equilibrium model simulation of the eluted carbon loading for the continuous counter-current elution of Figure 8.35.

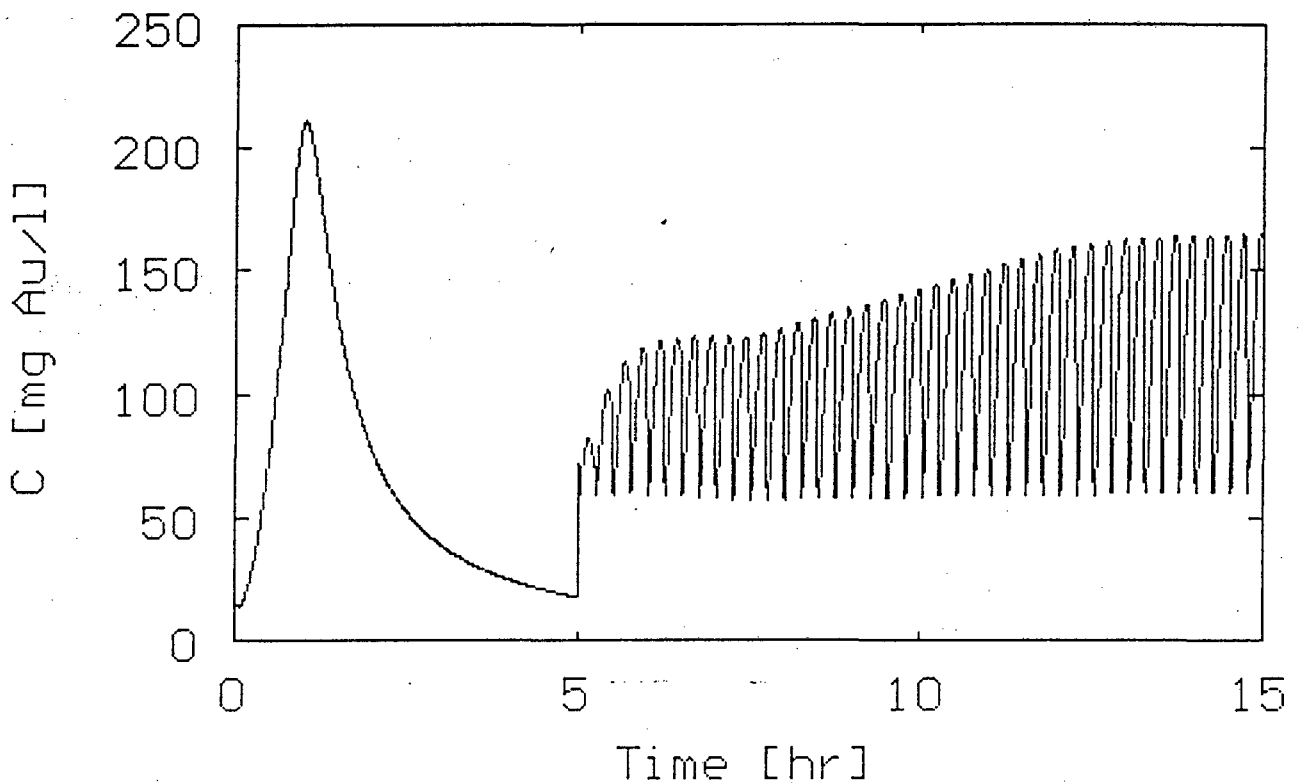


Figure 8.37 Equilibrium model simulation of the gold cyanide profile for a continuous counter-current elution with twice the carbon flow rate as for Figure 8.32.

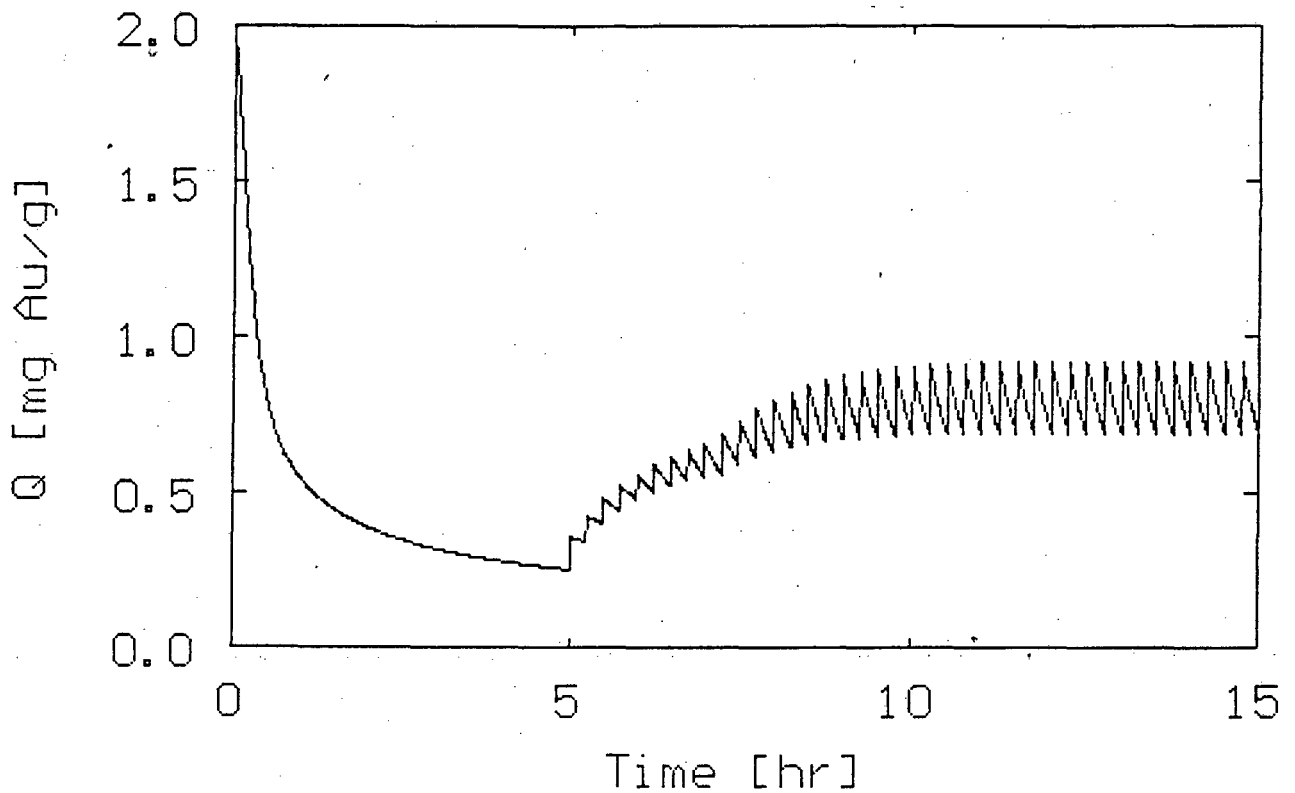


Figure 8.38 Equilibrium model simulation of the eluted carbon loading for the continuous counter-current elution of Figure 8.37.

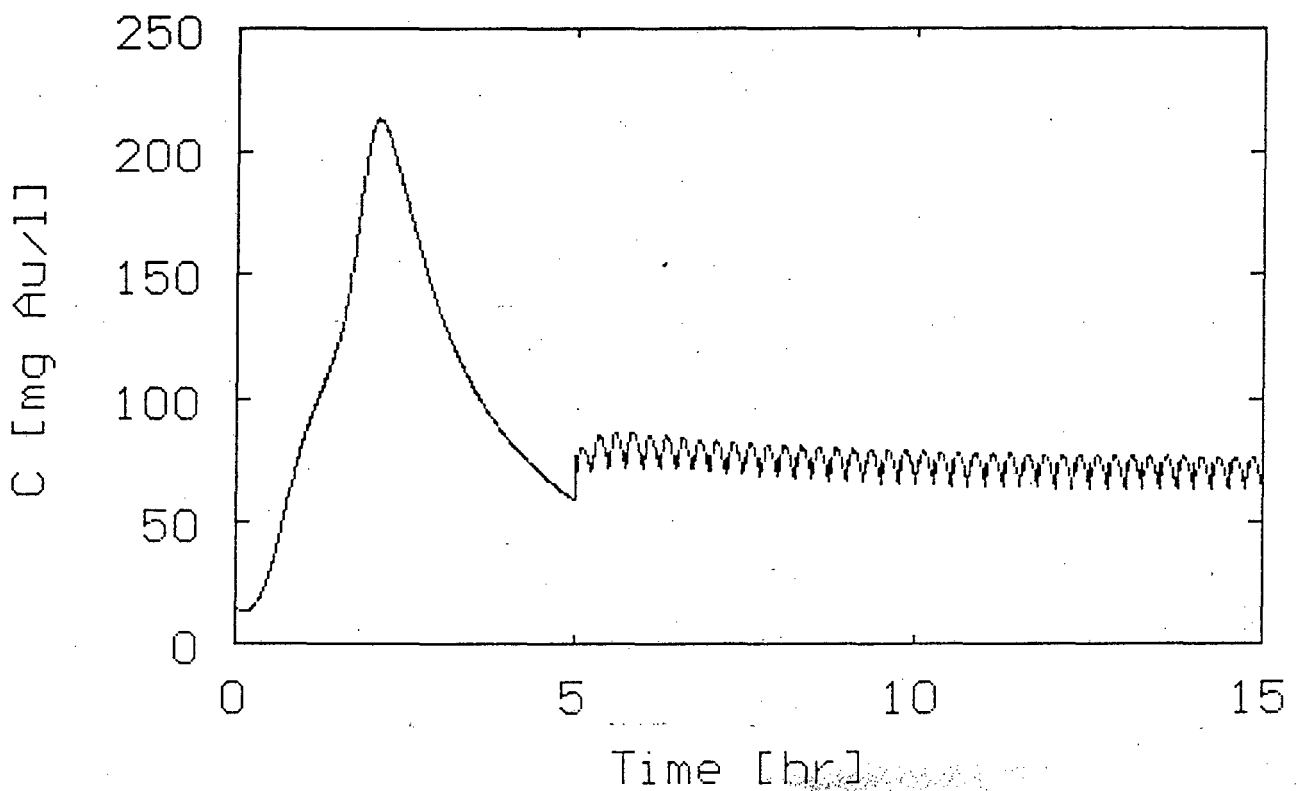


Figure 8.39 Equilibrium model simulation of the gold cyanide profile from a continuous counter-current elution column of twice the height of that in Figure 8.32.

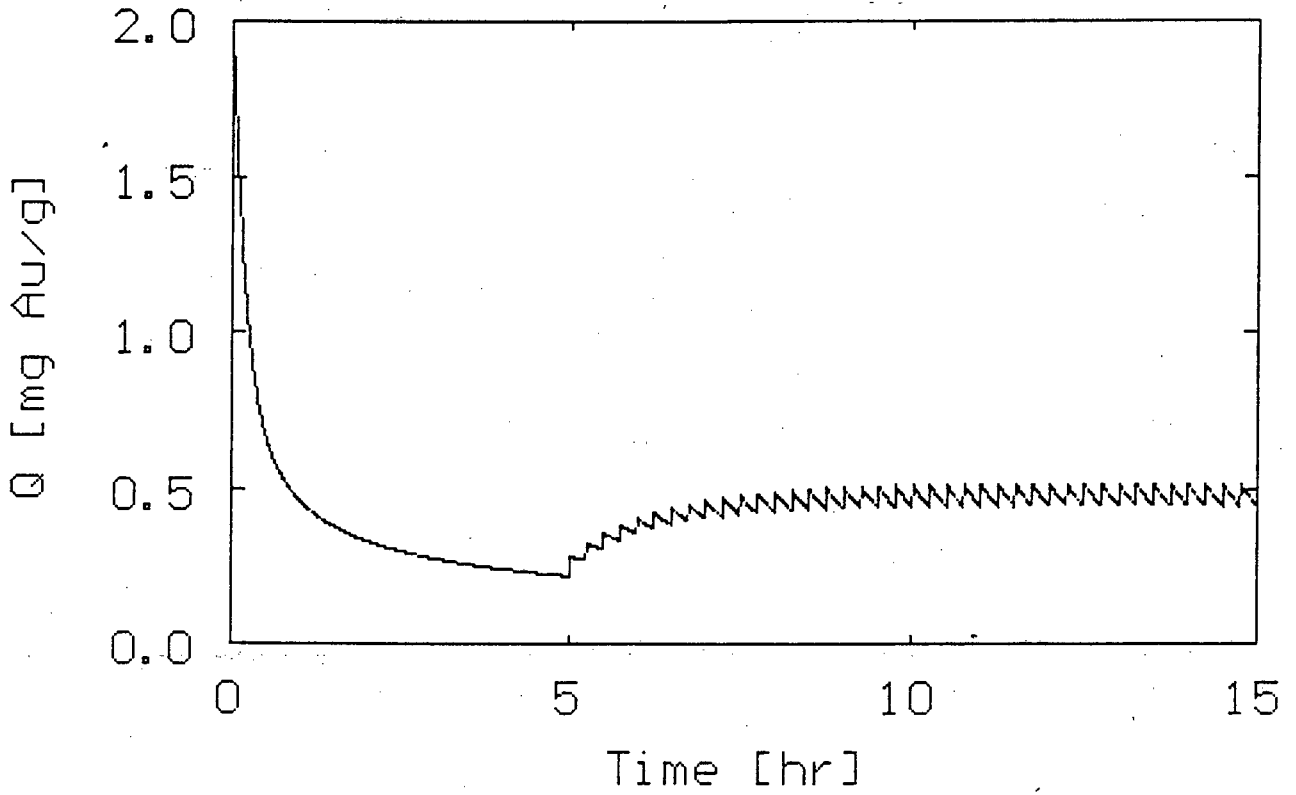


Figure 8.40 Equilibrium model simulation of the eluted carbon loading for the continuous counter-current elution of Figure 8.39.

9

CONCLUSIONS**9.1 CONCLUSIONS AND SIGNIFICANCE**

- (a) Oxygen does not take part in the adsorption reaction of metal cyanides on activated carbon. Although the dissolved oxygen concentration determines the equilibrium metal cyanide loading, the consumption of oxygen by the activated carbon is not increased by the adsorption of metal cyanides. Oxygen is believed to act as a surfactant which, depending on the concentration thereof, can promote or depress the adsorption of metal cyanides.
- (b) Oxygen is not required for the decomposition of $\text{Au}(\text{CN})_2^-$ to AuCN . If this reaction does occur, however, the consumption of oxygen would be increased because of its reaction with the free cyanide that is formed during the formation of AuCN .
- (c) Gold is adsorbed onto activated carbon as $\text{Au}(\text{CN})_2^-$ and AuCN . The ratio of these species is determined by the pH and temperature of the solution, and by the carbon itself. It was found that while some carbons contain both species, others contain only $\text{Au}(\text{CN})_2^-$. Under conditions of high temperature and low pH (as in a hot acid wash), both of these species are reduced to metallic gold, $\text{Au}^{(0)}$.
- (d) The three most important sub-processes occurring during the elution of gold cyanide from activated carbon were identified as the mass transfer and reactions of (i) aurocyanide, (ii) cyanide and (iii) the counter-cations such as K^+ , Na^+ and Ca^{2+} . Because of the effects of (ii) and (iii) on the aurocyanide equilibrium, a kinetic model for the elution of gold cyanide also has to account for changes in the cyanide and cation concentrations.

- (e) Cations (M^{n+}) depress the desorption of gold cyanide by the formation of the neutral $M(Au(CN)_2)_n$ species on the carbon. The formation of this species is promoted by the presence of high concentrations of cations in the solution, as found in the pretreatment step of an AARL elution. The horizontal position of the gold peak in an AARL elution profile is therefore a function of the kinetics of the removal of the cations present in the carbon bed after the pretreatment step.
- (f) The free cyanide present in the wash cycle of an AARL elution is of minor importance in comparison with the cyanide in the pretreatment step. During a cyanide pretreatment, cyanide reacts with the functional groups on the carbon surface and thereby passivates the carbon for the adsorption of anionic metal cyanides. It is this passivation, and not the free cyanide carried over from the pretreatment step, which causes the elution of the gold in the elution step of an AARL elution. The same passivation occurs in a Zadra elution, except that it happens during the elution.
- (g) Under strong elution conditions, the desorption of gold cyanide from activated carbon is no longer diffusion controlled and it becomes insensitive to flow rate and to the initial distribution of gold through the carbon particles. It was shown that the resistance to mass transfer decreased with a reduction in the equilibrium isotherm.
- (h) A general model was developed which describes the change in the free cyanide concentration during both the AARL and Zadra elution procedures. It was found, however, that there is little incentive in simulating the change in cyanide concentration during an AARL elution, because of the low sensitivity of an AARL elution to free cyanide in the elution step.
- (i) Potassium co-adsorbs mainly with CN^- or metalcyanides, such as $Au(CN)_2^-$, onto activated carbon. On the contrary, little adsorption of K^+ could be measured in the presence of a weakly adsorbed anion such as Cl^- . Although it was possible to simulate

the initial removal of the bulk of the potassium from the carbon bed with relatively simple models, the long tail in the measured profiles required the use of a more complicated model which accounted for accumulation in two porous regions with different resistances to mass transfer.

- (j) The proposed equilibrium model was shown to describe the elution of gold cyanide from activated carbon accurately under a wide variety of conditions. This model is a simplification of the fundamentally more correct surface diffusion model. It was only necessary to account for resistance to mass transfer under conditions of poor elution. Such unfavourable elution conditions would however not be acceptable in most industrial applications.
- (k) The equilibrium model was found to be highly sensitive to the gold cyanide equilibrium. Because of the low equilibrium isotherms applicable to the elution process, a small change to the isotherm or to the gold loading on the carbon results in a large shift in the concentration of gold in solution. A constant shift in the equilibrium isotherm can be accomplished with a change in the concentration of organic solvent or cation in the eluant, a change in operating temperature or a change in pretreatment conditions.
- (l) Because of the insensitivity of the elution of potassium and gold cyanide to the h/d ratio of the elution column, the elution profiles obtained from laboratory scale columns will be the same as for full scale columns, provided that large deviations from plug flow do not occur and that the same flow rate of eluant (in bed volumes per hour) is used.
- (m) The fluctuation in the gold concentration in the eluate of a continuous counter-current elution process is a function of the fraction of the carbon bed removed during each transfer of carbon. A higher frequency of carbon transfer at a fixed carbon flow rate will result in a more constant concentration of gold in the eluate.

- (n) For a continuous counter-current elution process with a fixed flow rate of carbon and a fixed gold loading on the eluted carbon, the concentration of gold in the eluate can be increased marginally by the use of a larger elution column. The gold elution efficiency was found, however, to be fairly insensitive to the size or geometry of the column and to carbon transfer rates (for a constant mass flow rate of carbon). Improved gold elution efficiencies from continuous operations will therefore depend on the same factors as batch operated processes, namely higher temperature, better pretreatment and the addition of organic solvents to the eluant.

9.2 RECOMMENDATIONS FOR FUTURE RESEARCH

- (a) Very little is known about the effect of an acid wash and the kinetics of the decomposition reactions of $\text{Au}(\text{CN})_2^-$ to AuCN and $\text{Au}^{(0)}$. The destruction of cyanide in a cyanide pretreatment because of residual acid from the acid wash has never been quantified. It should be investigated if the cyanide in the pretreatment cannot be utilized better if the AARL pretreatment step is split into a hydroxide pretreatment followed by a cyanide pretreatment.
- (b) It was shown that AuCN is formed on certain carbons during the adsorption of gold from alkaline solutions. No answers could however be supplied to why certain carbons promote the decomposition of $\text{Au}(\text{CN})_2^-$. The redox potential of the carbon is one characteristic which will have to be taken into account in such a study.
- (c) No work has yet been published on the reaction kinetics of $\text{Au}^{(0)}$ and AuCN to $\text{Au}(\text{CN})_2^-$ in a cyanide pretreatment. This will have a significant bearing on the minimum time required for a cyanide pretreatment following after an acid wash. It could also affect the desorption kinetics of gold in a Zadra elution if $\text{Au}^{(0)}$ or AuCN is present on the gold loaded carbon.

- (d) Only potassium was considered in the elutions in this thesis. More work is required to account for other cations and mixtures thereof. Furthermore, the model developed for the elution of cations does not account for the adsorption thereof. Because of the large effect of the cation concentration on the gold elution equilibrium, a more accurate model for the elution of the cations will increase the accuracy of the gold elution profiles.
- (e) The competitive adsorption of metal cyanides on activated carbon was investigated by Van Deventer (1986b). However, no work has been published yet in which the competition between different metal cyanides in the elution stage is studied.
- (f) It was illustrated that reactivation of the carbon towards the adsorption of metal cyanides occurs during the elution step of an AARL elution after a cyanide pretreatment at room temperature. This was however not the case at higher pretreatment temperatures. A detailed study is needed to determine the mechanism and kinetics of this reactivation and to determine whether the reactivation is the result of reversible carbon surface reactions with cyanide or just the desorption of some physically adsorbed cyanide.
- (g) The effect of the cyanide pretreatment has not been quantified yet. Elution experiments must be conducted after cyanide pretreatments with various initial cyanide concentrations, different pretreatment periods and different temperatures. It was shown that carbons with the same cyanide-age, but obtained at different pretreatment temperatures, result in different gold elutions. It will therefore be important to distinguish between the effects of adsorbed and decomposed cyanide.
- (h) Cyanide apparently deactivates the carbon surface towards the decomposition of more cyanide. This was studied at room temperature and might be because of the adsorption of cyanide and not the decomposition thereof. The decomposition of cyanide plays an important role in the Zadra elution procedure. It is therefore

necessary to quantify the deactivation of carbon towards cyanide at higher temperatures.

- (i) Although there is little reason to doubt that the models developed in this thesis will be applicable to continuous counter-current elution processes and to elutions with organic solvents, this remains to be proved.

REFERENCES

- Acton, C.F. (1982), "The technology of gold and silver extraction", *AIChE Symposium Series*, 78 (216), pp.127-137.
- Adams, D.M. (1967), "Metal-ligand and related vibrations", Edward Arnold (Publishers) Ltd., London, pp.164 and 172.
- Adams, M.D. (1990a), "The kinetics of the elution of gold from activated carbon by the Zadra method", *Trans. Inst. Min. Metall, Sect.C : Mineral Process. Extr. Metall.*, 99, pp.C71-C79.
- Adams, M.D. (1990b), "The chemical behaviour of cyanide in the extraction of gold. 1. Kinetics of cyanide loss in the presence and absence of activated carbon", *J.S.Afr.Inst.Min.Metall.*, 90 (2), pp.37-44.
- Adams, M.D. and Fleming, C.A. (1989), "The mechanism of adsorption of aurocyanide onto activated carbon", *Metall. Trans. B*, 20B, pp.315-325.
- Adams, M.D. and Nicol, M.J. (1986), "The kinetics of the elution of gold from activated carbon", *Gold 100: Proceedings of the International Conference on Gold*. vol. 2, (eds.) Fivaz, C.E. and King R.P., S.Afr.Inst.Min.Metall., Johannesburg, South Africa, pp. 111-121.
- Adams, M.D., McDougall, G.J. and Hancock, R.D. (1987a), "Models for the adsorption of aurocyanide onto activated carbon. Part II : Extraction of aurocyanide ion pairs by polymeric adsorbents", *Hydrometall.*, 18, pp. 139-154.
- Adams, M.D., McDougall, G.J. and Hancock, R.D. (1987b), "Models for the adsorption of aurocyanide onto activated carbon. Part III : Comparison between the extraction of aurocyanide by activated carbon, polymeric adsorbents and 1-pentanol", *Hydrometall.*, 19, pp. 95-115.
- Bailey, P.R. (1985), "A review of the Zadra process for the elution of gold from activated carbon", Workshop on CIP Technology, Lecture 16 of workshop course presented at Mintek, Johannesburg, pp. 16.1-16.46.
- Bailey, P.R. (1987), "Application of activated carbon to gold recovery", *The Extractive Metallurgy of Gold in South Africa* vol.1, (ed.) Stanley, G.G., Johannesburg, South Africa, SAIMM, pp. 379-614.

- Bernardin, F.E. (1970), "Detoxification of cyanide by adsorption and catalytic oxidation on granular activated carbon", *Proc. 4th Mid-Atlantic Industrial Waste Conference*, Newark, Delaware, pp. 203-228.
- Briggs, A.P.W. (1983), "Problems encountered during the commissioning of the carbon-in-pulp plant at Beisa Mine", *J.S.Afr.Inst.Min.Metall.*, 83 (10), pp. 246-253.
- Brittan, M. (1988), "The AARL carbon elution process", *Randol Gold Forum 88*, Scottsdale, Arizona, pp. 315-320, January 1988.
- Cashion, J.D., McGrath, A.C., Volz, P. and Hall, J.S. (1988), "Direct analysis of gold species on activated carbon by Mössbauer spectroscopy", *Trans. Instn. Min. Metall. (Sect. C: Mineral Process. Extr. Metall.)*, 97, pp. 129-133.
- Cho, E.H. and Pitt, C.H. (1979a), "Kinetics and thermodynamics of silver cyanide adsorption on activated charcoal", *Metall. Trans. B*, 10B, pp. 165-169.
- Cho, E.H. and Pitt, C.H. (1979b), "The adsorption of silver cyanide on activated charcoal", *Metall. Trans. B*, 10B, pp. 159-164.
- Cho, E.H., Dixon, S.N. and Pitt, C.H. (1979), "The kinetics of gold cyanide adsorption on activated carbon", *Metall. Trans. B*, 10B, pp. 185-189.
- Clauss, C.R.A. and Weiss, K. (1977), "Adsorption of aurocyanide on carbon : preliminary screening of functional groups", *CSIR report CENG 206*, Pretoria, 9 p., September 1977.
- Cook, R., Crathorne, E.A., Monhemius, A.J. and Perry, D.L. (1989), "An XPS study of the adsorption of gold(I) cyanide by carbons", *Hydrometall.*, 22, pp. 171-182.
- Costello, M.C., McLean, E. and Burdett, B. (1988), "Gold adsorption, elution and electrowinning of gold ores with up to 4:1 silver to gold ratios", *Randol Conference on Gold and Silver*, Perth, Australia, pp. 273-282, October 1988.
- Cussler, E.L. (1984), "Diffusion, Mass transfer in fluid systems", Cambridge University Press, Cambridge.
- Davidson, R.J. (1974), "The mechanism of gold adsorption on activated charcoal", *J.S.Afr.Inst.Min.Metall.*, 75 (4), pp. 67-76.

- Davidson, R.J. (1986a), "A review of the AARL process for the elution of gold from activated carbon", Lecture 15, S.A.I.M.M. "C.I.P. School", Randburg, 23 p., February 1986.
- Davidson, R.J. (1986b), "A pilot plant study on the effects of cyanide concentration on the CIP process", *Gold 100, Proceedings of the International Conference on Gold*, Vol.2 : Extractive Metallurgy of Gold, Johannesburg, SAIMM, 1986.
- Davidson, R.J. and Duncanson, D. (1977), "The elution of gold from activated carbon using deionized water", *J.S.Afr.Inst.Min.Metall.*, 77 (12), pp. 254-261.
- Davidson, R.J. and Veronese, V. (1979), "Further studies on the elution of gold from activated carbon using water as the eluant", *J.S.Afr.Inst.Min.Metall.*, 79 (19), pp. 437-169.
- Davidson, R.J., Veronese, V. and Nkosi, M.V. (1979), "The use of activated carbon for the recovery of gold and silver from gold-plant solutions", *J.S.Afr.Inst.Min.Metall.*, 79 (10), pp. 281-297.
- Dixon, S., Cho, E.H. and Pitt, C.H. (1978), "The interaction between gold cyanide, silver cyanide, and high surface area charcoal", *A.I.Ch.E. Symposium Series*, 74 (173), pp. 75-83.
- Edeskuty, F.J. and Amundson, N.R. (1952), "Effect of intraparticle diffusion, agitated nonflow adsorption systems", *Ind. Eng. Chem.*, 44 (7), pp. 1698-1703.
- Elmore, C.L., Brison, R.J. and Kenny, C.W. (1988), "The Kamy CILCO process", *Randol Conference on Gold and Silver*, Perth, Australia, pp. 197-201, October 1988.
- Espiell, F., Roca, A., Cruells, M. and Núñez, C. (1987), "Novel procedure for desorption of gold loaded carbon by organic solvent - water mixtures without cyanide", *11th International Precious Metals Institute Conference*, Brussels, June 1987, pp.23-30.
- Espiell, F., Roca, A., Cruells, M. and Núñez, C. (1988), "Gold desorption from activated carbon with dilute NaOH/organic solvent mixtures", *Hydrometall.*, 19, pp. 321-333.
- Finkelstein, N.P. (1972), "The chemistry of the extraction of gold from its ores", *Gold Metallurgy in South Africa*, (ed.) Adamson, Chamber of Mines of S.A., Johannesburg, p. 305.

- Fleming, C.A. (1983), "Recent developments in Carbon-in-pulp technology in South Africa", *Proceedings of the 3rd International Symposium on Hydrometallurgy*, 112th AIME Annual Meeting, Atlanta, Georgia, March 6-10, 1983, pp.839-857.
- Fleming, C.A. (1988), "The loading of gold cyanide onto activated carbon - The reversibility of adsorption and the interpretation of adsorption isotherms", *Mintek Confidential Communication No.530*, Mintek, Johannesburg, 19 pp., 6 June 1980.
- Fritz, W., Merk, W. and Schlünder, E.U. (1981), "Competitive adsorption of two dissolved organics onto activated carbon - II", *Chem. Eng. Sci.*, 36, pp. 731-741.
- Furusawa, T. and Smith, J.M. (1973), "Fluid-particle and intraparticle mass transport rates in slurries", *Ind. Eng. Chem. Fundam.*, 12 (2), pp. 197-203.
- Groszek, A.J. (1970), "Selective adsorption at graphite/ hydrocarbon surfaces", *Proc. Roy. Soc. Lond.*, A.314, pp. 473-498.
- Hall, K.R., Eagleton, L.C., Acrivos, A. and Vermeulen, T. (1966), "Pore- and solid-diffusion kinetics in fixed-bed adsorption under constant-pattern conditions", *Ind. Eng. Chem. Fundam.*, 5 (2), pp. 212-223.
- Hashimoto, K., Miura, K. and Nagata, S. (1975), "Intraparticle diffusivities in liquid-phase adsorption with nonlinear isotherms", *J. Chem. Eng. Japan*, 8 (5), pp. 367-373.
- Hassler, J.W. (1974), "Purification with activated carbon", Chemical Publishing Co., Inc., New York, N.Y., p. 330.
- Hoecker, W. and Muir, D. (1987), "Degradation of cyanide", *Proc. Symp. on Res. and Dev. in Extr. Metall.*, Aus.I.M.M., Adelaide, pp. 29-37, May 1987.
- Hughes, H.C., Muir, D.M., Tsuchida, N. and Dalton, R. (1984), "Oxidation reduction potential of activated carbon during anion loading", *The Aus.I.M.M. Perth and Kalgoorlie Branches, Regional Conference on "Gold-Mining, Metallurgy and Geology"*, pp. 151-157, October 1984.
- Jackson, E. (1986), "Hydrometallurgical extraction and reclamation", John Wiley and Sons, New York, pp.100-108.
- Jansen Van Rensburg, P. (1986), "Mathematical simulation of the adsorption of metal cyanides onto activated carbon in columns", *M.Eng. Thesis*, University of Stellenbosch, 296 p.

- Jansen Van Rensburg, P. and Van Deventer, J.S.J. (1985), "Simulation of adsorption of metal cyanides in packed beds of activated carbon", *Extraction Metallurgy '85, Symp. IMM*, pp. 289-308.
- Jones, W., Klauber, C. and Linge, H.G. (1988), "The adsorption of $\text{Au}(\text{CN})_2^-$ onto activated carbon", *Randol Conference on Gold and Silver*, Perth, Australia, pp. 243-248, October 1988.
- Komiyama, H. and Smith, J.M. (1974a), "Intraparticle mass transport in liquid-filled pores", *A.I.Ch.E.J.*, 20 (4), pp. 728-734.
- Komiyama, H. and Smith, J.M. (1974b), "Surface diffusion in liquid-filled pores", *A.I.Ch.E.J.*, 20 (6), pp. 1110-1117.
- La Brooy, S. and Ariti, J. (1988), "Water conservation in the elution of gold by the Anglo process", *Randol Conference on Gold and Silver*, Perth, Australia, pp. 284-287, October 1988.
- Laxen, P.A., Fleming, C.A., Holtum, D.A. and Rubin, R. (1982), "A review of pilot-plant testwork conducted on the carbon-in-pulp process for the recovery of gold", *Proceedings, 12th CMMI Congress*, H.W. Glen (ed.), Johannesburg, S. Afr. Inst. Min. Metall., pp. 551-560.
- Levenspiel, O. (1972), "Chemical reaction engineering", 2nd ed., John Wiley & Sons, Inc., New York, 578 p.
- Leyva, R.R. (1981), "Surface diffusion in liquid-filled pores of activated carbon", *Ph.D. Thesis*, The Ohio State University, 498 p.
- Mansour, A.R., Shahalam, A.B., Von Rosenberg, D.U. and Sylvester, N.D. (1984), "A general nonequilibrium multicomponent adsorption model: Numerical solution", *Separation Sci. and Tech.*, 19 (8&9), pp. 479-496.
- McDougall, G.J. (1982), "Adsorption on activated carbon", *Chem SA*, pp. 24-27, April 1982
- McDougall, G.J. and Fleming, C.A. (1987), "Extraction of precious metals on activated carbon", *Ion Exchange and sorption processes in hydrometallurgy*, Streat, M. and Naden, D. (eds.), Society of Chemistry and Industry, Wiley, Chichester, pp. 56-126.
- McDougall, G.J., Adams, M.D. and Hancock, R.D. (1987), "Models for the adsorption of aurocyanide onto activated carbon. Part I: Solvent extraction of aurocyanide ion pairs by 1-pentanol", *Hydrometall.*, 18, pp. 125-138.
- McDougall, G.J., and Hancock, R.D. (1980), "Activated carbons and gold - a literature survey", *Minerals Sci. Engng.*, 12 (2), pp.85-99.

- McDougall, G.J., Hancock, R.D., Nicol, M.J., Wellington, O.L. and Copperthwaite, R.G. (1980), "The mechanism of the adsorption of gold cyanide on activated carbon", *J.S.Afr.Inst.Min.Metall.*, 80 (9), pp. 344-356.
- Menne, D. (1987), "The adsorption and desorption of aurocyanide from activated carbon", *Nedpac Engineering Report*, Perth, 25 p..
- Muir, D.M., Aziz, A. and Hoecker, W. (1988), "Cyanide losses under C.I.P. conditions and effect of carbon on cyanide oxidation", *Proc. 1st Int. Hydrometall. Conf.*, Beijing, Eds. Yulian, Z. and Jiazhong, X., Int. Academic Publishers, pp. 461-465, October 1988.
- Muir, D.M., Hinchliffe, W.D. and Griffin, A. (1985a), "Elution of gold from carbon by the Micron Solvent Distillation procedure", *Hydrometall.*, 14, pp. 151-169.
- Muir, D.M., Hinchliffe, W.D. Tsuchida, N. and Ruane, M. (1985b), "Solvent elution of gold from C.I.P. carbon", *Hydrometall.*, 14, pp. 47-65.
- Nicol, M.J. (1986), "Elution theory", Lecture 14, *S.A.I.M.M. "C.I.P. School"*, Randburg, 26 p., February 1986.
- Parentich, A. and Kinsella, B. (1984), "Titrimetric studies on activated carbons", *The Aus.I.M.M. Perth and Kalgoorlie Branches, Regional Conference on "Gold-Mining, Metallurgy and Geology"*, pp.141-149, October 1984.
- Paterson, M.R. (1987), "Atmospheric continuous elution", *Nedpac Engineering Report*, Perth, Western Australia, 22 p.
- Peel, R.G. and Benedeck, A. (1981), "A simplified driving force model for activated carbon adsorption", *Canadian J. Chem. Eng.*, 59, pp. 688-692.
- Prober, R., Pyeha, J.J. and Kidon, W.E. (1975), "Interaction of activated carbon with dissolved oxygen", *A.I.Ch.E.J.*, 21 (6), pp. 1200-1204.
- Satterfield, C.N., Colton, C.K. and Pitcher, W.H. (1973), "Restricted diffusion in liquids within fine pores", *A.I.Ch.E.J.*, 19 (3), pp. 628-635.
- Stange, W. (1990), "The simulation and optimization of the CIP process", *Cyanide in Gold Processing : The next 100 years*, Johannesburg, 5,6 November 1990.
- Stange, W. and King, R.P. (1990), "The optimization of the CIP process", *XXII International Symposium APCOM*, Berlin, West-Germany, pp. 371-382, September 1990.

- Tsuchida, N. (1984), "Studies on the mechanism of gold adsorption and elution in the carbon-in-pulp process", *Ph.D. thesis*, Murdoch University, 212 p.
- Tsuchida, N. and Muir, D.M. (1986a), "Potentiometric studies on the adsorption of $\text{Au}(\text{CN})_2^-$ and $\text{Ag}(\text{CN})_2^-$ onto activated carbon", *Metall. Trans. B*, 17B, pp. 523-528.
- Tsuchida, N. and Muir, D.M. (1986b), "Studies on role of oxygen in the adsorption of $\text{Au}(\text{CN})_2^-$ and $\text{Ag}(\text{CN})_2^-$ onto activated carbon", *Metall. Trans. B*, 17B, pp. 529-533.
- Tsuchida, N., Ruane, M. and Muir, D.M. (1985), "Studies on the mechanism of gold adsorption on carbon", Proceedings of *MINTEK 50 : International conference on mineral science and technology* vol.2, (ed.) Haughton, L.F., MINTEK, South Africa, pp. 647-656.
- Van der Merwe, P.F. and Van Deventer, J.S.J. (1988), "The influence of oxygen on the adsorption of metal cyanides on activated carbon", *Chem. Eng. Commun.*, 65, pp.121-138.
- Van der Merwe, P.F. and Van Deventer, J.S.J. (1990), "Generalized simulation of Zadra and AARL elution columns", *Proc. of 14th Congress of CMMI*, Edinburgh, Scotland, July 1990.
- Van Deventer, J.S.J. (1984), "Kinetic model for the adsorption of metal cyanides on activated charcoal", *Ph.D. Thesis*, University of Stellenbosch, 337 p.
- Van Deventer, J.S.J. (1985), "Kinetic models for the adsorption of gold onto activated carbon", Proceedings of *MINTEK 50 : International conference on mineral science and technology* vol. 2, (ed.) Haughton, L.F., MINTEK, South Africa, pp. 487-494.
- Van Deventer, J.S.J. (1986a), "Kinetic model for the reversible adsorption of gold cyanide on activated carbon", *Chem. Eng. Commun.*, 44, pp. 257-274.
- Van Deventer, J.S.J. (1986b), "Competitive equilibrium adsorption of metal cyanides on activated carbon", *Sep. Sci. and Tech.*, 21 (10), pp. 1025-1037.
- Vegter, N.M., and Sandenbergh, R.F. (1990), "The kinetics of the organic elution of gold cyanide from activated granular carbon", *Cyanide in Gold Processing : The next 100 years*, Johannesburg, 5,6 November 1990.

- Vermeulen, T. (1958), "Separation by adsorption methods", *Advances in Chemical Engineering Vol.2*, Drew, T.B. and Hoopes, J.W. (eds.), Academic Press Inc., New York, pp.148-190.
- Wakeman, R.J. (1976), "Diffusional extraction from hydrodynamically stagnant regions in porous media", *Chem. Eng. J.*, 11, pp. 39-56.
- Weast, R.C. (ed.) (1985), "Handbook of Chemistry and Physics", 64th ed., CRC Press, Inc., Boca Raton, Florida, p.B-95.
- Weber, W. and Chakravorti, R.K. (1974), "Pore and solid diffusion models for fixed-bed adsorbers", *A.I.Ch.E.J.*, 20 (2), pp. 228-238.
- Zadra, J.B. (1950), "A process for the recovery of gold from activated carbon by leaching and electrolysis", *U.S. Bureau of Mines Report of Investigations no.4672*.

APPENDIX A

LEVENSPIEL'S DISPERSION MODEL

Levenspiel (1972) presented a model for high degrees of dispersed plug flow as follows :

$$C_{\theta} = \frac{1}{2\sqrt{\pi\theta(D_L/uh)}} \exp - \frac{(1-\theta)^2}{4\theta(D_L/uh)} \quad [\text{A.1}]$$

The variables C_{θ} and θ in Equation A.1 were defined (Levenspiel, 1972) as :

$$\theta = t/t_{\text{ave}} \quad [\text{A.2}]$$

and

$$C_{\theta} = dF/d\theta = t_{\text{ave}}(dF/dt) \quad [\text{A.3}]$$

with t_{ave} the mean residence time in the reactor, and

$$F = (C_i - C)/C_i \quad [\text{A.4}]$$

By substituting Equation A.4 in A.3, Equation A.3 could be written as :

$$dC/dt = -(C_i/t_{\text{ave}}) \cdot C_{\theta} \quad [\text{A.5}]$$

Equation A.5 could now be integrated from 0 to t to calculate the value of the outlet concentration C at any time t :

$$C = C_i - (C_i/t_{\text{ave}}) \int_0^t C_{\theta} \cdot dt \quad [\text{A.6}]$$

The integral in Equation [A.6] was solved numerically by means of the trapesium rule.

The linear velocity in Equation A.1 was calculated as :

$$u = V/(a \cdot \epsilon) \quad [\text{A.7}]$$

Both t_{ave} and D_L were treated here as unknown parameters to be determined from fitting the model to experimental data. The following values were used in the calculation of the curve in Figure 5.1 :

$$V = 1.5 \times 10^{-8} \text{ m}^3 \cdot \text{s}^{-1}$$

$$\epsilon = 0.292$$

$$a = 1.2 \times 10^{-4} \text{ m}^2$$

$$h = 0.139 \text{ m}$$

$$C_i = 5000 \text{ g} \cdot \text{m}^{-3}$$

$$t_{ave} = 700 \text{ s}$$

$$D_L = 1 \times 10^{-5}$$

APPENDIX B

"STAGNANT REGION" MODEL

A mathematical model was developed (Wakeman, 1976) to describe flow through a packed bed of spherical, porous particles which has been drained before washing. The model accounts for the retainment of solute in the porous particles as well as the particle contact points.

Three partial differential equations were derived to describe material balances for solute in the flow channels around the particles, solute in the stagnant regions at the particle contact points, and solute in the porous particles. These equations were solved by Laplace transformations and the solution to the model presented as a single dimensionless equation as in equation [B.1]. a_1 to a_{13} represent the functional groups given in Equations [B.3] to [B.15].

$$C^* = a_1 \cdot (a_2 + a_3) + a_4 \cdot (a_5 + a_6 + a_7) + a_8 \cdot (a_9 - a_9 \cdot a_{10} + a_{13}) \quad [\text{B.1}]$$

with

$$C^* = (C - C_w) / (C_i - C_w) \quad [\text{B.2}]$$

$$a_1 = s / \{\xi^2 \cdot \pi \cdot W \cdot (1-s)\}^{0.5} \quad [\text{B.3}]$$

$$a_2 = X_1 - 2 \cdot (X_1 - X_2) \cdot \exp\{-\xi^2 \cdot (1-s)/W\} \quad [\text{B.4}]$$

$$a_3 = 2 \sum_{n=0}^{\infty} (-1)^n \cdot \{X_1 - X_2 \cdot (n+2)^2\} \cdot \exp\{-\xi^2 \cdot (n+2)^2 \cdot (1-s)/W\} \quad [\text{B.5}]$$

$$a_4 = 3 \cdot (1-\epsilon) \cdot \epsilon^* / (\epsilon \cdot \eta \cdot \{\pi \cdot W \cdot (1-s)\}^{0.5}) \quad [\text{B.6}]$$

$$a_5 = X_3 - (1/\eta) \cdot \{\pi \cdot W / (1-s)\}^{0.5} \cdot \{1 + 3 \cdot (1-\epsilon) \cdot \epsilon^* / (2 \cdot (1-s) \cdot \epsilon \cdot \eta)\} \quad [\text{B.7}]$$

$$a_6 = 2 \cdot (X_3 - X_4) \cdot \exp\{-\eta^{0.5} \cdot (1-s)/W\} \quad [\text{B.8}]$$

$$a_7 = 2 \sum_{n=0}^{\infty} \{X_3 - X_4 \cdot (n+2)^2\} \cdot \exp\{-\eta^2 \cdot (n+2)^2 \cdot (1-s)/W\} \quad [\text{B.9}]$$

$$a_8 = a_4 \cdot s / \xi \quad [\text{B.10}]$$

$$a_9 = 1 / \{\eta \cdot (1-s)\} \quad [\text{B.11}]$$

$$a_{10} = 2 \sum_{n=0}^{\infty} (-1)^n \cdot \exp\{-\xi^2 \cdot (n+1)^2 \cdot (1-s)/W\} \quad [\text{B.12}]$$

$$a_{11} = -(1-s) \cdot \{(n+1) \cdot \xi^{0.5} + (m+1) \cdot \eta^{0.5}\}^2 / W \quad [\text{B.13}]$$

$$a_{12} = (n+1) \cdot \xi / W + (m+1) \cdot \eta / W \quad [\text{B.14}]$$

$$a_{13} = \sum_{m=0}^{\infty} \sum_{n=0}^{\infty} (-1)^n \cdot a_{12} \cdot \exp(a_{11}) \quad [\text{B.15}]$$

X_1 to X_4 were defined as :

$$X_1 = 1 + \{(1-s)/(4.W)\} \quad [\text{B.16}]$$

$$X_2 = \frac{1}{2} \cdot \{\xi \cdot (1-s)/W\}^2 + (s/W) \quad [\text{B.17}]$$

$$X_3 = X_1 + 3 \cdot (1-\epsilon) \cdot \epsilon^* / (\epsilon \cdot (1-s) \cdot \eta^{0.5}) \quad [\text{B.18}]$$

$$X_4 = \frac{1}{2} \cdot \{\eta \cdot (1-s)/W\}^{0.5} + 3 \cdot (1-\epsilon) \cdot \epsilon^* / (\epsilon \cdot W) \quad [\text{B.19}]$$

Each of Equations B.5, B.9, B.12 and B.15 was approximated here with a finite series with the last term in each series chosen as the first term with an absolute value of less than 1×10^{-6} . Equation [B.1] only becomes valid once the bed is completely filled. The time to fill the bed (t_{fill}) was calculated as :

$$t_{\text{fill}} = (1-s) \cdot h \cdot a \cdot \epsilon / V \quad [\text{B.20}]$$

The rest of the variables in the above equations were calculated as follows :

$$\xi = b \cdot \{u/(D \cdot h)\}^{0.5} \quad [\text{B.21}]$$

$$\eta = (d_c/2) \cdot \{u/(D^* \cdot h)\}^{0.5} \quad [\text{B.22}]$$

$$W = u \cdot t \cdot (1-s)/h \quad [\text{B.23}]$$

$$\epsilon^* = V_p \cdot \rho \quad [\text{B.24}]$$

with

$$u = V / \{\epsilon \cdot a \cdot (1-s)\} \quad [\text{B.25}]$$

The following nomenclature is not defined in the thesis and is used only in Appendix B :

- b Side channel length [m], Estimated as $0.38 \cdot d_c$ (Wakeman, 1976)
- C Solute concentration in eluate [$\text{g} \cdot \text{m}^{-3}$]
- C_w Solute concentration in feed [$\text{g} \cdot \text{m}^{-3}$]
- C_i Initial solute concentration in retained liquid [$\text{g} \cdot \text{m}^{-3}$]
- D Diffusivity of solute from side pores [$\text{m}^2 \cdot \text{s}^{-1}$]

- D^* Diffusivity of solute from particles [$m^2.s^{-1}$]
 s Saturation volume of retained liquor per unit volume of bed voids external to the particles
 u Solvent velocity [$m.s^{-1}$]
 W Voids volume of solvent as defined in Eq. B.23
 ϵ^* Porosity of particles
 ξ Mass transfer parameter defined in Eq. B.21
 η Mass transfer parameter defined in Eq. B.22

The following values were used in the calculation of the curve in Figure 5.2 :

$$d_c = 0.00142 \text{ m}$$

$$V = 3.7 \times 10^{-6} \text{ m}^3.s^{-1}$$

$$\epsilon = 0.292$$

$$V_p = 6.3 \times 10^{-4} \text{ m}^3.kg^{-1}$$

$$\rho = 838.8 \text{ kg.m}^{-3}$$

$$a = 7.9 \times 10^{-3} \text{ m}^2$$

$$h = 0.749 \text{ m}$$

$$C_i = 15000 \text{ g.m}^{-3}$$

$$C_w = 0 \text{ g.m}^{-3}$$

$$D = 1 \times 10^{-9} \text{ m}^2.s^{-1}$$

$$D^* = 1 \times 10^{-11} \text{ m}^2.s^{-1}$$

$$s = 0.15$$

APPENDIX C

PORE DIFFUSION MODEL WITH NO RESISTANCE TO FILM TRANSPORT

Assumptions

1. Spherical particles
2. The pores of the particles are subdivided in macro and micropores. A volume fraction β_K of the pores is considered as macropores for the diffusion of the cation.
3. The adsorption of the cation is negligible.
4. Resistance to mass transfer through the external liquid layer around the particles is negligible.

Macropore mass balance

A mass balance over the macropores in a radial section (thickness = Δr) of the particle is given by :

$$\beta_K \cdot \Delta r \cdot 4\pi r^2 \cdot \rho \cdot V_p \frac{\partial C_{Km}}{\partial t} = 4\pi (r^2 \bar{n})_{r+\Delta r} - 4\pi (r^2 \bar{n})_r - \Delta r \cdot 4\pi r^2 \cdot \rho \cdot V_p \cdot k_b (C_{Km} - C_{Kb}) \quad [C.1]$$

Divide by $4\pi r^2$ and let $\Delta r \rightarrow 0$. Equation [C.1] then becomes :

$$\beta_K \cdot r^2 \cdot \rho \cdot V_p \frac{\partial C_{Km}}{\partial t} = \frac{\partial (r^2 \bar{n})}{\partial r} - r^2 \cdot \rho \cdot V_p \cdot k_b (C_{Km} - C_{Kb}) \quad [C.2]$$

The mass flux is calculated from Fick's law as :

$$\bar{n} = \beta_K \cdot \rho \cdot V_p \cdot D_p \frac{\partial C_{Km}}{\partial r} \quad [C.3]$$

Substitution of Equation C.3 in C.2 yields :

$$\beta_K \cdot r^2 \frac{\partial C_{Km}}{\partial t} = \beta_K \cdot D_p \frac{\partial}{\partial r} r^2 \frac{\partial C_{Km}}{\partial r} - r^2 \cdot k_b (C_{Km} - C_{Kb}) \quad [C.4]$$

The average concentration of cation in the macropores, $C_{Km,ave}$, and the

micropores, $C_{Kb,ave}$, are defined as :

$$C_{Km,ave} = \frac{3}{R^3} \int_0^R C_{Km} \cdot r^2 \cdot dr \quad \text{and} \quad [C.5]$$

$$C_{Kb,ave} = \frac{3}{R^3} \int_0^R C_{Kb} \cdot r^2 \cdot dr \quad [C.6]$$

Integration of Equation C.4 from $r=0$ to R and substitution with Equations C.5 and C.6 yield :

$$\frac{dC_{Km,ave}}{dt} = \frac{3D_p}{R} \left. \frac{\partial C_{Km}}{\partial r} \right|_{r=R} - \frac{k_b}{\beta_K} (C_{Km,ave} - C_{Kb,ave}) \quad [C.7]$$

Hall *et al.* (1966) approximated the loading gradient at the external particle surface by a quadratic driving force. It was assumed here that a similar gradient exists for the liquid phase concentration at the particle surface and that this can be written as :

$$\left. \frac{\partial C_{Km}}{\partial r} \right|_{r=R} = \frac{5\psi}{R} \frac{(C_K^{(j)})^2 - C_{Km,ave}^2}{2C_{Km,ave}} \quad [C.8]$$

where $C_K^{(j)}$ is the interparticle concentration in the j 'th height section of the column. By replacing the concentration gradient at the surface with Equation C.8, Equation C.7 changes to :

$$\frac{dC_{Km,ave}}{dt} = \frac{60\Gamma_p}{d_c^2} \frac{(C_K^{(j)})^2 - C_{Km,ave}^2}{2C_{Km,ave}} - \frac{k_b}{\beta_K} (C_{Km,ave} - C_{Kb,ave}) \quad [C.9]$$

$$\text{where } \Gamma_p = \psi \cdot D_p \quad [C.10]$$

To avoid the derivative in Equation C.9 to become infinite when the macropore concentration is zero, a similar transformation was made as that used by Van Deventer (1984) :

$$\text{Let } c_{Km} = C_{Km,ave}^2 \quad [C.11]$$

Equation C.9 thus changes to :

$$\frac{dc_{Km}}{dt} = \frac{60\Gamma_p}{d_c^2} \{ (C_K^{(j)})^2 - c_{Km} \} - \frac{2k_b}{\beta_K} (c_{Km} - C_{Kb,ave} \cdot c_{Km}^{\frac{1}{2}}) \quad [C.12]$$

Micropore mass balance

As for the macropores, a mass balance over the micropores yields :

$$(1-\beta_K) \cdot \Delta r \cdot 4\pi r^2 \cdot \rho \cdot V_p \frac{\partial C_{Kb}}{\partial t} = \Delta r \cdot 4\pi r^2 \cdot \rho \cdot V_p \cdot k_b (C_{Km} - C_{Kb}) \quad [C.13]$$

By doing the same integration and substitutions as shown in Equations C.5, C.6 and C.11, Equation C.13 becomes :

$$(1-\beta_K) \frac{dC_{Kb}}{dt} = k_b (c_{Km}^{\frac{1}{2}} - C_{Kb}) \quad [C.14]$$

Interparticle mass balance

A mass balance over the interparticle solution in the j'th height section of the column is :

$$a \cdot \Delta h \cdot \epsilon \frac{dC_K^{(j)}}{dt} = V(C_K^{(j-1)} - C_K^{(j)}) - \bar{n}_{r=R} \cdot a \cdot \Delta h \cdot (1-\epsilon) \cdot a_c \quad [C.15]$$

For a spherical particle :

$$a_c = 6/d_c \quad [C.16]$$

The mass flux, $\bar{n}_{r=R}$, is obtained by combining Equations C.3, C.8, C.10 and C.11. Equation C.15 then becomes :

$$\frac{dC_K^{(j)}}{dt} = m_1 (C_K^{(j-1)} - C_K^{(j)}) - m_2 \frac{(C_K^{(j)})^2 - c_{Km}}{c_{Km}^{\frac{1}{2}}} \quad [C.17]$$

with

$$m_1 = -V/(a \cdot \Delta h \cdot \epsilon) \quad \text{and} \quad [C.18]$$

$$m_2 = 30 \cdot D_p \cdot \beta_K \cdot (1-\epsilon) \cdot V_p \cdot \rho / (d_c^2 \cdot \epsilon) \quad [C.19]$$

Numerical solution

By dividing the column in N equal height increments, Equations C.12, C.14 and C.17 could be solved simultaneously for $j=1$ to N at each time interval with a Runge Kutta method as shown in Appendix D. The concentration at $j=0$ was taken as constant and equal to the concentration in the eluant.

The following parameters and boundary conditions were used in the simulations in Figures 5.3 to 5.5 :

$$d_c = 0.00142 \text{ m}$$

$$\rho = 838.8 \text{ kg.m}^{-3}$$

$$\epsilon = 0.292$$

$$V_p = 6.34 \times 10^{-4} \text{ m}^3.\text{kg}^{-1}$$

$$a = 1.2 \times 10^{-4} \text{ m}^2$$

$$h = 0.143 \text{ m}$$

$$N = 10$$

$$\Delta t = 10 \text{ s}$$

$$C_{K_m}(t=0,j) = C_{K_b}(t=0,j) = 14000 \text{ g.m}^{-3}, \text{ thus } c_{K_m}(t=0,j) = 1.96 \times 10^8 \text{ g}^2.\text{m}^{-6}$$

$$C_K(t=0,j) = C_K(t,j=0) = 0 \text{ g.m}^{-3}$$

Figure	5.3	5.4	5.5
$V \text{ [m}^3.\text{s}^{-1}\text{]}$	1.4×10^{-8}	1.4×10^{-8}	17.6×10^{-8}
$\Gamma_p \text{ [m}^2.\text{s}^{-1}\text{]}$	8×10^{-11}	1.5×10^{-10}	1.5×10^{-10}
$k_b \text{ [s}^{-1}\text{]}$	1×10^{-15}	3.0×10^{-5}	3.0×10^{-5}
β_K	0.999	0.6	0.6

APPENDIX D

EXAMPLE OF 4TH-ORDER RUNGA KUTTA METHOD

Let the set of ordinary differential equations be :

$$(dC_1/dt) = f_1(C_1, C_2) \quad [D.1]$$

$$(dC_2/dt) = f_2(C_1, C_2, C_3) \quad [D.2]$$

$$(dC_3/dt) = f_3(C_1, C_3) \quad [D.3]$$

The following K-values are now defined :

$$K_{1,1} = \Delta t \cdot f_1(C_1^{(t)}, C_2^{(t)}) \quad [D.4]$$

$$K_{1,2} = \Delta t \cdot f_2(C_1^{(t)}, C_2^{(t)}, C_3^{(t)}) \quad [D.5]$$

$$K_{1,3} = \Delta t \cdot f_3(C_1^{(t)}, C_3^{(t)}) \quad [D.6]$$

$$K_{2,1} = \Delta t \cdot f_1(C_1^{(t)} + \frac{1}{2}K_{1,1}, C_2^{(t)} + \frac{1}{2}K_{1,2}) \quad [D.7]$$

$$K_{2,2} = \Delta t \cdot f_2(C_1^{(t)} + \frac{1}{2}K_{1,1}, C_2^{(t)} + \frac{1}{2}K_{1,2}, C_3^{(t)} + \frac{1}{2}K_{1,3}) \quad [D.8]$$

$$K_{2,3} = \Delta t \cdot f_3(C_1^{(t)} + \frac{1}{2}K_{1,1}, C_3^{(t)} + \frac{1}{2}K_{1,3}) \quad [D.9]$$

$$K_{3,1} = \Delta t \cdot f_1(C_1^{(t)} + \frac{1}{2}K_{2,1}, C_2^{(t)} + \frac{1}{2}K_{2,2}) \quad [D.10]$$

$$K_{3,2} = \Delta t \cdot f_2(C_1^{(t)} + \frac{1}{2}K_{2,1}, C_2^{(t)} + \frac{1}{2}K_{2,2}, C_3^{(t)} + \frac{1}{2}K_{2,3}) \quad [D.11]$$

$$K_{3,3} = \Delta t \cdot f_3(C_1^{(t)} + \frac{1}{2}K_{2,1}, C_3^{(t)} + \frac{1}{2}K_{2,3}) \quad [D.12]$$

$$K_{4,1} = \Delta t \cdot f_1(C_1^{(t)} + K_{2,1}, C_2^{(t)} + K_{2,2}) \quad [D.13]$$

$$K_{4,2} = \Delta t \cdot f_2(C_1^{(t)} + K_{2,1}, C_2^{(t)} + K_{2,2}, C_3^{(t)} + K_{2,3}) \quad [D.14]$$

$$K_{4,3} = \Delta t \cdot f_3(C_1^{(t)} + K_{2,1}, C_3^{(t)} + K_{2,3}) \quad [D.15]$$

The integrated equations D.1 to D.3 are written in terms of these K-values as :

$$C_1^{(t+\Delta t)} = C_1^{(t)} + (K_{1,1} + 2K_{2,1} + 2K_{3,1} + K_{4,1})/6 \quad [D.16]$$

$$C_2^{(t+\Delta t)} = C_2^{(t)} + (K_{1,2} + 2K_{2,2} + 2K_{3,2} + K_{4,2})/6 \quad [D.17]$$

$$C_3^{(t+\Delta t)} = C_3^{(t)} + (K_{1,3} + 2K_{2,3} + 2K_{3,3} + K_{4,3})/6 \quad [D.18]$$

APPENDIX E

SOLUTION OF COMBINATION MODEL WITH A LINEAR ISOTHERM

The relationship between C_m and Q_m with a linear equilibrium isotherm is :

$$Q_m = A \cdot C_m \quad [E.1]$$

Equations 6.6, 6.7 and 6.10 can thus be written as a function of C , C_m and Q_b as follows :

$$(\alpha A + \beta V_p) \frac{\partial C_m}{\partial t} = (\alpha D_s A + \beta D_p V_p) \frac{\partial^2 C_m}{\partial r^2} - k_b (A C_m - Q_b) + \frac{2(\alpha D_s A + \beta D_p V_p)}{r} \frac{\partial C_m}{\partial r} \quad [E.2]$$

$$(1 - \alpha) \frac{\partial Q_b}{\partial t} = k_b (A C_m - Q_b) \quad [E.3]$$

and,

$$k_s (C - C_{m, r=R}) = (\alpha D_s \rho A + \beta D_p \rho V_p) \left. \frac{\partial C_m}{\partial r} \right|_{r=R} \quad [E.4]$$

Numerical solution for a batch reactor

The mass balance over the liquid phase in a stirred batch reactor is written as :

$$v \frac{dC}{dt} = \frac{6k_s m_c}{\rho d_c} (C_{m, r=R} - C) \quad [E.5]$$

Equations E.2 to E.5 were discretised by substituting the derivatives with finite difference approximations as follows :

$$\frac{dC}{dt} = \frac{C(t+\Delta t) - C(t)}{\Delta t} \quad [E.6]$$

$$\frac{\partial C_m}{\partial t} = \frac{C_m(t+\Delta t, r) - C_m(t, r)}{\Delta t} \quad [E.7]$$

$$\frac{\partial C_m}{\partial r} = \frac{C_m(t+\Delta t, r+\Delta r) - C_m(t+\Delta t, r)}{\Delta r} \quad [E.8]$$

$$\frac{\partial^2 C_m}{\partial r^2} = \frac{C_m(t+\Delta t, r+\Delta r) - 2C_m(t+\Delta t, r) + C_m(t+\Delta t, r-\Delta r)}{(\Delta r)^2} \quad [E.9]$$

$$\frac{\partial Q_b}{\partial t} = \frac{Q_b(t+\Delta t, r) - Q_b(t, r)}{\Delta t} \quad [E.10]$$

and setting

$$C_m = C_m(t+\Delta t, r) \quad [E.11]$$

$$C = C(t+\Delta t) \quad [E.12]$$

$$Q_b = Q_b(t+\Delta t, r) \quad [E.13]$$

With the above substitutions, Equation E.3 changes to :

$$(M_1+1)Q_b(t+\Delta t, r) - AM_1C_m(t+\Delta t, r) = Q_b(t, r) \quad [E.14]$$

with

$$M_1 = k_b \cdot \Delta t / (1-\alpha) \quad [E.15]$$

Equation E.5 becomes :

$$(M_2+1)C(t+\Delta t) - M_2C_m(t+\Delta t, R) = C(t) \quad [E.16]$$

with

$$M_2 = 6k_s m_c \cdot \Delta t / (\rho d_c v) \quad [E.17]$$

and Equation E.4 changes to :

$$C_m^{(t+\Delta t, R+\Delta r)} = (1-M_3)C_m^{(t+\Delta t, R)} + M_3C_m^{(t+\Delta t)} \quad [E.18]$$

with

$$M_3 = \frac{\Delta r \cdot k_s}{\beta D_p \rho V_p + \alpha A D_s \rho} \quad [E.19]$$

Equation E.2 can be discretized within the boundaries of $0 < r < R$ to yield :

$$-(M_7+M_4+M_8+M_5)C_m^{(t+\Delta t, r+\Delta r)} - (M_7+M_4)C_m^{(t+\Delta t, r-\Delta r)} - k_b Q_b^{(t+\Delta t, r)} + (M_9+M_6+2M_7+2M_4+M_8+M_5+k_b A)C_m^{(t+\Delta t, r)} = (M_9+M_6)C_m^{(t, r)} \quad [E.20]$$

where

$$M_4 = \beta D_p V_p / (\Delta r)^2 \quad [E.21]$$

$$M_5 = 2M_4 \cdot \Delta r / r \quad [E.22]$$

$$M_6 = \beta V_p / \Delta t \quad [E.23]$$

$$M_7 = \alpha D_s A / (\Delta r)^2 \quad [E.24]$$

$$M_8 = 2\alpha D_s A / (r \cdot \Delta r^2) \quad [E.25]$$

$$M_9 = \alpha A / \Delta t \quad [E.26]$$

Special provision has to be made to enable the use of Equation E.2 when $r=0$. By assuming that C_m is symmetric with relation to the center of the particle, the derivative of C_m at $r=0$ is :

$$\left. \frac{\partial C_m}{\partial r} \right|_{r=0} = 0 \quad [E.27]$$

It then follows from the Taylor expansion :

$$\left. \frac{\partial C_m}{\partial r} \right|_r = \left. \frac{\partial C_m}{\partial r} \right|_{r=0} + \left. \frac{\partial^2 C_m}{\partial r^2} r \right|_{r=0} + O(r^2) \quad [E.28]$$

that

$$\lim_{r \rightarrow 0} \frac{1}{r} \left. \frac{\partial C_m}{\partial r} \right|_r = \left. \frac{\partial^2 C_m}{\partial r^2} \right|_{r=0} \quad [E.29]$$

Furthermore, because of the symmetry :

$$C_m(t, \Delta r) = C_m(t, -\Delta r) \quad [E.30]$$

By substituting Equation E.29 in E.2, Equation E.2 can now be discretized at $r=0$ to give :

$$\begin{aligned} (M_9 + M_6 + 6M_7 + 6M_4 + k_b A) C_m(t + \Delta t, 0) - 6(M_7 + M_4) C_m(t + \Delta t, \Delta r) \\ - k_b Q_b(t + \Delta t, 0) = (M_9 + M_6) C_m(t, 0) \end{aligned} \quad [E.31]$$

If r is substituted with R in Equation E.20, the term $C_m(t + \Delta t, R + \Delta r)$ is produced. This can be eliminated by substitution with Equation E.18. At $r=R$ Equation E.20 thus becomes :

$$\begin{aligned} \{ (M_7 + M_4 + M_8 + M_5)(M_1 - 1) + M_9 + M_6 + 2M_7 + 2M_4 + M_8 + M_5 + k_b A \} \cdot C_m(t + \Delta t, R) \\ - (M_7 + M_4) C_m(t + \Delta t, R - \Delta r) - k_b Q_b(t + \Delta t, R) - M_1(M_7 + M_4 + M_8 + M_5) C(t + \Delta t) \\ = (M_9 + M_6) C_m(t, R) \end{aligned} \quad [E.32]$$

Equations E.14, 16, 20, 31 and 32 can be written in matrix form as follows :

$$B \cdot \begin{bmatrix} C_m(t + \Delta t, 0) \\ C_m(t + \Delta t, \Delta r) \\ C_m(t + \Delta t, 2\Delta r) \\ \\ C_m(t + \Delta t, R) \\ Q_b(t + \Delta t, 0) \\ Q_b(t + \Delta t, \Delta r) \\ Q_b(t + \Delta t, 2\Delta r) \\ \\ Q_b(t + \Delta t, R) \\ C(t + \Delta t) \end{bmatrix} = \begin{bmatrix} (M_9 + M_6) C_m(t, 0) \\ (M_9 + M_6) C_m(t, \Delta r) \\ (M_9 + M_6) C_m(t, 2\Delta r) \\ \\ (M_9 + M_6) C_m(t, R) \\ Q_b(t, 0) \\ Q_b(t, \Delta r) \\ Q_b(t, 2\Delta r) \\ \\ Q_b(t, R) \\ C(t) \end{bmatrix} \quad [E.33]$$

The matrix in Equation E.33 has to be solved at each time step to produce the concentrations at $(t + \Delta t)$.

It was assumed that all the gold on the loaded carbon was present in the adsorbed state. The initial macro pore concentrations in the elution were thus calculated from the final loading in the adsorption ($Q_m^{(ads,r)}$) by a mass balance over the macro pores :

$$\alpha Q_m^{(0,r)} + \beta V_p C_m^{(0,r)} = \alpha Q_m^{(ads,r)} \quad [E.34]$$

By substituting $Q_m^{(0,r)}$ with the linear isotherm expression, Equation E.34 becomes :

$$C_m^{(t=0,r)} = \alpha Q_m^{(ads,r)} / (\alpha A + \beta V_p) \quad [E.35]$$

The values of the parameters used for the simulations in Chapter 6 with this model are :

$$C^{(0)} = 0 \text{ g.m}^{-3}$$

$$Q_m^{(0,r)} = Q_b^{(0,r)} = Q^{(ads)} = 10 \text{ g.kg}^{-1}$$

$$m_c = 0.01 \text{ kg}$$

$$v = 0.001 \text{ m}^3$$

$$k_s = 1 \times 10^{-5} \text{ m.s}^{-1}$$

$$\alpha = 0.4$$

$$\beta = 0.95$$

$$k_b = 1 \times 10^{-5} \text{ s}^{-1}$$

$$d_c = 0.00142 \text{ m}$$

$$\Delta r = 0.000142 \text{ m}$$

$$\rho = 838.8 \text{ kg.m}^{-3}$$

$$V_p = 6.34 \times 10^{-4} \text{ m}^3.\text{kg}^{-1}$$

The values of the macropore diffusivities and isotherm constants are given in the respective figure captions.

APPENDIX F

THE RELATIONSHIP BETWEEN α AND β

The following nomenclature is defined for use in this appendix only :

Pore	Macro	Micro
Pore diameter [m]	D	d
Pore length [m]	L	l
Pore volume [m ³]	V	v
Fraction of pore area	α	1- α
Fraction of pore volume	β	1- β
Total pore area [m ²]	A	

The total equivalent length of the pores can be calculated for specific diameters, D and d, from the total pore area as follows :

$$L = \alpha.A/(\pi.D) \quad [F.1]$$

$$l = (1-\alpha).A/(\pi.d) \quad [F.2]$$

The volume of the macropores is :

$$V = \frac{1}{4}.\pi.D^2.L = \frac{1}{4}.\pi.\beta.(D^2.L + d^2.l) \quad [F.3]$$

By substituting L and l with Equations F.1 and F.2, Equation F.3 becomes :

$$1/\beta = 1 + \frac{(1-\alpha)d}{\alpha D} \quad [F.4]$$

Macropores and micropores are classified (McDougall and Hancock, 1980) in terms of their diameters as follows :

Macropores : D = 50 to 2000 nm

Micropores : d = 0.8 to 5 nm.

It follows from these diameters that :

$$(d/D)_{\max} = 0.1 \quad [F.5]$$

$$(d/D)_{\min} = 0.0004 \quad [F.6]$$

The range of β can now be calculated from Equations F.4 to F.6 for a given value of α .

A typical value of α for the adsorption of metal cyanides onto activated carbon is 0.4 (Van Deventer, 1984, Jansen van Rensburg, 1986). For $\alpha = 0.4$, the macropore volume fraction is calculated as $0.87 \leq \beta \leq 0.999$. This means that even though more than half of the adsorption area is found in the micropores, the macropores contain nearly all of the pore volume.

APPENDIX G

TURBO PASCAL PROGRAM FOR COMBINATION MODEL WITH LINEAR ISOTHERM

This program solves the matrix (Equation E.33) presented in Appendix E. The program was written in Turbo Pascal version 4.0 and uses the unit "grph" presented in Appendix J for the creation of menu's and graphics. The output of the program is in the form of a graph of solute concentration or fractional desorption versus time.

Structure of main program

A flow scheme of the main program is presented in Figure G.1.

The program starts by setting the input parameters equal to default values stored in a text file called "parslin.dat". This file should contain a vertical list of the values of the parameters and conditions in the same order as specified in procedure "defaults". These default values are displayed and the user is given the opportunity to make changes to them. Once the input of data is completed, the screen is put into graphics mode by procedure "init" (see Appendix J), an axes system is drawn and experimental points are plotted if required. Files containing experimental concentration vs. time data should be in ASCII format with one t and one C-value, separated by one or more spaces, per line. The program will now perform procedure "model" in which the concentration vs. time profile is calculated and plotted as a curve on the screen. When the maximum specified time is reached, or the 'Q' key is pressed, the calculation of further values is stopped and the graph will remain on the screen until the ENTER key [CR] is pressed. A menu is then displayed from which the user can choose to change the input values, to repeat the calculation with the new values, or to quit the program. Before leaving the program, the user will be asked whether the input values should be saved so that they can be used as defaults for a next run.

Algorithm of procedure "model" (Figure G.2)

The concentration vs. time profile is calculated in procedure "model". This procedure starts by setting the time equal to 0. It then sets the initial values of the interparticle concentration, $C[0]$, and the loading in the micropores, $Qb[0]$. The loading and concentration in the macropores, $Qm[0]$ and $Cm[0]$, are calculated with the mass balance presented in Equation E.35. As a changing time-step length is used, the values of constants which are independent of Δt , such as m_3 , are calculated outside the time loop. The time-step length is increased from 1/60 sec to a maximum of 120 sec with a 1/60 sec increment every time the time loop is repeated. The small initial time-step lengths ensure stability of the integration procedure. Once Δt is calculated, the time is set at $(t+\Delta t)$ and the extended matrix B (including the array $[(M_9+M_6)C_m^{(t,0)} \dots C^{(t)}]$ in Equation E.33) is constructed. After the matrix is solved, the values of the concentrations at $(t+\Delta t)$, i.e. $C[1]$, $Qb[1]$, $Qm[1]$ and $Cm[1]$, are calculated by back substitution and the result plotted on the screen. The initial concentrations for the next time step are then set equal to the values calculated for the present time. The time loop is repeated until the maximum specified time is reached or the 'Q' key is pressed.

As Turbo Pascal does not distinguish between normal, uppercase, superscript and subscript characters, the following nomenclature was used in procedure "model" :

Program	Thesis	Program	Thesis	Program	Thesis
a	A	dens	ρ	Qb	Q_b
alfa	α	Dp	D_p	Qbo	Q_{bi}
beta	β	dr	Δr	Qi	Q_i
C	C	Ds	D_s	Qm	Q_m
Ci	C_i	kb	k_b	Qmo	Q_{mi}
Cm	C_m	ks	k_s	time	t
dc	d_c	m1-m9	M_{1-9}	vol	v
delt	Δt	mc	m_c	Vp	V_p

Program listing

```

program parslin;
uses crt,graph,grph;

const k=5;                                     {number of radial increments}
      mmks=12;                                 {mmks=(2*k)+2}
      mmkspl=13;                              {mmkspl=mmks+1}
var   rn,cred,a,vol,mc,dc,dens,Ci,Dp,Ds, kb,ks,alfa,beta,
      Qi,dummy,Qt, hours,dr,m1,m2,m3,m4,m6,m7,m9,Vp,delt,time:double;
      C:array[0..1] of double;
      Cm,Qb:array[0..k,0..1] of double;
      Q,Qmo,Qbo,Qm:array[0..k] of double;
      m5,m8:array[1..k] of double;
      B:array[0..mmks,0..mmkspl] of double;   {B[row,column]}
      cntn,chg:yn;
      wrn,n,tel,mde,ver,rpt:integer;
      st:text;
      xx,yy:pnt;
      nxy:array[1..4] of integer;

procedure model;                               {start of model}
begin
  time:=0;
  C[0]:=Ci;
  dr:=dc/(2*k);
  for j:=0 to k do Qb[j,0]:=Qbo[j];
  for j:=0 to k do
    begin
      Cm[j,0]:=alfa*Qmo[j]/(alfa*a+beta*Vp);
      Qm[j]:=a*Cm[j,0];
    end;
  case mde of 1: cred:=Ci;
              2: cred:=0;
              end;
  moveto(xscr(time),yscr(cred));
  m3:=dr*ks/(beta*Dp*dens*Vp+alfa*a*Dp*dens);
  m4:=beta*Vp*Dp/sqr(dr);
  m7:=alfa*Dp*a/sqr(dr);
  for j:=1 to k do
    begin
      m5[j]:=2*m4/j;
      m8[j]:=2*alfa*Dp*a/(j*sqr(dr));
    end;
  tel:=0;
repeat                                     {time loop}
  tel:=tel+1;
  delt:=tel/60;
  if delt>120 then delt:=120;
  m1:=kb*delt/(1-alfa);
  m2:=6*ks*mc*delt/(dens*dc*vol);
  m6:=beta*Vp/delt;
  m9:=alfa*a/delt;
  time:=time+delt;
  hours:=time/3600;

```

```

for j:=0 to mmks do for i:=0 to mmkspl do B[j,i]:=0;

j:=0;
B[j,0]:=m9+m6+6*m7+6*m4+kb*a;
B[j,1]:=-6*(m4+m7);
B[j,k+1]:=-kb;
B[j,mmkspl]:=(m6+m9)*Cm[j,0];

for j:=1 to (k-1) do
  begin
    B[j,j-1]:=-(m4+m7);
    B[j,j]:=m9+m6+2*m7+2*m4+m8[j]+m5[j]+kb*a;
    B[j,j+1]:=-(m4+m5[j]+m8[j]+m7);
    B[j,k+j+1]:=-kb;
    B[j,mmkspl]:=(m6+m9)*Cm[j,0];
  end;

j:=k;
B[j,j-1]:=-(m7+m4);
B[j,j]:=(m3-1)*(m7+m4+m8[j]+m5[j])+m9+m6+2*(m7+m4)+m8[j]+m5[j]+kb*a;
B[j,mmks-1]:=-kb;
B[j,mmks]:=-m3*(m7+m4+m8[j]+m5[j]);
B[j,mmkspl]:=(m6+m9)*Cm[j,0];

for j:=(k+1) to (mmks-1) do
  begin
    B[j,j]:=m1+1;
    B[j,j-k-1]:=-a*m1;
    B[j,mmkspl]:=Qb[j-k-1,0];
  end;

j:=mmks;
B[j,k]:=-m2;
B[j,j]:=m2+1;
B[j,mmkspl]:=C[0];

for j:=0 to mmks do
  begin
    dummy:=B[j,j];
    for i:=0 to mmkspl do B[j,i]:=B[j,i]/dummy;
    for n:=0 to mmks do
      begin
        if n<>j then
          begin
            dummy:=B[n,j];
            for i:=0 to mmkspl do B[n,i]:=B[n,i]-dummy*B[j,i];
          end;
        end;
      end;
  end;

for j:=0 to k do
  begin
    Cm[j,1]:=B[j,mmkspl];
    Qm[j]:=a*Cm[j,1];
  end;

```

(matrix routine)

```

for j:=0 to k do Qb[j,1]:=B[j+k+1,mmksp1];
C[1]:=B[mmks,mmksp1];

Qt:=Qi+(((Ci-C[1])*vol)/mc);
case mde of 1: cred:=C[1];
           2: cred:=(Qi-Qt)/Qi;
           end;
lineto(xscr(hours),yscr(cred));
C[0]:=C[1];
for j:=0 to k do
  begin
    Cm[j,0]:=Cm[j,1];
    Qb[j,0]:=Qb[j,1];
  end;
if keypressed then cntn:=upcase(readkey);
until (cntn='Q') or (time>=xmx*3600);
end;

```

```

procedure dat_gen;                                     {input of model parameters}
begin
  clrscr;
  writeln('Model parameters');
  writeln('-----');
  gotoxy(1,4);
  str(Ci:3:1, wrd[1]); str(Qi:3:1, wrd[2]); str(mc:6:4, wrd[3]);
  str(vol:6:4, wrd[4]); str(a:6:5, wrd[5]); str(ks:6, wrd[6]);
  str(Dp:6, wrd[7]);
  str(Ds:6, wrd[8]); str(alfa:4:2, wrd[9]); str(beta:4:2, wrd[10]);
  str(kb:6, wrd[11]); str(dc:7:5, wrd[12]); str(dens:3:0, wrd[13]);
  str(Vp:6, wrd[14]);
  writeln('Ci [mg/l] = ');
  writeln('Qi (total) [mg/g] = ');
  writeln('Mass of carbon [kg] = ');
  writeln('Volume [m3] = ');
  writeln('A in linear isotherm = ');
  writeln('Film transf coeff. [m/s] = ');
  writeln('Macropore diff. [m2/s] = ');
  writeln('Macro surf. diff. [m2/s] = ');
  writeln('Fraction macropore area = ');
  writeln('Fraction macropore vol. = ');
  writeln('Micropore diff. [1/s] = ');
  writeln('Particle diameter [m] = ');
  writeln('Particle density [kg/m3] = ');
  writeln('Pore volume [m3/kg] = ');
  selectno(4,18,28,1,num, wrd);
  Ci:=num[1]; Qi:=num[2]; mc:=num[3]; vol:=num[4]; a:=num[5]; ks:=num[6];
  Dp:=num[7]; Ds:=num[8]; alfa:=num[9]; beta:=num[10]; kb:=num[11];
  dc:=num[12]; dens:=num[13]; Vp:=num[14];
  gotoxy(1,20);
  writeln('Choose the values to be displayed :');
  wrd[1]:='Concentration = C [mg/l]';
  wrd[2]:='(Qi-Q)/Qi (for Qi > 0)';
  select(21,23,1,mde, wrd);
  case mde of 1: capt[2]:='C [mg/l]';
              2: capt[2]:='(Q-Qi)/Qi';
              end;
end;

```

```

repeat
  clrscr;
  writeln('Initial loading profiles in pores');
  writeln('-----');
  writeln;
  writeln('      Macro   Micro');
  for i:=0 to k do writeln(i:2,' : ',Qmo[i]:6:3,' ',Qbo[i]:6:3);
  gotoxy(1,22);
  ver:=3;
  wrd[1]:='Read loading profile from disk';
  wrd[2]:='Set all loadings equal to Qi';
  wrd[3]:='Keep values as displayed';
  select(22,25,1,ver,wrd);
  case ver of 1: begin
    gotoxy(1,22); delline; delline; delline;
    gotoxy(1,22);
    write('Give data file for pore loadings : ');
    readln(fname[5]);
    writeln('Insert disk with data file and ...');
    pause;
    assign(st,fname[5]);
    reset(st);
    for j:=0 to k do readln(st,Qmo[j],Qbo[j]);
    close(st);
    end;
  2: for j:=0 to k do
    begin
      Qmo[j]:=Qi; Qbo[j]:=Qi;
    end;
  end;
until ver=3;
end;

procedure st_dat;                                     (saving default values)
begin
  assign(st,'parslin.dat');
  rewrite(st);
  for i:=3 to 6 do writeln(st,capt[i]);
  writeln(st,ks); writeln(st,Dp); writeln(st,Ds); writeln(st,alfa);
  writeln(st,beta); writeln(st,kb); writeln(st,Ci); writeln(st,Qi);
  writeln(st,mc); writeln(st,vol); writeln(st,a); writeln(st);
  writeln(st,dc);
  writeln(st,dens); writeln(st,Vp); writeln(st,capt[1]);
  writeln(st,capt[2]);
  writeln(st,xmn); writeln(st,xmx); writeln(st,ymn); writeln(st,ymx);
  writeln(st,nx); writeln(st,ny); writeln(st,np);
  for i:=1 to np do
    begin
      writeln(st,fname[i]);
      writeln(st,plt[i]);
      writeln(st,join[i]);
      writeln(st,ltp[i]);
    end;
  writeln(st,key);
  if key='Y' then
    begin

```

```

    writeln(st,nv,' ',xv,' ',yv);
    for i:=1 to (np+nv) do writeln(st,lgnd[i]);
  end;
writeln(st,ex);
if ex='Y' then
  begin
    writeln(st,ni);
    for i:=1 to ni do
      begin
        writeln(st,ins[i]);
        writeln(st,xi[i],' ',yi[i]);
      end;
    end;
  close(st);
end;

procedure defaults;                                {setting default values}
begin
  default; size:=4; fnt:=0; fntsize:=1; lgndsize:=1; mde:=1;
  assign(st,'parslin.dat');
  reset(st);
  for i:=3 to 6 do readln(st,capt[i]);
  readln(st,ks); readln(st,Dp); readln(st,Ds); readln(st,alfa);
  readln(st,beta); readln(st,kb); readln(st,Ci); readln(st,Qi);
  readln(st,mc); readln(st,vol); readln(st,a); readln(st); readln(st,dc);
  readln(st,dens); readln(st,Vp); readln(st,capt[1]); readln(st,capt[2]);
  readln(st,xmn); readln(st,xmx); readln(st,ymn); readln(st,ymx);
  readln(st,nx); readln(st,ny); readln(st,np);
  for i:=1 to np do
    begin
      readln(st,fname[i]);
      readln(st,plt[i]);
      readln(st,join[i]);
      readln(st,ltp[i]);
    end;
  readln(st,key);
  if key='Y' then
    begin
      readln(st,nv,xv,yv);
      for i:=1 to (np+nv) do readln(st,lgnd[i]);
    end;
  readln(st,ex);
  if ex='Y' then
    begin
      readln(st,ni);
      for i:=1 to ni do
        begin
          readln(st,ins[i]);
          readln(st,xi[i],yi[i]);
        end;
      end;
    end;
  x1:=xmx-xmn;
  y1:=ymx-ymn;
  if nx>0 then xin:=x1/nx else xin:=x1;
  if ny>0 then yin:=y1/ny else yin:=y1;
end;

```

```

{----- MAIN PROGRAM -----}
begin
pc:=3;
ver:=9;
defaults;
while ver=9 do
begin
clrscr;
gotoxy(1,5);
writeln('          DESORPTION IN BATCH');
writeln('Combination model with linear isotherm');
writeln('-----');
pause;
dat_gen;
scale;
datname;
rpt:=1;
repeat
  if (rpt=1) and (np>0) then
  begin
  clrscr;
  gotoxy(1,8);
  writeln('Insert the disk with the following files :');
  writeln;
  for i:=1 to np do writeln(fname[i]);
  writeln;
  pause;
  wrn:=0;
  for i:=1 to np do
  begin
  if plt[i]='Y' then
  begin
  wrn:=wrn+1;
  pat[i]:=cha[wrn];
  end
  else pat[i]:=0;
  end;
  for i:=1 to np do readplot(fname[i],xx,yy,nxy[i],i);
  rpt:=0;
  end;
  Init(pc,size,fnt,fntsize);
  Axes;
  for i:=1 to np do Plot(xx,yy,nxy[i],join[i],pat[i],ltp[i],i);

  model;

  readln;
  if key='Y' then legend;
  if ex='Y' then extra;
  readln;
  CloseGraph;
  clrscr;
  gotoxy(1,8);
  writeln('Conditions after ',hours:5:2,' hr');
  writeln;

```

```

writeln('C = ',C[1]:5:3);
writeln('Q = Qi+(Ci-C)*V/m = ',Qt:5:3);
Qt:=0;
Q[0]:=0;
for j:=1 to k do
  begin
    Q[j]:=sqr(j)*(alfa*Qm[j]+(1-alfa)*Qb[j,1]+beta*Vp*Cm[j,1]);
    Qt:=Qt+0.5*(Q[j]+Q[j-1]);
  end;
Qt:=3*Qt/power(k,3);
writeln('Q = ',Qt:5:3);
writeln;
writeln('      MacroQ          MacroC          MicroQ');
for j:=0 to k do writeln(Qm[j]:12:8,Cm[j,1]:16:8,Qb[j,1]:16:8);
pause;
repeat;
  clrscr;
  gotoxy(1,5);
  writeln('Changes');
  writeln('-----');
  wrd[1]:='Plots and legends';
  wrd[2]:='Captions';
  wrd[3]:='Scale';
  wrd[4]:='Extra text';
  wrd[5]:='Model parameters';
  wrd[6]:='Repeat simulation with changes';
  wrd[7]:='Start a new run';
  wrd[8]:='Quit';
  ver:=6;
  select(8,16,1,ver, wrd);
  case ver of 1: begin
    datname;
    rpt:=1;
    end;
    2: caption;
    3: scale;
    4: extratext;
    5: dat_gen;
    8: begin
    gotoxy(1,20);
    write('Save data ? (Y/N) ');
    quest(chg);
    if chg='Y' then st_dat;
    write('Back to DOS ? (Y/N) ');
    quest(chg);
    if chg='N' then ver:=1;
    end;
  end;
until ver>5;
until ver>6;
end;
end.

```

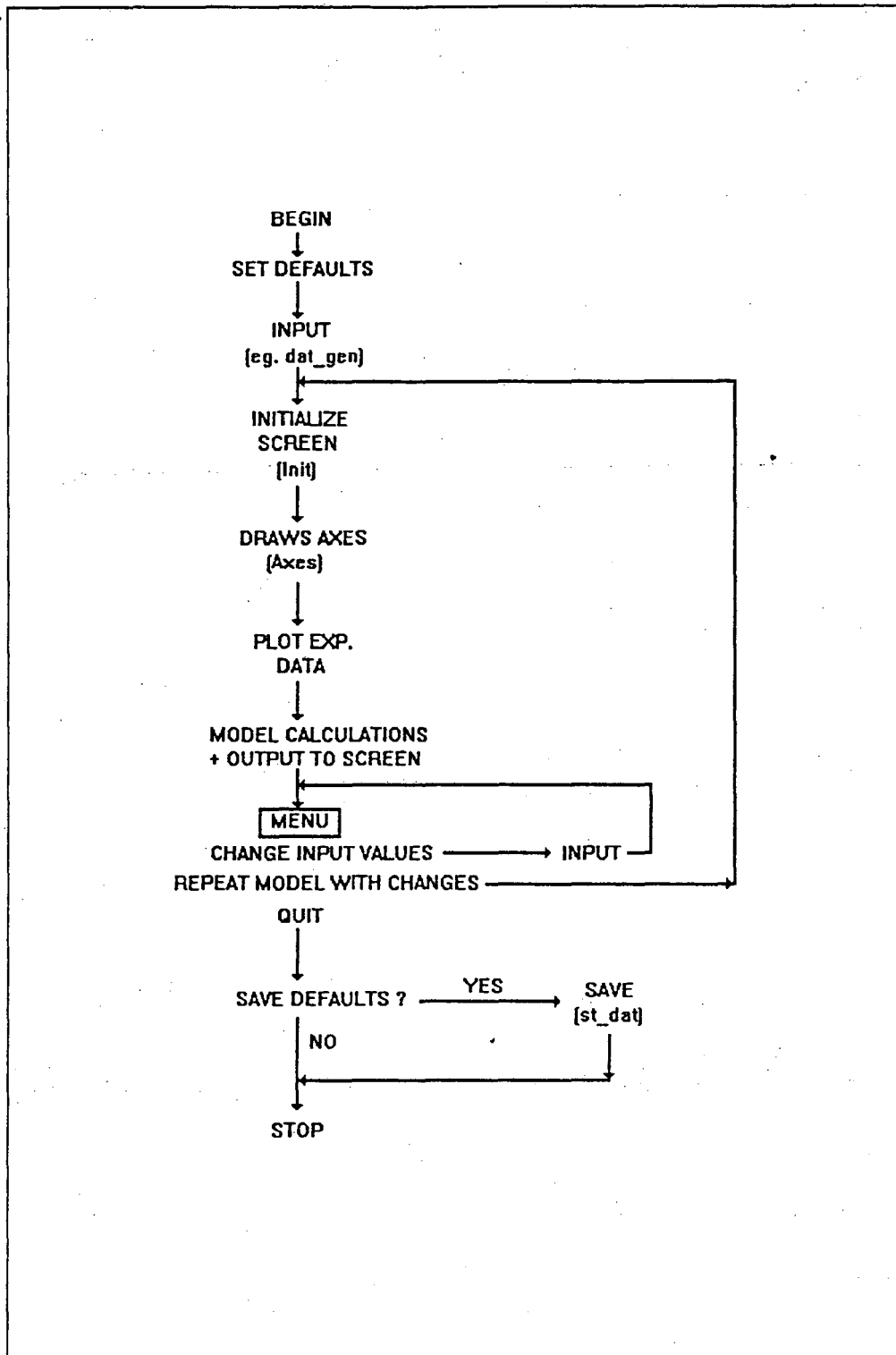


Figure G.1 Flow diagram of main program

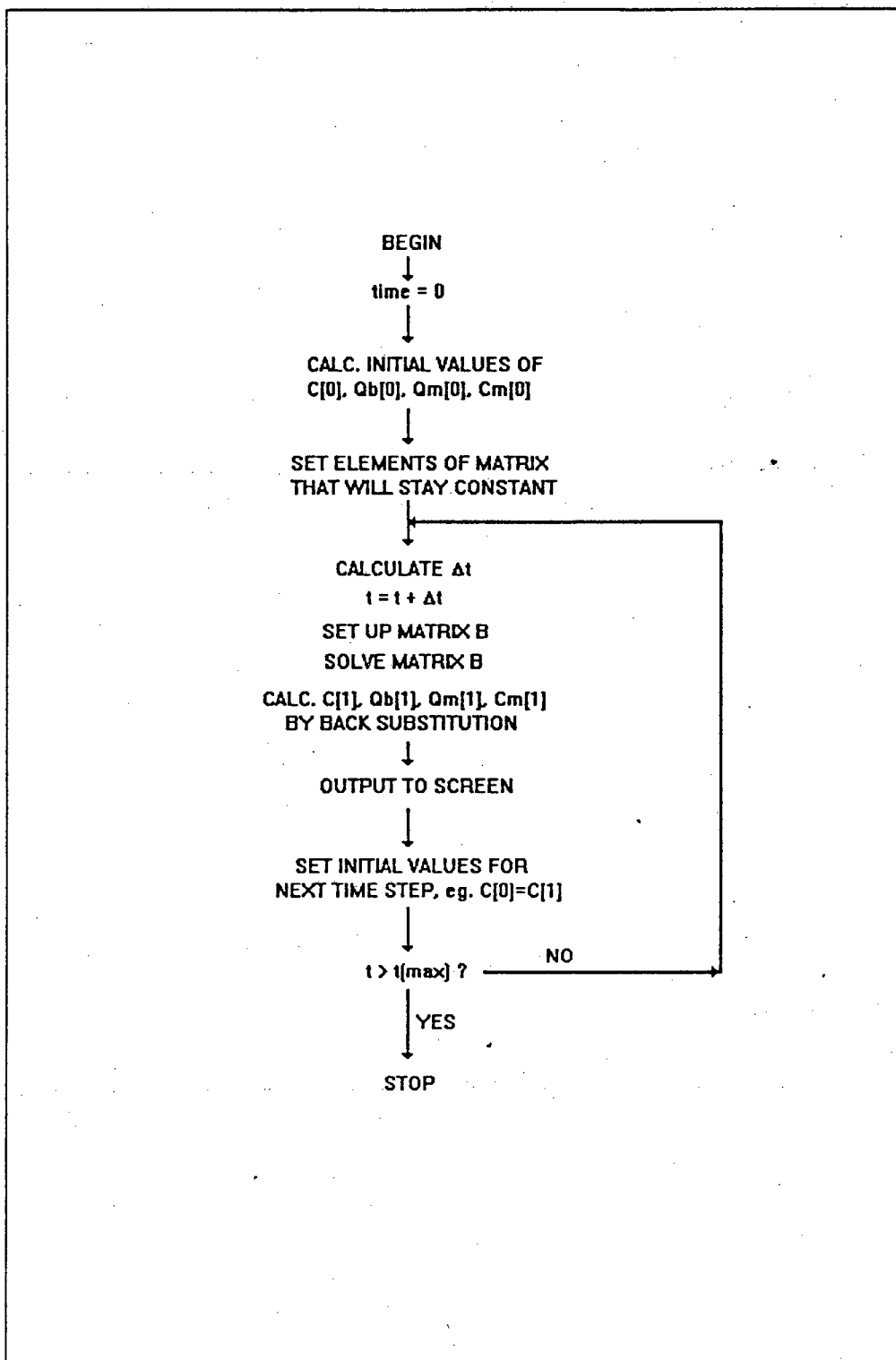


Figure G.2 Flow diagram of procedure "model" in program "parslin"

APPENDIX H

TURBO PASCAL PROGRAM FOR SURFACE DIFFUSION MODEL

This program describes the elution of gold cyanide from a packed bed of activated carbon by using a combination of the following models :

- (1) The model for the elution and decomposition of cyanide developed in Chapter 4,
- (2) The nonideal flow model for the elution of potassium described in Chapter 5, and
- (3) The surface diffusion model for the elution of gold cyanide developed in Chapter 6.

The program utilizes the unit "grph" in Appendix J for the creation of menu's and graphics. Program "surfdiff", described below, produces a graph of any of the following :

C_G in the eluate vs. t or V_B
 C_N in the eluate vs. t or V_B
 C_K in the eluate vs. t or V_B
 Q_G on the eluted carbon vs. t or V_B
 C_G/C_{Gi} vs. t or V_B for a CSTR ($C_{Gi} \neq 0$)
 $(Q_{Gi} - Q_G)/Q_{Gi}$ vs. t or V_B for a CSTR ($Q_{Gi} \neq 0$)

Structure of main program

The structure of the main program is the same as that of the combination model described in Appendix G.

Algorithm of procedure "model" (Figure H.1)

Procedure "model" starts by setting $t=0$ and by calculating the initial concentrations from the input values. If the bed was drained before the introduction of eluant, the bed is filled by using procedure "fill" which will be discussed later. Once the liquid level is equal to h , the time is set equal to $(t+\Delta t)$ and the models for potassium, cyanide and gold

calculated in each height section of the column from the inlet ($i=0$) to the outlet ($i=N$). (The algorithm of the model for the elution of the gold is discussed in the next paragraph.) The initial values for the next time step are then set equal to the values calculated in the present time step and the calculations for $i=0$ to N repeated for the next time step. This is continued until transfer of carbon has to occur (if $nt>1$, i.e. counter-current elution) or the maximum specified time is reached. In the case of counter-current elution, the liquid concentrations remain unchanged and the carbon concentration in each section is set equal to the value on the carbon which moves into that position. The calculation of the potassium, cyanide and gold models as a function of height and time is repeated until the next transfer of carbon. This is terminated after nt carbon transfers have occurred.

Algorithm of procedure "mod_au" (Figure H.2)

Procedure "mod_au" calculates the gold concentrations on the carbon and in the liquid phases at $(t+\Delta t)$ for any specified height section i . As procedure "mod_au" follows on procedures "mod_cat" and "mod_cn", the concentrations of cyanide and potassium are known and the gold cyanide equilibrium can be calculated at the height and time steps concerned. The value of C_{Gs} (cgs) is estimated immediately before "mod_au" and Q_{Gs} (qs) can thus be calculated from the equilibrium isotherm. The values of Q_{Gm} (qm), Q_{Gb} (qb) and C_G (cg) are then calculated by solving Equations 6.20, 6.21 and 6.25 simultaneously with a Runge Kutta routine. If the values of qm, cs and qs do not satisfy Equation 6.22, a new value of cs is estimated by determining the value of qs that will satisfy Equation 6.22. New values of qm, qb and cg are calculated with the new estimate of cs until convergence is obtained. The calculation procedure used in procedure "mod_au" is the same as that used by Van Deventer (1984a) for the adsorption of gold in a batch stirred tank reactor.

Algorithm of procedure "fill" (Figure H.3)

This procedure is only used if the void fraction of the carbon bed is not filled with liquid initially, i.e. $s<1.0$. For the fill procedure, the liquid level (hh) is defined as the highest height section of the bed that is filled with eluate. This is initially set equal to zero. A loop

is then entered in which the liquid level is increased by one height section per cycle. The concentrations of cyanide, potassium and gold in the height sections below the liquid level are calculated with procedures "mod_cat", "mod_cn" and "mod_au". For section hh, the intraparticle concentrations and loadings are assumed to remain unchanged while the section is filled. The interparticle concentrations in section hh are calculated as the weighted average of the concentrations in the remaining pretreatment solution and the liquid moving in from section (hh-1). When the bed is completely filled (i.e. hh=N), the procedure is terminated.

The following nomenclature was used in program "surfdiff" :

Program	Thesis	Program	Thesis	Program	Thesis
a	A	crossb	X_b	nd	N_d
acn	C_2	crossm	X_m	ndd	$N_d - N_d$
alfa	α	dc	d_c	nt	N_t
an	b	dens	ρ	p	p
ao	A_o	dh	Δh	q	q
area	a	dt	Δt	qb	Q_{bG}
beta	β	dtfill	Δt_{fill}	qbo	Q_{bGi}
bn	B	ea	E_a/R_o	qcn	Q_{cN}
c	C	ecn	E_{aN}	qm	Q_{mG}
cat	C_K	en	n	qmo	Q_{mGi}
catb	C_{bK}	eps	ϵ	qo	Q_{oGi}
catbo	C_{Kdi}	fillt	t_{fill}	qocn	Q_{oNi}
catm	C_{mK}	h	h	qs	Q_{sG}
cato	C_{KF}	k1-k3	k_{1-3}	s	s
catpo	C_{Kpi}	kb	k_b	s0-s5	S_{0-5}
cg	C_G	kcn	k_N	temp	T
cgs	C_{sG}	kcnp	k_{Np}	v	V
cn	C_N	kfcn	k_{sN}	vp	V_p
cnbo	C_{Ndi}	kocn	k_{oN}		
cno	C_{NF}	kocnp	C_i		
cnp	C_{Np}	ks	k_s		
cnpo	C_{Npi}	mmb	m_{mb}		
co	C_{Gi}	n	N		

Program listing

```

program surfdiff;
uses crt,graph,grph;

const n_max=50;                                {max number of height sections}
      n_maxx=51;                                {n_max+1}
type timevar=array[0..n_maxx,1..2] of double;
var  xmde,ymde,mnu,rpt,n,hh,i,j,jj,nt,ndd,nd:integer;
     qm,qb,cg,cgs,cat,catm,catb,cn,cnp,qcn:timevar;
     temp,dh,dtfill,dt,h,ti,v,eps,dc,fillt,sec,hours,vp,k1,k2,k3,
     crossb,crossm,s,cato,catpo,catbo,cath,beta,m1,m2,m3,m4,m5,m6,
     mm1,mm2,mm3,mm4,mb1,mb2,mb3,mb4,mcl,mc2,mc3,mc4,valx,valy,pp,qq,
     rr,ao,p,ea,f,c,nbvi,q,en,co,qo,mmb,qmo,qbo,an,bn,cshalf,
     chalf,save,epsi,km,kb,ks,dens,ttime,part1,alfa,area,sum,qt,
     a,qsf,csf,qs,kcn,kcnp,kocn,kocnp,acn,ecn,kfcn,cno,
     cnpo,cnbo,qocn,s0,s1,s2,s3,s4,s5:double;
     cntn,chg:yn;
     st:text;
     nxy:array[1..4] of integer;
     xx,yy:pnt;
label new;

{----- model starts -----}
procedure model;

procedure iso (ct,cyan,qcyan:double);          {gold isotherm}
begin
  nbvi:=(hours*3600*v*n/(area*i*h));
  a:=(ao/(c*qcyan+1))*exp(ea/(temp+273.15))*power(ct+50,p)
    *power(cyan+1,f)*power(nbvi+1,q);
  en:=an*a+bn;
end;

procedure draw(line:integer);                 {line draw procedure}
begin
  case ymde of 1: valy:=cg[n,1];
              2: begin
                  if qo<>0 then
                    begin
                      qt:=alfa*sqrt(qm[1,1])+(1-alfa)*qb[1,1];
                      valy:=(qo-qt)/qo;
                    end
                  else valy:=cg[1,1]/co;
                end;
              3: begin
                  valy:=0;
                  for jj:=1 to nd do
                    valy:=valy+alfa*sqrt(qm[jj,1])+(1-alfa)*qb[jj,1];
                  valy:=valy/nd;
                end;
              4: valy:=cat[n,1];
              5: valy:=cn[n,1];
            end;
end;

```

```

case xmde of 1: valx:=hours;
              2: valx:=hours*3600*v/(area*h);
              end;
case line of 0: moveto(xscr(valx),yscr(valy));
              1: lineto(xscr(valx),yscr(valy));
              end;
end;

function fm (var csf,qmf,qbf:double):double;           {gold}
begin
  qsf:=a*power(csf,en);
  fm:=m5*(sqr(qsf)-qmf) - m6*(qmf-(qbf*sqrt(qmf)));
end;

function fb (var qmf,qbf:double):double;             {gold}
begin
  fb:=m4*(sqrt(qmf)-qbf);
end;

function fc (var cf,csf,cff:double):double;         {gold}
begin
  fc:=m2*(cf-csf)+m1*(cf-cff);
end;

function balance (var qsf,qmf,cf:double):double;    {gold}
begin
  csf:=power(qsf/a,1/en);
  balance:=m3*((qsf*qsf)-qmf)-(ks*dc*(cf-csf)*sqrt(qmf));
end;

procedure increase;                                  {gold}
begin
  qs:=1.0005*qs;
  if balance(qs,qm[i,2],cg[i,2])<0 then increase;
end;

procedure reduce;                                    {gold}
begin
  qs:=0.9995*qs;
  if balance(qs,qm[i,2],cg[i,2])>0 then reduce;
end;

procedure mod_au (var deltd,delh:double);           {model for gold cyanide}
begin
  iso(cat[i,2],cn[i,2],qcn[i,2]);
  qs:=a*power(cgs[i,2],en);
  mml:=fm(cgs[i,1],qm[i,1],qb[i,1]);
  mbl:=fb(qm[i,1],qb[i,1]);
  mcl:=fc(cg[i,1],cgs[i,1],cg[i-1,1]);
  repeat
    cshalf:=(cgs[i,1]+cgs[i,2])/2;
    chalf:=(cg[i-1,1]+cg[i-1,2])/2;
    pp:=qm[i,1]+((deltd*mml)/2);
    qq:=qb[i,1]+((deltd*mbl)/2);
    rr:=cg[i,1]+((deltd*mcl)/2);
  end repeat;
end;

```

```

mm2:=fm(cshalf,pp,qq);
mb2:=fb(pp,qq);
mc2:=fc(rr,cshalf,chalf);
pp:=qm[i,1]+((delt*mm2)/2);
qq:=qb[i,1]+((delt*mb2)/2);
rr:=cg[i,1]+((delt*mc2)/2);
mm3:=fm(cshalf,pp,qq);
mb3:=fb(pp,qq);
mc3:=fc(rr,cshalf,chalf);
pp:=qm[i,1]+(delt*mm3);
qq:=qb[i,1]+(delt*mb3);
rr:=cg[i,1]+(delt*mc3);
mm4:=fm(cgs[i,2],pp,qq);
mb4:=fb(pp,qq);
mc4:=fc(rr,cgs[i,2],cg[i-1,2]);
qm[i,2]:=qm[i,1]+((delt/6)*(mm1+(2*mm2)+(2*mm3)+mm4));
qb[i,2]:=qb[i,1]+((delt/6)*(mb1+(2*mb2)+(2*mb3)+mb4));
cg[i,2]:=cg[i,1]+((delt/6)*(mc1+(2*mc2)+(2*mc3)+mc4));
save:=qs;
if balance(qs,qm[i,2],cg[i,2])=0 then epsi:=0
else
begin
if balance(qs,qm[i,2],cg[i,2])<0 then increase else reduce;
cgs[i,2]:=power(qs/a,1/en);
epsi:=abs((save-qs)/qs);
end;
until epsi<=0.001;
end;

```

procedure mod_cat (var delh,delh:double); {model for elution of cation}

```

function fk (var kt,ktt,ktm:double):double;
begin
fk:=k1*(ktt-kt)+k1*crossm*(ktm-kt);
end;

function fkm (var kt,ktb,ktm:double):double;
begin
fkm:=k2*(kt-ktm)+k2*crossb*(ktb-ktm);
end;

function fkb (var ktb,ktm:double):double;
begin
fkb:=k3*(ktm-ktb);
end;

begin
k1:=v/(area*eps*delh);
k2:=crossm*v/(beta*area*delh*dens*vp*(1-eps));
k3:=crossm*crossb*v/((1-beta)*area*delh*dens*vp*(1-eps));
mcl:=fk(cat[i,1],cat[i-1,1],catm[i,1]);
mm1:=fkm(cat[i,1],catb[i,1],catm[i,1]);
mb1:=fkb(catb[i,1],catm[i,1]);
pp:=catm[i,1]+((delt*mm1)/2);
qq:=catb[i,1]+((delt*mb1)/2);

```

```

rr:=cat[i,1]+((delt*mc1)/2);
cath:=(cat[i-1,1]+cat[i-1,2])/2;
mc2:=fk(rr,cath,pp);
mm2:=fkm(rr,qq,pp);
mb2:=fkb(qq,pp);
pp:=catm[i,1]+((delt*mm2)/2);
qq:=catb[i,1]+((delt*mb2)/2);
rr:=cat[i,1]+((delt*mc2)/2);
mc3:=fk(rr,cath,pp);
mm3:=fkm(rr,qq,pp);
mb3:=fkb(qq,pp);
pp:=catm[i,1]+(delt*mm3);
qq:=catb[i,1]+(delt*mb3);
rr:=cat[i,1]+(delt*mc3);
mc4:=fk(rr,cat[i-1,2],pp);
mm4:=fkm(rr,qq,pp);
mb4:=fkb(qq,pp);
cat[i,2]:=cat[i,1]+((delt/6)*(mc1+(2*mc2)+(2*mc3)+mc4));
catm[i,2]:=catm[i,1]+((delt/6)*(mm1+(2*mm2)+(2*mm3)+mm4));
catb[i,2]:=catb[i,1]+((delt/6)*(mb1+(2*mb2)+(2*mb3)+mb4));
end;

```

```

procedure mod_cn(delt,delh:double); {model for cyanide}

```

```

begin
kcnp:=kocnp/power(1+qcn[i,1],acn);
s0:=1+(6*kfcn*delt/(dens*vp*dc))+(kcnp*delt);
s1:=1/s0;
s2:=6*kfcn*delt/(dens*vp*dc*s0);
s3:=6*kfcn*(1-eps)*delt/(eps*dc);
s4:=v*delt/(area*eps*delh);
s5:=1+s4+(kcn*delt)+(s3*(1-s2));
cn[i,2]:=(cn[i,1]+(s4*cn[i-1,2])+(s3*s1*cnp[i,1]))/s5;
cnp[i,2]:=(s1*cnp[i,1])+(s2*cn[i,2]);
qcn[i,2]:=qcn[i,1]+(vp*kcnp*cnp[i,2]*delt);
end;

```

```

procedure fill; {filling up of drained bed}

```

```

begin
fillt:=(1-s)*h*area*eps/v;
dtfill:=fillt/n;
hh:=0;
repeat {time loop}
  sec:=sec+dtfill;
  hh:=hh+1; {hh = liquid level}
  if hh=1 then cgs[hh,2]:=0.1
  else
  begin
  for i:=1 to (hh-1) do mod_cn(dtfill,dh);
  if (cato<>catpo) or (cato<>catbo) then
    for i:=1 to (hh-1) do mod_cat(dtfill,dh)
  else
  for i:=1 to (hh-1) do
  begin
  catm[i,2]:=catm[i,1];

```

```

        catb[i,2]:=catb[i,1];
        cat[i,2]:=cat[i,1];
    end;
    if ymde<4 then for i:=1 to (hh-1) do
        begin
            cgs[i,2]:=cgs[i,1];
            mod_au(dtfill,dh);
        end;
    cgs[hh,2]:=cgs[hh-1,2];
    end;
    cnp[hh,2]:=cnp[hh,1];           {concentrations at liquid level}
    cn[hh,2]:=(cnbo*s)+(cn[hh-1,2]*(1-s));
    cat[hh,2]:=(catbo*s)+(cat[hh-1,2]*(1-s));
    catb[hh,2]:=catb[hh,1];
    catm[hh,2]:=catm[hh,1];
    cg[hh,2]:=cg[hh-1,2]*(1-s);
    qm[hh,2]:=qm[hh,1];
    qb[hh,2]:=qb[hh,1];
    for i:=1 to hh do
        begin
            cat[i,1]:=cat[i,2];
            catm[i,1]:=catm[i,2];
            catb[i,1]:=catb[i,2];
            cg[i,1]:=cg[i,2];
            cgs[i,1]:=cgs[i,2];
            qm[i,1]:=qm[i,2];
            qb[i,1]:=qb[i,2];
            cn[i,1]:=cn[i,2];
            cnp[i,1]:=cnp[i,2];
            qcn[i,1]:=qcn[i,2];
        end;
    until sec>=fillt;
end;                                     {end of fill procedure}

begin
    cntn:='a';
    sec:=0;
    kcn:=kocn*exp(-ecn/(8.314*(273.15+temp)));
    m1:=-v/(eps*area*dh);
    m2:=-6*ks*(1-eps)/(eps*dc);
    m3:=5*km*alfa*dens;
    m4:=kb/(1-alfa);
    m5:=60*km/sqr(dc);
    m6:=2*kb/alfa;
    n:=round(h/dh);
    ndd:=n-nd;
    for i:=1 to n_max do
        begin
            qm[i,1]:=sqr(qmo); qb[i,1]:=qbo; cg[i,1]:=co; cgs[i,1]:=co;
            catm[i,1]:=catpo; catb[i,1]:=catpo; cat[i,1]:=catbo;
            cn[i,1]:=cnbo; cnp[i,1]:=cnpo; qcn[i,1]:=qocn;
        end;
    for j:=1 to 2 do
        begin
            cg[0,j]:=co;

```

```

if (catpo=cato) and (catbo=cato) then
  for i:=0 to n_max do cat[i,j]:=cato
  else cat[0,j]:=cato;
if (cno=0) and (cnpo=0) and (cnbo=0) then
  for i:=0 to n_max do
    begin
      cn[i,j]:=0;
      cnp[i,j]:=0;
      qcn[i,j]:=qocn;
    end
  else cn[0,j]:=cno;
end;

if s<>1 then fill;

hours:=sec/3600;
draw(0);

for j:=1 to nt do {carbon transfer loop}
  begin
    if nt=1 then
      begin
        case xmde of 1: ttime:=xmx*3600;
                    2: ttime:=xmx*area*h/v;
        end;
      end
    else
      begin
        if j=1 then ttime:=ti*3600
        else
          begin
            case xmde of 1: ttime:=(xmx-ti)*3600/(nt-1);
                        2: ttime:=((xmx*area*h/v)-ti*3600)/(nt-1);
          end;
        end;
      end;
    end;
  sec:=0;
  repeat {time loop}
    sec:=sec+dt;
    if (cato<>catpo) or (catbo<>cato) then
      for i:=1 to n do mod_cat(dt,dh)
      else for i:=1 to n do
        begin
          catm[i,2]:=catm[i,1];
          catb[i,2]:=catb[i,1];
          cat[i,2]:=cat[i,1];
        end;
      if (cnpo<>0) or (cno<>0) or (cnbo<>0) then
        for i:=1 to n do mod_cn(dt,dh)
        else for i:=1 to n do
          begin
            cn[i,2]:=0;
            cnp[i,2]:=0;
            qcn[i,2]:=qocn;
          end;

```

```

if ymde<4 then for i:=1 to n do
    begin
        if (hours=0) and (i=1) then cgs[i,2]:=0.1
        else if (hours=0) then cgs[i,2]:=cgs[i-1,2]
        else cgs[i,2]:=cgs[i,1];
        mod_au(dt,dh);
    end;
for i:=1 to n do
    begin
        cat[i,1]:=cat[i,2];
        catm[i,1]:=catm[i,2];
        catb[i,1]:=catb[i,2];
        cg[i,1]:=cg[i,2];
        cgs[i,1]:=cgs[i,2];
        qm[i,1]:=qm[i,2];
        qb[i,1]:=qb[i,2];
        cn[i,1]:=cn[i,2];
        cnp[i,1]:=cnp[i,2];
        qcn[i,1]:=qcn[i,2];
    end;
hours:=hours+(dt/3600);
draw(1);
if keypressed then cntn:=upcase(readkey);
until (cntn='Q') or (sec>=ttime);
if (cntn<>'Q') and (j<>nt) then {transfer of carbon}
    begin
        for i:=1 to ndd do
            begin
                qm[i,1]:=qm[i+nd,2];
                qb[i,1]:=qb[i+nd,2];
                catm[i,1]:=catm[i+nd,2];
                catb[i,1]:=catb[i+nd,2];
                cnp[i,1]:=cnp[i+nd,2];
                qcn[i,1]:=qcn[i+nd,2];
            end;
        for i:=ndd+1 to n do
            begin
                catm[i,1]:=catpo;
                catb[i,1]:=catpo;
                cnp[i,1]:=cnpo;
                qm[i,1]:=sqr(qmo);
                qb[i,1]:=qbo;
                qcn[i,1]:=qocn;
            end;
        end;
    end;
end;
end;
{-----end of model-----}

procedure defaults; {sets default values}
begin
default;
xmde:=2; size:=4; fnt:=0; fntsize:=1; pc:=3; lgndsize:=1; ymde:=1;
assign(st,'surfdiff.dat');
reset(st);

```

```

readln(st,co); readln(st,qmo); readln(st,qbo); readln(st,mmb);
readln(st,qo);
readln(st,h); readln(st,v); readln(st,ao); readln(st,p); readln(st,ea);
readln(st,f); readln(st,c); readln(st,an); readln(st,bn);
readln(st,ks);
readln(st,km); readln(st,alfa); readln(st,dc); readln(st,dens);
readln(st,kb); readln(st,vp); readln(st,temp); readln(st,cato);
readln(st,catpo); readln(st,cno); readln(st,cnpo); readln(st,kfcn);
readln(st,kocn); readln(st,ecn); readln(st,acn); readln(st,eps);
readln(st,area); readln(st,s); readln(st,nt); readln(st,dh);
readln(st,nd);
readln(st,dt); readln(st,crossm); readln(st,crossb); readln(st,beta);
readln(st,catbo); readln(st,cnbo); readln(st,qocn); readln(st,q);
readln(st,kocnp);
close(st);
end;

```

```

procedure st_dat;                                     {saves default values}
begin
  assign(st,'surfdiff.dat');
  rewrite(st);
  writeln(st,co); writeln(st,qmo); writeln(st,qbo); writeln(st,mmb);
  writeln(st,qo); writeln(st,h); writeln(st,v); writeln(st,ao);
  writeln(st,p);
  writeln(st,ea); writeln(st,f); writeln(st,c); writeln(st,an);
  writeln(st,bn);
  writeln(st,ks); writeln(st,km); writeln(st,alfa); writeln(st,dc);
  writeln(st,dens); writeln(st,kb); writeln(st,vp); writeln(st,temp);
  writeln(st,cato); writeln(st,catpo); writeln(st,cno); writeln(st,cnpo);
  writeln(st,kfcn); writeln(st,kocn); writeln(st,ecn); writeln(st,acn);
  writeln(st,eps); writeln(st,area); writeln(st,s); writeln(st,nt);
  writeln(st,dh); writeln(st,nd); writeln(st,dt); writeln(st,crossm);
  writeln(st,crossb); writeln(st,beta); writeln(st,catbo);
  writeln(st,cnbo);
  writeln(st,qocn); writeln(st,q); writeln(st,kocnp);
  close(st);
end;

```

```

procedure dat_gen;                                   {input of working parameters}
begin
  clrscr;
  gotoxy(1,5);
  writeln('Working parameters');
  writeln('-----');
  gotoxy(1,8);
  str(h:8:6, wrd[1]); str(area:12, wrd[2]); str(dc:8:6, wrd[3]);
  str(dens:4:1, wrd[4]); str(vp:11, wrd[5]); str(eps:8:6, wrd[6]);
  str(v:12, wrd[7]); str(temp:3:1, wrd[8]); str(s:4:3, wrd[9]);
  str(nd:1, wrd[10]); str((nt-1):1, wrd[11]); str(dh:8:6, wrd[12]);
  str(dt:1:0, wrd[13]);
  writeln('Bed height [m]                               = ');
  writeln('Flow area of empty column [m2]              = ');
  writeln('Particle diameter [m]                         = ');
  writeln('Apparent density of particles [kg/m3]        = ');

```

```

writeln('Pore volume of particles [m3/kg]                = ');
writeln('Void fraction of bed                          = ');
writeln('Volumetric flow rate [m3/s]                  = ');
writeln('Working temperature [°C]                      = ');
writeln('Fraction of void fraction containing pretreatment reagent = ');
writeln('Number of height sections discharged in counterflow = ');
writeln('Number of carbon transfers during run            = ');
writeln('Incremental height [m]                          = ');
writeln('Time step [s]                                    = ');
selectno(8,21,61,1,num, wrd);
h:=num[1]; area:=num[2]; dc:=num[3]; dens:=num[4]; vp:=num[5];
eps:=num[6];
v:=num[7]; temp:=num[8]; s:=num[9]; nd:=round(num[10]);
nt:=1+round(num[11]);
dh:=num[12]; dt:=num[13];
if nt>1 then
  begin
    gotoxy(1,23);
    write('Time interval before first transfer of carbon (hr) : ');
    readln(ti);
    end;
end;

procedure dat_draw;                                     {specification of value to be displayed}
begin
  clrscr;
  writeln('Choose the value to be displayed');
  writeln('-----');
  wrd[1]:='Metal cyanide concentration [mg/l]';
  if co<>0 then wrd[2]:='C/Ci';
  if qo<>0 then wrd[2]:='(Qi-Q)/Qi';
  wrd[3]:='Eluted carbon loading [mg/g]';
  wrd[4]:='Cation concentration [mg/l]';
  wrd[5]:='Cyanide concentration [mg/l]';
  select(4,9,1,ymde, wrd);
  case ymde of 1: capt[2]:='C [mg/l]';
                2: if co<>0 then capt[2]:='C/Ci' else capt[2]:='(Qi-Q)/Qi';
                3: capt[2]:='Q [mg/g]';
                4: capt[2]:='K [mg/l]';
                5: capt[2]:='CN [mg/l]';
  end;
  gotoxy(1,12);
  wrd[1]:='Time [hr]'; wrd[2]:='No. of bed volumes';
  if v<>0 then
    begin
      writeln('Values on x-axis :');
      select(12,14,20,xmde, wrd);
    end
  else xmde:=1;
  case xmde of 1: capt[1]:=wrd[1];
                2: capt[1]:=wrd[2];
  end;
end;

```

```

procedure dat_met;                               {input of gold cyanide parameters}
begin
repeat
  clrscr;
  writeln('Metal cyanide concentration');
  writeln('-----');
  gotoxy(1,4);
  str(co:4:2, wrd[1]); str(qo:5:3, wrd[2]); str(mmb:5:3, wrd[3]);
  str(alfa:4:3, wrd[4]);
  writeln('Feed concentration [mg/l]           = ');
  writeln('Initial concentration on carbon [mg/g] = ');
  writeln('Qi(micro)/Qi(macro)                   = ');
  writeln('Macropore fraction                     = ');
  selectno(4,8,42,1,num, wrd);
  co:=num[1]; qo:=num[2]; mmb:=num[3]; alfa:=num[4];
  qmo:=qo/(alfa+(1-alfa)*mmb);
  qbo:=mmb*qmo;
  gotoxy(1,11);
  writeln('Calculated pore concentrations :');
  writeln('Qo (macro) [mg/g] = ', qmo:5:3);
  writeln('Qo (micro) [mg/g] = ', qbo:5:3);
  writeln;
  write('Change above values ? (Y/N) ');
  quest(chg);
until chg='N';
end;

```

```

procedure dat_iso;                               {input of gold cyanide parameters}
begin
  clrscr;
  writeln('Metal cyanide isotherm');
  writeln('-----');
  writeln;
  writeln('A=Ao*exp(ea/(T+273.15))*power(K+1,p)*power(CN+1,f)');
  writeln('  *(1/(c*qCN+1))*power(BV+1,q)');
  gotoxy(1,7);
  str(ao:6:5, wrd[1]); str(ea:4:3, wrd[2]); str(p:6:4, wrd[3]);
  str(f:6:4, wrd[4]); str(c:7:5, wrd[5]); str(q:5:3, wrd[6]);
  writeln('Ao-value                               = ');
  writeln('Temperature dependency (ea) = ');
  writeln('Cation dependency (p)         = ');
  writeln('Free cyanide dependency (f) = ');
  writeln('Cyanide-age dependency (c) = ');
  writeln('Change in activity (q)       = ');
  selectno(7,13,32,1,num, wrd);
  ao:=num[1]; ea:=num[2]; p:=num[3]; f:=num[4]; c:=num[5]; q:=num[6];
  gotoxy(1,15);
  writeln('n = an*A + bn');
  gotoxy(1,17);
  str(an:9:7, wrd[1]); str(bn:9:7, wrd[2]);
  writeln('Slope (an)                               = ');
  writeln('Intercept (bn)                            = ');
  selectno(17,19,32,1,num, wrd);
  an:=num[1]; bn:=num[2];
end;

```

```

procedure dat_dif;          {input of gold cyanide mass transfer parameters}
begin
  clrscr;
  writeln('Mass transfer coefficients of the metal cyanide');
  writeln('-----');
  gotoxy(1,4);
  str(ks:11, wrd[1]); str(km:11, wrd[2]); str(kb:11, wrd[3]);
  writeln('Film transfer coefficient [m/s] = ');
  writeln('Combined surface diffusivity in macro pores [m2/s] = ');
  writeln('Coeff. for transfer between micro and macro pores [1/s] = ');
  selectno(4,7,65,1,num, wrd);
  ks:=num[1]; km:=num[2]; kb:=num[3];
end;

procedure dat_cat;          {input of potassium parameters}
begin
  clrscr;
  writeln('Cation parameters');
  writeln('-----');
  gotoxy(1,4);
  str(catpo:1:0, wrd[1]); str(catbo:1:0, wrd[2]); str(cato:1:0, wrd[3]);
  str(crossm:5, wrd[4]); str(crossb:5, wrd[5]); str(beta:4:3, wrd[6]);
  writeln('Initial pore concentration [mg/l] = ');
  writeln('Initial interparticle conc. [mg/l] = ');
  writeln('Feed concentration [mg/l] = ');
  writeln('Macropore cross flow ratio = ');
  writeln('Micropore cross flow ratio = ');
  writeln('Macropore volume fraction = ');
  selectno(4,10,45,1,num, wrd);
  catpo:=num[1]; catbo:=num[2]; cato:=num[3]; crossm:=num[4];
  crossb:=num[5];
  beta:=num[6];
end;

procedure dat_cn;          {input of cyanide parameters}
begin
  clrscr;
  writeln('Cyanide');
  writeln('-----');
  gotoxy(1,4);
  str(cnpo:1:0, wrd[1]); str(cnbo:1:0, wrd[2]); str(cno:1:0, wrd[3]);
  str(kfcn:5, wrd[4]); str(kocn:5, wrd[5]); str(ecn:4:0, wrd[6]);
  str(kocnp:5, wrd[7]); str(acn:5:3, wrd[8]); str(qocn:3:1, wrd[9]);
  writeln('Initial pore concentration [mg/l] = ');
  writeln('Initial interparticle concentration = ');
  writeln('Feed concentration [mg/l] = ');
  writeln('Film transfer coefficient = ');
  writeln(' ko in bulk solution [1/s] = ');
  writeln(' E in bulk solution [J/mol] = ');
  writeln('k in pores at zero cyanide-age. [1/s] = ');
  writeln('Deactivating factor = ');
  writeln('Initial cyanide "loading" [mg/g] = ');
  selectno(4,13,45,1,num, wrd);
  cnpo:=num[1]; cnbo:=num[2]; cno:=num[3]; kfcn:=num[4]; kocn:=num[5];

```

```
ecn:=num[6]; kocnp:=num[7]; acn:=num[8]; qocn:=num[9];
end;
```

```
{----- MAIN PROGRAM -----}
```

```
begin
clrscr;
highvideo;
fnt:=0;
fntsize:=2;
grdvr:=detect;
initgraph(grdvr,grmd,'');
xo:=round(getmaxx/10);
xm:=round(getmaxx/1.1);
yo:=round(getmaxy/20);
ym:=round(getmaxy/1.05);
xg:=xm-xo;
yg:=ym-yo;
setviewport(xo,yo,xm,ym,false);
moveto(0,0);
linere1(xg,0);
linere1(0,yg);
linere1(-xg,0);
linere1(0,-yg);
xg:=xm div 10;
yg:=ym div 10;
floodfill(1,1,white);
setcolor(black);
setttextstyle(fnt,horizdir,fntsize);
setttextjustify(lefttext,toptext);
outtextxy(xg,yg,'Surface diffusion model for');
outtextxy(xg,2*yg,'the elution of gold from a');
outtextxy(xg,3*yg,'bed of activated carbon');
outtextxy(xg,5*yg,'by');
outtextxy(xg,7*yg,'P.F. van der Merwe');
setttextstyle(0,horizdir,1);
outtextxy(5*xg,9*yg,'Press ENTER to continue...');
defaults;
readln;
closegraph;
new:
dat_gen;
dat_met;
dat_iso;
dat_dif;
dat_cat;
dat_cn;
dat_draw;
scale;
datname;
rpt:=1;
repeat
  if (rpt=1) and (np>0) then
  begin
    clrscr;
    gotoxy(1,8);
```

```
writeln('Insert the disk containing the following files :');
writeln;
for i:=1 to np do writeln(fname[i]);
writeln;
pause;
j:=0;
for i:=1 to np do
  begin
    if plt[i]='Y' then
      begin
        j:=j+1;
        pat[i]:=cha[j];
      end
    else pat[i]:=0;
  end;
for i:=1 to np do readplot(fname[i],xx,yy,nxy[i],i);
rpt:=0;
end;
Init(pc,size,fnt,fntsize);
Axes;
for i:=1 to np do plot(xx,yy,nxy[i],join[i],pat[i],ltp[i],i);

model;

if key='Y' then legend;
if ex='Y' then extra;
readln;
CloseGraph;
clrscr;
repeat;
  clrscr;
  writeln('Changes');
  writeln('-----');
  gotoxy(1,4);
  mnu:=12;
  wrd[1]:='Plots and legend';
  wrd[2]:='Scale';
  wrd[3]:='Working parameters';
  wrd[4]:='Metal cyanide parameters';
  wrd[5]:='Metal cyanide isotherm';
  wrd[6]:='Metal cyanide transfer coefficients';
  wrd[7]:='Cation parameters';
  wrd[8]:='Cyanide parameters';
  wrd[9]:='Values to be displayed';
  wrd[10]:='Captions';
  wrd[11]:='Extra text';
  wrd[12]:='Repeat simulation with changes';
  wrd[13]:='Start a new run';
  wrd[14]:='Quit';
  select(4,18,1,mnu, wrd);
  case mnu of 1: begin
    datname;
    rpt:=1;
    end;
    2: scale;
```

```
3: dat_gen;
4: dat_met;
5: dat_iso;
6: dat_dif;
7: dat_cat;
8: dat_cn;
9: dat_draw;
10: caption;
11: extratext;
14: begin
    gotoxy(1,19);
    write('Save data ? (Y/N) ');
    quest(chg);
    if chg='Y' then st_dat;
    write('Quit program ? (Y/N) ');
    quest(chg);
    if chg='N' then mnu:=1;
    end;
end;
until (mnu>11);
if mnu=13 then goto new;
until (mnu=14);
end.
```

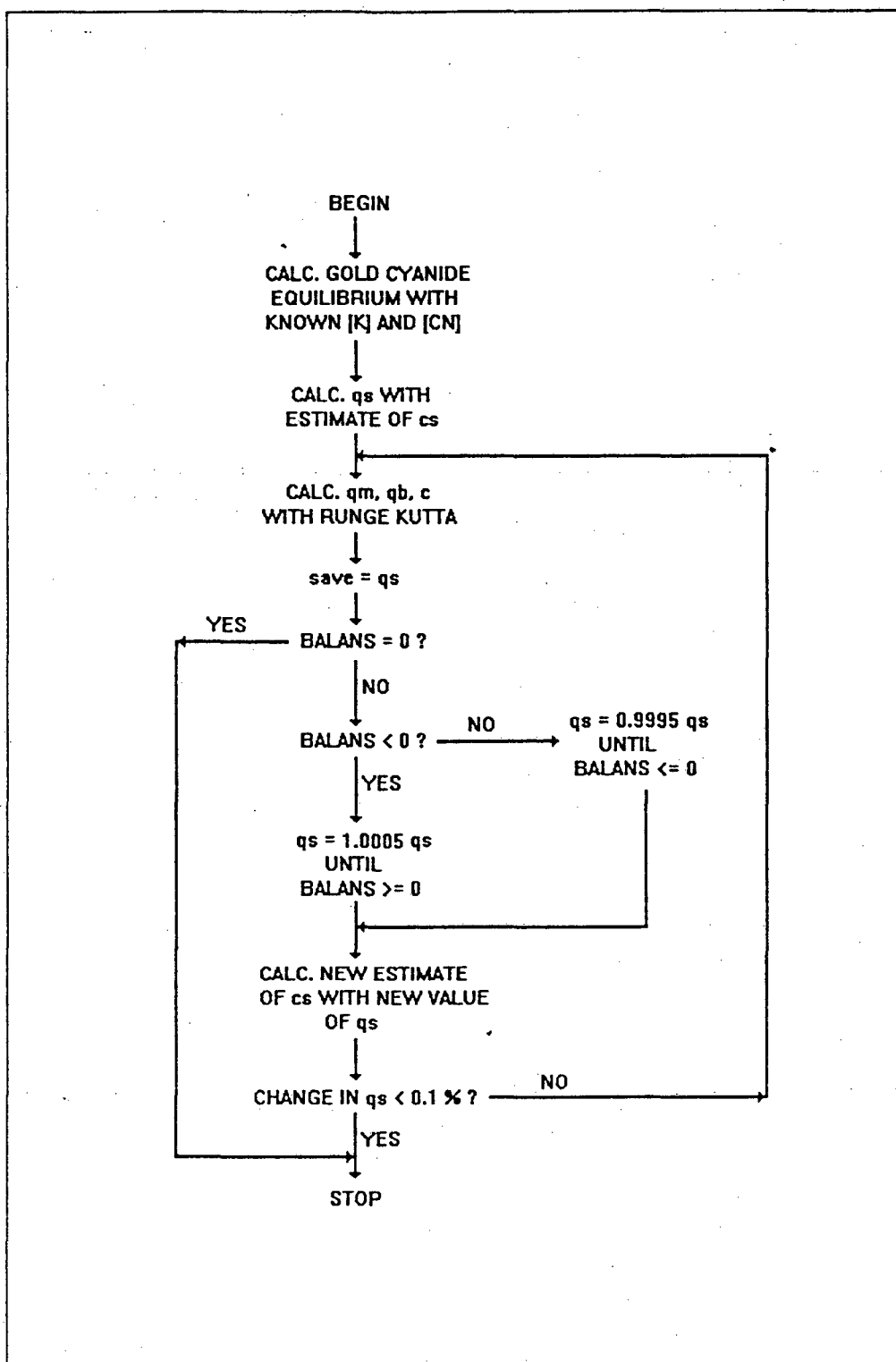



Figure H.2 Flow diagram of procedure "mod_au" in program "surfdiff"

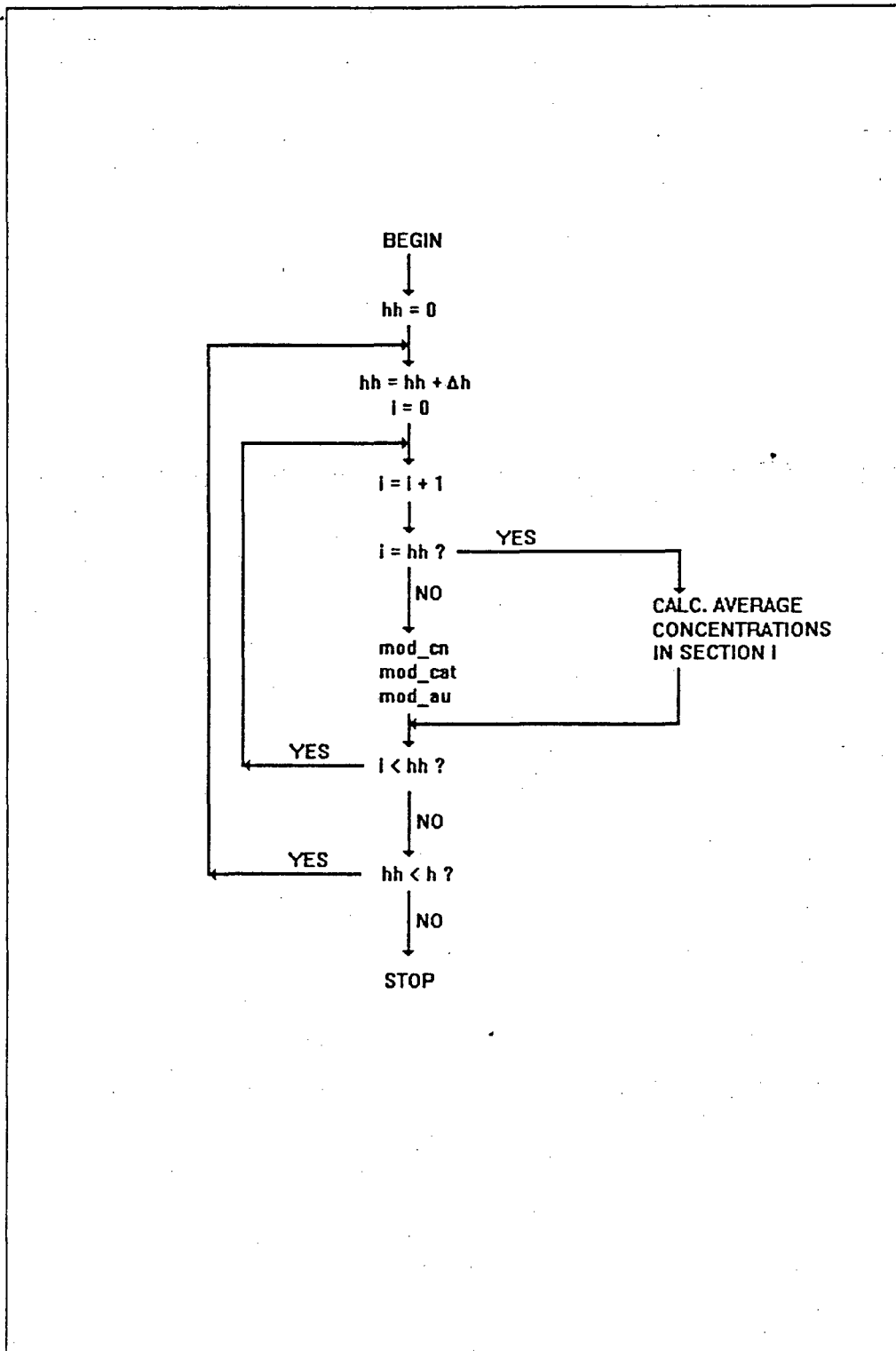


Figure H.3 Flow diagram of procedure "fill" in program "surfdiff"

APPENDIX I

TURBO PASCAL PROGRAM FOR EQUILIBRIUM MODEL

This program describes the elution of gold cyanide from a packed bed of activated carbon by using a combination of the following models :

- (1) The model for the elution and decomposition of cyanide developed in Chapter 4,
- (2) The nonideal flow model for the elution of potassium described in Chapter 5, and
- (3) The equilibrium model for the elution of gold cyanide developed in Chapter 6.

Program "equilib" is basically identical to program "surfdiff" described in Appendix H, except for the different model used in procedure "mod_au". The same output combinations are possible as for program "surfdiff".

Structure of main program

The structure of the main program is the same as that of the combination model described in Appendix G.

Algorithm of procedure "model"

The structure of procedure "model" is the same as that in program "surfdiff" (see Figure H.1 in Appendix H), except that no c_s -value is estimated before procedure "mod_au" in program "equilib". The structure of the fill procedure is also the same as described in Appendix H.

Algorithm of procedure "mod_au"

Procedure "mod_au" calculates the gold concentrations on the carbon and in the liquid phase by using the equilibrium model derived in Chapter 6. In each time step, the potassium and cyanide concentrations are calculated before procedure "mod_au". This enables the calculation of the equilibrium constant A for the height section concerned. The derivative (dA/dt) is then calculated with Equation 6.34. Equation 6.31

(function "fc") is solved with a Runge Kutta routine to produce the value of C_G (cg) at $(t+\Delta t)$.

The nomenclature is the same as in Appendix H, except for the following additions :

<u>Program</u>	<u>Thesis</u>
m1	m_1
m2	m_2
dadt	dA/dt
qg	Q_G

Program listing

```

program equilib;
uses crt,graph,grph;

const n_max=50;           {maximum number of height increments}
      n_maxx=51;         {n_max+1}
type timevar=array[0..n_maxx,1..2] of double;
var xmde,ymde,mnu,rpt,n,hh,i,j,jj,nt,ndd,nd:integer;
    a,cg,catm,catb,cat,cn,cnp,qcn:timevar;
    qg:array[0..n_maxx] of double;
    temp,dh,h,ti,v,eps,dc,fillt,hours,vp,cp,dt,
    dtfill,sec,k1,k2,k3,crossb,crossm,s,cato,
    catpo,catbo,beta,cath,nbvi,q,m1,m2,mm1,mm2,
    mm3,mm4, valx,mb1,mb2,mb3,mb4,mc1,mc2,mc3,mc4, valy,pp,
    qq,rr,ao,p,ea,f,c,
    co,qo,an,bn,dens,ttime,part1,area,sum,dadt,kcn,
    kcnp,kocn,kocnp,
    acn,ecn,kscn,cno,cnbo,cnpo,qocn,s0,s1,s2,s3,s4,s5:double;
    cntn,chg:yn;
    st:text;
    nxy:array[1..4] of integer;
    xx,yy:pnt;
label new;

function iso (ct,cyan,qcyan:double):double;           {gold isotherm}
begin
  nbvi:=(hours*3600*v*n/(area*i*h));
  iso:=(ao/(c*qcyan+1))*exp(ea/(temp+273.15))*power(nbvi+1,q)
    *power(ct+50,p)*power(cyan+1,f);
end;

function en (aa:double):double;                       {exponent in gold isotherm}
begin
  en:=an*aa+bn;
end;

```

```

procedure init1 (q0,cp0,aa:double;   {calculation of initial gold values}
                var c0:double);
var tail,r1,r2,r3,f1,f2,f3:double;
begin
tail:=q0+(m1-vp)*c0+vp*cp0;
r1:=0;
r2:=co+power(q0/aa,1/en(aa));
f1:=-tail;
f2:=aa*power(r2,en(aa))+m1*r2-tail;
repeat
  r3:=r1-(f1*(r1-r2)/(f1-f2));
  f3:=aa*power(r3,en(aa))+m1*r3-tail;
  if f3>0 then
    begin
      r2:=r3;
      f2:=f3;
    end
  else if f3<0 then
    begin
      r1:=r3;
      f1:=f3;
    end;
until abs(f3)<1e-8;
c0:=r3;
end;

```

```

{----- model starts -----}
procedure model;

```

```

procedure draw(line:integer);           {line draw procedure}
begin
  case ymde of 1: valy:=cg[n,1];
                2: valy:=cg[n,1]/co;
                3: begin
                    valy:=0;
                    for jj:=1 to nd do valy:=valy+qg[jj];
                    valy:=valy/jj;
                    end;
                4: valy:=cat[n,1];
                5: valy:=cn[n,1];
                end;
  case xmde of 1: valx:=hours;
                2: valx:=hours*3600*v/(area*h);
                end;
  case line of 0: moveto(xscr(valx),yscr(valy));
                1: lineto(xscr(valx),yscr(valy));
                end;
end;

```

```

procedure mod_au (var deltd,delh:double);   {model for gold cyanide}

```

```

function fc (var cf,ccf,af:double) : double;
begin
  part1:=m2*(ccf-cf)-(power(cf,en(af))*dadt
    -(af*an*power(cf,en(af))*dadt*ln(cf));

```

```

fc:=part1/(af*en(af)*power(cf,en(af)-1)+m1);
end;

begin
a[i,2]:=iso(cat[i,2],cn[i,2],qcn[i,2]);
dadt:=(a[i,2]-a[i,1])/delt;
mm1:=fc(cg[i,1],cg[i-1,1],a[i,1]);
pp:=cg[i,1]+((delt*mm1)/2);
qq:=(cg[i-1,1]+cg[i-1,2])/2;
rr:=(a[i,1]+a[i,2])/2;
mm2:=fc(pp,qq,rr);
pp:=cg[i,1]+((delt*mm2)/2);
mm3:=fc(pp,qq,rr);
pp:=cg[i,1]+(delt*mm3);
mm4:=fc(pp,cg[i-1,2],a[i,2]);
cg[i,2]:=cg[i,1]+((delt/6)*(mm1+(2*mm2)+(2*mm3)+mm4));
qg[i]:=a[i,2]*power(cg[i,2],en(a[i,2]));
end;

procedure mod_cat (var delh,delh:double); {model for elution of cation}

function fk (var kt,ktt,ktm:double):double;
begin
fk:=k1*(ktt-kt)+k1*crossm*(ktm-kt);
end;

function fkm (var kt,ktb,ktm:double):double;
begin
fkm:=k2*(kt-ktm)+k2*crossb*(ktb-ktm);
end;

function fkb (var ktb,ktm:double):double;
begin
fkb:=k3*(ktm-ktb);
end;

begin
k1:=v/(area*eps*delh);
k2:=crossm*v/(beta*area*delh*dens*vp*(1-eps));
k3:=crossm*crossb*v/((1-beta)*area*delh*dens*vp*(1-eps));
mcl:=fk(cat[i,1],cat[i-1,1],catm[i,1]);
mm1:=fkm(cat[i,1],catb[i,1],catm[i,1]);
mb1:=fkb(catb[i,1],catm[i,1]);
pp:=catm[i,1]+((delt*mm1)/2);
qq:=catb[i,1]+((delt*mb1)/2);
rr:=cat[i,1]+((delt*mcl)/2);
cath:=(cat[i-1,1]+cat[i-1,2])/2;
mc2:=fk(rr,cath,pp);
mm2:=fkm(rr,qq,pp);
mb2:=fkb(qq,pp);
pp:=catm[i,1]+((delt*mm2)/2);
qq:=catb[i,1]+((delt*mb2)/2);
rr:=cat[i,1]+((delt*mc2)/2);
mc3:=fk(rr,cath,pp);
mm3:=fkm(rr,qq,pp);

```

```

mb3:=fkb(qq,pp);
pp:=catm[i,1]+(delt*mm3);
qq:=catb[i,1]+(delt*mb3);
rr:=cat[i,1]+(delt*mc3);
mc4:=fk(rr,cat[i-1,2],pp);
mm4:=fkm(rr,qq,pp);
mb4:=fkb(qq,pp);
cat[i,2]:=cat[i,1]+((delt/6)*(mc1+(2*mc2)+(2*mc3)+mc4));
catm[i,2]:=catm[i,1]+((delt/6)*(mm1+(2*mm2)+(2*mm3)+mm4));
catb[i,2]:=catb[i,1]+((delt/6)*(mb1+(2*mb2)+(2*mb3)+mb4));
end;

```

```

procedure mod_cn(delt,delh:double); {model for cyanide}

```

```

begin
kcnp:=kocnp/power(1+qcn[i,1],acn);
s0:=1+(6*kscn*delt/(dens*vp*dc))+(kcnp*delt);
s1:=1/s0;
s2:=6*kscn*delt/(dens*vp*dc*s0);
s3:=6*kscn*(1-eps)*delt/(eps*dc);
s4:=v*delt/(area*eps*delh);
s5:=1+s4+(kcn*delt)+(s3*(1-s2));
cn[i,2]:=(cn[i,1]+(s4*cn[i-1,2])+(s3*s1*cnp[i,1]))/s5;
cnp[i,2]:=(s1*cnp[i,1])+(s2*cn[i,2]);
qcn[i,2]:=qcn[i,1]+(vp*kcnp*cnp[i,2]*delt);
end;

```

```

procedure fill; {start filling up}

```

```

begin
fillt:=(1-s)*h*area*eps/v;
dtfill:=fillt/n;
hh:=0;
repeat {time loop}
  sec:=sec+dtfill;
  hh:=hh+1; {hh = liquid level}
  if hh<>1 then
    begin
    for i:=1 to (hh-1) do mod_cn(dtfill,dh);
    cn[hh,2]:=(cn[hh,2]*s)+(cn[hh-1,2]*(1-s));
    if (cato<>catpo) or (cato<>catbo) then
      for i:=1 to (hh-1) do mod_cat(dtfill,dh)
    else
      for i:=1 to (hh-1) do
        begin
          catm[i,2]:=catm[i,1];
          catb[i,2]:=catb[i,1];
          cat[i,2]:=cat[i,1];
        end;
      if ymde<4 then for i:=1 to (hh-1) do mod_au(dtfill,dh);
    end;
    cnp[hh,2]:=cnp[hh,1]; {concentrations at liquid level}
    cn[hh,2]:=(cnbo*s)+(cn[hh-1,2]*(1-s));
    cat[hh,2]:=(catbo*s)+(cat[hh-1,2]*(1-s));
    catb[hh,2]:=catb[hh,1];
    catm[hh,2]:=catm[hh,1];
    cg[hh,2]:=cg[hh-1,2]*(1-s);
  end;
end;

```

```

a[hh,2]:=iso(cat[hh,2],cn[hh,2],qcn[hh,2]);
initl(qo,0,a[hh,2],cg[hh,2]);
qg[hh]:=a[hh,2]*power(cg[hh,2],en(a[hh,2]));
for i:=1 to hh do
  begin
    cat[i,1]:=cat[i,2];
    catm[i,1]:=catm[i,2];
    catb[i,1]:=catb[i,2];
    cg[i,1]:=cg[i,2];
    cn[i,1]:=cn[i,2];
    cnp[i,1]:=cnp[i,2];
    qcn[i,1]:=qcn[i,2];
    a[i,1]:=a[i,2];
  end;
until sec>=fillt;
end;
                                     {end of fill procedure}

begin
  cntn:='a';
  sec:=0;
  kcn:=kocn*exp(-ecn/(8.314*(273.15+temp)));
  m1:=vp+(eps/((1-eps)*dens));
  m2:=v/((1-eps)*area*dh*dens);
  n:=round(h/dh);
  ndd:=n-nd;
  for i:=1 to n_max do
    begin
      catm[i,1]:=catpo; catb[i,1]:=catpo; cat[i,1]:=catbo; cn[i,1]:=cnbo;
      cnp[i,1]:=cnpo; qcn[i,1]:=qocn; cg[i,1]:=co;
    end;
  for j:=1 to 2 do
    begin
      cg[0,j]:=co;
      if (catpo=cato) and (catbo=cato) then
        for i:=1 to n_max do cat[i,j]:=cato
      else cat[0,j]:=cato;
      if (cno=0) and (cnpo=0) and (cnbo=0) then
        for i:=0 to n_max do
          begin
            cn[i,j]:=0;
            cnp[i,j]:=0;
            qcn[i,j]:=qocn;
          end
        else cn[0,j]:=cno;
    end;

  if s<>1 then fill;

  hours:=sec/3600;
  draw(0);

  for j:=1 to nt do
    begin
      if nt=1 then

```

{carbon transfer loop}

```

begin
case xmde of 1: ttime:=xmx*3600;
              2: ttime:=xmx*area*h/v;
              end;
end
else
begin
if j=1 then ttime:=ti*3600
else
begin
case xmde of 1: ttime:=(xmx-ti)*3600/(nt-1);
              2: ttime:=((xmx*area*h/v)-ti*3600)/(nt-1);
              end;
end;
end;
sec:=0;
repeat
sec:=sec+dt;
if (cato<>catpo) or (catbo<>cato) then
for i:=1 to n do mod_cat(dt,dh)
else for i:=1 to n do
begin
catm[i,2]:=catm[i,1];
catb[i,2]:=catb[i,1];
cat[i,2]:=cat[i,1];
end;
if (cnbo<>0) or (cno<>0) or (cnpo<>0) then
for i:=1 to n do mod_cn(dt,dh)
else for i:=1 to n do
begin
cn[i,2]:=0;
cnp[i,2]:=0;
qcn[i,2]:=qocn;
end;
if ymde<4 then
begin
if hours=0 then
begin
for i:=1 to n do
begin
a[i,2]:=iso(cat[i,2],cn[i,2],qcn[i,2]);
cg[i,2]:=cg[i,1];
init1(qo,0,a[i,2],cg[i,2]);
qg[i]:=a[i,2]*power(cg[i,2],en(a[i,2]));
end;
end
else for i:=1 to n do mod_au(dt,dh);
end;
for i:=1 to n do
begin
cat[i,1]:=cat[i,2];
catm[i,1]:=catm[i,2];
catb[i,1]:=catb[i,2];
cg[i,1]:=cg[i,2];
a[i,1]:=a[i,2];

```

```

    cn[i,1]:=cn[i,2];
    cnp[i,1]:=cnp[i,2];
    qcn[i,1]:=qcn[i,2];
    end;
    hours:=hours+(dt/3600);
    draw(1);
    if keypressed then cntn:=upcase(readkey);
until (cntn='Q') or (sec>=ttime);
if (cntn<>'Q') and (j<>nt) then {transfer of carbon}
begin
for i:=1 to ndd do
begin
catm[i,1]:=catm[i+nd,1];
catb[i,1]:=catb[i+nd,1];
cnp[i,1]:=cnp[i+nd,1];
qcn[i,1]:=qcn[i+nd,1];
qg[i]:=qg[i+nd];
cp:=cg[i+nd,1];
if ymde<4 then
begin
a[i,1]:=iso(cat[i,1],cn[i,1],qcn[i,1]);
initl(qg[i],cp,a[i,1],cg[i,1]);
qg[i]:=a[i,1]*power(cg[i,1],en(a[i,1]));
end;
end;
for i:=ndd+1 to n do
begin
catm[i,1]:=catpo;
catb[i,1]:=catpo;
cnp[i,1]:=cnpo;
qcn[i,1]:=qocn;
if ymde<4 then
begin
a[i,1]:=iso(cat[i,1],cn[i,1],qcn[i,1]);
initl(qo,0,a[i,1],cg[i,1]);
qg[i]:=a[i,1]*power(cg[i,1],en(a[i,1]));
end;
end;
end;
end;
end;
}-----end of model-----}

procedure defaults; {setting default values}
begin
default;
xmde:=2; size:=4; fnt:=0; fntsize:=1; lgndsize:=1; ymde:=1; pc:=3;
assign(st,'equilib.dat');
reset(st);
readln(st,co); readln(st,qo); readln(st,h); readln(st,v);
readln(st,ao);
readln(st,p); readln(st,ea); readln(st,f); readln(st,c); readln(st,q);
readln(st,an); readln(st,bn); readln(st,dc); readln(st,dens);
readln(st,vp);
readln(st,temp); readln(st,cato); readln(st,catpo); readln(st,cno);

```

```

readln(st,cnbo); readln(st,kscn); readln(st,kocn);
readln(st,acn); readln(st,eps); readln(st,area); readln(st,s);
readln(st,nt);
readln(st,dh); readln(st,nd); readln(st,dt); readln(st,crossm);
readln(st,crossb); readln(st,beta); readln(st,catbo); readln(st,cnpo);
readln(st,qocn); readln(st,kocnp); readln(st,ecn);
close(st);
end;

```

```

procedure st_dat;                                {saving new default values}
begin
  assign(st,'equilib.dat');
  rewrite(st);
  writeln(st,co); writeln(st,qo); writeln(st,h); writeln(st,v);
  writeln(st,ao);
  writeln(st,p); writeln(st,ea); writeln(st,f); writeln(st,c);
  writeln(st,q);
  writeln(st,an); writeln(st,bn); writeln(st,dc); writeln(st,dens);
  writeln(st,vp); writeln(st,temp); writeln(st,cato); writeln(st,catpo);
  writeln(st,cno); writeln(st,cnbo); writeln(st,kscn); writeln(st,kocn);
  writeln(st,acn); writeln(st,eps); writeln(st,area);
  writeln(st,s); writeln(st,nt); writeln(st,dh); writeln(st,nd);
  writeln(st,dt); writeln(st,crossm); writeln(st,crossb);
  writeln(st,beta);
  writeln(st,catbo); writeln(st,cnpo); writeln(st,qocn);
  writeln(st,kocnp); writeln(st,ecn);
  close(st);
end;

```

```

procedure dat_gen;                               {input of working parameters}
begin
  clrscr;
  gotoxy(1,5);
  writeln('Working parameters');
  writeln('-----');
  gotoxy(1,8);
  str(h:6:4, wrd[1]); str(area:12, wrd[2]); str(dc:8:6, wrd[3]);
  str(dens:4:1, wrd[4]); str(vp:11, wrd[5]); str(eps:5:3, wrd[6]);
  str(v:12, wrd[7]); str(temp:3:1, wrd[8]); str(s:4:3, wrd[9]);
  str(nd:1, wrd[10]); str((nt-1):1, wrd[11]); str(dh:7:5, wrd[12]);
  str(dt:1:0, wrd[13]);
  writeln('Bed height [m] = ');
  writeln('Flow area of empty column [m2] = ');
  writeln('Particle diameter [m] = ');
  writeln('Apparent density of particles [kg/m3] = ');
  writeln('Pore volume of particles [m3/kg] = ');
  writeln('Void fraction of bed = ');
  writeln('Volumetric flow rate [m3/s] = ');
  writeln('Working temperature [°C] = ');
  writeln('Fraction of void fraction containing pretreatment reagent = ');
  writeln('Number of height sections discharged in counterflow = ');
  writeln('Number of carbon transfers during run = ');
  writeln('Incremental height [m] = ');
  writeln('Time step [s] = ');
  selectno(8,21,61,1,num, wrd);

```

```

h:=num[1]; area:=num[2]; dc:=num[3]; dens:=num[4]; vp:=num[5];
eps:=num[6];
v:=num[7]; temp:=num[8]; s:=num[9]; nd:=round(num[10]);
nt:=1+round(num[11]);
dh:=num[12]; dt:=num[13];
if nt>1 then
  begin
    gotoxy(1,23);
    write('Time interval before first transfer of carbon (hr) : ');
    readln(ti);
    end;
end;

procedure dat_draw;           {specification of value to be displayed}
begin
  repeat
    clrscr;
    writeln('Choose the value to be displayed');
    writeln('-----');
    wrd[1]:='Metal cyanide concentration [mg/l]';
    if co<>0 then wrd[2]:='C/Ci' else wrd[2]:='C/Co (not available)';
    wrd[3]:='Eluted carbon loading [mg/g]';
    wrd[4]:='Cation concentration [mg/l]';
    wrd[5]:='Cyanide concentration [mg/l]';
    select(4,9,1,ymde, wrd);
    case ymde of 1: capt[2]:='C [mg/l]';
                2: capt[2]:='C/Ci';
                3: capt[2]:='Q [mg/g]';
                4: capt[2]:='K [mg/l]';
                5: capt[2]:='CN [mg/l]';
    end;
    gotoxy(1,12);
    writeln('Values on x-axis :');
    wrd[1]:='Time [hr]'; wrd[2]:='No. of bed volumes';
    select(12,14,20,xmde, wrd);
    case xmde of 1: capt[1]:=wrd[1];
                2: capt[1]:=wrd[2];
    end;
  until (co<>0) or (ymde<>2);
end;

procedure dat_met;           {input of gold cyanide parameters}
begin
  clrscr;
  writeln('Metal cyanide');
  writeln('-----');
  writeln;
  writeln('A=Ao*exp(ea/(T+273.15))*power(K+50,p)*power(CN+1,f)');
  writeln(' *(1/(c*qCN+1))*power(BV+1,q)');
  str(co:4:2, wrd[1]); str(qo:5:3, wrd[2]); str(ao:6:5, wrd[3]);
  str(ea:4:3, wrd[4]); str(p:6:4, wrd[5]); str(f:6:4, wrd[6]);
  str(c:7:5, wrd[7]); str(q:7:5, wrd[8]);
  gotoxy(1,7);
  writeln('Feed concentration [mg/l] = ');
  writeln('Initial concentration on carbon [mg/g] = ');

```

```

writeln('Ao-value (ao)                = ');
writeln('Temperature dependency (ea)   = ');
writeln('Cation dependency (p)          = ');
writeln('Free cyanide dependency (f)     = ');
writeln('Cyanide-age dependency (c)       = ');
writeln('Change in activity (q)           = ');
selectno(7,15,42,1,num, wrd);
co:=num[1]; qo:=num[2]; ao:=num[3]; ea:=num[4]; p:=num[5]; f:=num[6];
c:=num[7]; q:=num[8];
gotoxy(1,17);
writeln('n = an*A + bn');
gotoxy(1,19);
str(an:9:7, wrd[1]); str(bn:9:7, wrd[2]);
writeln('Slope (an)                        = ');
writeln('Intercept (bn)                     = ');
selectno(19,21,42,1,num, wrd);
an:=num[1]; bn:=num[2];
end;

```

```

procedure dat_cat;                                {input of cation parameters}
begin
  clrscr;
  writeln('Cation parameters');
  writeln('-----');
  gotoxy(1,4);
  str(catpo:1:0, wrd[1]); str(catbo:1:0, wrd[2]); str(cato:1:0, wrd[3]);
  str(crossm:5, wrd[4]); str(crossb:5, wrd[5]); str(beta:4:3, wrd[6]);
  writeln('Initial pore conc. [mg/l]      = ');
  writeln('Initial interparticle conc. [mg/l] = ');
  writeln('Feed concentration [mg/l]          = ');
  writeln('Macropore cross flow ratio          = ');
  writeln('Micropore cross flow ratio          = ');
  writeln('Macro pore volume fraction          = ');
  selectno(4,10,45,1,num, wrd);
  catpo:=num[1]; catbo:=num[2]; cato:=num[3]; crossm:=num[4];
  crossb:=num[5]; beta:=num[6];
end;

```

```

procedure dat_cn;                                {input of cyanide parameters}
begin
  clrscr;
  writeln('Cyanide');
  writeln('-----');
  gotoxy(1,4);
  str(cnpo:1:0, wrd[1]); str(cnbo:1:0, wrd[2]); str(cno:1:0, wrd[3]);
  str(kscn:5, wrd[4]); str(kocn:5, wrd[5]); str(ecn:4:0, wrd[6]);
  str(kocnp:5, wrd[7]); str(acn:5:3, wrd[8]); str(qocn:3:1, wrd[9]);
  writeln('Initial pore concentration [mg/l]   = ');
  writeln('Initial interparticle concentration = ');
  writeln('Feed concentration [mg/l]          = ');
  writeln('Film transfer coefficient           = ');
  writeln('ko in bulk solution [1/s]           = ');
  writeln('E in bulk solution [J/mol]          = ');
  writeln('k in pores at zero cyanide-age [1/s] = ');
  writeln('Deactivating factor                 = ');
end;

```

```
writeln('Initial cyanide "loading" [mg/g]          = ');
selectno(4,13,45,1,num,wrđ);
cnpo:=num[1]; cnbo:=num[2]; cno:=num[3]; kscn:=num[4]; kocn:=num[5];
ecn:=num[6]; kocnp:=num[7]; acn:=num[8]; qocn:=num[9];
end;
```

```
{----- MAIN PROGRAM -----}
begin
clrscr;
highvideo;
fnt:=0;
fntsize:=2;
grdvr:=detect;
initgraph(grdvr,grmd,'');
xo:=round(getmaxx/10);
xm:=round(getmaxx/1.1);
yo:=round(getmaxy/20);
ym:=round(getmaxy/1.05);
xg:=xm-xo;
yg:=ym-yo;
setviewport(xo,yo,xm,ym,false);
moveto(0,0);
linere1(xg,0);
linere1(0,yg);
linere1(-xg,0);
linere1(0,-yg);
xg:=xm div 10;
yg:=ym div 10;
floodfill(1,1,white);
setcolor(black);
settextstyle(fnt,horizdir,fntsize);
settextjustify(lefttext,toptext);
outtextxy(xg,yg,'Equilibrium model for the');
outtextxy(xg,2*yg,'elution of gold from a');
outtextxy(xg,3*yg,'bed of activated carbon');
outtextxy(xg,5*yg,'by');
outtextxy(xg,7*yg,'P.F. van der Merwe');
settextstyle(0,horizdir,1);
outtextxy(5*xg,9*yg,'Press ENTER to continue...');
defaults;
readln;
closegraph;
new:
dat_gen;
dat_met;
dat_cat;
dat_cn;
dat_draw;
scale;
datname;
rpt:=1;
repeat
  if (rpt=1) and (np>0) then
    begin
      clrscr;
```

```
gotoxy(1,8);
writeln('Insert the disk containing the following files :');
writeln;
for i:=1 to np do writeln(fname[i]);
writeln;
pause;
j:=0;
for i:=1 to np do
  begin
    if plt[i]='Y' then
      begin
        j:=j+1;
        pat[i]:=cha[j];
      end
    else pat[i]:=0;
    end;
  for i:=1 to np do readplot(fname[i],xx,yy,nxy[i],i);
  rpt:=0;
end;
Init(pc,size,fnt,fntsize);
Axes;
for i:=1 to np do plot(xx,yy,nxy[i],join[i],pat[i],ltp[i],i);

model;

if key='Y' then legend;
if ex='Y' then extra;
readln;
CloseGraph;
clrscr;
repeat;
  clrscr;
  writeln('Changes');
  writeln('-----');
  gotoxy(1,4);
  mnu:=10;
  wrd[1]:='Plots and legend';
  wrd[2]:='Scale';
  wrd[3]:='Working parameters';
  wrd[4]:='Metal cyanide parameters';
  wrd[5]:='Cation parameters';
  wrd[6]:='Cyanide parameters';
  wrd[7]:='Values to be displayed';
  wrd[8]:='Captions';
  wrd[9]:='Extra text';
  wrd[10]:='Repeat simulation with changes';
  wrd[11]:='Start a new run';
  wrd[12]:='Quit';
  select(4,16,1,mnu, wrd);
  case mnu of 1: begin
    datname;
    rpt:=1;
    end;
    2: scale;
    3: dat_gen;
```

```
4: dat_met;
5: dat_cat;
6: dat_cn;
7: dat_draw;
8: caption;
9: extratext;
12: begin
    gotoxy(1,19);
    write('Save data ? (Y/N) ');
    quest(chg);
    if chg='Y' then st_dat;
    write('Quit program ? (Y/N) ');
    quest(chg);
    if chg='N' then mnu:=1;
    end;
end;
until (mnu>9);
if mnu=11 then goto new;
until (mnu=12);
end.
```

APPENDIX J

TURBO PASCAL SUB-ROUTINES FOR MENU'S AND GRAPHICS

The same graphics routines were used for the programs listed in Appendices G to I. These routines were combined in the Turbo Pascal unit "grph" presented below. The function of each procedure is noted in the program listing.

Program listing

```

unit grph;
interface
uses dos,graph,crt;

type  oneitem=string[50];
      filename=string[30];
      yn=string[1];
      pnt=array[1..4,1..100] of double;
      wrds=array[1..20] of oneitem;
      realstr=array[1..20] of double;
var   num:realstr;
      wrd:wrds;
      dat:text;
      scan,grdvr,grmd,inc,j,nx,ny,np,nv,xo,yo,xm,ym,lngth,
      hght,xb,yb,plc,fnt,
      lgndsize,fntsize,ni,xg,yg,xe,ye,xv,yv,i,xd,yd,w0,h0,ls,
      pc,size:integer;
      xmx,xmn,ymx,ymn,xl,yl,xin,yin,g:real;
      mrk:string[5];
      capt:array[1..8] of oneitem;
      plt,join:array[1..4] of yn;
      ch,ex,key,choice:char;
      test:string[1];
      lgnd,ins:array[1..6] of string[50];
      xi,yi:array[1..6] of integer;
      ltp,pat:array[1..6] of integer;
      fname:array[1..5] of filename;
      wc:yn;
const cha:array[1..8] of integer=(4,10,11,12,120,42,43,9);

function Xscr (x:double) :integer;
function Yscr (y:double) :integer;
procedure Default;
procedure Init (pc,size,fnt,fntsize:integer);
procedure Caption;
procedure Des (var numb:real;
              var ndes:integer);
procedure Scale;
procedure Datname;

```

```

procedure Readplot(var fnm:filename;
                  var x,y:pnt;
                  var npts,i:integer);
procedure Plot(var x,y:pnt;
              var npts:integer;
              var jn : yn;
              var car,tpe,i : integer);
procedure Axes;
procedure Extratext;
procedure Position(var xp,yp,hp,lp:integer);
procedure Extra;
procedure Legend;
procedure Quest (var ans:yn);
procedure Pause;
function Power (xm,ym:double) : double;
procedure KeyScan;
procedure SelectWrd (lg,hg,x,i:integer;
                   var items:wrds);
procedure SelectNo (lg,hg,x,i:integer;
                  var v:realstr;
                  var items:wrds);
procedure Select(lg,hg,x:integer;
                var i:integer;
                var items:wrds);

implementation

function Xscr (x:double) :integer;      {converts x to screen co-ordinate}
begin
  xscr:=round((x-xmn)*xg/xl);
end;

function Yscr (y:double) :integer;      {converts y to screen co-ordinate}
begin
  yscr:=yg-round((y-ymn)*yg/yl);
end;

procedure Default;                      {default settings}
begin
  key:='N';ex:='N';size:=4;fnt:=0;
  fntsize:=1; lgndsize:=1; xv:=10; yv:=10;
  for i:=1 to 8 do capt[i]:='';
  for i:=1 to 6 do
    begin
      xi[i]:=0;
      yi[i]:=0;
      lgnd[i]:='';
      ins[i]:='';
    end;
  for i:=1 to 4 do
    begin
      ltp[i]:=0;
      fname[i]:='a:\';
      plt[i]:='Y';
      join[i]:='N';
    end;
  end;

```

```

    end;
    xd:=3; yd:=3; ni:=0; np:=0; nv:=0;
    xmn:=0; ymn:=0; xmx:=10; ymx:=1; nx:=5; ny:=5;
end;

procedure Init (pc,size,fnt,fntsize:integer); {sets screen in graph mode}
begin
    if pc=1 then
        begin
            {pc = 1 = AT&T = Olivetti}
            {pc = 2 = Hercules      }
            {pc = 3 = CGA, other    }
            grdvr:=8;
            grmd:=3;
            initgraph(grdvr,grmd,'');
            setgraphmode(att400hi);
        end
    else
        begin
            grdvr:=detect;
            initgraph(grdvr,grmd,'');
        end;
    settxtstyle(fnt,horizdir,fntsize);
    if pc=3 then
        begin
            {sets size of graph}
            xo:=round(getmaxx/6);
            if (size=1) or (size=2) then
                xm:=round(getmaxx/1.5) else xm:=round(getmaxx/1.05);
            yo:=round(getmaxy/50);
            if (size=4) or (size=2) then ym:=round(getmaxy/1.3)
                else ym:=round(getmaxy/1.6);
            inc:=textheight('0');
        end
    else
        begin
            if (fnt=0) or (fntsize=5) then xo:=round(getmaxx/8)
                else xo:=round(getmaxx/6);
            if (size=1) or (size=2) then xm:=round(getmaxx/1.15)
                else xm:=round(getmaxx/1.06);
            yo:=round(getmaxy/50);
            if (size=4) or (size=2) then ym:=round(getmaxy/1.2)
                else ym:=round(getmaxy/1.4);
            inc:=round(1.5*textheight('0'));
        end;
    end;

procedure Caption;
begin
    {input of captions}
    clrscr;
    gotoxy(1,3);
    for i:=1 to 8 do wrd[i]:=capt[i];
    writeln('Captions');
    writeln('-----');
    writeln;
    writeln('X-axis  :');
    writeln('Y-axis  :');
    writeln('Heading :');
    writeln('      :');

```

```

writeln('      :');
writeln('      :');
writeln('      :');
writeln('      :');
select wrd(6,14,13,1, wrd);
for i:=1 to 8 do capt[i]:= wrd[i];
end;

procedure Des(var numb:real;           {calculates number of decimals}
              var ndes:integer);
var str10:string[10];
begin
  str(numb:10:3, str10);
  ndes:=3;
  plc:=11;
  repeat
    plc:=plc-1;
    test:=copy(str10,plc,1);
    if test='0' then ndes:=ndes-1;
  until (test<>'0') or (ndes=0);
end;

procedure Scale;                       {input of axes scales}
begin
  repeat
    clrscr;
    str(xmn:5:3, wrd[1]); str(xmx:5:3, wrd[2]); str(ymn:5:3, wrd[3]);
    str(ymx:5:3, wrd[4]); str(nx:1, wrd[5]); str(ny:1, wrd[6]);
    gotoxy(1,8);
    writeln('Scale');
    writeln('-----');
    writeln;
    writeln('X-minimum   :');
    writeln('X-maximum   :');
    writeln('Y-minimum   :');
    writeln('Y-maximum   :');
    writeln('X-divisions  :');
    writeln('Y-divisions  :');
    select no(11,17,16,1, num, wrd);
    xmn:=num[1]; xmx:=num[2]; ymn:=num[3]; ymx:=num[4];
    nx:=round(num[5]); ny:=round(num[6]);
    xl:=xmx-xmn;
    yl:=ymx-ymn;
    if nx>0 then xin:=xl/nx else xin:=xl;
    if ny>0 then yin:=yl/ny else yin:=yl;
  until (xl>0) and (yl>0);
end;

procedure Datname;                     {input of data files to be plotted}
begin
  clrscr;
  writeln;
  writeln('Plots');
  write('-----');

```

```

writeln('-----');
writeln('Filename');
writeln;
for i:=1 to 4 do wrd[i]:=fname[i];
SelectWrd (6,10,1,1, wrd);
for i:=1 to 4 do fname[i]:=wrd[i];
gotoxy(1,4);
writeln('Filename          P');
for i:=1 to 4 do wrd[i]:=plt[i];
SelectWrd (6,10,22,1, wrd);
for i:=1 to 4 do
  begin
    plt[i]:=copy(wrd[i],1,1);
    if plt[i]='y' then plt[i]='Y';
  end;
gotoxy(1,4);
writeln('Filename          P  J');
for i:=1 to 4 do wrd[i]:=join[i];
SelectWrd (6,10,26,1, wrd);
test:='N';
for i:=1 to 4 do
  begin
    join[i]:=copy(wrd[i],1,1);
    if join[i]='y' then join[i]='Y';
    if join[i]='Y' then test:='Y';
  end;
if test='Y' then
  begin
    gotoxy(1,4);
    writeln('Filename          P  J  L');
    for i:=1 to 4 do str(ltp[i]:1, wrd[i]);
    SelectNo (6,10,30,1, num, wrd);
    for i:=1 to 4 do ltp[i]:=round(num[i]);
  end;
np:=0;
for i:=1 to 4 do if fname[i]<>'a:\' then np:=i;
gotoxy(1,4);
writeln('Filename          P  J  L  Legend entry');
for i:=1 to 4 do wrd[i]:=lgnd[i];
SelectWrd (6,10,34,1, wrd);
nv:=0;
for i:=1 to 4 do
  begin
    lgnd[i]:=wrd[i];
    if lgnd[i]<>' ' then
      begin
        key:='Y';
        nv:=i;
      end;
  end;
if key='Y' then nv:=nv-np;
end;

procedure Readplot(var fnm:filename;          {reads data from disk}
                   var x,y:pnt;

```

```

                var npts,i:integer);
begin
  assign(dat,fnm);
  reset(dat);
  npts:=0;
  while not eof(dat) do
    begin
      npts:=npts+1;
      readln(dat,x[i,npts],y[i,npts]);
    end;
  close(dat);
end;

procedure Plot(var x,y:pnt;                                {plots data on screen}
               var npts:integer;
               var jn : yn;
               var car,tpe,i : integer);

begin
  settextstyle(defaultfont,horizdir,1);
  xb:=xscr(x[i,1]);
  yb:=yscr(y[i,1]);
  xe:=xb;
  ye:=yb;
  if (car<>0) then outtextxy(xe,ye,chr(car));
  settextjustify(centertext,centertext);
  for j:=2 to npts do
    begin
      xe:=xscr(x[i,j]);
      ye:=yscr(y[i,j]);
      if car<>0 then outtextxy(xe,ye,chr(car));
      if jn='Y' then
        begin
          setlinestyle(tpe,solidln,normwidth);
          line(xb,yb,xe,ye);
        end;
      xb:=xe;
      yb:=ye;
    end;
  setlinestyle(0,solidln,normwidth);
  if car<>0 then outtextxy(xe,ye,chr(car));
end;

procedure Axes;                                          {draws axes}
var xee,yee:double;
begin
  des(xin,xd);
  des(yin,yd);
  xg:=xm-xo;
  yg:=ym-yo;
  settextstyle(fnt,horizdir,fntsize);
  w0:=textwidth('0');
  h0:=textheight('0');
  if pc=3 then ls:=round(h0/3);
  if pc=1 then if (fnt=0) then ls:=round(1.3*h0) else ls:=round(h0/1.5);

```

```

if pc=2 then ls:=w0 div 2;
setviewport(xo,ym,xm,getmaxy,false);
if (nx>0) then
begin
for i:=0 to nx do
begin
g:=xmn+(i*xin);
plc:=0;
str(g:5:xd,mrk);
repeat
plc:=plc+1;
test:=copy(mrk,1,1);
if test=' ' then mrk:=copy(mrk,2,5-plc);
until (test<>' ') or (plc>4);
settextjustify(centertext,toptext);
outtextxy(round(i*xg/nx),ls,mrk);
end;
end;
settextjustify(centertext,toptext);
outtextxy(xg div 2,h0+2*ls,capt[1]);

setviewport(0,yo,xo,ym,false);
if (ny>0) then
begin
for i:=0 to ny do
begin
g:=ymx-(i*yin);
str(g:1:yd,mrk);
settextjustify(righttext,centertext);
outtextxy(xo-w0,round(i*(ym-yo)/ny),mrk);
end;
end;
str(ymx:1:yd,mrk);
settextstyle(fnt,vertdir,fntsize);
settextjustify(righttext,centertext);
if (fnt=1) or (fntsize>5) then xb:=2 else xb:=3;
xee:=xo-textwidth(mrk)-xb*w0;
outtextxy(round(xee),(ym-yo) div 2,capt[2]);

setviewport(0,ym,xm,getmaxy,false);
settextstyle(0,horizdir,1);
settextjustify(lefttext,toptext);
if (fnt=0) or (fntsize=5) then
for i:=1 to 6 do outtextxy(round(xee),(2+i)*h0+3*ls,capt[i+2]) else
for i:=1 to 6 do outtextxy(round(xee),(2+i)*h0+2*ls,capt[i+2]);

setviewport(xo,yo,xm,ym,true);
moveto(0,0);
linere1(xg,0);
linere1(0,yg);
linere1(-xg,0);
linere1(0,-yg);
if (nx>1) and (ny>1) then
begin
for i:=1 to (nx-1) do

```

{x-axis}

{y-axis}

{caption}

{graph window}

```

begin
  moveto(round(i*xg/nx),0);
  linere1(0,3);
  moveto(round(i*xg/nx),yg);
  linere1(0,-3);
end;
for j:=1 to (ny-1) do
  begin
    moveto(0,round(j*yg/ny));
    linere1(5,0);
    moveto(xg,round(j*yg/ny));
    linere1(-5,0);
  end;
end;
xee:=xmn;
yee:=0;
moveto(xscr(xee),yscr(yee));
xee:=xmx;
lineto(xscr(xee),yscr(yee));
xee:=0;
yee:=ymn;
moveto(xscr(xee),yscr(yee));
yee:=ymx;
lineto(xscr(xee),yscr(yee));
end;

procedure Extratext;                                     {input of extra text}
begin
  clrscr;
  gotoxy(1,8);
  writeln('Extra Text in graph window');
  writeln('-----');
  gotoxy(1,11);
  for i:=1 to 6 do
    begin
      writeln('Entry ',i:1,' : ');
      wrd[i]:=ins[i];
    end;
  select wrd(11,17,13,1,wrd);
  for i:=1 to 6 do
    begin
      ins[i]:=wrd[i];
      if ins[i]<>' ' then
        begin
          ex:='Y';
          ni:=i;
        end;
    end;
end;

procedure Position(var xp,yp,hp,lp:integer);           {determines position of}
var pix1,pix2:word;                                   {legend and extra text }
begin                                                 { on screen }
  pix1:=getpixel(xp,yp);

```

```

pix2:=getpixel(xp+lp,yp+hp);
putpixel(xp,yp,getcolor);
putpixel(xp+lp,yp+hp,getcolor);
inc:=4;
repeat
  ch:=readkey;
  putpixel(xp,yp,pix1);
  putpixel(xp+lp,yp+hp,pix2);
  case ord(ch) of
    72: yp:=yp-inc;
    73: inc:=2*inc;
    81: if inc>1 then inc:=inc div 2;
    75: xp:=xp-inc;
    77: xp:=xp+inc;
    80: yp:=yp+inc;
  end;
  pix1:=getpixel(xp,yp);
  putpixel(xp,yp,getcolor);
  pix2:=getpixel(xp+lp,yp+hp);
  putpixel(xp+lp,yp+hp,getcolor);
until ord(ch)=13;
putpixel(xp,yp,pix1);
putpixel(xp+lp,yp+hp,pix1);
end;

```

```

procedure Legend;                                     {output of legend on screen}
begin
  settextstyle(fnt,horizdir,lgndsize);
  if pc=3 then ls:=textheight('0')
    else if (fnt=0) or (lgndsize=5) then ls:=round(1.6*textheight('0'))
    else ls:=textheight('0');
  lngth:=textwidth(lgnd[1]);
  for i:=2 to (np+nv) do
    if textwidth(lgnd[i])>lngth then lngth:=textwidth(lgnd[i]);
  lngth:=lngth+2*textwidth('0');
  hght:=(np+nv-1)*ls;
  position(xv,yv,hght,lngth);
  settextjustify(centertext,centertext);
  settextstyle(defaultfont,horizdir,1);
  for i:=1 to np do
    begin
      if pat[i]<>'0' then outtextxy(xv,yv,chr(pat[i]));
      yv:=yv+ls;
    end;
  settextstyle(fnt,horizdir,lgndsize);
  yv:=yv-(np*ls);
  settextjustify(lefttext,centertext);
  for i:=1 to (np+nv) do
    begin
      outtextxy(xv+2*textwidth('0'),yv,lgnd[i]);
      yv:=yv+ls;
    end;
  yv:=yv-(np+nv)*ls;
end;

```

```

procedure Extra;                                     {output of extra text on screen}
begin
  settxtstyle(fnt,horizdir,lgndsize);
  for i:=1 to ni do
    begin
      lngth:=textwidth(ins[i]);
      hght:=0;
      position(xi[i],yi[i],hght,lngth);
      settxtjustify(lefttext,centertext);
      outtextxy(xi[i],yi[i],ins[i]);
    end;
end;

procedure Quest (var ans:yn);                       {input of Y/N type of questions}
begin
  ans:='a';
  repeat
    ans:=upcase(readkey);
  until (ans='Y') or (ans='N');
  writeln(ans);
end;

procedure Pause;                                   {pause until key pressed}
begin
  gotoxy(51,25);
  write('Press any key to continue ...');
  wc:='w';
  wc:=readkey;
end;

function Power (xm,ym:double) : double;           {raises xm to the power ym}
begin
  if xm>0 then power:=exp(ym*ln(xm))
  else if xm<0 then
    begin
      closegraph;
      clrscr;
      write('Argument of power function smaller than 0,');
      writeln(' Press Ctrl Break');
      readln;
    end
  else if ym>0 then power:=0
  else
    begin
      closegraph;
      clrscr;
      write('Division by 0 in power function,');
      writeln(' Press Ctrl Break');
      readln;
    end;
end;

end;

procedure KeyScan;                                 {rest of procedures : used for creation of menu's}
var reg : Registers;
    ascii:integer;

```

```

begin
  reg.ax := 0;
  intr ($16,reg);
  ascii := lo(reg.ax);
  scan := hi(reg.ax);
  ch := char(ascii);
end;

procedure Tab(var x,y:integer; var item:oneitem);
var k:integer;
begin
  textbackground(black);
  textcolor(white);
  gotoxy(x,y);
  for k:=1 to length(item) do write(' ');
  item:='';
  gotoxy(x,y);
end;
{TAB key - deletes line}

procedure Del(var x,y:integer; var item:oneitem);
begin
  textbackground(black);
  textcolor(white);
  gotoxy(x+length(item)-1,y);
  write(' ');
  item:=copy(item,1,length(item)-1);
  gotoxy(x,y);
  write(item);
end;
{BACKSPACE key - deletes character}

procedure Up(var x,y,hg,lg,i:integer; var items:wrds);
begin
  gotoxy(x,y);
  textbackground(black);
  textcolor(white);
  write(items[i]);
  if y>lg then begin y:=y-1; i:=i-1; end
  else begin y:=hg-1; i:=hg-1; end;
  gotoxy(x,y);
  textbackground(lightgray);
  textcolor(black);
  write(items[i]);
end;
{UP arrow}

procedure Down(var x,y,hg,lg,i:integer; var items:wrds);
begin
  gotoxy(x,y);
  textbackground(black);
  textcolor(white);
  write(items[i]);
  if y<hg-1 then begin y:=y+1; i:=i+1; end
  else begin y:=lg; i:=1; end;
  gotoxy(x,y);
  textbackground(lightgray);
  textcolor(black);
end;
{DOWN arrow}

```

```

    write(items[i]);
end;

procedure SelectWrd( lg,hg,x,i:integer;   {Permits changes to text menus}
                    var items:wrds);
var loop,pix,j,y : integer;

begin
  pix:=0;
  scan:=1;
  highvideo;
  for j:=1 to (hg-lg) do
    begin
      gotoxy(x,j+lg-1);
      writeln(items[j]);
    end;
  y:=lg+i-1;
  repeat
    gotoxy(x,y);
    textbackground(lightgray);
    textcolor(black);
    write(items[i]);
    loop := 1;
    while loop < 11 do begin
      if scan=28 then scan:=80 else
        begin
          repeat
            KeyScan
          until scan in [2..28,30..41,43..53,72,80]
          end;
        case scan of
          72 : up(x,y,hg,lg,i,items);
          80 : down(x,y,hg,lg,i,items);
          28 : begin
                pix:=1;
                loop:=11;
              end;
          15 : tab(x,y,items[i]);
        else begin
              textbackground(black);
              textcolor(white);
              if scan=14 then del(x,y,items[i])
              else
                begin
                  gotoxy(x,y);
                  items[i] := items[i] + ch;
                  write(items[i]);
                end;
            repeat
              repeat KeyScan
            until scan in [2..28,30..41,43..53,57];
            case scan of
              14 : del(x,y,items[i]);
              15 : tab(x,y,items[i]);
              28 : begin end;
            end;
          end;
        end;
    end;
  end;
end;

```

```

                else begin
                    items[i] := items[i] + ch;
                    write(ch);
                    end;
                end;
            until scan=28;
        end;
    end;
    until pix=1;
    textbackground(black);
    textcolor(white);
end;

procedure SelectNo(lg,hg,x,i:integer; {Permits changes to numeric values}
    var v:realstr;
    var items:wrds);
var loop,pix,j,y : integer;
    code:integer;

begin
    pix:=0;
    scan:=1;
    highvideo;
    for j:=1 to (hg-lg) do
        begin
            gotoxy(x,j+lg-1);
            writeln(items[j]);
            end;
    y:=lg+i-1;
    repeat
        gotoxy(x,y);
        textbackground(lightgray);
        textcolor(black);
        write(items[i]);
        loop := 1;
        while loop < 11 do begin
            if scan=28 then scan:=80 else
                begin
                    repeat KeyScan until scan in [2..12,83,28,52,72,80]
                end;
            case scan of
                72: up(x,y,hg,lg,i,items);
                80: down(x,y,hg,lg,i,items);
                28: begin
                    pix:=1;
                    loop:=11;
                    end;
            else begin
                tab(x,y,items[i]);
                items[i] := items[i] + ch;
                write(items[i]);
                repeat
                    repeat KeyScan until scan in [2..12,14,18,52,28];
                    case scan of

```

```

        14 : del(x,y,items[i]);
        28 : begin end;
        else begin
            items[i] := items[i] + ch;
            write(ch);
            end;
        end;
    until scan=28;
end;
end;
end;
for j:=1 to 20 do val(items[j],v[j],code);
until pix=1;
textbackground(black);
textcolor(white);
end;

procedure Select(lg,hg,x:integer;                                {Selection of option}
                var i:integer;                                  {no change possible }
                var items:wrds);

var loop,pix,j,y : integer;

begin
    pix:=0;
    scan:=1;
    highvideo;
    for j:=1 to (hg-lg) do
        begin
            gotoxy(x,j+lg-1);
            writeln(items[j]);
            end;
    y:=lg+i-1;
    repeat
        gotoxy(x,y);
        textbackground(lightgray);
        textcolor(black);
        write(items[i]);
        loop := 1;
        while loop < 11 do begin
            repeat KeyScan until scan in [28,72,80];
            case scan of
                72: up(x,y,hg,lg,i,items);
                80: down(x,y,hg,lg,i,items);
                28: begin
                    pix:=1;
                    loop:=11;
                    end;
            end;
        end;
    until pix=1;
    textbackground(black);
    textcolor(white);
end;

end.

```

APPENDIX K

TABULATION OF EXPERIMENTAL RESULTS

Experiment no.1

Zeta potentials of carbons A and B as a function of solution pH.

Carbon A		Carbon B	
pH	ξ [mV]	pH	ξ [mV]
2.01	-9.18	1.46	111.38
2.78	-23.44	2.92	-31.36
3.52	-37.12	3.83	-51.77
4.69	-67.60	5.52	-99.96
5.46	-92.35	6.41	-103.8
5.55	-89.27	9.34	-99.01
6.89	-98.14		
8.8	-89.84		
10.24	-94.31		
11.08	-82.96		

Experiment no.2

Particle size distribution of carbon BTX.

$-d_{c1}+d_{c2}$ [μm]	m_c [g]	ψ	d_c [μm]
-2360+2000	1.8029	0.052	2173
-2000+1700	5.3469	0.155	1844
-1700+1400	10.852	0.315	1543
-1400+1180	8.2232	0.239	1086
-1000+850	2.5241	0.073	922
-850+0	0.7064	0.020	29
$m_{c(\text{total})}$	34.466	$d_{c(\text{ave})}$	1417

 d_{c1}, d_{c2} = Sieve sizes

$$d_c = \sqrt{d_{c1} \cdot d_{c2}}$$

$$d_{c(\text{ave})} = \sum \psi \cdot d_c$$

Experiment no.3

Equilibrium adsorption of gold cyanide on carbon A from solutions in contact with air, i.e. $[O_2] = 9 \text{ mg/l}$.

$v_i = 1000 \text{ ml}$

m_c [g]	C_{ig} [g/m ³]	v_e [ml]	C_{eg} [g/m ³]	Q_{eg} [g/kg]
1.2081	30.6	945	3.0	23.0
1.0817	30.6	955	3.8	24.9
0.9745	30.6	960	4.9	26.6
0.8985	30.6	1000	5.9	27.5
0.8266	30.6	965	7.0	28.9
0.7667	30.6	945	7.9	30.2
0.7116	30.6	955	8.9	31.1
0.6238	30.6	955	11.1	32.1
1.1006	48.0	1015	11.6	32.9
0.5562	30.6	965	12.5	33.3
0.5064	30.6	965	13.5	34.7
0.9820	48.0	1010	13.6	34.9
2.0018	86.1	950	15.2	35.8
0.8492	48.0	1045	16.5	36.2
0.7751	48.0	1020	19.5	36.3
0.7130	48.0	1000	21.1	37.7
1.7555	86.1	955	21.1	37.6
0.5337	48.0	1041	26.0	39.2
1.5510	86.1	940	28.0	38.6
1.3660	86.1	985	31.1	40.6
1.2033	86.1	935	36.8	43.0
1.0552	86.1	950	43.0	42.9
1.2010	96.0	1020	46.3	40.6
0.9138	86.1	965	48.0	43.5
1.0009	96.0	990	51.3	45.2
0.7814	86.1	970	54.0	43.2
0.6583	86.1	965	57.4	46.7
0.8399	96.0	995	58.0	45.6
0.5383	86.1	960	63.4	46.9
0.6836	96.0	985	64.0	48.2
0.5419	96.0	1000	69.0	49.8
0.4265	86.1	960	69.2	46.1
0.3138	86.1	945	74.6	49.7

$$Q_{eg} = 18.97 C_{eg}^{0.2194}$$

Experiment no.4

Equilibrium adsorption of gold cyanide on carbon A from solutions with a constant $[O_2] = 4.4 \text{ mg/l}$.

$v_i = 1000 \text{ ml}$

m_c [g]	C_{iG} [g/m ³]	v_e [ml]	C_{eG} [g/m ³]	Q_{eG} [g/kg]
1.4312	13.8	890	0.3	9.5
1.1864	13.8	890	0.5	11.3
0.7570	13.8	875	1.8	16.2
0.4938	13.8	895	4.3	20.2
0.3326	13.8	880	7.1	22.7
0.2067	13.8	895	10.0	23.5
1.6800	57.4	870	12.7	27.6
1.3875	57.4	900	19.2	28.9
0.9410	57.4	885	28.6	34.1
0.5844	57.4	900	41.6	34.2

$$Q_{eG} = 13.478 C_{eG}^{0.2636}$$

Experiment no.5

Equilibrium adsorption of gold cyanide on carbon A from deaerated solutions, i.e. $[O_2] = 0$ mg/l.

$$V_e = V_i$$

m_c [g]	V_i [ml]	C_{iG} [g/m ³]	C_{eG} [g/m ³]	Q_{eG} [g/kg]
1.8968	1000	13.4	0.8	6.6
1.2751	950	10.0	1.0	6.7
0.9621	950	10.0	1.4	8.5
1.3946	1000	13.4	1.6	8.5
0.7349	950	10.0	2.3	9.95
1.1153	1000	13.4	2.3	9.95
0.4852	950	10.0	3.6	12.5
0.7833	1000	13.4	4.5	11.4
1.6310	950	29.0	5.9	13.5
0.3085	1000	13.4	9.1	13.9
1.1129	950	29.0	10.0	16.2
2.4208	1000	54.6	11.1	18.0
0.6922	950	29.0	14.9	19.4
1.9511	1000	54.6	16.6	19.5
1.2560	950	47.6	21.0	20.1
1.2707	1000	54.6	28.0	20.9
0.5949	950	47.6	33.0	23.3
0.7717	1000	54.6	35.8	24.4
0.3564	1000	54.6	45.1	26.7

$$Q_{eG} = 7.302 C_{eG}^{0.3387}$$

Experiment no.6

Equilibrium adsorption of gold cyanide on carbon A from solutions with a constant $[O_2] = 14.5 \text{ mg/l}$.

$v_i = 1000 \text{ ml}$

m_c [g]	C_{iG} [g/m ³]	v_e [ml]	C_{eG} [g/m ³]	Q_{eG} [g/kg]
1.1124	48.0	975	11.9	32.7
0.9834	48.0	985	15.0	33.8
0.7743	48.0	970	20.4	36.4
0.7123	48.0	970	22.6	36.6
0.6427	48.0	960	24.2	38.5
0.5385	48.0	980	27.0	40.0
1.2056	96.0	995	46.7	41.1
1.1103	96.0	980	49.0	43.2
0.9994	96.0	980	52.0	45.1
0.8411	96.0	980	58.0	46.6
0.6835	96.0	990	64.0	47.8
0.5400	96.0	1000	69.0	50.0

$$Q_{eG} = 18.47 C_{eG}^{0.226}$$

Experiment no.7

Equilibrium adsorption of silver cyanide on carbon A from solutions in contact with air, i.e. $[O_2] = 9 \text{ mg/l}$.

$v_i = 1000 \text{ ml}$

m_c [g]	C_{iv} [g/m ³]	v_e [ml]	C_{ev} [g/m ³]	Q_{ev} [g/kg]
4.5026	37.2	1000	0.4	8.2
3.6003	37.2	1000	0.5	10.2
3.2000	37.2	1000	0.6	11.4
3.0017	37.2	1000	0.8	12.1
2.2008	37.2	1000	1.3	16.3
2.0044	37.2	1000	1.6	17.8
1.9020	37.2	1000	1.7	18.7
1.6036	37.2	1000	3.0	21.4
1.5005	37.2	1000	3.3	22.6
1.3418	37.2	1000	4.5	24.4
1.3011	37.2	1000	4.7	25.0
1.1502	37.2	1000	5.7	27.4
1.5035	47.0	1030	6.7	26.7
1.0029	37.2	1000	6.8	30.3
1.4138	47.0	1000	7.0	28.3
0.9030	37.2	1000	7.6	32.8
1.1350	47.0	1000	9.3	33.2
0.7015	37.2	1000	10.4	38.2
0.9799	47.0	1060	14.2	32.6
0.7571	47.0	990	17.9	38.7
0.5700	47.0	1000	21.9	44.0
1.5015	102.0	1047	26.2	49.7
1.3187	102.0	1065	29.0	53.9
1.1656	102.0	1068	31.5	58.7
0.8998	102.0	1078	45.5	58.9
0.6859	102.0	1050	51.0	70.6

$$Q_{ev} = 13.62 C_{ev}^{0.398}$$

Experiment no.8

Equilibrium adsorption of silver cyanide on carbon A from solutions with a constant $[O_2] = 4.4$ mg/l.

$v_i = 1000$ ml

m_c [g]	C_{iv} [g/m ³]	v_e [ml]	C_{ev} [g/m ³]	Q_{ev} [g/kg]
1.1822	4.7	885	0.2	3.8
0.7593	4.7	895	0.3	5.8
0.5828	4.7	905	0.4	7.4
0.3767	4.7	915	1.0	10.1
0.2180	4.7	905	2.0	13.3
1.6037	28.6	900	5.7	14.6
1.2246	28.6	915	8.5	17.0
0.9638	28.6	910	10.1	20.1
0.6090	28.6	895	14.3	26.0
0.3585	28.6	905	18.6	32.8
0.9099	55.0	910	26.1	34.3
0.5359	55.0	905	37.6	39.1
0.2455	55.0	895	47.0	52.7

$$Q_{ev} = 8.92 C_{ev}^{0.409}$$

Experiment no.9

Equilibrium adsorption of silver cyanide on carbon A from deaerated solutions, i.e. $[O_2] = 0$ mg/l.

$v_i = v_e = 950$ ml

m_c [g]	C_{iv} [g/m ³]	C_{ev} [g/m ³]	Q_{ev} [g/kg]
3.0000	11.1	1.6	3.0
2.5050	11.1	2.1	3.4
1.6011	11.1	4.1	4.2
2.6910	47.0	21.2	9.1
1.9997	47.0	23.7	11.1
1.4735	47.0	27.1	12.8
1.0683	47.0	31.0	14.2
0.7122	47.0	35.0	16.0
0.2223	47.0	43.0	17.1

$$Q_{ev} = 2.192 C_{ev}^{0.5295}$$

Experiment no.10

Equilibrium adsorption of silver cyanide on carbon A from solutions at a constant $[O_2] = 14.5 \text{ mg/l}$.

$v_i = 1000 \text{ ml}$

m_c [g]	C_{iv} [g/m ³]	v_e [ml]	C_{ev} [g/m ³]	Q_{ev} [g/kg]
1.5031	47.0	1000	11.1	23.9
1.4109	47.0	1000	11.2	25.4
0.9752	47.0	990	20.0	27.9
0.7521	47.0	970	22.4	33.6
0.5700	47.0	995	24.4	39.9
1.4999	102.0	1000	33.0	46.0
1.3148	102.0	1010	46.4	41.9
1.1630	102.0	1000	50.0	44.7
0.9000	102.0	1005	54.0	53.0
0.6823	102.0	975	61.0	62.3

$$Q_{ev} = 7.603 C_{ev}^{0.482}$$

Experiment no.11

Equilibrium adsorption of gold cyanide on carbon B from solutions in contact with air, i.e. $[O_2] = 9 \text{ mg/l}$.

$v_i = 1000 \text{ ml}$

m_c [g]	C_{ig} [g/m ³]	v_e [ml]	C_{eg} [g/m ³]	Q_{eg} [g/kg]
1.6132	62.5	922	0.8	38.3
1.5312	62.5	930	1.2	40.1
1.3915	62.5	920	2.6	43.2
1.3317	62.5	920	4.0	44.2
1.2500	62.5	938	4.2	46.8
1.1028	62.5	921	7.8	50.2
1.0388	62.5	920	9.6	51.7
0.9481	62.5	920	13.3	53.0
0.8278	62.5	900	15.5	58.6
0.7197	62.5	900	22.8	58.3
0.6289	62.5	912	27.2	59.9
0.5198	62.5	935	33.2	60.5
1.4060	125.0	916	39.2	63.4
1.3242	125.0	880	46.4	63.6
1.2612	125.0	900	49.2	64.0

$$Q_{eg} = 38.646 C_{eg}^{0.1309}$$

Experiment no.12

Equilibrium adsorption of gold cyanide on carbon B from solutions with a constant $[O_2] = 4.2 \text{ mg/l}$.

$$v_i = 1000 \text{ ml}$$

$$C_{iG} = 41.3 \text{ g/m}^3$$

m_c [g]	v_e [ml]	C_{eG} [g/m ³]	Q_{eG} [g/kg]
1.7028	930	0.1	24.2
1.5015	935	0.2	27.4
1.3028	935	0.4	31.4
1.1527	930	0.8	35.2
1.0288	915	1.9	38.5
0.8102	930	5.8	44.3
0.5520	950	13.4	51.8
0.3016	935	24.1	62.2

$$Q_{eG} = 35.37 C_{eG}^{0.159}$$

Experiment no.13

Equilibrium adsorption of gold cyanide on carbon B from deaerated solutions, i.e. $[O_2] = 0 \text{ mg/l}$.

$$v_i = v_e = 950 \text{ ml}$$

$$C_{iG} = 39.2 \text{ g/m}^3$$

m_c [g]	C_{eG} [g/m ³]	Q_{eG} [g/kg]
2.4050	0.1	15.4
2.0020	0.3	18.5
1.5998	1.4	22.4
1.2015	4.6	27.4
1.0020	8.0	29.6
0.8013	12.3	31.9
0.6006	16.7	35.6
0.4042	22.9	38.3
0.2132	29.6	42.8

$$Q_{eG} = 22.02 C_{eG}^{0.1683}$$

Experiment no.14

Equilibrium adsorption of silver cyanide on carbon B from solutions in contact with air, i.e. $[O_2] = 9 \text{ mg/l}$.

$v_i = 1000 \text{ ml}$

m_c [g]	C_{iv} [g/m ³]	v_e [ml]	C_{ev} [g/m ³]	Q_{ev} [g/kg]
0.9450	22.0	1053	0.7	22.5
0.8725	22.0	1048	0.9	24.1
0.7626	22.0	1068	1.3	27.0
1.4120	44.0	1020	1.8	29.9
1.1883	44.0	1020	4.0	33.6
1.0739	44.0	1005	4.1	37.1
0.9713	44.0	950	4.4	41.0
0.8447	44.0	975	6.7	44.4
0.6605	44.0	998	8.5	53.8
1.5036	88.0	942	16.5	48.2
1.3010	88.0	1058	23.0	48.9
1.0898	88.0	990	27.5	55.8
0.8704	88.0	1023	31.5	64.1
1.1754	125.0	1055	46.0	65.1
1.0548	125.0	1052	49.0	69.6
0.8239	125.0	982	59.0	81.4
0.7126	125.0	945	67.0	86.6
1.2889	176.0	980	82.0	74.2
1.0746	176.0	1020	84.0	84.0

$$Q_{ev} = 25.357 C_{ev}^{0.2626}$$

Experiment no.15

Equilibrium adsorption of silver cyanide on carbon B from solutions with a constant $[O_2] = 4.2 \text{ mg/l}$.

$$v_i = 1000 \text{ ml}$$

$$C_{iv} = 38.3 \text{ g/m}^3$$

m_c [g]	v_e [ml]	C_{ev} [g/m ³]	Q_{ev} [g/kg]
0.6535	935	14.0	38.6
0.9566	940	7.9	32.3
1.4045	935	3.2	25.1
1.6887	935	1.8	21.7
1.9057	930	1.2	19.5
2.4599	905	0.5	15.4
2.8514	930	0.4	13.3

$$Q_{ev} = 18.134 C_{ev}^{0.286}$$

Experiment no.16

Equilibrium adsorption of silver cyanide on carbon B from deaerated solutions, i.e. $[O_2] = 0 \text{ mg/l}$.

$$v_i = v_e = 950 \text{ ml}$$

m_c [g]	C_{iv} [g/m ³]	C_{ev} [g/m ³]	Q_{ev} [g/kg]
0.4049	38.3	30.1	19.2
0.8038	38.3	24.5	16.3
1.6080	38.3	14.1	14.3
0.2057	9.9	7.0	13.4
0.5069	9.9	3.6	11.8
0.8013	9.9	1.5	10.0
1.0011	9.9	0.6	8.8
1.2013	9.9	0.2	7.7
1.4015	9.9	0.2	6.6
1.8027	9.9	0.1	5.2

$$Q_{ev} = 9.206 C_{ev}^{0.1935}$$

Experiment no.17

The effect of purging with pure oxygen on the adsorption of gold cyanide onto carbon A from an alkaline solution.

$v = 1000 \text{ ml}$

$\text{pH} = 8.5$

$C_{iG} = 20.0 \text{ g/m}^3$

(a) Purge solution with pure oxygen, $[\text{O}_2] = 40 \text{ mg/l}$, $m_c = 1.3303 \text{ g}$

(b) Purge solution with air, $[\text{O}_2] = 9.0 \text{ mg/l}$, $m_c = 1.3310 \text{ g}$

Time [h]	(a)		(b)	
	C_G [g/m ³]	C_G/C_{iG}	C_G [g/m ³]	C_G/C_{iG}
0.000	20.0	1.000	20.0	1.000
0.100	19.6	0.980	19.8	0.990
0.317	19.1	0.955	19.2	0.960
0.800	18.8	0.940	18.9	0.945
1.083	18.5	0.925	18.3	0.915
1.950	17.9	0.895	18.0	0.900
3.467	17.2	0.860	17.0	0.850
4.817	16.7	0.835	16.2	0.810
9.117	15.5	0.775	13.6	0.680
21.083	12.9	0.645	9.4	0.470
22.233	12.6	0.630	9.2	0.460
24.767	12.4	0.620	8.6	0.430
27.583	12.2	0.610	8.2	0.410
30.167	11.8	0.590	7.7	0.385
33.600	11.6	0.580	7.2	0.360
45.550	10.5	0.525	5.7	0.285
48.650	10.4	0.520	5.3	0.265
51.500	9.9	0.495	5.0	0.250
70.383	9.1	0.455	3.7	0.185

Experiment no.18

The effect of purging with pure oxygen on the adsorption of gold cyanide onto carbon A from an acidic solution.

$v = 1500 \text{ ml}$

$\text{pH} = 3.5$

$C_{iG} = 30.3 \text{ g/m}^3$

(a) Purge solution with air, $[\text{O}_2] = 9.0 \text{ mg/l}$, $m_c = 2.0010 \text{ g}$

(b) Purge solution with pure oxygen, $[\text{O}_2] = 40 \text{ mg/l}$, $m_c = 2.0015 \text{ g}$

Time [h]	(a)		(b)	
	C_G [g/m ³]	C_G/C_{iG}	C_G [g/m ³]	C_G/C_{iG}
0.000	30.3	1.000	30.3	1.000
0.250	24.0	0.792	23.6	0.779
0.500	21.0	0.693	20.0	0.660
1.000	16.4	0.541	15.3	0.505
2.250	10.9	0.360	8.6	0.284
3.500	7.0	0.231	5.6	0.185
5.167	4.7	0.155	3.7	0.122
6.300	3.6	0.119	2.6	0.086
8.750	2.0	0.066	1.4	0.046
11.800	1.1	0.036	0.7	0.023
14.370	0.6	0.020	0.5	0.017
23.500	0.4	0.013	0.3	0.010
32.750	0.3	0.010	0.3	0.010
47.500	0.3	0.007	0.2	0.007
56.900	0.2	0.007	0.2	0.007

Experiment no.19

Effect of dissolved oxygen concentration on the adsorption of $\text{Hg}(\text{CN})_2$.

Adsorption period = 2 days

$\text{pH} = 8.5$

$v = 1500 \text{ ml}$

	(a)	(b)	(c)	(d)
Carbon	A	A	BTX	BTX
m_c [g]	2.0	2.0	1.5	1.5
C_i [g Hg/m ³]	34.0	34.0	34.7	34.7
Purge	Air	N_2	Air	O_2
$[\text{O}_2]$ [mg/l]	9.0	0.0	9.0	40.0
C_f [g Hg/m ³]	9.5	10.0	14.7	14.7

Experiment no.20

The effect of oxygen on the adsorption of gold cyanide onto an experimental weak-base ion exchange fibre.

$v = 1000 \text{ ml}$

$\text{pH} = 9.86$

$C_{iG} = 19.6 \text{ g/m}^3$

(a) Purge solution with nitrogen, $[O_2] = 0.0 \text{ mg/l}$, $m_{\text{fibre}} = 0.2011 \text{ g}$

(b) Purge solution with air, $[O_2] = 9.0 \text{ mg/l}$, $m_{\text{fibre}} = 0.2018 \text{ g}$

Time [h]	(a)	(b)
	C_G [g/m ³]	C_G [g/m ³]
0.167	18.6	18.5
0.333	18.0	18.4
0.517	18.4	18.0
0.767	17.7	17.3
1.033	17.2	17.7
1.600	16.7	16.9
2.050	16.1	16.1
2.800	15.6	15.8
6.117	13.0	13.0
8.450	11.8	11.6

Experiment no.21

The effect of oxygen on the zeta potential of carbon A in distilled water.

$v = 1000 \text{ ml}$

$m_c = 0.005 \text{ g}$

$\text{pH} = 5.5$ (pH not adjusted)

$[O_2] \text{ [mg/l]}$	0.0	9.0	40.0
$\xi \text{ [mV]}$	-71.3	-64.5	-56.7

Experiment no.22

The effect of a step change in the oxygen concentration on the adsorption of gold cyanide on carbon A.

$v = 1500 \text{ ml}$

$\text{pH} = 8.5$

- (a) Purged solution with nitrogen for whole duration of experiment, $C_{iG} = 10.1 \text{ g Au/m}^3$, $m_c = 3.0005 \text{ g}$.
- (b) Purged solution with air for whole duration of experiment, $C_{iG} = 9.4 \text{ g Au/m}^3$, $m_c = 3.0012 \text{ g}$.
- (c) Purged solution with air for first 24 hours of experiment and then switched to nitrogen, $C_{iG} = 9.4 \text{ g Au/m}^3$, $m_c = 3.0050 \text{ g}$.

(a)		(b)		(c)	
Time [h]	C_G [g/m ³]	Time [h]	C_G [g/m ³]	Time [h]	C_G [g/m ³]
0.167	9.4	0.683	9.1	0.083	9.4
0.333	9.1	1.183	8.2	0.333	9.4
0.583	8.9	2.200	7.6	0.533	9.1
0.833	8.8	3.383	6.7	0.767	9.0
1.083	8.7	5.067	5.9	1.083	8.6
1.550	8.3	5.750	5.3	1.500	8.3
2.117	8.0	7.783	4.5	2.000	8.0
2.617	7.9	9.800	3.5	2.867	7.4
3.417	7.6	16.233	1.9	4.083	6.6
4.450	7.6	20.283	1.2	5.033	6.1
6.417	7.2	27.383	0.5	6.000	5.5
7.883	6.9	32.967	0.2	7.050	5.0
8.667	6.9	40.000	0.1	9.067	3.8
10.750	6.7			11.000	2.9
13.750	6.4			12.267	2.9
15.500	6.3			23.400	0.9
22.667	5.2			24.000	(N ₂)
25.167	4.9			24.617	0.9
27.750	4.8			25.000	0.9
30.400	4.8			25.933	0.9
33.667	4.6			29.500	1.0
36.400	4.4			36.133	1.0
39.117	4.3			47.370	0.9
47.783	4.0			53.750	0.9
52.083	3.8			74.100	0.8
56.367	3.5				

Experiment no.23

The effect of the dissolved oxygen concentration on the desorption of gold cyanide loaded onto carbon A from aerated solutions.

Conditions for each of the three experiments (a,b and c) :

Adsorption conditions :

$v = 1500 \text{ ml}$

$\text{pH} = 8.5$

$m_c = 2.0 \text{ g}$

$C_{iG}^c = 29.3 \text{ g/m}^3$

$T = 20 \text{ }^\circ\text{C}$

Adsorption period = 2 days

(a) $C_{fG} = 9.7 \text{ g/m}^3$

(b) $C_{fG} = 9.4 \text{ g/m}^3$

(c) $C_{fG} = 10.1 \text{ g/m}^3$

Desorption conditions :

$v = 1500 \text{ ml}$

$\text{pH} = 12$

$T = 20 \text{ }^\circ\text{C}$

(a) $Q_{iG} = 14.7 \text{ g/kg}$

(b) $Q_{iG} = 14.9 \text{ g/kg}$

(c) $Q_{iG} = 14.4 \text{ g/kg}$

(a) [O ₂] = 9 mg/l			(b) [O ₂] = 40 mg/l			(c) [O ₂] = 0 mg/l		
t	C _G	ψ	t	C _G	ψ	t	C _G	ψ
0.333	1.3	0.066	0.350	1.3	0.065	0.383	1.3	0.068
0.667	1.8	0.092	0.683	1.9	0.095	0.700	1.8	0.094
1.083	2.5	0.128	1.100	2.5	0.126	1.117	2.4	0.125
1.667	3.1	0.158	1.683	3.2	0.161	1.700	3.0	0.156
2.617	4.1	0.209	2.633	4.2	0.211	2.633	4.0	0.208
3.933	4.8	0.245	3.950	5.0	0.251	3.967	4.8	0.250
5.617	5.6	0.286	5.633	5.8	0.291	5.633	5.5	0.286
7.000	6.0	0.306	7.000	6.2	0.312	7.017	5.9	0.307
8.400	6.4	0.327	8.417	6.6	0.332	8.433	6.3	0.328
11.383	6.7	0.347	11.400	7.1	0.357	11.400	6.8	0.354
22.850	7.2	0.367	22.867	7.6	0.382	22.883	7.4	0.385

t = Time [h]

C_G = Gold concentration [g/m³]

$\psi = \frac{Q_i - Q}{Q_i} = \text{Fraction of } Q_i \text{ desorbed}$

Experiment no.24

The effect of the dissolved oxygen concentration on the desorption of gold cyanide loaded onto carbon A from deaerated solutions.

Conditions for each of the three experiments (a,b and c) :

Adsorption conditions :

$v = 1500 \text{ ml}$

$\text{pH} = 8.5$

$m_c = 2.0 \text{ g}$

$C_{iG} = 45.6 \text{ g/m}^3$

$T = 20 \text{ }^\circ\text{C}$

Adsorption period = 7 days

(a) $C_{fG} = 26.5 \text{ g/m}^3$

(b) $C_{fG} = 27.2 \text{ g/m}^3$

(c) $C_{fG} = 26.5 \text{ g/m}^3$

Desorption conditions :

$v = 1500 \text{ ml}$

$\text{pH} = 12$

$T = 20 \text{ }^\circ\text{C}$

(a) $Q_{iG} = 14.3 \text{ g/kg}$

(b) $Q_{iG} = 13.8 \text{ g/kg}$

(c) $Q_{iG} = 14.3 \text{ g/kg}$

(a) [O ₂] = 0 mg/l			(b) [O ₂] = 40 mg/l			(c) [O ₂] = 9 mg/l		
t	C _G	ψ	t	C _G	ψ	t	C _G	ψ
0.167	0.5	0.026	0.167	0.5	0.027	0.167	0.5	0.026
0.700	0.8	0.042	0.700	0.8	0.043	0.700	0.8	0.042
1.167	1.1	0.058	1.167	1.0	0.054	1.167	1.1	0.058
2.167	1.6	0.084	2.167	1.5	0.082	2.167	1.6	0.084
3.200	2.1	0.110	3.200	1.9	0.103	3.200	2.1	0.110
4.867	2.8	0.147	4.867	2.5	0.133	4.867	2.8	0.147
6.167	3.2	0.168	6.167	2.8	0.152	6.167	3.2	0.168
7.033	3.5	0.183	7.033	2.9	0.158	7.033	3.5	0.183
11.033	4.3	0.225	11.033	3.6	0.196	11.033	4.3	0.225
13.333	4.7	0.246	13.333	3.7	0.201	13.333	4.6	0.241
22.400	5.5	0.288	22.400	4.1	0.223	22.400	5.0	0.262
25.167	5.8	0.304	25.167	4.3	0.234	25.167	5.2	0.272
28.533	6.1	0.319	28.533	4.6	0.250	28.533	5.4	0.283
30.000	6.4	0.335	30.000	4.8	0.261	30.000	5.6	0.293

t = Time [h]

C_G = Gold concentration [g/m³]

$\psi = \frac{Q_i - Q}{Q_i} = \text{Fraction of } Q_i \text{ desorbed}$

Experiment no.25

The consumption of oxygen by carbon A in distilled water.

2.0 g Carbon A was contacted with 500 ml distilled water in a tightly sealed bottle for a period of two weeks. A similar bottle of distilled water without carbon was used as a reference for the measurement of the oxygen concentrations.

Oxygen concentrations after 2 weeks :

Reference solution : 8.8 mg/l

Carbon/water mixture : 7.0 mg/l

Oxygen consumption : $1.8 \text{ mg/l} \times (v/m_c) = 0.45 \text{ mg O}_2/\text{g}$

Experiment no.26

Measurement of the dissolved oxygen concentration during the adsorption of gold cyanide on carbon A in a closed vessel.

$$v = 1475 \text{ ml}$$

$$m_c = 2.0 \text{ g}$$

$$\text{pH} = 8.5$$

$$C_{iG} = 21.3 \text{ g Au/m}^3$$

The reliability of the oxygen measurements was investigated by repeating Experiment 26(a) in 26(b), (c) and (d). The gold concentration was measured for (a) and (c) and found to be the same.

(a)			(b)	(c)		(d)
t	C_G	C_x	C_x	t	C_x	C_x
0.000	21.3	8.3	8.3	0.000	8.3	8.9
0.100	21.3	8.2	8.1	0.083	8.3	8.7
0.183	21.2	8.2	8.1	0.167	8.2	8.6
0.283	21.0	8.1	8.0	0.333	8.1	8.5
0.367	20.9	8.0	8.2	0.500	8.0	8.4
0.450	20.7	8.0	8.1	0.867	7.8	8.2
0.617	20.6	7.9	8.0	1.417	7.6	8.3
1.617	20.4	7.6	7.8	2.050	7.4	8.0
2.183	19.7	7.2	7.6	2.450	7.3	8.0
2.500		7.1	7.5	4.867	7.1	7.6
3.650	19.4			6.683	6.9	7.5
5.117		6.8	7.3	9.800	6.8	7.4
6.733	17.5			19.300	7.3	7.2
9.317	16.8	7.0	6.5	19.500	7.2	7.1
17.933	14.9			21.300	6.8	7.1
18.700		6.1	7.1	24.667	6.7	7.0
20.433	14.2	6.0	7.1	27.283	6.9	6.8
23.050	13.8	5.9	7.0	30.750	6.5	6.9
25.033	13.5	5.8	7.1	33.583	6.4	6.9
26.783	12.6	5.7	7.1	44.083	6.6	6.7
34.117	12.3	5.5	7.0	46.250	6.3	6.7
42.900	11.3	5.4	7.0	48.583	6.2	6.6
48.650	11.3	5.2	7.0			

t = Time [h]

C_x = Oxygen concentration [mg/l]

C_G = Gold concentration [g/m³]

Experiment no.27

The consumption of dissolved oxygen by activated carbon in closed containers.

All the experiments were conducted in Schott Duran 2000ml and 1000ml bottles with plastic screw tops. The tops were sealed with candle wax. The bottles were rolled for the whole duration of the experiments. At the end of the experiments, the oxygen concentrations were measured and subtracted from the oxygen concentration in a reference solution. The reference solutions were distilled water that was treated in exactly the same way as the rest of the experiments, except that no carbon or metal cyanides were added.

Experiment 27(a) : 2280 ml distilled water was purged with N_2 for 2 hours before the bottle was sealed and rolled for 93 hours. The bottle was then opened and the oxygen concentration measured as 0.5 mg O_2 /l.

No.	(b)	(c)	(d)	(e)	(f)
Carbon	A	A	A	A	A
Carbon conc. [g/l]	1.33	1.33	1.77	1.77	1.77
Carbon pretreatment*	D,S	D,S	D	D	D
Drying temp. [°C]	110	110	110	110	110
Open/Closed bottle	C	O	C	C	C
Volume [ml]	1170	1475	2260	2260	2260
pH	8.5	8.5	11.2	9.1	3.2
Metal cyanide (M)	Au	Au			
$C_i(M)$ [g/m ³]	22.8	19.7			
Duration [h]	19	19	90	90	90
$C_f(M)$ [g/m ³]	10.9	9.6			
$C_f(M)/C_i(M)$	0.478	0.487			
$[O_2]_{diff.}$ [mg/l]	0.2		1.4	1.2	1.4

No.	(g)	(h)	(i)	(j)	(k)	(l)
Carbon	A	A	A	A	A	A
Carbon conc. [g/l]	1.34	1.34	1.77	1.77	1.77	1.77
Carbon pretreatment*	D,S	D,S		D	D	D
Drying temp. [°C]	110	110		110	200	300
Open/Closed bottle	C	O	C	C	C	C
Volume [ml]	1170	1170	2260	2260	2260	2260
pH	8.5	8.5				
Metal cyanide (M)	Ag	Ag				
$C_i(M)$ [g/m ³]	23.2	23.2				
Duration [h]	90	90	90	90	90	90
$C_f(M)$ [g/m ³]	14.7	10.2				
$C_f(M)/C_i(M)$	0.634	0.440				
$[O_2]_{diff.}$ [mg/l]	0.5		-0.2	1.3	1.8	0.3

No.	(m)	(n)	(o)	(p)	(q)	(r)
Carbon	A	BTX	BTX	BTX	BTX	BTX
Carbon conc. [g/l]	1.75	1.75	1.75	1.75	1.75	1.75
Carbon pretreatment*		D				
Drying temp. [°C]		110				
Open/Closed bottle	C	C	C	C	C	C
Volume [ml]	2280	2280	2280	2280	2280	2280
pH				8.8		3.9
Metal cyanide (M)	CN			Au	CN	Au
$C_i(M)$ [g/m ³]	409			70.5	409	70.5
Duration [h]	93	93	93	93	93	93
$C_f(M)$ [g/m ³]	385			28.2	390	10.4
$C_f(M)/C_i(M)$	0.941			0.400	0.954	0.148
$[O_2]_{diff.}$ [mg/l]	0.6	0.2	-0.5	0.5	3.2	0.7

*Carbon pretreatment :

D = Oven dried at specified temperature for 24 hrs

S = Soaked in aerated, distilled water for 24 hrs

Experiment no. 28

The consumption of oxygen during the adsorption of gold cyanide in a column packed with carbon A.

Characteristics of carbon bed :

$h = 225$ mm, $d = 31$ mm, Packed with 94.7 g carbon A (-1.7+1.4 mm sieve size fraction), Flow direction = upward, Inserted oxygen electrode through a rubber plug into the top of the glass column.

In the instruction booklet of the oxygen electrode, the required stirring rate of the solution is specified as at least 10 cm/s. As a very low flowrate was used in the column, the measured concentration of O_2 in the column was calibrated against the concentration of O_2 measured in the same solution on a magnetic stirrer :

$[O_2]$ in column [mg/l]	7.4	5.6	4.6
$[O_2]$ (stirred) [mg/l]	8.7	6.3	5.0

Let :

$C_{X(1)}$ = Oxygen concentration as measured in column,

$C_{X(2)}$ = Oxygen concentration as calculated from calibration.

The following relationship was obtained from a least squares fit on the calibration data : $C_{X(2)} = 1.33.C_{X(1)} - 1.13$

Feed solution :

$C_{iG} = 14.9$ g Au/m³

$C_{iX} = 9.0$ mg O_2 /l

pH = 8.5

Time [h]	V [ml/min]	C_G [g/m ³]	$C_{X(1)}$ [mg/l]	$C_{X(2)}$ [mg/l]
0.000			7.6	9.0
0.033			7.4	8.7
0.067			7.5	8.8
0.100	47	0.2	7.4	8.7
0.433		0.3	7.4	8.7
0.767	46	0.7	7.4	8.7
1.550	46	1.8	7.3	8.6
2.583	45	3.1	7.3	8.6
3.600		4.1	7.3	8.6
4.983	45	5.2	7.4	8.7
5.783	46		7.4	8.7
7.683	46	7.0	7.4	8.7
10.383	44	8.1	7.5	8.8
14.933		9.2	7.5	8.8

Experiment no. 29

Determination of irreversibly adsorbed gold cyanide species on carbon A by elution with distilled water.

Adsorption :

$$C_{iG} = 48.0 \text{ g/m}^3$$

$$m_c = 0.7123 \text{ g}$$

$$v^c = 1000 \text{ ml}$$

$$\text{pH} = 8.5$$

$$[\text{O}_2] = 9.0 \text{ mg/l}$$

$$\text{Time} = 21 \text{ days}$$

$$C_{fG} = 22.6 \text{ g/m}^3$$

Desorption :

$$Q_{iG} = 36.6 \text{ g/kg}$$

$$\text{pH} = 12$$

$$T = 20 \text{ }^\circ\text{C}$$

Elution no.	Duration [h]	v [ml]	C_G [g/m ³]	ψ [%]
1	24	1650	7.4	46.7
2	48	1510	4.3	71.6
3	48	1620	2.3	85.8
4	48	1515	1.0	91.6
5	96	1615	0.8	96.6
6	96	1600	0.4	99.0
% AuCN				0

$$\psi = \frac{Q_i - Q}{Q_i} \times 100 = \% \text{ of initial metal loading eluted}$$

Experiment no. 30

Determination of irreversibly adsorbed silver cyanide species on carbon A by elution with distilled water.

Adsorption :

$$C_{iv} = 47.0 \text{ g/m}^3$$

$$m_c = 0.7521 \text{ g}$$

$$v_c = 1000 \text{ ml}$$

$$\text{pH} = 8.5$$

$$[\text{O}_2] = 9.0 \text{ mg/l}$$

$$\text{Time} = 21 \text{ days}$$

$$C_{fv} = 22.4 \text{ g/m}^3$$

Desorption :

$$Q_{iv} = 33.6 \text{ g/kg}$$

$$\text{pH} = 12$$

$$T = 20 \text{ }^\circ\text{C}$$

Elution no.	Duration [h]	v [ml]	C_v [g/m ³]	ψ [%]
1	3.5	1500	1.2	7.1
2	4.5	1455	0.9	12.3
3	10	1455	1.2	19.0
4	24	1450	1.4	26.9
5	24	1465	0.9	32.0
6	46	1460	0.2	33.2
7	48	1435	0.4	35.6
8	96	1475	0.3	37.2
9	72	1440	0.3	38.7
% AgCN				61

$$\psi = \frac{Q_i - Q}{Q_i} \times 100 = \% \text{ of initial metal loading eluted}$$

Experiment no.31

The effect of the dissolved oxygen concentration on the formation of an irreversibly adsorbed gold cyanide species on carbon B.

The results of two experiments (a and b) are presented here. These experiments were conducted with different oxygen concentrations in the adsorption stage, but similar $[O_2]$'s (= 0 mg/l) in the elutions.

Adsorption :

$$C_{iG} = 19.2 \text{ g/m}^3$$

$$m_c = 1.00 \text{ g}$$

$$v = 1000 \text{ ml}$$

$$\text{pH} = 8.5$$

$$\text{Time} = 24 \text{ h}$$

$$\text{(a) } [O_2] = 0.0 \text{ mg/l, } C_{fG} = 5.6 \text{ g/m}^3$$

$$\text{(b) } [O_2] = 9.0 \text{ mg/l, } C_{fG} = 0.0 \text{ g/m}^3$$

Desorption :

$$v = 1500 \text{ ml}$$

$$\text{pH} = 12$$

$$T = 20 \text{ }^\circ\text{C}$$

$$[O_2] = 0.0 \text{ mg/l}$$

$$\text{(a) } Q_{iG} = 13.6 \text{ g/kg}$$

$$\text{(b) } Q_{iG} = 19.2 \text{ g/kg}$$

Elution no.	Time [h]	(a)		(b)	
		C_G [g/m ³]	ψ [%]	C_G [g/m ³]	ψ [%]
1	4	1.8	19.9	1.9	14.8
2	4	1.3	34.2	1.7	28.0
3	16	0.7	48.5	2.2	45.2
4	24	0.7	56.2	1.6	57.7
5	36	0.4	63.9	1.0	65.5
6	36	0.4	68.3	0.7	71.0
7	48	0.3	71.6	0.5	74.9
8	52	0.3	74.9	0.5	78.8
% AuCN			25		20

$$\psi = \frac{Q_i - Q}{Q_i} \times 100 = \% \text{ of initial metal loading eluted}$$

Experiment no. 32

Determination of irreversibly adsorbed gold cyanide species on carbon BTX by elution with distilled water.

Adsorption :

$$C_{iG} = 41.8 \text{ g/m}^3$$

$$m_c = 0.9982 \text{ g}$$

$$v^c = 1000 \text{ ml}$$

$$\text{pH} = 8.5$$

$$[\text{O}_2] = 9.0 \text{ mg/l}$$

$$\text{Time} = 3 \text{ days}$$

$$C_{\text{end}} = 15.6 \text{ g/m}^3$$

Desorption :

$$Q_{iG} = 26.2 \text{ g/kg}$$

$$\text{pH} = 12$$

$$T = 20 \text{ }^\circ\text{C}$$

$$v = 1500 \text{ ml}$$

Elution no.	Duration [h]	C_G [g/m ³]	ψ [%]
1	2.5	2.7	15.5
2	4.5	2.4	29.2
3	9	2.8	45.2
4	9	2.0	56.7
5	18	2.0	68.2
6	45	2.0	79.7
7	49	1.7	89.4
8	40	1.5	98.0
9	72	0.8	102.6
% AuCN			0

$$\psi = \frac{Q_i - Q}{Q_i} \times 100 = \% \text{ of initial metal loading recovered}$$

Experiment no.33

The effect of a high dissolved oxygen concentration on the formation of an irreversibly adsorbed gold cyanide species on carbon A at a low pH.

The results of two experiments (a and b) are presented here. These experiments were conducted with different oxygen concentrations in the adsorption stage, but similar $[O_2]$'s in the elutions.

Adsorption :

$$C_{iG} = 30.3 \text{ g/m}^3$$

$$m_c = 2.00 \text{ g}$$

$$v = 1500 \text{ ml}$$

$$\text{pH} = 3.35$$

$$\text{Time} = 57 \text{ h}$$

$$(a) \quad [O_2] = 9.0 \text{ mg/l}$$

$$C_{fG} = 0.2 \text{ g/m}^3$$

$$(b) \quad [O_2] = 40 \text{ mg/l}$$

$$C_{fG} = 0.2 \text{ g/m}^3$$

Desorption :

$$v = 1500 \text{ ml}$$

$$\text{pH} = 12$$

$$T = 20 \text{ }^\circ\text{C}$$

$$[O_2] = 9.0 \text{ mg/l}$$

$$(a) \quad Q_{iG} = 22.6 \text{ g/kg}$$

$$(b) \quad Q_{iG} = 22.6 \text{ g/kg}$$

Elution no.	Time [h]	(a)		(b)	
		C_G [g/m ³]	ψ [%]	C_G [g/m ³]	ψ [%]
1	3.5	4.4	14.6	4.3	14.3
2	4.5	4.3	28.9	4.4	28.9
3	10	5.0	45.5	5.1	45.8
4	24	5.4	63.4	5.4	63.7
5	24	3.4	74.7	3.7	76.0
6	46	0.5	76.3	0.4	77.3
7	48	1.2	80.3	1.5	82.3
8	96	0.6	82.3	1.2	86.3
9	72	0.6	84.3	0.8	89.0
% AuCN			16		11

$$\psi = \frac{Q_i - Q}{Q_i} \times 100 = \% \text{ of initial metal loading eluted}$$

Experiment no.34

Equilibrium isotherm for desorption of gold cyanide from carbon B.

The carbon was loaded with gold cyanide for a period of 5 days whereafter it was separated from the gold solutions and transferred to beakers with distilled water at the same pH and temperature as used in the determination of the adsorption isotherm (Experiment no.11).

Adsorption :

$v = 1000 \text{ ml}$

$C_{fg} = 159 \text{ g Au/m}^3$

$\text{pH} = 8.5$

$T = 20 \text{ }^\circ\text{C}$

Desorption :

$v_i = 1000 \text{ ml}$

$\text{pH} = 8.5$

$T = 20 \text{ }^\circ\text{C}$

Adsorption			Desorption		
m_c [g]	C_{fg} [g/m ³]	Q_{fg} [g/kg]	v_e [ml]	C_{eg} [g/m ³]	Q_{eg} [g/kg]
0.4035	130.0	71.9	990	5.3	58.9
0.6005	120.0	64.9	985	6.2	54.7
0.9071	93.0	72.8	985	7.1	65.1
1.2140	76.0	68.4	985	6.9	62.8
1.5026	62.0	64.6	990	6.5	60.3
1.8038	46.5	62.4	985	5.3	59.5
2.1424	34.0	58.3	990	4.0	56.5
2.4790	22.0	55.3	990	3.3	54.0
2.8448	12.5	51.5	990	2.0	50.8

Experiment no.35

Equilibrium isotherm for desorption of gold cyanide from carbon A.

The carbon was loaded with gold cyanide for a period of 5 days whereafter it was separated from the gold solutions and transferred to beakers with distilled water at the same pH and temperature as used in the determination of the adsorption isotherm (Experiment no.3).

Adsorption :

$v = 1000 \text{ ml}$

$\text{pH} = 8.5$

$T = 20 \text{ }^\circ\text{C}$

Desorption :

$v_i = 1000 \text{ ml}$

$\text{pH} = 8.5$

$T = 20 \text{ }^\circ\text{C}$

Adsorption			Desorption		
m_c [g]	C_{ig} [g/m ³]	C_{fg} [g/m ³]	v_e [ml]	C_{eg} [g/m ³]	Q_{eg} [g/kg]
0.2070	45.4	40.8	985	1.2	16.5
0.5012	45.4	32.4	985	2.0	22.0
1.0009	45.4	24.0	990	1.6	19.8
0.6519	190.0	159.0	990	9.4	33.3
1.0028	190.0	147.5	985	11.8	30.8
1.5160	190.0	126.0	990	16.2	31.6
2.0034	190.0	106.0	985	16.7	33.7
2.5200	190.0	85.5	985	17.9	34.5
3.0106	190.0	77.0	985	15.7	32.4

Experiment no.36

Equilibrium adsorption of gold cyanide on carbon BTX from solutions in contact with air, i.e. $[O_2] = 9 \text{ mg/l}$.

$v_i = 1000 \text{ ml}$
 $\text{pH} = 8.5$

m_c [g]	C_{iG} [g/m ³]	v_e [ml]	C_{eG} [g/m ³]	Q_{eG} [g/kg]	A^*
1.2010	23.8	985	0.2	19.7	32.43
0.9040	23.8	990	0.3	26.0	32.28
1.0018	23.8	990	0.3	23.5	33.15
0.7999	23.8	995	0.6	29.0	33.37
0.7046	23.8	990	0.8	32.7	34.13
0.6058	23.8	990	1.6	36.7	32.19
0.5037	23.8	990	3.0	41.4	33.12
0.4020	23.8	990	5.5	45.7	30.18
0.3135	23.8	985	8.3	49.8	27.80
1.6007	88.0	990	12.0	47.6	25.92
1.4015	88.0	990	14.8	52.3	37.30
1.2000	88.0	990	21.2	55.8	30.48
1.0007	88.0	990	22.7	65.5	35.71
0.8024	88.0	990	36.6	64.5	29.27
0.6119	88.0	990	42.0	75.9	29.69
0.3981	88.0	985	63.2	64.7	27.85

* Calculated with $n = -0.002688.A + 0.2902$

From least squares fit on equilibrium data :

$$Q_{eG} = 31.485 C_{eG}^{0.204}$$

From average of calculated A-values :

$$Q_{eG} = 31.55 C_{eG}^{0.205}$$

Experiment no.37

Equilibrium isotherm for desorption of gold cyanide from carbon BTX.

The carbon was loaded with gold cyanide for a period of 5 days whereafter it was separated from the gold solutions and transferred to beakers with distilled water at the same pH and temperature as used in the determination of the adsorption isotherm (Experiment no.36).

Adsorption :
 $v = 1000 \text{ ml}$
 $\text{pH} = 8.5$
 $T = 20 \text{ }^\circ\text{C}$
 $C_{iG} = 138 \text{ g/m}^3$

Desorption :
 $v_i = 1000 \text{ ml}$
 $\text{pH} = 8.5$
 $T = 20 \text{ }^\circ\text{C}$

Adsorption		Desorption		
m_c [g]	C_{fG} [g/m ³]	v_e [ml]	C_{eG} [g/m ³]	Q_{eG} [g/kg]
0.4004	115.5	995	4.9	44.0
0.8023	108.0	995	2.3	34.5
1.2727	82.0	995	3.9	41.0
1.6055	59.0	995	7.1	44.8
2.0045	49.0	995	3.5	42.7
2.4011	28.0	990	5.3	43.6

Experiment no. 38

Determination of irreversibly adsorbed gold cyanide species on carbon BTX after drying at 150 °C.

Adsorption :

$$C_{iG} = 102.8 \text{ g/m}^3$$

$$v = 1000 \text{ ml}$$

$$\text{Time} = 18.5 \text{ h}$$

$$m_c = 1.5031 \text{ g}$$

$$\text{pH} = 8.5$$

$$C_{fG} = 69.3 \text{ g/m}^3$$

Oven drying of carbon after adsorption step :

$$T = 150 \text{ }^\circ\text{C}$$

$$\text{Time} = 18 \text{ h}$$

Desorption :

$$Q_{iG} = 22.3 \text{ g/kg}$$

$$T = 20 \text{ }^\circ\text{C}$$

$$\text{pH} = 12$$

$$v = 1500 \text{ ml}$$

Elution no.	Duration [h]	C_G [g/m ³]	ψ [%]
1	3	3.0	13.4
2	3.6	1.8	21.5
3	16	2.8	34.0
4	7.5	1.3	39.9
5	15	1.3	45.7
6	28	1.3	51.5
7	44	1.1	56.4
% AuCN			40

$$\psi = \frac{Q_i - Q}{Q_i} \times 100 = \% \text{ of initial metal loading recovered}$$

Experiment no. 39

The effect of $\text{Au}^{(0)}$ on the equilibrium adsorption of $\text{Au}(\text{CN})_2^-$.

The adsorption of $\text{Au}(\text{CN})_2^-$ on a sample of $\text{Au}^{(0)}$ loaded carbon BTX (Exp. (a)) was compared to that on a fresh sample of carbon BTX (Exp. (b)). The amount of irreversibly adsorbed gold on sample (a) was determined with an identically treated sample (c).

Samples (a) and (c) were taken from a batch of carbon treated in the following way :

Adsorption :

$$m_c = 10.0131 \text{ g}$$

$$v_c = 5000 \text{ ml}$$

$$C_{iG} = 38.3 \text{ g/m}^3$$

pH not adjusted

$$\text{Time} = 60 \text{ h}$$

$$C_{fG} = 0.9 \text{ g/m}^3$$

$$Q_{fG} = 18.7 \text{ g/kg}$$

Acid treatment :

Boil carbon for 25.5 h in 1000 ml 3 vol.% of 33 mass % HCl solution. Dried at 110 °C for 4 days.

Determination of irreversibly adsorbed gold cyanide species on sample (c) :

$$m_c = 1.000 \text{ g}$$

$$\text{pH} = 12$$

$$T = 20 \text{ }^\circ\text{C}$$

$$v = 1000 \text{ ml}$$

Elution no.	Duration [h]	C_G [g/m ³]	ψ [%]
1	18	0.6	3.2
2	50	0.5	5.9
3	22	0.6	9.1
4	25	0.7	12.8
5	24	0.5	15.5
% $\text{Au}(\text{CN})_2^-$			< 20

Comparison of adsorption of $\text{Au}(\text{CN})_2^-$ onto samples (a) and (b) :

Time = 3 weeks

pH = 8.5

$C_{iG} = 30.5 \text{ g/m}^3$

$T = 20 \text{ }^\circ\text{C}$

$v = 1000 \text{ ml}$

	(a)	(b)
m_c [g]	0.5772	0.5771
Q_{iG} [g/kg]	18.7	0.0
v_e [ml]	995	995
C_{eG} [g/m ³]	4.3	4.7
Q_{eG} [g/kg]	45.4+18.7	44.7

Experiment no. 40

The elution of gold cyanide from carbon BTX loaded over a period of 72 h.

Adsorption :

$$m_c = 9.4091 \text{ g}$$

$$v = 2000 \text{ ml}$$

$$C_{iG} = 22.8 \text{ g/m}^3$$

$$\text{Time} = 72 \text{ h}$$

$$C_{fG} = 0.1 \text{ g/m}^3$$

$$Q_{fG} = 4.83 \text{ g/kg}$$

Cyanide pretreatment :

Soaked loaded carbon in 20 ml of a 20 g KCN/l solution at room temperature for 30 min. $C_{iN} = 7886 \text{ g/m}^3$, $C_{iK} = 12300 \text{ g/m}^3$, $C_{fN} = 4567 \text{ g/m}^3$, $C_{fK} = 7200 \text{ g/m}^3$.

Elution :

In glass column, $h = 143 \text{ mm}$, $T = 70 \text{ }^\circ\text{C}$, eluant = distilled water

t [h]	V [ml/h]	V_B	C_G [g/m ³]	pH	C_N [g/m ³]	C_K [g/m ³]
0.050		0.175	16.2			3400
0.133	60.0	0.465		10.42	1327	
0.183		0.634	22.2			1818
0.333	52.2	1.090			292	
0.417		1.344	64.4	10.62		501
0.717	50.7	2.230			37	
0.767		2.377	112.0			214
1.133		3.433	119.4			159
1.300	49.0	3.910		10.82	32	
1.500		4.520	113.4			130
1.833	57.8	5.640	103.5			110
2.350	45.7	7.020	92.5			108
2.933	51.7	8.775	82.5	10.74	8	95
3.633	55.4	11.040	65.1			85
4.550	47.9	13.590		10.68		
5.550	45.0	16.220	45.0	10.58		58

$$V_{ave} = 1.386 \times 10^{-8} \text{ m}^3 \cdot \text{s}^{-1}$$

Experiment no. 41

Relationship between exponent n and constant A in Freundlich isotherm for gold on various carbons.

The values for the carbons other than carbons A,B and BTX were obtained from Van Deventer (1984a).

Carbon	[O ₂]	T [°C]	A	n
Le Carbone G210 AS	9.0	20	49.90	0.091
Le Carbone G210 AS	< 9.0	20	19.03	0.207
Le Carbone G210 AS	9.0	20	50.10	0.075
Extruded coal-based	9.0	20	54.00	0.074
Coconut shell	9.0	20	19.90	0.300
Norit	9.0	20	41.70	0.120
Brazilian coconut	9.0	20	28.10	0.210
Sutcliffe Speakman	9.0	20	40.10	0.110
Peach pip	9.0	20	27.80	0.180
Sentrachem	9.0	20	39.50	0.130
Haycarb	9.0	20	26.90	0.162
BTX	9.0	20	31.48	0.204
BTX	9.0	30	25.79	0.209
BTX	9.0	40	21.84	0.251
BTX	9.0	60	13.43	0.247
A	0.0	20	7.31	0.338
A	4.4	20	13.44	0.264
A	9.0	20	18.32	0.229
B	0.0	20	22.03	0.168
B	4.2	20	35.37	0.159
B	9.0	20	38.65	0.131

Experiment no.42

Equilibrium adsorption of gold cyanide on carbon BTX from solutions at 30 °C in open containers.

$$v_i = 1000 \text{ ml}$$

$$\text{pH} = 8.5$$

$$C_{iG} = 30.5 \text{ g/m}^3$$

m_c [g]	v_e [ml]	C_{eG} [g/m ³]	Q_{eG} [g/kg]	A *
0.2038	960	21.4	48.9	24.62
0.3978	965	14.1	42.5	23.27
0.6210	965	6.4	39.2	26.05
0.8075	955	3.1	34.1	26.63
1.2376	955	0.6	24.2	27.04
1.6022	960	0.3	18.9	24.74

* Calculated with $n = -0.002688.A + 0.2902$

From least squares fit on equilibrium data :

$$Q_{eG} = 25.79 C_{eG}^{0.2095}$$

From average of calculated A-values :

$$Q_{eG} = 25.39 C_{eG}^{0.222}$$

Experiment no.43

Equilibrium adsorption of gold cyanide on carbon BTX from solutions at 40 °C in open containers.

$$v_i = 1000 \text{ ml}$$

$$\text{pH} = 8.5$$

$$C_{iG} = 27.8 \text{ g/m}^3$$

m_c [g]	v_e [ml]	C_{eG} [g/m ³]	Q_{eG} [g/kg]	A *
0.2053	935	19.9	44.78	22.53
0.6074	895	6.5	36.19	23.68
1.0058	945	1.8	25.95	22.68
1.4070	1025	0.6	19.32	21.75
1.8055	915	0.3	15.25	20.26
2.2099	985	0.1	12.54	21.42

* Calculated with $n = -0.002688.A + 0.2902$

From least squares fit on equilibrium data :

$$Q_{eG} = 21.84 C_{eG}^{0.2508}$$

From average of calculated A-values :

$$Q_{eG} = 22.05 C_{eG}^{0.231}$$

Experiment no.44

Equilibrium adsorption of gold cyanide on carbon BTX from solutions at 60 °C in open containers.

$$v_i = 1000 \text{ ml}$$

$$\text{pH} = 8.5$$

m_c [g]	C_{iG} [g/m ³]	v_e [ml]	C_{eG} [g/m ³]	Q_{eG} [g/kg]	A^*
0.2019	27.5	970	22.8	26.67	11.90
0.6006	27.5	785	15.2	25.92	12.93
1.0042	27.5	650	7.4	22.60	13.60
2.2068	27.5	1080	1.1	11.92	11.63
1.2043	30.3	895	4.0	22.19	15.74
1.6094	30.3	610	2.5	17.88	14.19

* Calculated with $n = -0.002688.A + 0.2902$

From least squares fit on equilibrium data :

$$Q_{eG} = 13.43 C_{eG}^{0.247}$$

From average of calculated A-values :

$$Q_{eG} = 13.33 C_{eG}^{0.254}$$

Experiment no.45

Effect of pH on equilibrium adsorption of gold cyanide on carbon BTX from solutions at 20 °C in open containers.

$$v_i = 1000 \text{ ml}$$

$$C_{iG} = 37.8 \text{ g/m}^3$$

The initial pH's were adjusted by the addition of KOH. KCl was added to give equimolar potassium concentrations.

m_c [g]	v_e [ml]	pH_e	C_{eK} [g/m ³]	C_{eG} [g/m ³]	Q_{eG} [g/kg]	A^*
0.5087	995	12.65	1003	21.0	33.2	15.59
0.5025	995	10.68	1137	17.6	40.4	20.60
0.5063	995	8.20	1188	11.5	52.1	31.55
0.5005	1000	7.60	1191	10.5	54.6	34.23
0.5019	995	6.90	1190	9.0	57.5	38.05

* Calculated with $n = -0.002688.A + 0.2902$

$$A = 113.4 \exp(-0.16 \text{ pH}_e)$$

Experiment no.46

Effect of pH on equilibrium adsorption of gold cyanide on carbon BTX from solutions at 40 °C in open containers.

$$v_i = 1000 \text{ ml}$$

$$C_{iG} = 29.8 \text{ g/m}^3$$

The initial pH's were adjusted by the addition of KOH. KCl was added to give equimolar potassium concentrations.

m_c [g]	v_e [ml]	pH_e	C_{eK} [g/m ³]	C_{eG} [g/m ³]	Q_{eG} [g/kg]	A^*
0.5019	940	7.57	1678	8.0	44.4	28.46
0.5017	895	11.89	1705	19.5	24.6	11.38
0.5026	920	12.39	1538	20.1	22.5	10.23
0.5018	940	8.49	1679	11.3	38.2	21.80
0.5037	900	12.68	1523	21.3	21.1	9.38
0.5025	925	12.89	1372	21.6	19.5	8.60

* Calculated with $n = -0.002688.A + 0.2902$

$$A = 137.7 \exp(-0.21 pH_e)$$

Experiment no.47

Effect of cyanide concentration on equilibrium adsorption of gold cyanide on carbon BTX from solutions at 20 °C in open containers.

$$v_i = v_e = 1000 \text{ ml}$$

$$C_{iG} = 38 \text{ g/m}^3$$

KCl was added to give equimolar potassium concentrations.

m_c [g]	C_{eK} [g/m ³]	pH _e	C_{eN} [g/m ³]	C_{eG} [g/m ³]	Q_{eG} [g/kg]	A *
1.5046	1221	8.62	15.9	1.9	23.99	20.63
1.5118	1230	9.09	37.2	2.8	23.28	18.16
1.5080	1232	9.52	85.0	4.2	22.41	15.70
1.5037	1223	9.73	135.4	5.2	21.81	14.41
1.4967	1219	9.92	199.2	5.6	21.65	14.01
1.5063	1218	10.09	259.0	5.9	21.31	13.58
1.5039	1212	10.26	358.5	6.5	20.95	12.99
1.5131	1183	10.23	398.3	6.8	20.62	12.62
1.5100	1200	10.31	471.4	7.5	20.23	12.05
1.5094	1209	10.51	564.3	7.7	20.07	11.84

* Calculated with $n = -0.002688.A + 0.2902$

$$A = 31.8 (C_{eN} + 1)^{-0.155}$$

Experiment no.48

Effect of potassium concentration on equilibrium adsorption of gold cyanide on carbon BTX from solutions at 20 °C in open containers.

$$v_i = 1000 \text{ ml}$$

$$C_{iG}^i = 37.8 \text{ g/m}^3$$

KCl was added to adjust the potassium concentrations.

m_c [g]	v_e [ml]	pH_e	C_{eK} [g/m ³]	C_{eG} [g/m ³]	Q_{eG} [g/kg]	A *
0.5073	1000	7.70	14	12.6	49.7	29.03
0.5260	995	7.47	67	10.8	51.4	31.52
0.5026	995	7.29	249	10.9	53.6	33.16
0.5045	1000	7.15	1119	8.9	57.3	37.98
0.5125	1000	7.02	3104	7.2	59.7	42.09

* Calculated with $n = -0.002688.A + 0.2902$

$$A = 23.6 (C_{eK} + 1)^{0.069}$$

Experiment no.49

Effect of calcium concentration on equilibrium adsorption of gold cyanide on carbon BTX from solutions at 20 °C in open containers.

$$v_i = 1000 \text{ ml}$$

$$C_{iG}^i = 59.7 \text{ g/m}^3$$

CaCl₂ was added to adjust the calcium concentrations.

m_c [g]	v_e [ml]	pH_e	C_{eCa} [g/m ³]	C_{eG} [g/m ³]	Q_{eG} [g/kg]	A *
0.4767	980	7.64	326	20.0	84.1	54.9
0.4783	990	7.53	860	18.0	87.6	60.7
0.4779	990	7.38	2010	16.0	91.8	68.3
0.4796	990	7.31	3720	14.4	94.8	74.7
0.4790	995	7.18	4920	13.9	95.8	76.9

* Calculated with $n = -0.002688.A + 0.2902$

$$A = 26.0 (C_{eCa} + 1)^{0.127}$$

Experiment no. 50

The elution of gold cyanide from carbon BTX loaded over a period of 22 h.

Adsorption :

$$m_c = 9.4061 \text{ g}$$

$$v_c = 2000 \text{ ml}$$

$$C_{iG} = 22.8 \text{ g/m}^3$$

$$\text{Time} = 22 \text{ h}$$

$$C_{fG} = 0.0 \text{ g/m}^3$$

$$Q_{fG} = 4.85 \text{ g/kg}$$

Cyanide pretreatment :

Soaked loaded carbon in 20 ml of a 20 g KCN/l solution at room temperature for 30 min. $C_{iN} = 7886 \text{ g/m}^3$, $C_{iK} = 12300 \text{ g/m}^3$, $C_{fN} = 4593 \text{ g/m}^3$, $C_{fK} = 7380 \text{ g/m}^3$.

Elution :

In glass column, $h = 143 \text{ mm}$, $T = 70 \text{ }^\circ\text{C}$, eluant = distilled water

t [h]	V [ml/h]	V_B	C_G [g/m ³]	pH	C_N [g/m ³]	C_K [g/m ³]
0.067		0.209	18.2			3053
0.167	53.7	0.522			1600	
0.317		0.978	40.6	10.35		1200
0.450	50.8	1.373			159	
0.567		1.723	105.6			324
0.783	52.7	2.388		10.58	69	
0.883		2.695	122.4			204
1.117	52.3	3.406		10.72	29	
1.167		3.557	121.8			150
1.983		5.770	105.6			112
2.117	45.6	6.125		10.78	11	
2.550	56.7	7.556				
2.650		7.884	92.4			90
3.133	54.0	9.405		10.77	11	
3.200		9.614	78.0			80
3.950	52.7	11.918	60.0			70
4.700	35.0	13.447	55.8			72
4.783	54.5	13.712		10.69		
5.367	48.3	15.354	46.4		8	56
6.117		17.540	41.0	10.42		

$$V_{ave} = 1.367 \times 10^{-8} \text{ m}^3 \cdot \text{s}^{-1}$$

Experiment no. 51

The elution of gold cyanide from carbon BTX after a sodium cyanide pretreatment.

Adsorption :

$$m_c = 9.4061 \text{ g}$$

$$v_c = 2000 \text{ ml}$$

$$C_{iG} = 24.9 \text{ g/m}^3$$

$$\text{Time} = 22 \text{ h}$$

$$C_{fG} = 0.0 \text{ g/m}^3$$

$$Q_{fG} = 5.29 \text{ g/kg}$$

Cyanide pretreatment :

Soaked loaded carbon in 20 ml of a 15 g NaCN/l solution at room temperature for 30 min. $C_{iN} = 7766 \text{ g/m}^3$, $C_{iNa} = 6896 \text{ g/m}^3$, $C_{fN} = 4846 \text{ g/m}^3$, $C_{fNa} = 4494 \text{ g/m}^3$.

(Subscript Na = sodium)

Elution :

In glass column, $h = 143 \text{ mm}$, $T = 70 \text{ }^\circ\text{C}$, eluant = distilled water

t [h]	V [ml/h]	V_B	C_G [g/m ³]	pH	C_N [g/m ³]	C_{Na} [g/m ³]
0.067		0.193	16.7			1592
0.217	49.6	0.626	13.0	10.342	1261	1046
0.500	51.0	1.468	80.0		372	280
0.767	49.8	2.242	116.0	10.370	106	166
1.050		3.044	131.6		26	116
2.033	53.9	5.921	104.4			65
2.500	51.4	7.319	90.6	10.766		57
3.167	48.7	9.211	79.0			50
3.783	40.0	10.648	68.0	10.711		48
4.583	51.5	13.049	56.1			41
5.217	48.9	14.854	46.8	10.702		39
6.117	49.9	17.471	38.4			34

$$V_{ave} = 1.361 \times 10^{-8} \text{ m}^3 \cdot \text{s}^{-1}$$

Experiment no. 52

The elution of gold cyanide from carbon BTX after a KOH/KCl pretreatment.

Adsorption :

$$m_c = 9.4055 \text{ g}$$

$$v = 2000 \text{ ml}$$

$$C_{iG} = 24.0 \text{ g/m}^3$$

$$\text{Time} = 24 \text{ h}$$

$$C_{fG} = 0.1 \text{ g/m}^3$$

$$Q_{fG} = 4.95 \text{ g/kg}$$

Pretreatment :

Soaked loaded carbon in 20 ml of a solution of 0.965 g KOH/l and 21.66 g KCl/l at room temperature for 30 min. (This solution had the same pH and C_{iK} as the 20 g KCN/l solutions used in most of the other elution experiments in the glass column.) $\text{pH}_i = 12.379$, $C_{iK} = 11696 \text{ g/m}^3$, $\text{pH}_f = 11.012$, $C_{fK} = 8712 \text{ g/m}^3$.

Elution :

In glass column, $h = 143 \text{ mm}$, $T = 70 \text{ }^\circ\text{C}$, eluant = distilled water

t [h]	V [ml/h]	V_B	C_G [g/m ³]	pH	C_K [g/m ³]
0.050		0.150	3.2		2766
0.150	51.5	0.450			3856
0.183		0.552	2.6	9.152	
0.350	56.4	1.100	5.2		474
0.600	50.0	1.828	8.8	9.549	154
1.017	46.8	2.964	11.8		64
1.350	54.3	4.019	12.1	9.660	47
1.683	51.2	5.014		10.029	
2.267		6.762	10.1		33
2.517	51.5	7.512			
2.783	48.9	8.271	8.8	9.873	25
3.517	46.0	10.237	7.5	9.754	19
4.283	49.1	12.431	5.9		11
5.183		15.006		9.276	5

$$V_{ave} = 1.38 \times 10^{-8} \text{ m}^3 \cdot \text{s}^{-1}$$

Experiment no. 53

The prolonged effect of a cyanide pretreatment on the elution of gold cyanide from carbon BTX.

Adsorption :

$$m_c = 9.4061 \text{ g}$$

$$v = 2000 \text{ ml}$$

$$C_{iG} = 24.0 \text{ g/m}^3$$

$$\text{Time} = 23 \text{ h}$$

$$C_{fG} = 0.6 \text{ g/m}^3$$

$$Q_{fG} = 4.98 \text{ g/kg}$$

Cyanide pretreatment :

Soaked loaded carbon in 20 ml of a 20 g KCN/l solution at 35 °C for 44 h, boiled for 1 h, and left at room temperature for a further 20 h. $C_{iN} = 7886 \text{ g/m}^3$, $C_{iK} = 12300 \text{ g/m}^3$, $C_{fN} = 80 \text{ g/m}^3$, $C_{fK} = 7380 \text{ g/m}^3$.

Elution :

In glass column, $h = 143 \text{ mm}$, $T = 70 \text{ }^\circ\text{C}$.

Conducted elution in 2 phases : A KCl solution with a $C_K = 1972 \text{ g/m}^3$ was used as the eluant for the first 2.5 bed volumes. For the second part of the elution the KCl solution was replaced with distilled water.

t [h]	V [ml/h]	V _B	C _G [g/m ³]	pH	C _K [g/m ³]
0.067		0.190	20.9		
0.200	49.0	0.571	21.4		
0.367	56.7	1.122	29.6		
0.633	49.9	1.897	39.9	11.072	2226
0.883	47.1	2.446			
0.900		2.646	39.9		2196
1.017	58.9	3.046	40.8		2055
1.267	53.2	3.821	49.0	11.109	2050
1.450	51.5	4.372	115.0		827
1.683	48.4	5.030	155.5		395
1.983	43.7	5.794	200.0	11.746	336
2.217	48.3	6.451	191.0		290
2.483	53.1	7.276	167.2	11.616	250
2.700	54.4	7.963	160.8		230
3.150	51.1	8.901	138.0		198
3.867	47.6	11.263	120.6		156
4.583	48.8	13.301	91.0	11.104	129
5.200	43.5	14.864	79.5		116

**

** Replaced KCl eluant with distilled water.

$$V_{ave} = 1.36 \times 10^{-8} \text{ m}^3 \cdot \text{s}^{-1}$$

Experiment no. 54

Deactivation of carbon BTX towards the adsorption of gold cyanide by pretreatment with cyanide.

Pretreatment of carbon :

- (a) Soaked 1.0027 g carbon BTX in 10 ml of a 20 g KCN/l solution for 40 h at room temperature, rinsed in glass column with 3.2 l of distilled water at room temperature and a flow rate of 35 ml/min.
- (b) Soaked 1.0037 g carbon BTX in 10 ml distilled water for 40 h at room temperature.

Adsorption :

$$v = 1000 \text{ ml}$$

$$C_{iG} = 24.3 \text{ g/m}^3$$

$$\text{pH} = 9.5$$

Time [h]	(a)		(b)	
	C_G [g/m ³]	C_G/C_{iG}	C_G [g/m ³]	C_G/C_{iG}
0.250	23.6	0.971	23.4	0.963
0.583	23.6	0.971	21.9	0.901
1.367	23.4	0.963	20.6	0.848
2.000	23.2	0.955	20.0	0.823
3.750	22.2	0.914	18.3	0.753
8.000	20.2	0.833	16.1	0.664
13.000	17.9	0.738	13.6	0.559
17.000	16.1	0.662	11.5	0.475
22.167	13.7	0.564	8.9	0.366
26.667	11.3	0.465	5.9	0.243
94.667	2.7	0.111	0.9	0.037

Experiment no. 55

Effect of cyanide-age on desorption of gold cyanide from carbon BTX.

Adsorption :

 $v = 1000 \text{ ml}$ $C_{iG} = 63.3 \text{ g/m}^3$

Time = 44 h

	(a)	(b)	(c)	(d)	(e)
$m_c \text{ [g]}$	2.8627	2.8629	2.8619	2.8607	2.8649
$C_{fG} \text{ [g/m}^3\text{]}$	3.2	3.2	2.4	3.2	2.4

Pretreatment :

Soaked in 10 ml of cyanide solution for 45 min. at room temperature.
Potassium concentrations all adjusted to $18000 \text{ g K}^+/\text{m}^3$ by addition of KCl.

	(a)	(b)	(c)	(d)	(e)
$C_{iN} \text{ [g/m}^3\text{]}$	0	2057	3983	7700	11550
$C_{fN} \text{ [g/m}^3\text{]}$	0	730	1693	4447	7567
$Q_{fN} \text{ [g/kg]}$	0	4.64	8.00	11.37	13.90
$C_{fG} \text{ [g/m}^3\text{]}$	6.5	27.0	48.0	84.0	102.5

Desorption :

In batch, 75 ml each, distilled water at $70 \text{ }^\circ\text{C}$.

	(a)	(b)	(c)	(d)	(e)
$C_G \text{ (22 h)}$	18.0	69.0	101.0	158.0	192.0
$C_G \text{ (52 h)}$	7.0	48.0	77.0	120.0	129.5
$C_G \text{ (94 h)}$	3.0	27.6	52.5	91.0	107.5
After 94 h :					
pH	7.883	9.725	10.158	10.528	10.689
C_K	445	458	499	511	544
Q_G	20.89	20.15	19.71	18.30	18.05
A	15.92	8.28	6.71	5.27	4.94
$A/\exp(-0.2 \text{ pH})$	77.03	57.90	51.20	43.28	41.90

A-values calculated with $n = -0.002688 A + 0.2902$

Experiment no.56

Reactivation of carbon BTX towards gold cyanide after pretreatment with cyanide.

Adsorption :

(a)
 $v_i = 1000 \text{ ml}$
 $m_c = 3.0073$
 $C_{iG}^c = 48.9 \text{ g/m}^3$
 Time = 21 days
 $v_e = 985 \text{ ml}$
 $C_{eG}^e = 0.1 \text{ g/m}^3$

(b)
 $v_i = 1000 \text{ ml}$
 $m_c = 3.0073$
 $C_{iG}^c = 21.1 \text{ g/m}^3$
 Time = 21 days
 $v_e = 975 \text{ ml}$
 $C_{eG}^e = 0.0 \text{ g/m}^3$

Pretreatment :

Soaked each sample of loaded carbon in 5 ml of a $7300 \text{ g CN}^-/\text{m}^3$ solution for 30 min. at room temperature, $C_{fN} = 3319 \text{ g/m}^3$.

Desorption :

$v = 500 \text{ ml}$ of distilled water

$T = 60 \text{ }^\circ\text{C}$

$\text{pH}_i = 11.103$

(a) $Q_{iG} = 16.25 \text{ g.kg}^{-1}$ (b) $Q_{iG} = 7.0 \text{ g.kg}^{-1}$

(a)			(b)			
t [h]	C_G	C_K	t [h]	C_G	C_K	pH
0.167	15.0		0.167	7.1		9.072
0.417	20.6	59	0.417	10.2	62	
0.917	26.4		0.883	12.8		
1.750	34.5	67	1.717	13.2	68	
3.200	34.8		3.167	13.3		8.878
4.633	35.7		4.600	13.1		
5.667	35.1	72	5.633	13.0	72	
6.950	34.3		6.917	12.8		9.237
23.283	31.3		23.250	9.4		10.757
26.167	29.4		26.133	9.1		
29.133	29.0		29.100	9.0		10.950

Experiment no.57

Effect of a water insoluble gold species on elution from carbon BTX.

Adsorption :

(a)	(b)	(c)
$v = 1000 \text{ ml}$	$v = 1000 \text{ ml}$	$v = 1000 \text{ ml}$
$m_c = 1.5046 \text{ g}$	$m_c = 1.5031 \text{ g}$	$m_c = 1.5024 \text{ g}$
$C_{iG} = 102.8 \text{ g/m}^3$	$C_{iG} = 102.8 \text{ g/m}^3$	$C_{iG} = 102.8 \text{ g/m}^3$
Time = 18.5 h	Time = 18.5 h	Time = 18.5 h
$C_{fG} = 69.3 \text{ g/m}^3$	$C_{fG} = 69.3 \text{ g/m}^3$	$C_{fG} = 67.2 \text{ g/m}^3$
$Q_{fG} = 22.3 \text{ g/kg}$	$Q_{fG} = 22.3 \text{ g/kg}$	$Q_{fG} = 23.7 \text{ g/kg}$

Pretreatment :

(a), (b) : Dried at 150 °C for 18 h before desorption.
 (c) : Desorption directly after adsorption.

Desorption :

$v = 1000 \text{ ml}$ of distilled water with 1 g KCN/l
 $T = 20 \text{ }^\circ\text{C}$
 $\text{pH} = 11.25$

(a)			(c)	
t [h]	C_G	ψ	C_G	ψ
0.083	1.0	0.030	0.8	0.022
0.250	1.5	0.045	1.6	0.045
0.417	2.1	0.063	2.2	0.062
0.667	2.8	0.084	3.3	0.093
0.917	3.4	0.101	3.9	0.110
2.967	6.9	0.206	8.3	0.233
3.983	8.1	0.242	9.7	0.272
6.417	9.9	0.296	12.2	0.343

where $\psi = (Q_{iG} - Q_G)/Q_{iG}$

Determination of water insoluble species on (a) and (b) by elution of $\text{Au}(\text{CN})_2^-$ from sample (b) with distilled water :

Each elution : $v = 1500 \text{ ml}$, $\text{pH} = 11.5$

Des.no	t [h]	C_{FG}	Q_{FG}
1	3.0	3.0	19.3
2	3.6	1.8	17.5
3	16.3	2.8	14.7
4	7.5	1.3	13.4
5	15.2	1.3	12.1
6	27.9	1.3	10.8
7	44.2	1.1	9.7

% Water insoluble species = $100 * (9.7/22.3) = 43.6 \%$

Experiment no.58

Effect of particle size on elution of gold from carbon BTX in the presence of a water insoluble gold species.

Adsorption :

$$v = 5000 \text{ ml}$$

$$m_c = 10.0131 \text{ g}$$

$$d_c = -1.7 + 1.4 \text{ mm}$$

$$C_{iG} = 38.3 \text{ g/m}^3$$

$$\text{Time} = 60 \text{ h}$$

$$C_{fG} = 0.9 \text{ g/m}^3$$

$$Q_{fG} = 18.7 \text{ g/kg}$$

Pretreatment :

Boil carbon for 26 h in 1000 ml water to which 30 ml of a 33 wt.% HCl solution was added, rinsed with distilled water and dried at 110 °C for 4 days.

Desorptions :

$$v = 1000 \text{ ml of distilled water with } C_{iN} = 342 \text{ g/m}^3$$

$$\text{pH}_i = 11.0$$

$$T = 20 \text{ }^\circ\text{C}$$

$$(a) m_c = 1.0030 \text{ g powdered carbon (from above batch)}$$

$$(b) m_c = 1.0035 \text{ g granular carbon (from above batch)}$$

(a)			(b)	
t [h]	C_G	ψ	C_G	ψ
0.250	1.6	0.085	0.4	0.021
0.750	2.0	0.107	0.5	0.027
2.417	2.8	0.149	0.9	0.048
3.750	3.2	0.171	1.2	0.064
6.000	3.5	0.187	1.6	0.085
8.250	3.6	0.192	1.9	0.101
13.917	3.5	0.187	2.4	0.128
22.000	3.4	0.182	2.9	0.155
25.083	3.6	0.192	3.0	0.160

$$\text{where } \psi = (Q_{iG} - Q_G) / Q_{iG}$$

$$C_{fN} = 275 \text{ g/m}^3$$

$$\text{pH}_f = 11.05$$

Determination of water insoluble species on (a) and (b) by elution of $\text{Au}(\text{CN})_2^-$ from 1.00 g of the dried carbon with distilled water :

Each elution : $v = 1000 \text{ ml}$, $\text{pH} = 12$

Des.no	t [h]	C_{fG}	Q_{fG}
1	18	0.6	18.1
2	50	0.5	17.6
3	22	0.7	16.9
4	25	0.8	16.1
5	24	0.7	15.4

% Water insoluble species = $100 * (15.4/18.7) = 82.4 \%$

Experiment no. 59

The elution of gold cyanide from loaded carbon BTX stored in distilled water for 6 months.

Adsorption :

$$m_c = 3.6 \text{ kg}$$

$$v_c = 60 \text{ l}$$

$$C_{ig} = 167 \text{ g/m}^3$$

$$\text{Time} = 10 \text{ days}$$

$$C_{fg} = 0.0 \text{ g/m}^3$$

$$Q_{fg} = 2.78 \text{ g/kg}$$

Stored loaded carbon in distilled water for 6 months after adsorption.

Cyanide pretreatment :

Loaded 9.143 g of the above batch of carbon into glass column filled with distilled water. Replaced distilled water with pretreatment solution by feeding 10 ml of 20 g KCN/l solution to the column. Soaked at room temperature for 16 h. Switched on water bath and heated up bed to 80 °C over a period of 1.5 h.

Elution :

In glass column, $h = 139 \text{ mm}$, $T = 80 \text{ °C}$, eluant = distilled water. Started flow of distilled water directly after temperature of bed reached 80 °C. (The pretreatment solution was not drained from the bed.)

t [h]	V [ml/h]	V _B	C _G [g/m ³]	pH	C _N [g/m ³]	C _K [g/m ³]
0.033		0.103	13.5			4932
0.167	51.7	0.517	15.2	10.094	929	3484
0.350	50.2	1.068	61.5	10.269	491	605
0.600	50.7	1.828	107.5	10.784	106	260
1.000	51.3	3.058	129.0		45	192
1.250	48.1	3.779	118.0	11.190		175
1.500	50.0	4.529				
1.667		5.035	106.5			151
1.917	51.6	5.808	100.8	11.147		131
2.417	46.9	7.214	81.6			120
3.150	49.5	9.390	61.8	11.078		
4.317	53.9	13.160	43.6			74
4.883	51.9	14.923	30.5	10.930		
5.617	49.4	17.095	25.1			57

$$V_{ave} = 1.45 \times 10^{-8} \text{ m}^3 \cdot \text{s}^{-1}$$

Experiment no. 60

The elution of gold cyanide from loaded carbon BTX stored in distilled water for 6 months.

Adsorption :

$$m_c = 3.6 \text{ kg}$$

$$v_c = 60 \text{ l}$$

$$C_{ig} = 167 \text{ g/m}^3$$

$$\text{Time} = 10 \text{ days}$$

$$C_{fg} = 0.0 \text{ g/m}^3$$

$$Q_{fg} = 2.78 \text{ g/kg}$$

Stored loaded carbon in distilled water for 6 months after adsorption.

Cyanide pretreatment :

Loaded the above carbon into distilled water in the stainless steel column. Replaced distilled water with pretreatment solution by pumping 4000 ml of 20 g KCN/l solution through the column. Soaked at room temperature for 16 h. Switched on oil heaters and heated up bed to 80 °C over a period of 1.5 h.

Elution :

In stainless steel column, $h = 749 \text{ mm}$, $T = 80 \text{ }^\circ\text{C}$, eluant = distilled water. Started flow of distilled water directly after temperature of bed reached 80 °C. (The pretreatment solution was not drained from the bed.)

t [h]	V [ml/ min]	V _B	C _G [g/m ³]	pH	C _N [g/m ³]	C _K [g/m ³]
0.083	261	0.222	6.9	9.819	929	4320
0.250	299	0.730				
0.283		0.832	15.9	10.101	531	1025
0.450	298	1.338	55.5	10.325	159	431
0.583	295	1.739	83.5	10.566	106	308
0.833	301	2.506	106.0	10.940	53	212
1.083	307	3.290	110.0	11.072	40	184
1.367	309	4.183	111.5	11.171	40	171
1.717	305	5.271	107.5		26	150
2.133	307	6.576	92.5	11.155		139
2.750	305	8.494	82.8			111
3.750	308	11.635	59.1	11.141		91
5.000	307	15.549	45.6			
5.667	306	17.631	33.4	11.030		63
6.333	306	19.709	27.3			
6.917	304	21.519	25.0	10.899		53

Temperature profile through column during run :

t [h]	TI ₀	TI ₁	TI ₂	TI ₃	TI ₄	TI ₅
0.024	74	77	76	69	76	77
0.072	76	76	75	62	73	80
0.200	77	70	69	74	71	81
0.338	77	76	77	77	77	81
0.498	80	80	80	79	80	81
0.684	80	80	80	79	79	80
0.881	79	79	79	78	79	80
1.142	79	79	79	78	78	79
1.415	79	79	79	78	78	80
1.757	78	78	78	77	78	79
2.171	78	78	78	77	77	79
2.792	78	78	78	77	78	79
3.719	78	78	77	77	77	79
5.045	78	78	77	77	77	79
5.949	77	78	77	77	77	78
6.945	77	77	77	77	77	78

See definition of TI₀ - TI₅ in Figure 3.2.

$$V_{\text{ave}} = 5.08 \times 10^{-6} \text{ m}^3 \cdot \text{s}^{-1}$$

Experiment no. 61

The elution of gold cyanide from carbon BTX at a flowrate of 5.9 bed volumes per hour.

Adsorption :

$$m_c = 9.4061 \text{ g}$$

$$v = 2000 \text{ ml}$$

$$C_{iG} = 23.5 \text{ g/m}^3$$

$$\text{Time} = 23 \text{ h}$$

$$C_{fG} = 0.6 \text{ g/m}^3$$

$$Q_{fG} = 4.869 \text{ g/kg}$$

Cyanide pretreatment :

Soaked loaded carbon in 20 ml of a 20 g KCN/l solution at room temperature for 30 min. $C_{iN} = 7169 \text{ g/m}^3$, $C_{iK} = 12300 \text{ g/m}^3$, $C_{fN} = 3983 \text{ g/m}^3$, $C_{fK} = 7015 \text{ g/m}^3$.

Elution :

In glass column, $h = 143 \text{ mm}$, $T = 70 \text{ }^\circ\text{C}$, eluant = distilled water

t [h]	V [ml/h]	V _B	C _G [g/m ³]	pH	C _N [g/m ³]	C _K [g/m ³]
0.033		0.204	20.6	10.569		3340
0.100	104.9	0.611	29.8		1261	1396
0.217	108.2	1.347	66.0	10.461	332	499
0.333	99.1	2.021	117.5		80	290
0.483	106.4	2.951	129.0	10.866	50	190
0.633	99.2	3.818	118.0			163
0.800	111.4	4.900	105.2	11.050		129
1.133	102.1	6.883	84.0			106
1.317	105.3	8.008	66.4	10.900		94
1.950	98.3	11.636	52.8			
2.367	100.8	14.084	48.0			61
2.967	101.1	17.619	29.2	10.455		
3.783	100.8	22.416	22.9			42
5.033	99.5	29.664	15.4	10.255		33

$$V_{ave} = 2.809 \times 10^{-8} \text{ m}^3 \cdot \text{s}^{-1}$$

Experiment no. 62

The elution of gold cyanide from carbon BTX at a flowrate of 37 bed volumes per hour.

Adsorption :

$$m_c = 9.4073 \text{ g}$$

$$v_c = 2000 \text{ ml}$$

$$C_{iG} = 24.1 \text{ g/m}^3$$

$$\text{Time} = 22 \text{ h}$$

$$C_{fG} = 0.0 \text{ g/m}^3$$

$$Q_{fG} = 5.12 \text{ g/kg}$$

Cyanide pretreatment :

Soaked loaded carbon in 20 ml of a 20 g KCN/l solution at room temperature for 30 min.

$$C_{iN} = 7766 \text{ g/m}^3, \quad C_{iK} = 12300 \text{ g/m}^3,$$

$$C_{fN} = 4248 \text{ g/m}^3, \quad C_{fK} = 7380 \text{ g/m}^3.$$

Elution :

In glass column, $h = 143 \text{ mm}$, $T = 70 \text{ }^\circ\text{C}$, eluant = distilled water

t [h]	V [ml/h]	V _B	C _G [g/m ³]	pH	C _N [g/m ³]	C _K [g/m ³]
0.017		0.612	29.3			1423
0.042	630	1.530			< 80	
0.050		1.834	94.0			288
0.067	618	2.434		11.024		
0.100		3.596	94.4			183
0.150	568	5.251	84.4			137
0.200	690	7.261	62.4			86
0.217		7.925		11.251		
0.267	664	9.860	52.0			
0.333	658	12.415	41.6			61
0.383	660	14.339	30.9			
0.433	641	16.207	29.9			50
0.483	624	18.025		11.214		
0.500		18.636	23.7			43
0.550	645	20.516	22.6			
0.633	631	23.579	19.1			39
0.733	667	27.466	15.0	10.976		
0.817	652	30.633	13.3			33
0.933	622	34.862	11.6			
1.017	580	37.679	10.3	10.522		29

$$V_{ave} = 1.767 \times 10^{-7} \text{ m}^3 \cdot \text{s}^{-1}$$

Experiment no. 63

Effect of distribution of gold through carbon particles on elution from carbon BTX.

Adsorption :

$v = 1000 \text{ ml}$

$C_{iG} = 10.0 \text{ g/m}^3$

(a) $m_c = 1.0033 \text{ g}$

Time = 25.4 h

$C_{fG} = 0.5 \text{ g/m}^3$

(b) $m_c = 1.0094 \text{ g}$

Time = 46.8 h

$C_{fG} = 0.2 \text{ g/m}^3$

(c) $m_c = 1.0025 \text{ g}$

Time = 144.3 h

$C_{fG} = 0.2 \text{ g/m}^3$

Desorption :

$v = 1000 \text{ ml}$ of distilled water

$\text{pH}_i = 12.37$

$T = 22 \text{ }^\circ\text{C}$

$C_K = 390 \text{ g/m}^3$

(a)			(b)		(c)	
t [h]	C_G	ψ	C_G	ψ	C_G	ψ
0.067	0.2	0.021	0.1	0.010	0.1	0.010
0.133	0.2	0.021	0.2	0.020	0.15	0.015
0.250	0.3	0.032	0.2	0.020	0.15	0.015
0.417	0.4	0.042	0.3	0.031	0.2	0.020
0.733	0.5	0.053	0.4	0.041	0.3	0.031
1.167	0.7	0.074	0.5	0.051	0.4	0.041
2.217	1.1	0.116	0.9	0.092	0.6	0.061
3.167	1.4	0.147	1.1	0.112	0.8	0.082
6.133	2.0	0.211	1.7	0.173	1.1	0.112
8.250	2.2	0.232	2.0	0.204	1.4	0.143
21.850	2.5	0.263	2.4	0.245	2.0	0.204
23.683	2.4	0.253	2.4	0.245	1.9	0.194
28.433	2.5	0.263	2.4	0.245	2.0	0.204
29.183	2.5	0.263	2.4	0.245	2.0	0.204
47.433	2.2	0.232	2.3	0.235	1.9	0.194
74.267	1.7	0.179	1.6	0.163	1.5	0.153
94.100	1.4	0.147	1.2	0.122	1.1	0.112

where $\psi = (Q_{iG} - Q_G)/Q_{iG}$
 $\text{pH}_f = 11.0$

Experiment no. 64

The elution of gold cyanide from carbon BTX after a cyanide pretreatment at 100 °C.

Adsorption :

$$m_c = 9.4115 \text{ g}$$

$$v = 2000 \text{ ml}$$

$$C_{iG} = 22.9 \text{ g/m}^3$$

$$\text{Time} = 48 \text{ h}$$

$$C_{fG} = 0.3 \text{ g/m}^3$$

$$Q_{fG} = 4.80 \text{ g/kg}$$

Cyanide pretreatment :

Soaked loaded carbon in 10 ml of a 20 g KCN/l solution at 100 °C for 30 min. $C_{iN} = 7733 \text{ g/m}^3$, $C_{iK} = 12300 \text{ g/m}^3$, $C_{fN} = 1128 \text{ g/m}^3$, $C_{fK} = 4245 \text{ g/m}^3$.

The cyanide concentration in a "control" solution of 10 ml 20 g KCN/l without any carbon decreased to $C_{fN} = 7435 \text{ g/m}^3$ under the above conditions.

Elution :

In glass column, $h = 143 \text{ mm}$, $T = 70 \text{ °C}$, eluant = distilled water

t [h]	V [ml/h]	V_B	C_G [g/m ³]	pH	C_N [g/m ³]	C_K [g/m ³]
0.050		0.142	18.0			1479
0.167	48.6	0.473			478	1668
0.250		0.705	34.0			
0.483	46.1	1.331	72.8		305	458
0.750	49.6	2.103	137.6	9.950		192
1.167		3.416	180.0			103
1.283	55.3	3.790			26	
1.517	52.0	4.499	160.3	10.042		89
2.167	48.0	6.317	137.4			72
2.750	44.5	7.829	120.0			
3.450	44.3	9.636	96.6	10.366		61
4.167	40.3	11.320	80.0			
4.833	54.5	13.435	63.5			47
5.583	49.5	15.599	55.5			
6.083	47.2	16.974	49.5	10.427		41

$$V_{ave} = 1.33 \times 10^{-8} \text{ m}^3 \cdot \text{s}^{-1}$$

Experiment no. 65

The elution of gold cyanide from carbon BTX after an acid wash.

Adsorption :

$$m_c = 9.4086 \text{ g}$$

$$v_c = 2000 \text{ ml}$$

$$C_{iG} = 24.2 \text{ g/m}^3$$

$$\text{Time} = 22 \text{ h}$$

$$C_{fG} = 0.0 \text{ g/m}^3$$

$$Q_{fG} = 5.14 \text{ g/kg}$$

Acid wash :

Soaked loaded carbon in 10 ml of a 3 vol.% x 33 mass% HCl solution at 70 °C for 45 min. Rinsed with distilled water and soaked for 20 min. at room temperature in 10 ml of distilled water with a $\text{pH}_i = 11.907$, $\text{pH}_f = 2.291$.

Cyanide pretreatment :

Soaked loaded carbon in 10 ml of a 20 g KCN/l solution at 100 °C for 30 min. $C_{iN} = 7567 \text{ g/m}^3$, $C_{iK} = 12300 \text{ g/m}^3$, $C_{fN} = 200 \text{ g/m}^3$, $C_{fK} = 6447 \text{ g/m}^3$. The cyanide concentration in a "control" solution of 10 ml 20 g KCN/l without any carbon decreased to $C_{fN} = 7435 \text{ g/m}^3$ after 30 min. at 100 °C.

Elution :

In glass column, $h = 143 \text{ mm}$, $T = 70 \text{ °C}$, eluant = distilled water

t [h]	V [ml/h]	V_B	C_G [g/m ³]	pH	C_N [g/m ³]	C_K [g/m ³]
0.050		0.142	7.3			1908
0.217	48.9	0.618	7.0		133	1382
0.417	53.7	1.243	17.6		133	504
0.617	51.4	1.842		8.863		
0.833	49.8	2.471	53.6		80	155
1.117	46.6	3.241	69.6	9.012		102
1.600	49.2	4.626			< 26	
1.650		4.770	85.0			56
2.000	51.3	5.817	98.5			
2.250	57.7	6.657				
2.450	54.5	7.293	94.5	9.273		37
3.083	49.9	9.134	79.2			
3.750	47.0	10.960	72.0			28
4.550	50.2	13.301	60.3	9.413		
5.250	46.8	15.210	54.6			20

$$V_{ave} = 1.38 \times 10^{-8} \text{ m}^3 \cdot \text{s}^{-1}$$

Experiment no. 66

The effect of temperature on the decomposition of cyanide in the absence of carbon.

$v = 1500 \text{ ml}$

- (a) $T = 54 \text{ }^\circ\text{C}$, $C_{iN} = 727 \text{ g.m}^{-3}$
 (b) $T = 76 \text{ }^\circ\text{C}$, $C_{iN} = 727 \text{ g.m}^{-3}$
 (c) $T = 91 \text{ }^\circ\text{C}$, $C_{iN} = 709 \text{ g.m}^{-3}$
 (d) $T = 100 \text{ }^\circ\text{C}$, $C_{iN} = 709 \text{ g.m}^{-3}$

(a)			(b)		
t [h]	C_N	C_N/C_{Ni}	t [h]	C_N	C_N/C_{Ni}
0.750	711	0.978	0.617	714	0.982
6.617	703	0.967	2.717	693	0.953
20.370	687	0.945	6.550	669	0.920
26.880	685	0.942	10.930	637	0.876
44.870	653	0.898	20.320	557	0.766
			26.830	512	0.704
			44.820	403	0.554

(c)			(d)		
t [h]	C_N	C_N/C_{Ni}	t [h]	C_N	C_N/C_{Ni}
0.500	685	0.966	0.350	663	0.935
2.633	627	0.884	2.583	523	0.738
6.467	528	0.745	6.417	342	0.483
10.880	432	0.610	10.830	218	0.307
20.200	260	0.367	20.150	64	0.090
26.780	186	0.262	26.750	42	0.059
44.770	82	0.116	44.720	11	0.016

Calculated first order rate constants :

- (a) $k_N = 5.167 \times 10^{-7} \text{ s}^{-1}$
 (b) $k_N = 3.603 \times 10^{-6} \text{ s}^{-1}$
 (c) $k_N = 1.353 \times 10^{-5} \text{ s}^{-1}$
 (d) $k_N = 2.644 \times 10^{-5} \text{ s}^{-1}$

Experiment no. 67

The effect of carbon particle size on the decomposition of cyanide.

$v = 1000 \text{ ml}$

$C_{iN} = 1 \text{ g KCN/l}$

$\text{pH} = 10.97$

$T = 20 \text{ }^\circ\text{C}$

(a) $m_c = 1.5035 \text{ g}$ powdered carbon BTX

(b) $m_c = 1.5023 \text{ g}$ carbon BTX with $d_c = -1.7 +1.4 \text{ mm}$

Time [h]	(a)		(b)	
	C_N [g/m ³]	C_N/C_{iN}	C_N [g/m ³]	C_N/C_{iN}
0.00	372	1.000	372	1.000
20.72	268	0.721	281	0.757
41.97	194	0.529	202	0.543

Experiment no. 68

The effect of mixing speed on the decomposition of cyanide on carbon BTX.

$v = 1000 \text{ ml}$

$C_{iN} = 1 \text{ g KCN/l}$

$\text{pH} = 11.53 = 29 \text{ }^\circ\text{C}$

(a) $m_c = 1.5077 \text{ g}$, $N = 700 \text{ rpm}$

(b) $m_c = 1.4993 \text{ g}$, $N = 1350 \text{ rpm}$

(c) $m_c = 1.5021 \text{ g}$, $N = 1500 \text{ rpm}$

(a)			(b)		(c)		
t [h]	C_N	C_N/C_{iN}	C_N	C_N/C_{iN}	t [h]	C_N	C_N/C_{iN}
0.000	380	1.000	380	1.000	0.000	380	1.000
0.167	377	0.992	377	0.992	0.167	380	1.000
0.783	377	0.992	376	0.989	0.783	376	0.989
3.833	369	0.971	369	0.971	3.833	359	0.945
17.417	324	0.853	305	0.803	17.417	290	0.763
26.883	281	0.739	276	0.726	26.883	256	0.674
42.667	268	0.705	223	0.587	42.667	178	0.468
66.250	210	0.553	162	0.426	66.250	98	0.258

Experiment no. 69

The elution of gold cyanide from carbon BTX with a constant concentration of cyanide in the eluant.

Adsorption :

$$m_c = 9.4085 \text{ g}$$

$$v_c = 2000 \text{ ml}$$

$$C_{ig} = 22.8 \text{ g/m}^3$$

$$\text{Time} = 22 \text{ h}$$

$$C_{fg} = 0.3 \text{ g/m}^3$$

$$Q_{fg} = 4.78 \text{ g/kg}$$

No pretreatment was conducted.

Elution :

In glass column, $h = 143 \text{ mm}$, $T = 70 \text{ }^\circ\text{C}$, eluant = solution of 0.5 g KCN/l , $C_N = 191 \text{ g/m}^3$, $\text{pH} = 10.65$.

t [h]	V [ml/h]	V _B	C _G [g/m ³]	pH	C _N [g/m ³]	C _K [g/m ³]
0.083		0.259	2.2	8.72		101
0.250		0.777	2.1			
0.500	53.3	1.550			5.3	
0.583		1.809	1.8			145
0.667	50.5	2.060	2.0			
0.750		2.300		8.39		
0.917		2.770			5.3	
0.950		2.860	2.1			
1.050	45.5	3.130	2.2	8.87	21.2	183
1.333		3.860	2.7			
1.750	41.1	4.890	3.0		23.9	
2.000	51.4	5.570				227
2.667	45.0	7.440	6.1		79.7	
3.050		8.440	7.1			
4.000		10.830	9.6	9.87	117	
4.167	42.0	11.240	9.7			254
4.833	48.1	12.990	12.3		141	
5.900	57.4	16.270		10.09		259

$$V_{ave} = 1.315 \times 10^{-8} \text{ m}^3 \cdot \text{s}^{-1}$$

Experiment no. 70

The deactivation of carbon BTX towards the decomposition of cyanide.

$$v = 350 \text{ ml}$$

$$C_{iN} = 525 \text{ g/m}^3$$

$$T = 18 \text{ }^\circ\text{C}$$

$$m_c = 21 \text{ g}$$

The same sample of carbon BTX was repeatedly contacted with a fresh solution of cyanide as follows :

No.	t [h]	Q_{iN}	C_{fN}	$-\ln(C_f/C_i)$	$k_N[\text{h}^{-1}]$
1	1.533	0.00	404	0.262	0.171
2	1.817	2.02	441	0.174	0.096
3	4.118	3.42	449	0.156	0.038
4	2.333	4.68	475	0.100	0.043
5	1.417	5.52	496	0.057	0.040

Experiment no. 71

The elution of potassium from carbon BTX after a KCl pretreatment.

Pretreatment :

Soaked 9.4069 g dry carbon BTX in 20 ml KCl solution at 20 °C for 30 min.
 $C_{iK} = 11921 \text{ g/m}^3$, $C_{fK} = 12740 \text{ g/m}^3$.

Elution : In glass column, h = 143 mm, T = 20 °C, eluant = distilled H₂O

t [h]	V [ml/h]	V_B	$C_K [\text{g/m}^3]$
0.067	62.6	0.243	6012
0.167	48.8	0.528	4587
0.250	48.5	0.763	1800
0.367	49.6	1.100	729
0.533	46.8	1.555	246
0.683	48.8	1.981	107
0.933		2.697	56
1.250	49.6	3.613	41
1.583	45.7	4.500	34
2.033	50.9	5.835	23
2.333	47.6	6.667	21
2.883	51.4	8.315	15
3.500	47.8	10.033	13
4.050	47.8	11.565	8

$$V_{ave} = 1.361 \times 10^{-8} \text{ m}^3 \cdot \text{s}^{-1}$$

Experiment no. 72

The adsorption of potassium onto carbon BTX during a KCN pretreatment.

- (a) Soaked 9.4067 g dry carbon BTX in 20 ml of a 20 g KCN/l solution at 20 °C for 30 min. $C_{iN} = 7435 \text{ g/m}^3$, $C_{iK} = 12481 \text{ g/m}^3$, $C_{fN} = 5841 \text{ g/m}^3$, $C_{fK} = 10213 \text{ g/m}^3$.
- (b) Soaked 9.4060 g dry carbon BTX in 20 ml of a 20 g KCN/l solution at 70 °C for 30 min. $C_{iN} = 7435 \text{ g/m}^3$, $C_{iK} = 12481 \text{ g/m}^3$, $C_{fN} = 5310 \text{ g/m}^3$, $C_{fK} = 10178 \text{ g/m}^3$.

Molar ratio of adsorbed $K^+ : CN^-$

- (a) $Q_K : Q_N = 1 : 1.03$ (b) $Q_K : Q_N = 1 : 1.37$

Note that dry carbon was used in the above experiments to eliminate the dilution effect of the pore volume solution.

Experiment no. 73

The elution of gold cyanide from carbon BTX at room temperature.

Adsorption :

$$m_c = 9.4056 \text{ g}$$

$$v = 2000 \text{ ml}$$

$$C_{iG} = 119 \text{ g/m}^3$$

$$\text{Time} = 21 \text{ h}$$

$$C_{fG} = 10.3 \text{ g/m}^3$$

$$Q_{fG} = 23.1 \text{ g/kg}$$

Cyanide pretreatment :

Soaked loaded carbon in 20 ml of a 20 g KCN/l solution at 20 °C for 30 min. $C_{iN} = 7766 \text{ g/m}^3$, $C_{iK} = 12300 \text{ g/m}^3$, $C_{fN} = 4593 \text{ g/m}^3$, $C_{fK} = 7380 \text{ g/m}^3$

Elution : In glass column, $h = 143 \text{ mm}$, $T = 20 \text{ }^\circ\text{C}$, eluant = distilled H_2O

t [h]	V [ml/h]	V_B	C_G [g/m ³]	pH	C_N [g/m ³]	C_K [g/m ³]
0.250	31.9	0.465	10.8	11.051	1062	3171
0.583	29.0	1.028	17.0		1261	1356
0.867	29.5	1.516	41.6		498	510
1.183	30.3	2.074	66.8	10.911	432	290
1.633	30.2	2.866	89.6		106	191
2.083		3.768	104.8			146
2.633	31.9	4.701	107.6	11.144	40	
3.067	31.7	5.501	111.2			107
3.867	30.0	6.900	111.2			
4.333	30.3	7.723	110.0	11.373		92
5.250	30.7	9.364	104.8			
6.000	31.5	10.741	105.2			79
7.050	29.5	12.546	96.8	11.320		
7.500	32.5	13.398	90.4			69

$$V_{ave} = 8.515 \times 10^{-9} \text{ m}^3 \cdot \text{s}^{-1}$$

Experiment no. 74

The elution of gold cyanide from carbon BTX with a 2 wt.% KCN solution.

Adsorption :

$$m_c = 9.4061 \text{ g}$$

$$v_c = 2000 \text{ ml}$$

$$C_{iG} = 22.8 \text{ g.m}^{-3}$$

$$\text{Time} = 23 \text{ h}$$

$$C_{fG} = 0.3 \text{ g.m}^{-3}$$

$$Q_{fG} = 4.78 \text{ g.kg}^{-1}$$

Cyanide pretreatment :

Soaked loaded carbon in 20 ml of a 20 g KCN/l solution at room temperature for 30 min. $C_{iN} = 7726 \text{ g.m}^{-3}$, $C_{iK} = 12200 \text{ g.m}^{-3}$, $C_{fN} = 4461 \text{ g.m}^{-3}$, $C_{fK} = 7154 \text{ g.m}^{-3}$.

Elution :

In glass column, $h = 143 \text{ mm}$, $T = 70 \text{ }^\circ\text{C}$, eluant = distilled water containing 20 g KCN/l ($C_N = 7726 \text{ g.m}^{-3}$, $C_K = 12200 \text{ g.m}^{-3}$)

t [h]	V [ml/h]	V_B	C_G [g/m ³]	pH	C_N [g/m ³]	C_K [g/m ³]
0.033		0.159	19.9		5177	
0.083	82.0	0.398				9070
0.167		0.738	21.1		6107	
0.300	50.4	1.130		10.776		
0.367		1.327	24.6		6532	11060
0.500	51.5	1.727				
0.583		1.970	26.2			
0.750	48.1	2.437		11.019		
0.833		2.680	27.6		7195	11300
0.967	52.5	3.088				
1.050		3.331	28.4			
1.217	48.0	3.797		11.204		
1.400		4.342	29.7			
1.917	54.8	5.968	31.8	11.380		11870
2.667	48.2	8.075		11.508	7517	
3.250	48.6	9.727	34.6			11840
3.833	49.1	11.395		11.649		
4.533	48.2	13.361	35.1		7633	
5.550	40.2	15.743	36.3			12200
5.750	53.1	16.362		11.864		

$$V_{ave} = 1.356 \times 10^{-8} \text{ m}^3 \cdot \text{s}^{-1}$$

Experiment no. 75

The elution of gold cyanide from carbon BTX with a solution containing $559 \text{ g K}^+ \cdot \text{m}^{-3}$.

Adsorption :

$$m_c = 9.4067 \text{ g}$$

$$v_c = 2000 \text{ ml}$$

$$C_{ig} = 22.2 \text{ g} \cdot \text{m}^{-3}$$

$$\text{Time} = 21 \text{ h}$$

$$C_{fg} = 0.1 \text{ g} \cdot \text{m}^{-3}$$

$$Q_{fg} = 4.70 \text{ g} \cdot \text{kg}^{-1}$$

Cyanide pretreatment :

Soaked loaded carbon in 20 ml of a 20 g KCN/l solution at room temperature for 30 min. $C_{iN} = 7567 \text{ g} \cdot \text{m}^{-3}$, $C_{iK} = 12450 \text{ g} \cdot \text{m}^{-3}$, $C_{fN} = 4315 \text{ g} \cdot \text{m}^{-3}$, $C_{fK} = 6312 \text{ g} \cdot \text{m}^{-3}$.

Elution :

In glass column, $h = 143 \text{ mm}$, $T = 70 \text{ }^\circ\text{C}$, eluant = distilled water containing $559 \text{ g K}^+ \cdot \text{m}^{-3}$ (by addition of KCl).

t [h]	V [ml/h]	V_B	C_G [g/m ³]	pH	C_N [g/m ³]	C_K [g/m ³]
0.050		0.157	17.3			3035
0.183	54.0	0.576			1328	
0.217		0.682	16.0			2553
0.400	51.7	1.233			372	
0.450		1.383	25.9			1066
0.583	50.1	1.771		10.229	133	
0.667		2.014	30.2			830
0.833	48.6	2.484			56	
0.917		2.727	30.2			715
1.083	51.5	3.225		10.180		
1.167		3.473	30.1			660
1.417	48.6	4.182			26	
1.700		5.017	28.4			623
1.917	52.2	5.677		10.129		
2.500	48.2	7.314	25.2			608
2.933	50.0	8.576	22.8			604
3.433	47.9	9.972	22.2			598
4.050	50.9	11.802	20.5	10.045		578
4.667	45.0	13.420				
5.083	54.3	14.736	19.1			577
5.417	49.7	15.704		10.090		
6.000	47.5	17.317	17.5			577

$$V_{ave} = 1.376 \times 10^{-8} \text{ m}^3 \cdot \text{s}^{-1}$$

Experiment no. 76

The elution of gold cyanide from carbon BTX in the stainless steel column after drainage of the pretreatment solution.

Adsorption :

$$m_c = 3.6 \text{ kg}$$

$$v = 75 \text{ l}$$

$$C_{ig} = 85.9 \text{ g/m}^3$$

$$\text{Time} = 24 \text{ days}$$

$$C_{fg} = 0.0 \text{ g/m}^3$$

$$Q_{fg} = 1.79 \text{ g/kg}$$

Cyanide pretreatment :

Loaded the above carbon into distilled water in the stainless steel column. Drained column and added 1.9l of the following KCN/KOH solution at 70 °C to the top of the bed : 22 g KCN/l, 18.75 g KOH/l. Measured composition of pretreatment solution : $C_N = 8496 \text{ g.m}^{-3}$, $C_K = 25600 \text{ g.m}^{-3}$, pH = 13.56. Soaked for 30 min. at 70 °C before draining the bed. Composition of drain solution : $C_N = 1062 \text{ g.m}^{-3}$, $C_K = 3308 \text{ g.m}^{-3}$, pH = 10.61, $C_G = 0.5 \text{ g.m}^{-3}$.

Elution :

In stainless steel column, $h = 749 \text{ mm}$, $T = 80 \text{ }^\circ\text{C}$, eluant = distilled water. Started flow of distilled water directly after draining of pretreatment solution. $t=0$ was recorded at the moment when the eluant pump was switched on.

t [h]	V [ml/ min]	V _B	C _G [g/m ³]	pH	C _N [g/m ³]	C _K [g/m ³]
0.217	3.18	0.494	5.4	12.48	1168	6075
0.400	3.64	0.910	12.3	12.29	148	1450
0.583	3.65	1.327	20.6	12.13	53	790
0.817	3.74	1.860	29.6	11.99	32	515
1.083	3.77	2.465	41.4	11.85		365
1.417	3.72	3.225	46.6	11.78	16	278
1.750	3.76	3.983	50.0	11.67		230
2.100	3.75	4.780	52.6	11.62	16	196
3.100	3.74	7.056	45.8	11.43		135
4.000	3.78	9.104	39.2	11.28	5	109
5.333	3.68	12.138	27.5	11.11		81
6.300		14.339	22.0	11.06	10	68
7.833	3.71	17.828	16.4	10.94		54
9.917	3.80	22.572	10.9	10.83	8	42
11.917	3.82	27.124	7.7	10.56		34
14.917	3.81	33.952	4.3	10.25	5	24
18.850	3.77	42.904	2.2	10.18		15
22.417	3.80	51.022	1.2	9.99	10	9

$$V_{ave} = 3.719 \times 10^{-6} \text{ m}^3 \cdot \text{s}^{-1}$$

Temperature profile through column during run :

t [h]	TI ₀	TI ₁	TI ₂	TI ₃	TI ₄	TI ₅
0.002	75	84	86	84	86	68
0.069	75	85	87	75	84	83
0.191	84	84	80	79	79	82
0.306	81	80	80	79	79	82
0.443	79	80	80	80	79	81
0.595	79	80	80	79	79	81
0.811	79	80	79	79	79	80
1.084	78	78	78	78	77	79
1.422	77	78	78	79	78	81
1.784	78	79	79	79	78	80
2.117	78	79	79	79	79	80
3.096	79	79	79	79	79	80
4.044	78	79	79	79	79	80
5.343	78	79	79	79	78	80
6.347	78	79	79	78	78	80
7.834	78	79	79	78	78	80
9.926	77	78	78	78	78	80
11.896	78	78	78	78	78	80
14.919	78	78	78	78	78	80
18.900	77	78	78	77	77	80
22.425	78	79	79	78	78	80

See definition of TI₀ - TI₅ in Figure 3.2.

Experiment no. 77

Kinetics of adsorption and desorption of aurocyanide on carbon BTX in batch.

Adsorption :

$$m_c = 0.5106 \text{ g}$$

$$V_c = 1500 \text{ ml}$$

$$C_{iG} = 20.1 \text{ g.m}^{-3}$$

Both adsorption and elution were conducted in batch in open 2000 ml bottles with magnetic stirring at 1350 rpm and at room temperature.

t [h]	C_G [g/m ³]	pH	C_G/C_{iG}
0.000	20.1	6.80	1.000
0.083	19.9	6.89	0.990
0.167	20.3		1.010
0.250	20.2	6.66	1.005
0.400	19.6		0.975
0.600	19.6	6.55	0.975
1.050	18.7		0.930
2.950	18.1	6.58	0.900
6.083	17.2		0.856
16.783	14.6		0.726
19.167	14.6	6.80	0.726
21.950	14.1		0.701
24.117	13.8		0.687
30.083	13.0		0.647
41.583	12.0	6.90	0.597

Elution :

Eluant = 1500 ml distilled water with $\text{pH}_i = 11.87$ and $C_K = 90 \text{ g.m}^{-3}$ (by addition of KOH), $Q_{iG} = 23.8 \text{ g.kg}^{-1}$

t [h]	C_G [g/m ³]	pH	$\frac{Q_{iG} - Q_G}{Q_{iG}}$
0.083	0.2		0.025
0.167	0.3		0.037
0.283	0.3	11.87	0.037
0.400	0.3		0.037
0.533	0.3		0.037
0.883	0.5		0.062
1.567	0.8		0.099
3.083	1.2	11.82	0.148
5.500	1.6		0.198
7.200	1.9		0.235
11.367	2.5		0.309
23.333	3.0	11.26	0.370
25.867	3.0		0.370
28.800	3.0		0.370
32.367	3.1		0.383
36.183	3.1		0.383
47.367	3.1	10.32	0.383

Experiment no. 78

Kinetics of adsorption and desorption of aurocyanide on carbon BTX in batch.

Adsorption :

$$m_c = 1.0031 \text{ g}$$

$$v = 1500 \text{ ml}$$

$$C_{iG} = 20.1 \text{ g.m}^{-3}$$

Both adsorption and elution were conducted in batch in open 2000 ml bottles with magnetic stirring at 1350 rpm and at room temperature.

t [h]	C_G [g/m ³]	pH	C_G/C_{iG}
0.000	20.1	6.80	1.000
0.083	19.9	6.86	0.990
0.167	19.5		0.968
0.250	19.4	6.64	0.965
0.400	18.7		0.930
0.600	18.4	6.53	0.915
1.050	17.8		0.886
2.950	16.4	6.60	0.816
6.083	14.6		0.726
16.783	10.2		0.507
19.167	9.9	7.01	0.493
21.950	9.2		0.458
24.117	8.7		0.433
30.083	7.5		0.373
41.583	5.5	7.07	0.274

Elution :

Eluant = 1500 ml distilled water with $\text{pH}_i = 11.87$ and $C_K = 90 \text{ g}\cdot\text{m}^{-3}$ (by addition of KOH), $Q_{Gi} = 21.83 \text{ g}\cdot\text{kg}^{-1}$

t [h]	C_G [g/m ³]	pH	$\frac{Q_{iG} - Q_G}{Q_{iG}}$
0.083	0.3		0.021
0.167	0.3		0.021
0.283	0.4	11.87	0.027
0.400	0.5		0.034
0.533	0.6		0.041
0.883	0.9		0.062
1.567	1.3		0.089
3.083	2.1	11.82	0.144
5.500	2.9		0.199
7.200	3.3		0.226
11.367	4.0		0.274
23.333	4.4	11.29	0.301
25.867	4.3		0.295
28.800	4.4		0.301
32.367	4.4		0.301

Experiment no. 79

Kinetics of adsorption and desorption of aurocyanide on carbon BTX in batch.

Adsorption :

$$m_c = 0.7029 \text{ g}$$

$$v = 1500 \text{ ml}$$

$$C_{iG} = 11.4 \text{ g.m}^{-3}$$

$$\text{pH} = 7.0$$

Both adsorption and elution were conducted in batch in open 2000 ml bottles with magnetic stirring at 1350 rpm and at room temperature.

t [h]	C_G [g/m ³]	C_G/C_{iG}
0.000	11.4	1.000
0.083	11.6	1.018
0.167	11.3	0.991
0.333	11.1	0.974
0.500	11.0	0.965
1.467	10.2	0.895
4.350	9.2	0.807
5.533	8.7	0.763
7.883	8.1	0.711
14.500	6.4	0.561
22.950	5.3	0.465
25.000	5.2	0.456
27.017	4.7	0.412
31.583	4.5	0.395
35.117	4.3	0.377
37.000	4.4	0.386
46.850	3.4	0.298

Elution :

Eluant = 1500 ml distilled water with $\text{pH}_i = 11.05$, $C_{iN} = 382 \text{ g.m}^{-3}$ and $C_K = 597 \text{ g.m}^{-3}$ (by addition of KOH and KCN), $Q_{iG} = 17.07 \text{ g.kg}^{-1}$

t [h]	C_G [g/m ³]	pH	C_N [g/m ³]	$\frac{Q_{iG} - Q_G}{Q_{iG}}$
0.000	0.0	11.05	382	0.000
0.083	0.8			0.100
0.233	0.8	11.00		0.100
0.417	0.9			0.113
0.617	1.0			0.125
1.183	1.2			0.150
2.000	1.6	10.90	372	0.200
3.333	2.1			0.263
4.900	2.6	10.84		0.325
6.700	3.1	10.82		0.388
14.530	3.8			0.475
25.583	4.0		363	0.500
28.783	4.0	10.52		0.500
32.167	4.1			0.513
35.367	4.2		356	0.525

Experiment no. 80

Kinetics of adsorption and desorption of aurocyanide on carbon BTX in batch.

Adsorption :

$$m_c = 1.5038 \text{ g}$$

$$v = 1500 \text{ ml}$$

$$C_{i6} = 11.4 \text{ g.m}^{-3}$$

$$\text{pH} = 7.0$$

Both adsorption and elution were conducted in batch in open 2000 ml bottles with magnetic stirring at 1350 rpm and at room temperature.

t [h]	C_G [g/m ³]	C_G/C_{i6}
0.000	11.4	1.000
0.083	11.1	0.974
0.167	10.9	0.956
0.333	10.4	0.912
0.500	10.0	0.877
1.467	8.7	0.763
4.350	6.4	0.561
5.533	5.7	0.500
7.883	4.8	0.421
14.500	2.6	0.228
22.950	1.2	0.105
25.000	1.1	0.096
27.017	0.9	0.079
31.583	0.7	0.061
35.117	0.6	0.053
37.000	0.6	0.053
46.850	0.5	0.044

Elution :

Eluant = 1500 ml distilled water with $\text{pH}_i = 11.05$, $C_{iN} = 382 \text{ g.m}^{-3}$ and $C_K = 597 \text{ g.m}^{-3}$ (by addition of KOH and KCN), $Q_{iG} = 10.87 \text{ g.kg}^{-1}$

t [h]	C_G [g/m ³]	pH	C_N [g/m ³]	$\frac{Q_{iG} - Q_G}{Q_{iG}}$
0.000	0.0	11.05	382	0.000
0.083	0.6			0.055
0.233	0.7	11.00		0.064
0.417	0.8			0.073
0.617	0.9			0.083
1.183	1.1			0.101
2.000	1.6	10.90	369	0.147
3.333	2.0			0.183
4.900	2.4	10.84		0.220
6.700	2.8	10.83	377	0.257
14.530	3.2			0.294
25.583	3.1		366	0.284
28.783	3.0	10.55		0.275
32.167	3.1			0.284
35.367	3.1		356	0.284

Experiment no. 81

Kinetics of desorption of aurocyanide from carbon BTX in batch.

Adsorption :

$m_c = 0.6594 \text{ g}$

$v_i = 1000 \text{ ml}$

$v_e = 990 \text{ ml}$

$C_{iG} = 49.9 \text{ g.m}^{-3}$

$C_{eG} = 13.3 \text{ g.m}^{-3}$

$\text{pH}_e = 7.04$

$T = 20 \text{ }^\circ\text{C}$

Adsorption period = 21 days, i.e. adsorption to equilibrium.

Elution :

In open 1000 ml beaker with magnetic stirring at 1350 rpm

$v = 1000 \text{ ml}$

$T = 20 \text{ }^\circ\text{C}$

$Q_{iG} = 55.7 \text{ g.kg}^{-1}$

$C_K = 1872 \text{ g.m}^{-3}$ (from addition of KOH)

$C_N = 0 \text{ g.m}^{-3}$

$\text{pH} = 12.59$

t [h]	C_G [g/m ³]	$\frac{Q_{iG} - Q_G}{Q_{iG}}$
0.050	0.1	0.003
0.150	0.3	0.008
0.250	0.4	0.011
0.450	0.7	0.019
0.733	1.1	0.030
1.117	1.5	0.041
1.667	2.0	0.054
2.600	3.0	0.082
3.717	4.0	0.109
4.817	4.8	0.131
6.000	5.6	0.152
7.083	6.1	0.166
10.383	7.6	0.207
13.350	8.3	0.226
22.450	10.0	0.272
23.750	10.4	0.283
26.000	10.8	0.294
28.750	11.1	0.302
34.500	12.5	0.340

Experiment no. 82

Kinetics of desorption of aurocyanide from carbon BTX in batch.

Adsorption :

$m_c = 0.8000 \text{ g}$

$v_i = 1000 \text{ ml}$

$v_e = 975 \text{ ml}$

$C_{iG} = 49.9 \text{ g.m}^{-3}$

$C_{eG} = 7.0 \text{ g.m}^{-3}$

$\text{pH}_e = 7.36$

$T = 20 \text{ }^\circ\text{C}$

Adsorption period = 21 days, i.e. adsorption to equilibrium.

Elution :

In open 1000 ml beaker with magnetic stirring at 1350 rpm

$v = 1000 \text{ ml}$

$T = 20 \text{ }^\circ\text{C}$

$Q_{iG} = 53.8 \text{ g.kg}^{-1}$

$C_K = 690 \text{ g.m}^{-3}$ (from addition of KCN)

$C_{iN} = 441 \text{ g.m}^{-3}$

$C_{fN} = 284 \text{ g.m}^{-3}$

$\text{pH} = 11.1$

t [h]	C_G [g/m ³]	$\frac{Q_{iG} - Q_G}{Q_{iG}}$
0.067	0.4	0.009
0.167	0.8	0.019
0.250	1.1	0.026
0.417	1.7	0.039
0.667	2.4	0.056
1.083	3.4	0.079
1.417	4.1	0.095
2.550	6.1	0.142
4.467	8.6	0.200
6.317	10.6	0.246
7.217	11.3	0.262
9.717	13.1	0.304
18.000	16.5	0.383
23.533	18.1	0.420
26.050	18.7	0.434
29.783	19.4	0.450

Experiment no. 83

Kinetics of desorption of aurocyanide from carbon BTX in batch.

Adsorption :

$$m_c = 1.6042 \text{ g}$$

$$v_c = 1000 \text{ ml}$$

$$C_{iG} = 49.9 \text{ g.m}^{-3}$$

$$C_{eG} = 0.2 \text{ g.m}^{-3}$$

$$pH_e = 7.49$$

$$T_e = 20 \text{ }^\circ\text{C}$$

Adsorption period = 21 days, i.e. adsorption to equilibrium.

Elution :

The elution was conducted in a 2000 ml round-bottomed flask fitted with a total reflux condenser. The flask was submerged in a water bath and stirred magnetically at 1350 rpm,

$$v = 1000 \text{ ml}$$

$$T = 52 \text{ }^\circ\text{C}$$

$$Q_{iG} = 30.98 \text{ g.kg}^{-1}$$

$$C_K < 10 \text{ g.m}^{-3} \text{ (no KOH or KCN added)}$$

$$pH = 6.5$$

t [h]	C_G [g/m ³]	$\frac{Q_{iG} - Q_G}{Q_{iG}}$
0.067	0.3	0.006
0.167	0.5	0.010
0.250	0.7	0.014
0.417	0.9	0.018
0.667	1.1	0.022
1.083	1.4	0.028
1.417	1.4	0.028
2.550	1.7	0.034
4.467	2.0	0.040
6.317	2.1	0.042
7.217	2.1	0.042
9.717	2.2	0.044
18.000	2.2	0.044
23.533	2.2	0.044
26.050	2.4	0.048
29.783	2.3	0.046

Experiment no. 84

Kinetics of desorption of aurocyanide from carbon BTX in batch.

Adsorption :

$$m_c = 1.8145 \text{ g}$$

$$v_i = 1000 \text{ ml}$$

$$v_e = 970 \text{ ml}$$

$$C_{ig}^e = 49.9 \text{ g.m}^{-3}$$

$$C_{ig}^{eff} = 0.1 \text{ g.m}^{-3}$$

$$pH_e^{eff} = 7.47$$

$$T_e = 20 \text{ }^\circ\text{C}$$

Adsorption period = 21 days, i.e. adsorption to equilibrium.

Elution :

The elution was conducted in a 2000 ml round-bottomed flask fitted with a total reflux condenser. The flask was submerged in a water bath and stirred magnetically at 1350 rpm,

$$v = 1000 \text{ ml}$$

$$T = 90 \text{ }^\circ\text{C}$$

$$Q_{ig} = 27.45 \text{ g.kg}^{-1}$$

$$C_K < 10 \text{ g.m}^{-3} \text{ (no KOH or KCN added)}$$

$$pH = 6.5$$

t [h]	C_G [g/m ³]	$\frac{Q_{ig} - Q_G}{Q_{ig}}$
0.067	1.2	0.024
0.167	2.0	0.040
0.250	2.8	0.056
0.417	3.4	0.068
0.667	4.2	0.084
1.083	5.4	0.108
1.417	5.7	0.114
2.550	7.1	0.143
4.467	8.6	0.173
6.317	9.4	0.189
7.217	10.0	0.201
9.717	10.4	0.209
18.000	10.8	0.217
23.533	11.3	0.227
26.050	11.6	0.233
29.783	11.8	0.237

Experiment no. 85

The elution of gold cyanide from carbon BTX with distilled water at 70 °C.

Adsorption :

$$m_c = 9.407 \text{ g}$$

$$v = 2000 \text{ ml}$$

$$C_{iG} = 95.0 \text{ g.m}^{-3}$$

$$\text{Time} = 23 \text{ h}$$

$$C_{fG} = 9.5 \text{ g.m}^{-3}$$

$$Q_{fG} = 18.18 \text{ g.kg}^{-1}$$

Pretreatment :

NONE

Elution :

In glass column, $h = 143 \text{ mm}$, $T = 70 \text{ °C}$, eluant = distilled water

t [h]	V [ml/h]	V _B	C _G [g/m ³]	pH
0.083	49.6	0.241	81.0	
0.217	41.0	0.559	55.8	
0.433	42.9	1.101	62.1	8.552
0.650	45.0	1.669	64.5	8.636
0.900	43.9	2.309	62.7	8.779
1.167	46.3	3.028	57.9	
1.517	46.6	3.979	53.1	8.828
1.900	45.0	4.984	44.4	
2.400	42.6	6.225	34.8	
3.083	40.3	7.830	25.3	8.434
3.650	44.7	9.306	21.1	
4.300	42.3	10.909	17.9	
4.967	42.4	12.556	16.0	7.917
5.617	44.9	14.257	15.4	
6.250	43.8	15.873	14.4	8.027
6.900	41.3	17.437	13.4	

$$V_{ave} = 1.205 \times 10^{-8} \text{ m}^3 \cdot \text{s}^{-1}$$

Experiment no. 86

The elution of gold cyanide from carbon BTX with a 12 g KCl/l solution.

Adsorption :

$$m_c = 9.4078 \text{ g}$$

$$v_c = 2000 \text{ ml}$$

$$C_{iG} = 22.8 \text{ g.m}^{-3}$$

$$\text{Time} = 23 \text{ h}$$

$$C_{fG} = 0.2 \text{ g.m}^{-3}$$

$$Q_{fG} = 4.805 \text{ g.kg}^{-1}$$

Cyanide pretreatment :

Soaked loaded carbon in 20 ml of a 20 g KCN/l solution at room temperature for 30 min. $C_{iN} = 7726 \text{ g.m}^{-3}$, $C_{iK} = 12450 \text{ g.m}^{-3}$, $C_{fN} = 4461 \text{ g.m}^{-3}$, $C_{fK} = 7154 \text{ g.m}^{-3}$.

Elution :

In glass column, $h = 143 \text{ mm}$, $T = 70 \text{ }^\circ\text{C}$, eluant = distilled water containing 12 g KCl/l ($C_K = 6300 \text{ g.m}^{-3}$)

t [h]	V [ml/h]	V_B	C_G [g/m ³]	pH	C_N [g/m ³]	C_K [g/m ³]
0.067		0.319	14.2			6750
0.100	81.8	0.477	15.7	10.50	1062	6540
0.183		0.810	13.0			6540
0.300	51.4	1.161	12.5	10.01	212	
0.350		1.307	11.2			6540
0.467	46.8	1.626	10.8		90	
0.600		1.988	10.6			6660
0.717	46.7	2.306		9.66	50	
0.850		2.669	9.6			6462
1.017	47.0	3.126			32	
1.150		3.481	8.8			6300
1.300	44.4	3.869		9.59		
1.517		4.426	7.9			6168
1.933	43.3	5.475	7.4	9.56	21	6198
2.600	45.6	7.248	6.6			6180
3.017	40.0	8.220	6.5	9.43		6132
3.850	52.0	10.744	5.8	9.41	8	6372
4.350		12.154	5.6			6300
4.850	44.8	13.460	5.4			

$$V_{ave} = 1.323 \times 10^{-8} \text{ m}^3 \cdot \text{s}^{-1}$$

Experiment no. 87

The elution of gold cyanide from carbon BTX with a 3.9 g KCl/l solution.

Adsorption :

$$m_c = 9.4061 \text{ g}$$

$$v_c = 2000 \text{ ml}$$

$$C_{iG} = 22.8 \text{ g.m}^{-3}$$

$$\text{Time} = 22 \text{ h}$$

$$C_{fG} = 0.0 \text{ g.m}^{-3}$$

$$Q_{fG} = 4.848 \text{ g.kg}^{-1}$$

Cyanide pretreatment :

Soaked loaded carbon in 20 ml of a 20 g KCN/l solution at room temperature for 30 min. $C_{iN} = 7726 \text{ g.m}^{-3}$, $C_{iK} = 12450 \text{ g.m}^{-3}$, $C_{fN} = 4461 \text{ g.m}^{-3}$, $C_{fK} = 7154 \text{ g.m}^{-3}$.

Elution :

In glass column, $h = 143 \text{ mm}$, $T = 70 \text{ }^\circ\text{C}$, eluant = distilled water containing 3.9 g KCl/l ($C_K = 2100 \text{ g.m}^{-3}$)

t [h]	V [ml/h]	V_B	C_G [g/m ³]	pH	C_N [g/m ³]	C_K [g/m ³]
0.067		0.221	17.4			4140
0.183	56.6	0.604	13.6	10.19	1088	
0.267		0.872	16.6			3210
0.567	48.9	1.727	18.3			2400
0.767		2.286	17.8			
1.017	46.8	2.967	17.5	9.90	80	
1.083		3.145	16.9			
1.350	44.4	3.836				
1.600		4.572	15.2			2180
1.767	54.5	5.102		10.06		
2.517		6.086	12.8			
2.767	50.5	6.821	12.4		11	
2.983		7.451	11.7	9.64		2130
3.350	50.0	8.520				
3.483		8.869	11.5			
4.267	40.6	10.724	11.0			
4.433	48.9	11.197		9.59		
4.767		12.112	10.8			
5.267	45.5	13.437	10.9			2124
5.767	52.0	14.953	10.6			

$$V_{ave} = 1.239 \times 10^{-8} \text{ m}^3 \cdot \text{s}^{-1}$$

Experiment no. 88

The elution of gold cyanide from carbon BTX loaded with gold over a short period of time.

Adsorption :

$$m_c = 9.4061 \text{ g}$$

$$v_c = 2000 \text{ ml}$$

$$C_{iG} = 22.8 \text{ g.m}^{-3}$$

$$\text{Time} = 7.25 \text{ h}$$

$$C_{fG} = 3.1 \text{ g.m}^{-3}$$

$$Q_{fG} = 4.189 \text{ g.kg}^{-1}$$

Cyanide pretreatment :

Soaked loaded carbon in 20 ml of a 20 g KCN/l solution at room temperature for 30 min. $C_{iN} = 7674 \text{ g.m}^{-3}$, $C_{iK} = 12450 \text{ g.m}^{-3}$, $C_{fN} = 4514 \text{ g.m}^{-3}$, $C_{fK} = 7154 \text{ g.m}^{-3}$.

Elution :

In glass column, $h = 143 \text{ mm}$, $T = 70 \text{ }^\circ\text{C}$, eluant = distilled water.

t [h]	V [ml/h]	V_B	C_G [g/m ³]	pH	C_N [g/m ³]	C_K [g/m ³]
0.067		0.234	26.2			3350
0.233	60.0	0.815			1328	
0.250		0.873	25.2			1940
0.400	50.0	1.310		10.528	478	
0.567	52.5	1.821	69.0			378
0.900	42.8	2.652				
0.983		2.860	78.6			230
1.567	44.4	4.371		11.060	40	
1.667		4.657	84.0			138
1.817	56.5	5.151				
2.233	50.4	6.373	78.0	11.081		110
2.483	44.4	7.020				
2.733		7.715	70.0			97
3.067	52.2	8.731		11.089		
3.317	47.0	9.416	62.0			86
3.900	45.9	10.975		10.966		
3.922		11.034	60.4			77
4.483	50.7	12.692		10.933		
4.733		13.424	51.2			
5.617	48.7	15.933	45.2			

$$V_{ave} = 1.352 \times 10^{-8} \text{ m}^3 \cdot \text{s}^{-1}$$

Experiment no. 89

The elution of gold cyanide from carbon BTX with a high initial gold loading.

Adsorption :

$$m_c = 9.4053 \text{ g}$$

$$v = 2000 \text{ ml}$$

$$C_{iG} = 57.3 \text{ g.m}^{-3}$$

$$\text{Time} = 48 \text{ h}$$

$$C_{fG} = 0.1 \text{ g.m}^{-3}$$

$$Q_{fG} = 12.16 \text{ g.kg}^{-1}$$

Cyanide pretreatment :

Soaked loaded carbon in 20 ml of a 20 g KCN/l solution at room temperature for 30 min. $C_{iN} = 7634 \text{ g.m}^{-3}$, $C_{iK} = 12450 \text{ g.m}^{-3}$, $C_{fN} = 4447 \text{ g.m}^{-3}$, $C_{fK} = 7154 \text{ g.m}^{-3}$.

Elution :

In glass column, $h = 143 \text{ mm}$, $T = 70 \text{ }^\circ\text{C}$, eluant = distilled water

t [h]	V [ml/h]	V_B	C_G [g/m ³]	pH	C_N [g/m ³]	C_K [g/m ³]
0.083		0.268	61.8			2925
0.217	55.5	0.702		10.266	1221	
0.250		0.807	103.0			1830
0.383	51.6	1.207		10.234	401	
0.467		1.455	207.0			620
0.633	49.1	1.930		10.259	133	
0.717		2.170	308.0			320
1.033		3.063	354.0			217
1.183	48.3	3.486	355.5			190
1.467	49.0	4.297		10.444	20	
1.550		4.532	331.5			181
1.717	47.8	4.998				
2.050	50.9	5.985		10.619		
2.167		6.333	290.0			127
2.650	51.4	7.780	245.0			
3.350	49.5	9.799	190.0	10.696		94
3.983	45.6	11.481	160.0			
4.683	47.1	13.402	135.0			78
5.600	43.6	15.722	107.2			
6.050		16.860	93.6			65

$$V_{ave} = 1.328 \times 10^{-8} \text{ m}^3 \cdot \text{s}^{-1}$$

Experiment no. 90

The elution of gold cyanide from carbon BTX after a pretreatment with a 4 g KCN/l solution.

Adsorption :

$$m_c = 9.4050 \text{ g}$$

$$v_c = 2000 \text{ ml}$$

$$C_{iG} = 24 \text{ g.m}^{-3}$$

$$\text{Time} = 24 \text{ h}$$

$$C_{fG} = 0.2 \text{ g.m}^{-3}$$

$$Q_{fG} = 5.061 \text{ g.kg}^{-1}$$

Cyanide pretreatment :

Soaked loaded carbon in 25 ml of a 4 g KCN/l solution at room temperature for 65 h. $C_{iN} = 1593 \text{ g.m}^{-3}$, $C_{iK} = 2420 \text{ g.m}^{-3}$, $C_{fN} < 50 \text{ g.m}^{-3}$, $C_{fK} = 1500 \text{ g.m}^{-3}$.

Elution :

In glass column, $h = 143 \text{ mm}$, $T = 70 \text{ }^\circ\text{C}$, eluant = distilled water

t [h]	V [ml/h]	V_B	C_G [g/m ³]	pH	C_K [g/m ³]
0.050		0.158	11.2		522
0.133	54.2	0.421			
0.217		0.674	12.1		471
0.367	48.3	1.096		9.920	
0.417		1.243	18.2		275
0.533	54.7	1.614			
0.650		1.966	29.0		152
0.750	49.1	2.252		10.190	
0.933		2.750	30.3		109
1.117	44.1	3.221		10.263	
1.250		3.582	31.2		93
1.583	52.4	4.600			
1.767	49.3	5.127	34.8	10.426	69
2.617	44.3	7.321	36.9	10.387	59
3.417		9.725	34.7		
4.083	57.6	11.962	33.9		40
4.350	58.4	12.870	32.4		37
5.217	54.1	15.602	29.4		
5.417	51.5	16.202			
5.583		16.694	27.1		30
6.083	47.8	18.086			
6.583		19.479	27.1	10.130	

$$V_{ave} = 1.41 \times 10^{-8} \text{ m}^3 \cdot \text{s}^{-1}$$

Experiment no. 91

The elution of gold cyanide from carbon BTX at 50 °C.

Adsorption :

$$m_c = 9.4053 \text{ g}$$

$$v = 2000 \text{ ml}$$

$$C_{iG} = 21.6 \text{ g.m}^{-3}$$

$$\text{Time} = 22 \text{ h}$$

$$C_{fG} = 0.0 \text{ g.m}^{-3}$$

$$Q_{fG} = 4.593 \text{ g.kg}^{-1}$$

Cyanide pretreatment :

Soaked loaded carbon in 20 ml of a 20 g KCN/l solution at room temperature for 30 min. $C_{iN} = 7726 \text{ g.m}^{-3}$, $C_{iK} = 12450 \text{ g.m}^{-3}$, $C_{fN} = 4461 \text{ g.m}^{-3}$, $C_{fK} = 7119 \text{ g.m}^{-3}$.

Elution :

In glass column, $h = 143 \text{ mm}$, $T = 50 \text{ °C}$, eluant = distilled water

t [h]	V [ml/h]	V_B	C_G [g/m ³]	pH	C_N [g/m ³]	C_K [g/m ³]
0.050		0.157	10.1			2360
0.233	54.0	0.734	8.9		1328	1535
0.433	50.1	1.318	17.9		425	570
0.783	51.8	2.375	47.8	10.821	132	239
1.300	47.4	3.802	59.0		30	159
1.567	50.0	4.579	62.0			137
1.950	45.6	5.598	58.0			123
2.350	50.9	6.784	57.0	11.014		101
2.733	49.8	7.895	54.4			
3.450	47.6	9.884	50.0			82
4.000	45.0	11.327	42.3	11.024		
4.583	51.0	13.060	40.8			63
5.167	49.8	14.753	30.5			
5.867	47.9	16.707	29.3	10.846		53

$$V_{ave} = 1.357 \times 10^{-8} \text{ m}^3 \cdot \text{s}^{-1}$$

Experiment no. 92

The elution of gold cyanide from carbon BTX at 80 °C.

Adsorption :

$$m_c = 9.4051 \text{ g}$$

$$v = 2000 \text{ ml}$$

$$C_{iG} = 23.4 \text{ g.m}^{-3}$$

$$\text{Time} = 22 \text{ h}$$

$$C_{fG} = 0.0 \text{ g.m}^{-3}$$

$$Q_{fG} = 4.976 \text{ g.kg}^{-1}$$

Cyanide pretreatment :

Soaked loaded carbon in 20 ml of a 20 g KCN/l solution at room temperature for 30 min. $C_{iN} = 7501 \text{ g.m}^{-3}$, $C_{iK} = 12450 \text{ g.m}^{-3}$, $C_{fN} = 4315 \text{ g.m}^{-3}$, $C_{fK} = 6916 \text{ g.m}^{-3}$.

Elution :

In glass column, $h = 143 \text{ mm}$, $T = 80 \text{ °C}$, eluant = distilled water

t [h]	V [ml/h]	V_B	C_G [g/m ³]	pH	C_N [g/m ³]	C_K [g/m ³]
0.050		0.142	29.8			2960
0.233	48.7	0.662	33.6		1195	1908
0.433	57.4	1.331	132.0	10.291	266	466
0.700	48.0	2.077	182.4	10.415	106	268
1.150	44.3	3.239	196.8		80	172
1.833	46.2	5.078	153.3	10.756	26	130
2.217	46.3	6.113	133.8			112
3.067	45.5	8.367	103.0	10.814		94
4.217	42.1	11.188	80.0			80
4.933	55.1	13.489	60.3	10.740		62
5.767	41.7	15.514	50.4			57
6.683	37.3	17.507	43.8	10.557		50

$$V_{ave} = 1.249 \times 10^{-8} \text{ m}^3 \cdot \text{s}^{-1}$$

Experiment no. 93

The elution of gold cyanide from carbon BTX at 130 °C.

Adsorption :

$$m_c = 3.626 \text{ kg}$$

$$v = 50 \text{ l}$$

$$C_{iG} = 178.5 \text{ g/m}^3$$

$$\text{Time} = 37 \text{ h}$$

$$C_{fG} = 0.1 \text{ g/m}^3$$

$$Q_{fG} = 2.46 \text{ g/kg}$$

Cyanide pretreatment :

Loaded the above carbon into distilled water in the stainless steel column. Replaced distilled water with pretreatment solution by pumping 4000 ml of a 20 g KCN/l solution through the column. Switched on oil heaters and heated up bed to 125 °C over a period of 1.5 h.

Elution :

In stainless steel column, $h = 749 \text{ mm}$, $T = 130 \text{ °C}$, $P = 280 \text{ kPa(g)}$, eluant = distilled water. Started flow of distilled water directly after temperature of bed reached 130 °C. (The pretreatment solution was not drained from the bed.)

t [h]	V [ml/ min]	V _B	C _G [g/m ³]	pH	C _N [g/m ³]	C _K [g/m ³]
0.133	226	0.307	81.5	9.529	531	4285
0.200	163	0.418	163.1			1922
0.417	216	0.896	639.6	9.945	199	719
0.667	222	1.462	630.0			402
0.917	228	2.043	409.5	9.883	40	313
1.167	206	2.568	273.0			
1.417	239	3.178	152.0	10.014		194
1.917	258	4.493	69.9			
2.417	266	5.850	27.4	10.424		121
2.917	274	7.247	16.2			
3.417	245	8.496	9.8	10.629		103
4.167	239	10.324	5.7			
4.917	236	12.130	4.1	10.796		88
6.083	233	14.902	2.6			
6.917	223	16.797	1.7	10.219		67

Temperature profile through column during run :

t [h]	TI ₀	TI ₁	TI ₂	TI ₃	TI ₄	TI ₅
0.001	117	126	125	121	125	123
0.093	121	125	121	117	116	131
0.252	120	121	124	127	123	135
0.447	129	129	130	128	127	135
0.758	129	130	130	129	128	134
0.947	130	130	131	129	128	134
1.218	130	130	131	129	128	134
1.707	129	130	130	129	128	133
2.046	130	130	132	131	129	135
2.356	132	132	133	132	130	136
2.903	131	132	132	131	130	134
3.228	130	131	131	129	129	134
3.819	129	130	130	130	128	134
4.157	129	130	131	130	128	134
4.922	130	131	131	130	129	135
6.051	130	131	132	131	129	135
6.895	130	131	132	131	129	135

See definition of TI₀ - TI₅ in Figure 3.2.

$$V_{\text{ave}} = 3.966 \times 10^{-6} \text{ m}^3 \cdot \text{s}^{-1}$$

Experiment no. 94

The elution of gold cyanide from carbon BTX at 20 °C.

Adsorption :

$$m_c = 9.4053 \text{ g}$$

$$v = 2000 \text{ ml}$$

$$C_{iG} = 119 \text{ g.m}^{-3}$$

$$\text{Time} = 21 \text{ h}$$

$$C_{fG} = 10.3 \text{ g.m}^{-3}$$

$$Q_{fG} = 23.11 \text{ g.kg}^{-1}$$

Cyanide pretreatment :

Soaked loaded carbon in 20 ml of a 20 g KCN/l solution at room temperature for 30 min. $C_{iN} = 7766 \text{ g.m}^{-3}$, $C_{iK} = 12450 \text{ g.m}^{-3}$, $C_{fN} = 4713 \text{ g.m}^{-3}$, $C_{fK} = 7154 \text{ g.m}^{-3}$.

Elution :

In glass column, $h = 143 \text{ mm}$, $T = 20 \text{ °C}$, eluant = distilled water

t [h]	V [ml/h]	V_B	C_G [g/m ³]	pH	C_N [g/m ³]	C_K [g/m ³]
0.050	133.3	0.388	12.7	11.112	1261	2646
0.117	123.7	0.869	30.0		929	797
0.200	118.5	1.444	68.0	11.009	318	452
0.283	119.2	2.023	89.2		159	265
0.400	117.3	2.821	105.2		106	190
0.550	123.5	3.900	118.8	11.203	79	143
0.683	117.1	4.810	116.4		50	
0.950	114.3	6.586	111.2	11.278		98
1.217	111.3	8.316	105.6			84
1.467	133.4	10.260	95.2			
1.767	117.9	12.321	90.4			66
2.067	108.3	14.214	80.0	11.321		
2.367	123.5	16.373	70.8			57
2.683	125.8	18.694	68.8			
3.017	115.2	20.933	65.6	11.201		
3.800		23.671	57.2			
4.217	121.3	26.617	41.6			41
4.633	121.6	29.569	40.0	11.202		
5.050	111.7	32.282	38.4			37

$$V_{ave} = 3.047 \times 10^{-8} \text{ m}^3 \cdot \text{s}^{-1}$$

APPENDIX L

PUBLICATION OF RESULTS FROM OXYGEN RELATED WORK

Published in Chem. Eng. Comm., 65, pp. 121-138, 1988.

THE INFLUENCE OF OXYGEN ON THE ADSORPTION OF METAL CYANIDES ON ACTIVATED CARBON

P. F. VAN DER MERWE and J. S. J. VAN DEVENTER†

Department of Metallurgical Engineering
University of Stellenbosch
Stellenbosch 7600
South Africa

(Received August 13, 1987; in final form September 9, 1987)

Activated carbon adsorbs insignificant quantities of oxygen from aerated water. This consumption is increased drastically during the adsorption of anionic metal cyanides. The equilibrium loadings of gold and silver cyanides increased with an increase in the level of dissolved oxygen. However, for both gold and silver cyanides an oxygen concentration occurred above which the metal loading showed no further increase. FTIR scans were used to confirm the presence of AuCN and Au(CN)₂⁻ on the loaded carbons. It was suggested that gold and silver cyanides adsorb in two ways: (1) where oxygen is consumed for the oxidation of the active sites, and (2) where adsorption takes place without the use of oxygen. A multicomponent Freundlich-type isotherm proved to be adequate in predicting the equilibrium metal loadings for the competitive adsorption of gold and silver cyanides on activated carbon. The level of dissolved oxygen did not affect the competition between these two solutes significantly.

KEYWORDS Activated carbon Adsorption Oxygen Metal cyanides

INTRODUCTION

Activated carbon is being used worldwide as the main adsorbent for gold and silver from cyanided pulps. In most plants the activated carbon is contacted with the pulp in counter-current cascades of open stirred reactors. Factors such as pH, temperature, free cyanide concentration and ionic strength influencing this process have been investigated thoroughly (Fleming *et al.*, 1984; Tsuchida *et al.*, 1984; Davidson, 1986). Although it is known that oxygen also plays a role in the adsorption of metal cyanides onto activated carbon, it has received less attention.

Dixon *et al.* (1978) observed that less gold was adsorbed in the presence of nitrogen instead of air. They concluded that the exclusion of oxygen reduces the number of available adsorption sites on the carbon. From the changes in redox potential observed for charcoal in different solutions, Hughes *et al.* (1984) proposed an oxidation-reduction mechanism for the loading of various anions. They stated that the loading of complexes, such as Au(CN)₂⁻, is controlled by the supply of an oxidant such as oxygen or quinone groups.

† Author to whom correspondence should be addressed.

In a detailed study of the mechanism of gold adsorption on activated carbon, Tsuchida and co-workers (1984) suggested that up to half of the adsorbed gold was oxidized to neutral AuCN by oxygen and/or quinone groups and that the released CN^- was oxidized via CNO^- to CO_3^{2-} and NH_3 . Consequently, the effect of oxygen cannot be investigated without due consideration of the nature of the adsorbed species.

Dixon *et al.* (1978) found that the zeta potential of the carbon became more negative as more silver cyanide was absorbed. This agrees with a mechanism in which the adsorbate is an anion such as $\text{Ag}(\text{CN})_2^-$. McDougall *et al.* (1980) measured the molar ratios of nitrogen to gold to be lower than 2:1 for all their loaded carbons. This suggested that not all of the adsorbed gold was in the $\text{Au}(\text{CN})_2^-$ form. A mechanism was proposed in which the gold is adsorbed as the $\text{M}^{n+}[\text{Au}(\text{CN})_2]_n$ ion pair ($\text{M}^{n+} = \text{Na}^+, \text{K}^+, \text{Ca}^{2+}, \text{H}^+$), followed by reduction to a sub-stoichiometric $\text{Au}(\text{CN})_x$ surface species or a cluster-type compound of gold.

As summarized by Tsuchida *et al.* (1984), it is widely assumed that the gold is adsorbed in mainly two forms, i.e. (a) AuCN, or (b) $\text{Au}(\text{CN})_2^-$, where the latter can be part of an ion pair, a cluster-type species or adsorbed in a double layer.

Although the importance of oxygen is recognized, there is still disagreement on its function and its influence on the nature and distribution of the adsorbed species. Up to now, no quantitative studies have been published on the uptake of oxygen during the adsorption of metal cyanides onto activated carbon. These aspects, as well as the effect of oxygen on the competitive adsorption of gold and silver cyanides, will be discussed here. An understanding of the role of oxygen is important in the modelling of the adsorption of metal cyanides in columns of carbons, while knowledge of the form of the adsorbed species is essential in studying the desorption process.

EXPERIMENTAL PROCEDURE

Materials

Two types of experimental coconut shell carbon, designated A and B, were used. Figure 1 shows their zeta potential versus pH curves determined at 25°C with a Rank Brothers Mark II instrument. In order to measure the zeta potential, 50 mg of carbon was mixed with 1 litre of distilled water and conditioned for 20 min. Both carbons revealed a point of zero charge at a pH of 1.8, and a natural pH in distilled water of 5.5. Carbons A and B had apparent densities of 1080 and 1004 kg/m³ respectively. The iodine test described by Hassler (1974) was performed on both carbons. Carbon A adsorbed 48% of the available iodine and carbon B 53%. For all experiments the carbon was dried at 120°C for 3 days before being weighed. Only the 1.7 to 2 mm sieve size fraction was used.

The gold and silver were obtained as $\text{KAu}(\text{CN})_2$ and AgCN from Barry Colne & Co. The silver was dissolved in a 10% more than stoichiometric KCN solution at a pH of 10 and a temperature of 95°C. Mercury in the form of $\text{Hg}(\text{CN})_2$ was used in comparative experiments. The concentrations of metals in solution were

determined with a Varian AA-1275 atomic absorption spectrophotometer, and the loadings on the carbon calculated by mass balance. Distilled water was used in all experiments. HCl and KOH were used to adjust the pH.

Adsorption

All the adsorption experiments were carried out at a pH of 8.5 and a room temperature of 17 to 22°C. Although most gold extraction plants still use pH values higher than 10, there is a tendency towards lower pH's with the improvement in control systems. Equilibrium conditions were assumed after 3 weeks. Constant oxygen concentrations were maintained by a continuous supply of air-nitrogen or air-oxygen mixtures to the solution. The level of dissolved oxygen was monitored with a Schott Geräte model CG867 oxygen meter.

Elution

In order to determine the molar ratio of MCN to $\text{M}(\text{CN})_2^-$ ($\text{M} = \text{Au}$ or Ag) on the loaded carbon, the $\text{M}(\text{CN})_2^-$ was eluted at room temperature in the absence of free cyanide and at a pH of 11. The eluant was replaced repeatedly until less than 1% of the initial loading of the adsorbent could be recovered over an elution period of 96 hours.

Infrared measurements

Fourier Transform Infrared (FTIR) scans of the carbons were obtained with a Perkin-Elmer model 1710 infrared spectrophotometer. Owing to the intense background caused by organic groups on the carbon, sufficiently high loadings of gold were required in order to observe the $\nu(\text{CN})$ vibrations of the AuCN and the $\text{Au}(\text{CN})_2^-$. For this purpose 0.5 g of powdered carbon was contacted for 5 days with 0.8 litre of solution containing 200 mg Au/l at a pH of 8.5. The carbon was then filtered, washed with distilled water and analysed immediately.

RESULTS AND DISCUSSION

Adsorbed species

In the absence of free cyanide AuCN is practically insoluble (Weast, 1985). The $\text{Au}(\text{CN})_2^-$ could therefore be eluted with distilled water, and the difference between the loaded and eluted gold accounted for as AuCN. Proper mass balances could not be obtained using conventional desorption conditions (i.e. temperatures >70°C and pH > 12) without the addition of free cyanide. A yellow precipitate was observed in such solutions and identified as AuCN by FTIR spectrophotometry. This means that the $\text{Au}(\text{CN})_2^-$ is reduced to AuCN at high temperatures in the absence of free cyanide. Thus cold water had to be used in further elution tests.

TABLE I

Determination of the $\text{MCN}/\text{M}(\text{CN})_2^-$ ratio ($\text{M} = \text{Au}$ or Ag)

Carbon	A	A	A	A	B
M	Au	Au	Au	Ag	Au
$[\text{O}_2]$ during adsorption	9.0	9.0	14.5	9.0	9.0
pH during adsorption	8.5	3.5	3.5	8.5	8.5
Time of adsorption (days)	21	2	2	21	1
Loading (mg M/g carbon)	36.6	22.6	22.6	33.6	28.4
Recovery by elution (%)	100	85	85	38	80
$\text{MCN}/\text{M}(\text{CN})_2^-$	0.0	0.18	0.18	1.63	0.33

The results of the tests conducted at room temperature are summarized in Table I. All the gold loaded onto carbon A under alkaline conditions and an oxygen concentration of 9 mg/l could be recovered without the addition of cyanide. This means that even after a loading period of 3 weeks no $\text{Au}(\text{CN})_2^-$ changed to AuCN . Under the same adsorption conditions 62% of the adsorbed silver was reduced to AgCN . The silver cyanide complex, $\text{Ag}(\text{CN})_2^-$, is therefore less stable than the corresponding gold complex. When the initial pH during adsorption was dropped to 3.5, it was impossible to recover more than 85% of the gold adsorbed over a much shorter period of time. An increase in the level of dissolved oxygen at the lower pH did not result in a higher ratio of AuCN to $\text{Au}(\text{CN})_2^-$. For carbon B however, a maximum of only 80% of the gold adsorbed under alkaline conditions and an oxygen concentration of 9 mg/l could be eluted in this way.

To confirm the above results, FTIR scans of the gold loaded carbons were obtained. The $\nu(\text{CN})$ vibrations of the two gold cyanide species have been published (Adams, 1967) as follows:

$\text{Au}(\text{CN})_2^-$ in aqueous solution: 2147 cm^{-1} , and
 AuCN in the solid state: 2239 cm^{-1} .

The peaks within 2 cm^{-1} from these values are marked in Figures 2 and 3 for gold loaded carbons A and B respectively. Only the $\text{Au}(\text{CN})_2^-$ peak is observed for carbon A, while both the $\text{Au}(\text{CN})_2^-$ and AuCN peaks appeared in the case of carbon B.

The methods used to characterize the carbons proved to be of little value. Whereas carbons A and B have nearly identical zetapotential versus pH curves (Figure 1) they differ significantly in the adsorption of metal cyanides. The iodine test suggested a difference of 10% in the adsorption behaviour of the two carbons, while their equilibrium metal cyanide loadings differed by approximately 30% and 12% for gold and silver respectively.

The influence of oxygen

When the adsorption of gold or silver cyanide onto activated carbon occurs in a closed vessel, a decrease in the oxygen concentration can be monitored, as shown in Figure 4. In the absence of gold or silver cyanide, it was found that only

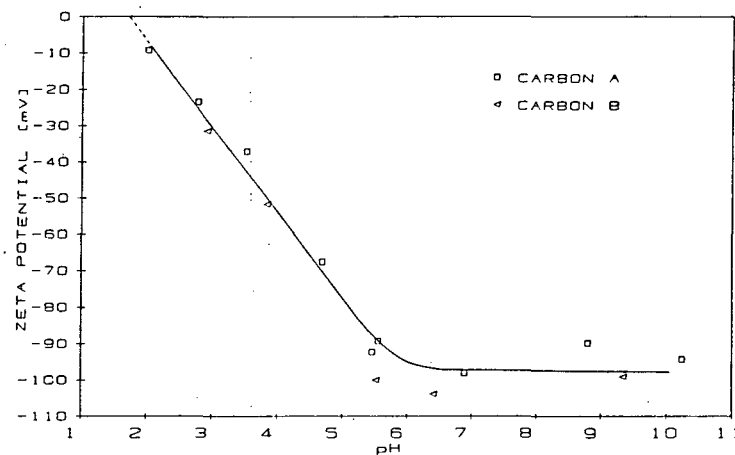


FIGURE 1 Zeta potential of carbon as a function of solution pH.

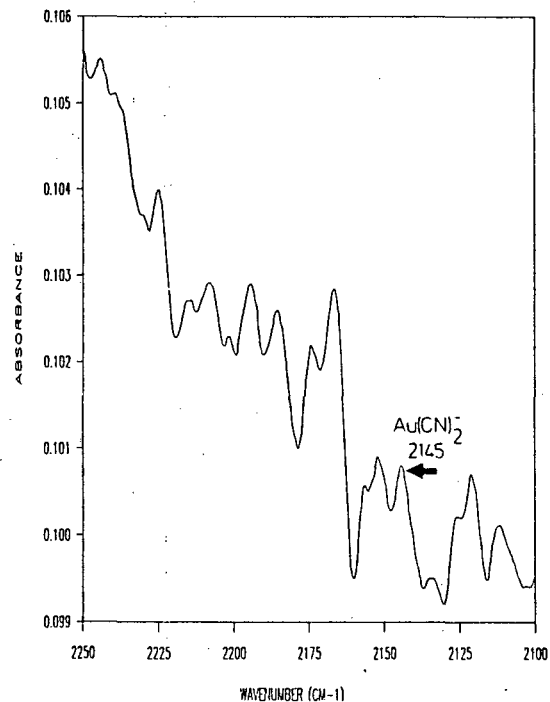


FIGURE 2 FTIR spectrograph of carbon A loaded with gold cyanide.

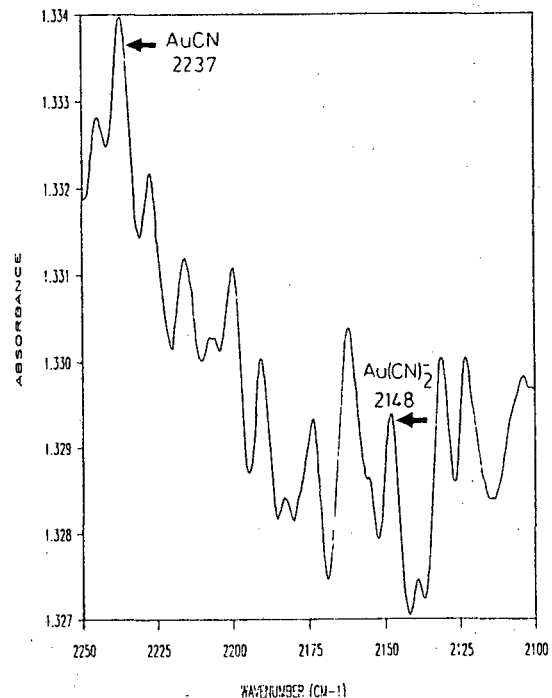


FIGURE 3 FTIR spectrograph of carbon B loaded with gold cyanide.

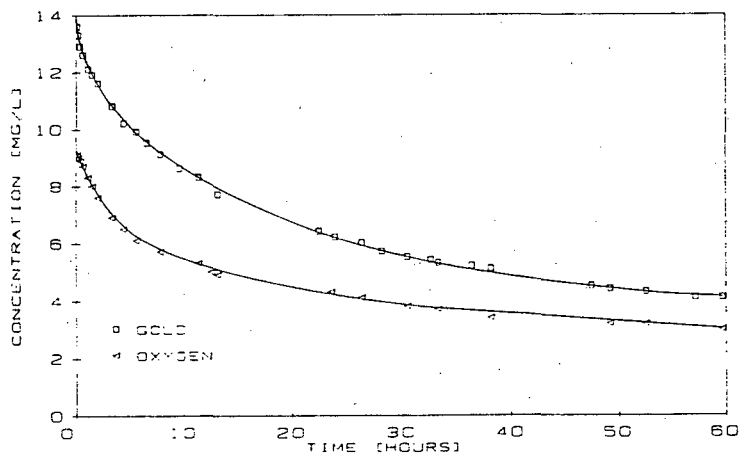


FIGURE 4 Concentration decay curves for the simultaneous uptake of gold and oxygen by carbon A in a closed system. $C_0(\text{Au}) = 13.8 \text{ mg/l}$, $C_0(\text{O}_2) = 9.2 \text{ mg/l}$. Dosage of carbon = 2 g/l.

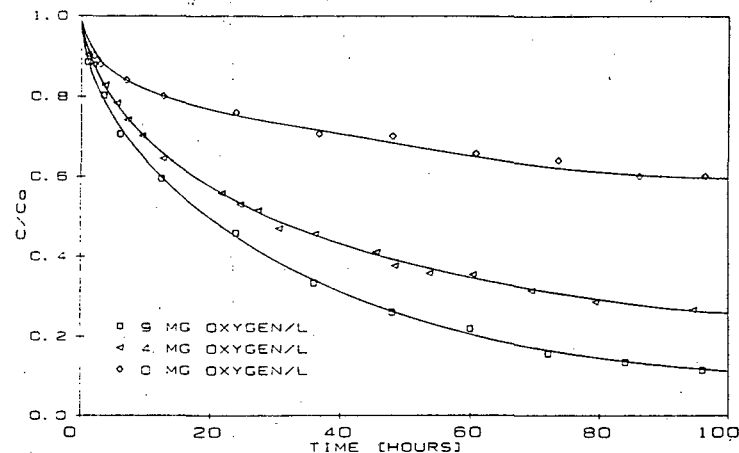


FIGURE 5 Rate curves for the adsorption of silver cyanide on carbon A at different constant levels of dissolved oxygen. $C_0(\text{Ag}) = 40 \text{ mg/l}$. Dosage of carbon = 3 g/l.

0.45 mg O_2/g carbon was adsorbed over a period of 2 weeks. For the experiment illustrated in Figure 4 nine times more oxygen was consumed in 60 hours. The finding that the oxygen is consumed during the adsorption process was further emphasized by an experiment where one sample of carbon was pretreated in water saturated with oxygen and the other in water saturated with nitrogen. Both of these carbons exhibited identical behaviour during the adsorption of gold or silver cyanide in the absence of oxygen.

Figure 5 shows that dissolved oxygen levels lower than that in equilibrium with air (i.e. $[\text{O}_2] < 9 \text{ mg/l}$) caused decreased adsorption of silver cyanide. In further work it was found that the adsorption of the neutral $\text{Hg}(\text{CN})_2$ was, however, unaffected by the presence or absence of oxygen. Consequently, it was observed that the oxygen concentration in a closed system remained constant during the adsorption of $\text{Hg}(\text{CN})_2$. As no AuCN was formed on carbon A under alkaline conditions, the oxygen taken up during the adsorption of anionic complexes could not have been used to change $\text{Au}(\text{CN})_2^-$ to AuCN , as suggested by Tsuchida *et al.* (1984). The neutral mercuric species seems to be adsorbed in a way which differs from that of the negative silver and gold complexes.

The influence of oxygen on the equilibrium loading of gold and silver is demonstrated in Figures 6, 7 and 8 for carbon A, and Figures 9 and 10 for carbon B. Tables II and III show the equilibrium constants for the Freundlich equation (Eq. 1) fitted to the experimental data.

$$Q_e = KC_e^n \quad (1)$$

Characteristic equilibrium gold and silver isotherms could be obtained at each dissolved oxygen level. Therefore, it is not only the presence of oxygen that is

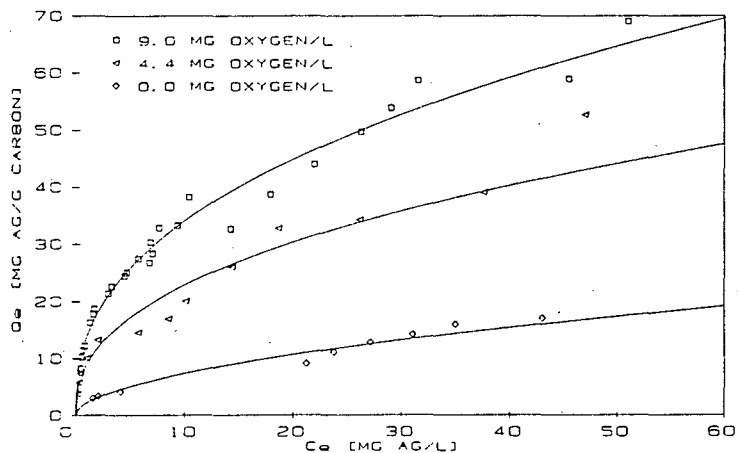


FIGURE 6 Equilibrium adsorption of silver cyanide on carbon A at different constant levels of dissolved oxygen.

important, but also its concentration. For both carbons there exist oxygen levels above which the equilibrium loadings of gold and silver show no further increase. For carbon A this point for both gold and silver is approximately 9 mg O₂/l. Figure 7 shows that oxygen levels higher than 9 mg/l cause a decreased silver loading on carbon A. The maximum loading of gold on carbon B has already

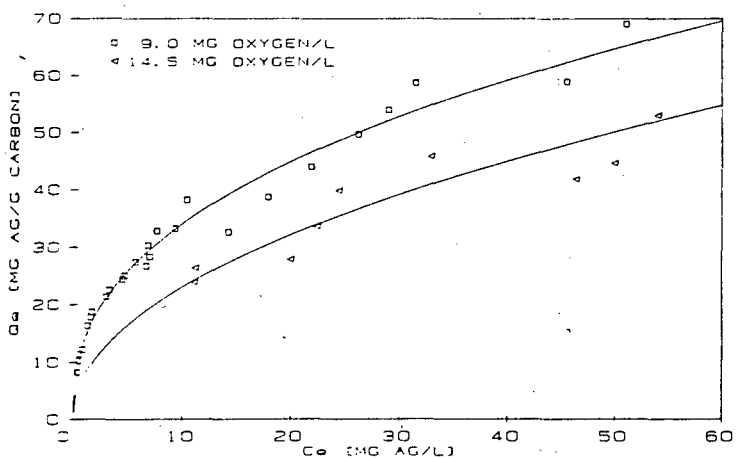


FIGURE 7 The effect of oxygen-enriched air on the equilibrium adsorption of silver on carbon A.

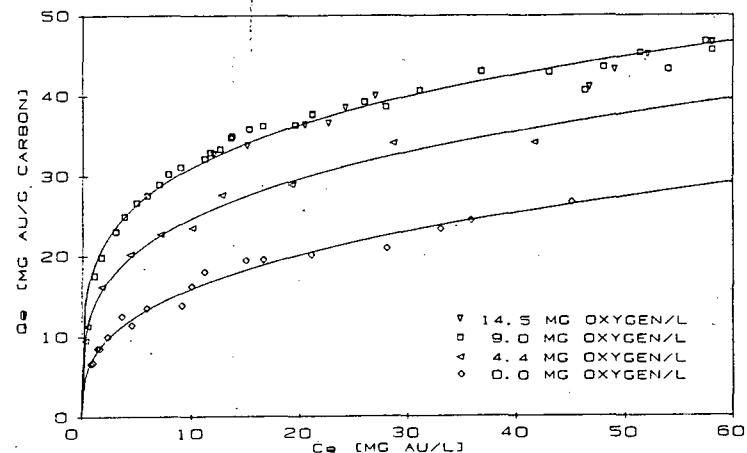


FIGURE 8 Equilibrium adsorption of gold cyanide on carbon A at different constant levels of dissolved oxygen.

been reached at an oxygen concentration of 4.2 mg/l, while this point appears to be slightly higher for silver. Furthermore, significant loadings of gold and silver were obtained even in the absence of oxygen. This implies that these metals are adsorbed in two ways: 1) where oxygen is consumed during the adsorption, and 2) where adsorption takes place without the use of oxygen.

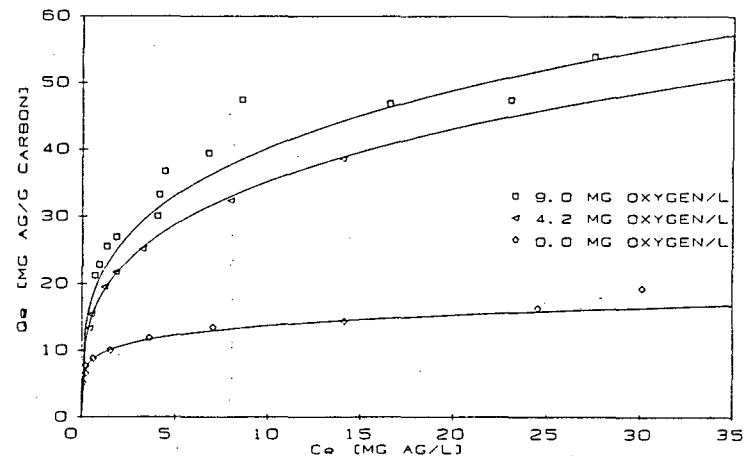


FIGURE 9 Equilibrium adsorption of silver cyanide on carbon B at different constant levels of dissolved oxygen.

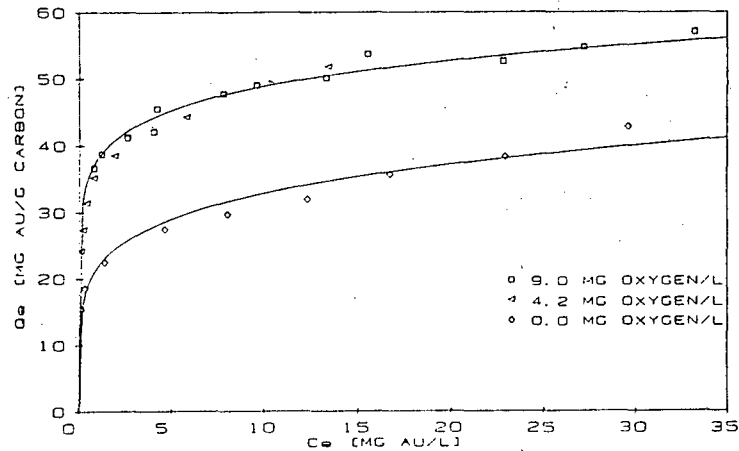


FIGURE 10 Equilibrium adsorption of gold cyanide on carbon B at different constant levels of dissolved oxygen.

It is possible to increase the equilibrium loading of gold and silver at 0 mg O₂/l by increasing the level of dissolved oxygen. However, the adsorption process cannot be reversed only by lowering the oxygen concentration. The step-wise decrease in the oxygen concentration in Figure 11 retarded the adsorption, but did not cause the loaded gold to desorb. This indicates that the oxygen is not

TABLE II

Values of *K* and *n* in Eq. (1) for adsorption on carbon A

[O ₂]	Gold		Silver	
	<i>K</i>	<i>n</i>	<i>K</i>	<i>n</i>
0.0	7.306	0.338	2.190	0.530
4.4	13.438	0.264	8.947	0.480
9.0(atm.)	18.315	0.229	13.637	0.398
14.5	18.315	0.229	7.578	0.483

TABLE III

Values of *K* and *n* in Eq. (1) for adsorption on carbon B

[O ₂]	Gold		Silver	
	<i>K</i>	<i>n</i>	<i>K</i>	<i>n</i>
0.0	21.706	0.180	9.464	0.160
4.2	37.963	0.110	18.083	0.290
9.0(atm.)	37.963	0.110	21.132	0.280

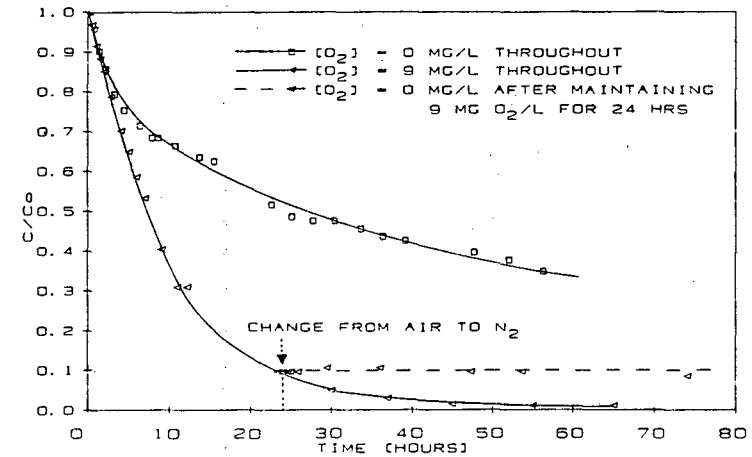


FIGURE 11 The effect of lowering the oxygen concentration from 9 to 0 mg/l during the adsorption of gold cyanide onto carbon A. C₀(Au) = 9.5 mg/l. Dosage of carbon A = 2 g/l.

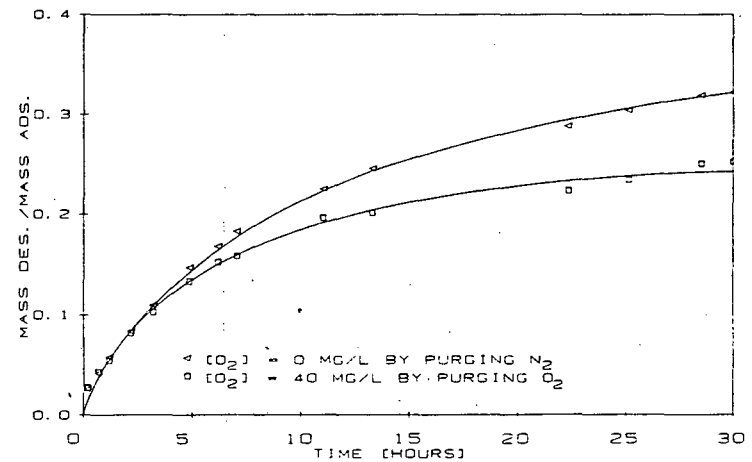
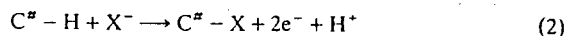


FIGURE 12 The effect of oxygen on the desorption of gold loaded onto carbon A in the absence of oxygen. Desorption conditions: Q₀ = 9.6 mg Au/g carbon, dosage of carbon = 1.33 g/l, pH = 12, 20°C.

physically adsorbed, but consumed in the adsorption reaction. Similar behaviour is observed in the elution process. When carbon was loaded in open containers, it was observed that the oxygen level had no effect on the elution of the gold. In Figure 12 however, the presence of oxygen had a small negative effect on desorption from carbon loaded in the absence of oxygen.

No stoichiometric relationship could be found between the amount of gold adsorbed and the oxygen consumed in a closed vessel. Figure 13 shows the molar ratios of oxygen to gold adsorbed in closed containers with different initial oxygen concentrations. All the curves have the same shape, but the higher the initial oxygen level, the more oxygen is consumed for each mole of gold adsorbed. This is in agreement with the suggestion that the gold is adsorbed in two separate ways. The driving-force for adsorption associated with the consumption of oxygen is increased with an increase in the initial oxygen concentration. This leads to a larger fraction of the gold being adsorbed via the use of oxygen, and therefore a higher molar ratio of oxygen consumed to the total amount of gold adsorbed (Figure 13).

The adsorption reaction during which oxygen is consumed, may involve the oxidation of the surface functional groups where the adsorption takes place. Hughes *et al.* (1984) illustrated this by the reaction of an anion (X^-) at the chromene sites (designated C^H):



The transformation of oxygen to OH^- in the accompanying reduction reaction agrees with the finding that the adsorption process cannot be reversed by only lowering the oxygen concentration. During the second type of adsorption (i.e.

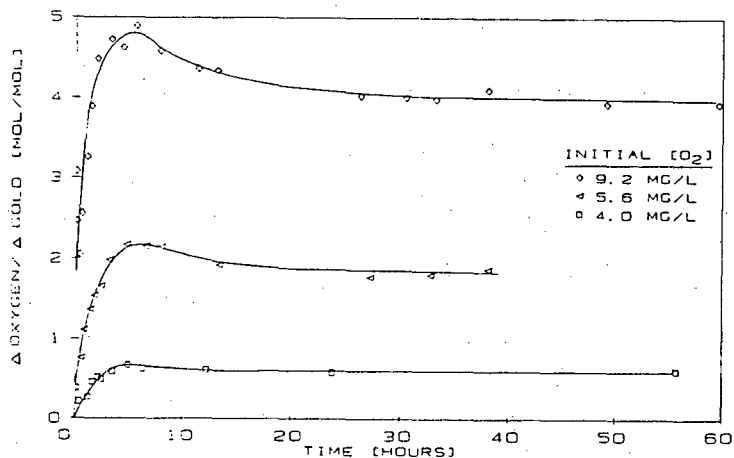


FIGURE 13 Molar ratios of O_2 consumed to Au adsorbed in closed vessels with different initial oxygen concentrations. $C_0(Au) = 20$ mg/l. Dosage of carbon = 1.33 g/l.

where no oxygen is required) the metal cyanide may also be adsorbed as in Eq. (2), but with surface functional groups such as quinone groups acting as the oxidant.

Effect of oxygen on competitive adsorption

In most studies on the simultaneous adsorption of organics onto activated carbon the Ideal Adsorbed Solution (IAS) theory was used to correlate results. As stated by Fritz *et al.* (1981), the IAS theory does not hold for partially dissociated solutes. Therefore, the IAS theory cannot be applied to the adsorption of metal cyanide complexes. Consequently, the more empirical Freundlich multicomponent isotherm derived by Sheindorf *et al.* (1981) was used here.

With this isotherm applied to the simultaneous adsorption of gold and silver cyanides the equilibrium adsorption of each component is given by:

$$Q_{eR} = K_R C_{eR} (C_{eR} + a_{RS} C_{eS})^{nR-1}; \quad (3)$$

$$Q_{eS} = K_S C_{eS} (C_{eS} + a_{SR} C_{eR})^{nS-1}; \quad (4)$$

where K and n are the constants in the single solute Freundlich isotherm (Eq. 1). Equations 3 and 4 can be written in the form:

$$f(C_{eR}) = (K_R C_{eR} / Q_{eR})^{1/(1-nR)} - C_{eR} = a_{RS} C_{eS}; \quad (5)$$

$$f(C_{eS}) = (K_S C_{eS} / Q_{eS})^{1/(1-nS)} - C_{eS} = a_{SR} C_{eR}. \quad (6)$$

With $f(C_{eR})$ and $f(C_{eS})$ plotted against C_{eS} and C_{eR} respectively, the competition coefficients a_{RS} and a_{SR} can be obtained from the slopes of the curves. From the derivation of the above isotherm it follows that $a_{RS} = 1/a_{SR}$. Sheindorf *et al.* (1981) used this criterion in the testing of their isotherm.

The values of K and n in Tables II and III have been used together with the C_e

TABLE IV

Competitive adsorption of gold and silver on carbon A

Experimental data				Predictions			
C_{eS}	C_{eR}	Q_{eS}	Q_{eR}	\hat{Q}_{eS}	r_S	\hat{Q}_{eR}	r_R
0.8	1.0	9.5	16.2	16.8	1.038	7.3	0.773
2.7	1.3	16.2	15.5	15.8	1.022	15.6	0.962
1.8	1.9	12.4	19.7	19.2	0.974	10.7	0.866
1.6	1.2	12.9	16.1	16.6	1.033	11.4	0.881
3.6	2.1	16.0	19.0	18.3	0.961	16.7	1.046
4.0	3.6	15.4	22.3	21.9	0.980	15.5	1.008
2.1	1.9	11.6	19.6	18.9	0.964	12.0	1.033
4.1	3.7	15.2	22.3	22.0	0.987	15.7	1.030
5.2	5.3	17.4	23.9	24.2	1.012	16.6	0.952
8.4	7.2	20.0	24.9	25.5	1.023	21.2	1.058
9.2	7.8	20.7	25.6	25.9	1.012	22.0	1.063
Mean deviation from 1.000:				0.025		0.073	

TABLE V

Competitive adsorption of gold and silver on carbon B

Experimental data					Predictions			
[O ₂]	C _{rs}	C _{rg}	Q _{rs}	Q _{rg}	Q _{rg}	r _g	Q _{rs}	r _s
9.0	17.5	10.6	20.0	33.8	33.3	0.985	19.7	0.986
	24.8	12.6	24.5	29.3	32.0	1.092	23.7	0.967
	15.6	5.0	21.3	23.4	24.0	1.026	25.5	1.196
	4.3	1.6	18.3	19.8	22.6	1.142	16.7	0.913
	1.6	0.3	13.9	14.0	13.4	0.956	16.3	1.170
	5.9	8.2	8.7	37.9	39.5	1.042	9.1	1.049
	3.7	3.7	8.0	32.4	33.9	1.047	9.7	1.216
	9.1	17.3	6.4	48.8	45.0	0.922	8.5	1.326
	4.2	14.5	10.5	19.4	37.6	35.1	0.933	15.2
9.3		4.4	16.8	29.6	27.8	0.939	16.5	0.980
2.3		1.6	12.1	30.8	28.2	0.916	9.1	0.751
0.9		0.4	10.1	23.0	20.8	0.906	8.6	0.852
0.4		0.2	8.1	17.8	20.2	1.133	6.4	0.796
0.2		0.1	6.8	14.6	18.7	1.280	5.3	0.775
0.0	15.3	12.3	5.4	26.5	25.6	0.968	4.5	0.825
	13.3	8.4	5.6	23.2	22.5	0.969	5.1	0.903
	7.1	7.1	2.8	22.5	24.4	1.084	3.4	1.221
	5.2	3.4	3.4	19.6	19.3	0.984	4.3	1.253
	3.9	2.1	3.6	17.1	16.7	0.977	4.6	1.267
	2.7	1.2	3.6	14.8	14.2	0.957	4.8	1.327
	1.7	0.6	3.6	13.0	11.5	0.882	5.0	1.386
	0.5	0.2	3.3	10.7	9.9	0.923	3.9	1.168
	10.9	7.3	4.7	25.5	22.3	0.874	4.7	1.006
	9.6	5.8	5.0	21.8	20.8	0.953	4.9	0.985
	6.9	2.7	5.4	17.6	15.7	0.889	5.9	1.098
Mean deviation from 1.000:						0.007		0.167

and Q_e values in Tables IV and V to calculate the f(C_r) values plotted in Figures 14 to 17. For carbon A the competition coefficients were determined as a_{gs} = 0.147 and a_{rg} = 1.131, which means that a_{gs} = 1/a_{rg} is not being satisfied. Therefore the assumptions used by Sheindorf *et al.* (1981) are not applicable to the competitive adsorption of silver and gold on carbon A. From the ratios of predicted to experimental values, r_g and r_s, in Table IV it is nevertheless evident that this model is adequate for the prediction of the equilibrium loadings of gold and silver cyanides.

For carbon B the competitive adsorption of silver and gold was studied at oxygen levels of 0, 4.2 and 9 mg O₂/l. Figures 16 and 17 illustrate that it is statistically unexceptionable to correlate the results for these three levels separately. A combined regression on all these data yielded slopes of a_{gs} = 0.334 and a_{rg} = 3.883. It is shown in Table V that reasonable predictions could be obtained by use of these aggregate coefficients. This implies that, although the oxygen concentration affects the equilibrium loadings of both metals, it appears to have

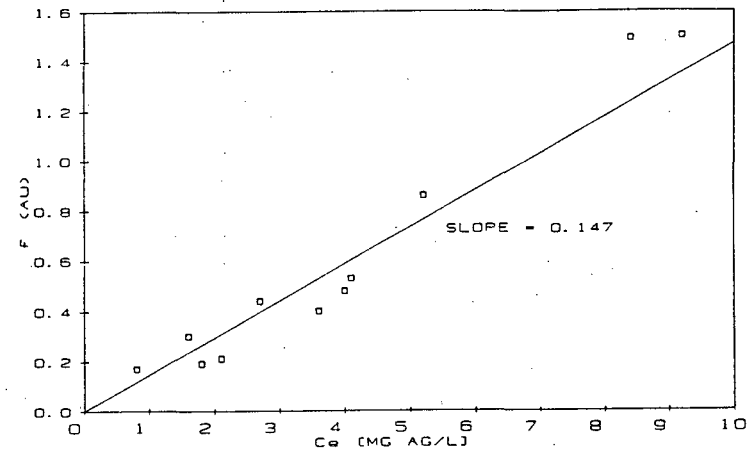


FIGURE 14 Estimation of the competition coefficient a_{gs} for the competitive adsorption of gold and silver cyanides on carbon A at [O₂] = 9 mg/l.

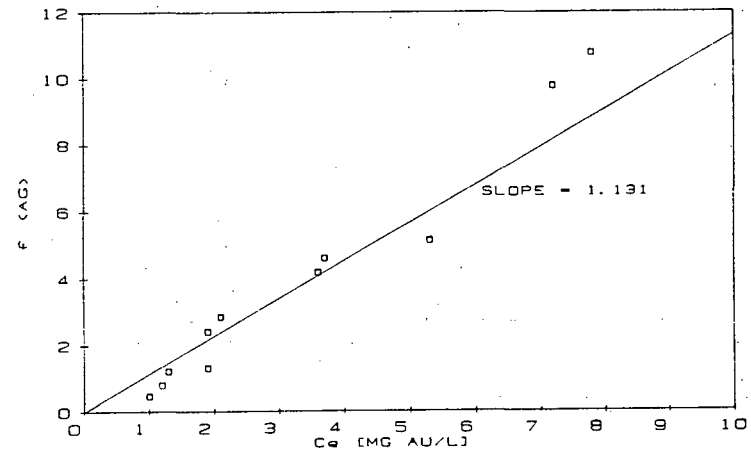


FIGURE 15 Estimation of the competition coefficient a_{rg} for the competitive adsorption of gold and silver cyanides on carbon A at [O₂] = 9 mg/l.

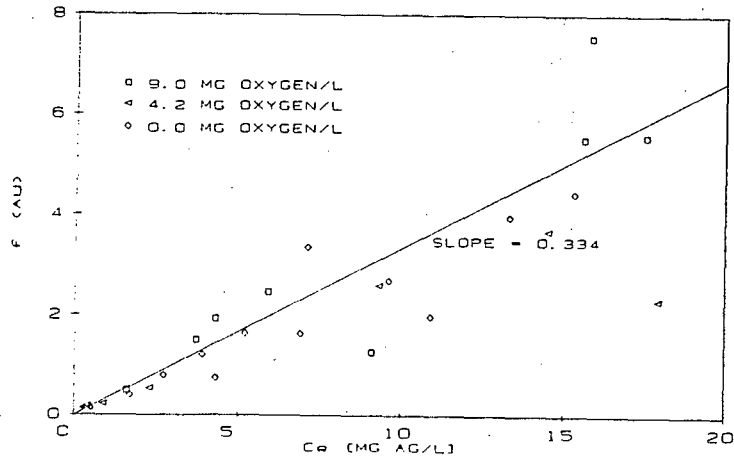


FIGURE 16 Competitive adsorption of gold and silver cyanides on carbon *B* at different oxygen levels: estimation of a_{gr} .

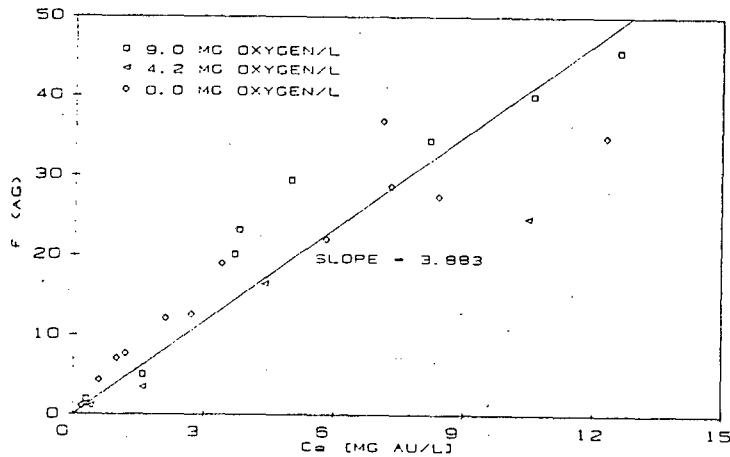


FIGURE 17 Competitive adsorption of gold and silver cyanides on carbon *B* at different oxygen levels: estimation of a_{gr} .

little influence on the competition between the gold and silver. With $1/a_{gr} = 3$ the competitive adsorption of gold and silver on carbon *B* approximates the criterion for the validity of the isotherm used.

CONCLUSIONS

The fraction of gold loaded as AuCN is a function of the type of carbon as well as the temperature and pH during adsorption. It remains to be investigated whether a relationship exists between the redox poten of the carbon and the ratio of $AuCN/Au(CN)_2^-$.

Whereas activated carbon adsorbs insignificant quantities of oxygen in water, considerable quantities of oxygen are consumed during the adsorption of anionic metal cyanides. The gold (or silver) cyanide is adsorbed in two ways: (1) where oxygen is required for the oxidation of the surface functional groups used for adsorption, and (2) where the adsorption takes place without the use of oxygen. The existence of oxygen levels above which the equilibrium loadings of metal cyanides show no further increase cannot be explained at present.

A Freundlich-type multicomponent isotherm yielded a reasonable description of the competitive equilibrium adsorption of gold and silver cyanides on both carbons tested. However, the assumptions of this isotherm do not appear to be valid for all systems. While the level of dissolved oxygen affects the equilibrium loadings of both metals, it has little influence on the competition coefficients.

ACKNOWLEDGEMENT

The authors sincerely appreciate the financial sponsorship provided by the General Mining-Union Corporation Ltd.

NOMENCLATURE

- a* competition coefficient in multicomponent isotherms
- C* solution phase concentration (mg/l)
- f* function defined in Eqs. (5) and (6)
- K* Freundlich isotherm coefficient
- n* Freundlich isotherm exponent
- [O₂] level of dissolved oxygen (mg O₂/l)
- r* ratio of predicted to experimental metal loading
- Q* metal loading on carbon (mg metal/g carbon)

Greek symbol

Δ amount of specified component consumed (mol)

subscripts

e equilibrium condition
g gold
0 initial condition
s silver

superscript

\wedge predicted or calculated value

REFERENCES

- Adams, D.M., "Metal-ligand and related vibrations", Edward Arnold (Publishers) Ltd., London, pp. 164 and 172 (1967).
- Cho, E.H., and Pitt, C.H., "The adsorption of silver cyanide on activated charcoal", *Metall. Trans.* **10B**, 159 (1979).
- Davidson, R.J., "A pilot plant study on the effects of cyanide concentration on the CIP process", *Gold 100: Proceedings of the International Conference on Gold*, vol. 2, (eds.) Fivaz, C.E. and King R.P., SAIMM, Johannesburg, South Africa, 209 (1986).
- Dixon, S., Cho, E.H., and Pitt, C.H., "The interaction between gold cyanide, silver cyanide, and high surface area charcoal", *A.I.Ch.E. Symposium Series* **74** (173), 75 (1978).
- Fleming, C.A., and Nicol, M.J., "The adsorption of gold cyanide onto activated carbon. III. Factors influencing the rate of loading and the equilibrium capacity", *J.S. Afr. Inst. Min. Metall.* **84** (4), 85 (1984).
- Fritz, W., Merk, W., and Schlünder, E.U., "Simultaneous adsorption of organic solutes in water by activated carbon", *Int. Chem. Eng.* **21**(3), 384 (1981).
- Hassler, J.W., "Purification with activated carbon", Chemical Publishing Co., Inc., New York, N.Y., p. 330 (1974).
- Hughes, H.C., Muir, D.M., Tsuchida, N., and Dalton, R., "Oxidation reduction potential of activated carbon during anion loading", *Regional Conference on "Gold-Mining, Metallurgy and Geology"*, Aus. I.M.M., Perth, 151 (1984).
- McDougall, G.J., Hancock, R.D., Nicol, M.J., Wellington, O.L., and Copperthwaite, R.G., "The mechanism of the adsorption of gold cyanide on activated carbon", *J.S. Afr. Inst. Min. Metall.* **80**(9), 344 (1980).
- Sheindorf, C.H., Rebhun, M., and Sheintuch, M., "A Freundlich-type multicomponent isotherm", *J. Colloid and Interface Sci.* **79**(1), 136 (1981).
- Tsuchida, N., Ruane, M., and Muir, D.M., "Studies on the mechanism of gold adsorption on carbon", Proceedings of MINTEK 50: *International conference on mineral science and technology* vol. 2, (ed.) Haughton L.F., MINTEK, South Africa, 647 (1984).
- Weast, R.C. (ed.), "Handbook of Chemistry and Physics", 64th ed., CRC Press, Inc., Boca Raton, Florida, p. B-95 (1985).

APPENDIX M

CONFERENCE PRESENTATION OF RESULTS WITH SURFACE DIFFUSION MODEL

Presented at the 14th Congress of CMMI, Edinburgh, Scotland, 2-6 July
1990.

GENERALIZED SIMULATION OF ZADRA AND AARL ELUTION COLUMNS

P.F. VAN DER MERWE & J.S.J. VAN DEVENTER

Department of Metallurgical Engineering
 University of Stellenbosch
 Stellenbosch 7600
 South Africa
 FAX : (02231) 774336

ABSTRACT

Most modelling work on activated carbon systems has been concerned only with the adsorption process. If the adsorption and desorption processes occur at the same rate, and if the isotherm of adsorption is completely reversible, modelling of the desorption process is quite simple. Unfortunately, this seldom occurs in practice, so that a more involved procedure of simulation has to be followed. In this paper the mechanism of elution and the difficulties encountered during the simulation thereof are discussed.

It is demonstrated that it is possible to simulate both the Zadra and the AARL elution processes with the same fundamental model. The model that has been proposed, accounts for the change in eluate composition, as well as the change in the activity of the carbon towards the decomposition of CN^- and the adsorption of $Au(CN)_2^-$. These changes have been incorporated in a shifting equilibrium isotherm that is assumed to apply at the liquid-solid interface.

Simulations of experimental data are presented as proof of the validity of the model. Furthermore, the model is used to perform a parametric sensitivity test and to predict the elution profile during a continuous elution process.

INTRODUCTION

Mainly three methods of elution are employed at present⁽¹⁾:

- (1) The Anglo American Research Laboratory (AARL) method which consists of a pretreatment step, in which the loaded carbon is soaked in a hot cyanide solution, followed by elution with hot deionised water,
- (2) The Zadra method in which a warm cyanide solution is recycled through an elution column and electrowinning cell in series, and
- (3) The organic solvent methods in which large quantities of organic solvents such as methanol, ethanol, acetone or acetonitrile are added to the eluants of the above mentioned procedures.

Even though cyanide is used in all of these processes, it has been shown^(2,3) that, in the absence of an acid wash, elution yields of 100% can be accomplished without the addition of cyanide. This is in contrast with adsorption mechanisms in which it is postulated that up to half of the aurocyanide is decomposed to AuCN after it has been adsorbed^(4,5).

These claims necessitated an investigation⁽⁶⁾ into the form of the adsorbed species and the factors involved in the transformation of one species into another. In the absence of free cyanide, AuCN is practically insoluble. The $Au(CN)_2^-$ could therefore be eluted with distilled water, and the difference between the remaining and eluted gold accounted for as AuCN. It was found that AuCN is formed only on some carbons. The % of $Au(CN)_2^-$ that will be transformed depends on the pH and temperature of the solution, and most likely on the redox potential of the carbon. If no AuCN is present on the gold loaded carbon, all the gold can be eluted without the addition of cyanide. If cyanide enhances the elution of the gold as $Au(CN)_2^-$, this effect cannot be ascribed to the solvation of the AuCN species.

Little work has been done on the modelling of the elution of gold cyanide from activated carbon. The only attempt to do so was the modelling of the Zadra elution process by Adams and Nicol⁽³⁾. Even though the authors claim that they could successfully simulate the Zadra process, they did so after making the following assumptions:

1. A single average mass transfer coefficient was used to describe the intraparticle diffusion.
2. The equilibrium between the gold on the carbon and that in solution was described by a single linear isotherm (i.e. $Q_{pg} = A C_{pg}$); and
3. The elution conditions was assumed to remain constant during the course of the process.

The assumption of a linear isotherm will be applicable only under conditions of low solution phase concentrations as was the case for the continuous stirred tank reactor in which they have performed their tests. Adams and Nicol⁽³⁾ included an extension of their model to describe

elution in a column, but provided no experimental evidence for the applicability thereof.

As far as the modelling of the AARL elution process is concerned, no attempts have been published yet. The main reasons for this are probably the following :

1. The lack of understanding the need for the pretreatment process,
2. The change in the chemical composition of the eluate during the elution, and
3. The apparent complexity of the opposing effects of high ionic strength and high cyanide concentrations.

This paper describes the development of a fundamental model that can be used for the simulation of both the AARL as well as the Zadra process. Although it has not yet been proven, it is assumed that it will also be applicable to elution with organic solvents. Apart from its prediction and simulation functions, the model can be used in combination with existing models for CIP or CIL to optimize plant designs. It can also be used for the training of operators in order to develop their feeling for the dynamics of the process as well as the sensitivity thereof to changes in elution conditions. A computer program was developed for the numerical solution of the simulation model. This program can be used on an IBM compatible XT type personal computer with an 8087 math coprocessor and takes less than 4 min. to simulate an 8 hour long elution run. It is obvious that this simulation will be significantly faster if a high frequency AT machine is used.

EXPERIMENTAL

All the experimental data were collected by using eluted carbon from the Beatrix mine in South Africa. This carbon was acid washed and rinsed with deionised water to remove as much impurities as possible. The carbon was tested for the formation of AuCN as described⁽⁶⁾ previously. It was found that no AuCN was formed on the carbon during adsorption from alkaline solutions at room temperature. A BET surface area of $792 \text{ m}^2 \cdot \text{g}^{-1}$ and an apparent density of $838.8 \text{ kg} \cdot \text{m}^{-3}$ were measured for the carbon. The pore volume of the carbon was determined as $9 \times 10^{-4} \text{ m}^3 \cdot \text{kg}^{-1}$ by measuring the weight loss upon oven drying of a sample of carbon saturated with water. The average particle size was 1.42 mm and provided a void fraction of 0.292 in a packed column.

Most of the elution runs were conducted in a glass column with a temperature controlled water jacket. A stainless steel column with a hot oil jacket was used to test the models on a larger scale. The dimensions of the columns are summarized in Table I. The glass column contained 9.4 g and the stainless steel column 3500 g of the above mentioned dry carbon.

In order to simplify the investigation, it was decided to use only the potassium salts of aurocyanide, cyanide and hydroxide. In more complex systems other cations, or combinations thereof, can be treated similarly to K'. Distilled water was used in all the experiments.

Batch experiments were conducted in 1000 ml stirred reactors and the equilibrium conditions measured after a period of 3 weeks.

Table I : Dimensions of columns.

Column	Glass	Steel
Height [m]	0.143	0.749
h/d ratio	11.57	7.49
Flow area [m ²]	1.2×10^{-4}	7.854×10^{-3}
Bed volume [cm ³]	17.16	5883

ELUTION SUB-PROCESSES

After the pretreatment step in the AARL process, the gold is normally eluted with a high quality softened water to minimize the ionic strength of the eluant and thereby promoting the desorption of the gold. The elution step contains three important sub-processes that occur simultaneously. The most obvious of these is the desorption of the gold, followed by the diffusion thereof out of the carbon into the interparticle solution. The other two sub-processes involve the removal of the pretreatment reagents from the carbon bed. These two processes are defined as, firstly, the diffusion of cations from the pores of the carbon, and, secondly, the decomposition and diffusion of the cyanide from the carbon pores.

Figure 1 shows a typical elution profile obtained at 70°C in the glass column described previously. The concentrations of the gold, cyanide and potassium have been normalized for comparative reasons. Note the sharp decline in the cyanide and potassium concentrations within the first two bed volumes. The tailing effect is because of the reagents being trapped in the pores of the carbon. The peak in the gold profile appears only once the bulk of the pretreatment reagents have been removed. The pH remains high for the whole duration of the run, even though the pH of the water supply has not been adjusted.

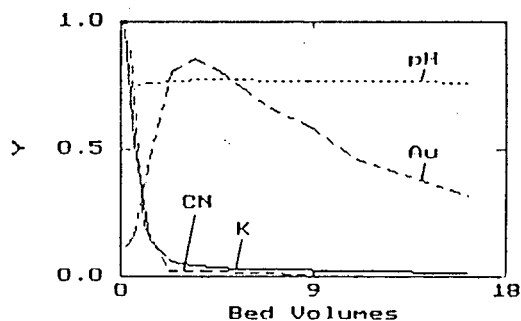


Figure 1 : Normalized AARL elution profiles. $C(\text{Au}) = 140 \cdot Y \text{ mg/l}$, $C(\text{K}) = 3500 \cdot Y \text{ mg/l}$, $\text{pH} = 14 \cdot Y$, $C(\text{CN}) = 1500 \cdot Y \text{ mg/l}$

MATHEMATICAL MODELS

In the modelling of the elution process, the temperature and pH are assumed as constant for a particular run. This leaves the concentrations of aurocyanide, cyanide and potassium as variables. As the potassium and cyanide concentrations affect the gold isotherm, it is important to know their concentrations at any time and height in the elution column. Therefore, the displacement of the pretreatment reagents had to be modelled together with the modelling of the elution of the gold. For modelling purposes, the carbon particles were assumed to be spherical.

Potassium

The elution of the cations was modelled with a mechanism that accounts for accumulation in two types of pores, which present different resistances to diffusion (viz. macropores and micropores). The micropores had to be included to provide the long tail of potassium that was observed in the experimental work. To simplify the model, the resistance to film transport was assumed to be negligible. The amount of potassium co-adsorbed with the $\text{Au}(\text{CN})_2^-$ or CN^- was assumed to be small compared to the accumulation in the pore liquid and omitted. The mathematical model for the displacement of the potassium consists of the following equations:

Mass balance over the macropores:

$$\frac{\partial C_{mk}}{\partial t} = \frac{D_{mk}}{r^2} \frac{\partial}{\partial r} \left[r^2 \frac{\partial C_{mk}}{\partial r} \right] - \frac{k_{bk}}{a_k} (C_{mk} - C_{bk}) \quad (1)$$

Mass balance over the micropores:

$$(1 - \alpha_k) \frac{\partial C_{bk}}{\partial t} = k_{bk} (C_{mk} - C_{bk}) \quad (2)$$

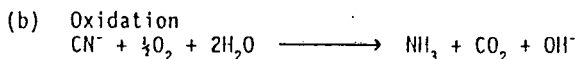
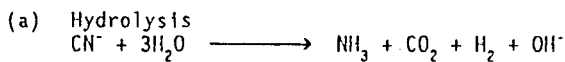
Mass balance over the interparticle solution:

$$a\epsilon \frac{\partial C_k}{\partial t} = -V \frac{\partial C_k}{\partial h} - \frac{6}{d_c} \alpha_k a v_p \rho D_{mk} (1 - \epsilon) \frac{\partial C_k}{\partial r} \Big|_{r=R} \quad (3)$$

Equations (1) and (2) were transformed to ordinary differential equations by the use of average concentrations in the pores and solved by a 4th order Runge-Kutta routine. Equation (3) was discretized by a backwards-difference method and solved simultaneously with equations (1) and (2).

Cyanide

Under normal, alkaline gold elution conditions, cyanide is decomposed via several reactions. Of these, the following reactions are considered to be the most important:



The oxidation reaction is catalyzed by the presence of activated carbon. Measurement^[7] of

the decomposition rate of cyanide revealed first order kinetics for both the hydrolysis and oxidation reactions.

The physical adsorption of cyanide on activated carbon at room temperature was found^[7] to be relatively insignificant compared to the decomposition thereof. Furthermore, it can be assumed that the adsorption of cyanide, like $\text{Au}(\text{CN})_2^-$, will decrease with an increase in temperature and that it will become negligible under typical elution conditions.

It was found that the reaction rate was independent of particle size, but strongly dependent on mixing speed. This means that resistance to film transfer is dominant and that a uniform concentration of cyanide can be assumed throughout the carbon particles.

A model consisting of equations (4) and (5) adequately describes the removal of cyanide from the carbon bed. Although the rate of cyanide decomposition in the pores of the carbon will differ from that in the interparticle solution, an average rate constant (k_N) is used to minimize the number of parameters.

Pore mass balance:

$$\frac{\partial C_{pN}}{\partial t} = \frac{6k_{rN}}{d_c v_p \rho} (C_N - C_{pN}) - k_N C_{pN} \quad (4)$$

Mass balance over the interparticle solution:

$$a\epsilon \frac{\partial C_N}{\partial t} = -V \frac{\partial C_N}{\partial h} - \frac{6}{d_c} k_{rN} a (1 - \epsilon) (C_N - C_{pN}) - a\epsilon k_N C_N \quad (5)$$

These equations were discretized with a backwards-difference method and could be combined in a single equation.

Gold

It has been shown^[8] that the adsorption of $\text{Au}(\text{CN})_2^-$ is fully reversible if no AuCN is present on the gold loaded carbon. It can therefore be assumed that the intraparticle transport mechanism for the $\text{Au}(\text{CN})_2^-$ will be similar for adsorption and desorption. While a mechanism of surface diffusion is favoured^[9] for the adsorption of gold onto activated carbon, Hall et al.^[10] reported pore diffusion to be dominant under conditions of high pore fluid concentration, and conversely for surface diffusion. As high solution phase concentrations are reached during elution, pore diffusion is expected to make a significant contribution to the intraparticle transport of the gold. Nevertheless, a comparison of simulations with models for pore diffusion, surface diffusion, and a combination thereof revealed that the same results could be obtained with any of these models. It was decided to model the elution with a mechanism of surface diffusion for the following reasons:

1. The model for a surface diffusion mechanism is mathematically easier to solve, and therefore consumes less computing time,
2. The surface diffusion model involves fewer

parameters than the fundamentally more appropriate combination model, and

3. Adsorption breakthrough curves^[11] calculated with either a pore or surface diffusion model for an unfavourable isotherm (i.e. poor adsorption) showed little difference.

The following main assumptions have been made in the development of the model :

1. Accumulation of metal cyanide in the pore liquid is negligible,
2. The pores of the carbon can be classified as macropores and micropores which are homogeneously distributed throughout the particle,
3. The surface of the carbon is separated from the bulk liquid by a liquid film surrounding the particle,
4. Local equilibrium exists at the carbon surface, and
5. No accumulation of metal cyanide occurs at the external particle surface.

The model is similar to Van Deventer's model^[9] for adsorption and consists of equations (6) to (10).

Macropore mass balance :

$$\frac{\partial Q_{mG}}{\partial t} = \frac{D_{mG}}{r^2} \frac{\partial}{\partial r} \left[r^2 \frac{\partial Q_{mG}}{\partial r} \right] - \frac{k_{bG}}{\alpha_G} (Q_{mG} - Q_{bG}) \quad (6)$$

Micropore mass balance :

$$(1 - \alpha_G) \frac{\partial Q_{bG}}{\partial t} = k_{bG} (Q_{mG} - Q_{bG}) \quad (7)$$

Mass balance at external particle surface :

$$k_{fG} (C_G - C_{sG}) = \alpha_G D_{mG} \rho \left. \frac{\partial Q_{mG}}{\partial r} \right|_{r=R} \quad (8)$$

Mass balance over interparticle solution :

$$a\epsilon \frac{\partial C_G}{\partial t} + V \frac{\partial C_G}{\partial h} + \frac{6}{d_c} k_{fG} a (1 - \epsilon) (C_G - C_{sG}) = 0 \quad (9)$$

Local equilibrium at particle surface :

$$Q_{sG} = A C_{sG}^n \quad (10)$$

Equations (6) and (7) were transformed to ordinary differential equations by the use of average metal loadings in the pores. The value of C_{sG} is guessed at each step and the calculation of equations (1) and (2) repeated with a 4th order Runge-Kutta method until condition (8) is satisfied. By approximating the loading gradient at the external particle surface by a quadratic driving force^[10], equation (8) was written as a normal algebraic equation. Equation (9) was discretized and solved together with the other equations.

EQUILIBRIUM STUDIES

It is assumed that local equilibrium exists at the solid-liquid interface. The aurocyanide equilibrium is a function of the chemical and physical conditions prevailing at the carbon surface at that moment. The most significant influences on the elution of gold have been listed^[3,12], in order of decreasing importance, as follows : temperature, cyanide and hydroxide concentrations; and the ionic strength of the eluant.

As the composition of the surrounding liquid constantly changes during an AARL elution, it will be impossible to model the process with a single constant equilibrium condition. This makes it necessary to know the equilibrium at all possible combinations of temperature, pH, cyanide concentration and ionic strength.

At any one combination of these factors the equilibrium can be described by a Freundlich isotherm,

$$Q_{eG} = A C_{eG}^n \quad (11)$$

The problem is that, if the conditions are changed, the value of A as well as n change. In an attempt to minimize the number of variables, the values of A and n determined for more than 10 different carbons under different adsorption conditions have been plotted in Figure 2. From this plot it is clear that n decreases linearly with an increase in A. It was found that the isotherm for the carbon used in this study can be written as :

$$Q_{eG} = A C_{eG}^{-0.002688 \cdot A + 0.2902} \quad (12)$$

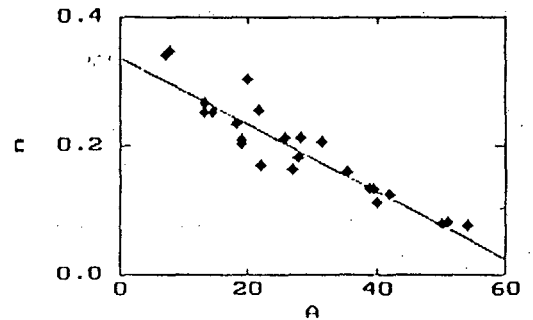


Figure 2 : Freundlich isotherm parameters for the equilibrium adsorption of gold on various carbons.

With only the one unknown constant A in the isotherm expression, it was now possible to describe the equilibrium at any given set of conditions with only one value of Q_{eG} and C_{eG} . It was further postulated that A can be written as a function of temperature, pH, cyanide concentration (C_N) and potassium concentration (C_K) as follows :

$$A = f_1(T) \cdot f_2(pH) \cdot f_3(C_N) \cdot f_4(C_K) \quad (13)$$

Because different cations, even with the same charge, have different effects on the adsorption and desorption of $\text{Au}(\text{CN})_2^-$, it was decided to treat each cation separately and not to include the ionic strength as such. Each of the functions f_1 to f_4 was determined by changing the variable of f_1 that specific function while keeping the other variables constant. By following this procedure, eq. (13) adopted the following form :

$$A = A_0 \exp(b_1/T) \exp(b_2 \cdot \text{pH}) (C_H+1)^{b_3} (C_K+1)^{b_4} \quad (14)$$

By fitting equation (14) to equilibrium adsorption data determined at different combinations of pH, C_H and C_K in the temperature range 18°C to 60°C, the parameters were determined as :

$$A_0 = 0.13, \quad b_1 = 2044, \quad b_2 = -0.2014, \\ b_3 = -0.0888, \quad \text{and} \quad b_4 = 0.041.$$

Even though the values of the parameters have to be changed under certain conditions, the relationships remain the same. If other cations are to be added to the system, the equation for A can be extended by adding more functions or by grouping the different cations together.

PRETREATMENT

In an AARL elution, the cyanide that is carried over from the pretreatment to the elution step seems to be of little importance, as it is washed out of the bed within the first 2 bed volumes of eluant that passes through the column. If, however, the carbon was pretreated with a solution with the same pH and potassium concentration as in a normal pretreatment, but omitting the cyanide, the elution process was inhibited. It has to be stressed that this was not because of the presence of an irreversibly adsorbed gold species as no acid wash had been performed, and it is known that all the gold adsorbed onto this specific carbon was in the $\text{Au}(\text{CN})_2^-$ form.

An experiment (see Figure 3) was then devised to investigate the effect of the cyanide pretreatment. In the pretreatment step the gold loaded carbon was soaked in 1 bed volume of a 20 g KCN/l solution for 40 h at room temperature, followed by 1 hr at 100°C to decompose any remaining free cyanide. The elution step consisted of two stages : During the first stage an eluant containing 2000 mg K⁺/l was pumped through the carbon bed. The high cation concentration suppressed the elution of the gold and provided 4 bed volumes of eluant to completely rinse the carbon of any cyanide that was carried over from the pretreatment stage. For the second stage of the elution the potassium rich eluant was replaced with distilled water. The gold peak appeared almost immediately.

From this experiment the following conclusions could be drawn :

1. The cyanide in the elution step is of secondary importance to that in the pretreatment.
2. With only $\text{Au}(\text{CN})_2^-$ on the carbon, the cyanide could not have been used to alter

the gold species.

3. Cyanide displaces very little gold via a mechanism of competitive adsorption, because that would have led to more gold being desorbed in the pretreatment stage.
4. The horizontal position of the gold peak is a function of the kinetics of the removal of the cations carried over from the pretreatment stage.

As it was found that the cyanide ion does not displace or alter the adsorbed aurocyanide, it is speculated that the cyanide that is decomposed on the surface of the carbon during the pretreatment stage changes the functional groups on the surface in such a way that the surface becomes less receptive to adsorption.

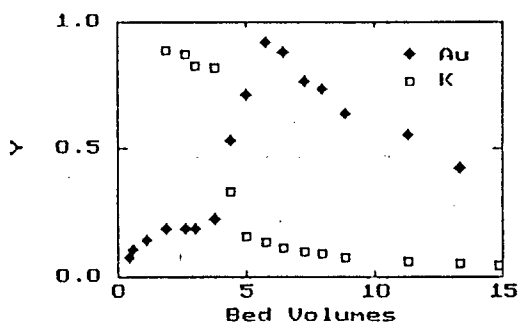


Figure 3 : The prolonged effect of cyanide pretreatment on elution. $C(\text{Au}) = 220 \cdot Y \text{ mg/l}$, $C(\text{K}) = 2500 \cdot Y \text{ mg/l}$

SIMULATIONS OF EXPERIMENTAL DATA

Potassium

Figure 4 shows the displacement of a potassium solution with distilled water from a bed of carbon that has been soaked in a KCl solution. This experiment was conducted in the stainless steel column described in the Experimental section. The portion of Figure 4 containing values lower than 300 mg K⁺/l are enlarged in Figure 5. It can be seen that the model accurately describes the experimental profile right down to the lowest values that have been measured. The conditions and parameters used in the simulations are summarized in Table II.

The intraparticle parameters were determined as follows :

$$D_{mk} = 1 \times 10^{-10} \text{ m}^2 \cdot \text{s}^{-1}, \quad \alpha_k = 0.8, \quad k_{bk} = 3 \times 10^{-5} \text{ s}^{-1}$$

It was found that the same parameters could be used in simulations of experimental data collected from both the stainless steel column as well as the more than 300 times smaller glass column.

Cyanide

The simulation in Figure 6 can be taken as representative of the accuracy of the predictions with the simple model described above. In this case carbon particles with a pore concentration

Table II : Conditions and parameters for simulations

Figure no.	4,5	6,8	9	10	7,12	Std
Column	SS	G	G	SS	G	SS
V [bed vol./h]	1.68	3.0	3.0	3.11	3.17	3.0
T [°C]	20	70	70	80	70	80
pH		10.6	10.2	10.8	9.5	10.8
Q_{16} [mg/g]	0	4.85	4.80	2.78	4.76	3.0
m_{mb}		0.5	0.5	1.0	0.5	0.7
α_6		0.5	0.6	0.9	0.9	0.8
A_0		0.37	0.10	0.12	6.5	0.15
b_3		0.0	0.0	0.0	-0.18	0.0
b_4		0.2	0.40	0.25	0.0	0.2
b_5		0.0	0.0	0.0	0.07	0.0
C_{IK} [mg/l]	1932	7380	4245	5000	260	5000
C_{FK} [mg/l]	0	0	0	0	260	0
C_{IN} [mg/l]	0	4593	1128	1070	0	1000
C_{FN} [mg/l]	0	0	0	0	190	0
Pretreatment	1	2	3	4	0	

Pretreatment procedures :

0. None.
1. Soaked carbon for 48 h at 20°C in 2 bed volumes of a 4 g KCl/l solution.
2. Soaked carbon for 30 min. at 20°C in 20 ml of a 20 g KCN/l solution.
3. Soaked carbon for 30 min. at 100°C in 10 ml of a 20 g KCN/l solution.
4. Soaked carbon for 15 h at 20°C in 1 bed volume of a 20 g KCN/l solution, switched on heaters and soaked for further 1.5 h while raising temperature of column.

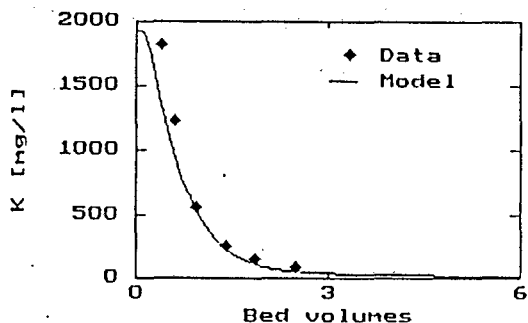


Figure 4 : Simulation of the displacement of potassium from a bed of carbon.

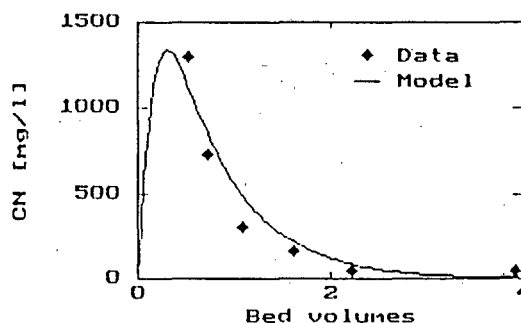


Figure 6 : Simulation of removal of cyanide during an AAIL elution

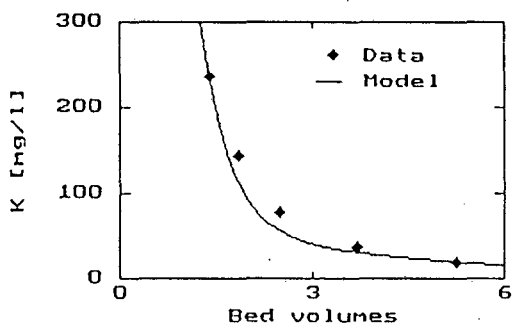


Figure 5 : Enlargement of lower portion of Figure 4

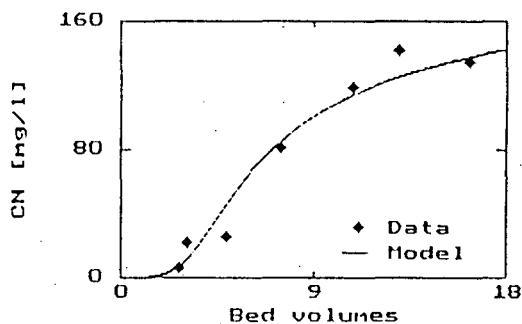


Figure 7 : Simulation of decomposition of cyanide during a Zadra elution

of 4593 mg CN/l were dropped into the glass column containing distilled water at 70°C. The cyanide was then washed out with distilled water at the same temperature. This experiment is equivalent to the decomposition and displacement of cyanide in an AARL elution process where the pretreatment step has been conducted in a separate vessel. The following parameters have been used in this simulation :

$$k_{rN} = 2 \times 10^{-7} \text{ m.s}^{-1} \quad k_{oN} = 7.3 \times 10^7 \text{ s}^{-1}, \\ E_N = 73000 \text{ kJ.mol}^{-1}$$

In an ideal Zadra operation, a constant concentration of cyanide is maintained in the eluant. The eluate concentration during a Zadra elution at 70°C with a constant feed concentration of 190 mg CN/l is plotted in Figure 7. It can be seen that the fraction of cyanide that is decomposed decreases with time. This can be ascribed to the deactivation of the carbon as related to the decomposition of cyanide. The amount of cyanide previously decomposed on a sample of carbon will be referred to here as the "cyanide-age" (Q_N) of the carbon, with the dimensions of mg CN/g carbon. By measuring the rate constant of cyanide decomposition in the presence of carbons with different cyanide-ages, the following relationship was found to describe the change in the rate constant :

$$k_N = \frac{k_{oN}}{(Q_N + 1)^{b_6}} \quad (15)$$

For the simulation in Figure 7 the values for k_{rN} and E_N were as above. The other parameters were :

$$k_{oN} = 5 \times 10^9 \text{ s}^{-1}, \text{ and } b_6 = 3.5.$$

It has to be stressed that the values presented here are combinations of values for different reactions and that they have been determined by fitting the model to the experimental data.

Gold

During the simulation of gold elution, the cyanide and potassium concentrations are first calculated at each incremental height and timestep in order to establish the gold equilibrium at that specific condition. As the temperature and pH remains constant during the elution, equation (14) has been used in the form :

$$A = A_0 (C_N + 1)^{b_3} (C_K + 1)^{b_4} \quad (16)$$

In equation (16) the value of A_0 is determined by the pretreatment of the loaded carbon and the temperature and pH of the elution. The conditions and parameters used in the simulations are summarized in Table II. The following transport coefficients have been used in all the simulations of gold elutions :

$$k_{rG} = 5 \times 10^{-6} \text{ m.s}^{-1}, \quad D_{mG} = 1 \times 10^{-11} \text{ m}^2.\text{s}^{-1}, \text{ and } \\ k_{bG} = 1 \times 10^{-5} \text{ s}^{-1}.$$

Figure 8 shows the simulation of an AARL elution at 70°C after a pretreatment step in which the carbon has been soaked for 30 min. in a 20 g KCN/l solution at room temperature. The value of m_{mb} (the initial ratio of loading in the micro pores to that in the macro pores) is less than 1.0 because equilibrium has not been attained in the foregoing adsorption. The conditions for the elution in Figure 9 are the same as those in Figure 8, except for the pretreatment step that has been conducted at 100°C. By comparing the α_6 values of these two runs, it seems that the pretreatment conditions have an influence on the micro-macro behaviour of the carbon.

From the definition of an ideal plug flow reactor it follows that the gold elution profile will be independent of the dimensions of the column, provided that the same flow rate (in bed volumes/hr) is used and that the flow in the column does not deviate from plug flow. This is illustrated in Figure 10 in which the experimental data have been collected from an elution run in the stainless steel column, whereas the parameters used for the simulated profile have been determined under the same conditions in the small glass column. Because the gold loaded carbon used in this run had been stored in distilled water for a period of 6 months before the elution, it was assumed that the gold was distributed homogeneously throughout the carbon, so that a value of $m_{mb} = 1.0$ had to be used in the simulation.

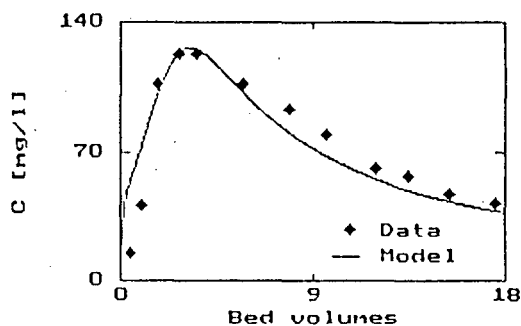


Figure 8 : Simulation of gold profile during an AARL elution

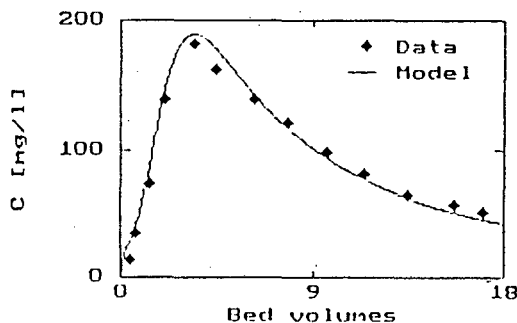


Figure 9 : Simulation of gold profile during an AARL elution

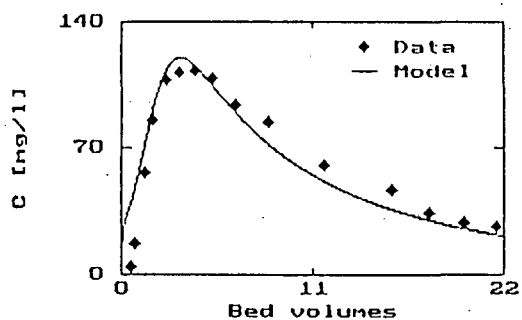


Figure 10 : Prediction of AARL elution on larger scale with parameters from experiment in glass column.

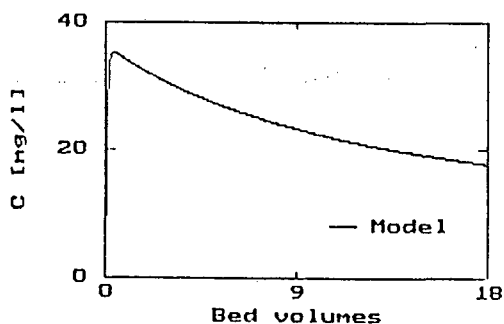


Figure 11 : Simulation of gold profile during Zadra elution in a CSTR. Equilibrium assumed to be constant.

The same model can also be used for the simulation of a Zadra elution. The run in Figure 11 has been performed with a constant equilibrium isotherm. By using only one height increment in the simulation, the profile represents that of an elution in a CSTR. From Figure 7 it is clear however that the cyanide concentration in the interparticle solution changes drastically during a Zadra elution in a column. As the gold equilibrium is affected by the solution phase cyanide concentration as well as the cyanide-age of the carbon, it is impossible to simulate the process with a single equilibrium isotherm. The experimental data from a Zadra elution in a column is plotted in Figure 12.

$$A = A_0 \frac{(C_N+1)^{b_3}}{(b_5 \cdot Q_N+1)} \quad (17)$$

MODEL PREDICTIONS

The parameters used for the simulations in this section can be found in Table 11 where it has been designated as "Std". Those values that have been changed, are supplied in the respective figure captions.

Figure 13 illustrates the sensitivity of gold elution to temperature. The effect of temperature on the adsorption isotherms was

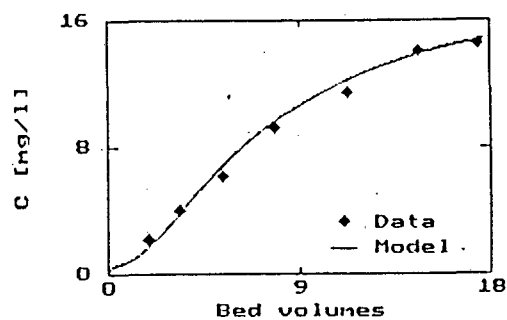


Figure 12 : Simulation of the gold profile during a Zadra elution in a column

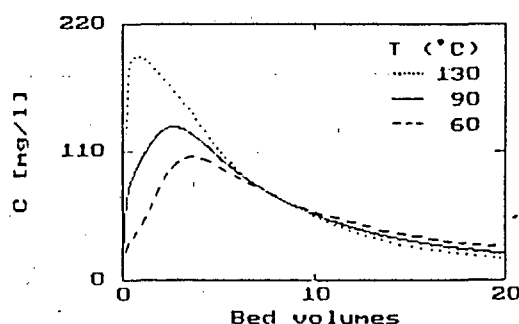


Figure 13 : Prediction of effect of temperature on AARL elution

included in the equation for A (Eq.14) as :

$$A = 0.095 \exp(2044/T) (C_k+1)^{0.2} \quad (18)$$

Although it has not been quantified yet, it seems that the effect of the potassium concentration (b_4) increases with temperature. This implies that the difference in the horizontal positions of the peaks in Figure 13 will be less in practice. Furthermore, the value of $b_1 = 2044$ has been determined over the temperature range 20°C to 60°C and can result in large errors if extrapolated to such high temperatures as 130°C.

The initial gold loading on the carbon has a small effect on the form of the elution profile, but results in drastic changes in the peak height (Figure 14). After elution with 20 bed volumes of water, the curves in Figure 14 represented elution efficiencies of 61%, 74% and 77% for initial loadings of 1.5, 3.0 and 4.0 mg Au/g respectively. This will have a large effect on the cost of elution^[12].

In order to simulate the effect of water quality on AARL elution, the elution profiles in Figure 15 have been determined with 0, 300 and 1000 mg K⁺/l in the eluant. The calculated elution efficiencies after 20 bed volumes of eluant decreased with increasing potassium concentration as follows : 74%, 61% and 54%. As mentioned earlier, the effect of potassium seems to vary with temperature and may result in larger or smaller differences in the simulations of Figure 15.

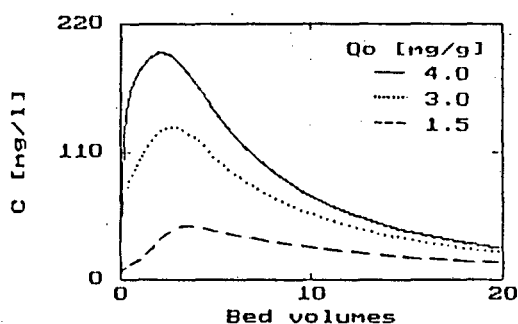


Figure 14 : Effect of initial gold loading on AARL elution

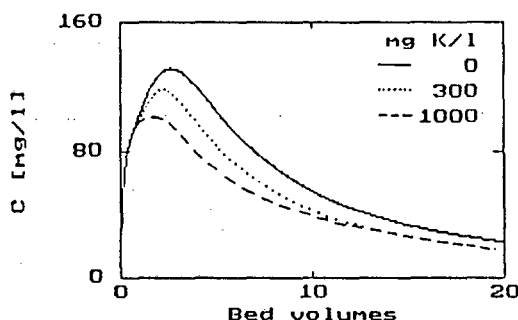


Figure 15 : Effect of water quality on AARL elution.

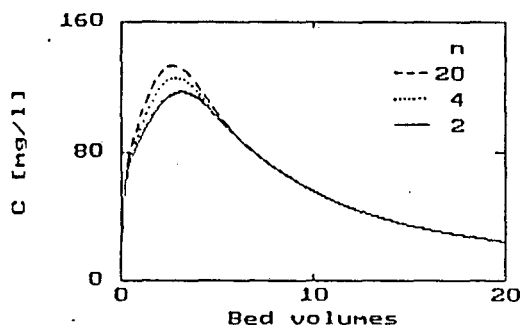


Figure 16 : Simulation of deviation from plug flow by back-mixing. n = number of height increments.

Menne^[13] presented elution profiles obtained from laboratory scale columns with h/d ratios ranging from 1.5:1 to 12:1. No apparent effect could be observed. Variations due to different h/d ratios on large columns were attributed mainly to deviations from plug flow. Deviations from plug flow were investigated in Figure 16 by decreasing the number of incremental height sections in the simulation. The relatively small effect implies that the degree of back mixing can be considered as of minor importance and that larger variations are probably caused by channelling or bypassing of portions of the carbon bed. Such occurrences can be simulated by sub-dividing the column into two or more parallel columns with different film transfer coefficients.

The computer program also accommodates the simulation of a continuous elution column as developed by Nedpac Engineering, Australia^[14]. In such an operation the carbon and eluant moves in counterflow through the column. The pretreatment reagents are circulated through the top section of the column. As the eluted carbon is extracted from the bottom of the column, carbon from the pretreatment stage moves down into the elution stage. The step changes in the simulated elution profile in Figure 17 indicate the transfer of carbon. In this simulation the bottom 10% of the carbon bed was removed during each transfer. To prevent the discharge of carbon with high gold loadings, a start-up period of 5 hours was allowed before the first transfer of carbon. The eluted carbon values have been plotted in Figure 18. The larger than normal step change at 12.5 h represents the extraction of the last 10% of the carbon from the start-up period. It follows from these two figures that the total volume of such a column will be of great importance. For a constant feed of loaded carbon, the retention time of the carbon will be determined by the capacity of the column. The choice of the optimum retention time will involve a compromise between the lowest possible gold loading on the eluted carbon and the highest possible gold concentration in the eluate.

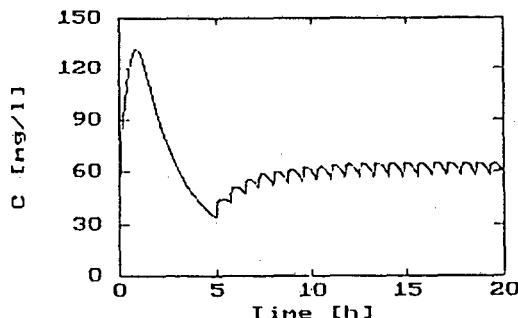


Figure 17 : Prediction of elution profile for continuous elution.

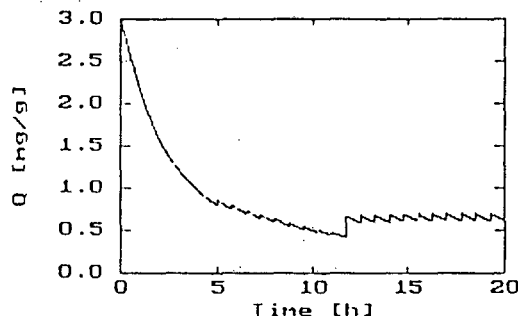


Figure 18 : Eluted carbon values during continuous elution.

CONCLUSIONS

It is possible to model both the Zadra and the AARL elution process with the same fundamental model. Because of the complexity of the system, it is impossible to model the elution of the gold without due consideration of the sub-processes involved. It was found that the shape of the gold elution profile for an AARL process is a function of mainly the removal of the cations transferred from the pretreatment stage. While the cyanide pretreatment plays a major role in the height of the elution peak and the efficiency of elution, the small amount of cyanide present during the initial stage of the elution is of little importance.

In a Zadra elution, the cyanide in the eluant is decomposed by the carbon that acts as a deactivating catalyst. If the composition of the eluant is kept constant, the gold elution profile was found to be a function of the amount of cyanide that has been decomposed on the carbon, as well as the concentration of free cyanide in the elution.

Although this paper presents the first generalized attempt to model the complex elution process, many questions remain unanswered. Further research on elution at the University of Stellenbosch will hopefully shed more light on these problems and the complex behaviour of activated carbon.

ACKNOWLEDGEMENT

The financial support of General Mining, Metals and Minerals Ltd. for this work is gratefully acknowledged.

NOMENCLATURE

a	Flow area of column [m ²]
A	Parameter in Freundlich isotherm expression
b ₁₋₅	Parameters in isotherm expression
b ₆	Deactivation parameter
C	Solution phase concentration [mg/l]
d	Column diameter [m]
D	Diffusion coefficient [m ² /s]
d _c	Particle diameter [m]
E _a	Activation energy [kJ/mol]
h _N	Bed height [m]
k _b	Rate coefficient for transport between macropores and micropores [1/s]
k _f	Film transfer coefficient [m/s]
k _N	Reaction rate constant [1/s]
k _{oN}	Frequency factor in Arrhenius' law [1/s]
m _{mb}	Ratio of metal loading in micropores to metal loading in macropores
n	Exponent in Freundlich isotherm
Q	Concentration of adsorbent on carbon surface [mg/g]
R	Outside particle radius [m]
r	Radial variable [m]
t	Time variable [s]
T	Temperature [K]
V	Volumetric flow rate [m ³ /s]
V _p	Pore volume of carbon [m ³ /kg]
Y ^p	Dimensionless concentration

Greek symbols

α	Fraction of pores available as macropores
ε	Void fraction in bed of carbon
ρ	Apparent density of carbon [kg/m ³]

Subscripts

b	Micropores
e	Equilibrium
F	Feed
G	Gold
i	Initial value
K	Potassium
m	Macropores
N	Cyanide
P	Pores
s	Carbon surface

REFERENCES

- McDougall, G.J. and Fleming, C.A., "Extraction of precious metals on activated carbon", *Ion Exchange and sorption processes in hydrometallurgy*, Streat, M. and Naden, D. (eds.), Society of Chemistry and Industry, Wiley, Chichester, p.56 (1987).
- Jones, W., Klauber, C. and Linge, H.G., "The adsorption of Au(CN)₂ onto activated carbon", *Randol Conference on Gold and Silver*, Perth, Australia, p.243 (Oct.1988).
- Adams, M.D. and Nicol, M.J., "The kinetics of the elution of gold from activated carbon", *Gold 100: Proceedings of the International Conference on Gold*, vol. 2, (eds.) Fivaz, C.E. and King R.P., S.Afr.Inst.Min.Metall., Johannesburg, South Africa, p.111 (1986).
- Tsuchida, N., "Studies on the mechanism of gold adsorption and elution in the carbon-in-pulp process", *Ph.D. thesis*, Murdoch University, (1984).
- Cook, R., Crathorne, E.A., Monhemius, A.J. and Perry, D.L., "An XPS study of the adsorption of gold(I) cyanide by carbons", *Hydrometall.*, 22, p.171 (1989).
- Van der Merwe, P.F. and Van Deventer, J.S.J., "The influence of oxygen on the adsorption of metal cyanides on activated carbon", *Chem. Eng. Comm.*, 65, p.121 (1988).
- Muir, D.M., Aziz, A. and Hoecker, W., "Cyanide losses under C.I.P. conditions and effect of carbon on cyanide oxidation", *Proc. 1st Int. Hydrometall. Conf.*, Beijing, Eds. Yulian, Z. and Jiazhong, X., Int. Academic Publishers, (Oct. 1988).
- Van der Merwe, P.F. and Van Deventer, J.S.J., "Studies on the interaction between metal cyanides, oxygen and activated carbon", *Randol Conference on Gold and Silver*, Perth, Australia, p.258 (Oct.1988).
- Van Deventer, J.S.J., "Kinetic model for the reversible adsorption of gold cyanide on activated carbon", *Chem. Eng. Commun.*, 44, p.257 (1986).
- Hall, K.R., Eagleton, L.C., Acrivos, A. and Vermeulen, T., "Pore- and solid-diffusion kinetics in fixed-bed adsorption under constant-pattern conditions", *Ind. Eng. Chem. Fundam.*, 5 (2), p.212 (1966).

11. Weber, W. and Chakravorti, R.K., "Pore and solid diffusion models for fixed-bed adsorbers", *A.I.Ch.E.J.*, 20 (2), p.228 (1974).
12. Davidson, R.J., "A review of the AARL process for the elution of gold from activated carbon", Lecture 15, *S.A.I.M.M. "C.I.P. School"*, Randburg, (Feb. 1986).
13. Menne, D., "The adsorption and desorption of aurocyanide from activated carbon", *Nedpac Engineering Report*, Perth, (1987).
14. Paterson, M.R., "Atmospheric continuous elution", *Nedpac Engineering Report*, Perth, (1987).

LIST OF SYMBOLS

a	Flow area of column [m^2]
A	Parameter in Freundlich isotherm expression
a_c	Specific external area of carbon [$m^2.m^{-3}$]
A_o	Constant in generalized isotherm, Equation 3.1
b	Constant in generalized isotherm, Equation 3.1
B	Constant in generalized isotherm, Equation 3.1
C	Liquid phase concentration [$g.m^{-3}$]
c	Parameter describing effect of cyanide age on gold equilibrium
$c_{1,2}$	Parameters as defined in Equations 3.21 and 4.7
c_m	Squared macropore concentration [$g^2.m^{-6}$]
d	Column diameter [m]
D	Molecular diffusivity [$m^2.s^{-1}$]
d_c	Particle diameter [m]
D_L	Dispersion coefficient
D_p	Effective pore diffusion coefficient in macropores [$m^2.s^{-1}$]
D_s	Effective surface diffusion coefficient in macropores [$m^2.s^{-1}$]
E_a	Activation energy [J/mol]
f	Parameter describing effect of free CN^- on gold equilibrium
h	Bed height [m]
j	Height increment number
K	Distribution coefficient = Q_e/C_e
K	Equilibrium constant
$k_{1,2,3}$	Constants defined in Equations 5.10, 5.13, 5.14
k_b	Rate coefficient for transport between macropores and micropores [s^{-1}]
k_N	Reaction rate constant for decomposition of cyanide [s^{-1}]
k_{oN}	Frequency factor in Arrhenius' law [s^{-1}]
k_s	Film transfer coefficient [$m.s^{-1}$]
$m_{1,2}$	Constants defined for the equilibrium model in Chapter 6
M_{1-9}	Constants defined for the general model in Chapter 6
m_c	Mass of carbon [kg]
m_{mb}	Ratio of metal loading in micropores to metal loading in macropores
n	Exponent in Freundlich isotherm expression

\bar{n}	Mass flux [$\text{g}\cdot\text{m}^{-2}\cdot\text{s}^{-1}$]
N	Total number of height increments = $h/\Delta h$
N_d	Number of height sections discharged in counter-current elution
N_t	Frequency of carbon transfers during counter-current elution [hr^{-1}]
P	Gauge pressure [kPa]
p	Parameter describing effect of K^+ on gold equilibrium
p_h	Parameter describing effect of pH on gold equilibrium
Q	Concentration of adsorbent on carbon surface [$\text{g}\cdot\text{kg}^{-1}$]
q	Reactivating factor in generalized isotherm
q_m	Squared macropore loading [$\text{g}^2\cdot\text{kg}^{-2}$]
R	Outside particle radius [m]
r	Radial variable [m]
R_o	Ideal gas constant = 8.314 [$\text{J}\cdot\text{mol}^{-1}\cdot\text{K}^{-1}$]
s	Saturation volume of retained liquor per unit volume of bed voids external to the particles
S_{0-5}	Constants defined for the cyanide model in Chapter 4
T	Temperature [K]
t	Time variable [s]
u	Linear velocity [$\text{m}\cdot\text{s}^{-1}$]
v	Volume of liquid [m^3]
V	Volumetric flow rate [$\text{m}^3\cdot\text{s}^{-1}$]
V_B	Number of bed volumes
V_{cross}	Flow rate to and from deadwater regions in nonideal flow model for elution of potassium
V_p	Pore volume of carbon [$\text{m}^3\cdot\text{kg}^{-1}$]
X	Cross flow ratio in nonideal flow model for elution of potassium
Y	Normalized concentration

GREEK SYMBOLS

α	Fraction of pore surface available as macropores
β	Fraction of pore volume available as macropores
ϵ	Void fraction in bed of carbon
ϵ_c	Porosity of carbon particle
ρ	Apparent density of carbon [$\text{kg}\cdot\text{m}^{-3}$]

ξ	Zeta potential [mV]
δ	Tortuosity factor
ψ	Fraction or correction factor
ψ_N	Ratio of cyanide concentration in pore liquid to cyanide concentration in interparticle solution at end of pretreatment
Δ	Increment
Γ	Combined diffusion coefficient [$\text{m}^2 \cdot \text{s}^{-1}$]

SUBSCRIPTS

ave	Average value
b	Micropores
Ca	Calcium
cat	Cation
d	Interparticle solution
e	Equilibrium
f	Final value
F	Feed
fill	Fill procedure for drained beds
G	Gold
i	Initial value
K	Potassium
m	Macropores
max	Maximum
N	Cyanide
Na	Sodium
p	Pores
pred	Predicted value
s	Carbon surface
V	Silver
X	Oxygen